INFLUENCE OF SURFACTANTS ON THE FORMATION AND DISSOCIATION OF GAS HYDRATES IN FIXED BED MEDIA

A THESIS

Submitted in partial fulfilment of the
requirements for the award of the degree
of
DOCTOR OF PHILOSOPY

in

CHEMICAL ENGINEERING

by

AMIT ARORA

DEPARTMENT OF CHEMICAL ENGINEERING
INDIAN INSTITUTE OF TECHNOLOGY ROORKEE
ROORKEE 247667 (INDIA)
FEBRUARY 2016

INFLUENCE OF SURFACTANTS ON THE FORMATION AND DISSOCIATION OF GAS HYDRATES IN FIXED BED MEDIA

Ph.D THESIS

by

AMIT ARORA

DEPARTMENT OF CHEMICAL ENGINEERING
INDIAN INSTITUTE OF TECHNOLOGY ROORKEE
ROORKEE 247667 (INDIA)
FEBRUARY 2016

INDIAN INSTITUTE OF TECHNOLOGY ROORKEE
ROORKEE

CANDIDATE'S DECLARATION

I hereby certify the work which is being presented in the thesis, entitled **"INFLUENCE OF SURFACTANTS ON THE FORMATION AND DISSOCIATION OF GAS HYDRATES IN FIXED BED MEDIA"** in partial fulfilment of the requirements for the award of the degree of Doctor of philosophy and submitted in the Department of Chemical Engineering Indian Institute of Technology, Roorkee is an authentic record of my own work carried out during a period from January 2013 to February 2016 under the supervision of Dr. C.B Majumder , Professor Chemical Engineering Department, Indian Institute of Technology, Roorkee and Dr. Rajnish Kumar, Senior Scientist, Chemical Engineering and Process Development Division, National Chemical Laboratory, Pune, India.

The matter presented in the thesis has not been submitted by me for the award of any other degree of this or any other institute.

(Amit Arora)

This is to certify that the above statement made by the candidate is correct to the best of our knowledge.

(Rajnish Kumar)
Supervisor

(C.B.Majumder)
Supervisor

The PhD. Viva- Voice Examination of **Mr. Amit Arora**, Research scholar, has been held on 20-07-2016.

Chairman, SRC **Signature of External Examiner**

This is to certify that the student has made all the corrections in the thesis.

Signature of Supervisor (s) **Head of the Department**
Dated: _____

ABSTRACT

Rapid growth in energy demand with depleting energy resources, along with anthropological discharge of CO_2 in environment has lead to search for unconventional energy resources like Natural Gas Hydrates (NGH), of which Methane Hydrates are the most commonly encountered Hydrates [Demirbas, 2010] found Naturally in abundance. The worldwide organic carbon in the Gas Hydrates is estimated to be roughly about 10000 X 10^{15} grams which is almost double the carbon content in total fossil fuel reserves of the world [Satoh et al, 1996, Collett, 2002]. Methane Gas Hydrates is source of Methane Gas found as crystalline ice like structure in permafrost regions and under the sea in outer continental margins.

Gas Hydrates belong to a class of inclusion compounds that are commonly known as clathrates. Gas Hydrates are solid nonstoichiometric crystalline compound having cage like structure comprising of water as host and Gas as a guest molecule formed at high pressure and low temperature [Sloan, 1998]. Gas Hydrates have tremendous application potential in the fields of energy and the environment [Koh et al, 2011] like Methane and Natural Gas storage as well as transportation in the form of synthetic Gas Hydrate [Gudmundsson et al, 2006, Kim et al, 2010], Hydrate based carbon dioxide capture, Hydrate based Gas separation [Babu et al, 2014].

Successful commercialization of NGH would require efficient and safe technology for their generation, Dissociation, storage and transportation; extensive research programmes are being conducted to find less energy intensive, economic, clean and green technology for the promotion of Gas Hydrates Formation. Although synthetic surfactant promote Hydrate Formation but at the same time their limited biodegradability and toxicity hinders them from adopting their use as Hydrates promoters.

The microbes like *Bacillus subtilis* and Members of gammaproteobacteria are identified in Gulf of Mexico Gas Hydrate mounds [Lanoil et al, 2001] and are found to produce Surfactin and Rhamnolipids biosurfactants respectively which influence the induction time and rate of Formation of Gas Hydrates (GH). It is anticipated that secondary metabolites from

gammaproteobacteria like *Pseudomonas aeruginosa* may have beneficial effect on Gas Hydrate Formation.

Despite plethora of efforts to develop Hydrate-based technology, none has been established effectively for practical application. Hydrate based CO_2 capture and separation process can be commercialized by increasing the Hydrate Formation rate and reducing the operating pressure conditions. Hydrate Formation in quiescent condition is very slow; a thin film of Hydrate is formed on the water surface which stops effective migration of Gas further into the system resulting in slower kinetics of Hydrate Formation. In this context, higher solubility of Gas in water and larger contact area between host molecule i.e. water and guest molecules i.e. Gases are very vital so as to enhance the Hydrate Formation rate [Linga et al, 2012, Kumar et al, 2013, Kang et al, 2010]. Synthetic surfactants as a chemical additive has been useful in enhancing Hydrate Formation rate by increasing Gas solubility, supporting micelle Formation and providing the nucleation sites for Hydrate Formation [Saw et al, 2014]. Use of synthetic surfactant such as sodium dodeccyl sulphate (SDS), sodium tetradecyl sulphate (STS), sodium hexadecyl sulphate (SHS) has shown good results and enhance the Hydrate growth considerably. However its use in Natural environment for enhancing NGH generation may be detrimental for the living organisms [Michael et al, 1991, Banat et al, 2014].

Desire to have environmentally compatible surfactants has propelled search for a substitutes from biological origin which are considered better than their synthetic counterparts for their lower toxicity, environment-friendly nature and stability under extreme conditions like high temperature, pH, and high salinity [Banat et al, 2014]. Very few studies pertaining to influence of biosurfactants on NGH Formation has restricted our knowledge and thus, limiting the potential application of biosurfactants in Gas Hydrate generation, storage and transportation [Rogers et al, 2003, Rogers et al, 2003, Woods, 2004]. Moreover, the studies have largely concentrated on kinetics and related parameters [Rogers et al, 2003, Carvajal et al, 2013, Woods, 2004]. Influence of microbial surfactant like Rhamnolipids and surfactin on thermodynamics of Gas Hydrates Formation has not been reported in literature. Thus, limiting the potential application of biosurfactants in Gas Hydrates generation, storage and transportation.

As discussed above, Hydrate promoters has proven application in Gas Hydrate based technological processes. Similarly, design and application of Gas Hydrate inhibitors is also very

important. Unlike Hydrate promoters, inhibitors are required to reduce the possibility of Hydrate nucleation and growth. Gas Hydrate Formation has been considered as a nuisance in oil and Gas industries because of plugging problem of Gas pipelines and these industries are very concerned about this problem as Hydrates can destroy the whole pipeline and can be a danger for human life. Formation of gas hydrates leads to the blocking of pipe lines actually hydrate propagation gradually forms a plug which separates the pipe into two pressure zones: a pressure zone between the well and the plug and the second section at low pressure between the plug and recovery division. In the upstream section a pipe blast can take place due to pressure rise. The plug behaves like a projectile which destroys the pipe when the pressure difference between the upstream and downstream section increases. Both these events can destroy the whole pipeline.

Traditionally this problem has been sorted out by using thermodynamic Hydrate inhibitors (methanol, glycol etc.) which change the phase equilibria of Hydrate Formation, however, they are not considered environment friendly. To address this problem few polymeric compounds like Polyvinylpyrrolidone (PVP), Polyvinylcaprolactam (PVCAP), Polyethylene oxide (PEO) etc. have been explored as kinetic Hydrate inhibitors (KHI) [Kelland, 2006, Freer et al, 2000]. These chemicals do not prevent Hydrate Formation but they delay Hydrate Formation in pipelines as they pass through the Hydrate sensitive zone. Although these compounds are successful at very low concentrations but because of their limited biodegradability they are not certified for use in all regions (for example the North Sea).Recently Anti Freeze Proteins (AFP) has been utilized to inhibit Gas Hydrates Formation in laboratory scale experimentation. However, extracting AFP in large scale is commercially not viable and thus there is a strong motivation for inventing economic green biodegradable inhibitor. During the course of this thesis we have tried lignin an abundant biomass as inhibitor which is economic and has never been reported as a Gas Hydrate inhibitor. Lignocelluloses are attractive materials due to their renewability and availability i.e. 1.8 trillion tons of annual production [McKendry, 2002].

The energy intensive mechanical agitation processes used for Gas Hydrate Formation needs to be replaced by less energy intensive process using fixed bed media. So the current study explores the use of its bed media FDM for the hydrate based CO_2 Capture which can lead to replace the energy intensive processes like agitation used for the hydrate formation. In this thesis, the performance of SDS for carbon dioxide GH Formation in two different fixed bed media: Silica

sand and zeolites (5A and 13X) was evaluated as a base line case. The concentration of SDS was always fixed at 0.5 wt% of water used in the experiment Experiments were carried out in batch mode with the initial pressure fixed at 3.0 MPa, and the temperature was kept constant at 274.65 K. The experiments were conducted at 3.0 MPa at 274.65 K because this pressure leads to the formation of carbon dioxide gas hydrate at this temperature as this much pressure is sufficient to give the required driving force. It was found that the effect of SDS is media dependant. In the case of Silica sand, SDS greatly impacted the Hydrate Formation kinetics whereas it did not have such a marked effect in the case of zeolites. Presence of SDS in the system was found to lower the induction time.

Again to understand the base case kinetics, various porous media were evaluated in a fixed bed reactor (FBR) and also compared to stirred tank reactor (STR). Carbon dioxide Hydrate Formation experiments were carried out at a pressure 3.0 MPa and constant temperature of 274.5K. Silica sand, Silica Gel (100 nm and 5 nm pore size) and a blend of Silica Gel (5nm) with zeolite 5A were used as a porous media in FBR. The results have shown that the kinetics of Hydrate Formation and conversion of water to Hydrate in a FBR system is significantly greater than that in a STR system. Among all the different porous media studied, 100 nm pore size Silica Gel was found to be a good candidate to enhance Hydrate Formation kinetics. There was a significant increase in the rate of Hydrate Formation in the case of FBR whereas STR was found to be not a suitable approach for scaling up the Hydrate based Gas capture and separation processes because the power required for mechanical agitation is very significant and it is also plagued by other limitations such as the low Gas uptake and low water to Hydrate conversions. Further with Silica Gel and zeolite as packing media effect of porosity on CO_2 Gas Hydrate Formation kinetics was studied. Silica Gel of mesh size 230-400 and certain percentage of zeolite as a solid additive have been used as a medium of Hydrate Formation from distributed water in its pores. Zeolite 3A (beads) and zeolite 5A (beads) were used with different water saturation amount. Above study revealed that zeolite certainly performs well as Silica Gel and enhances the Hydrate Formation rate and conversion.

Biosurfactant synthesized from strain A11 was found to be Rhamnolipids after characterizing with techniques such as Thin layer chromatography (TLC), Fourier transform infrared spectroscopy (FTIR), Nuclear magnetic resonance (NMR), Liquid Chromatography-Mass

Spectrometry (LC-MS), Matrix-assisted laser desorption/ionization (MALDI). Purified Rhamnolipids produced by strain A11 can reduce the surface tension of water from 72 mN/m to 36 mN/m with critical micelles concentration CMC of 70 mg/L. Rhamnolipids produced by strain A11 has dirhamnolipids ($RhaRhaC_{10}C_{10}$) as most dominant congener. Apart from $RhaRhaC_{10}C_{10}$ olefinic Rhamnolipids $RhaC_{22}$, $RhlRhaC_{10}C_{10}$/ $RhlRhaC_{10}C_{12}$, $RhaRhaC_{10}C_{10}$ / $RhaRhaC_{10}C_{12}$ were also produced by strain A11.

Biosurfactant synthesized from strain A21 was found to be Surfactin after characterizing with techniques such as TLC, FTIR, High Performance Liquid Chromatography (HPLC), MALDI, NMR, Amino Acids Sequence (AAS) . Purified Surfactin produced by strain A21 can reduce the surface tension of water from72 mN/m to 29 mN/m with CMC of 33 mg/L.

The purpose of this set of experiments was to explore the feasibility of using glycolipids (Rhamnolipids) type biosurfactant as Methane Hydrate generation promoter. Rhamnolipids (glycolipids) type biosurfactant was produced by rhizobacteria, *Pseudomonas aeruginosa* strain A11. Study compares Methane Hydrate Formation in the quiescent water and fixed bed system of water saturated C type Silica Gel in the presence of different concentration of biosurfactants. The thermodynamics and kinetics of Gas Hydrate Formation were studied to gain a better understanding of the process. Using Rhamnolipids solution in C type Silica Gel increased the rate of Methane Hydrate Formation as compared to other systems, increased in the number of moles of Methane consumed in Hydrate Formation and reduction in induction time. Presence of Rhamnolipids also shifted Methane Hydrate Formation temperature to higher values relative to the system without biosurfactant. The Dissociation behaviour of Methane Hydrate using thermal stimulation technique was also studied. The enthalpies of Dissociation were also calculated. Results from thermodynamic and kinetic studies suggest that Rhamnolipids can be applied as environment-friendly Methane Hydrate promoter.

The goal of this set of experiments was to understand the thermodynamics and kinetics of Methane Hydrate Formation in quiescent water system and fixed bed system of porous media i.e C type Silica Gel amended with different concentration of cyclic biosurfactant i.e Surfactin (lipopeptide). Biosurfactants was produced by rhizospheric bacteria *Bacillus Subtilis* strain A21. Saturating Silica Gel surfactin solution increased the rate of Methane Hydrate Formation when compared to other systems. Addition of surfactin solution also increased the number of moles of Methane consumed in Hydrate Formation, Methane Hydrate Formation rate, increased

percentage conversion and reduced the induction time significantly. Surfactin also shifted Methane Hydrate Formation temperature to higher values relative to the system without biosurfactant. The Dissociation behaviour of Methane Hydrate using thermal stimulation technique was also studied. Results from thermodynamic and kinetic studies suggest that surfactin can act as environment-friendly additive for Methane Hydrate promoter.

In this study, we have investigated experimentally a bio-surfactant i.e. Calcium lignosulphonate (CaLS) generated from waste of pulp and paper for inhibiting the nucleation or growth of Methane and Natural Gas Hydrate Formation. Calcium lignosulphonate was characterized by FTIR, Ultraviolet – Visible Spectrometry (UV-VIS), Carbon Hydrogen Nitrogen Sulphur Analysis (CHNS), Gel Permeation Chromatography (GPC), Field Emission Scanning Electron Microscopy (FE-SEM), Energy Dispersive X-ray Spectroscopy (EDS), FE-SEM Mixing, Inductively Coupled Plasma Mass Spectroscopy (ICPMS), Thermo gravimetric analysis (TGA) and Solid NMR and was found to be the same. All techniques have given signatures of various elements present in calcium lignosulphonate and the molecular weight determined from Gel permeation chromatography has confirmed its polymeric nature. Different dosage (0.1, 1 and 5 wt %) of bio-surfactant is used in Hydrate Formation in presence of Methane and Natural Gas Hydrate decomposition behaviour of Methane Hydrates was also investigated in the presence of inhibitor. The induction time was delayed to 11.2 hours in presence of 1 wt% CaLS from 44 minutes when it is not present .Hence, there is a major shift in the induction time of Gas Hydrates.

The outcome of the thesis is that an economic and less energy intensive fixed bed media of Silica Gel (100 nm) was found to be more efficient amongst fixed bed of Silica sand, Silica Gel (5 nm), blend of Silica Gel (5nm) and zeolites and stirred tank rectors for Hydrate based carbon dioxide capture. Fixed bed media are capable of replacing the expensive and energy intensive method of mechanical agitation used for Gas Hydrate. Rhamnolipids and surfactin were found to be dual promoters i.e kinetic as well as thermodynamic promoter for Methane Hydrate Formation. These Biosurfactants are capable of replacing their counter parts i.e synthetic surfactants which are toxic, non-environment-friendly and non-biodegradable. Hence these biosurfactants can help in designing a green, clean, biodegradable and environment-friendly technology for promoting the Formation of Natural Gas Hydrates. Methane Gas Hydrates are

fuels of the future generation provided an economical viable technology is developed. Thermal stimulation technique is found to be very effective for Dissociation of Methane Hydrates. The small dosage of Rhamnolipids produced by *Pseudomonas aeruginosa* Strain A11 and Surfactin produced by *Bacillus subtilis* Strain A21 must clear the role of these biosurfactants as promoter in Natural Gas Hydrate sites (as in Gulf of Mexico). Calcium LignoSulphonate (CaLS) is found to be an economic, low dose, green and biodegradable kinetic inhibitor for Methane as well as Natural Gas Hydrates which can replace their very expansive low dose antifreeze proteins (AFP) used currently by industry for inhibition of Natural Gas Hydrates.

Overall, this study has shown the significance of Biosurfactants i.e. Rhamnolipids and Surfactin on Methane Hydrate Formation. In addition, the production and characterization protocol of biosurfactants were discussed. The role of microbes at Natural Gas Hydrate sites, the insight of using Biosurfactants as Hydrate promotes so that Hydrate based technologies can use biodegradable and environment-friendly promoters and an economic green biosurfactant inhibitor were also discussed. As the future lies in Hydrate based CO_2 Capture, Hydrate based Natural Gas transportation and storage and designing an economical viable technology like CO_2 sequestration to exploit this vast source of energy. So in the current study the fixed bed media (FBM) approach was found to be more effective, economic and efficient for Hydrate based CO_2 capture. The present study reports the significance of microorganisms and their metabolites. Biosurfactant are produced in the ocean floor which catalyze the Gas Hydrates Formation, so, the above thesis has lighten the Formation of Gas Hydrates in marine conditions and given the better understanding of the Formation of Natural Gas Hydrates in ocean floor.

ACKNOWLEDGEMENT

First of all I would like to thank almighty **God** for his constant grace.

I am really indebted to my supervisor **Dr. C.B Majoumdar**, Professor and Head of Chemical Engineering Department, Indian Institute of Technology Roorkee, India who bestowed me with his invaluable guidance. His supervision widened my horizon as a research scholar and his dedication for true research is always a motivating force for me. My research work is outcome of his experience, accurate guidance, valuable suggestions, exceptional leadership and his passion towards science.

I put on record my indebtedness to my supervisor **Dr. Rajnish Kumar**, Senior Scientist, Chemical Engineering and Process Development Division, National Chemical Laboratory, Pune, India for not only his exceptional guidance, but also for inspiration as an incredibly creative and capable individual. His knowledge and infectious enthusiasm towards research have contributed immensely towards the completion of this thesis. In addition, his work ethics and dedication always motivated me to move out of my comfort zone and work on a challenging and very interesting multidisciplinary project. I will be forever grateful to him for all the things he has taught me over the course of this thesis.

I Would like to extend my sincere gratitude to **Dr. Girish Sahni** , **Director General CSIR** then Director of IMTECH, Chandigarh who allowed me to work in his lab.

I fall short of words to thank Senior Principal Scientist **Dr. Swanjit Singh Cameotra**, IMTECH Chandigarh who allowed me to work in his lab and making me learn few important fundamentals in the field of Biosurfactants. I am grateful to him for showing continued interest in my work, and patiently answering questions and teaching me about the field of microbiology.

My heart felt thanks to **Dr. Pushpendra Kumar** Co-ordinator National Gas Hydrate Programme 02 from ONGC, Dehradun for constant oasis of ideas, which exceptionally inspired and enriched my growth as a student, and as a researcher. I also thank him for several stimulating discussions on gas hydrate systems and for greatly improving my technical writing skills.

I would like to acknowledge **Professor Sukumar Laik**, Department of Petroleum Engineering, Indian School of Mines Dhanbad for allowing me to conduct few experiments in his gas hydrate laboratory.

I wish to extend my sincere thanks **Head, Institute Instrumentation Centre**, IIT Roorkee for providing me necessary facilities to pursue my research work smoothly.

I am highly obliged all members of **Student Research Committee** and all faculty members of Department of Chemical Engineering IIT Roorkee for timely assessment of my work in progress and persistent encouragement

I offer my sincere regards **Mrs. B. Santhakumari**, Centre for Material Characterization, National Chemical Laboratory, Pune, India for LC-MS and MALDI analysis of Biosurfctants.

I acknowledge the help of **Dr. Rajmohan** from NCL, Pune for NMR of Biosurfactants.

My sincere thanks to **Dr. S. Mayadevi** from Chemical Engineering and Process Development Division, National Chemical Laboratory for BET of Silica Gel Samples.

I am very much obliged to Dr. Anil Kumar Singh for making me learn few fundamentals in microbiology.

I am also grateful to my lab colleagues from IIT Roorkee, NCL Pune, IMTECH Chandigarh and my friends for their constant support.

I am also grateful to the ministerial staff of my department in helping me in various ways.

I articulate my sincere gratitude to my parents, **Sh. Tilak Raj Arora and Late Smt. Sudershan Kumari** without their love, care and support I would have not come so far in life. They are strong pillars of my life and always a source of inspiration for me in facing the struggles of life. Their boundless love, meticulous care, timely help and relentless encouragement helped me to combat my weak moments.

I am thankful to my affectionate wife, **Garima** , whom I found at all times enthusiastic about my research work and she always spared time for me from her own busy work schedule . I am grateful to her for her unconditional love and support. I acknowledge that without her co-operation this work was doubtfully possible. I regret the loss of blissful moments which I could not spend with my doting son, **Aloukik** and Daughter **Arushi** without their sacrifices this work

would have not been possible. They desperately desired my company but I could hardly spare time for them due to my tight schedule.

I dedicate this thesis to my father Sh. Tilak Raj Arora, my mother Late Smt. Sudershan Kumari, my wife Garima, my son Aloukik Arora and my Daughter Arushi Arora

Dated: February , 2016 **(Amit Arora)**

CONTENTS

		Page No.
	CANDIDATE'S CERTIFICATE	
	ABSTRACT	i
	ACKNOWLEDGEMENT	viii
	CONTENTS	xi
	LIST OF TABLES	xxiii
	LIST OF FIGURES	xxvi
	LIST OF ABBREVIATIONS AND NOTATIONS	xl
Chapter-1	**INTRODUCTION**	1-3
Chapter -2	**LITERATURE REVIEW**	4-110
2	Introduction	4
2.1	Gas Hydrates	7
2.2	Historical Perspective	11
	2.2.1 *Period I: Hydrate as a Laboratory Interest*	11
	2.2.2 *Period II: Hydrate as an Issue to the Natural Gas Industry*	11
	2.2.3 *Period III: Hydrate as an Untapped Energy Resource*	12
2.3	Energy Potential	12
2.4	Hydrate Fundamentals	13
	2.4.1 *Structure of Gas Hydrates*	14
2.5	Classification of Gas Hydrate Accumulation	16
2.6	Occurrence of Gas Hydrates	17
	2.6.1 *Global Scenario*	17
	2.6.2 *Indian Scenario*	19
2.7	Current Techniques for Dissociation of Gas Hydrates	21
	2.7.1 *Depressurization*	21
	2.7.2 *Inhibitor Injection*	21
	2.7.3 *Thermal Stimulation*	21
	2.7.4 *Gas Exchange (CO_2 Sequestration)*	22
2.8	Environmental Impact of the Use of this Energy Source and advantages and disadvantages of Hydrates	23

2.8.1 *The Benefits of Clathrate Hydrates* 23
2.8.2 *The disadvantages of Clathrate Hydrates i.e Pipeline Clogging* 27
2.9 Global Efforts 28
2.9.1 Indian scenario 28
2.9.1.1 *Sites of NGHP Expedition 01* 29
2.9.2 *Global Scenario* 29
2.9.2.1 *Alaska Site* 29
2.9.2.2 *Mallik Site* 31
2.9.2.3 *Nankai Trough* 32
2.10 Future Prospective of Gas Hydrates 34
2.11 Economic Issues 34
2.12 Role of Microbes in Gas Hydrates 36
2.12.1 *Relationship Between Gas Hydrates and Biosurfactants* 37
2.13 Biosurfactants 37
2.13.1 Microorganisms producing biosurfactants 38
2.13.2 *Rhamnolipids* 40
2.13.3 *Lipopeptides and Lipoproteins Surfactin* 41
2.13.4 *Phospholipid and Fatty Acids* 43
2.13.5 *Polysaccharide-Lipid Complex Snomax* 44
2.13.6 *Hydroxylated Fatty Acid* 44
2.14 Influence of Surfactants on Formation of Gas Hydrate 45
2.15 Formation of Gas Hydrate in Presence of Fixed Bed Media. 69
2.16 Effects of Biosurfactants on Gas Hydrate Formation 76
2.17 Influence of inhibitors on Gas Hydrate Formation 84
2.18 Hydrate Based CO_2 Capture 95
2.19 Biosurfactant as a Promoter of Methane Hydrate Formation 101
2.20 Influence of Biosurfactant as Inhibitor on Formation of Natural Gas Hydrate and Methane Hydrate 104
2.20.1 LingoSulphonates 107
2.20.2 Calcium LignoSulphonate (CaLS) 108
2.21 Gaps Identified 108

2.22	Objectives of Present Study	109
Chapter-3	**EXPERIMENTAL PROGRAMMES**	111-120
3.1	Effect of Different Fixed Bed Media on the Performance of Sodium Dodecyl Sulphate for Hydrate Based CO_2 Capture	111
3.2	Carbon dioxide Hydrate Formation in Fixed Bed and Stirred Tank Reactor Systems	112
3.3	Influence of 3A and 5A Zeolites in Presence of Silica Gel on Carbon Dioxide Gas Hydrate Formation	113
3.4	Production of Rhamnolipids from Strain A11 and its Characterization	114
3.5	Production of Surfactin from Strain A21 and its Characterization	115
3.6	Biosurfactant i.e. Rhamnolipids as a Promoter of Methane Hydrate Formation in fixed bed of Silica Gel: Thermodynamic and Kinetic Studies.	117
3.7	Surfactin a Lipopeptide Biosurfactant Promoting Methane Hydrate Formation in Fixed Bed of Silica Gel: Thermodynamic and Kinetic Studies.	117
3.8	Characterization of Biosurfactant Calcium LignoSulphonate (CaLS)	118
3.9	Influence of Biosurfactant i.e. Calcium LignoSulphonate as Inhibitor on Formation of Natural Gas Hydrate and Methane Hydrate	119
Chapter-4	**EXPERIMENTAL SETUP**	121-144
4.1	Effect of Different Fixed Bed Media on the Performance of Sodium Dodecyl Sulphate for Hydrate Based CO_2 Capture	121
	4.1.1 Apparatus and Hydrate Formation procedure	121
4.2	Carbon dioxide Hydrate Formation in Fixed Bed and Stirred Tank Reactor Systems	125
	4.2.1. Fixed bed reactor (FBR)	125
	4.2.2. Stirred tank reactor (STR)	126
4.3	Influence of 3A and 5A Zeolites in Presence of Silica Gel on Carbon Dioxide Gas Hydrate Formation	128
	4.3.1 Experimental Setup	128
4.4	The Experimental Setup for Methane Gas Hydrate Formation and	129

Dissociation in Presence of Biosurfactants namely Rhamnolipids, Surfactin, Calcium LignoSulphonate (CaLS) using Large Reactor: Thermodynamics and Kinetic Studies

4.4.1 Experimental Setup for Hydrate Formation and Dissociation Procedure 129

4.4.2 Instrumentation Section 132

4.4.3 *The pictorial representations of various material used* 137

4.4.4 The Experimental Setup for Methane and Natural Gas Hydrate Formation in Presence of Biosurfactant Calcium LignoSulphonate (CaLS) using Medium Reactor 143

Chapter-5 MATERIALS AND METHODS 145-185

5.1 Effect of Different Fixed Bed Media on the Performance of Sodium Dodecyl Sulphate for Hydrate Based CO_2 Capture 145

5.1.1 Materials 145

5.1.2 Zeolites 145

5.1.3 Field Emission Scanning Electron Microscopy FE-SEM of 5A and 13X Zeolites 146

5.1.4 Zeolite 5A 146

5.1.5 Zeolite 13X 148

5.1.6 Summary of the systems used in the present study is as shown table 5.1.4. 150

5.2 Carbon dioxide Hydrate Formation in Fixed Bed and Stirred Tank Reactor Systems 152

5.2.1 Materials 152

5.2.2 The Summary of the systems used in present study 153

5.2.3 Brunauer-Emmett-Teller (BET) analysis of C-type Silica Gel (Rankem) 153

5.3 Influence of Zeolites on Carbon Dioxide Gas Hydrate Formation 155

5.3.1 Materials 155

5.3.2 Field Emission Scanning Electron Microscopy (FE-SEM) of 3A Zeolite 156

5.3.3 Zeolite 3A 156
5.3.4 The Summary of the systems used in present study 158
5.4 Biosurfactant Rhamnolipids as a Promoter of Methane Hydrate Formation: Thermodynamic and Kinetic Studies 159
5.4.1 Materials 159
5.4.2 Pseudomonas aeruginosa strain A11growing on nutrient agar Plate 160
5.4.3 Microorganism and growth medium composition 161
5.4.4 Biosurfactant production and purification 161
5.4.5 Determination of Biomass and Biosurfactant Concentration 162
5.4.6 Surface tension and Critical Micelle Concentration (CMC) 167
5.4.7 Characterization of Biosurfactant namely Rhamnolipids 169
5.4.7.1 TLC 169
5.4.7.2 FTIR 169
5.4.7.3 NMR 169
5.4.7.4 LC-MS 169
5.4.7.5 MALDI-TOF 170
5.4.7.6 Zeta potential measurements 170
5.4.7.7 Micelle Size 171

5.5 Brunauer–Emmett–Teller (BET) Analysis of C-type of Silica Gel (Merck) 171
5.6 Lipopeptide Biosurfactant Surfactin Promoting Methane Hydrate Formation in Fixed Bed of Silica Gel: Thermodynamic and Kinetic Studies 173
5.6.1 Materials 173
5.6.2 Bacillus subtilis strain A21 growing on nutrient agar plate 174
5.6.3 Microorganism and growth medium composition 175
5.6.4 Biosurfactant production and purification 175
5.6.5 Biosurfactant purification 175
5.6.6 Surface tension and Critical Micelle Concentration (CMC) 176

5.6.7 Characterization of Biosurfactant Surfactin 176
5.6.7.1 TLC 176
5.6.7.2 FTIR 178
5.6.7.3 NMR 178
5.6.7.4 MALDI-TOF 178
5.6.7.5 Amino acid analysis 178
5.6.7.6 HPLC 178
5.6.7.7 Zeta potential measurements 178
5.6.7.8 Micelle Size 178
5.7 Influence of a Novel Green Kinetic Inhibitor on Formation of Natural Gas Hydrate and Methane Hydrate 178
5.7.1 Materials 179
5.7.2 Method of Gas Chromatography of Natural Gas 182
5.7.3 Characterization of Calcium LignoSulphonate 182
5.7.3.1 FTIR 182
5.7.3.2 Ultra Violet Spectroscopy 182
5.7.3.3 CHNS 182
5.7.3.4 ICPMS 182
5.7.3.5 GPC 183
5.7.3.6 FE-SEM 183
5.7.3.7 TGA 184
5.7.3.8 NMR 184
5.8 Analysis of C-type Silica Gel (Merck) before and after growing through Methane Hydrate Formation Experience 184
5.8.1 FTIR of C-type silica Gel (Merck) before and after growing through Methane Hydrate Formation Experience 185
5.8.2 Scanning Electron Microscopy (SEM) of C- type Silica Gel (Merck) before and after going for Gas Hydrate Formation Experience 185

Chapter-6 RESULTS AND DISCUSSION 186-354

6.1 Effect of Different Fixed Bed Media on the Performance of Sodium Dodecyl Sulphate for Hydrate Based CO_2 Capture 186

6.1.1 Induction Time and Gas Consumption 186

6.1.2 Typical Hydrate Formation-Dissociation Curve along with Pressure and Temperature Profile Acquired from Zeolite 5A/Water System 187

6.1.3 The comparison of Gas consumption for Hydrate growth measured in a fixed bed media of zeolite 5A and 13X with the Gas consumption without any Hydrate growth in dry zeolite 5A 187

6.1.4 The comparison of Gas uptake for Hydrate growth measured in fixed bed media of zeolite 13X and Silica sand in presence /absence of SDS 189

6.1.5 Conclusion of this Task 191

6.2 Carbon dioxide Hydrate Formation in Fixed Bed and Stirred Tank Reactor Systems 192

6.2.1 Typical pressure -temperature curve (P-T profile) of CO_2 Hydrate Formation in a fixed bed of spherical Silica Gel (pore size 100 nm) at 3.0 MPa and 274.5 K 192

6.2.2 Hydrate Formation curves (pressure profile) along with visualization of Hydrates obtained with pure CO_2 in a stirred tank reactor 193

6.2.3 The comparison of Gas consumption during Hydrate growth (mol of Gas/mol of water) infixed bed of Silica Gel (pore size 100 nm) Silica Sand and stirred tank reactor systems 194

6.2.4 Gas uptake curves received for the two types of water saturated Silica Gels having larger pore size (100 nm) and Silica Gel having lower pore size (5nm) 195

6.2.5 Comparison of Gas uptake during Hydrate growth (mol of Gas/mol of water) in a fixed bed reactor containing Silica Gel (5 nm) and blend of Silica Gel with zeolite 5A 196

6.2.6 Water to Hydrate conversion of various systems investigated during this study 197
6.2.7 Conclusion of this Task 198
6.3 Influence of 3A and 5A Zeolites in Presence of Silica Gel on Carbon Dioxide Gas Hydrate Formation 199
6.3.1 Moles of CO_2 consumed in a fixed bed reactor containing Silica Gel (5 nm, Rankem) and blend of Silica Gel with zeolite 3A and 5A Zeolite 199
6.3.2 Moles of CO_2 consumed/ moles of water in a fixed bed reactor containing Silica Gel (5 nm, Rankem) and blend of Silica Gel with zeolite 3A and 5A Zeolite 200
6.3.3 Percentage Conversion of water to Hydrate 202
6.3.3.1 Percentage conversion at 100% saturation 202
6.3.3.2 Percentage conversion at 50% saturation 202
6.3.3.3 Percentage conversion for different experiments till the end of experiments 203
6.3.4 Conclusion of this Task 204
6.4 Production of Biosurfactant Rhamnolipids from Strain A11 and its Characterization 204
6.4.1 Biosurfactant producing microorganism 204
6.4.2 Biosurfactant production 205
6.4.3 Surface Tension, Critical Micelle Concentration (CMC) and stability of Biosurfactant 208
6.4.4 Characterization of Rhamnolipids Produced from Strain A11 211
6.4.4.1 TLC 211
6.4.4.2 FTIR 213
6.4.4.3 NMR 214
6.4.4.4 LC-MS 216
6.4.4.5 MALDI 220
6.4.4.6 Zeta Potential (Charge on Biosurfactant) 223
6.4.4.7 Micelle Size 223

6.5 Production of Biosurfactant Surfactin from Strain A21 and its Characterization 224
6.5.1 Biosurfactant producing microorganism 224
6.5.2 Biosurfactant Production 225
6.5.3 Surface tension, Critical Micelle Concentration (CMC) and Stability of Biosurfactant 227
6.5.4 Characterization of Biosurfactant Surfactin produced by Bacillus subtilis strain A21 229
6.5.4.1 TLC 229
6.5.4.2 FTIR 231
6.5.4.3 HPLC 232
6.5.4.4 MALDI 232
6.5.4.5 NMR 234
6.5.4.6 Amino Acids Analysis 237
6.5.4.7 Zeta Potential (Charge on Biosurfactant) 237
6.5.4.8 Micelle Size 238
6.6 Characterization of a Novel Green Kinetic Inhibitor Calcium LignoSulphonate (CaLS) 238
6.6.1 FTIR of CaLS 238
6.6.2 UV of CaLS 239
6.6.3 CHNS Analysis of CaLS 240
6.6.4 ICPMS 240
6.6.5 GPC 242
6.6.6 FE-SEM and Mapping 244
6.6.6.1 FE-SEM 244
6.6.6.2 FE-SEM Mapping 244
6.6.7 EDS 246
6.6.8 TGA 247
6.6.9 NMR 248
6.7 Biosurfactant Rhamnolipids as a Promoter of Methane Hydrate Formation: Thermodynamic and Kinetic Studies 249

6.7.1 Thermodynamic Study 249
6.7.1.1 Methane Hydrate Formation-Dissociation 249
6.7.1.2 Comparison of nucleation temperature of Methane Hydrate Formation for different Systems 253
6.7.1.3 Comparison of phase equilibrium of Methane Hydrate Formation for different Systems 254
6.7.1.4 Dissociation enthalpy of Methane Hydrate 255
6.7.2 Kinetic Study 258
6.7.2.1 Induction Time 258
6.7.2.2 Moles of Methane consumed 263
6.7.2.3 Moles of Methane consumed per mole of water 263
6.7.2.4 The growth curve of Methane Hydrate Formation for different Systems 264
6.7.2.5 The rate of Methane Hydrate Formation for different experimental conditions 268
6.7.2.6 Water to Hydrate conversion 289
6.7.3 Conclusion of this task 299
6.8 Lipopeptide Biosurfactant Surfactin Promoting Methane Hydrate Formation in Fixed Bed of Silica Gel Thermodynamic and Kinetic Studies 300
6.8.1 Thermodynamic Study 300
6.8.1.1 Methane Hydrate Formation-Dissociation 300
6.8.1.2 Comparison of nucleation temperature of Methane Hydrate Formation for different Systems 304
6.8.1.3 Comparison of phase equilibrium of Methane Hydrate Formation for different Systems 305
6.8.1.4 Dissociation enthalpy of Methane Hydrate 306
6.8.2 Kinetic Study 308
6.8.2.1 Induction Time 309
6.8.2.2 Moles of Methane consumed 311
6.8.2.3 Moles of Methane consumed per mole of water 312

6.8.2.4 The growth curve of Methane Hydrate Formation for different Systems 313
6.8.2.5 The rate of Methane Hydrate Formation for different experimental conditions 315
6.8.2.6 Water to Hydrate conversion 327
6.8.3 Conclusion of this task 334
6.9 Influence of a Novel Green Kinetic Inhibitor Calcium LignoSulphonate (CaLS) on Formation of Natural Gas Hydrate and Methane Hydrate 335
6.9.1 Results for Medium Reactor 335
6.9.1.1 Induction Time for Natural Gas Hydrate Formation 335
6.9.1.2 Normalized growth of Natural Gas Hydrate Formation 336
6.9.1.3 Induction Time for Methane Hydrate Formation 337
6.9.2 Results for Large Reactor 337
6.9.2.1 Thermodynamics Study 337
6.9.2.1.1 Methane Hydrate Formation and Dissociation in large reactor in presence of CaLS 337
6.9.2.1.2 Dissociation enthalpy of Methane Hydrate 339
6.9.2.2 Kinetic Study 340
6.9.2.2.1 Induction Time 340
6.9.2.2.2 Gas consumption 341
6.9.2.2.3 The rate of Methane Gas Hydrate Formation for different experimental conditions 343
6.9.3 FTIR of Silica C- type Silica Gel (Merck) 351
6.9.4 Scanning Electron Microscopy (SEM) 352
6.9.5 Conclusion of this task 354

Chaptetr-7	**CONCLUSIONS**	355-356
Chapter-8	**SCOPE FOR FUTURE WORK**	357-358
	PUBLICATIONS	359-363
	REFERENCES	364-408
	ANNEXURE	409-411

LISTS OF TABLES

Table No.	Title	Page No.
2.1.1	Conventional Gas Consumption, Reserves and Gas Hydrate Reserves and Usage Years in Major Countries (BP: British Petroleum)	10
2.13.1	Various Types of Biosurfactants produced by Microorganisms	39
2.13.2	Amino Acids present in Surfactin.	42
2.14.1	Influence of Surfactants on Formation of Gas Hydrate	54
2.15.1	Gas Hydrate Formation in Presence of Various Fixed Bed Media	73
2.16.1	Effects of Biosurfactants on Gas Hydrate Formation	80
2.17.1	Influence of Low Dose Kinetic Inhibitors on Gas Hydrates Formation	86
2.17.2	Effects of Thermodynamic Inhibitors on Gas Hydrates Formation	91
4.4.1	Reactor Parameter	132
5.1.1	Materials used along with suppliers used in the present study	145
5.1.2	The Weight % and Atomic % of different elements in 5A	148
5.1.3	The Weight % and Atomic % of Different Elements in 13 X	150
5.1.4	Summary of the systems used in the study	150
5.2.1	Materials used along with suppliers used in the present study	152
5.2.2	Summary of the systems used in the present study	153
5.2.3	Surface characteristics of the C-type Silica Gel (Rankem)	155
5.3.1	Materials used and their suppliers	155
5.3.2	The Weight % and Atomic % of different elements in Zeolite 3A	158
5.3.3	Summary of the systems used in the present study	158
5.4.1	Materials used and their suppliers	159
5.5.1	Surface characteristics of C-type Silica Gel (Merck)	172
5.6.1	Materials used and their suppliers	173

5.7.1	Materials used in present study	179
6.1.1	Summary of experiments: induction time and Gas consumption; experimental pressure and temperature used were 3.0 MPa and 274.65 K respectively. Amount of water used for all the experiment was 50 cm^3 except experiment-1(no water). Amount of SDS used was 0.5 wt%	186
6.3.1	Percentage conversion for different experiments till the end of experiments.	203
6.4.1	Assignment of all rhamnolipids mass peaks found by LCMS mass spectrometry of biosurfactant produce by *Pseudomonas aeruginosa* strain A11	220
6.4.2	Assignment of all rhamnolipids mass peaks obtained by MALDI-TOF mass spectrometry of biosurfactant produce by *Pseudomonas aeruginosa* strain A11	222
6.5.1	Exhibits the mass peak and assignments of Surfactin identified in the MALDI of strain A21	234
6.6.1	CHNS of CaLS	240
6.6.2	Gel Permeation Chromatography of CaLS	243
6.6.3	Electron Dispersive Spectroscopy analysis of CaLS	246
6.6.4	Nuclear Magnetic Resonance ^{13}C of CaLS	248
6.7.1	Methane Hydrate Formation and Dissociation parameters in presence of different test sample	253
6.7.2	Equilibrium temperature, pressure and Dissociation enthalpy calculated by Clausius-Clapeyron equation	257
6.7.3	Induction time for various experiments	261
6.7.4	The rate of Methane Gas Hydrate Formation for different experimental condition	288
6.8.1	Methane Hydrate Formation and Dissociation parameters in presence of different test sample	303
6.8.2	Equilibrium temperature, pressure and calculated enthalpy of Dissociation	307

6.8.3	Induction time for various experiments	310
6.8.4	The rate of Methane Gas Hydrate Formation for different experimental condition	327
6.9.1	Methane Hydrate Formation parameters for various types of samples	338
6.9.2	Equilibrium temperature, pressure and calculated Dissociation enthalpy	340
6.9.3	Induction time for various experiments	340
6.9.4	The rate of Methane Gas Hydrate Formation for different experimental condition	351

LIST OF FIGURES

Fig. No.	Title	Page No.
2.1	Primary Energy Consumption by Fuel in the Reference Case, 1990-2040	5
2.1.1	Distribution of Organic Carbon on Earth (Total 18,777 Gt)	11
2.4.1	Gas Hydrate Synthesized in Lab	14
2.4.2	The Structure of Gas Hydrates sI	15
2.4.3	The Structure of Gas Hydrate sII.	15
2.4.4	The Structures of Gas Hydrate sH.	16
2.5.1	Representation of Class 1, Class 2 and Class 3 Gas Hydrate	17
2.6.1	Distribution of Known Gas Hydrate Reserves throughout the world.	18
2.6.2	Overview Map Showing the Locations of Sites for Gas Hydrate Coring/Drilling in India.	19
2.6.3	Calculated Gas in-Place in Hydrate Bearing Sediments, Total Median=43,311 tcf (Median, tcf (trillion cubic feet)) Released by Hydrate Energy International (HEI).	20
2.13.1	Structure of Biosurfactant.	38
2.13.2 (a)	Structure of Monorhamnolipid: $RhaC_{10}C_{10}$	40
2.13.2 (b)	Structure of Dirhamnolipid: $RhaRhaC_{10}C_{10}$	40
2.13.3 (a)	Structure of Surfactin	41
2.13.3 (b)	Lipid Chains of Surfactin Molecule	41
2.13.4	Structure of Surfactin.	42
2.13.5	Structure of DMPC	43
2.13.6	Structure of DPPS.	43

2.13.7	Structure of POPC.	44
2.13.8	Structure of Hydroxystearic Acid.	45
3.1.1	Effect of Different Fixed Bed Media on the Performance of Sodium Dodecyl Sulphate for Hydrate Based CO_2 Capture	112
3.2.1	Carbon dioxide Hydrate Formation in Fixed Bed and Stirred Tank Reactor Systems	113
3.3.1	Influence of 3A and 5A Zeolites in Presence of Silica Gel on Carbon Dioxide Gas Hydrate Formation	114
3.4.1	Production of Rhamnolipids from Strain A11 and its Characterization	115
3.5.1	Production of Surfactin from Strain A21 and its Characterization	116
3.6.1	Microbial Surfactant Promotes Methane Hydrates Formation in Fixed Bed Porous Silica Gel System	117
3.7.1	Role of surfactin as Biosurfactant in Methane Gas Hydrate Formation Kinetics	118
3.8.1	Characterization of Calcium LignoSulphonate	119
3.9.1	Inhibition of Methane and Natural Gas Hydrates in Presence of Calcium LignoSulphonate	120
4.1.1	Line diagram of Experimental Setup to Study the Effects of Zeolite 5A, Zeolite 13X, Silica Sand on CO_2 Hydrate Formation	122
4.1.2	Experimental Setup to Study the Effects of Zeolite 5A, Zeolite 13X, Silica Sand on CO_2 Hydrate Formation	123
4.1.3	Showing the Location of Three Thermocouples in the Reactor used in present study	124
4.2.1	Line diagram of the Experimental Setup for Studying the Effects of Silica Sand, Silica Gel (5nm and 100nm) and Zeolite 5A on CO_2 Hydrate Formation	125

4.2.2	Line diagram of Stirred Tank Reactor for CO_2 Hydrate Formation	126
4.2.3	Experimental set up of Stirred Tank Reactor (STR) Along with Transparent Window used in present study	127
4.3.1	Line diagram of Experimental Setup for Influence of 3A and 5A Zeolites in Presence of Silica Gel on Carbon Dioxide Gas Hydrate Formation	128
4.4.1	Line diagram of the Experimental Setup for Methane Hydrate Formation for Various Experimental Conditions	130
4.4.2	Experimental setup of Methane Hydrate Formation	131
4.4.3	Hydrate Cell in Close Condition	133
4.4.4	Hydrate Cell in Open Condition	133
4.4.5	Thermostatic bath for both cooling and heating	135
4.4.6	Thermostatic Bath Containing Cell in Pressurised Conditions	135
4.4.7	Display of Pressure, Temperature and Bath Set Point Temperature while Methane Hydrate Formation on Computer	136
4.4.8	Online video pictures of Methane Hydrate Formation after Nucleation	136
4.4.9	C-type Silica Gel (Merck)	137
4.4.10	A Solution of 1000 ppm Rhamnolipids	138
4.4.11	C-type Silica Gel (Merck) getting Saturated with 1000 ppm Rhamnolipids Solution	139
4.4.12	C-type Silica Gel (Merck) Saturated with 1000 ppm Rhamnolipids Solution	139
4.4.13	Fixed Bed of C-type Silica Gel (Merck) Saturated with 1000 ppm Rhamnolipids Solution	140
4.4.14	C-type Silica Gel (Merck) Saturated with distilled water	140
4.4.15	Fixed Bed of C-type Silica Gel (Merck) Saturated with distilled water	141

4.4.16	Solution of 1 wt.% Calcium LignoSulphonate and C-type Silica Gel (Merck)	141
4.4.17	Fixed bed of C-type Silica Gel (Merck) Saturated with 1 wt.% Calcium LignoSulphonate	142
4.4.18	C-type Silica Gel (Merck) after going through Methane Hydrate Formation Experience	142
4.4.19	Line diagram of Experimental Setup for Methane and Natural Gas Hydrate Formation in Presence of Biosurfactant Calcium LignoSulphonate(CaLS) using Medium Reactor	143
5.1.1	EDS Analysis of Zeolite 5A	147
5.1.2	The morphology of the procured sample Zeolite 5A	147
5.1.3	EDS Analysis of Zeolite 13X	149
5.1.4	The morphology of the procured sample Zeolite 13X	149
5.1.5	The Zeolite 5A and 13X	151
5.1.6	The 13X Zeolite saturated with distilled water	151
5.2.1	Pore Diameter of 5 nm pore size Silica Gel	154
5.2.2	Pore Volume and Surface Area of 5 nm pore size Silica Gel	154
5.3.1(a)	Sample of 3A Zeolite	156
5.3.1(b)	Sample of 5A Zeolite	156
5.3.1(c)	Sample of C-type Silica Gel (Rankem)	156
5.3.2	EDS Analysis of 3A Zeolite	157
5.3.3	The morphology of the procured sample Zeolite 3A	157
5.4.1	*Pseudomonas aeruginosa* strain A11growing on nutrient agar plate	160
5.4.2	Bottles Containing Mother Liquor and Biomass after Centrifugation	163
5.4.3	Mother Liquor Collected from all bottles as shown above	163
5.4.4	Bottles Containing Biomass after collecting Mother Liquor	164
5.4.5	Acidified Mother Liquor kept in cold room over night	164

5.4.6	The bottles containing Mother Liquor as shown above and crude Biosurfactant after centrifugation	165
5.4.7	Rotary Dryer for Solvent removal	165
5.4.8	Lyophilizer used for Lyophilization of Biosurfactants	166
5.4.9	DuNouy Tensiometer for measurement of Surface Tension of Biosurfactants	167
5.4.10	Platinum-Iridium Ring Detachment Method for measuring Surface Tension of Biosurfactants	168
5.5.1	Pore Diameter of C-type Silica Gel (Merck)	171
5.5.2	Pore Volume and Surface Area of C-type Silica Gel (Merck)	171
5.6.1	*Bacillus subtilis* strain A21 growing on nutrient agar plate	174
5.6.2	TLC of Surfactin synthesized from strain A21 and standard from Sigma Aldrich, USA	177
5.7.1	Sample of Calcium LignoSulphonate	180
5.7.2(a)	Distilled water containing 1 wt.% CaLS	180
5.7.2(b)	C-type Silica Gel(Merck)	180
5.7.2(c)	Reactor Packed with 90% saturated (Distilled water with 1wt.% CaLS) Silica Gel (Merck)	180
5.7.3	The distilled water containing 5wt.%, 1wt.%, 0.1 wt.% of CaLS	181
6.1.1	Typical Hydrate Formation-Dissociation curve along with temperature profile (Experimental pressure and temperature was 3.0 MPa and 274.65K. Inset shows the location of three thermocouples inside the reactor)	188
6.1.2	Comparison of Gas consumption for Hydrate growth measured in a fixed bed media of zeolite 5A and 13X with the Gas consumption in dry zeolite 5A. Time zero in the graph corresponds to nucleation point (induction time) for the Hydrate experiments	189
6.1.3	Comparison of Gas consumption for Hydrate growth measured in a fixed bed media of zeolite 13X and Silica sand in presence	190

	/absence of SDS. Time zero in the graph corresponds to nucleation point (induction time) for the experiments	
6.2.1	Typical pressure-temperature curve (P-T profile) of CO_2 Hydrate Formation in a fixed bed of spherical Silica Gel (100 nm) at 3.0 MPa and 274.5 K	193
6.2.2	Pressure profile obtained during CO_2 Hydrate Formation in a stirred tank reactor at 400 rpm along with visual presentation of Hydrates at 3.0 MPa and 274.5 K	194
6.2.3	Comparison of Gas consumption during Hydrate growth (mol of Gas/mol of water) in FBR and STR systems. Time zero corresponds to induction for all the experiment	195
6.2.4	Comparison of Gas consumption during Hydrate growth (mol of Gas/mol of water) in fixed bed reactor containing Silica Gel of different pore size (5 and 100 nm). Time zero corresponds to induction for all the experiment	196
6.2.5	Comparison of Gas consumption during growth of Hydrate (mol of Gas/mol of water) in fixed bed reactor containing Silica Gel and blend of Silica Gel with zeolite 5A. Time zero corresponds to induction for all the experiment	197
6.2.6	Comparison of water to Hydrate conversion for the different systems studied; the data is shown for 3 hours of Hydrate growth after nucleation	198
6.3.1	Comparison between 100% saturation of Silica Gel, Silica Gel+ 30wt.% Zeolite 3A, Silica Gel+ 30wt.% Zeolite 5A	199
6.3.2	Comparison between 50% saturation of Silica Gel, Silica Gel+ 30wt.% Zeolite 3A, Silica Gel+ 30wt.% Zeolite 5A	200
6.3.3	Comparison between 100% saturation of Silica Gel, Silica Gel+ 30wt.% Zeolite 3A, Silica Gel+ 30wt.% Zeolite 5A	201
6.3.4	Comparison between 50% saturation of Silica Gel, Silica Gel+ 30wt.% Zeolite 3A, Silica Gel+ 30wt.% Zeolite 5A	201
6.3.5	Comparison of water to Hydrate conversion for CO_2 Hydrate	202

	Formation at 100% saturation for 13.6 h	
6.3.6	Comparison of water to Hydrate conversion for CO_2 Hydrate Formation at 50% saturation for 6.43 h.	202
6.4.1	Growth kinetics of *Pseudomonas aeruginosa* A11.Time course of growth and surface tension reduction of growth medium	206
6.4.2	Growth kinetics of *Pseudomonas aeruginosa* A11.Time course of dry cell biomass and rhamnolipids yield. Strain A11 was grown in glycerol supplemented MSM containing TES at 30^o C with stirring done at 200 rpm. The values provided are mean ± S.D. of three independent experiments	207
6.4.3	pH and reduction in surface tension relationship of Rhamnolipids produced from strain A11	209
6.4.4	Temperature and reduction in surface tension relationship of Rhamnolipids produced from strain A11	210
6.4.5	CMC of Rhamnolipids produced from strain A11	210
6.4.6	TLC of Rhamnolipids produced by standard and strain A11	212
6.4.7	FTIR spectrum of Rhamnolipids produced from strain A11	213
6.4.8	^{1}H NMR of Rhamnolipids produced by strain A11	214
6.4.9	^{13}C NMR of Rhamnolipids produced by strain A11	215
6.4.10	Chromatogram of rhamnolipids produced by *Pseudomonas aeruginosa* strain A11	216
6.4.11	LCMS of purified rhamnolipids produced by *Pseudomonas aeruginosa* A11	217
6.4.12	LCMS of purified Rhamnolipids produced by *Pseudomonas aeruginosa* A11	217
6.4.13	LCMS of purified Rhamnolipids produced by *Pseudomonas aeruginosa* A11strain A11	218
6.4.14	LCMS of purified Rhamnolipids produced by *Pseudomonas aeruginosa* A11	218
6.4.15	LCMS of purified Rhamnolipids produced by *Pseudomonas*	219

	aeruginosa A11	
6.4.16	Structure of RhaRha C_{10} C_{10}	219
6.4.17	MALDI-TOF mass spectra of purified rhamnolipids produced by *Pseudomonas aeruginosa* A11	221
6.4.18	MALDI-TOF mass spectra of purified rhamnolipids produced by *Pseudomonas aeruginosa* A11	221
6.4.19	DLS analysis of Rhamnolipids produced from strain A11	224
6.5.1	Growth and surface tension reduction kinetics of *Bacillus subtilis* strain A21. Strain A21 was grown in sucrose supplemented mineral salt medium at 30^o C with stirring done at 200 rpm. Values given are mean ± S.D. of three independent experiments	225
6.5.2	Time course of growth and surfactin production from *Bacillus subtilis* strain A21. Strain A21 was grown in sucrose supplemented mineral salt medium at 30^o C with stirring done at 200 rpm. Values given are mean ± S.D. of three independent experiments	226
6.5.3	pH and reduction in surface tension relationship of Surfactin produced from strain A21	228
6.5.4	Temperature and reduction in surface tension relationship of Surfactin produced from strain A21	228
6.5.5	CMC of Surfactin produced from strain A21	229
6.5.6	TLC of Surfactin produced by standard and strain A21	230
6.5.7	Fourier transform infrared spectrum of purified surfactin produced by *Bacillus subtilis* strain A21	231
6.5.8	HPLC of Surfactin from Strain A21 and Standard	232
6.5.9	MALDI-TOF mass spectrum of purified surfactin produced by *Bacillus subtilis* strain A21	233
6.5.10	^{1}H NMR of biosurfactant i.e Surfactin produced by *Bacillus subtilis* strain A21	235
6.5.11	^{13}C NMR of biosurfactant i.e Surfactin produced by *Bacillus*	236

	subtilis strain A21	
6.5.12	Chromatogram of amino acid analysis of Surfactin produced by *Bacillus subtilis* strain A21	237
6.5.13	Diameter of surfactin produced from strain A21	238
6.6.1	FTIR of CaLS	239
6.6.2	UV of CaLS	239
6.6.3	Calibration Curve of Sodium (Na)	240
6.6.4	Calibration Curve of Magnesium (Mg)	241
6.6.5	Calibration Curve of Potassium (K)	241
6.6.6	Calibration Curve of Calcium (Ca)	242
6.6.7	Gel Permeation Chromatography of CaLS	243
6.6.8	FE-SEM of CaLS	244
6.6.9	FE-SEM showing mapping of various elements of CaLS where Blue, Red, Green are Sulphur, Oxygen, Calcium respectively where Red + Blue = Magenta (showing the presence of Oxygen and Sulphur)	245
6.6.10	FE-SEM showing mapping of various elements of CaLS where Blue, Red, Green are Sulphur, Carbon, Calcium respectively where Red+ Green = Yellow (showing the presence of Carbon and Calcium)	245
6.6.11	Electron Dispersive Spectroscopy of CaLS	246
6.6.12	DTG Analysis of CaLS	247
6.6.13	Nuclear Magnetic Resonance ^{13}C of CaLS	248
6.7.1	Temperature and Pressure profile of Methane Hydrate Formation and Dissociation in presence of C-type Silica Gel (Merck)	250
6.7.2	Temperature and Pressure profile of Methane Hydrate Formation and Dissociation in presence of C-type Silica Gel (Merck) containing 100 ppm Rhamnolipids	251
6.7.3	Temperature and Pressure profile of Methane Hydrate Formation and Dissociation in presence of C-type Silica Gel	252

(Merck) containing 1000 ppm Rhamnolipids

6.7.4	Comparison of Methane Hydrate Formation nucleation temperature	254
6.7.5	Comparison of phase equilibrium parameters	255
6.7.6	The (P,T) data of equilibrium are plotted as lnP vs 1000/T	258
6.7.7	Induction Time for Methane Hydrate Formation in quiescent water	259
6.7.8	Induction Time for Methane Hydrate Formation in C-type Silica Gel (Merck)	260
6.7.9	Induction Time for Methane Hydrate Formation in C-type Silica Gel (Merck) containing 100ppm Rhamnolipids	260
6.7.10	Induction Time for Methane Hydrate Formation in C-Type Silica Gel (Merck) containing 1000ppm Rhamnolipids	261
6.7.11	Moles of Methane consumed while Methane Hydrate Formation for various experimental conditions	263
6.7.12	Moles of Methane/Moles of Water consumed while Methane Hydrate Formation for various experimental runs	264
6.7.13	The growth curve of Methane Hydrate Formation for Quiescent water	266
6.7.14	The growth curve of Methane Hydrate Formation in presence of C-type Silica Gel	266
6.7.15	Growth curve of Methane Hydrate Formation in C-type Silica Gel in presence of 100 ppm Rhamnolipids	267
6.7.16	The growth curve of Methane Hydrate Formation in C-type Silica Gel containing 1000 ppm Rhamnolipids	267
6.7.17	N/No vs Time Plot for Methane Hydride Formation with quiescent water	269
6.7.18	Semi-logarithmic plot of change of moles of Gas while Methane Hydrate Formation with quiescent water	270-272
6.7.19	N/No vs Time Plot for Methane Hydrate Formation in presence of C-type Silica Gel	273

6.7.20	Semi-logarithmic plot of change of moles of Gas while Methane Hydrate Formation in presence of C-type Silica Gel	274-276
6.7.21	N/No vs Time Plot for Methane Hydrate Formation in presence of C-type Silica Gel containing 100 ppm Rhamnolipids	276
6.7.22	Semi-logarithmic plot of change of moles of Gas while Methane Hydrate Formation in presence of C-type Silica Gel containing 100 ppm Rhamnolipids	277-279
6.7.23	N/No vs Time Plot for Methane Hydrate Formation in presence of C-type Silica Gel containing 1000 ppm Rhamnolipids	280
6.7.24	Semi-logarithmic plot of change of moles of Gas while Methane Hydrate Formation in presence of C-type Silica Gel containing 1000 ppm Rhamnolipids	281-283
6.7.25	Methane Hydrate Formation rate for time zone 0 to 20 minutes	284
6.7.26	Methane Hydrate Formation rate for time zone 20 to 40 minutes	285
6.7.27	Methane Hydrate Formation rate for time zone 40 to 80 minutes	285
6.7.28	Methane Hydrate Formation rate for time zone 80 to 160 minutes	286
6.7.29	Methane Hydrate Formation rate for time zone 160 to 260 minutes	286
6.7.30	Comparison of rates of Methane Gas Hydrate Formation for different time zone in different experiment condition	287
6.7.31	% Conversion of Methane Hydrate for various experiments	289
6.8.1	Temperature and Pressure profile of Methane Hydrate Formation and Dissociation in presence of C-type Silica Gel containing 100 ppm surfactin	301
6.8.2	Temperature and Pressure profile of Methane Hydrate Formation and Dissociation in presence of C-type Silica Gel	302

	containing 1000 ppm surfactin	
6.8.3	Methane Hydrate Formation parameters in presence of different test samples	304
6.8.4	Phase Equilibrium conditions for various test samples	305
6.8.5	The (P,T) data of equilibrium are plotted as lnP vs 1000/T	308
6.8.6	Induction Time for Methane Hydrate Formation in C-type Silica Gel (Merck) containing 100ppm Surfactin	309
6.8.7	Induction Time for Methane Hydrate Formation in C-type Silica Gel (Merck) containing 1000 ppm Surfactin	310
6.8.8	Moles of Methane consumed while Methane Hydrate Formation for various experimental conditions	312
6.8.9	Moles of Methane consumed / moles of water consumed while Methane Hydrate Formation for various experimental conditions	313
6.8.10	Growth curve of Methane Hydrate Formation in C-type Silica Gel in presence of 100 ppm Surfactin	314
6.8.11	The growth curve of Methane Hydrate Formation in C-type Silica Gel containing 1000 ppm Surfactin	315
6.8.12	N/No vs Time Plot for Methane Hydrate Formation in presence of C-type Silica Gel (Merck) containing 100 ppm Surfactin	316
6.8.13	Semi-logarithmic plot of change of moles of Gas while Methane Hydrate Formation in presence of C-type Silica Gel (Merck) containing 100 ppm Surfactin	317-319
6.8.14	N/No vs Time Plot for Methane Hydrate Formation in presence of C-type Silica Gel containing 1000 ppm Surfactin	319
6.8.15	Semi-logarithmic plot of change of moles of Gas while Methane Hydrate Formation in presence of C-type Silica Gel containing 1000 ppm Surfactin	320-322
6.8.16	Methane Hydrate Formation rate for time zone 0 to 20 minutes	323
6.8.17	Methane Hydrate Formation rate for time zone 20 to 40	323

	minutes	
6.8.18	Methane Hydrate Formation rate for time zone 40 to 80 minutes	324
6.8.19	Methane Hydrate Formation rate for time zone 80 to 160 minutes	324
6.8.20	Methane Hydrate Formation rate for time zone 160 to 260 minutes	325
6.8.21	Comparison of rates of Methane Gas Hydrate Formation for different time zone in different experiment condition	326
6.8.22	Conversion (%) of Methane Hydrate for various experiments	328
6.9.1	Induction Time of Natural Gas Hydrate Formation for various experimental conditions	336
6.9.2	Normalized growth of Natural Gas Hydrate Formation for various experimental conditions	336
6.9.3	Induction Time of Methane Hydrate Formation for various experimental conditions	337
6.9.4	Temperature and pressure profile of Methane Hydrate Formation and Dissociation in presence of 1 wt.% CaLS	339
6.9.5	Induction Time for Methane Hydrate Formation in presence of 1 wt.% CaLS	341
6.9.6	Moles of Methane Gas consumed	342
6.9.7	Methane Gas consumption and Pressure drop as function of time in presence 1 wt.% CaLS	343
6.9.8	Change of moles of Methane during Methane Hydrate Formation in presence of 1 wt.% CaLS	344
6.9.9	Semi-logarithmic plots of change of moles of Gas during Hydrate Formation in presence of 1 wt.% CaLS	345-347
6.9.10	Comparison of rates of Methane Gas Hydrate Formation for different time zone in different experiment condition	348
6.9.11	Comparison of rates of Methane Gas Hydrate Formation for time zone (0-20 min) in different experiment condition	348

6.9.12	Comparison of rates of Methane Gas Hydrate Formation for time zone(20-40 min) in different experiment condition	349
6.9.13	Comparison of rates of Methane Gas Hydrate Formation for time zone(40-80 min) in different experiment condition	349
6.9.14	Comparison of rates of Methane Gas Hydrate Formation for time zone(80-160 min) in different experiment condition	350
6.9.15	Comparison of rates of Methane Gas Hydrate Formation for time zone (160-280 min) in different experiment condition	350
6.9.16	FTIR of C-Type Silica Gel before and after Going for Gas Hydrate Experience	352
6.9.17(a)	Scanning Electron Microscopic Image of C-Type Silica Gel before Hydrate Formation	353
6.9.17(b)	Scanning Electron Microscopic Image of C-Type Silica Gel after Hydrate Formation	353

ABBREVIATION AND NOTATIONS

ABBREVIATIONS

NGH	Natural gas hydrates
GH	Gas Hydrate
SDS	Sodium Dodecyl Sulphate
STS	Sodium Tetradecyl Sulphate
SHS	Sodium Hexadecyl Sulphate
PVP	Polyvinylpyrrolidone
PVCAP	Polyvinylcaprolactam
PEO	Polyethylene oxide
KHI	Kinetic Hydrate Inhibitors
AFP	Anti Freeze Proteins
FBR	Fixed Bed Reactor
STR	Stirred Tank Reactor
TLC	Thin Layer Chromatography
FTIR	Fourier Transform Infrared Spectroscopy
NMR	Nuclear Magnetic Resonance
LC-MS	Liquid Chromatography-Mass Spectrometry
MALDI	Matrix-assisted Laser Desorption/Ionization
CMC	Critical Micelles Concentration
HPLC	High Performance Liquid Chromatography
AAS	Amino Acids Sequence
CaLS	Calcium lignosulphonate
UV-VIS	Ultraviolet – Visible Spectrometry
CHNS	Carbon Hydrogen Nitrogen Sulphur Analysis
GPC	Gel Permeation Chromatography
FE-SEM	Field Emission Scanning Electron Microscopy
EDS	Energy Dispersive X-ray Spectroscopy
ICPMS	Inductively Coupled Plasma Mass Spectroscopy
TGA	Thermo Gravimetric Analysis
FBM	Fixed Bed Media

LNG	Liquefied Natural Gas
NGHP	National Gas Hydrate Programme
LPG	Liquefied Petroleum Gas
K-G	Krishna – Godavari
RLNG	Regassified Liquefied Natural Gas
G	Guest Molecule
TCF	Trillion Cubic Feet
GIP	Gas-In-Place
K-K	Kerela-Konkan
GHSZ	Gas Hydrate Stability Zone
HEI	Hydrate Energy International
IIASA	International Institute for Applied System Analysis
HBGS	Hydrate Base Gas Separation
THF	Tetrahydrofuran
HFC	Hydro fluorocarbon
PCM	Phase Change Material
TBAB	Tetra-n-Butyl Ammonium Bromide
CFC	Chloroflurocarbons
QAB	Quaternary Ammonium Bromide
LWD	Logging While Drilling
MWD	Measurement While Drilling
USGS	United States Geological Survey
MDT	Modular Dynamic Testing
SCF	Standard Cubic Feet
BSR	Bottom Simulating Reflectors
CSEM	Controlled Source Electro Magnetic
PCCT	Pressure Core Characterization Tools
STP	Standard Temperature and Pressure
HAA	Hydroxyalkanoyloxy Alkanoic Acid
Val	Valine
Asp	Aspartic Acid

Leu	Leucine
Glu	Glutamic Acid
DMPC	1, 2-Dimyristoyl-sn-glycero-3-phosphocholine
DPPS	1, 2 Dipalmitoyl-sn-glycero-3-phospho-L-serine sodium salt
POPC	1-palmitoyl-2-oleoyl-sn-glycero-3-phosphocholine
LABSA	Linear Alkyl Benzene Sulfonic Acid
DAM	Quaternary Ammonium Salt
Brij-58	Polyoxyethylene (20) cetyl ether
PAAA	Poly-Acryl amide-co-Acrylic Acid
PVA	Poly Vinyl Alcohol
Igepal-520	Polyoxyethylene (5) nonylphenyl ether
Tween-40	Polyoxyethylene (20) sorbitan monopalmitate
LABS	Linear Alkyl Benzene Sulfonate
ENP	Ethoxylated Nonylphenol
CTAB	Cationic Surfactant Cetyl Trimethyl Ammonium Bromide
CCD	Charge Coupled Device
HTABr	Hexa Decyl Trimethyl Ammonium Bromide
SDBS	Sodium Dodecyl Benzene Sulfonate
CuO	Copper Oxide
TDS	Total Dissolved Salts
PVC	Polyvinyl Chloride
LDKI	Low Dose Kinetic Inhibitor
THI	Thermodynamic Inhibitor
PAP	Polyacryloylpyrrolidine
IPCC	International Panel on Climate Change
MOF	Metal Organic Framework
US DOE	United States Department of Energy
JOGMEC	Japan Oil, Gas and Metals National Corporation
HBCC	Hydrate Based Carbon Dioxide Capture
TBAF	Tetrabutyl Ammonium Salts of Fluoride
TBAC	Tetrabutyl Ammonium Salts of Chloride

TBAB	Tetrabutyl Ammonium Salts of Bromide
CAC	Carbon Dioxide Adsorption Capacity
LDHI	Low Dose Kinetic Inhibitor
NaCl	Sodium Chloride
HP-DSC	High Pressure Differential Scanning Calorimetry
LS	Lingo Sulfonate
CR	Crystallizer
SV	Supply Vessel
P	Pressure Transducer
T	Thermocouples
DAQ	Data Acquisition System
ER	External Refrigerator
SPV	Safety Pressure Valve
TCWB	Temperature Controlled Water Bath
GC	Gas Chromatography
S	Stirrer
R	Reservoir
MFC	Mass Flow Controller
V1	Valve 1
V2	Valve 2
V3	Value 3
BET	Brunauer, Emmett, and Teller
EDX	Energy Dispersive X-Rays
BJH	Barret- Joyner-Halenda
IUPAC	The International Union of Pure and Applied Chemistry
MSM	Minimal Salt Medium
EDTA	Ethylene Diaminetetraacetic Acid
TES	Trace Element Salts
NaOH	Sodium Hydroxide
HCL	Hydrochloric Acid
NB	Nutrient Broth

OD	Optical Density
CFS	Cell-Free Supernatant
$NaHCO_3$	Sodium Bicarbonate
KBr	Potassium Bromide
$CdCl_3$	Trichloro(^2H) methane
TMS	Tetramethyl Silane
UHPLC	Ultra High Performance Liquid Chromatography
ACN	Acetonitrile
CHCA	Cyano 4-Hydroxy Cinnamic Acid
DMSO	Deuterated Dimethyl Sulfoxide
TFAA	Trifluoroacetic Acid
TCD	Thermal Conductivity Detector
SEM	Scanning Electron Microscope
PGP	Plant-Growth Promoting
MMR	Multi-Metal-Resistant
DTG	Differential Thermogravimetry
DTAB	Dodecyl Trimethyl Ammonium Bromide
CPS	Counts Per Second

NOTATIONS

Gt	gigatones
MPa	Mega Pascal
$\triangle H_f$	Molar Enthalpy of Formation of Gas Hydrate (KJ/mol)
$\triangle H_d$	Molar Enthalpy of Dissociation of Gas Hydrate (KJ/mol)
ppm	parts per million
rpm	revolution per minute
K	Kelvin
ppt	parts per trillion
µm	Micrometer
nm	nanometer
^0C	Degree Celcius

pH	Power of hydrogen
ml	mililiter
μ	Specific growth rate was
M_n	Number average molecular weight
M_w	Weight average molecular weight
M_p	Molecular weight of highest peak M_z,
M_{z+1}	The higher average molecular weights
Δn_H	Total number of moles of gas consumed for Hydrate Formation
V_{CR}	Volume of the Gas Phase of the Crystallizer
Z	Compressibility Factor
R	Universal Gas Constant
P_r	Critical Pressure
T_r	Critical Temperature
β^0	Empirical Constant
β^1	Empirical Constant
ω	Acentric factor
P1	Initial Pressure
P2	Final Pressure
T1	Initial Temperature
T2	Final Temperature
ΔH_{diss}	Molar enthalpy of Dissociation of Methane Gas Hydrate
N	Total number of moles at time t
N_0	Initial number of moles
k	Rate Constant
n_{H_2O}	The total number of moles of water in the system
N_h	Hydration number
θ_L	Fractional occupancy of the large cavity
θ_S	Fractional occupancy of the large cavity

CHAPTER- 1

INTRODUCTION

As there are limited resources of Conventional fuels like Coal, Petroleum and Natural Gas, hence with the available resources the demands for the energy of the world can be met for a limited time. Gas Hydrates are seen as white gold provided a viable technology is developed for their exploitation. Natural Gas is being exploited through conventional means such as drilling, but in order to harness the full potential of this highly promising energy resource, a lot of other non-conventional sources are being looked into with great confidence. Some of the promising non-conventional energy sources are shale Gas and Methane Hydrates. Beyond conventional sources of Natural Gas, tapping of Gas Hydrates opens new horizons as this unconventional energy source has recently got discovered in India and its cost effective utilization is crucial to India's energy security and it is also likely to reduce India's import bills of LNG (Liquefied Natural Gas) substantially. Rapid growth in energy demand, coupled with the worry of anthropological discharge of CO_2 into the environment has seen extraordinary increase in consumption of Natural Gas. The scientific evidence of global warming and its link to anthropogenic activities has been stabilized [Tchapda et al, 2014]. Exhaustion of traditional stock of non-renewable fuels [Rawool et al, 2005] has resulted in the rise of their price which has led to exploitation of novel resources through modern technologies. Methane Gas Hydrates is one such source of Methane Gas which is captured in crystalline ice like structure in permafrost regions and under the sea in outer continental margins but mostly they are present in oceanic deposit below the ocean floor where the depths are approximately more than 500 m. It was evident from the NGHP 01 (National Gas Hydrate Programme) expedition that the Gas Hydrates are distributed in the Krishna-Godavari, Mahanadi and Andaman off shores in Indian context. They are seen as the future potential energy resource. An enormous quantity of Methane is available in the Gas Hydrates. It is evaluated that total quantity of carbon in the form of Methane clathrate is much greater than the carbon content in all the non-renewable fuel sources put together and hence these are seen as the potential future energy resource.

The energy requirements of the world can be met even if a small percentage of Gas Hydrates can be exploited. If exploited properly, Gas Hydrates will be the next generation energy resource. US department of energy has said that if only 1% of Methane stored in Hydrates can be exploited, it

is almost more than the current supply of Natural Gas in the country [Holder et al, 1987, Haq et al, 1998].

Gas Hydrates are non-stoichiometric crystalline compounds that are formed when small guest molecules (Gases and liquids) get entrapped in cages made up of hydrogen bonded host (water) molecules at suitable conditions of temperature and pressure. [Davidson et al, 1973, Englezos et al, 1993, Sloan et al, 2008]. The most common guest molecules are CH_4, C_2H_6, C_3H_8, iso- C_4H_{10}, n-C_4H_{10}, N_2, H_2, H_2S and CO_2, of which Methane or Natural Gas Hydrates occur abundantly in nature [Kumar et al, 2015, Babu et al, 2013, Makogon et al, 2007] and are also known as crystalline form of Natural Gas. They are also known as Methane clathrates. They are formed by intermingling of two compounds as there is no bonding between them. Pure CO_2 and CH_4 Hydrates form type I structure [Sloan et al, 2008]. The worldwide organic carbon in the Gas Hydrates is approximated to be roughly about 10000 X 10^{15} grams which is almost double the carbon content in total non-renewable fuel sources (Natural Gas, crude oil and coal) of the world [Kvenvolden, 1993, Satoh et al, 1996, Collett, 2002]. Methane Hydrates contain high amount of Methane as 1 m^3 of Methane Hydrate contains 0.8 m^3 of water and more than 160 m^3 of Methane at standard temperature-pressure-condition [Sloan et al, 2008]. Hence, Methane and Natural Gas storage and transportation in the form of synthetic Gas Hydrate appeals an economical process [Gudmundsson et al, 2006, Kim et al, 2010]. Hydrates are seen as clean form of energy.

Hydrates have various applications such as carbon dioxide capture, desalination, storage and transportation of Natural Gas. Hence, a lot of research is going on to find a less energy intensive, economic, clean and green technology for the promotion of Gas Hydrates. Although synthetic surfactants promote Hydrate Formation but at the same time their non-biodegradability and toxicity hinders them from being used as Hydrates promoters. Hydrate Formation is also promoted by mechanical agitation but this method is very energy intensive so the solution lies in designing fixed bed media for Hydrate Formation. Hence industry is looking towards biosurfactants as Hydrates promoters in order to make Hydrate based technologies green, clean and biodegradable. The drawback of Hydrates is pipeline plugging which is a threat in oil and Gas industry as they can destroy the whole pipeline and can be a danger for human life. So lot of work is going on for finding economical biodegradable inhibitors for Gas Hydrates Formation.

CO_2 capturing is gaining high attention as it is a major greenhouse Gas. The latest research going in the field of exploitation of this resource of energy is through CO_2 sequestration. Hence, this energy source can be obtained by dumping CO_2 in sea. CO_2 sequestration of Gas Hydrates can take out Methane from Gas Hydrates by reducing the global warming, hence attaining two objectives i.e giving new resource of energy Methane, the burning fuel side by side reducing pollution. This technology has been effective and successful at the laboratory scale. Pilot scale production tests have been completed in permafrost region and in marine Gas Hydrate deposit to test the possible Gas recovery technology from Hydrate bearing reservoir by CO_2 sequestration. Moreover, when combustion of Methane takes place 25% lesser CO_2 is released in comparison to when the same mass of coal is combusted and additionally Methane does not emit the Nitrogen and Sulphur oxides which makes it more environment friendly.

The microbe community is active with the Gas Hydrates. *Bacillus subtilis* and members of gammaproteobacteria are identified in Gulf of Mexico Gas Hydrate mounds [Lanoil et al, 2001]. These microbes produce Surfactin and Rhamnolipids biosurfactants respectively. Thus, anticipation that secondary metabolites from gammaproteobacteria like *Pseudomonas aeruginosa* may have beneficial effect on Gas Hydrate Formation would not be an exaggeration. The biosurfactants influence the induction time and rate of Formation of Gas Hydrates. The induction time is known as the time passed till the measurable amount of Hydrate phase appears or until the measurable number of moles of Gas forming the Hydrates are consumed and it is also known as the Hydrate nucleation time. Biosurfactants enhance the Formation rate of Gas Hydrates after their Critical Micelles Concentration (CMC) [Zhong et al, 2000].

CHAPTER - 2
LITERATURE REVIEW

2. Introduction

About 60% of the energy requirement of the world's population of over 7 billion people is fulfilled by oil and Gas. The rest of the 40% is supplied by nuclear, hydroelectric power and coal, renewable sources of energy like solar, tidal power, wind and biomass products such as firewood. The present worldwide demand of oil is about 90.1 million barrels per day. This requirement is growing every year. According to the forecasts, the global demand for energy will rise by about 40% by 2030. In order to fulfil the global energy requirements in a reasonable way, huge investments are necessary to eventually generate volumes which would be good enough to cater to our energy demands. Study at Rice University's Baker Institute, Houston, US, reported an investment of approximately 2 trillion dollars are needed by the year 2030 so that the expected global demand of oil can be fulfilled. In order to meet higher energy demand in countries like India and China low-carbon technologies will play a vital role [Stephen et al, 2014]. Other options like hydrogen are also worth investigating as it can be changed into different forms of energy in many ways than any other fuel [Sherif et al, 1999, Sherif et al, 2003, Sherif et al, 2005]. Reservoirs contain hydrogen which is found in small amounts mixed with Natural Gas [Sherif et al, 2014].

The ever increasing energy demand and depletion of fossil fuels reservoirs has forced researchers to investigate for alternative fuel resources. Fossil fuels have been an important and reliable energy source for society since the advent of the industrial revolution in the late 17^{th} century. However, excessive use, restricted resource content and environmental concerns have forced the present world to look for suitable alternative energy sources.

Owing to its distinct set of benefits Natural Gas has indisputably come forth as the future of energy industry. The Natural Gas majorly comprises of Methane which is a colourless, volatile, odourless, flammable Gas [Rahimi et al, 2015]. It helps in reducing the air pollution as it releases smaller amount of air pollutants when burnt. Furthermore, it has also got some very useful properties due to which a huge amount of Natural Gas can be transported to other countries in

the form of compressed LNG (Liquefied Natural Gas). LNG is the Natural Gas that has been cooled to about -162° C due to this the Gas changes into liquid thereby reducing the volume by 600 times. This remarkable decrease in volume allows it to be transported securely and efficiently using specifically designed LNG containers. When it reaches its destination, LNG is reheated to restore it to its Gaseous state and distributed to the Natural Gas consumers via local pipelines. When Natural Gas is burnt in a good quality burning system, it can establish combustion efficiency as high as 95% which is superior as compared to LPG which can establish combustion efficiency of 90%. As the weight of Natural Gas is less than air, it rapidly ascends upwards and gets scattered if there is any case of leakage. Therefore, Natural Gas is quite safe in contrast to other fuels such as solid and liquid fuels. All the big energy companies are investing billions of dollars in the Natural Gas industry as the potential returns appear to be exceptionally good, in view of the prominent benefits of Natural Gas. According to report published by US Energy Information Administration (2015) in Annual Energy Outlook (2015), the energy consumption in the form of Natural Gas has increased substantially over the last couple of decades and it is bound to increase even more as shown by the projected consumption of energy in Figure 2.1.

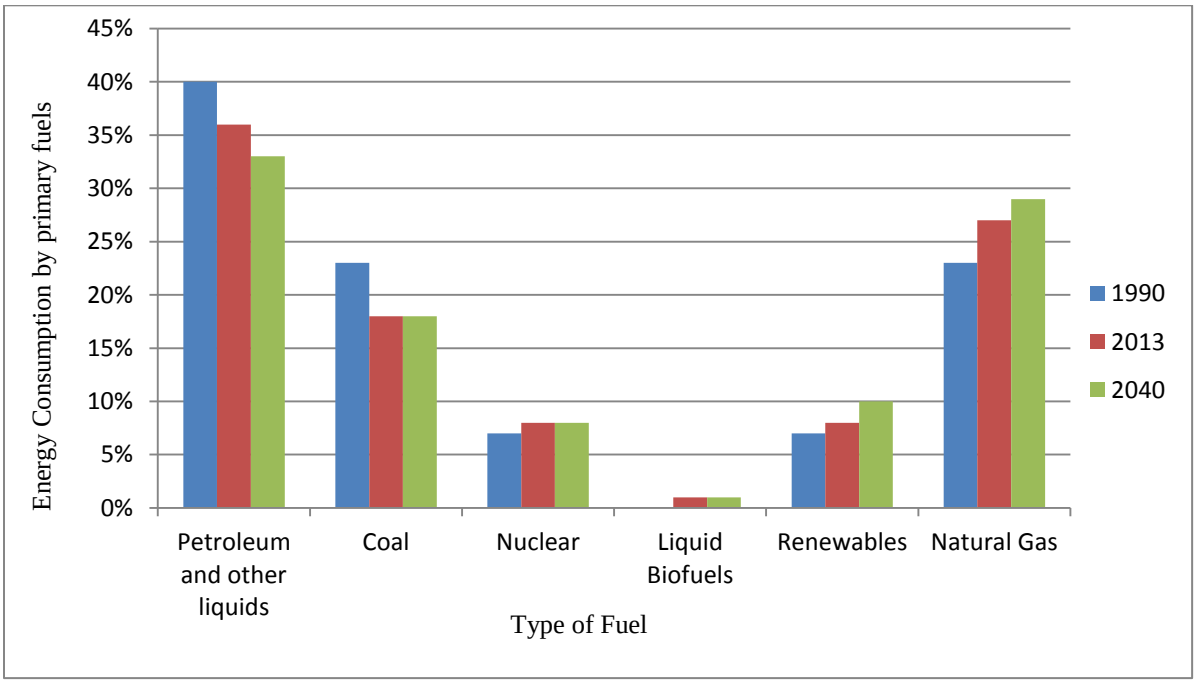

Figure 2.1: Primary Energy Consumption by Fuel in the Reference Case, 1990-2040

Natural Gas is being exploited through conventional means such as drilling but in order to harness the full potential of this highly promising energy resource, a lot of other non-conventional sources are being looked into with great confidence. Some of the non-conventional energy sources are shale Gas and Methane Hydrates. A large amount of money is being invested on year basis considering that these non-conventional energy sources are competent enough to alter the dynamism within the global energy industry by satisfying the rapidly growing demand for energy at a much reasonable cost for customers.

Beyond conventional sources of Natural Gas, tapping of Gas Hydrates opens new horizons as an unconventional energy source as its been recently discovered in India and its cost effective tapping is crucial to India's future energy security. It is also likely to reduce India's import bills of Liquefied Natural Gas (LNG) substantially. The contribution of Natural Gas in the energy mix of India is likely to increase to 20% in 2025 as compared to 11% in 2010. For fulfilling this demand Indian Natural Gas sources in conventional form are insufficient and currently not as promising, as they rely on costly foreign technology. To overcome this, India must self-equip itself with the right technological capabilities leading to world class innovations in the field of Gas Hydrates as source of energy. In view of this we have taken a great step forward in research on Methane Gas Hydrates by launching National Gas Hydrate Programme (NGHP-01). During NGHP-01 drilling/coring operations were performed in four areas of India offshore from 28th April to 19th August 2006. The NGHP Expedition 01 has revealed the existence of Gas Hydrates in Mahanadi, Krishna-Godavari (K-G) and Andaman basins. NGHP 02 expedition has been recently completed in 2015.

When we consider sources of energy as a resource then they are of national importance because energy security today has emerged out as one of the most challenging issue being faced by the world especially in the fast developing countries such as India and China which are some of the biggest importers of sources of energy mostly oil and Gas. India, as we know, is a huge importer of oil and Gas products typically petrol, diesel and Natural Gas in the form of RLNG (ReGassified Liquefied Natural Gas). This cost huge to our county leading to rapid increase in current account deficit.

We have used various sources of energy from wood and animal fat, to fossil fuels to provide us with heat, produce our goods, and travel around the earth. Since the birth of civilization, the energy needs of the mankind has progressed through various degrees of development. In the realm of energy Research & Development Natural Gas Hydrate is the latest addition as a promising energy resource for the future.

2.1 Gas Hydrates

Gas Hydrates are non-stoichiometric crystalline compounds, which are formed when small guest molecules (Gases and liquids) get entrapped in cages made up of hydrogen bonded host (water) molecules at suitable conditions of temperature and pressure. [Davidson et al, 1973, Englezos et al, 1993, Sloan , 1998, Sloan et al, 2003, Sloan et al, 2008, Kang et al, 2014]. The most common guest molecules are CH_4, C_2H_6, C_3H_8, iso-C_4H_{10}, n-C_4H_{10}, N_2, H_2, H_2S and CO_2, of which Methane/Natural Gas Hydrates occur abundantly in nature [Kumar et al, 2015, Babu et al, 2013, Makogon et al, 2007, Mahajan et al, 2007]. Pure CO_2 and Methane Hydrates form type I structure [Sloan et al, 2008]. Gas Hydrates are inclusion compounds formed by water as host and Gas as a guest molecule at high pressure and low temperature [Sloan, 1998]. Naturally occurring Gas Hydrates are present in permafrost regions and seafloors of continental margins [Hester et al, 2009, chong et al, 2015].

Today Gas Hydrates are known as one of the potential source of Methane and therefore it is sometimes called as fuel of the future. Methane Gas Hydrates have captured double amount of carbon in comparison to fossil fuels. They are considered as future generation fuels. It is estimated that under the sea huge amount of Methane of the order of trillion in the form of Gas Hydrate is present [Buffett et al, 2004]. Hydrates are Naturally occurring materials that are present on regions of arctic permafrost and submarine continental margins [Kvenvolden et al, 1993, Kvenvolden et al, 1998, Sloan et al, 1998, Durham et al, 2003]. Their presence is also supposed to be on large icy to medium-sized moons of the outer solar system [Loveday et al, 2001, Lunine et al, 1985] and also on the polar regions of Mars [Miller et al, 1970, Jakosky et al, 1995]. Gas Hydrates can store a huge percentage of Gas per unit volume due to arrangement of Gas molecules within this structure. Hydrates are inter-grown, white-to-grey and yellow crystals, transparent-to-translucent and with poorly defined crystal form in appearance. Hydrates may occur in pore spaces in uncemented sediment grains or they may cement sediment in which they

occur. Hydrates can occur in large, continuous deposits and occupy large percentage of pore space in high-porosity sediments.

Gas Hydrates were discovered by Sir Humphrey Davy in 1881. He observed that water and chlorine can form a crystalline substance under certain conditions of temperature and pressure and it was called chlorine Hydrate. Later in 1930's, it was observed that solid Gas Hydrate developed in the oil and Gas transmission pipelines in the U.S. were accountable for the clogging of pipelines. After this, Gas Hydrate was seen as a nuisance. Today Gas Hydrates are considered as one of the potential resource of Methane and it is also called as fuel of the future. Gas Hydrates (clathrate) are solid and non stoichiometric crystalline compound consisting of water called host molecules and low molecular weight hydrocarbons Gases called guest molecules. Water molecules arrange itself in a cage like Formation which encapsulates a Gas molecule. At low temperature and high pressure condition, guests and host interact with each other through Van der Waal's interaction and stabilize the structure and there is no chemical bonding between them. Thermodynamically, Hydrate Formation is favoured at high pressure, low temperature and low salt concentration [Sloan, 1990, Sloan et al, 2008]. These type of conditions can occur in ocean-bottom sediments where depth of the water is less than 500 m [Kvenvolden, 1993] and in permafrost region. Gas Hydrates constitute a tremendous reserve of Natural Methane in the earth [Dobryin et al, 1981, Sloan, 1998] for example, $1m^3$ of Hydrate disassociates at atmospheric pressure and temperature to form 164 m^3 of Natural Gas plus 0.8 m^3 of water [Kvenvolden, 1993]. Gas Hydrates can remain stable till temperatures up to 291 K with the use of pressurization. Density of Gas Hydrate is 0.79 kg/L [Suess et al, 2002].

In recent past Natural Gas Hydrates (NGH) have been highlighted as a potential next generation sources of energy [Chong et al, 2015, Zhang et al, 2012]. The amount of Gas present in Natural Hydrate reservoirs is estimated to possess two times as much energy as contained in the total conventional fuel reservoirs [Demirbas, 2010]. Huge amount of untapped Gas Hydrates present in nature is considered as a new source of sustainable energy. Among all known Natural Gas Hydrates, the Methane Hydrates are the most commonly encountered Hydrates [Demirbas, 2010]. Gas Hydrates have tremendous application potential in the discipline of environment and energy [Koh et al, 2011]. Apart from the alternative energy source the Gas Hydrates have also drawn a lot of attention for its possible uses in storage, separation, transportation and capture of several Gases (like Methane, propane, carbon dioxide, and hydrogen) and water desalination

[Hester et al, 2009, Sloan et al, 2003, Wang et al 2012, Wang et al 2013]. Storage and transportation of Natural Gas as a solid Gas Hydrate is considered an alternative method to liquefied Natural Gas (LNG). Compared to LNG, Gas Hydrates are easier and safer to handle because of their low explosion potential. This physical property of Gas Hydrates inspired researchers to develop Hydrate technology as a new means of storage and transportation of Gas. It is reported that Hydrate could be stored at -15^{o} C under atmospheric pressure for fifteen days, holding on to nearly all the Gas. Significant amount of money will be saved if the Natural Gas in transported in Hydrate form as compared to liquefied Natural Gas [Klein et al, 2000, Gudmundsson et al, 1998, Gudmundsson et al, 1999, Taylor et al, 2001, Gudmundsson et al, 2003]. The successful commercialization of NGH would require efficient and safe technology for their generation, Dissociation, storage and transportation

The estimate of global Methane Hydrate reserves is still uncertain. At standard pressure and temperature the total quantity of Methane present *in situ* Methane Hydrate is approximately between 200 and 3,000,000 trillion m^3 [Boswell et al, 2011]. In this the quantity of global Methane Hydrates reserves in the most frequently quoted estimates is approximately about 20,000 trillion m^3 the total amount of organic carbon contents are about 10 trillion metric tons. This is about twice the amount of presently known global conventional fuels (oil, coal, Natural Gas) [Kvenvolden, 1998]. In the present scenario, due to scarcity of non-renewable fuels energy sources, countries from all over the world such as Canada, China, India, Japan, South Korea and USA are competing in the investigation of the Gas Hydrate resources.

Gas Hydrates are also emerging as a one of the cleaner fuels in the 21st century. Their total amount is approximately 100 times the entire Natural Gas resources in the world. Presuming that we are able to harness 10% of the entire resources, they can still be used for around 600 years as shown in Table 2.1.1 [British Petroleum, 2013, Lu, 2015].

Table 2.1.1: Conventional Gas Consumption, Reserves and Gas Hydrate Reserves and Usage Years in Major Countries (BP: British Petroleum, 2013 Lu 2015)

Country	Conventional Gas consumption (billion cubic meter)	Conventional Gas reserve (trillion cubic meter)	Gas Hydrate (trillion cubic meter)	Usage year
US	722.1	8.5	9060	12547
Canada	100.7	2.0	43.6-809	433-8034
Taiwan	16.3	--	50-230	50-230
Japan	116.7	--	4.7-7.4	40-63
India	54.6	1.3	1894-14572	34689-266886
China	143.8	3.1	107.7	749
World	3314.4	187.3	20,000	6034

Methane that is entrapped in the marine deposits as a Hydrate shows an enormous carbon reserve that it is worthy of being deemed a governing factor in estimation of renewable energy sources. On earth, Natural Gases such as ethane, Methane and propane mostly exist in Gas phase [Kvenvolden, 1993]. The worldwide organic carbon in the Gas Hydrates is approximated to be roughly about 10000 X 10^{15} grams which is almost two times the carbon content in total conventional fuel (Natural Gas, crude oil and coal) sources of the world.

The comparison of the sources of global organic carbon is shown in Figure 2.1.1.

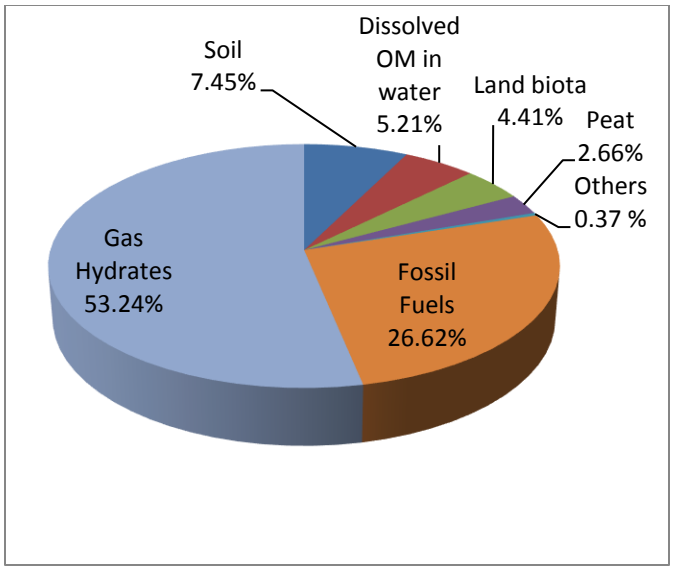

Where OM stands for Organic Matter in the above figure.

Figure 2.1.1: Distribution of Organic Carbon on Earth (Total 18,777 Gt) [Kvenvolden, 1993, Satoh et al, 1996, Collett, 2002].

2.2 Historical Perspective

The history of Natural Gas Hydrates has developed over three key periods as described below:

2.2.1 *Period I: Hydrate as a Laboratory Interest*

As discussed above, Natural Gas Hydrates were accidently detected by Sir Humphrey Davy in 1800's [Davy, 1811]. Since then, Gas Hydrates remained an academic curiosity for almost five decades. Scientists experimented to identify all of the compounds which can form Hydrates and their physical and chemical properties. By the end of the 19th century Villard [Villard, 1888, Villard, 1890] observed that hydrocarbons like Methane, ethane, propane etc. can form Hydrates. First tabulated results were recorded by de Forcrand, 1902 (a collaborator of Villard).

2.2.2 *Period II: Hydrate as an Issue to the Natural Gas Industry*

In 1930's, it was observed that solid Gas Hydrates developed in the oil and Gas transmission pipelines in the U.S. were accountable for the clogging of pipelines. After this, Gas Hydrates were seen as a nuisance. The first such example responsible for blocking the pipes due to Gas Hydrate was provided by Hammerschmidt in 1934. Hammerschmidt in 1939 invented the first algorithm for calculating the amount of methanol to inhibit the Formation of Natural Gas

Hydrates. Deaton et al in 1946 examined the effects of several chloride salts on Hydrate Formation and noticed that these salts inhibit Gas Hydrate Formation.

2.2.3 *Period III: Hydrate as an Untapped Energy Resource*

About 60 years ago Natural Gas Hydrates were located for the first time as Gas Hydrate deposit in Siberia .Since then they are seen as potential fossil fuel reserves. Makogon in 1997 provided the background on the up to date sole continuous Gas production in the Messoyakha field, Siberia from Natural Gas Hydrates. After that it was recognized that the low temperature and high pressure conditions are the necessity for the Hydrate Formation which should be present extensively around the globe, under the deep oceans and in permafrost region. The occurrence of Gas Hydrates in oceanic sediments was first estimated based on seismic observations [Tucholke et al, 1977, Shipley et al, 1979]. In 1992, the Ocean Drilling Programme was started deliberately to identify Hydrate deposits which resulted in samples being brought to the surface for more investigation [Farkhondeh et al, 2002].During the last decade the efforts of research and development in the field of Gas Hydrates has resulted into the detection of existence of Gas Hydrates in the continental margin areas [Gupta, 2004].

2.3 Energy Potential

Gas Hydrates are seen as a probable alternative renewable energy source [Ramana et al, 2009]. Gas Hydrates have gained a major focus because of the increasing demand of hydrocarbons coupled with their diminishing quantities [Satyavani et al, 2002]. The amount of Methane stored in the form of Gas Hydrates is more than 1500 times of current Natural Gas reserve of India. The energy demand of the country can be met for 100 years if only 10% of this resource can be harnessed [Sain, 2012]. There is uncertainty in the amount of Methane caught in Gas Hydrates. The idea given by the studies in pre-1990 of the amount of Methane caught in global Gas Hydrates deposits were in the range from ~10^{17} ft^3 or 10^5 trillion cubic feet (TCF) (McIver, 1981) to 10^8 TCF [Trofimuk et al, 1977]. Within the same period, [Kvenvolden, 1988, Gornitz et al, 1994, Harvey et al, 1995] has also given similar ideas. In the mid 1990 numerical modelling evaluation have given the total volume of Gas sequestered in Gas Hydrates from 1.4 to 1.7x10^5 TCF [Milkov, 2004, Buffett et al, 2004] to 4.2x10^6TCF [Klauda et al, 2003] with some intermediate estimates [Wood et al, 2008]. In the most recent review on the concerned subject Boswell et al. (2011) [Boswell et al, 2011] estimated 10^5 TCF of Methane caught in Gas

Hydrates (Gas-in-place or GIP). Among all renewable (Nuclear, Wind, Wave, Geothermal, Hydro, Solar, Bioprocess etc.) and non-conventional (Basin Centered Gas, Gas Shale, Gas Hydrates, Coal Bed Methane, Tight Gas Shale etc.) energy sources, Gas Hydrates are considered as one of the most relevant contender for cleaner fuels in this century. US department of energy has said that if only 1% of Methane stored in Hydrates can be exploited, it is almost more than the current supply of Natural Gas in the country [Holder et al, 1987, Haq et al, 1998]. Gas Hydrates will be a source of attention till their development capability is assessed [Grauls, 2001]. Methane Hydrates are assumed upcoming resource of hydrocarbon energy and will be a future fuel [Kvenvolden, 1993, Kvenvolden et al, 1980].

2.4 Hydrate Fundamentals

Natural Gas Hydrates are stable at a moderate to high pressure of the order of 1-30 Mega Pascal (MP) and at low temperature (-5^o - 20^o C). The Methane found in the marine sediments is either biogenic [Singh et al, 1999] or thermogenic [Vogt et al, 1999] or mixture of these two. Methane can have thermogenic or biogenic i.e origin it can be formed due to microbiological degeneration of organic matter in the absence of oxygen [Gupta, 2004]. In Gas Hydrates, Methane is predominantly produced due to bacterial anaerobic deterioration of organic material in environments containing low oxygen. During the diagenesis of organic matter bacterial Gas is formed. This Gas can be the part of the Gas Hydrate in continental shelf sediment. Similarly, deep sea Gas accumulation can lead to Formation of Gas Hydrate in the same continental shelf sediment if leakage of thermogenic Gas takes place to the surface. There are Hydrate forms in both primary and secondary pore space and fractures in sediments as a diagenetic mineral [Sloan, 1998].

Clathrates are formed as per the following reaction:-

$G + N_H H_2O = G.\ N_H H_2O$

G is the guest molecule which is 90 – 99% Methane in a Natural Gas Hydrate sample. N_H is the hydration number, which is average number of water molecules per guest molecules in a unit cell of crystalline Gas Hydrate compound and it can be used for calculating the amount of water molecules contained in the unit cell of a particular structure of Gas Hydrate. For a stable Gas Hydrate crystal, hydration number lies between 5.66 and 17; a lower hydration number will lead to higher saturation of Gas in the sample.

The Gas Hydrates synthesized in the lab is as shown in Figure 2.4.1.

Figure 2.4.1: Gas Hydrate Synthesized in Lab by Our Group

2.4.1 *Structure of Gas Hydrates*

With the help of X-ray diffraction methods von Stackelberg [Stackelberg, 1949, Stackelberg et al, 1954] provided the information of the detailed structure of Gas Hydrates. Vander Waals and Platteeuw gave the basis for calculating Gas Hydrate phase equilibria. Parrish and Prausnitz in the 70's of last century [Parrish et al, 1972] were the pioneer to provide additional assumptions on the occupation of the cages to Gas mixtures including Natural Gases and they also provided the first computer executable algorithm.

The structures I and II were first explained by von Stackelberg, structure H was invented by Ripmeester et al, 1987. Pure Methane forms structure I, if less than 0.1% propane is added then the structure changes to structure II, being formed by pure propane [Rock, 2002].

Three types of Methane Hydrate structures have been reported in Natural sediments known as sI, sII and sH Hydrate. All the three Hydrate structure has a cage of water molecule enclosing Methane known as pentagonal dodecahedron.

The three important structures are explained as follows:

(a) Structure I (sI): Structure I is cubic. There is a pentagonal dodecahedral (5^{12}) cage which is centred at the corners of the unit cell and in the centre of the cell a rotated dodecahedron is present. Pure Methane forms sI Hydrate and all large cages are occupied by it. CO_2 also forms structure I. The Structure I includes of 2 small cages consisting of 12 pentagonal surfaces i.e. 5^{12}

and 6 larger cages of again 12 pentagonal and two hexagonal surfaces i.e. 5^{12} 6^2 [Sloan, 2003] which is shown in Figure 2.4.2.

The unit cell consists of water molecules = ($2x5^{12}$ $+6x5^{12}$ 6^2 = 46) [Nixdorf, 1996].

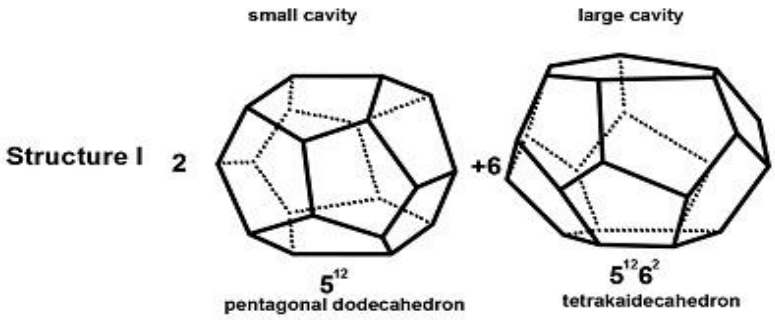

Figure 2.4.2: The Structure of Gas Hydrates sI [Gerami et al, 2006].

(b) Structure II (sII): Structure II is also cubic, in addition to common pentagonal dodecahedra, a large cage (hexakaidecahedral) made up of 12 pentagons rings and 4 hexagonal rings is also there. Large cage diameter in sI Hydrate is slightly lesser than the large cage diameter of sII Hydrate. Gases like ethane, propane, butane, Natural Gas forms sII Hydrates which is shown in Figure 2.4.3.

Structure II is made up of 16 small cages consisting of 12 pentagonal surfaces i.e. "5^{12}" and 8 larger cages of again 12 pentagonal and four hexagonal surfaces i.e. $5^{12}6^{4.}$

The unit cell consists of water molecules = ($16x5^{12}$+$8x5^{12}6^4$ = 136) [Nixdorf, 1996].

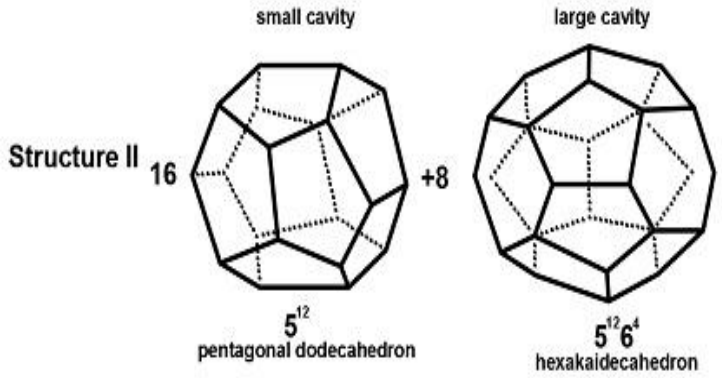

Figure 2.4.3: The Structure of Gas Hydrate sII [Nixdorf, 1996]

(c) Structure H (sH): It has hexagonal crystals having three pentagonal dodecahedron (5^{12}) cavities, two small irregular dodecahedron ($4^3 5^6 6^3$) cavities, one large icosahedron ($5^{12}6^8$) cavity, and it contains 34 water molecules in one unit cell and can accommodate larger molecules such as 2, 2-dimethylbutane in the bigger cavities only. Each icosahedrons ($5^{12}6^8$) barrel-shaped cavity is enclosed by six irregular dodecahedron ($4^3 5^6 6^3$) cavities around its central ring of six hexagons which is shown in Figure 2.4.4. The Structure H made up of 3 small cages consisting of 12 pentagonal surfaces i.e. "5^{12}", 6 larger cages of again 12 pentagonal and 1 hexagonal surfaces i.e. $5^{12}\ 6^8$ and two which is shown in Figure 2.4.4.

The unit cell consists of water molecules = ($3x5^{12} + 2x4^3 5^6 6^3 + 1x5^{12}\ 6^8 = 34$). [Sloan 1990, Moridis et al, 2003, Mazzini et al, 2004].

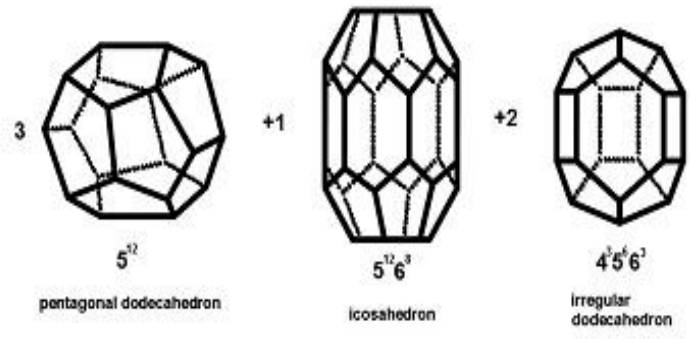

Figure 2.4.4: The Structures of Gas Hydrate sH [Sloan, 1990, Sloan, 2003].

2.5 Classification of Gas Hydrate Accumulation

Natural occurring Hydrate reservoir varies both in terms of geologic structure & thermodynamic conditions. Gas Hydrate deposits have been classified into four major classes:

Class-1: These are made up of two layers – the Hydrate layer and beneath two phase fluid zone containing free Gas and liquid water which is shown in Figure 2.5.1. Class I type of Hydrates are referred as "Hydrate capped Gas reservoirs" [Gerami et al, 2006].

Class-2: This is made up of two zones i.e. Hydrate layer overlying the zone of mobile water zone.

Class-3: Hydrate deposits comprise of a single zone of Hydrate interval and characterized by the absence of beneath zone of mobile fluids.

Class-4: Hydrate deposits are referred to oceanic accumulations and includes disperse, low saturation Hydrate deposits (< 10%) which fall short of confining geologic strata [Moridis et al, 2007].

They are classified into following categories as shown in **Figure 2.5.1** below:

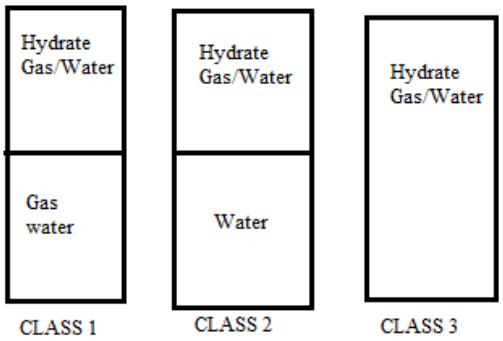

Figure 2.5.1: Representation of Class 1, Class 2 and Class 3 Gas Hydrate [Moridis et al, 2003].

2.6 Occurrence of Gas Hydrates

Natural Gas Hydrates are found at sub surface depths from one hundred thirty to eleven hundred meters in permafrost regions, also at water depths between eight hundred and four thousand meters and under the mean sea level in offshore continental margins [Vedachalam et at, 2015].

2.6.1 *Global Scenario*

The occurrence of Gas Hydrate has been known since the mid of 1960's when they were discovered in Russia. Shallow and deep coring, drilling and geophysical imaging have disclosed the Gas Hydrate occurrence along all major continental margins of Japan, Korea, India, New Zealand, Taiwan and China [Matsumoto et a, 2011]. Microbial decomposition of organic matter resulted into Methane accumulation in the coastal sediments [Gonsalves et al, 2011]. While due to the organic carbon degradation great amount of Methane are formed in situ depending on its concentration, solubility in pore water and relatively high pressure and low temperature may lead to Formation of Methane Hydrate [Sujith et al, 2014]. The bathymetry, total organic carbon content, seafloor temperature, rate of sedimentation, sediment-thickness, geothermal gradient are

good indicators that shallow sediments of Indian margins are good hosts of Gas Hydrates [Sain et al, 2014].

The existence of Gas Hydrates in oceanic sediments increase the velocity of composite medium [Chand et al, 2003]. Gas Hydrates are detected at lesser depths also. Methane-derived authigenic carbonates indicate high Methane flux region where also Gas Hydrates often occur [Kocherla et al, 2014, Kocherla et al, 2015]. The morphologies of the authigenic carbonates indicate the relative fluid flux rate [Kocherla et al, 2015]. These are present in oceanic sediments along continental margins as well as in polar continental settings [Paull et al, 2000]. Gas Hydrates are scattered from western and eastern margins of Japan, South Eastern coast of United States on the Black Ridge, in the Cascadian Basin near Oregon, Peru, the Gulf of Mexico, and the Middle America Trench.

The worldwide occurrence of Gas Hydrate is shown in Figure 2.6.1:

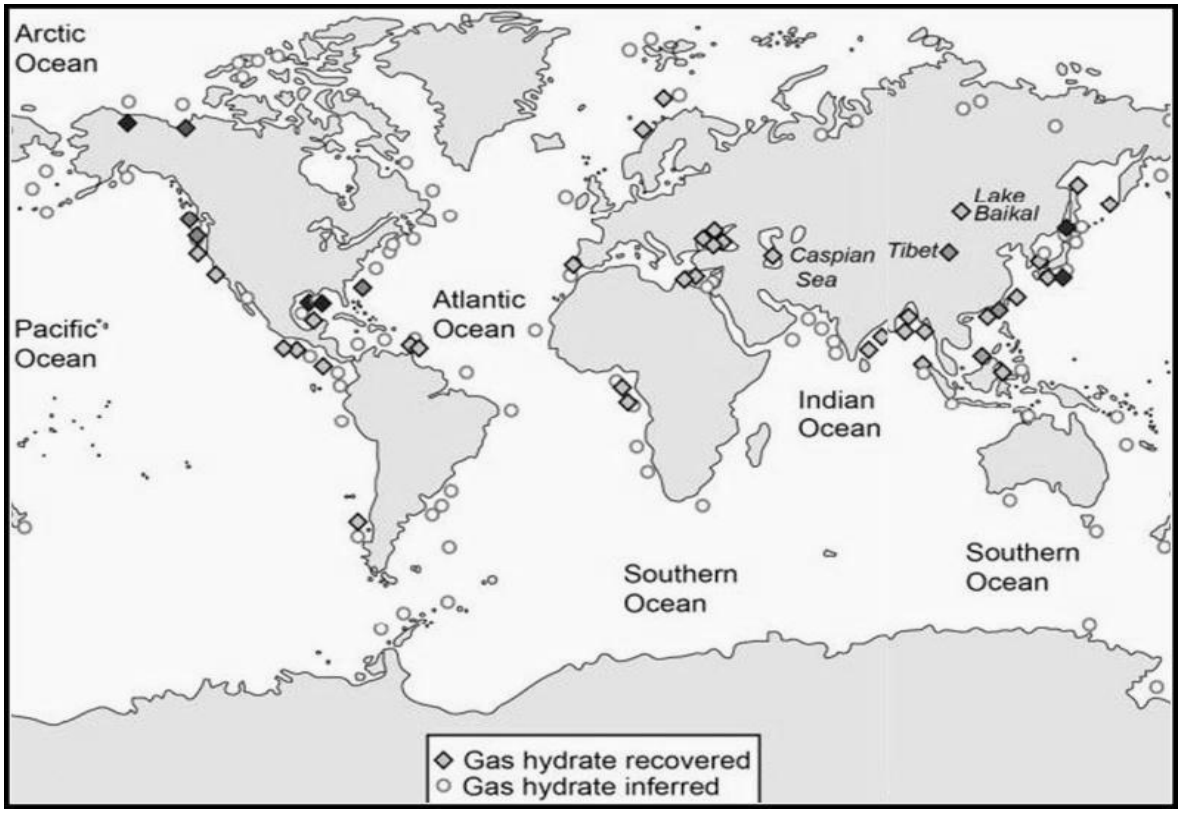

Figure 2.6.1: Distribution of Known Gas Hydrate Reserves throughout the World [Hester at al, 2009].

2.6.2 *Indian Scenario*

The Gas Hydrates are present in the Krishna - Godavri (K-G) basin, Mahanadi Offshore Basin and Andaman regions. In spite of no recovery of Gas Hydrates from the drill site in the Kerela-Konkan (K-K) basin, there has been indication of presence of Gas Hydrates in the Saurashtra and K-K basins in western India margins [Poropokari et al, 1993]. The thickness of Gas Hydrate stability zone (GHSZ) is mainly influenced by seafloor temperature, geothermal gradient, water depth, Gas composition and pore water salinity [Shankar et al, 2014].

The richest Gas Hydrate deposits (approximately 130 meter thick with approximately seventy percent saturation and sixty percent porous fractured shale) are in the Krishna-Godavari basin and the thickest (260-600 meters) in Andaman Sea as shown in Figure 2.6.2.

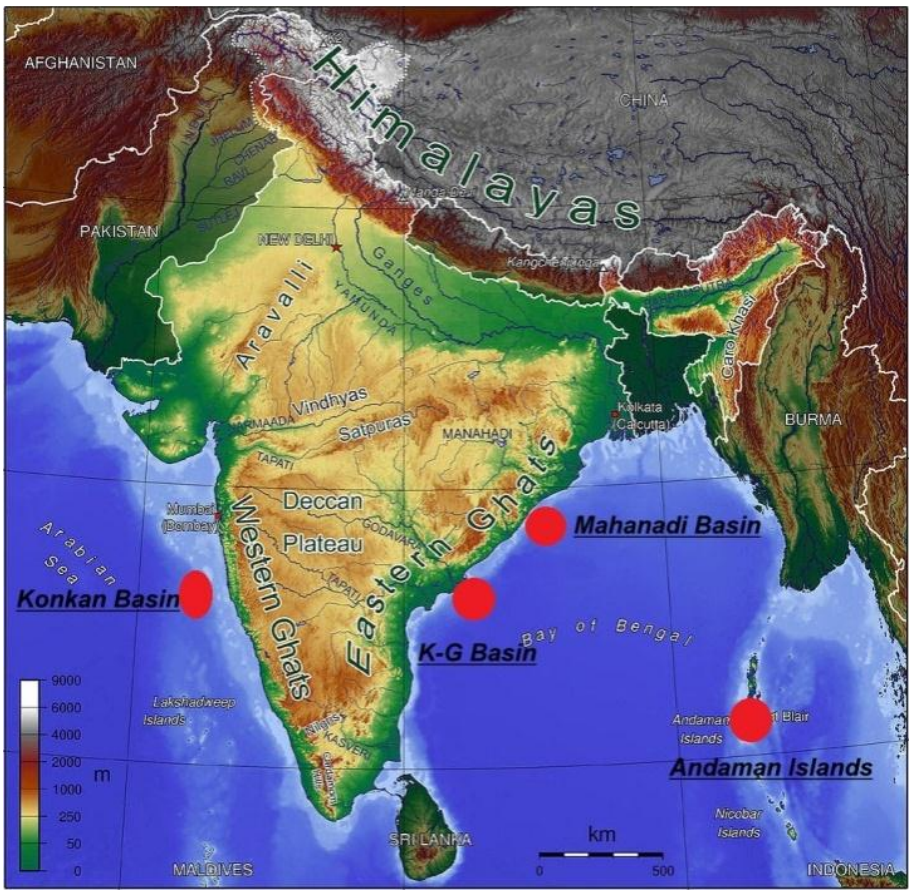

Figure 2.6.2: Overview Map Showing the Locations of Sites for Gas Hydrate Coring/Drilling in India [Kumar et al, 2014].

Figure 2.6.3 describes the global resources of Gas Hydrates as published by [Max et al, 2006, Collett et al, 2009]. Hydrate Energy International (HEI) has recently released Figure 2.6.3 as a part of global energy assessment conducted by International Institute for Applied System Analysis (IIASA).

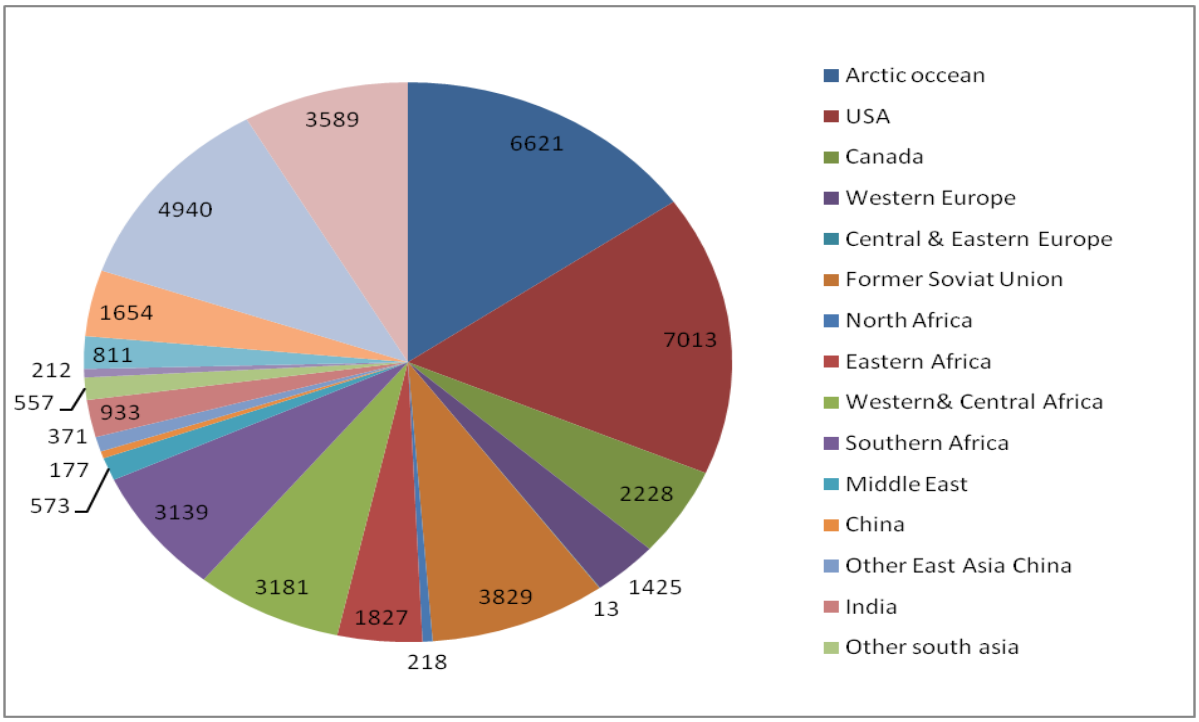

Figure 2.6.3: Calculated Gas in-Place in Hydrate Bearing Sediments, Total Median=43,311 tcf (Median, tcf (trillion cubic feet) Released by Hydrate Energy International (HEI).

There is considerable interest from large countries such as China and India which are growing at rapid pace and they are in the need of a dependable source of energy so that the growth rate can be maintained. Hence, the accessibility of such a source of energy becomes of great importance for India, if a commercially feasible recovery system can be developed. Countries like Japan, USA, and Korea also have restricted domestic reserves of conventional hydrocarbons; therefore Natural Gas Hydrates are of equal significance for them.

2.7 Current Techniques for Dissociation of Gas Hydrates

The extraction of Methane Gas from Gas Hydrates is of global interest. To understand the sediment response for production technique is very important [Pinkert et al, 2015]. Recently, the Dissociation method applicable to fine-grained clay-rich reservoir conditions in the Krishna-Godavari basin of India by introducing an electrode into a Gas Hydrate zone for Dissociation and then subsequently continuing with depressurization for production of Methane has been found effective [Ramesh et al, 2014]. The Current Techniques for Exploitation of Gas Hydrates are described as follows.

2.7.1 *Depressurization*

It is an extraction technique in which drilling of hole into the layer of Hydrate is involved which reduces the pressure beneath the Hydrate equilibrium initiating an endothermic process (i.e. absorbing heat from the surroundings) which results in to release of Methane Gas from the Hydrate flowing up the pipe [Moridis, 2002, Sung et al, 2003, Pooladi-Darvish, 2004]. The Dissociation continues until equilibrium is maintained at the lower temperature. Depressurization is advantageous because it is a most economical method and low energy consumption. Recently TOUGH + HYDRATE reservoir modelling studies have shown that Hydrate Dissociation occurs effectively in the depressurizing range between 80 and 90 bar [Vedachaalam et al, 2015]. This technique is applicable for Hydrates only in Polar Regions beneath the permafrost where the free Gas is found to be present under the Hydrate stability zone.

2.7.2 *Inhibitor Injection*

It is a technique to abolish the creation of Hydrates. In this technique, an injection of a chemical inhibitor is employed on Hydrates which disturb the Gas Hydrate equilibrium condition beyond the thermodynamic stability of the Gas Hydrate zone. Chemical inhibition injection method needs admirable porosity and moreover, the cost of various chemicals makes it an expensive technique. This method is like putting salt on icy road. This technology is used for inhibiting Gas Hydrates in pipelines.

2.7.3 *Thermal Stimulation*

It is an extraction technique which makes use of steam injection, hot brine solution, fire flooding and cyclic steam injection etc. which raises the temperature of the local reservoir outside the

Hydrate region. The rise in temperature will cause the Dissociation of the Hydrate, thus releasing free Gas which can be collected.

2.7.4 *Gas Exchange (CO_2 Sequestration)*

This technique exploits the greater solubility of CO_2 in water to displace Natural Gas and hence it achieves the two positive results in a single process i.e. extraction of Natural Gas from Gas Hydrates and removal of CO_2. The Gas exchange between CO_2 and CH_4 was first proven in lab by Ohgaki et al, 1994, Ohgaki et al, 1996. The experiment observed that there is a preference for CO_2 clathrate over CH_4 in Hydrate phase. Not only equilibrium consideration but the heat of CO_2 Hydrate Formation (-57.98 kJ/mol) is more than the heat of Dissociation of CH_4 (54.49 kJ/mol), which is favoring for the Natural exchange of CO_2 with CH_4 Hydrate, because Hydrate Formation change process is exothermic [Smith et al, 2001]. Multiphase exchange of CO_2 for CH_4 was given by Hirohama et al 1996. The author claimed much more rapid CH_4 recovery using Gaseous N_2. A mixture of CO_2 and N_2 can also be tried for exchange with CH_4 from Gas Hydrate. The enthalpy of CO_2 Hydrate Formation and enthalpy of Methane Hydrate Dissociation is shown as follow:

$$CO_2\,(g) + nH_2O \rightarrow CO_2\,(H_2O)_n \qquad \Delta H_f = -57.98 \text{ kJ /mol}$$

$$CH_4\,(H_2O)_n \rightarrow CH_4\,(g) + nH_2O \qquad \Delta H_d = 54.49 \text{ kJ /mol}$$

To make the Gas Hydrates exploitation economically viable and side by side making their exploitation environment-friendly the CO_2 Sequestration of Gas Hydrates seems an attractive and suitable option which have been studied in lab scale and as well as successfully carried out in field testing of Gas Hydrates. Actually by this technology the heat of Dissociation of Methane Hydrate is provided by heat of Formation of CO_2 Hydrates because heat of Formation of CO_2 Gas Hydrate exceeds the heat of Dissociation of Methane Hydrates. In order to make this technology economically viable intensive investigation is required which is going on. If we are able to make this technology successful then we can get tremendous amount of energy available by reducing the global warming. Global warming and Energy are the burning issues of the century. This technology can give Energy Simultaneously by reducing Global Warming.

2.8 Environmental Impact of the Use of this Energy Source and advantages and disadvantages of Hydrates

The latest research going on in the field of exploitation of this resource of energy is through CO_2 Sequestration, hence this energy source can be obtained by dumping CO_2 in sea which will help in reducing global warming. The only threat which is involved is the controlled release of Methane from the Gas Hydrates while CO_2 sequestration for which lot of research is going on. Even if it is dissociated in uncontrolled manner, there is no chance that the Methane released from the dissociated Gas Hydrate will reach the atmosphere, instead it may be transformed to CO_2 and sequestered by biosphere and hydrosphere before reaching the atmosphere. Moreover, while combustion of Methane takes place 25% lesser CO_2 is released in comparison to when the same mass of coal is combusted. Additionally Methane does not emit the nitrogen and sulphur oxides which makes it more environment friendly.

2.8.1 *The Benefits of Clathrate Hydrates*

Apart from its use as an energy source, further study in the CH_4 Hydrate system may speed up the development of other direct and indirect uses of Methane Hydrates. Hydrate is more or less seen as next generation technology for various application explained below:

(a) Marine Carbon Dioxide Sequestration

It has been observed that carbon dioxide emissions are the cause of 64% of the increased greenhouse effect [Bryant, 1997]. Out of this quantity more than 6 Gt/year are caused due to anthropogenic activities [Desideri et al, 1999]. As there is no doubt that greenhouse effect is the major culprit for global warming [Smith et al, 1993]. So it has become the chief environmental challenge to diminish the amount of carbon dioxide released into the atmosphere. Various methods have been found by which we can absorb the carbon dioxide partially. One of the way is chemical absorption in amines [Desideri et al, 1999, Chakma, 1997, Gray et al, 2004] and the other is sequestration in geological media and oceans [Hendriks et al, 1993, Brewer et al, 1999] by releasing carbon dioxide in water using the process adjusted to the injection depth [Brewer et al, 1999, Kojima et al, 2002]. This can be achieved when Gaseous carbon dioxide is injected down at 400 m depth of sea. It is then trapped by dissolution in water [Bachu et al, 2003]. At the depths of 1000 to 2000 m (deep water), carbon dioxide diffuses and dissolves in the ocean in liquid state [Liro et al, 1992]. The Hydrates of carbon dioxide can appear from 500 to 900 m in

sea water that is rich in carbon dioxide [Kojima et al, 2002] and subsequently they sink due to their high density [Holder et al, 1995] heading to the deep sea bottom where they become steady in the long term [Lee et al, 2003, Harrison et al, 1995]. Carbon dioxide sequestration in the sea water is currently at a preliminary phase, signifying additional research on CO_2 solubility [Kojima et al, 2002, Aya et al, 1997, Uchida et al, 1997, Yang et al, 2000]. CO_2-Hydrate Formation kinetics [Lee et al, 2003, Holder et al, 1995, Englezos, 1992, Circone et al, 2003] and CO_2 Hydrate stability [Harrison et al, 1995, Circone et al, 2003, Kang et al, 2000] is studied by various group.

(b) Separation Processes

Another application of Gas Hydrates is desalination and Gas-liquid fractionation. The possibility of desalination of sea water by using Hydrates revealed in the 1960's and early 1970's but the industrial development of the process didn't take place as it was not considered economically feasible [Englezos, 1993]. The procedure is based on the principal of Formation of Gas Hydrate by refrigerant injection in seawater. Pure water is retrieved after segregating the Hydrate crystals from the residual concentrated brine solution and further heating the Gas Hydrates. This breakdown of the Hydrate will give away fresh water and Hydrate former. The Hydrate Formation with the sea water can be continued if the Hydrate former is sent back to the system. It has been pointed by many authors [Mori et al, 1989] that due to the slurry texture of the Hydrates, it may be difficult to implement desalination process. The possibility of Gas Hydrates to behave as a Gas separating mechanism is being explored by the research work done by others so that carbon dioxide can be extracted from the flue Gas released by big power plants (Jean-Baptiste et al, 2003). A high pressure process for carbon dioxide separation is being developed by US department of energy. The focus of the process is on low temperature, SIMTECHE process in which pre cooled nucleated water is combined with a shifted synthesis Gas stream (carbon dioxide Hydrate slurry, hydrogen and other Gases) in a carbon dioxide Hydrate slurry reactor. The Hydrate slurry Gas separator divides the outlet mixture (carbon dioxide Hydrate slurry, hydrogen and other Gases) into two streams. One is the carbon dioxide Hydrate slurry and the other is hydrogen rich product Gas. A different process named Hydrate base Gas separation (HBGS) with Tetrahydrofuran (THF) chosen as a Hydrate promoter has been examined [Kang et al, 2000]. The purpose of THF is to lower pressure of Hydrate Formation and hence, expand the stability region of Gas Hydrate. The authors say that greater than ninety nine mol % of CO_2 from

the flue Gas can be possibly recovered by the HBGS process. The major benefits of this process are moderate operational temperatures in the range of 273–283 K and continuous operations, which makes it feasible to process a large amount of Gaseous stream.

(c). Natural Gas Storage and Transportation

The Gas Hydrates have got the ability to provide a huge concentration of Gas [Davidson et al, 1978]. As said above $1m^3$ of Gas Hydrate is capable of containing $164m^3$ of Natural Gas [Kvenvolden, 1993]. So for few years Hydrate based storage and transportation of Natural Gases seems attractive [Gudmundsson et al, 1996] and lot of research is going in this area to make this process commercial. The process involves three steps. The first step comprises of Hydrate production, the second step is transportation to the place of use and the recovery of the Gas by dissociating the Hydrate structure completes the process [Thomas et al, 2003]. The mixing of Gas and water under the conditions that favour Gas Hydrate Formation (275–283 K, 8–10 MPa) completes the first step [Thomas et al, 2003]. Surfactants can be put into the solution so that Hydrate Formation rate increases [Zhong et al, 2000, Sun et al, 2003, Sun et al, 2003]. The heating of a mixture of ice particles and Natural Gas initiates crystallization of Hydrate which is an innovative investigative production method [Stern et al, 2001]. The temperature of the Hydrates is lowered to 258 K at atmospheric pressure to make sure that they are stable while being stored in the insulated carriers during the transportation stage [Taylor et al, 2003]. The last step involves slow melting of Gas Hydrates, there by releasing the Gas from the resulting water. The reason due to which this storage and transportation process of Gas Hydrates is probable is the metastability of Methane Hydrates [Stern et al, 2001]. At atmospheric pressure and when temperature is maintained between 193 and 348 K then the Methane Hydrates do display metastable behaviour. If this process is carried out at higher temperature and lower pressure levels than those required for liquefaction and compression, respectively, then the feasibility of transportation of Gas using Hydrates is as good as these traditional processes. Additionally, in order to boost the storage capacity, the use of structure H [Aittomaki et al, 1997], or surfactant promoters is presently being considered [Sun et al, 2003, Gnanendran et al, 2003, Ganji et al, 2007].

(d) Cool Storage Application

Since the ratification of the Montreal Protocol, 1987 and the signing of the Kyoto Protocol 1997), it has become vital to develop refrigerating systems which have much lesser impact on the atmosphere. In order to face this problem, secondary refrigeration can be a potential substitute as it limits the decreased load of primary refrigerant hydroflurocarbon (HFC) in an engine room. The refrigerating capacity delivered to the secondary refrigerant is then transported towards the places of use [Inaba, 2000, Aittomäki et al, 1997, Lugo et al, 2002, Saito, 2002]. The energy of the system can be made better by applying a phase change material (PCM) in the secondary refrigerant [Tanasawa et al, 2002, Fournaison et al, 2004, Bel et al, 1999]. The PCM has got the latent heat of melting which adds to the heat transfer. The secondary refrigerants thus created may be ‘‘ice slurries’’ [Bel et al, 1999, Tanino et al, 2001, Ayel et al, 2003, Matsumoto et al, 2004] or ‘‘Hydrate slurries’’ [Tanasawa et al, 2002, Inaba, 2000, Bily et al, 2004]. The carrying fluid in the secondary refrigerant is an aqueous solution and the PCM ice or Hydrate crystals, respectively.

The first inference of clathrate Hydrates in refrigeration processes was associated with the crystallization of the refrigerant Hydrate. Unluckily, this had happened in expansion valves [Wittstruck et al, 1961]. Afterwards, the large heat of melting of clathrate Hydrates was confirmed by various authors [Tanasawa et al, 2002, Mori et al, 1989, Tanino, 2001, Tomlison, 1983, Carbajo, 1985, Akiya et al, 1987]. This led to favourable consideration of clathrate Hydrates, especially for the purpose of cold storage later. The use of Hydrate energy is significant in the domain of air conditioning as their phase change temperature is more than the freezing point of water [Tanasawa et al, 2002, Mori et al, 1989, Carbajo, 1985, Mori et al, 1989, Mori et al, 1991]. Moreover, up to the working solid concentrations, Hydrate slurries are fluid enough and hence they can flow easily through the refrigerant loop [Tanasawa et al, 2002, Mori et al, 1989, Inaba, 2000, Bily et al, 2004, Lubert-Martin et al, 2003]. Currently, advanced research is being done on Hydrate slurries. Guest molecules such as TBAB Hydrate are being used, which are more environmentally friendly than the CFC refrigerant [Tanasawa et al, 2002]. Other work is dedicated to application of the CO_2 Hydrate under medium pressure [Fournaison et al, 2004]. The heat of Dissociation could be connected to only the host structure of the Gas Hydrate, which consists of water molecules held collectively by hydrogen bonds [Sloan, 1998]. Hence, the attribute of guest molecule is not evident from the point of view of energy. If the

Hydrate heat of Dissociation is found using the Clausius–Clapeyron equation, we see that structure II is more energetic than structure I (apart from the less frequent existence of structure H) [Sloan et al, 1992]. It has been revealed by Kang and Lee [Kang et al, 2000], that transferring ($CO_2 + N_2$) Hydrate from structure I to structure II is possible by addition of THF in the aqueous solution.

2.8.2 *The disadvantage of Clathrate Hydrates i.e. Pipeline Clogging*

In 1934, Hammerschmidt pointed out that the blockages that were being caused in pipelines was due to the Formation of Gas Hydrates [Hammerschmidt, 1934]. Contemplating the considerable economic threats in oil and Gas industry, a lot of studies have been carried out by petroleum industry so that their occurrence can be prevented. The propagation of the Hydrate has an inclination to clog the pipe line, hence dividing it into two sections of different pressures i.e. the section between the well and the plug is under high pressure while the section between the plug and the recovery division is under low pressure. So there is a possibility of occurrence of blast in the upstream section which is a serious safety hazard. If there is an increase in pressure difference between the upstream and downstream sections then the plug behaves as a projectile and destroys the whole pipeline. The occurrence of both these events can be a cause of danger for the human life and the production equipment [Sloan, 2000]. The agglomeration of Hydrate takes place in very harsh environments, such as the Arctic where the temperature is extremely low and in subsea pipelines where pressure levels are too much elevated.

In order to combat the plugs that form in the pipelines and to make sure flow is maintained, four processes were explored. The first method i.e chemical method involves injection of additives in the pipe and it can help in either prevention or removal of plugs. The additives in the pipe behave differently according to the nature of the inhibitors as they are kinetic or thermodynamic. The thermodynamic inhibitors are used to alter the equilibrium temperature therefore enabling the crystallization of Gas Hydrate. The thermodynamic inhibitors generally used are methanol [Ng et al, 1985, Bishnoi et al, 1999, Jager et al, 2002] or glycols, [Elgibaly et al, 1999, Sun et al, 2001, Mahmoodaghdam et al, 2002] and/or aqueous electrolyte solutions [Jager et al, 2002, Englezos et al, 1988, Dholabhai et al, 1997]. The large quantities of additives employed (60% by weight) limits the efficiency of this process, which is, moreover, difficult to restore from H_2O, and by the corroding characteristics of salts (electrolytes) [Sloan, 1998]. The development of

new generation of additives such as dispersants like QAB (quaternary ammonium bromide) which prevents agglomeration of Hydrate [Koh et al, 2002], and kinetic inhibitors generally in the form of polymers which slow down the growth of Hydrate so that it can't disturb oil transport [Koh et al, 2002, Duncum et al, 1993, Sloan, 1995, Lederhos et al, 1996, Karaaslan et al, 2002]. They are a very economically attractive option as a small amount of dispersant and kinetic inhibitors are needed for prevention of clogging of pipeline.

The second method of removal of Hydrate is by depressurization. The permeable structure of Gas pipeline plugs makes this method a very capable option [Sloan, 2000, Kelkar et al, 1998]. However, this method is inappropriate for liquid hydrocarbons as depressurization leads to its vaporization.

The third method involves use of thermal energy. A local heat flow sent in the direction of plug through the pipe wall so that the system temperature can be increased over the point of Hydrate Formation. This procedure is not appropriate for subsea equipment however it is a good option for external pipelines [Sloan, 1998].

Fourthly a mechanical solution can be used such as pipeline pigging, which presents Hydrate plugs. The whole pipeline is placed with pipeline pigs which are driven by product flow. The obstructions or the deposits in the pipeline are then removed as they are encountered [Sloan, 2000].

2.9 Global Efforts

Global efforts have been put by various countries for exploiting this vast source of energy. India has already completed Nation Gas Hydrate Programme NGHP-01 and started NGHP-02. The field testing of Gas Hydrate is done globally as explained below:

2.9.1 *Indian scenario* (National Gas Hydrate Programme NGHP-01)

The drilling/coring operations were performed in four areas of India offshore while NGHP 01 from 28th April to 19th August 2006. Dedicated Gas Hydrate drilling/LWD (logging while drilling) / coring / MWD (Measurement while drilling) operations were implemented out while Indian Offshore during NGHP Expedition 01, 2006. The goal of this multi-disciplinary expedition was to characterize the occurrence and distribution of Gas Hydrates in the Indian continental margins [Priest et al, 2014]. NGHP-01 is explained as below:

2.9.1.1 *Sites of NGHP Expedition 01, 2006 Operational Programme*

The total of 39 holes were drilled at 21 sites in 4 areas in Indian Offshore (one site in Kerela-Konkan (K-K), fifteen sites in Krishna-Godavari (K-G), four sites in Mahanadi and one site in Andaman) [Kumar et al, 2014]. Existence of Gas Hydrates in the Krishna-Godavari (K-G) and Mahanadi offshore basins and the Andaman regions have been confirmed. During NGHP expedition 01 significant sand and Gas Hydrate were found at the site NGHP-01-15 in the KG basin, east coast off India [Riedel et al, 2011]. Thus, the KG offshore with its proven hydrocarbon potential seems to be a potential area for Gas Hydrate accumulation [Ramana et al, 2009]. Although occurrence of Gas Hydrates has not been confirmed in the Kerela--Konkan (K-K) basin, many geo-scientific studies have shown that Gas Hydrates may exist in the Saurashtra and Kerela- Konkan (KK) basins, western Indian margins [Poropkari et al, 1993, Karisiddaiah et al, 1998, Shankar et al, 2007].

The NGHP Expedition 01 has revealed the occurrence of Gas Hydrates in Mahanadi, Krishna-Godavari (K-G) and Andaman basins. NGHP-02 expedition has recently completed in 2015 by Operational experts on Gas Hydrates.

2.9.2 *Global Scenario*

Field testing for generating Natural Gas from Natural Gas Hydrates deposits of Alaska North Slope:-

2.9.2.1 *Alaska Site*

According to USGS assessment North Slope Alaska hosts about 85 tcf of unexplored exploitable Gas Hydrate resources [USGS Fact Sheet, 2008]. Mount Elbert site was selected for data acquisition and drilling operations were done in Mount Elbert site after doing a comparative study of 14 sites in Alaska. Alaska Mount Elbert Gas Hydrate test well project was carried out from February 3-19, 2007 which included the procurement of pressure transient data from four short-duration open-hole, Schlumberger's wireline Modular Dynamic Testing (MDT) was used for testing dual-packer pressure-drawdown [Hunter et al, 2011]. While this programme drilling, logging, coring, and transient pressure testing was performed at the Mount Elbert site.

Four 1 m thick zones were tested in the Mount Elbert well: two in unit D (tests D1 and D2) and two in unit C (tests C1 and C2). Each test has multiple stages of varying duration; along with that each stage has a period of fluid removal which reduced pressure enough to dissociate Gas Hydrate. Collection of water and Gas samples was done during selected periods of flow [Lorenson et al, 2011]. In the Mount Elbert unit D sand, the mobilized phase of water was calculated to be about 8 to 10 percent of total pore volume. In the unit C sand, its presence to upward range to roughly 15 percent, hence giving confirmation for application of depressurisation technique [Lee et al, 2011]. Cleaning and squeezing at the well site for Forty-six (46) samples were done to obtain pore water samples for interstitial water geochemical analyses [Bosewell et al, 2008].

For investigating the feasibility of carbon dioxide-Methane exchange in Gas Hydrate reservoirs, a first field programme was completed on 5th May, 2012 in Prudhoe Bay Unit of Alaska Methane Hydrate site by Conoco Phillips jointly with the Japan oil Gas and metal National Corporation and US department of energy. During 15 th - 28 th February 2012, 210,000 standard cubic feet (SCF) of blended mixture of carbon dioxide and nitrogen along with some volume of chemical was used to displace Methane from Hydrate sites. Mixture Gas is preferred over pure carbon dioxide because mixture Gas promotes interaction of carbon dioxide with Methane Gas Hydrate and prevents Formation of undesired Hydrates. The injected volume of 210,000 scf of mixture Gas into well, was locked in for reconfiguration of back flow. Well was shut off on 4th March 2012. Under its own energy a mixture of Gases was produced which carried on for 1.5 days before locking in. After that when well was shut off water and Methane Gas were produced at variable rates. Afterwards reinitiating of production was done on 23rd March 2012. For next nineteen days continuous flow was derived before final lock in on 11th April. Highest flow rate achieved was 175,000 scf/d but during last days of production testing, rates varied between 20,000 to 45,000 scf/d. There is environmental threat with increasing concentration of carbon dioxide and Methane in seawater which were recorded so as to maintain their optimum amount [Ignik Skumi, 2012].

CO_2-CH_4 exchange technique followed by depressurization forms the basis for the Ignik Sikumi field trials conducted on the Alaska North Slope during 2011 and 2012 [Anderson et al, 2014]. Free water was found in the reservoir in the 2011 programme. Based on this finding, a mixture was implemented as free water blocks injection of pure CO_2. Injection used mixture of CO_2

(23%), N_2 (77%) and chemical tracers. While CO_2 achieves 64% exchange efficiency mixed Gas injection improves it to 85% [Park et al, 2006].

Field testing for producing Natural Gas from Natural Gas Hydrates deposits of Mallik site:-

2.9.2.2 *Mallik Site*

Mallik site is located in Richards Island, Mackenzie Delta, North West Territories of Canada. In 1972 Hydrates were inferred while exploration drilling by Imperial oil Ltd. Mallik L-38 well was drilled during exploration [Bily et al, 1974, Wright et al, 2011]. In 1998 test were conducted under Mallik 2l-38 collectively undertaken by Japan and Canada. Gas Hydrate Research Well Program established that Mallik fields are one of the most concentrated Gas Hydrate reserves in the world. Well Mallik 2L-38 was drilled to 1150 meters [Scott et al, 2008, Dallimore et al, 1999]. Programme tests were carried out to confirm feasibility of Natural Gas production by depressurisation and by thermal stimulation techniques. New production well Mallik 5L-38 was drilled along with observation wells Mallik 3L-38 and Mallik 4L-38. It was a five day test. Mallik 3L-38 was drilled to 1188 m [Wright et al, 2011]. Results proved that Gas can be recovered. In this test 500 cubic meter of Methane Gas was produced from Gas Hydrates [Wright et al, 2011]. This test gave signature for the first time that there is a technical feasibility for the generation of Gas from Gas Hydrates.

Another test was carried out in 2007-2008. First phase was carried out in April 2007 for 12.5 hours [Birchwood et al, 2010], without sand control measures to monitor and measure direct Formation response to pressure drawdown. Well Mallik 2L-38(production well) was re occupied and hole section was further dug from 1150 to 1310 m. Production casing of 244.5 mm was installed to 1288 m. Another well Mallik 3L-38 (injection well) was dug from 1188 m to 1275 m [Dallimore et al, 2005]. In well Mallik 3L-38, 73 mm tubing casing was installed [Scott et al, 2008]. Two annulus wells were used, Gas produced was recovered up the annulus well head. Though this test produced 830 cubic meters of Gas which was more than Gas produced in tests done in 2002, it resulted in accumulation of significant amount of sand as expected [Birchwood et al, 2010]. Second phase of this test was done in winter of 2008 which consisted of field operations of six day pressure draw down, during which stable Gas flow was to be measured at the surface. Mallik 2L-38 production test well was re-entered, and a modified pumping system was used into the hole this time with sand control devices. The operation of the pump was started

in the afternoon of March 10, 2008 and extended until the 12 noon on March 16, 2008 i.e. 139 hr approximately. Successfully continuous Gas flow varied from roughly 2000 to 4000 m^3/day, was maintained and cumulative Gas production was approximately 13000 m^3 [Yamamoto et al, 2008]. Along with that water produced was less than roughly 850 barrels. This test grant liability to Gas production from Gas Hydrates by depressurization alone. Experiments were carried out on samples from Mallik 5L-38, which resulted in characterisation of effects of pore water salinity on in situ Hydrate stability. An in situ pore salinity of approximately 45 ppt was detected [Scott et al, 2008]. Sediment porosities in both wells range from 30 to 40 % [Scott et al, 2008]. This Site requires more fundamental experimental study for a kinetic Gas Hydrate model to qualify various scales which will be required for future reservoir simulations that may include investigation of larger areas.

Field testing for producing Natural Gas from Natural Gas Hydrates deposits of Nankai Trough:-

2.9.2.3 ***Nankai Trough***

Japanese government, in 1999, funded a drilling project in eastern Nankai Trough which indicated existence of bottom simulating reflectors (BSR) [Birchwood et al, 2010]. Under this project a test well 'MITI Nankai Trough' was drilled to study geological characteristics of BSRs [Ochiai et al, 2003]. In 2001, an optimal interpretation workflow to find exact location of Gas Hydrate rich zones, was developed which includes evaluation and integration of four indicators which are bottom simulating reflector (BSR), Turbidite sequence, Strong seismic reflector and relatively higher interval velocity. In this program, 2D, 3D seismic surveys were carried out and wells were drilled in water to depths of 722 to 2033 m. In this site base of Hydrate stability zone ranges from 177 to 345 m below sea floor. 12 wells were cored, 16 were logged with logging while drilling (LWD) tools, 1 was equipped with temperature sensors and in 2 wireline tools were used for logging [Takashashi et al, 2005]. After this test detailed analysis of Gas Hydrate rich sand samples and their geophysical properties was carried out for production test [Saeki et al, 2008]. Density-magnetic resonance technique used to determine Gas saturation in Gas reservoirs was used to estimate saturation from wireline logs [Birchwood et al, 2010].

In July 2012, two Controlled Source Electro Magnetic (CSEM) surveys were conducted over the West Svalbard margin on the basis of seismic data collected previously. Its aim was to check out Hydrate and free Gas saturations in submarine sediments. Offshore production test was carried

out at Daini Atsumi Knoll which is off the coasts of peninsulas, Atsumi and Shima. Test included preparatory drilling and flow tests along with well abandonment. Deep sea drilling vessel, Chikyu was used in this operation. Preparatory drilling commenced on 15th February, 2012. Vessel returned to Shimizu port on 26th March, 2012. Pressured core samples were acquired from 29th June to 7th July, 2012. In January, 2013, in Sapporo, Japan, a suite of instrumented pressure chambers, Pressure Core Characterization Tools (PCCT), developed at Georgia Tech, were deployed. These tools were used to measure electrical, biologic, hydraulic, and mechanical properties of Gas Hydrate-bearing pressure cores recovered from the Eastern Nankai Trough in 2012 [Bosewell, 2013]. An average daily Gas production of approximately 700,000 cubic feet was achieved and 4,200,000 cubic feet of cumulative volume of Gas were produced [Bosewell, 2013]. Test was conducted for six days during 12 th - 18 th March, 2013. Depressurization method for production was used [Yamamoto, 2014]. The pressure dropped to 5MPa from 13.5 MPa during the day with Gas production beginning at late morning. Six days of continuous Gas production with stability was observed. 11950 m^3 standard temperature and pressure (STP) of Gas at STP was produced in this time along with total water volume being 1162 m^3 [Yamamoto et al, 2014]. Methane was produced for first time from this site in 2013. A lot of efforts are going on to make this operation successful.

German project SUGAR tested thermal stimulation method by in situ combustion using counter current heat exchanger in the large reservoir simulator [Schicks et al, 2014]. The main advantage of this method is that there is no energy loss for transportation. The method involves catalytic combustion of CH_4 in air and transfer of heat to the reactor shell. 10wt% Pd supported on ZrO_2 was used as catalyst. In 12 hours of the test 288 litre of CH_4 was converted to CO_2 and H_2O and resulted in fluid expansion 23.5 litre at 8MPa (or 1880L at 0.1MPa). Thus, effectively 15% of produced CH_4 supplied the heat for Dissociation of the Hydrates. Later, this method was adopted as a borehole tool at site KTB in Windischeschenbach, Germany. This test proved safety of catalytic combustion of CH_4 at depth.

Several methods for Gas production were implemented in Muri Basin, Qilan Mountain Permafrost, China in 2011 [Guo et al, 2014]. These were the depressurisation method done by keeping water level below Hydrate layer in the borehole; thermal stimulation method done by injection of hot air or steam. In 84 hours, production by depressurisation yielded 81.97m^3. On the

other hand, hot air injection produced 9.73m^3 in 11 hours and steam injection produced 3.3m^3 in 42 minutes.

Tremendous amount of Methane is present in the form of the Gas Hydrates. They are present worldwide beneath the sea and in permafrost regions. They are considered as future generation fuel. From the NGHP 01 Expedition it was evident that the Gas Hydrates are distributed in the Krishna-Godavari (K-G), Mahanadi and Andaman off shores but were not observed in the Kerala Konkan(K-K) Basin. Long term production test are planned in USA and Japan to establish the viability of production technologies. Various lesson have been learnt from the field trial for Gas production from Gas Hydrate in Alaska North Slope Site, Mallik Site, Nankai Trough, if the experience gained from these trial is understood and applied properly then it can help in designing a novel technology for the exploitation of this Natural novel resource of energy which can meet the energy demand for centuries. However, there is a strong need to prepare a suitable technology for exploiting this untapped energy resource.

2.10 Future Prospectives of Gas Hydrates

As there are limited resources of Conventional fuels like Coal, Petroleum and Natural Gas, hence with the available resources the demands for the energy of world can be met for a limited time. As far as the amount of Gas Hydrates is concerned no other resource can match this upcoming resource of energy. They are seen as future generation fuels moreover they are also clean source of energy and their exploitation is possible by CO_2 sequestration as it is clear from the field testing. So, this resource of energy can be exploited by the reduction in Global Warming.

2.11 Economic Issues

The problem being faced for commercial exploitation of Methane Hydrate is that they can be exploited only when there is substantial increase in the prices of petroleum oil and conventional resources. The seeming plenitude of fossil fuels and their rather low prices are restricting research in the field of Gas Hydrates. There is a need to sustain research and development activities in this field. The key to commercialization of the Gas Hydrates is the supply and management of thermal energy and maintenance of artificial thermodynamic equilibrium so that Dissociation can be controlled and recovery of Methane is a safe process. The major obstacle in exploitation of this resource is deficiency of appropriate production technology.

Nonetheless, in the last five years there has been exciting advancements in drilling techniques for oil and Gas in deep water areas where the Hydrate sediments are found. During this time deep water development costs have also seen a decline. The above developments are progressive considering the challenges that are being faced in Hydrate research and development. The established technology that is being employed at present for the purpose of exploitation of oil and Gas reserves in deep sea water, can be duly implemented to exploit the Hydrate sediments.

Most of the locations of the Hydrate sediments were found accidently by the scientists when they were looking again at the existent seismic data. The initial efforts did not require much spending. The scientists understood the large potential of these Hydrates as fuel. Policy makers are also slowly realizing that the amount of energy that can be harnessed from Gas Hydrates is very beneficial in the long run and can really help the economies of their countries.

However, for the exploiting these Hydrates and producing Natural Gas we need to face the challenges that are being presented by the unfriendly and tricky atmosphere under the sea. For achieving this objective we need some substantial concentrated research and development endeavours in a variety of fields related to Gas Hydrates. However, monetary support for this purpose has been deficient. This is probably due to the fact that the cost of conservative hydrocarbons is low. The general perception is that this will be economically feasible only when their prices of traditional hydrocarbons and other fuels will rise significantly.

In contrast, if we analyse the locations of Hydrate sediments we can observe that these are situated in continental slopes and close to main markets of the industrialized nations. The countries that have robust economic foundation, or are showing great industrial development pace could possibly become self-sufficient in the field of energy. This event would have great influence on the international affairs and foreign policy. When Gas Hydrates are exploited the independence of the exploiting nations will have repercussions in world trade and foreign currency balance. The awareness of that such a condition can be faced has created some curiosity in the field of Natural Gas Hydrate research in a lot of nations. The possibility of energy self-sufficiency will spur on these countries to begin some initiatives for the exploitation of the Natural Gas Hydrates, the moment scientists and engineers come up with a reliable, safe and economically feasible method to exploit this vast reserve of energy.

The amount of research and development carried out in the field of Natural Gas Hydrate has been fairly small till now. These preliminary efforts did not need much spending. For the most part these efforts have been centred on the operations of Gas industry, with the purpose of finding the processes that are better and cost effective and make sure that there are no problems due to the Natural Gas Hydrates during the production, transfer and circulation of the Natural Gas that is being harnessed conventionally.

An important aspect which goes in the favour of Natural Gas Hydrates is that the conventional fossil fuels such as coal and oil are carbon intensive fuels whereas Methane is less carbon intensive as compared to them. Methane, whether it is extracted from Natural Gas Hydrates or from the conventional sources of Natural Gas generates carbon dioxide that is half in quantity as compared to coal and oil per unit of combustion products. In case of conventional fossil fuels such as coal and oil two third of the combustion product is carbon dioxide whereas if we take a look at Methane, one third of the combustion product is carbon oxide.

Hence, if we try and exploit the Methane that is entrapped in Natural Gas Hydrate, it would guarantee that we have adequate energy resources in the world for the future of the mankind. Furthermore, we would also be able to alleviate the problem of worldwide climate change that has been troubling mankind for a long time now as carbon dioxide released will be significantly reduced if we start exploiting the Methane that is captured in Natural Gas Hydrates.

2.12 Role of Microbes in Gas Hydrates

Methane Hydrates have high porosity their pore sizes vary from 100-400 nanometers and pore volumes range from twenty five to forty percent [Kuhs et al, 2000], and they permit potential substrate e.g. Sulphate to enter and products of microbial metabolism e.g. Sulphite to come out of the Gas Hydrate structure without any trouble. The microbe community are active with the Gas Hydrates. *Bacillus subtilis* and Members of *gammaproteobacteria* are identified in Gulf of Mexico Gas Hydrate mounds [Lanoil et al, 2001]. These microbes produce Surfactin and Rhamnolipids biosurfactants respectively.

Lanoil et al, 2001, reported direct physical contact between microbes and Gas Hydrate. They hypothesized that aforementioned interaction can have significant repercussion for geochemistry, composition and Gas Hydrate stability. Members of *gammaproteobacteria* have been reported in Gulf of Mexico Gas Hydrates sample [Lanoil et al, 2001]. Thus, anticipation that secondary

metabolites from *gammaproteobacteria* like *Pseudomonas aeruginosa* may have beneficial effect on Gas Hydrate Formation would not be an exaggeration. It was expected that rhamnolipids, a glycolipids type biosurfactant produced by *Pseudomonas aeruginosa* strain A11 and surfactin produced by *Bacillus Subtilis* strain A21 can execute beneficial influence on Gas Hydrate Formation by improving interfacial interaction between water and Methane.

The above generated biosurfactants i.e. Surfactin and Rhamnolipids decrease the surface tension of water and interfacial tension. They also produce carbon alkyl group chains which forms spherical micelles that dissolve hydrocarbon Gases [MacKerell, 1995]. Water partners around the circumference of the micelles in close vicinity to the solubilized Gas. This leads to micelles acting as nucleation sites for the growth of Hydrate crystals.

2.12.1 *Relationship between Gas Hydrates and Biosurfactants*

The Biosurfactants influence the induction time and rate of Formation of Gas Hydrate. The induction time is known as the time passed till the observable amount of Hydrate phase appears until the observable number of moles of the Gas forming the Hydrate is consumption and it is also known as the Hydrate nucleation time. Biosurfactants enhance the Formation rate of Gas Hydrates after their critical micelles concentration (CMC) [Zhong et al, 2000]. The surfactin is a strong biosurfactant which is capable of reducing the surface tension of water to 27 mN /m [Nakano et al, 1988]. Biosurfactants enhance the Gas Hydrate Formation in following ways: (1) They decrease the induction time of Gas Hydrate Formation (2) They enhance the Formation rate of Gas Hydrate (3) They dissolve guest Gases in micelles that pass through sands to a Hydrate zone.

2.13 Biosurfactants

Biosurfactants are amphiphilic molecules (water loving and fat loving) consisting of a hydrophilic head and a hydrophobic tail. The hydrophobic tail is a hydrocarbon whereas the hydrophilic head can be amphoteric or non-ionic positively or negatively charged [Georgiou et al, 1992, Desai et al, 1994].Which is as shown in Figure 2.13.1:

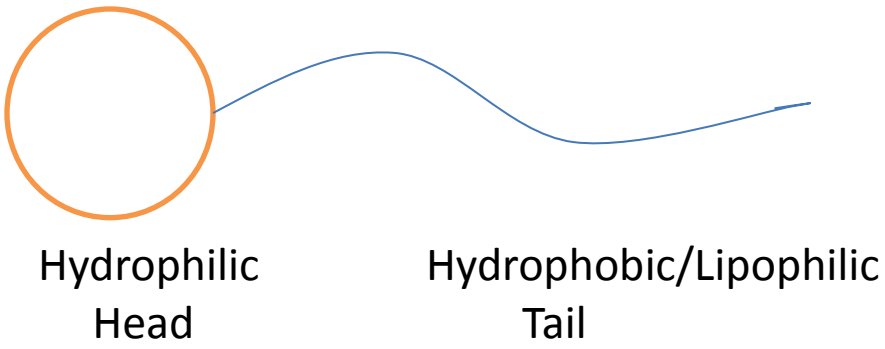

Figure 2.13.1: Structure of Biosurfactant.

Biosurfactants have a distinguish property that they can lower the surface and interfacial tension as well as (CMC) in both aqueous solution and hydrocarbon mixtures [Banat et al, 1995, Rahman et al, 2002]. CMC is the threshold concentration of a surfactant to form micelles. A good surfactant can lower the surface tension of water from 72 to 36 mN/m. Generally biosurfactants are more powerful and their CMC is almost 10-40 times belower in comparison to chemical surfactants, i.e. less amount of surfactant is necessarily required to get the greatest reduction in surface tension [Desai et al, 1997].

2.13.1 Microorganisms producing biosurfactants

Biosurfactants produced by microorganisms mainly bacteria, yeasts and fungi are diverse in chemical composition. The attributes and the quantity of biosurfactant produced depends on the category of microorganism producing it. Biosurfactants can be classified as: (1) Glycolipids (2) Phospholipid and Fatty acids (3) Lipopeptides and lipoproteins (4) Polymeric Surfactant (5) Particulate biosurfactants.

The various biosurfactants along with the micro-organisms producing them is as shown in Table 2.13.1.

Table 2.13.1: Various Types of Biosurfactants Produced by Microorganisms

S.No.	Biosurfactant Type	Biosurfactant	Microorganism	Reference
1.	Glycolipids	Rhamnolipids	*Pseudomonas aeruginosa, Pseudomonas chlororaphis*	(Jadhav et al, 2011).
		Diglycosyl Diglycerides	*Lactobacillus fermentum*	(Mulligam et al, 2001).
		Trehalose mycolates	*Rhodococcus erythropolis, Arthrobacter paraffineu, Mycobacterium phlei, Nocardia erythropolis*	(Muthusamy et al, 2008).
		Sophorolipids	*Candida bombicola, C. antartica, Torulopsis petrophilum C. botistae, C. apicola, C. riodocensis, C. stellata, C. Bogoriensis*	(Felse et al, 2007).
		Amino acids lipids	*Bacillus sp.*	(Cotter et al, 2005).
2.	Phospholipid and Fatty acids	Fatty acids/neutral lipids	*Clavibacter michiganensis subsp. Insidiosus*	(Herman et al, 2002).
		Phospholipids	*Acinetobacter sp.*	(Kosaric, 2001).
3.	Lipopeptides and lipoproteins	Peptide lipids	*Bacillus licheniformis*	(Begley et al, 2009).
		Serrawettin	*Serratia marcescens*	(Lai et al, 2009).
		Ornithine lipid	*Pseudomonas sp, Thiobacillust hiooxidans*	(Desai et al, 1997).
		Viscosin	*Pseudomonas fluorescens, Leuconostoc mesenteriods*	(Banat et al, 2010).
		Surfactin	*Bacillus subtilis*	(Arguelles et al, 2009).
		Subtilisin	*Bacillus subtilis*	(Sutyak et al, 2008).
		Lichenysin	*Bacillus licheniformis, Bacillus subtilis*	(Yakimov et al, 1997).
4.	Polymeric Surfactant	Protein PA	*Pseudomonas aeruginosa*	(Hisatsuka et al, 1971).
		Liposan	*Candida lipolytica*	(Cirigliano et al, 1984).
		Lipoheteropolysaccharide (Emulsan)	*Acinetobacter calcoaceticus RAG-1, Arethrobacter calcoaceticus*	(Choi et al, 1996).
		Polysaccharide-lipid complex (Snomax)	*Pseudomonas syringae*	(Skirvina et al, 2000).
		Alasan	*A. radio resistens*	(Barkay et al, 1999).
5.	Particulate biosurfactants	Whole cells	*Cyanobacteria*	(Levy et al, 1990).
		Vesicles	*Acinetobacter sp.*	(Desai et al, 1997).

2.13.2 *Rhamnolipids*

Rhamnolipids are produced by *Pseudomonas aeruginosa*. They have a glycosyl head group, a Rhamnose moiety, and a 3-(hydroxyalkanoyloxy) alkanoic acid (HAA) fatty acid tail. Mono-rhamnolipids and di-rhamnolipids are two main classes of rhamnolipids; containing one and two Rhamnose groups respectively. The length and the degree of branching of the HAA moiety is heterogeneous in rhamnolipids and it is also dependent on the growth media used and the environmental conditions. The CMC of rhamnolipids is much lower than the CMC of Sodium dodecyl Sulphate (SDS) [Herman et al, 2002, Thangamani et al, 1994, Churchill et al, 1995], and they can be adsorbed on sediment particle surfaces [Banat, 1995, Herman et al, 2002]. The size of the Micelles of rhamnolipids is much lower than the size of the micelles of SDS and it can easily pass through porous media [Herman et al, 2002, Bai et al, 1997]. In the analysis of sand related to the Gas Hydrates from Gulf of Mexico [Lanoil et al, 2001], the *Pseudomonas aeruginosa* bacterium was identified which must have generated rhamnolipids, The structure of rhamnolipids is shown in Figure 2.13.2(a) and 2.13.2(b).

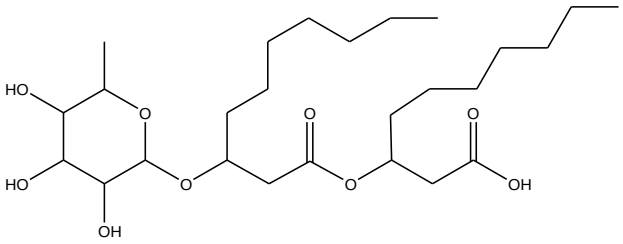

Figure 2.13.2(a): Structure of Monorhamnolipids: $RhaC_{10}C_{10}$

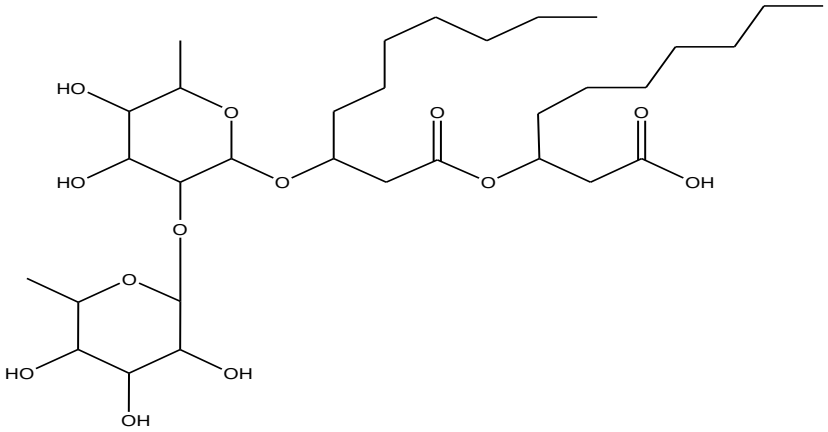

Figure 2.13.2(b): Structure of Dirhamnolipids: $RhaRhaC_{10}C_{10}$

2.13.3 *Lipopeptides and Lipoproteins Surfactin*

Surfactin is a lipopeptide formed from *Bacillus subtilis* bacterium. It is a lipopeptide that is composed of one β-hydroxy fatty acid, which has a long fatty acid moiety, and seven amino acids. Surface tension of water can be decreased from 72 to 27 mN/m by this lipopeptide [Nakano et al, 1988]. It is named surfactin due to its exceptional surfactant activity [Peypoux et al, 1999]. *Bacillus subtilis* bacterium was identified in the analysis of sand related to the Gas Hydrates in the Gulf of Mexico [Lanoil et al, 2001], which generated surfactin.

The Structure of Surfactin is shown in Figure 2.13.3 (a & b).

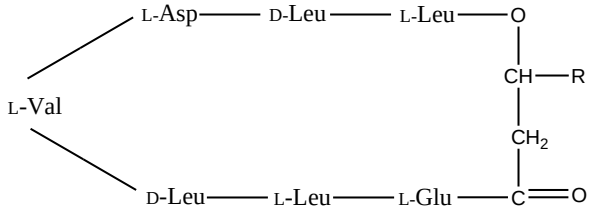

Figure 2.13.3 (a): Structure of Surfactin

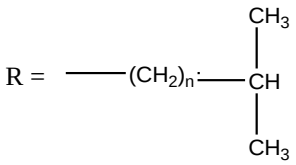

Figure 2.13.3 (b): Lipid Chains of Surfactin Molecule.

(Where 'n' can vary for various Surfactin Molecules as 7, 8, 9, and 10)

Various types of amino acids present in a Surfactin is as given in table 2.13.2.

Table 2.13.2: Amino Acids Present in Surfactin.

S.No	Letter	Name of Amino Acid	Molecular Formula	Mass (g/mol)
1.	Val	Valine	$C_5H_{11}NO_2$	117.151
2.	Asp	Aspartic acid	$C_4H_7NO_4$	133.11
3.	Leu	Leucine	$C_6H_{13}NO_2$	131.17
4.	Glu	Glutamic acid	$C_5H_9NO_4$	147.13

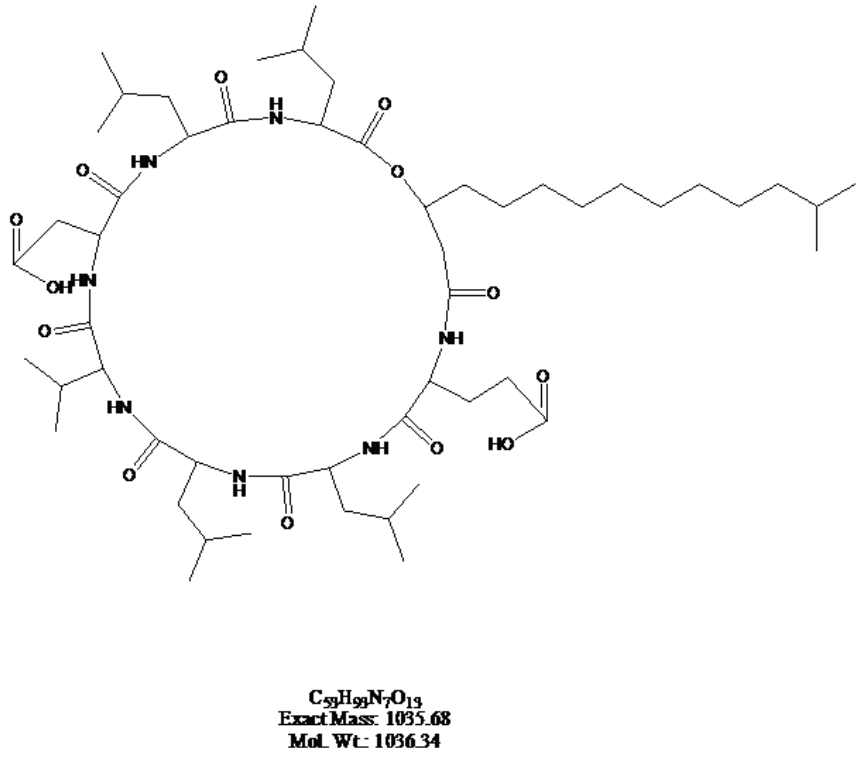

Figure 2.13.4: Structure of Surfactin.

2.13.4 *Phospholipids and Fatty Acids*

Phospholipids

Phospholipids are a class of lipids capable of forming lipid bi-layers and all cell membranes are majorly composed of them. Phospholipids generally contain a phosphate group, diglyceride and a simple organic molecule such as choline. The structure of the phospholipid molecule consists of a hydrophilic head and a hydrophobic tails. Phospholipids provide membrane fluidity and mechanical strength in eukaryotic cells. There are three types of phospholipids that are synthetically derived as described below.

(a) Phosphocholines (DMPC)

DMPC has a chemical name as 1, 2-Dimyristoyl-sn-glycero-3-phosphocholine. Its empirical formula is $C_{36}H_{72}NO_8P$ and has a molecular weight 677.93. The structure of DMPC is as shown in Figure 2.13.5.

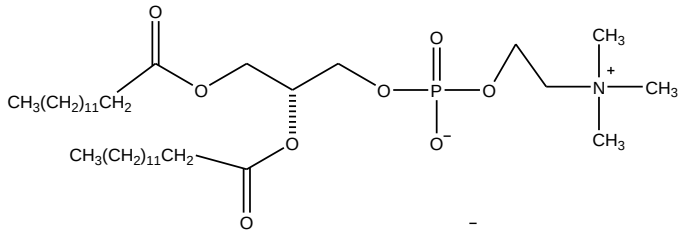

Figure 2.13.5: Structure of DMPC

(b) Phosphoserines (DPPS)

DPPS has a chemical name as 1, 2 Dipalmitoyl-sn-glycero-3-phospho-L-serine sodium salt. Its empirical formula is $C_{38}H_{73}NO_{10}PNa$ and has a molecular weight 757.95. The structure of DPPS is as shown in Figure 2.13.6.

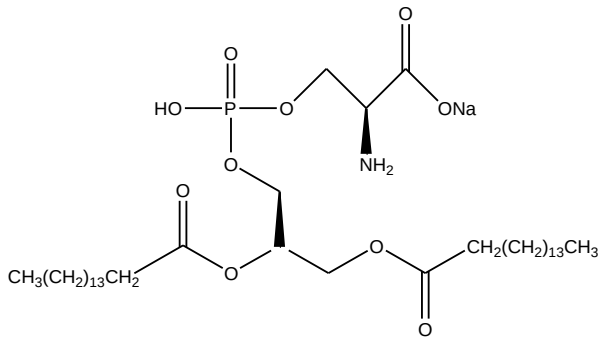

Figure 2.13.6: Structure of DPPS.

(c). Mixed Chain Phospholipids (POPC)

POPC has a chemical name as 1-palmitoyl-2-oleoyl-sn-glycero-3-phosphocholine. It is available commercially and synthetically. It is also Naturally present in eukaryotic cell. Its empirical formula is $C_{42}H_{82}NO_8P$ and has a molecular weight 760.08. The structure of POPC is as shown in Figure 2.13.7.

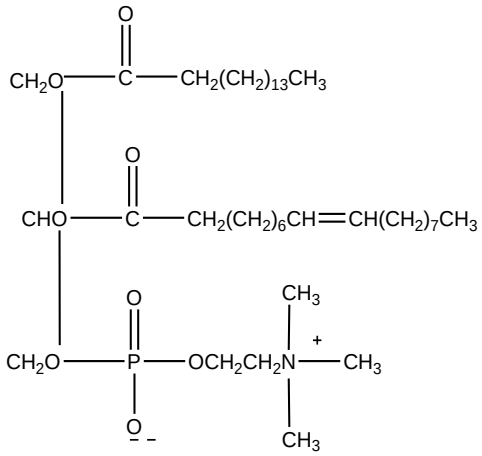

Figure 2.13.7: Structure of POPC.

2.13.5 *Polysaccharide-Lipid Complex Snomax*

Snomax is produced by *Pseudomonas syringae* bacterium. It has ice nucleation protein. It is a type of polysaccharide-lipid complex [Goodnow et al, 1990]. It contains 34% protein, fifteen percent mono and disaccharides, and eleven percent nucleic acids [Amende et al, 1999].

Emulsan is a type of polysaccharide-lipid complex produced by *Acinetobacter calcoaceticus* bacterium. The molecular weight of Emulsan is 89,000 [Shoham et al, 1983]. Emulsan can boost the Hydrate Formation by using its hydrophobic-hydrophilic moieties to unite the water and the host hydrocarbon. However micelles are not formed by Emulsan.

2.13.6 *Hydroxylated Fatty Acid*

DL-α-Hydroxystearic Acid

It is a synthetic fatty acid and has chemical name as DL-α-Hydroxystearic acid (2-Hydroxyoctadecanoic Acid) $C_{18}H_{36}O_3$, has a molecular weight 300.48. DL-α-Hydroxystearic Acid is a mixture of D and L-α-hydroxystearic Acid (2-Hydroxyoctadecanoic Acid)

enantiomers. It has surface properties similar to corynocycolic fatty acids [Rosenberg, 1986]. The structure of Hydroxystearic acid is as shown in Figure 2.13.8.

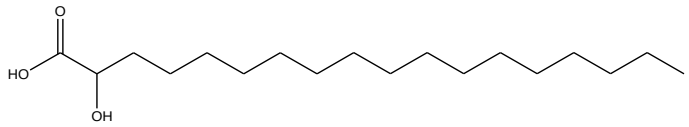

Figure 2.13.8: Structure of Hydroxystearic Acid.

2.14 Influence of Surfactants on Formation of Gas Hydrate

During the last two decades, many investigations have been carried out displaying a marked increase in Hydrate Formation rate when surfactants were added [Karaaslan et al, 2000, Sun et al, 2004, Mandal et al, 2008, Moraveji et al, 2010, Verret et al , 2012]. Surfactant molecules gets adsorbed at the water-Gas or the water-liquid interface with hydrophilic head groups aligning toward the aqueous phase and hydrophobic tails aligning toward the Gas or liquid phase. The head groups connect with water molecules while the tails connect with hydrocarbon molecules.

Surfactants tend to boost the Formation rate of Hydrates at the interface by decreasing the interfacial tension at the Gas or water interface, therefore promoting the transit of Gas associated with water. The finding of various research groups on the influence of surfactants on the Formation of Gas Hydrates is explained as below:

Zhong et al, 2000 studied the influence of SDS on the Formation of Hydrate mechanism using ethane and Natural Gas. In their studies they also observed that micelles behave by accelerating the solubility of hydrocarbon Gas in the aqueous phase and by generating the Formation of Hydrate crystals around the micelle in the bulk water phase under the Gas or water interface. Subsequently, there was an increment in the rate of Hydrate Formation by more than seven hundred times and the induction time for nucleation is reduced as compared to systems in which surfactants were not used. Equivalent results were noticed in other studies when different surfactant were used. However they required different mechanistic explanations, thereby questioning the CMC requirement (Zhang et al, 2004; Lee et al, 2010).

Karaaslan et al. (2000) in their study produced Natural Gas Hydrates from different types and concentrations of surfactants in a high pressure vessel. They used a non-ionic, a cationic and an

anionic surfactant to make solutions from deionized water. In order to create Gas Hydrate, a high pressure reactor was used which comprised of high pressure cylinder kept at a pressure of 576 psig and a magnetic stirrer which is kept at a constant speed of 500 rpm over the period of the study. The surfactants that were used in the study are linear alkyl benzene sulfonic acid (LABSA), quaternary ammonium salt (DAM), nonylphenol ethoxalate (ETHOXALATE). For each surfactant four experiments were done for different concentrations and one experiment was done without any surfactant for the purpose of comparison. While studying Hydrate Formation kinetics, the approximated initial Gas uptake rates for all the tests were compared. It showed that LABSA has prominent effect on the Hydrate Formation rate. The Gas uptake rates are always superior when LABSA is used as compared to the case where no surfactant is used. The promotional effect of DAM was similar to LABSA at lower concentrations of 0.005 wt% and 0.01 wt% but at higher concentrations the effect was reversed. However, in case of ETHOXYLATE the Gas consumption rates were constantly lower.

So, in this study it was revealed that in general the Hydrate Formation rate is enhanced by anionic surfactant for all the concentrations that were examined. The cationic surfactant showed conflicting behaviour at low and high concentrations. The non-ionic surfactant had less prominent effect on the Hydrate Formation rate as compared to the anionic surfactant. So they recommend the use of anionic surfactant as a Gas Hydrate promoter

Karaaslan et al, 2002 in their article studied the promotional effect of two polymers and three surfactants on the Formation rate of Methane Hydrates in a high pressure system. The chemicals they used in the study are Polyoxyethylene (20) cetyl ether (Brij-58), Poly-(acrylamide-co-acrylic acid) (PAAA), poly (vinyl alcohol) (PVA), Polyoxyethylene (5) nonylphenyl ether (Igepal-520) and Polyoxyethylene (20) sorbitan monopalmitate (Tween-40). The Formation rate of Hydrate was studied by preparing 1 wt% solutions for all the chemicals and then Methane Hydrate was produced in the solution. The system was kept at a constant pressure of 700 psig for all the experiments. A rocking system was also provided for the purpose of agitation and its speed was kept at 30 rpm. The results of all the chemicals were matched with CH_4 Hydrate Formation rate in pure H_2O. To ensure the reproducibility of the data two tests were done with pure water and fresh sample of water was taken to avoid the memory effect. Then the curves were plotted for free Gas mole vs time. The exponential nature of the curve implied that it was a first order reaction. By differentiating the first order equation, the Formation rate was found out.

These were then compared with the Formation rate for pure water. It was observed that for the PAAA Formation rate was very close to water. The rest of the chemicals had positive effect on the Formation rate. Igepal-520 gave the best performance among all of them as it increased the Formation rate by a factor of 2.4 as compared to the Formation rate of H_2O. They made an interesting observation that the more effective promoters PVA and Igepal have small molecular size as compared to other chemicals.

Lin et al, 2004 in their study have investigated the consequences of using sodium dodecyl sulphate (SDS) anionic surfactant on the Formation and Dissociation rate of CH_4 Hydrates. The experimental equipment used by them comprised of a cylindrical transparent sapphire cell that is set up in an air bath that enabled them to observe Gas Hydrate Formation visually. They didn't use any equipment to provide agitation to the Formation process. After that they experimented with different concentrations of SDS to study its promotional effect on the Gas Hydrate Formation. The pressure of the cell was fixed at 6.6 MPa and the concentration of SDS was varied from 0 to 2000 ppm. They plotted a curve of moles of Gas consumed per gram of H_2O as a function of time for different concentrations of SDS. The results depicts that presence of SDS enhances the Formation rate of CH_4 Hydrates.

Ganji et al, 2006 in their investigation, studied the effects of surfactants on the Formation, Dissociation and the storage capacity of Methane Hydrate. They used anionic surfactants linear alkyl benzene sulfonate (LABS) and sodium dodecyl sulphate (SDS), non-ionic surfactant Ethoxylated nonylphenol (ENP) and cationic surfactant Cetyl trimethyl ammonium bromide (CTAB). For each surfactant three concentrations were used 300 parts per million (ppm), 500 ppm and 1000 ppm. It was observed that among all the surfactants that were tested, SDS is the one that is more effective for speeding up the rate of Hydrate Formation. The experiment was done in a high pressure reactor in which pressure was fixed at 8.3 MPa and the stirrer speed was fixed at 200 rpm. The Formation of Methane Hydrate in pure water was examined for matching. During the study, SDS acted as a promoter for all the three concentrations as compared to other surfactants. The promotion effect was maximum at the concentration of 500 ppm and the steady state is achieved in approximately one hour. The induction time is also very less. When concentration is 300 ppm, the induction time is small just like 500 ppm case but the rate of Formation is reduced. For 1000 ppm, induction time is nearly 1 hour and the Formation ceases in approximately three hours. When LABS was used the Formation rate is enhanced for the

concentrations of 500 ppm and 1000 ppm as compared to the Formation rate in pure water. At 500 ppm, the induction time for Hydrate Formation was roughly equal to eight hours and the maximum conversion is achieved after 24 hours. This is much less as compared to the promotion effect of SDS. However, at 1000 ppm the promotion effect of LABS is equivalent to SDS. The induction time in this case is very short and the steady state of the Hydrate is achieved in around two hours. CTAB and ENP also improve the Hydrate Formation rate at 1000 ppm but the increase is slight as compared to SDS. The induction time is 18 hours and the time required for the completion of Hydrate Formation is 40 hours for 1000 ppm solution of CTAB. The induction time for the ENP solution at 1000 ppm is around 14 hours and steady state is achieved in 40 hours.

Hence, it can be said that among all the surfactants studied in present study. SDS is the best option for promoting the Hydrate Formation rate so that they can be used for storage and shipping purposes.

Lee et al, 2007 in their article have predicted Gas Hydrate phase equilibria when SDS is used. They have used a high pressure reactor of volume 450 ml and the mixture was not agitated. The quantity of SDS solution used for the tests was 150 ml and the initial pressure was 75 bar. The tests were conducted at two different temperatures of 271 and 274 K. The concentration of SDS was varied between 250 ppm to 10,000 ppm. The tests were done twice for any concentration and then the average induction time was calculated. From the observations it was found that the induction time is reduced when there is an increase in SDS concentration. However, this pattern is not observed at 70 bar and 274 K. At concentration of 10000 ppm there is a vast difference between the values of induction time for Hydrate Formation. For the first test its 0.4 hour and for the next run is 13 hours.

Zhang et al, 2008 looked into the effects of surfactants when they acted as promoters for the Formation of Gas Hydrate on induction time. They tried out three different three different types of tween solutions which had concentration of 0.001 mol/L. The three solutions consisted of T40, T40 and T80 in a ratio of 1:1 and T40 and T80 in a ratio of 4:1. The visual experimental equipment they had used was developed by them. They measured the induction time by direct observation method. The system comprises of a high pressure cell, an air bath of invariable a pressurizer, temperature, a system for measurement of pressure and temperature and a data

acquisition system. The experimental data and any alteration in the growth conditions are found through the visual window by using images and data logger system. The driving force for the Formation of Gas Hydrate is the super saturation of the Gas in the solution. So, in order to hasten the Formation of Gas Hydrate surfactants are added to enhance the solubility of Gas.

Christiansen and Sloan pointed out that in Methane and pure water system at 4.54 MPa and 275.15 K the Formation of Gas Hydrate had not finished even after twenty hours. In their study, the induction time for T40, T40 and T80 (1:1) and T40 and T80 (4:1) systems is 475 min, 584 min and 749 min respectively.

Mandal et al, 2008 in their article have formed ethane Hydrates in presence of SDS and studied how it changes their rate of Formation and Gas consumption. The equipment used for the study is composed of stainless steel having a volume of 500 cm^3. The study was conducted at different pressures and temperatures. The concentrations of SDS used were 300 ppm and 500 ppm and the results were compared with pure water and ethane mixture. The Formation rate of Gas Hydrate was enhanced as shown by the increase of Hydrate Formation temperature from 265K to 272 K as the concentration of SDS is increased from 0 to 500 ppm. Curves for Gas consumption were also plotted. It was observed that as the surfactant concentration increased the Gas consumption rate also increased. This can be attributed to the change in the energy of the intermolecular interaction and the change in equilibrium between water and Gas molecules.

Qiang et al, 2009 in their study studied the elevation in the Formation rate of Gas Hydrates by using surfactants in the solution. The surfactant used was sodium dodecyl sulphate (SDS) and its concentration fluctuated from 0.4 mol/L to 0.7 mol/L. The experimental equipment used for this study comprised of a visual cylindrical high pressure cell, a Gas pressing system, a thermo tank, a charge coupled device (CCD) image system and a data logging system. During the Formation of the Gas Hydrates the pressure was varied from 7 MPa to 9 MPa. The Gas consumption rate of the experiment can be found out by finding rate of change of pressure. Pressure and time curves were plotted for all the different concentrations of SDS solutions and for all the changes in pressure. It was found that when the steady state is achieved the rate of Gas consumption is approximately the same for different solutions of SDS. They classified the Formation of Gas Hydrate on the basis of Gas consumption rate into three periods. They are initial growth period, rapid growth period and stable period. The important point is that during the Formation of Gas

Hydrate, the phase of initial growth is the longest at 7 MPa. However, in the case of Formation process at 8 MPa and 9 MPa, the Gas Hydrates instantaneously proceeded into the growth period and subsequently become stable. This implies that the Gas Hydrate Formation can be permitted at higher pressures.

Linga et al, 2010 have used a new apparatus to capture carbon dioxide by using Hydrate crystallization which employs modular, mechanically stirred Gas inducing crystallizer. The crystallizer improves the contact of Gases which form Hydrate and thereby increases the Hydrate crystallization rate. They have used flue Gas (CO_2/N_2) and fuel Gas (CO_2/H_2) mixtures to denote the post combustion and pre combustion capture. In their study they have found that Hydrate crystallization is a proficient method to capture CO_2. But the downside of this process is that it necessitates the need for considerable amount of power. So they have finished off their study by pointing out the fact that in order to be used in industry Hydrate crystallization should be done without the mechanical agitation.

Moraveji et al, 2010 in their article have examined the kinetics of Formation of CH_4 Gas Hydrates. They have used sodium dodecyl sulphate (SDS) as an anionic surfactant to study its promotion effect. They have used equipment consisting of cylindrical high pressure cell equipped with magnetically coupled rotary impeller system. The speed of the impeller is maintained at 400 rpm and the pressure of the cell is fixed at 60 bar. The study was conducted for different concentrations of SDS and the results were compared with the experiment where no surfactant was used. The induction time for the Formation of Gas Hydrate in pure water was close to 320 minutes but when SDS was added in the solution the induction time was reduced by a big factor. The induction time was found out for concentrations of 500 ppm, 700 ppm, 900 ppm and 1100 ppm. Among all the concentrations of SDS, the highest promotional effect during the initial phase of Hydrate Formation was for 500 ppm. While for the concentrations of 900 ppm and 1100 ppm, the promotional effect was more prominent at the end of Hydrate Formation.

Torre et al, 2011 perfomed their study in a high pressure batch reactor in which a mixture of Tetrahydrofuran (THF) and sodium dodecyl sulphate (SDS) was used as a supplement. When THF and SDS are used collectively in appropriate concentration, they were able to achieve high efficiency for promoting the capture of CO_2.

Kwon et al, 2011 in their study studied surfactants with sodium sulfonic acid groups with different carbon chain lengths, how they impact the kinetics of Gas Hydrate Formation. They have used a high pressure vessel having a volume of 350 cc provided with a digital magnetic stirrer which is rotated at a constant speed of 500 rpm in this experiment. The temperature maintained during the experiment is 274.15 K and the pressure is varied between 3.5 - 4 MPa. The surfactants used in the study are SDS, C8DS, C10DS and C12DS. In one of the studies Hydrate Formation rate was examined at different concentrations of C8DS and at temperature and pressure of 274.15 K and 4 MPa and results were matched with pure water. The concentration was varied from 10 to 150 ppmw. The promotional effect increases with increase in concentration and is maximum at 50 ppmw, but starts decreasing if it is increased any further. However, it still remains more than pure water. In another study, the influence of carbon chain length on Hydrate Formation was observed by testing 50 ppmw of C8DS, C10DS and C12DS at 274.15 K and 3.5 MPa. The results were compared with SDS. It was observed that C8DS and C12DS showed the minimum. For C10DS Formation rate was comparable to C8DS. This showed that the promotional effect is more if the alkyl chain is shorter.

Fazlali et al, 2013 in their study studied have investigated the influence of Hexa decyl trimethyl ammonium bromide (HTABr), sodium dodecyl sulphate (SDS), mixtures of SDS with HTABr, Polyoxy ethylene(20) cetyl ether (Brij-58) on Methane Hydrate Formation kinetics. A high pressure cylindrical reactor made of stainless steel was used and the pressure was fixed up to 6 MPa. The speed of the magnetic stirrer was maintained at 400 rpm. 21 experiments were done with different combinations of all the surfactants to monitor induction time. In one of the tests no surfactant we used do that it can be used a reference study. The study revealed that in each test induction time was less as compared to the pure water test. This showed that all of the surfactants act as promoters for the Formation of Gas Hydrate. The induction time of 17 minutes was minimum for the mixture of HTABr (700 ppm) and SDS (500 ppm). However, there was no prediCTABle pattern between the induction time and the concentration and type of surfactant. Among all the surfactants, SDS at concentration of 500 ppm observed to be the best promotional effect. The mixtures of SDS with Brij-58 and HTABr had lesser promotional effect than SDS. The least amount of influence in the Hydrate Formation rate was shown by HTABr and Brij-58.

Zhou et al, 2013 in their study studied effects of sodium dodecyl benzene sulfonate (SDBS), polyethylene oxide - polypropylene oxide - polyethylene oxide tri-block copolymer (P123) and

hexadecyl tri-methyl ammonium bromide (CTAB) on the CO_2 Hydrate Formation. Maximum promotion effect of SDBS was found at 700 mg / kg which was comparable with that of CTAB at 300 mg / kg and P123 at 500 mg / kg. This investigation has a certain significance to improve the rate of Hydrate Formation.

Liu et al, 2014 in their study the effect of the addition of a surfactant on CH_4 Hydrate Formation. The ice powders, with different concentration of sodium dodecyl sulphate (SDS), was used to generate Methane Hydrates. The tests were carried out under the conditions of different pressure and temperature. The ice powders with 300ppm of SDS would make the Formation of the CH_4 Hydrates faster than others. The joint action of the high initial pressure and SDS addition significantly increases the degree of conversion of ice into hydrae.

Saw et al, 2014 in their article have used different concentrations of tergitol to study the Formation rate of Gas Hydrate. They have used a Gas Hydrate autoclave for this study in which the pressure was maintained at 11.6 MPa. The system also had a magnetic stirrer which had a fixed speed of 1000 rpm. The different concentrations of tergitol used were 1 parts per trillion (ppt), 5 ppt and 10 ppt. Kinetics study was also done on a sample containing no tergitol for the purpose of comparison. During the study of induction time, it was observed that it decreases when tergitol is added to the solution. The lowest induction time is observed when concentration if tergitol is 1 ppt. However, when concentration is increased further induction time also increases but it is still less than that in water. The Hydrate Formation rate is enhanced as the quantity of tergitol increases in the water. The increase in concentration of tergitol also increases the Gas uptake rate.

Najibi et al. (2015) in their article have observed the rate of Gas consumption and the induction time at different temperatures and pressures. The copper oxide nanoparticles used in the study have nominal diameter of 40 nm. The experiments are conducted in a stainless steel 316 vessel and it has also got a magnetic bar that stirs the contents of the cell up to the speed of 500 rpm. The tests are performed at the temperatures of 274.65 K and 276.65 K with the initial pressure being 5 and 6 MPa. During the experiments, the concentration of SDS is kept at 0.035% by weight and the concentration of copper oxide (CuO) nanoparticles is varied between 0.01 to 1 % by weight. At 5 MPa pressure and 274.65 K temperature, the induction time for the mixture of 0.035% SDS and 1% CuO is 4 minutes as compared to the induction time of 25 minutes when

pure water is used. When the temperature is kept constant and pressure is increased to 6 MPa, it was observed that the induction time for the mixture of 0.035% SDS and 1% CuO is 2.1 minutes as compared to the induction time of 17.5 minutes when pure water is used. In all the tests it was found out that induction time was increased on addition of SDS and CuO nanoparticles. The decrease was also proportional to the concentration of promoters on the mixtures. This can be attributed to the decrease in surface tension of water by SDS and improvement of heat and mass transfer characteristics of the solution due to CuO nanoparticles. Similar results were obtained when the mixtures were tested at 276.65 K

The work done by various research groups is compared in Table 2.14.1

Table 2.14.1 Influence of Surfactants on Formation Gas Hydrate

S. No.	Group	Title	Gas	Composition	Surfactant	Pexp	Dose	Induction time /consumption of Gas/ Moles of Gas/ moles of water consumed /rate of Hydrate Formation/conversion/storage capacity
1	Karaaslan et al, (2000)	Surfactants as Hydrate promoters	CH_4+C_2H_6+C_3H_8+I-C_4H_{10}+N-C_4H_{10}+I-C_5H_{12}+N-C_5H_{12}+N_2+CO	89.47%+5.39%+1.89%+0.40%+0.62%+0.28%+0.19%+1.58%+0.18 %	nonylphenol ethoxalate (ethoxalate) (nonionic)	3.97MPa (576 psig)	0 wt. %	7.143×10^{-9} mol/s
					ethoxalate (non-ionic)	3.97MPa (576 psig)	0.005 wt. %	3.799×10^{-9} mol/s
					ethoxalate (non-ionic)	3.97MPa (576 psig)	0.01 wt. %	4.393×10^{-9} mol/s
					ethoxalate (non-ionic)	3.95MPa (574 psig)	0.1 wt. %	5.197×10^{-9} mol/s
					ethoxalate (non-ionic)	3.97MPa (576 psig)	1 wt. %	8.832×10^{-9} mol/s

					linear alkyl benzene sulfonic acid LABSa (anionic)	3.97MPa (576 psig)	0 wt. %	7.143×10^{-9} mol/s
					LABSa (anionic)	3.97MPa (577 psig)	0.005 wt. %	2.452×10^{-8} mol/s
					LABSa (anionic)	3.97MPa (576 psig)	0.01 wt. %	2.553×10^{-8} mol/s
					LABSa (anionic)	3.96MPa (575 psig)	0.1 wt. %	1.773×10^{-8} mol/s
					LABSa (anionic)	3.96MPa (575 psig)	1 wt. %	1.343×10^{-8} mol/s
					quaternary ammonium salt (dam) (cationic)	3.97MPa (576 psig)	0 wt. %	7.143×10^{-9} mol/s
					dam (cationic)	3.97MPa (576 psig)	0.005 wt. %	2.931×10^{-8} mol/s
					dam (cationic)	3.97MPa (577	0.01 wt. %	2.417×10^{-8} mol/s

						psig)		
					dam (cationic)	3.97MPa (576 psig)	0.1 wt. %	6.687×10^{-8} mol/s
					dam (cationic)	3.98MPa (578 psig)	1 wt. %	2.285×10^{-8} mol/s
2	Karaaslan et al, (2002)	Promotion effect of polymers and surfactants on Hydrate Formation rate	CH_4	99.5 % CH_4	pure water	4.83MPa (700 psig)	1 wt. %	1.37e-08 lb-mole/s
					poly-(acrylamide-co-acrylic acid) (paaa)	4.83MPa (700 psig)	1 wt. %	1.40e-08 lb-mole/s
					polyxyethylene (20) cetyl ether (brij-58)	4.83MPa (700 psig)	1 wt. %	2.43e-08 lb-mole/s
					polyoxyethylene (20) sorbitan monopalmitate (tween-40)	4.83MPa (700 psig)	1 wt. %	3.03e-08 lb-mole/s
					poly (vinyl alcohol) pva	4.83MPa (700 psig)	1 wt. %	3.12e-08 lb-mole/s

					polyoxyethylene (5) nonylphenyl ether (igepal-520)	4.83MPa (700 psig)	1 wt. %	3.31e-08 lb-mole/s

3	Lin et al, (2004)	Effect of surfactant on the Formation and Dissociation kinetic behaviour of Methane Hydrate	CH_4		SDS(anionic)	6.6 M Pa	600 ppm	0.0075 mol/ g water
					SDS	6.6 M Pa	650 ppm	0.0085 mol/g water
					SDS	6.6 M Pa	800 ppm	0.008 mol/g water
					SDS	6.6 M Pa	1600 ppm	0.0075 mol/g water
4	Ganji et al, (2006)	Effect of different surfactants on Methane Hydrate Formation rate, stability and storage capacity	CH_4	99.99% CH_4	Pure water	8.3 M Pa	_	0.05 mole
					Sodium dodecyl sulphate (SDS) (anionic)	8.3 M Pa	300 ppm	0.52 mole
					SDS	8.3 M Pa	500 ppm	0.58 mole
					SDS	8.3 M Pa	1000 ppm	0.55 mole/155 v/v at std. Conditions
					Pure water	8.3 M Pa		0.03 mole

					Linear alkyl benzene sulfonate (LABS) (anionic)	8.3 M Pa	300 ppm	0.03 mole
					LABS	8.3 M Pa	500 ppm	0.5 mole
					LABS	8.3 M Pa	1000 ppm	0.53 mole/140 v/v at std. Conditions
					Pure water	8.3 M Pa		0.4 mole
					Cetyl trimethyl ammonium bromide (CTAB) (cationic)	8.3 M Pa	300 ppm	0.35 mole
					CTAB	8.3 M Pa	500 ppm	0.25 mole
					CTAB	8.3 M Pa	1000 ppm	0.63 mole/165 v/v at std. Conditions
					Pure water	8.3 M Pa		0.42 mole

					Ethoxylated nonylphenol (ENP)(non-ionic)	8.3 M Pa	300 ppm	0.2 mole
					ENP	8.3 M Pa	500 ppm	0.33 mole
					ENP	8.3 M Pa	1000 ppm	0.58 mole/158 v/v at std. Conditions
5	Lee et al, (2007)	Methane Hydrate equilibrium and Formation kinetics in the presence of an anionic surfactant	CH_4	99.99%	SDS(anionic)	7 MPa (70 bar)	250 ppm	11.4%
6	Zhang et al, (2008)	Effect of surfactant tween on induction time of Gas Hydrate Formation	$CH_4+C_2H_6+C_3H_8+CO_2$	87.66%+2.61%+ 6.19%+3.54%	T40(non-ionic)	24 M Pa	0.001 mol/l	475 min
					T40+t80(1:1)	19.4 M Pa	0.001 mol/l	584 min

					T40+t80(4:1)	22.55 M Pa	0.001 mol/l	749 min
7	Mandal et al, (2008)	Effect of the promoter on Gas Hydrate Formation and Dissociation	C_2H_6	99.99%	SDS(anionic)	2.94 MPa (30 kg/cm^2)	300ppm	0.040 mol
						3.24 MPa (33 kg/cm^2)	500ppm	0.045 mol
8	Qiang et al, (2009)	Kinetic promotion of sodium dodecyl sulphate on Formation rate of mine Gas Hydrate	CH_4+N_2+O_2	39.8%+50.1%+10.1%	SDS (anionic)	7 M Pa	0.4 mol/l	85 min
					SDS	7 M Pa	0.5 mol/l	93 min
					SDS	7 M Pa	0.6 mol/l	93 min
					SDS	7 M Pa	0.7 mol/l	93 min

9	Linga et al, (2010)	A new apparatus to enhance the rate of Gas Hydrate Formation: application to capture of carbon dioxide	CO_2+N_2	16.9%+83.1%(1 % mole thf)	_	1.2 M Pa	_	70.3 min/0.0098
			CO_2+N_2	16.9%+83.1%(1 % mole thf)	_	2.2 M Pa	_	12 min/0.0178
			$Co2+H_2+C_3H_8$	38.1%+59.4%+2. 5%	_	1.7 M Pa	_	8.7 min /0.0101
10	Moraveji et al, (2010)	Effect of an anionic surfactant on the Methane Hydrate Formation: induction time and stability	CH_4	99.995% CH_4	SDS	6MPa (60 bar)	0 ppm	320 min
					SDS	6MPa (60 bar)	500 ppm	48 min.
					SDS	6MPa (60 bar)	700 ppm	50 min.
					SDS	6MPa (60 bar)	900 ppm	50 min.
					SDS	6MPa (60 bar)	1100 ppm	48 min

11	Torre et al, (2011)	CO_2 capture by Hydrate Formation in quiescent conditions: in search of efficient kinetic additives	CO_2	99.995% CO_2 (4 wt% THF)	SDS	2.7 MPa (27 bar)	3000 ppm	66.66 min
12	Kwon et al, (2011)	Synthesis of anionic multichain type surfactant and its effect on Methane Gas Hydrate Formation	CH_4	Pure CH_4	Sodium sulfonic acid group with hydrophobic carbon chain lengths (C8) (anionic)	4 M Pa	Water	.0045
							5 ppm	.05
							10 ppm	.085
							25 ppm	.10
							50 ppm	.17
							100 ppm	.12
							150 ppm	.07

					Sodium sulfonic acid group with hydrophobic carbon chain lengths (C10)	3.5 M Pa	50 ppm	.11
					Sodium sulfonic acid group with hydrophobic carbon chain lengths (C12)	3.5 M Pa	50 ppm	.07
					Sodium dodecyl sulphate (SDS)	3.5 M Pa	250 ppm	.08
13	Fazlali et al, (2013)	Impact of different surfactants and their mixtures on Methane-Hydrate Formation	CH_4	CH_4	Sodium dodecyl sulphate (SDS) (anionic)	6MPa (60×10^5 Pa)	300ppm	20 min/2.27×10^{-4}mol s^{-1}
						6.1MPa (61×10^5 Pa)	500ppm	18 min/2.40×10^{-4}mol s^{-1}

					Hexa decyl trimethyl ammonium bromide (htabr)(cationic) (HTABR)	6MPa (60×10^5 Pa)	300ppm	44 min/5.64×10^{-5} mol s^{-1}
						6.1MPa (61×10^5 Pa)	500ppm	30 min /9.31×10^{-5} mol s^{-1}
						62×10^5 Pa	700 ppm	36 min/8.79×10^{-5} mol s^{-1}
					Polyoxy ethylene(20) cetyl ether (brij-58)(non-ionic)	6MPa (60×10^5 Pa)	300ppm	55 min/ 5.18×10^{-5} mol s^{-1}
						6.1MPa (61×10^5 Pa)	500ppm	49 min/ 6.54×10^{-5} mol s^{-1}
						6.2MPa (62×10^5 Pa)	700 ppm	52 min/ 7.94×10^{-5} mol s^{-1}
					Pure water	6MPa (60×10^5 Pa)	0 ppm	58 min/ 3.81×10^{-5} mol s^{-1}

					SDS+HTABR	6.1MPa (61×10^5 Pa)	300 ppm+300 ppm	50 min./ 1.19×10^{-4}mol s^{-1}
						6.1MPa (61×10^5 Pa)	300 ppm+500 ppm	23 min/ 1.49×10^{-4}mol s^{-1}
						6.1MPa (61×10^5 Pa)	300 ppm+700 ppm	32 min/ 1.35×10^{-4}mol s^{-1}
						6.1MPa (61×10^5 Pa)	500 ppm +300 ppm	34 min/ 1.63×10^{-4}mol s^{-1}
						6.1MPa (61×10^5 Pa)	500 ppm+500 ppm	19 min/ 1.99×10^{-4}mol s^{-1}
						6.1MPa (61×10^5 Pa)	500 ppm+700 ppm	17 min/ 2.09×10^{-4}mol s^{-1}
					SDS+Brij-58	6.1MPa (61×10^5 Pa)	300 ppm+300 ppm	42 min/ 1.14×10^{-4}mol s^{-1}

						6.1MPa (61×10^5 Pa)	300 ppm+500 ppm	53 min/1.26×10^{-4}mol s^{-1}
						6.1MPa (61×10^5 Pa)	300 ppm+700 ppm	46 min/ 1.30×10^{-4}mol s^{-1}
						6.2MPa (62×10^5 Pa)	500 ppm +300 ppm	40 min/ 1.55×10^{-4}mol s^{-1}
						6.2MPa (62×10^5 Pa)	500 ppm+500 ppm	25 min/ 1.66×10^{-4}mol s^{-1}
						6.2MPa (62×10^5 Pa)	500 ppm+700 ppm	29 min/ 1.76×10^{-4}mol s^{-1}
14	Saw et al,(2014)	Kinetics of Methane Hydrate Formation and its Dissociation in presence of non-ionic surfactant Tergitol	CH_4	99.99%	Tergitol (non-ionic)	11.6 M Pa	0 ppt	161 min/ 0.08 mol
					Tergitol	11.6 M Pa	1 ppt	20 min/ 0.24 mol
					Tergitol	11.6 M Pa	5 ppt	71 min/ 0.27 mol

					Tergitol	11.6 M Pa	10 ppt	100 min/ 0.32 mol
15	Najibi et al, (2015)	Experimental investigation of Methane Hydrate Formation in the presence of copper oxide nanoparticles and sds	CH_4,Cuo nanoparticles	99.9%	SDS (.035 wt.%) and CuO nanoparticles from .035 wt. % to 1 wt. %	5 M Pa	pure water	25 min/.035
							SDS (.035 wt. %) (anionic)	15.5 min/ .055
							SDS (.035 wt. %)+CuO nanoparticles .05 wt. %	13.5 min/.06
							SDS (.035 wt. %)+CuO nanoparticles .01 wt. %	9.4 min/ .07
							SDS(.035 wt. %)+CuO nanoparticles 1 wt. %	4 min/.075

2.15 Formation of Gas Hydrate in Presence of Fixed Bed Media.

The Hydrate Formation in presence of surfactants needs mechanical agitation which makes that process costly. So, in order to commercialize the process of Hydrate Formation some cheaper and less energy intensive process needs to be investigated. The use of fixed bed media is one suitable option which can replace energy intensive agitation process of Hydrate Formation. The fixed bed media of Silica Gels, Sand, Bentonite clay have been used by various research groups as discussed as per the following and shown in **table 2.15.1:**

Kang et al, 2008 in their article have studied the possibility of Gas storage technique by using porous material as storage media. On the basis of equilibrium data, the Gas consumption with respect to time was calculated and the results were converted to the rate and amount of Gas uptake. The Silica Gels used for the study had nominal diameters of 6 nm, 30 nm and 100 nm. When Methane Gas was used for the study the Silica Gels used had pore diameter of 30 nm and 100 nm. Silica Gel of pore diameter of 6 nm was not used for this study as it is not appropriate for Hydrate Formation at high pressure. For each of these Silica Gels sizes pressure was varied. The pressure maintained in the cells was 3.92 MPa, 5.88 MPa and 7.84 MPa and the volume of Silica Gels used was 350 cm^3. The results demonstrated that the rate of Formation of Methane Hydrate increased when the driving force is increased for all the samples. The quantity of Methane consumed was directly related to the driving force, except in the case of 100 nm Silica Gel at 7.84 MPa where the quantity of Gas used up was less than that at 5.88 MPa. The quantity of Methane consumed was very less for the tests done at 3.92 MPa for 30 and 100 nm. This led to the conclusion that at least in order to obtain suitable Gas Hydrate Formation rate, we need to provide a pressure of at least 5 MPa.

Linga et al, 2009 in their study studied used new equipment to acclimatize three volume beds of Silica particles of distinct sizes. They have used sand particles of average diameter of 329 micrometer (μm). The apparatus includes a crystallizer, which is cylindrical container made of stainless steel 316. To vary the quantity of Silica sand bed, 2 copper cylinders are positioned within the crystallizer. The quantity of Silica sand placed inside the crystallizer was 914.1 g. The height of the bed is fixed at 7 cm. When 1 copper cylinder is put in the crystallizer the quantity

of sand is reduced to 513.7 g as the sand bed is fixed at 7 cm. Similarly when 2 copper cylinders are positioned within the crystallizer, the quantity of sand is reduced to 228.5 g. In the cell the pressure was fixed at 8 MPa and the temperatures studies were done at 7 ^{0}C, 4 ^{0}C and 1 ^{0}C. They found multiple nucleation points at temperatures of 4 ^{0}C and 1 ^{0}C. This led to high conversion rate of water to Hydrates. The consequence of changing the sand bed size on the rate of Formation of Hydrate was also investigated. It was discovered that for all the trials the initial slow growth was succeeded by rapid growth till forty three to fifty three percent of the water was transformed to Hydrate. For the duration of last growth stage the conversion rate lies amid seventy four to ninety eight percent and the Gas consumption rate was also changed. They completed their study by mentioning that in order to model the Hydrate Formation rate in a porous bed, the effect of size of bed should also be considered.

Kang et al, 2009 in their study studied have covered the experimental data on the Formation kinetics of Gas Hydrates of CH_4 and CO_2 in Silica Gel pores at different pressures on the range of 0.5 MPa-4.85 MPa. The equipment consisted of a stainless steel cylindrical reactor which was dosed with 400 cm^3 of Silica Gel having pore water. The pore diameters of the Silica Gels used were 6 nm, 30 nm and 100 nm. The Formation rates of Gas Hydrate and induction time were found out over a wide range of driving forces and pore sizes. It was observed that driving force was strongly linked with the Hydrate Formation rate. The effect of pore size on the Hydrate Formation rate seemed to be insignificant. In case of the Methane Hydrate Formation, for pore size of 100 nm no Hydrate was formed while for pore size of 30 nm induction time was 1.8 minutes. When CO_2 was used with hundred nanometer Silica Gel pores the Formation rate was the quickest even when driving force was low. In most of the cases the Gas uptake to water ratio was high. They concluded their study by saying that Hydrate Formation rate observed while using Silica Gel pores was equivalent to mechanical agitation.

Kang et al. (2010) in their article have looked into the phase equilibrium and the kinetics of Formation of Gas Hydrates in porous Silica Gels in the domestic Natural Gas grid of Korea. Formation kinetics was determined in a specially built high pressure cell. They selected Silica Gels pore diameter 6 nm, 15 nm and 100 nm. For the past equilibria study all the 3 forms of Silica Gels were used. The Silica Gels used for the first reaction kinetics study had pore diameter of 100 nm and the quantity used was 250 cm^3. The pressure of the cell was fixed at 3.92 MPa.

The Formation kinetics study was conducted at different temperatures. The study revealed that there was small difference in the final Gas consumption for different temperatures. However, it was observed that initial Formation rate was fastest at 275.2 K. The study also brought to light the fact that the steady state was achieved in a shorter span of time without mechanical agitation. Hence, it was concluded that when porous media is used for Hydrate Formation, it can be beneficial if favourable conditions are provided even without agitation.

Saw et al. (2013) in their work has reported the effects of using bentonite clay in synthetic sea water. They had used a high pressure autoclave which also consisted of a magnetic stirrer to mix up the samples. The synthetic sea water had 3.5% of total dissolved salts (TDS). They used different concentrations of bentonite clay in synthetic sea water for the experiments. The concentrations of bentonite clay used were 3 wt. %, 7 wt.%, 10 wt.% and 15 wt.% and the results were compared with synthetic sea water which didn't have any bentonite clay particles. It was found that the induction time for the Formation of Hydrate is reduced when bentonite clay is introduced in the synthetic sea water. The induction time also varies according to the concentrations of bentonite clay in the samples. For each of the test samples the rate of Hydrate Formation is also different indicating that it is dependent on quantity of bentonite clay present in the system.

Mekala et al, 2014 in their study have used Toyoura sand in pure H_2O at 8 MPa and seawater at 8 MPa and 10 MPa. Saline water (3.03 wt. %) was acquired from Palau Tekong in Singapore. The equipment comprised of a stainless steel crystallizer which was filled with 645.16 g of sand. The pressure of 8 MPa and 10 MPa gave the driving force of 4.2 MPa and 6.2 MPa respectively at 277.15 K. Induction times and Gas uptake for the given conditions were found. From the study it was revealed that for pure H_2O the rate of Transformation was 72% for the driving force of 4.2 MPa, while for sea water the Transformation rate was only 11.6%. When the Gas consumption curves for pure water and sea water were compared, it was found out that for same temperature and pressure measurement the rate of Formation of Gas Hydrates in seawater is very less from the initial growth phase and continued like that till the end of the test.

Saw et al, 2014 in their article has studied the influence of particle of Silica sand individually as well as with a blend of bentonite and Silica sand on the Formation rate of Methane Hydrate. They used a high pressure Hydrate autoclave provided with a magnetic stirrer for agitating the

sample. The sea water had a TDS of 3.5%. They have used Silica Gel of mesh size 30-50 (500-300 µm), 52-60 (300-250 µm) and 60-100 (250-150 µm). The quantity of Silica sand and bentonite used was 10 wt. %. When the tests were done with different grain sizes of Silica sand, it was seen that they inhibited the Formation of Gas Hydrate. Silica sand also reduces the Gas uptake during the Formation of Gas Hydrate. When a blend of bentonite clay and Silica sand was used it was noted that the blend had much better effect on the Formation of Gas Hydrate in comparison to samples using only Silica sand or bentonite clay. It was concluded that induction time of the Formation of Gas Hydrate had reduced when Silica sand of smaller mesh size was used. Additionally it was found that if bentonite clay and Silica sand are used collectively, the induction time of Hydrate Formation is further decreased.

Gas Hydrate Formation in Presence of Various Fixed Bed Media are shown in Table 2.15.1 as follows:

Table 2.15.1: Gas Hydrate Formation in Presence of Various Fixed Bed Media

S. No	Group	Title	Gas	Composi-tion	Fixed Media	Pexp	Dose	Induction time /consumption of Gas/ Moles of Gas/ moles of water consumed /rate of Hydrate Formation
1	Kang et al, (2008)	Natural Gas Storage in Mesoporous Media Using Gas Hydrate	CH_4	99.99%	Silica Gel (30 nm)	3.92 MPa	350 cm^3	0.033 mol/mol
					Silica Gel (30 nm)	5.88 MPa	350 cm^3	0.118 mol/mol
					Silica Gel (30 nm)	7.84 MPa	350 cm^3	0.158 mol/mol
					Silica Gel (100 nm)	3.92 MPa	350 cm^3	0.005 mol/mol
					Silica Gel (100 nm)	5.88 MPa	350 cm^3	0.152 mol/mol
					Silica Gel (100 nm)	7.84 MPa	350 cm^3	0.122 mol/mol
2	Kang et al, (2009)	Kinetics of Methane and Carbon Dioxide Hydrate Formation in Silica Gel Pores	CH_4	99.99%	Silica Gel (6 nm) memory	7.85 MPa	400 cm^3	2.1 min/ 0.0632 mol/mol
					Silica Gel (30 nm) fresh	7.85 MPa	400 cm^3	1.8 min/ 0.1600 mol/mol
					Silica Gel (100 nm) fresh	3.92 MPa	400 cm^3	No Hydrate
			CO_2	99.99%	Silica Gel (6 nm) fresh	2.45 MPa	400 cm^3	0 min/ 0.0135 mol/mol
					Silica Gel (30 nm) fresh	1.96 MPa	400 cm^3	285.3 min/ 0.1272 mol/mol
					Silica Gel (100 nm) fresh	2.94 MPa	400 cm^3	30.7 min/ 0.1382 ml/mol

3	Linga et al, (2009)	Gas Hydrate Formation in a Variable Volume Bed of Silica Sand Particles	CH_4	99.99%	Silica Sand	8 MPa (at 7 °C)	914.1 g	130 min/ 0.0172
						8 MPa (at 7 °C)	914.1 g	206.7 min/ 0.018
						8 MPa (at 4 °C)	914.1 g	18.3-644.3 min/ 0.1215-0.1287
						8 MPa (at 1 °C)	914.1 g	123.7 min/ 0.1308
						8 MPa (at 1 °C)	914.1 g	87.7 min/ 0.135
						8 MPa (at 4 °C)	513.7 g	8.7-546.3 min/ 0.1244-0.1381
						8 MPa (at 4 °C)	228.5 g	7.3-11 min/ 0.1238-0.1603
4	Kang et al, (2010)	Formation Characteristics of Synthesized Natural Gas Hydrates in Meso- and Macroporous Silica Gels	CH_4+C_2H_6+C_3H_8+iso C_4H_{10}+ n-C_4H_{10}+ n-C_5H_{12}+ N_2	89.96%+6.40%+2.71%+0.48%+0.49%+0.02%+0.04%	Silica Gel (100 nm)	3.92 MPa (at 275.2 K)	250 cm^3	0.136 mol/mol
						3.92 MPa (at 278.2 K)	250 cm^3	0.132 mol/mol
						3.92 MPa (at 273.2 K	250 cm^3	0.128 mol/mol
6	Saw et al, (2013)	Methane Hydrate Formation and Dissociation in the Presence of Bentonite Clay Suspension	CH_4	99.99%	Synthetic sea water (SSW) (3.55 % TDS)	11.85 MPa	-	125 min
					Bentonite in SSW	11.85 MPa	3 wt%	95 min/ 0.015 mol
					Bentonite in SSW	11.85 MPa	7 wt %	40 min/ 0.08 mol
					Bentonite in SSW	11.85 MPa	10 wt %	25 min/ 0.09 mol
					Bentonite in SSW	11.85 MPa	15wt %	51 min/ 0.18 mol

7	Saw et al, (2014)	Methane Hydrate Formation and Dissociation in the presence of Silica Sand and Bentonite Clay	CH_4	99.99%	Silica sand (mesh size 30-52) in SSW	11.54 MPa	10 wt %	418 min/ 0.17 mol
					Silica sand (mesh size 52-60) in SSW	11.54 MPa	10 wt %	405 min/ 0.19 mol
					Silica sand (mesh size 60-100) in SSW	11.54 MPa	10 wt %	278 min/ 0.20 mol
					Bentonite in SSW	11.54 MPa	10 wt %	25 min
					Bentonite+Silica sand (mesh size 30-52) in SSW	11.54 MPa	10 wt % each	384 min/ 0.42 mol
					Bentonite+Silica sand (mesh size 52-60) in SSW	11.54 MPa	10 wt % each	343 min/ 0.5 mol
					Bentonite+Silica sand (mesh size 60-100) in SSW	11.54 MPa	10 wt % each	289 min/ 0.54 mol
8	Mekala et al, (2014)	Formation and Dissociation Kinetics of Methane Hydrates in Seawater and Silica Sand	CH_4	99.99%	Toyoura Silica sand (100−500 μm) (pure and fresh water)	8 MPa	645.16 g	0.3 min/ 0.1182 mol/mol
					Toyoura Silica sand (100−500 μm) (sea and fresh water)	8 MPa	645.16 g	3.7 min/ 0.0119 mol/mol
					Toyoura Silica sand (100−500 μm) (sea and fresh water)	10 MPa	645.16 g	2 min/ 0.0191 mol/mol

2.16 Effects of Biosurfactants on Gas Hydrate Formation

The synthetic surfactants put toxic and adverse effects on human beings and their environment. Hence, they need to be replaced by green biosurfactants for Hydrate Formation. The effects of bio surfactants on Gas Hydrate Formation revealed by various research groups is discussed as per follows and shown in table 2.16.1.

Rogers et al, 2003 in their article has used different biosurfactants and observed their effects on the Formation rate and induction time of the Natural Gas Hydrate. They have used biosurfactants of different origins such as Rhamnolipids, Surfactin, Phospholipids, Snomax and Emulsan and studied their effects on induction time by comparing it with control study where no biosurfactant was used. The concentration of biosurfactants in all the tests was 1000 ppm in sand or clay packs filled with seawater. They have used a two hundred fifty millilitre translucent plastic vessel and packed it with bentonite clay and sand to investigate the induction time and Formation rate of Hydrates. A 2.54 cm thick layer of sand was placed at the bottom of the cell. Then a 1.27 cm thick layer of bentonite clay was spread over the sand. This was followed by another layer of sand close to 1.27 cm from the top of the cell. The last layer of the container was split into two parts by using a vertical aluminium strip. One half was filled with bentonite clay and the other half was filled with sand. To ensure that Gas is diffused all through the sand and clay packing, twelve random holes of diameter 0.3175 cm were drilled in the container. The container's top was left open to Natural Gas that pressurizes the testing cell. After filling in the sand and bentonite clay, the cell was soaked with the solution of water and biosurfactant which was being observed. They water specimens used were from Gulf of Mexico. The extra solution was drained from the saturated packing so that only residual water is left. After that, the vessel was set on a translucent shelf in the test cell on top of cooling coils. A temperature probe is inserted into the lower clay layer up to a depth of 2.54 cm from the side of the packing. The sample was illuminated with the help of a fibre optics light source in the test cell. The pressure and temperature in the cell were maintained at 2.28 MPa and 294.3 K respectively. It was then purged with Natural Gas from Matheson Inc. The temperature of the fluid flowing through the cooling coils was 271 K and data compilation was started at onset of refrigeration. The 3900 ml stainless steel container housing the entire sample was temperature and pressure controlled with provisions for constantly recording the pressure and temperature. When they studied the

induction time from the equilibrium curve, they found that all the biosurfactants influenced the Formation of Gas Hydrates in a positive way in seawater sand or clay environment. Snomax and Emulsan had the least impact on induction time as in their case it was 20 to 44% less as compared to the control study in which no biosurfactant was used. For Rhamnolipids induction time was 58% less than the induction time noted in control study. Among all the biosurfactants Surfactin was the most effective promoter as it reduced the induction time by seventy one percent from the control study.

Rogers et al, 2003 in their study studied induction time and Formation rate of Gas Hydrates formed in seawater saturated in sand or clay packs in the presence of biosurfactants. The main purpose to conduct the study was to find whether biosurfactants promote the Formation of Gas Hydrates or there is any specific requirement when biosurfactants act in synergy with bentonite, kaolin and sand surfaces. They studied the effects of Rhamnolipids, Surfactin, Phospholipids, Snomax and Emulsan on the Formation rate of Natural Gas Hydrate in clay packs or seawater saturated sand. They compared the results with a reference sample where no biosurfactant was used. The Gas used in the experiments was Natural Gas found in Gulf of Mexico and the packing contained a blend of sand and bentonite clay or kaolin clay. The concentration of the biosurfactants used in the tests was 1000 ppm. The equipment was intended to monitor the induction time and Gas uptake rates, since these factors are important to study Formation rate of Gas Hydrates. The equipment was also aimed to permit the visual examination of Gas Hydrate Formation. The cells were made of stainless steel and provided with pressure and temperature monitoring systems. To observe the Formation of Hydrate visually, a 2 inch thick and 4 inch diameter quartz observing port was provided at the top of the cell. Two sapphire sealed observing ports that used image capture and fibre optic light entry acted as second visual observation_point.

After that the samples were cooled then pressure, temperature and time were recorded. This resulted in plotting of equilibrium curve for the given samples. From the observations, it was found that Surfactin was the best promoter among all the biosurfactants in presence of bentonite clay as it decreased the induction time by 71% as compared to the reference study. Rhamnolipids also decreased the induction time by approximately 58% from the control study containing bentonite. Emulsan, Snomax and Phospholipids also showed reduced induction times which were 20% to 44% less than the bentonite control study. However, some differences were

observed when kaolin was used in place of bentonite. In this case, Rhamnolipids show the best promoting effect as it reduces the induction time by 66% as compared to the control study containing kaolin clay. These results showed that the presence of biosurfactant can affect the Formation of Gas Hydrate and the induction time is also changed by the type of sand and clay. When Formation rates of Gas Hydrate were studied, it was found that kaolin gives reduced Hydrate Formation rates in comparison to bentonite. The Formation rates are further decreased in presence of Surfactin, Phospholipids, Snomax and Emulsan. However, when Rhamnolipids were used in the solution containing kaolin the Formation rate increased by 16 times. When bentonite is used, Surfactin gives increased Formation rate of almost four times but kaolin Surfactin collaboration inhibited the rate of Formation. From the study, it was found that generally the presence of biosurfactants reduced the induction times and in some cases rate of Hydrate Formation improvements were considerable.

Woods, 2004 in his thesis have studied the Gas Hydrate Formation rate and induction time in presence of biosurfactants. Rhamnolipids and Emulsan with various porous media surfaces. The various porous media used were Ottawa sand, bentonite clay, kaolinite clay, nontronite clay and aragonite. They fabricated a sample cup to replicate the behaviour of Natural Gas, water and sediments on the ocean floor. They used a 50 ml polypropylene cup in which a 2 inch long and 1/2 inch diameter Polyvinyl Chloride (PVC) pipe was glued to the centre of the cup as a container. Then they drilled holes into the side of the polypropylene cup and the PVC pipe so that greater amount of Gas can be transported to the porous media. The diameter of the holes is 1/16 of an inch and they were pierced along the periphery of the cup and the PVC pipe after every forty five degrees. The vertical distance between the holes was 1/2 inch. There were five more holes drilled in the bottom of the cup inside the inner PVC ring circle. The purpose of these holes was to drain excess water from the sample. They had used a pressure cell of volume 450 ml which was made of stainless steel 316 and could work at a maximum press of 2950 psi. The internal diameter of the cell was 2 ½ inches and the height of the cell was 5.94 inches. Two resistance temperature devices and a pressure transducer was provided to monitor pressure and temperature. A pressure relief valve was also fitted in which relief pressure had set at 500 psig. When a sample was prepared, firstly about 21 g of Ottawa sand was placed in the cup. Then a layer of required sediment weighing 1.25 g is spread on top of the sand layer. The above steps are repeated until four separate layers were formed. At last, a layer of Ottawa sand weighing 25 g

is placed over the fourth layer such that a thin semi-circular cavity is left at the top of the cup. This semi-circular cavity is filled with a 0.5 g layer of the sediment that was used in the Formation of earlier layers. After filling the pressure cell with the sample, it was plunged into water bath at temperature 0.5 ^{0}C. Then the temperature and pressure were noted after every 30 seconds. The Formation rate of Gas Hydrates was studied for different biosurfactants in presence of various sand and clay mixtures. From the Formation rate curves it was observed that Formation rates were radically high for Rhamnolipids for all the sediments used, but the concentration at which this happens was different for each case. For concentrations less than 100 ppm, Ottawa sand and the mixture of Ottawa sand and bentonite exhibited instant results. The most drastic increase was observed when Ottawa sand and bentonite mixture was used. However, when Kaolinite was used rise in Hydrate Formation rate was delayed. The only noteworthy increases were seen at concentrations ranging between 100 to 500 ppm. It was also observed that although all the porous media showed increased rate of Hydrate Formation at high concentrations of Rhamnolipids. All the sediments achieved approximately same rate at concentration of 1000 ppm. Tests with sediments like nontronite and aragonite also proved this. When Emulsan was used in the tests, it was seen that bentonite once again showed greater rate of Hydrate Formation for all the porous media. However, the usage of kaolinite didn't show any change in the rate of Hydrate Formation which was opposite to the behaviour shown by Ottawa sand and bentonite.

The effects of various biosurfactants on Gas Hydrate Formation are shown in Table 2.16.1.

Table 2.16.1 Effects of Biosurfactants on Gas Hydrate Formation

S N.	Group	Title	Gas and conditions	Fixed Media	Micro organism	Bio surfactants		Induction time (min)	rate (milli mole/hr)	Increase in Hydrate Formation rate
1	Rogers et al, (2003)	Catalysis of Gas Hydrates by Biosurfactants in Seawater-Saturated Sand/Clay ,	Natural Gas Sand/clay saturated with sea ,water , 90% Methane, 6% ethane, and 4% propane Test cell cool down at constant, Cooling rate biosurfactants at 1000 ppm in sea water, initial P=2.28Mpa ,T=294.3K	Sand+Bentonite	*Pseudomonas aeruginosa*	Rhamno lipid 1000 ppm		53	23	96% to 107%
					Bacillus subtilis	Surfactin 1000 ppm		35	50	288%
					Thiobacillus species	Phosph-olipid 1000 ppm	DPPS	67	27	96% to 107%
							POPC	90	24	
					Coryneba-cterium species		DMPC	100	22	
					Pseudomonas syringae	Snomax 1000 ppm		87	29	135%
					Acinetob-acter calcoaceti-cus	Emulsan 1000 Ppm		75	31	135%

2	Rogers et al, (2003)	Enhancement of Gas Hydrate Formation in Gulf of Mexico Sediments	Natural Gas , 90% Methane, 6% ethane, and 4% propane	Sand+Bentonite	*Pseudomonas aeruginosa*	Rhamno lipid 1000 ppm	53	23	76.92%
					Bacillus subtilis	Surfactin 1000 ppm	38	50	284.61%
					Thiobacillus species	Phosph-olipid 1000 ppm	84	24	84.61%
					Coryneba-cterium species				
					Pseudomonas syringae	Snomax 1000 ppm	86	29	123.07%
					Acinetob-acter calcoaceti-cus	Emulsan 1000 ppm	78	31	146.15%
				Sand+Kaolin	*Pseudomonas aeruginosa*	Rhamno lipid 1000 ppm	22	50	1900%
					Bacillus subtilis	Surfactin 1000 ppm	66	3.5	40%
					Thiobacillus species	Phosph-olipid 1000 ppm	48	4.5	80%
					Coryneba-cterium species				
					Pseudomonas syringae	Snomax 1000 ppm	43	7.5	240%

					Acinetob-acter calcoaceti-cus	Emulsan 1000 ppm		43	18	620%
3	Woods, (2004)	Examination of the effects of biosurfactant concentration on Natural Gas Hydrate Formation in seafloor porous media	Natural Gas 90% Methane, 6% ethane, and 4%	Ottawa Sand/ Bentonite/ Kaolinite/ Nontronite/ Aragonite	*Pseudomonas aeruginosa*	Rhamno lipid 100 ppm	Ottawa Sand		0.8	1.5
							Ottawa Sand/Bentonite		1.9	2.31
							Ottawa Sand/Kaolinite		0.4	3.23
						Rhamno lipid 500 ppm	Ottawa Sand		1.6	40.63
							Ottawa Sand/Bentonite		2.3	1.63
							Ottawa Sand/Kaolinite		1.2	4.94
						Rhamno lipid 1000 ppm	Ottawa Sand		1.6	9.04
							Ottawa Sand/Bentonite		1.5	14.77
							Ottawa Sand/Kaolinite		1.7	1.94
							Ottawa sand/Nontronite		1.6	6.38
							Ottawa sand/Aragonite		1.4	17.32

					Acinetob-acter calcoaceti-cus	Emulsan 100 ppm	Ottawa Sand	0.7	1.51
							Ottawa Sand/Bentonite	1.1	2.23
							Ottawa Sand/Kaolinite	0.4	10.88
						Emulsan 500 ppm	Ottawa Sand		10.8
							Ottawa Sand/Bentonite	1.8	3
							Ottawa Sand/Kaolinite	0.4	
						Emulsan 1000 ppm	Ottawa Sand	1.5	14.84
							Ottawa Sand/Bentonite	1.9	5.17
							Ottawa Sand/Kaolinite	0.4	3.48

2.17 Influence of inhibitors on Gas Hydrate Formation

Gas Hydrates block the flow in oil and Gas pipe lines. So some inhibitors are required to inhibit the Gas Hydrate Formation in pipe lines. Two types of inhibitors are used the industry as briefly explained below:

(a) Low Dose Kinetic Inhibitor (LDKI)

(b) Thermodynamic Inhibitor (THI)

(a). Influence of Low Dose Kinetic Inhibitor on Gas Hydrates Formation -These type of inhibitor are added at very low concentration(less than 1 wt. % in the aqueous phase) and they delay Hydrate nucleation which leads to decreased rate of Hydrate Formation for example Poly-N-Vinylpyrolidone(PVP), Poly-N-Vinyl Amides etc. Their advantage is their low cost, low dose requirement etc. The findings of various research groups is explained as per follows and shown in **table 2.17.1** as follows:

Lee et al, 2006 in their work have tested a mixture of Methane and ethane by using water droplets of size 5 mm. The equipment consisted of a crystallizer which had a magnetic bar for agitation. The Formation of Gas Hydrates was done at a constant pressure of 5.1 MPa. The inhibitors that were used in testing are GHI 101 and Polyvinylpyrrolidone (PVP). In one of the droplets no Inhibitor was added to use it as a comparison study. From the results, it was observed that Hydrate Formation was inhibited by GHI 101 leading to longer induction time as compared to PVP and pure water sample.

Villano et al, 2010 in their work have used Polyacryloylpyrrolidine (PAP) to find out how the tacticity effects the induction time of the Formation of synthetic Gas Hydrate. The experiments were conducted in a high pressure autoclave made of sapphire and stainless steel in which pressure was set at 90 bar and the stirrer was rotated at 600 rpm. The inhibitors used in the experiments are vinyl caprolactam/vinyl Pyrrolidone polymer (Luvicap 55W), Isotactic Polyacryloylpyrrolidine (PAP) and Atactic Polyacryloylpyrrolidine (PAP). They also did a test with no inhibitor in the solution for comparison.

The results showed that atactic PAP shows greater inhibition effect as compared to isotactic PAP and Luvicap 55W.

Daraboina et al, 2011 in their study have using Stirrer reactor experiments have looked into inhibition of Hydrates by using two commercial kinetic inhibitors and two antifreeze proteins. The kinetic inhibitors used were polyvinylpyrrolidone (PVP) and HIW85281 and the antifreeze proteins used are type I and type III. The apparatus consisted of crystallizer made of stainless steel fixed at a pressure of 8.1 MPa. The magnetic stirrer in the cell was fixed at 400 rpm. Testing was also done on pure water sample for reference. When the tests were conducted, it was found that the induction time had increased in the presence of kinetic inhibitors and antifreeze proteins. Among the samples, the highest induction time was recorded by the commercial Inhibitor HIW85281. When the results are compared with pure water samples, it was found that Hydrate nucleation was postponed by a factor of 1.4 by AFP-III, 2.2 by PVP, 3.2 by AFP-I and 33.6 by HIW85281.

Xu et al, 2015 in their article have used poly(N-vinyl) pyrrolidone, Inhibex501, and synthesized KHI-HY4 at different values of pressure and temperatures to gauge their effect on Formation rate. They used a high pressure stainless steel cell with a stirrer rotating at 550 rpm for all the experiments. HY4 was made by free-radical polymerization of N-vinyl-2-pyrrolidone in diethylene glycol monobutyl ether while PVPK90 and Inhibex501 (vinyl caprolactam/vinylpyrrolidone copolymer in butoxyethanol solution) are commercial KHI. The study also included tests done with no inhibitors for reference study. The results were compared for different pressures and different inhibitors and they were also compared with reference tests. The results indicated that among all the inhibitors studied HY4 gave the best performance and in one case it gave an induction time of 24.8 hours.

Influence of Low Dose Kinetic Inhibitors on Gas Hydrates Formation is shown in Table 2.17.1.

Table 2.17.1 Influence of Low Dose Kinetic Inhibitors on Gas Hydrates Formation

S. No.	Title	Group	Gas	Composition	Inhibitor	Pexp	Dose	Induction time
1	Natural Gas Hydrate Formation and Decomposition in the Presence of Kinetic Inhibitors. 2. Stirred Reactor Experiments	Daraboina et al, (2011)	CH_4+C_2H_6+ C_3H_8	93%+5%+ 2%	Water	8.1 MPa	0 wt %	7.3 min
					water +polyvinylpyrrolidone (PVP)	8.1 MPa	0.5 wt %	17.3 min
					water + HIW85281	8.1 MPa	0.5 wt %	182.8 min
					water + AFP I	8.1 MPa	0.5 wt %	23 min
					water + AFP III	8.1 MPa	0.5 wt %	10.2 min
2	Unusual kinetic inhibitor effects on Gas Hydrate Formation	Lee et al,(2006)	CH_4+C_2H_6	89.4%+10 .6%	Water (droplet A 5mm)	5.1 MPa	0 wt %	191 min
					Water + GHI 101 (droplet B 5mm)	5.1 MPa	0.5 wt %	252 min
					Water + PVP (droplet C 5mm)	5.1 MPa	0.5 wt %	191 min
3	Effect of Polymer Tacticity on the Performance of Poly(N,N-dialkylacrylamide)s as Kinetic Hydrate Inhibitors	Villano et al, (2010)	CH_4+C_2H_6+ C_3H_8+isoC$_4$ H_{10}+n-C_4H_{10}+N_2+ CO_2 (Synthetic Natural	80.67%+1 0.20%+4. 90%+1.53 %+0.76% +0.10%+1 .84%	no inhibitor	9MPa (90 bar)	0 wt %	< 50 min
					vinyl caprolactam/vinyl pyrrolidone polymer (Luvicap 55W)	9MPa (90 bar)	0.5 wt %	505 min

			Gas)		Isotactic polyacryloylpyrrolidine (PAP)	9MPa (90 bar)	0.5 wt %	869 min
					Isotactic polyacryloylpyrrolidine (PAP)	9MPa (90 bar)	0.5 wt %	611 min
					Atactic polyacryloylpyrrolidine (PAP)	9MPa (90 bar)	0.5 wt %	1137 min
					Atactic polyacryloylpyrrolidine (PAP)	9MPa (90 bar)	0.5 wt %	885 min
4	An Investigation of Kinetic Hydrate Inhibitors on the Natural Gas from the South China Sea	Xu et al, (2015)	Gas A (N_2+CO_2+CH_4+C_2H_6+C_3H_8+2-methyl propane+C_4H_{10}+1-methyl butane+C_5H_{12}+C_6H_{14})	0.41%+5.73%+87.16%+3.60%+1.43%+0.29%+0.30%+0.10%+0.03%+0.95%	no inhibitor	8.65 MPa	0 wt %	2.43 hr
					HY4 (synthesized by free-radical polymerization of N-vinyl-2-pyrrolidone in diethylene glycol monobutyl ether)	8.65 MPa	1 wt%	14.05 hr
					poly(N-vinyl) pyrrolidone, (PVP) K90	8.65 MPa	1 wt%	16.13 hr
					no inhibitor	6 MPa	0 wt %	4.56 hr

					HY4 (synthesized by free-radical polymerization of N-vinyl-2-pyrrolidone in diethylene glycol monobutyl ether)	6 MPa	1 wt%	24.89 hr
					Inhibex501 (vinyl caprolactam/vinylpyrrolidone copolymer in butoxyethanol solution (w = 0.5))	6 MPa	1 wt%	10.89 hr

(b) Effects of thermodynamic inhibitor on Gas Hydrates Formation –These type of inhibitor alters the energy of intermolecular interaction and thermodynamic equilibrium between molecules of Gas and H_2O. These are added at high concentrations (10-60 wt. %). They change the chemical potential of the aqueous or Hydrate phase due to which Hydrate Dissociation curve is displaced to higher pressure and lower temperature for example methanol, ethanol, ethylene glycol etc. Their advantage is that they are effective and predictable. The findings of various research groups is explained as per follows and shown in **table 2.17.2** as follows:

Maekawa, 2008 in his study have used different strengths of 1-propanol or 2-propanol aqueous solution to study their inhibition influence on the Formation of CH_4 Gas Hydrates. The experimental equipment used was a cylindrical stainless steel cell which also had an agitator to stir the mixture. During all the tests around 500 cm^3 of solution was put in the cell. During the Formation of Hydrates an abrupt decrease in pressure was seen. After that, the temperature of the system was raised by 0.1 K to dissociate the Gas Hydrates. Observations were recorded once equilibrium was reached at any temperature. The concentration of 2-propanol was varied between 0% to 20 % and equilibrium conditions were studied. The equilibrium pressures for the solution having 2-propanol at concentration of 2 mass % were higher when compared with pure water. This showed that 2-propanol inhibits Formation of structure I Hydrate. However, the equilibrium pressure decreases when concentration of 2-propanol is between 12% and 16.4% by mass. This happens as 2-propanol steadies the type II Hydrate structure with Methane. So in their study they found out that 2-propanol acts as an inhibitor until the concentration of structural transition is reached after which it stabilizes Hydrate with Methane.

Mohammaadi et al, 2008 in their article have studied the effect of ethanol on different Gas Hydrates. Their experimental equipment consisted of cylindrical vessel and an agitator to stir the solution. The Formation of Gas Hydrate is indicated by rapid drop in pressure and then temperature is decreased in steps by 0.1 K. The temperature is kept constant until equilibrium is attained in the vessel. The tests were performed on ethane and propane. The concentration of ethanol used was 5% and 10 % by mass and the observation were compared with pure water solution. The experimental data was compared with the thermodynamic model [Heriot Watt University, 2007] and the general correlation [Østergaard et al, 2005] predictions and it was found that the experimental data is in agreement to the predicted data.

Mohammadi et al, 2010 in their study studied have used isochoric pressure search method to compare the experimental Dissociation data for ethane and Methane to the corresponding literature data and further discussed the inhibition nature of methanol and ethylene glycol. They have used different apparatuses for ethane and Methane. For ethane the cylindrical vessel used could work at pressures up to 40 MPa and it also had a stirrer for agitating the solution to help it to reach equilibrium. For Methane the equipment used consisted of horizontal cylindrical vessel having two sapphire windows and it could endure pressures up to 60 MPa. It had a Rushton turbine stirred mixer for agitating the solution. Ethylene glycol was used with ethane and its concentration was varied from 0.1 mass fraction to 0.5 mass fraction. In case of Methane, methanol was used for the tests and its concentration ranged from 0.55 mass fractions to 0.65 mass fraction. The inhibition effect is shown if the conditions for Hydrate Dissociation are shifted towards high pressure or low temperature. From the study, it was found that the reported data in the literature for ethane was in agreement with their experimental data [Ng et al, 1985, Mohammadi et al, 2008]. However, for the Methane and methanol mixture the reported data [Mohammadi et al 2010, Robinson et al, 1986, Ng et al, 1987] doesn't seem to be reliable. As they have argued that at high concentrations of methanol, it may take part on the Formation of Gas Hydrate.

Lee et al, 2011 in their study have used Natural Gas circulated in the Korean domestic grid and investigated the inhibiting effects of methanol and ethylene glycol at different temperatures and pressures. They measured the equilibrium conditions in high pressure vessel which had a provision for agitation with the help of a mechanical stirrer. The concentration of methanol varied from 10-30 wt. % and the ethylene glycol's concentration was in the range of 10-50 wt. %. During the testing equilibrium curves were plotted for all the conditions. It was found that when inhibitors are used, the curves move to the inhibition region and this effect becomes more pronounced when inhibitor concentration is increased. When the inhibiting nature of methanol was compared with ethylene glycol, it was found that for increase in 10wt % of each of the inhibitors, methanol showed a higher temperature suppression of 5 K whereas ethylene glycol showed temperature suppression of 4 K. This happens due to the smaller molecular weight of methanol.

The influence of various thermodynamic inhibitors is shown in table 2.17.2 as follows.

Table 2.17.2 Effects of Thermodynamics Inhibitors on Gas Hydrates Formation

S. No.	Title	Group	Gas	Composition	Inhibitor	Dose	Teq	Peq
1	Equilibrium conditions for clathrate Hydrates formed from Methane and aqueous propanol solutions	Maekawa, (2008)	CH_4	99.90%	2-Propanol	0 mass %	274.6 K	3 MPa
							277.9 K	4.1 MPa
							281.6 K	6.1 MPa
						2 mass %	277.9 K	4.3 MPa
						3 mass %	277.9 K	2.9 MPa
							281.6 K	6.2 MPa
						4 mass %	277.9 K	4.0 MPa
						6 mass %	281.6 K	5.7 MPa
2	Experimental Data and Predictions of Dissociation Conditions for Ethane and Propane Simple Hydrates in the Presence of Distilled Water and Methane, Ethane, Propane, and Carbon Dioxide Simple Hydrates in the Presence of Ethanol Aqueous Solutions	Mohammadi et al, (2008)	C_2H_6	99.995%	Ethanol	0 mass %	275.2 K	0.60 MPa
							279.6 K	1.01 MPa
							282.1 K	1.40 MPa
						5 mass %	273.9 K	3.45 MPa
							275.6 K	4.02 MPa
							277.8 K	5.03 MPa
							280.1 K	6.2 MPa
						10 mass %	271.1 K	2.98 MPa
							273.8 K	4.01 MPa
							276.5 K	5.03 MPa
							280.2 K	7.42 MPa
			C_3H_8	99.995%		0 mass %	274.6 K	0.22 MPa
							277.1 K	0.4 MPa
							278.3 K	0.5 MPa
						5 mass %	272.5 K	0.2 MPa
							274.2 K	0.3 MPa
							275.1 K	0.35 MPa

							276.6 K	0.51 MPa
						10 mass %	272 K	0.25 MPa
							273.4 K	0.36 MPa
							274.5 K	0.44 MPa
							275 K	0.5 MPa
3	Gas Hydrate Phase Equilibrium in the Presence of Ethylene Glycol or Methanol Aqueous Solution	Mohammadi et al, (2010)	C_2H_6	99.995 (mol %)	Ethylene glycol	0.1 Mass Fraction	271.1 K	0.471 MPa
							272.4 K	0.55 MPa
							276.1 K	0.882 MPa
							278.5 K	1.2 MPa
						0.2 Mass Fraction	267.1 K	0.414 MPa
							270.4 K	0.622 MPa
							273.7 K	0.958 MPa
							275.3 K	1.182 MPa
						0.35 Mass Fraction	262.1 K	0.486 MPa
							265.4 K	0.745 MPa
							267.7 K	0.983 MPa
							269.4 K	1.287 MPa
						0.50 Mass Fraction	251.6 K	0.386 MPa
							254.3 K	0.567 MPa
							256.1 K	0.712 MPa
							259 K	1.002 MPa
			CH_4	99.995 (mol %)	Methanol	0.65 Mass Fraction	234.5 K	5.19 MPa
							235.9 K	6.01 MPa
							238.3 K	8.01 MPa

							240.3 K	10.31 MPa
						0.55 Mass Fraction	237.3 K	3.16 MPa
							239.5 K	3.99 MPa
							244.3 K	6.7 MPa
							248.4 K	10.76 MPa
4	Phase Equilibria of Natural Gas Hydrates in the Presence of Methanol, Ethylene Glycol, and NaCl Aqueous Solutions	Lee et al, (2011)	Natural Gas (CH_4+C_2H_6 +C_3H_8+iso-C_4H_{10}+n-C_4H_{10}+n-C_5H_{12}+N_2)	89.86%+6.40%+2.71%+0.48%+0.49%+0.02%+0.04%	Methanol	pure water	281.4 K	1.71 MPa
							283.3 K	2.18 MPa
							288.3 K	4.17 MPa
							290.1 K	5.29 MPa
							291.4 K	6.61 MPa
						10 wt %	277.8 K	2.08 MPa
							283 K	4.05 MPa
							285.9 K	6.16 MPa
							287.2 K	7.76 MPa
						20 wt %	274.5 K	2.21 MPa
							279 K	4.1 MPa
							281.5 K	6.07 MPa
							283.1 K	8.17 MPa
						30 wt %	273.1 K	3.8 MPa
							276 K	6.26 MPa
							276.4 K	7.08 MPa
							277 K	8.5 MPa
					Ethylene Glycol	pure water	281.4 K	1.71 MPa
							283.3 K	2.18 MPa
							288.3 K	4.17 MPa

							290.1 K	5.29 MPa
							291.4K	6.61 MPa
						10 wt %	275.7 K	1.52 MPa
							280.1 K	2.48 MPa
							284.5 K	4.26 MPa
							288 K	7.08 MPa
							289.2 K	8.22 MPa
						20 wt %	271.1 K	1.09 MPa
							277 K	2.27 MPa
							281.9 K	4.02 MPa
							284.6 K	5.97 MPa
							287.7 K	9.2 MPa
						30 wt %	266.2 K	0.99 MPa
							270.5 K	1.7 MPa
							278.6 K	4.48 MPa
							281.6 K	6.55 MPa
							283.7 K	8.64 MPa
						40 wt %	261.2 K	1.28 MPa
							265.7 K	2.23 MPa
							268 K	2.88 MPa
							272.2 K	4.83 MPa
							275.8 K	8.15 MPa
						50 wt %	264.6 K	4.04 MPa
							267.6 K	6.09 MPa
							268.9 K	7.32 MPa
							270.2 K	9.21 MPa

2.18 Hydrate Based CO_2 Capture

The ever increasing level of emissions of greenhouse Gases is having adverse effects on the environment, not least of which is global warming, a major environmental threat that needs our immediate attention. CO_2 is a greenhouse Gas and a major contributor to the greenhouse effect, contributing to 60% of global warming effects [Yamasaki, 2003]. The International Panel on Climate Change (IPCC) has predicted that, by the year 2100, CO_2 may cause the mean global temperature to rise by around 1.9°C and the mean sea level to increase by around 38 m by the year 2100 [Stewart et al, 2005]. Energy related activities are the major cause of CO_2 emissions with fossil fuel power plants contributing around 40 percent of the total CO_2 emissions [Carapellucci et al, 2003, Kumar et al, 2009]. Large point sources such as the combustion of fossil fuels (coal, Natural Gas, and oil) for energy production and transportation etc. are the primary causes for this CO_2 increment in the environment [Carapellucci et al, 2003, Kumar et al, 2009]. The increasing concentration of CO_2 in the environment is a global concern and various novel technologies are designed to capture CO_2. Carbon dioxide (CO_2) is emitted majorly through human activities which results in increasing greenhouse effect. The major cause of increment of CO_2 in the atmosphere is due to shrinkage of Natural forest (deforestation) and human activities are adding more CO_2 to the atmosphere. Many industries produce CO_2 by chemical reaction such as in the production of cement, metals etc. CO_2 content is emitted in large volume globally.

A lot of different approaches can be employed to capture CO_2 from its mixture or pure form. Conventional methods such as cryogenic fractionation, selective adsorption by solid adsorbents, Gas absorption, and membrane separation have been extensively studied in the past [Kumar et al, 2009, Barchas et al,1992, Kikkinides et al, 1993, White et al, 2003, Aaron et al, 2005]. The Hydrate based procedure for Gas separation and the use of metal organic frameworks (MOFs) are novel technologies for CO_2 capture, which need to be investigated exhaustively [Aaron et al, 2005, Alessandro et al, 2010]. The Hydrate based Gas separation process (HBGS) is a moderately new approach in which the sought Gas can be separated from its mixture through Hydrate Formation. This is now being thought of as a promising contender to nullify the short to medium term threats posed by the emission of CO_2 Gas from fossil fuel plants and the corresponding greenhouse effect [Kumar et al, 2014, Babu et al, 2013, Kumar et al, 2009, Linga et al, 2007, Klara et al, 2002, Budzianowski et al, 2010]. There are a lot of causes to investigate

Gas Hydrates. Natural Gas Hydrates occur on various parts of the earth and are the biggest untapped source of Natural Gas presently known to mankind at the moment [Makogon et al, 2007, Milkov et al, 2003, Klauda et al, 2005, Kumar et al, 2015, Kvenvolden et al, 1999, Kumar et al, 2008]. Hydrate based desalination, water treatment, Gas separation and sequestration and Gas storage are some of the other potential applications of Gas Hydrates [Babu et al, 2014, Thomas et al, 2003, Lee et al, 2011, Max et al, 2000, Gudmundsson et al, 2000, Veluswamy et al, 2014, Yang et al, 2015, Yang et al, 2013, Bhattacharjee et al, 2015]. One of these unconventional technologies being looked at with great interest is a Hydrate based CO_2 capture and separation from fuel and flue Gas mixtures [Kumar et al, 2009, Babu et al, 2013, Kumar et al, 2014, Linga et al, 2007]. CO_2 capture by Hydrate Formation could be the answer in the present context [Linga et al, 2007, Duc et al, 2007]. Capturing by Hydrate Formation is utilized for CO_2 sequestration and transportation [Fan et al, 2005, Chatti et al, 2005]. In addition to being a massive energy resource, Gas Hydrates find application in various other fields such as Gas storage, Gas fractionation, seawater desalination [Gudmundsson et al, 2000, Siangsai et al, 2015, Kang et al, 2014] and CO_2 storage, capture and sequestration [Tajima et al, 2004, Aaron et al, 2005, Alessandro et al, 2010, Englezos et al, 2005]. Various novel technologies are being designed to capture CO_2. Kumar et al, (2013) have investigated CO_2 capture using 100% water saturated Silica Gel and have reported that rate of Hydrate Formation is at par with Hydrate Formation in agitated tank reactor conditions, stating that existence of Silica Gel can enhance the Hydrate Formation rate compared to the quiescent system. Thus the presence of Silica Gel can enhance the Hydrate Formation rate compared to the quiescent system. The Hydrate Formation rate can be manipulated by using the porous medium as it tends to promote the Hydrate Formation by removing mass transfer barrier [Cha et al, 1988, Yan et al, 2005]. Kumar et al, 2014 have recently conducted the study on the Hydrate-based Gas separation (HBGS) procedure for Gas mixtures of CO_2+N_2 (flue Gas) and CO_2+H_2 (fuel Gas) and revealed that HBGS and presence of fly ash further facilitates this process for CO_2 capture Kumar et al, 2009 have investigated in detail the hybrid procedure for the capture of H_2 and CO_2 from a treated fuel Gas consisting of two Hydrate crystallization stages.

CO_2 sequestration has been extensively studied on a lab scale [Goel et al, 2006, Seo et al, 2001, Lee et al, 2003, Mastuo et al, 2004]. CO_2 sequestration in Natural Gas Hydrates can release Methane and simultaneously sequester CO_2. So, there is a strong motivation to attempt Hydrate

based CO_2 capture. In 2012, the United States Department of Energy (US DOE) in association with ConocoPhillips and Japan Oil, Gas and Metals National Corporation (JOGMEC) performed a field test in the Prudhoe Bay region of Alaska. The researchers attempted to pump CO_2 Gas down wells and into Hydrate deposits. The idea was to exchange the Methane molecules inside the Hydrates with CO_2 molecules leaving the water crystals intact and freeing the Methane to flow up the well [Schoderbek et al, 2013].

Continuous efforts are being made to improve the economics and efficiency of Hydrate based Gas capture. One approach to achieve this is the use of fixed bed reactors in place of more conventionally used, energy intensive stirred tank reactors. Conventional fixed bed media like Silica Gel and Silica sand have been used extensively to study Hydrate Formation kinetics [Kumar et al, 2015, Linga et al, 2012, Kumar et al, 2013, Babu et al, 2013, Zhang et al, 2013, Klauda et al, 2003, Jin et al, 2012, Seo et al, 2005, Clennell et al, 1999, Saw et al, 2013]. More recently, people have investigated the effects of using novel materials such as polyurethane foam and metallic packing as packing media on Hydrate Formation [Kumar et al, 2015]. The kinetics of Hydrate Formation can also be enhanced by the use of surfactants such as Sodium dodecyl sulphate (SDS) in small doses of the order of ppm as additives [Kumar et al, 2013, Zhong et al, 2000, Lee et al, 2007, Karaaslan et al, 2000, Zhang et al, 2004, Profio et al, 2005, Zhang et al, 2007, Zhang et al, 2007, Song et al, 2013, Yang et al, 2013, Saw et al, 2014]. Thus we can see that the use of porous fixed bed media and kinetics promoters (SDS) enhances the rate of Hydrate Formation.

The Hydrate based CO_2 capture and separation process can be commercialized by increasing the Hydrate Formation rate and reducing the operating pressure conditions. Hydrate Formation in quiescent condition is very slow. A thin film of Hydrate is formed on the H_2O surface which stops effective migration of Gas further into the system resulting in the slower kinetics of Hydrate Formation. In this context, higher solubility of Gas in water and larger contact area between host molecule, i.e. water and guest molecules, i.e. Gases are very vital so as to enhance the Hydrate Formation rate [Linga et al, 2012, Kumar et al, 2013, Kang et al, 2010]. Stirred tank reactor (STR) system is one of the arrangements to increase the Hydrate Formation rate as compared to the quiescent condition. However, certain limitations such as the stirring cost negatively influence the feasibility of using STR systems for Hydrate Formation [Linga et al, 2010]. Compared to STR systems, Fixed bed reactor (FBR) systems are having economical

operations (there is no stirring) and they help in providing a large surface area for Gas-liquid contact [Linga et al, 2012, Kumar et al, 2013]. So there is a requirement in evaluating the performance of the fixed bed reactor (various fixed bed media) with respect to an agitated tank container for CO_2 Hydrate Formation. To overcome the mass transfer limitation, FBR can be employed to enhance kinetics of Hydrate Formation.

Chun-Gang et al, 2014 in the study have explained Hydrate based separation of CO_2 from Gas mixture containing CO_2. It is considered as one of the novel technology to reduce the anthropological release CO_2 into the atmosphere. The article has critically discussed CO_2 Hydrate Formation equilibrium conditions, various Hydrate promoters, molecular level measurement methods and various equipments for Hydrate based CO_2 separation technologies. A novel computation model combining conventional model have been developed for more accurate prediction. Either kinetic additive or thermodynamic additive can solve all problems related to Hydrate based CO_2 separation hence combination of additives have been developed.

Jiafei et al, 2012 has discussed the exploitation of CH_4 from Natural Gas Hydrates by CO_2. It has given the latest information on the feasibility of replacement of CH_4 from Natural Gas Hydrate by CO_2 from kinetic and thermodynamic angle by experimental and simulation approach. The multistate simulation combined the phase field theory and molecular dynamic for analysing the replacement microscopic mechanism. The factor influencing replacement reaction is mainly phase of CO_2, initial temperature and pressure and additives. The efficiency of this replacement can be improved by further studying in this area.

Igboanusi et al, 2011 has discussed the global geographical distribution of Gas Hydrates and their occurrence. Particularly, it has explained the presence of Hydrates on the Nigerian continental shelf. The various aspects of Hydrate like Hydrates as potential energy resource, climate change, and ocean floor instability for large scale CO_2 sequestration have been discussed. The Nigerian Hydrates are biogenic in origin. At present Nigeria has no national program for Natural Gas Hydrates exploitation as other countries like USA, Japan, and India.

Sun et al, 2011 has discussed various Hydrates based technologies. Hydrates are considered to separate components of Gas mixtures like capturing greenhouse Gases, capturing organic contaminants, capturing hydrogen from mixture of hydrogen and light hydrocarbon, capturing Methane from coal bed, for separating ethane and Methane. Comparable to conventional

separating techniques this technique is more efficient. The only drawback of this technology is requirement of high pressure due to which it is not viable commercially. Additives are used to resolve this issue to some extent. They are considered for Methane Gas storage, due to their high safety and storage capacity, Hydrates are commercially appealing. Drawbacks of this technique are: Rate of Formation is slow, large amount water remains un-reacted, Problems regarding reliability, Economical aspect. Surfactants and additives are added to improve the Hydrate Formation rate.

Yanhong et al, 2013 in their study has discussed Hydrate based carbon dioxide capture (HBCC), technology is one of the best ways for CO_2 capture and storage. In this process Carbon Dioxide is stored in solid form. Carbon Dioxide requires lowest pressure at 270 K for combining with water cavities, hence it has highest affinity among above other Gases. So, Carbon Dioxide can be captured through Hydrate based technology. Carbon dioxide capture process based on Hydrate technology involves two separate processes for recovery and disposal. Carbon Dioxide from flue Gas, synthesis Gas and bioGas or Natural Gas can be separated using this technique. In recovery process these Gases are fed to Hydrate reactor which also gets water input and here water and Carbon Dioxide Hydrate are formed and sent to decomposing reactor and remaining Gases are sent for further processing. In decomposing section Carbon Dioxide is separated and recovered, water and slurry are recycled to Hydrate reactor. In disposal process, Gases containing Carbon Dioxide are fed to Hydrate reactor where Carbon Dioxide Hydrates are formed and like in recovery process remaining Gases are sent for processing. Additives are used for moderating Formation of carbon dioxide Hydrate. Additives used are Tetrabutyl ammonium salts of fluoride (TBAF), Tetrabutyl ammonium salts of chloride (TBAC), Tetrabutyl ammonium salts of bromide (TBAB) and other quaternary ammonium salts with low concentrations. Capturing process has problems related to pressure and kinetics which are to be taken into consideration and need to be studied further. Along with these, efficiency needs to be improved which depends on various factors including pressure-temperature, hydration rate of carbon dioxide, energy needed for process.

Wei et al, 2009 has explained various separation techniques for separating carbon dioxide from mixture of Gases. Being heaviest molecule of mixture, carbon dioxide can be separated by cryogenic distillation but it's a costly technique. Industrially absorption method is used for separating carbon dioxide. Various studies have been carried out to develop new techniques for

pre-combustion and post-combustion capture of carbon dioxide which are based on adsorption, ammonia carbonation, absorption, distillation, Hydrate Formation, membrane diffusion etc. Carbon dioxide capture through adsorption is a common thing. In this process emissions in Gas phase are not generated. Various adsorbents like Amine-immolated on MCM-41, SBA-15, Zeolite 13 X, Beta-zeolite, and Amine modified activated carbon FeZSM-5 etc. are used. Problems related with adsorption processes are Carbon dioxide adsorption capacity (CAC) and pore volume is reduced due to amine impregnation which leads to plugging of supporting pores. These adsorbents have lower CAC than 13X zeolite. Nitrogen oxide adsorption which is irreversible occurs. Carbon dioxide can be captured by solid sorbents like re-generable sodium carbonate, lithium Silicate etc. Besides these other techniques like electrochemical pumps, electrically supported absorption are observed. The Hydrate based separation of CO_2 seems very attractive but the requirement of high pressure for the Formation of Hydrates makes it less efficient. Further research is needed in order to make novel technique like CO_2 Sequestration of Gas Hydrate Formation economic and commercial.

Zeolite has been used in the past for capture of CO_2. Zeolite has found a place in the field of CO_2 capture, mainly as a solid adsorbent. It has been reported in literature that aluminoSilicate zeolites have large potential for CO_2 uptake owing to an idealized Silica lattice with large free volume [Kim et al, 2012]. A number of studies have been reported in literature for different types of zeolite as solid adsorbents for CO_2 capture [Chen et al, 2014, Lu et al, 2008, Hicks et al, 2008]. Additionally, zeolite imidazole frameworks have been used as novel MOFs to capture CO_2 [Banerjee et al, 2008, Banerjee et al, 2009, Phan et al, 2010]. In the field of Gas Hydrates, zeolites haven't been studied to a large extent. However, the effects of different types of Zeolite: 3A, 5A and 13X on Methane Hydrate Formation have been reported in the literature [Kim et al, 2015, Park et al, 2012, Zang et al, 2009].

Kim et al, 2015 have studied the role of Zeolite 5A and 13X as promoters for Methane Gas Hydrate Formation and concluded that 13X resulted in the highest Gas consumption, but thermodynamically they are not influencing Hydrate Formation [Kim et al, 2015]. Park et al, 2012 have investigated the Formation of CH_4 Hydrate in the presence of Natural zeolite and synthetic zeolite 5A and proved that both the compounds act as Gas Hydrate promoter, but the Gas consumption was more in the presence of 5A zeolite [Park et al, 2012]. Zang et al, 2009 has carried out Methane Hydrate Formation in water adsorbed zeolite and they have concluded

certain zeolite promote Gas Hydrate Formation rate [Zang et al, 2009]. However, it was not clear from their study [Kim et al, 2015, Park et al, 2012, Zang et al, 2009] whether the enhanced Hydrate Formation rate was due to better water to Gas contact as observed by Kumar et al, 2013 in Silica Gel or Zeolite indeed has induced some catalytic effect on Hydrate Formation.

There has been no study on carbon dioxide Hydrate Formation in the presence of zeolites in the literature as of now to the best of the author's knowledge so it was decided to address this issue which may lead to the development of this novel technology for carbon dioxide capture leading to reduction in greenhouse effect.

2.19 Biosurfactant as a Promoter of Methane Hydrate Formation

Gases present in Gas Hydrates are formed by group of *coccoid* and *bacilli archaea* known as methanogens or by thermal decomposition of organic matter [Demirbas, 2010]. Gas Hydrate Formation in a quiescent pure water-Gas system involves clustering of water molecules by hydrogen bonding in liquid phase and subsequently occluding Gas until a cluster of critical concentration and size is formed. This determines the critical nuclei for Formation of Hydrate. Following the induction, depending upon the system condition, agglomeration of nuclei takes place at water-Gas interface resulting in the Formation of a thin Hydrate film on the surface. The thin Hydrate film present on surface isolates the bulk water from Gas, thereby drastically slowing the rate of Hydrate Formation.

The viability of utilizing Gas Hydrates for various aforementioned industrial purposes has long been an exciting area of work for various researchers. Despite the plethora of efforts to develop Hydrate-based technology, none has been effectively set up for real world application. The two main hurdles inhibiting successful commercialization of Gas Hydrate are slow rate of Formation and low storage volume [Wang et al, 2012]. One of the major technical difficulties undermining the efforts is to devise a procedure to form Gas Hydrates at significantly high rates [Okutani et al, 2008 , Okutani et al, 2007]. Inadequate interfacial interaction between a Gas–solid or Gas–water slows the rate of Gas Hydrate Formation [Okutani et al, 2008, Saw et al, 2014]. Improving the interfacial interaction between Gas-water phases can improve Gas Hydrate storage and generation. Several methods have been reported for enhancing the Gas Hydrate Formation rate and capacity by increasing the interfacial contact between liquid water (or solid ice) and the Gas which ranges from energy intensive process like agitation (vigorous mixing) and application of

high pressure [Kuhs et al, 2000, Saw et al, 2014] to simple methods like use of chemical additives [Moraveji et al,2010, Saw et al, 2014, Rogers et al, 2007] and supports system has been favoured by several research groups as energy affordable options for enhancing Gas Hydrate Formation [Linga et al, 2012, Kumar et al, 2013, Chong et al, 2015, Okutani et al, 2008]. Mechanical agitation is an energy intensive process, thus the use of chemical additives is preferred. Synthetic surfactants as a chemical additive can enhance Hydrate Formation rate by increasing Gas solubility, supporting micelle Formation and providing the nucleation sites for Hydrate Formation [Moraveji et al, 2010, Saw et al, 2014, Saw et al, 2013, Saw et al, 2014, Mandal et al, 2008, Masakorala et al, 2010]. The use of surfactants, such as sodium dodecyl sulphate (SDS), Tergitol [Zhong et al, 2000, Saw et al, 2014, Zhang et al, 2007, Yoslim et al, 2010] and support system like Silica sand, bentonite clay [Kumar et al, 2013, Linga et al, 2012, Saw et al, 2014] has been favoured by several research groups as energy favourable options for enhancing Gas Hydrate Formation. Very often combinations of methods have been applied for enhancing the Gas Hydrate Formation [Kumar et al, 2013, Kumar et al, 2015]. However, successful industrial exploitation of Hydrates for transit and storage of Natural Gases has been hindered due to slow Formation rate [Wang et al, 2012]. The main cause for slow Gas Hydrate generation is low solubility of Methane Gas in water. This restricts the proper interaction of water and Methane molecules, one of the important requirements for Gas Hydrate Formation [Wang et al, 2012]. Enhancing the rate of Hydrate Formation by surfactants can have tremendous influence on commercialization prospect as this can facilitate the conversion of Natural Gas into solid Hydrates useful for storage and transportation of solid NGH.

Recently anionic surfactant sodium dodecyl sulphate (SDS) has been used along with the fixed bed system for reducing the induction time and hasten the carbon dioxide Hydrate growth. Kumar et al, 2015 and Link et al, 2003 reported that the best surfactant available for accelerating the rate of CH_4 Hydrate Formation is sodium dodecyl sulphate (SDS). However, toxicity associated with a synthetic surfactant such as SDS cannot be ignored [Forni et al, 2012, Arechabala et al, 1999] and thus, necessitating the search for environmentally compatible surfactant. Use of synthetic surfactant such as sodium dodecyl sulphate (SDS), sodium tetradecyl sulphate (STS), sodium hexadecyl sulphate (SHS) in a Natural environment for enhancing NGH generation could be a cause of concern as they have been reported to possess toxic effects for living organisms [Michael et al, 1991, Banat et al, 2014].

Desire to have environmentally compatible surfactants has propelled the search for substitutes of biological origin. Substituting synthetic surfactants with surface active agents of biological origin can provide environment-friendly means for enhanced NGH generation. Surface active agents of biological origin are commonly referred as biosurfactant and often considered as next generation surfactants. They are better than synthetic counterparts for their low toxicity, biodegradability, higher selectivity, specific activity, environment-friendly nature, stability at extreme conditions like pH, temperature, salinity and the ability to synthesize them from renewable substrates, [Muller et al 2012, Banat et al, 2014, Bezza et al 2014] and effectiveness even in extreme environmental conditions [Muller et al, 2012]. Another advantage associated with biosurfactant is their ability to be produced from alternative substrate such as agro and industrial wastes. This approach not only reduces the pollution associated with these wastes, but also reduces the production cost and thus making biosurfactant economically viable [Pacwa-Plociniczak et al, 2011]. Properties of biosurfactants have been explored for varieties of application ranging from simple household cleaning process to sophisticated enhanced oil recovery [Muller et al, 2012, Randhawa et al, 2014, Pacwa-plociniczak et al 2011, Singh et al 2013].

Biosurfactants are a diverse collection of amphipathic molecules generated by microorganisms like fungi, bacteria and yeast. Increasing environmental concerns, advancement in biotechnology and the development of more strict rules have drawn attention of researchers and policy-makers towards biosurfactants. Among all known biosurfactants, rhamnolipids is one of the most widely investigated microbial surfactants [Muller et al, 2012]. Rhamnolipids are surface-active glycolipids produced by bacteria belonging to various classes, namely *Actinobacteria, Bacilli, Betaproteobacteria, Deltaproteobacteria, and Gammaproteobacteria* [Abdel-Mawgoud et al, 2010]. Lanoil et al, 2001 reported presence of *Gammaproteobacteria* leading to generation of Rhamnolipids in the Gulf of Mexico Gas Hydrates samples and proposed direct association between microbes and Gas Hydrates. Lanoil et al, (2001) also reported the presence of *Firmicutes* like *Bacillus Subtilis* leading to generation of Surfactin in the Gulf of Mexico Gas Hydrate samples and proposed direct association between microbes and Gas Hydrates. These microbes and their metabolites are expected to have properties to overcome hurdle associated with the successful commercialization of Natural Gas Hydrates [Rogers et al, 2003].

The surfactants of biological origin have also been used in the fixed bed system for accelerating the rate of Gas Hydrate Formation rate [Wang et al, 2012, Rogers et al, 2003, Carvajal et al,

2013]. Microorganisms have been detected in Natural Gas Hydrate samples, thus propelling the researchers to believe that their metabolic competence may have an influence on the Gas Hydrates generation [Lanoil et al, 2001, Zhang et al, 2007] and may also provide means for overcoming the hurdles associated with commercial exploitation of Gas Hydrates [Rogers et al, 2003]. Very few studies pertaining to the influence of biosurfactants on NGH Formation have restricted our knowledge and thus, limiting the potential application of biosurfactants in Gas Hydrate generation, storage and transportation [Rogers et al, 2003, Rogers et al, 2003, Woods, 2004]. Moreover, the studies have largely concentrated on kinetics and related parameters [Rogers et al, 2003, Carvajal et al, 2013, Zhang et al, 2007, Woods, 2004]. Influence of microbial surfactant like rhamnolipids and surfactin on thermodynamics of Gas Hydrate Formation has not been reported in literature.

Microorganisms and their metabolites like biosurfactants have been expected to influence the Gas Hydrate Formation at Natural sites as well as possess property to overcome the obstacle associated with the successful commercialization of Gas Hydrates [Lanoil et al, 2001, Rogers et al, 2003].

2.20 Influence of Biosurfactant as Inhibitor on Formation of Natural Gas Hydrate and Methane Hydrate

Gas Hydrates create a lot of problems for flow of materials in oil and Gas industries. Gas Hydrate may lead to many hazards including plugging of oil/Gas pipelines They are formed within the pipeline and obstruct the flow [Hammerschmidt et al, 1934, Kelland, 2006, Englezos, 1996, Sloan et al, 2008, Sloan et al, 2009, Sloan, 2011, Kelland et al, 2009, Villano et al, 2010]. Their Formation may lead to explosion and lead to environmental threats. The explosions caused in the pipelines can lead to environmental and economic damage. So, it is necessary from economic, safety and environmental point of view to prevent their Formation.

In general, industry adds a large quantity of thermodynamic inhibitors such as methanol or glycols (20−50 wt. %) while Gas is being produced to avoid Hydrate Formation. These compounds shift the Natural Gas Hydrate equilibrium conditions to low temperatures and high pressures, but this method is costly because of requirement of high concentrations of thermodynamic inhibitors in aqueous phase to stop the Formation of Gas Hydrates in offshore developments [Sloan et al, 2008, Koh, 2002]. Prolonged induction time allows transit of fluids

from place of origin to the processing plants without crystallization of Hydrates in the system and such additives are regularly used in oil and Gas industry as Hydrate inhibitors [Kashchiev et al, 2003].

It is approximated that yearly operating costs can be more than $500,000,000 to stop the Formation of Hydrates by using thermodynamic inhibitor (methanol) injection [Lederhos et al, 1996].

Due to this reason the research in Gas Hydrates has shifted towards low dosage (<1 wt. %) kinetic inhibitors (LDHI). Generally, KHI are polymeric compounds which are soluble in water and stop or prevent Formation of Hydrates. A large number of different polymers like Polyvinylpyrrolidone (PVP), Polyvinylcaprolactam (PVCAP), Polyethylene oxide (PEO) etc. have been investigated as kinetic Hydrate inhibitors (KHI) [Kelland, 2006, Freer et al, 2000]. The Formation of Hydrates is not completely stopped by these chemicals but they postpone the Formation of Hydrate in pipelines when they go through Hydrate sensitive zone. These also include homo- and copolymers of the N-vinyl caprolactam (PVCAP) and N-vinyl pyrrolidone (PVP).

Although these compounds are successful at extremely low concentrations but because of their inferior biodegradability they are not authorised to be used in all regions (for example the North Sea) and they put environmental impacts which demanded an investigation for new environmentally favourable Hydrate inhibitors [Del et al, 2008, Daraboina et al, 2011]. Moreover, recently surfactants toxicity test was carried out on a marine alga called *skeletonema costatum* the results of the same have motivated industry to use green biodegradable environment-friendly inhibitor, so, a new class of green inhibitor i.e. Antifreeze proteins are used as kinetic Hydrate inhibitors these days. Recent investigations have proven that antifreeze proteins (AFP) are a suitable candidate for Green kinetic Hydrate inhibitor [Ohno et al, 2010, Daraboina et al, 2011, Daraboina et al, 2013].

Antifreeze proteins Type I (AFP) [Zeng et al, 2006] from *winter flounder, longhorn Beetle,Rhagium Mordax(RmAFP1)* [Perfeldt et al, 2014], Biological Type III (AFP) [Daraboina et al, 2011], can have significant effect on the Formation of C_3H_8 Hydrate and CH_4 Hydrate .Also, AFP can eradicate the “memory effect” in the reformation of Gas Hydrate. AFP-based polymers and polyaspartamides have also been studied for their ability to delay Hydrate

induction time in flow loops and autoclave chamber [Daraboina et al, 2011, Townson et al, 2012, Del et al, 2008].

Daraboina et al, 2013 have investigated the Formation and Dissociation of the Natural Gas Hydrates in the presence of Luvicap which is a kinetic inhibitor. Luvicap's performance was also studied under the effect of Sodium Chloride (NaCl) and poly ethylene oxide (PEO). The presence of PEO and NaCl promoted the nucleation inhibition of Luvicap. PEO has not affected the growth of Hydrate whereas NaCl can reduce the Hydrate growth both in presence as well as absence of Luvicap.

Kumar et al, 2008 has studied the morphology of Methane/propane Hydrates in presence of the kinetic inhibitor Poly (N-vinylpyrrolidone) or PVP on CH_4 or C_3H_8 Hydrate Formations. It was revealed that at the inhibitor concentration 0.1 wt. %, Hydrate Formation initiated as a film at the Gas/water interface matching the crystal behaviour without inhibitor. At the inhibitor concentration 0.5 wt. % Hydrate Formation was found at the wall above the Gas/water interface and at the Gas/water interface also. But, for inhibitor concentration 1.0 wt. %, the Hydrate began to form from water droplets adhered to the wall above the Gas/liquid interface and grew catastrophically.

Cha et al, 2013 have studied the influence of the concentration of kinetic Hydrate inhibitors, Polyvinylcaprolactam (PVCAP) and Polyvinylpyrrolidone (PVP) on the commencement and increase of synthetic Natural Gas Hydrates. When the concentration is increased from 0.5 to 3.0 wt. % the Hydrate onset time is prolonged PVP and PVCAP.

Daraboina et al, 2011 has also studied the effect of kinetic inhibitors, both biological (type III antifreeze protein) and chemical (PVP and H1W85281), on Natural Gas Hydrate Formation using high pressure differential scanning calorimetry (HP-DSC). When Hydrate inhibitors were not used the first nucleation event was seen after 48 minutes which was delayed by almost 10-20 minutes in the presence of AFP and PVP and more than 1.5 h with H1W85281.

Perfeldt et al, 2014 have reported that insect antifreeze protein from the *longhorn beetle, Rhagium mordax* (RmAFP1) can inhibit CH_4 Hydrates to the same effect as the synthetic polymeric inhibitor Polyvinylpyrrolidone (PVP).

Gordienko et al, 2010 has shown that antifreeze proteins (AFP) are capable to change the structures II (sII) tetrahydrofuran (THF) Hydrate crystal morphologies by binding to the Hydrate surface and inhibits the growth in a same way as the kinetic inhibitor poly-Nvinylpyrrolidone (PVP). The influence of AFP on the Formation and growth rate of high-pressure sII Gas mix Hydrate revealed that at AFPs are better Hydrate inhibitors compared to PVP.

Zeng et al, 2003 have reported that *Pleuronectes americanus* (winter flounder) antifreeze protein increases the induction time of THF Hydrate Formation as compared to PVP.

Zeng et al, 2006 also found that *Choristoneura fumiferana* (an insect AFP) is better than PVP in inhibiting THF Hydrate Formation.

Gilbert et al, 2005 reported a powerful bacterial AFP found in an Antarctic strain of the bacterium, *Marinomonas primoryensis.* It is Ca^{2+} dependent and has shown evidence of providing over 2 degrees Celsius of freezing point depression. Unlike AFP, it does not produce obvious crystal faceting during thermal hysteresis. This AFP might be capable of imparting freezing avoidance to *M. primoryensis* in ice-covered Antarctic lakes.

A lot of research is going on various types of Inhibitors for Gas Hydrate Formation but still the problem of inventing economic green biodegradable inhibitor has still not been attempted as using AFP is not economically viable. Inhibitors have to be flora and fauna friendly. So there is a strong motivation in attempting research for inventing economic green biodegradable inhibitor. So, keeping this into view lignin an abundant biomass was investigated as inhibitor which is very economical and has never been claimed to be an inhibitor for Gas Hydrate Formation to the best of author's knowledge so far in literature. Lignocellulosic materials are attractive due to their renewability and availability. It is found to be effective, economic, green and biodegradable inhibitor for Methane and Natural Gas Hydrate and has potential of replacing synthetic polymer which have environmental issue and antifreeze protein which are very very costly inhibitor currently used by oil and Gas industry.

2.20.1 *LignoSulphonates*

LignoSulfonates or Sulphonated lignin which are by-products of the paper and pulp industry and reported to be used as inhibitor for the Formation of Natural Gas and Methane Hydrates Formation in present study. Different chemical pulping processes yield different types of lignin

wastes [Hill Bembenic, 2011]. Herein, we claim, to the best of our knowledge, for the first time about using Lingo Sulfonate (LS), an inhibitor obtained from biomass to inhibit Formation of Natural Gas and Methane Hydrates with prolonged induction time which may generate a great influence on the practical application of inhibition of Gas Hydrates in pipelines from both the environmental and economical points of view. Worldwide production of LS is 9.8×10^5 tons per year [Gargulak et al, 1999]. The renewable nature of LS makes them specifically appealing for probable commercial applications in the future. The immense range of molecular mass of LignoSulphonate varies from few thousands to lakhs. The commercial LignoSulphonate contains 30% carboHydrates (reducing sugars).

2.20.2 *Calcium LignoSulphonate (CaLS)*

In these mixtures, metal cation such as of Calcium substitutes the hydrogen in the sulphonic group. Calcium LignoSulphonate is obtained using the sulphite pulping process of the softwood and is an amorphous light- yellow- brown powder. The average weight estimated for the Calcium LignoSulphonate is within the range of few thousands to few lakhs with greater than 90% ranging from 1,000 to 250,000 (Risk assessment report). It is soluble in water but insoluble in the organic solvents The framework of Calcium LignoSulphonate i.e. the basic units of the polymeric structure consist of three aromatics i.e coniferyl alcohol [4-(3-hydroxy-1-propenyl)-2-methoxyphenol], p-coumaryl alcohol [4-[(E)-3-hydroxyprop-1-enyl]phenol] and sinapyl alcohol [4-(3-hydroxyprop-1-enyl)-2,6-dimethoxyphenol] of which coniferyl alcohol represents the principle unit in lignin.

2.21 Gaps Identified

1. The energy intensive mechanical agitation processes used for Gas Hydrate Formation needs to be replaced by less energy intensive process using fixed bed media.
2. The synthetic surfactants used for Gas Hydrate Formation are toxic and not environment-friendly so there is an immediate need of replacing these synthetic surfactants with green biodegradable biosurfactants which can address environmental issues.
3. At present few synthetic polymer and anti-freeze proteins (AFP) are used as inhibitors for Gas Hydrates Formation. The synthetic polymer are not environment-friendly and AFP

are very expensive so, there is a need of low dose, economic, green biodegradable inhibitor for Gas Hydrates Formation.

2.22 Objectives of Present Study

1. To investigate different fixed bed media of Zeolite 5A, Zeolite 13X and Silica Sand to form carbon dioxide Hydrates in order to design an economical and less energy intensive fixed bed media for Hydrate Formation

2. To compare the performance of fixed bed media of C type Silica Gel (5 nanometer (nm)), Silica Gel (100 nm), C type Silica Gel (5nm) with Blend of Zeolite 3A and 5A ,Silica Sand with stirred tank reactors for Carbon Dioxide Hydrate Formation which can replace the expensive and energy intensive mechanical agitation used for Gas Hydrate Formation. So that the Hydrate technology can be used economically for applications such as carbon capture.

3 To synthesise the biosurfactant i.e. Rhamnolipids from strain A11 and characterise it with modern sophisticated techniques like TLC, FTIR, NMR, LC-MS, MALDI.

4. To synthesise the biosurfactant i.e. Surfactin from strain A21 and characterise it with modern sophisticated techniques like as TLC, FTIR, MALDI, NMR, AAS, HPLC.

5. To synthesize Methane Hydrates using above synthesized biosurfactant i.e. Rhamnolipids and Surfactin in presence of fixed bed media of C type Silica Gel for investigating the thermodynamics and kinetics behaviour of Methane Hydrate which can help in replacing the toxic, non-environment-friendly synthetic surfactants used at present for Gas Hydrate Formation.

6. To study the Dissociation behaviour of above formed Methane Hydrates using thermal stimulation technique.

7. To characterise a biosurfactant i.e. Calcium LignoSulphonate (CaLS) used as inhibitor for Methane and Natural Gas Hydrate Formation with modern sophisticated techniques like FTIR, UV, CHNS, ICPMS, GPC, FE-SEM, EDS, FE-SEM Mixing, TGA and NMR.

8. To investigate an economic, low dose, green and biodegradable inhibitor i.e Calcium LignoSulphonate (CaLS) for inhibition of Methane and Natural Gas Hydrate which can

replace synthetic polymers and very expensive low dose antifreeze proteins (AFP) used currently by oil Gas industry for inhibition of Gas Hydrates.

CHAPTER - 3

EXPERIMENTAL PROGRAMMES

3.1 Effect of Different Fixed Bed Media on the Performance of Sodium Dodecyl Sulphate for Hydrate Based CO_2 Capture

Sodium dodecyl sulphate (SDS) is used as a kinetic promoter in Formation of Gas Hydrate. The purpose of this set of experiments was to evaluate the performance of SDS for carbon dioxide Gas Hydrate Formation in two different fixed bed media: Silica sand and zeolite (5A and 13X) has been evaluated. The concentration of SDS was fixed at 0.5 wt. %. The experiments were done in batch mode with the initial pressure fixed at 3.0 MPa, and the temperature was kept constant at 274.65 K. Figure 3.1.1 shows the experimental programme for studying the Effect of Different Fixed Bed Media on the Performance of Sodium Dodecyl Sulphate for Hydrate Based CO_2 Capture.

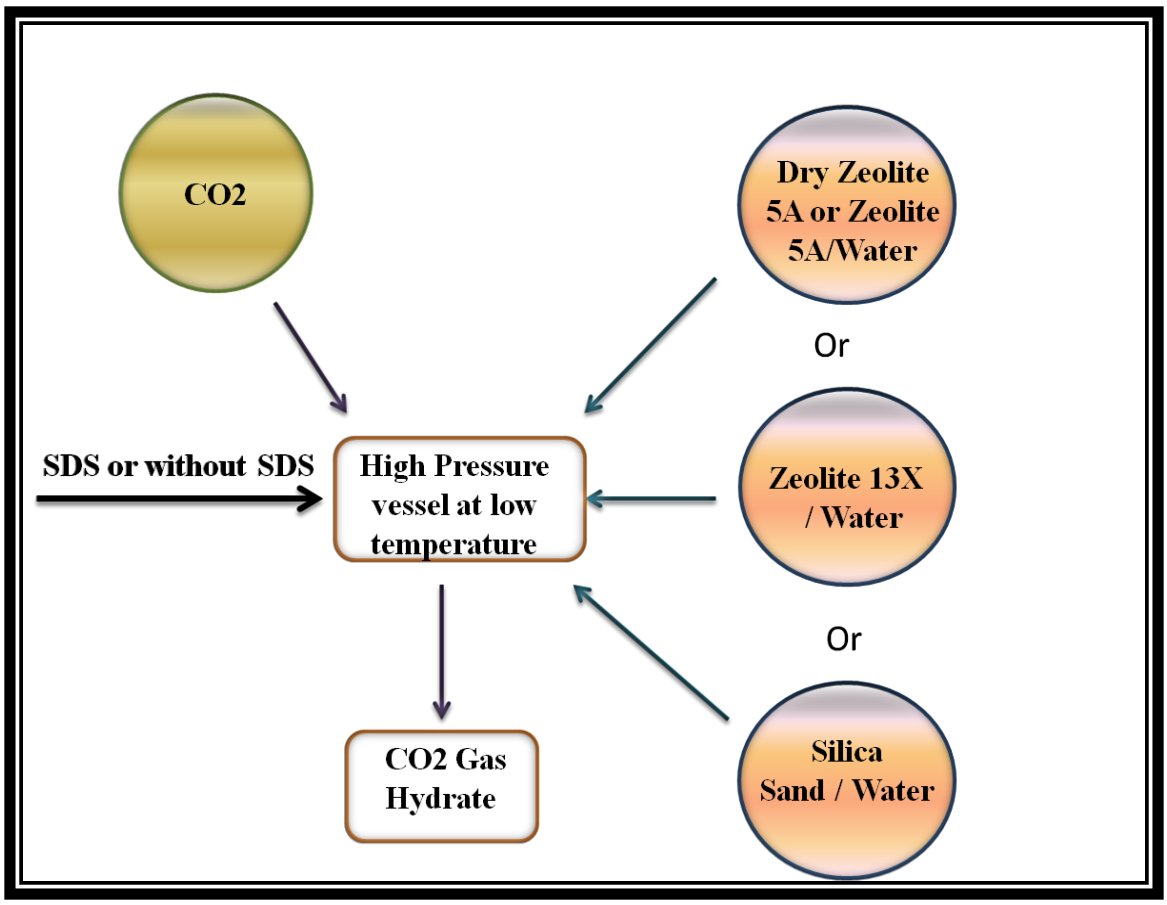

Figure 3.1.1: Effect of Different Fixed Bed Media on the Performance of Sodium Dodecyl Sulphate for Hydrate Based CO_2 Capture

3.2 Carbon dioxide Hydrate Formation in Fixed Bed and Stirred Tank Reactor Systems

The purpose of this set of experiments was to evaluate the performance of various porous media was evaluated in a fixed bed reactor (FBR). In addition to this, Hydrate Formation kinetics of FBR was compared to stirred tank reactor (STR). Carbon dioxide Hydrate Formation experiments were done at a pressure 3.0 MPa and constant temperature of 274.5K. Silica sand, Silica Gel (100 nm and 5 nm pore size) and a blend of Silica Gel (5nm) with zeolite 5A were used as a porous media in FBR. This work will be of interest to those dealing with Hydrate-based CO_2 capture and separation, Natural Gas recovery from Hydrates and storage of CO_2 (CO_2 sequestration). Figure 3.2.1 shows the experimental programme for studying the Carbon dioxide Hydrate Formation in Fixed Bed and Stirred Tank Reactor Systems.

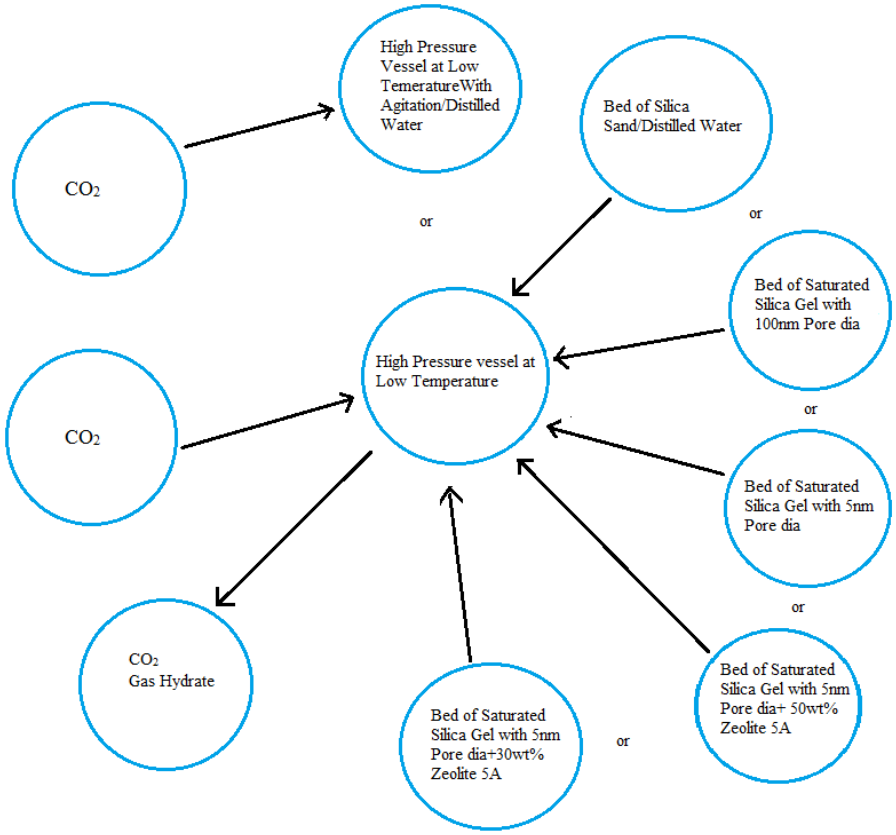

Figure 3.2.1: Carbon dioxide Hydrate Formation in Fixed Bed and Stirred Tank Reactor Systems

3.3 Influence of 3A and 5A Zeolites in Presence of Silica Gel on Carbon Dioxide Gas Hydrate Formation

Gas Hydrate Formation of carbon dioxide containing Gases has been proposed for separating mixtures. In this work, influence of porous medium on Gas Hydrate Formation kinetics has been studied in detail. Silica Gel of mesh size 230-400 and certain percentage of zeolite as a solid additive have been used as a medium of Hydrate Formation from distributed water in its pores. Zeolite 3A (beads) and zeolite 5A (beads) were used with different water saturation experiments amount. This done at 274.15 K temperature and 30 bar pressure. The moles of CO_2 consumed are compared for different cases. Goal of this set of experiments was to study the 100% water saturation and 50% water saturation. Figure 3.3.1 shows the experimental programme for

studying the Influence of 3A and 5A Zeolites in Presence of Silica Gel on Carbon Dioxide Gas Hydrate Formation.

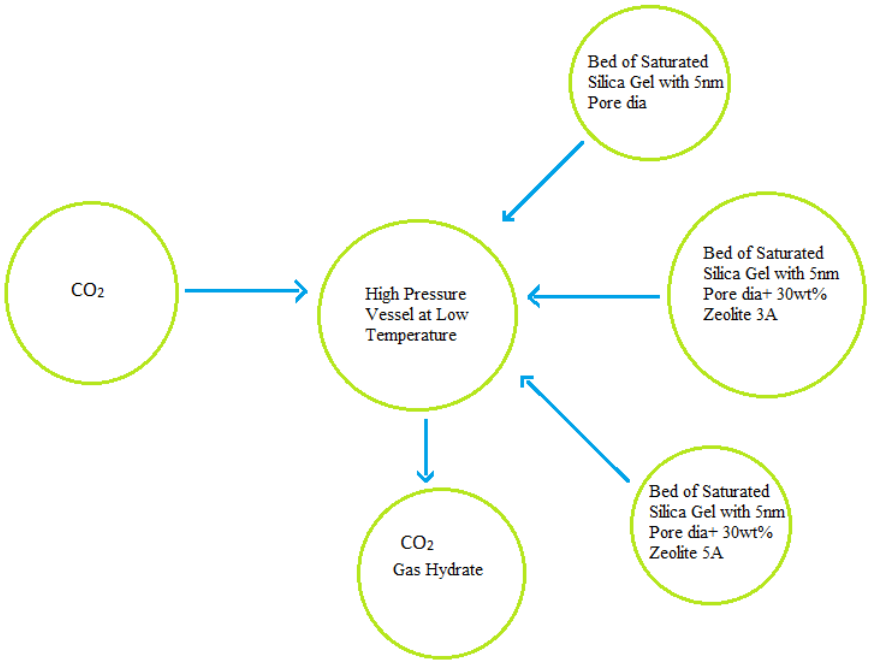

Figure 3.3.1: Influence of 3A and 5A Zeolites in Presence of Silica Gel on Carbon Dioxide Gas Hydrate Formation

3.4 Production of Rhamnolipids from Strain A11 and its Characterization

Figure 3.4.1 shows the experimental programme for studying the Production of Rhamnolipids from Strain A11 and its Characterization.

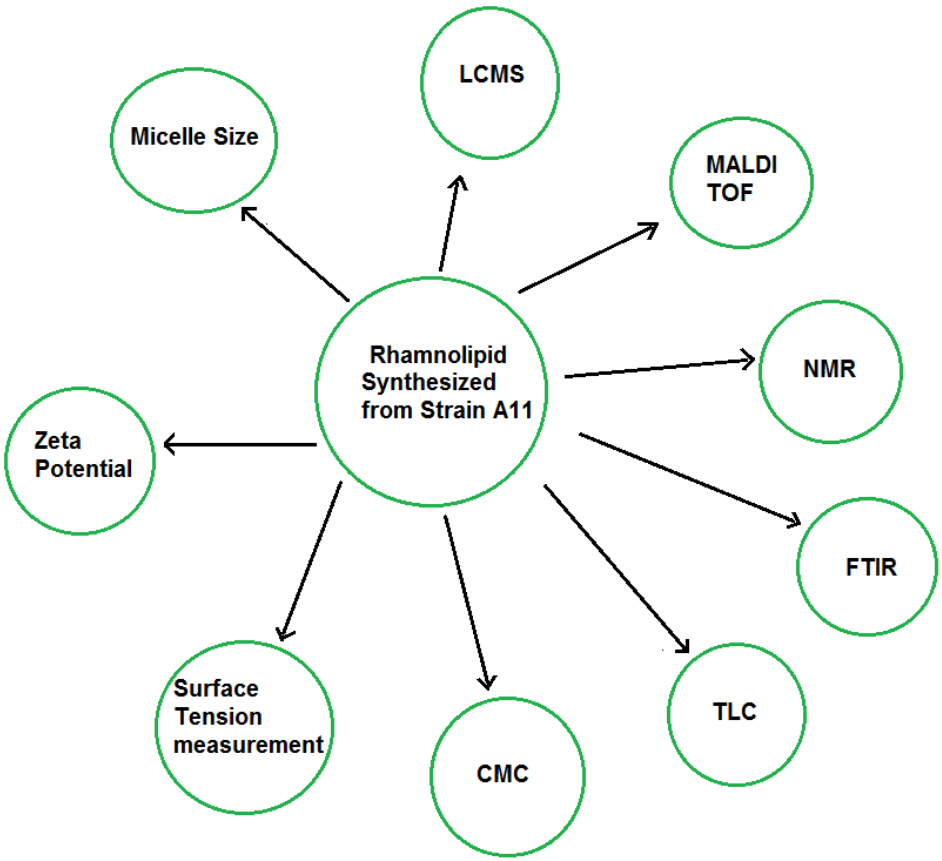

Figure 3.4.1: Production of Rhamnolipids from Strain A11 and its Characterization

3.5 Production of Surfactin from Strain A21 and its Characterization

Figure 3.5.1 Shows the experimental programme for studying the Production of Surfactin from Strain A21 and its Characterization.

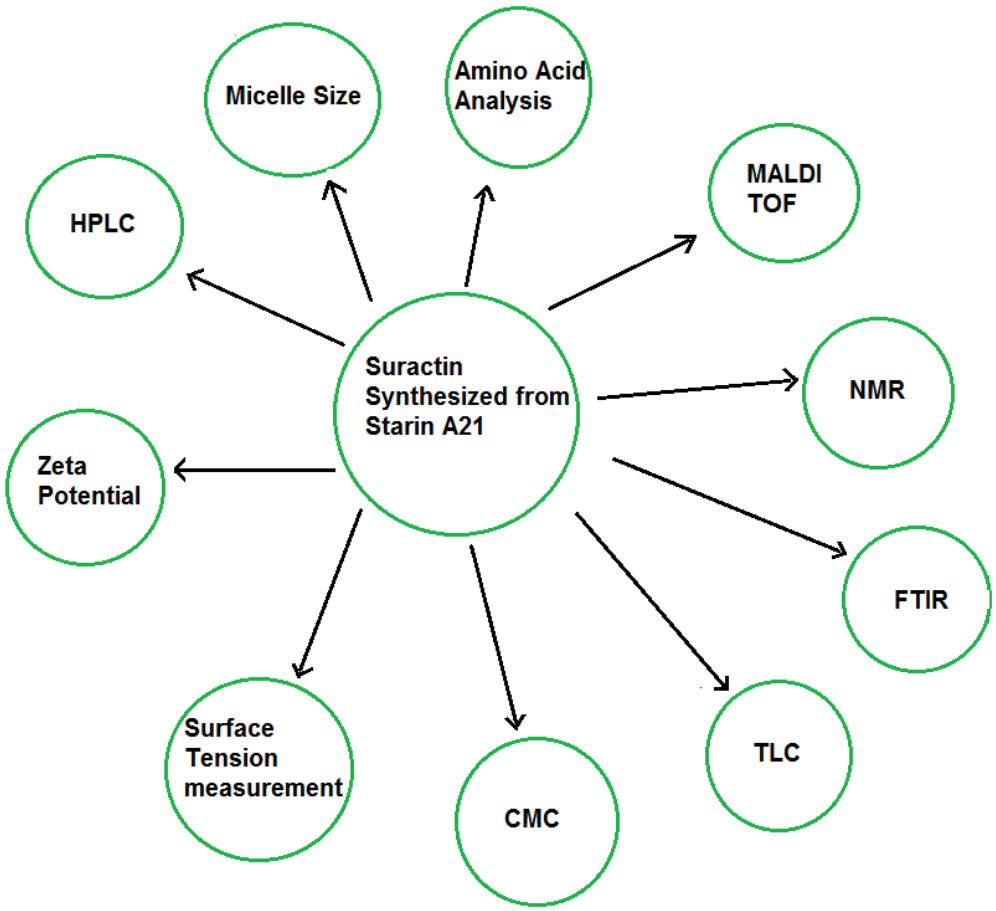

Figure 3.5.1: Production of Surfactin from Strain A21 and its Characterization

3.6 Biosurfactant i.e. Rhamnolipids as a Promoter of Methane Hydrate Formation in fixed bed of Silica Gel: Thermodynamic and Kinetic Studies

The goal of this set of experiment was to explore the feasibility of using glycolipids (Rhamnolipids) type biosurfactant as CH_4 Hydrate generation promoter. Study compares CH_4 Hydrate Formation in the quiescent water and fixed bed system of water saturated C type Silica Gel in the presence of different concentration of biosurfactant. The kinetics and thermodynamics of Gas Hydrate Formation was studied to have a better understanding of the process. The study will also help in understanding the role of microbial secondary metabolites on Methane Hydrate generation at Natural sites. Figure 3.6.1 Shows the experimental programme for studying the Microbial Surfactant Promotes Methane Hydrates Formation in Fixed Bed Porous Silica Gel System.

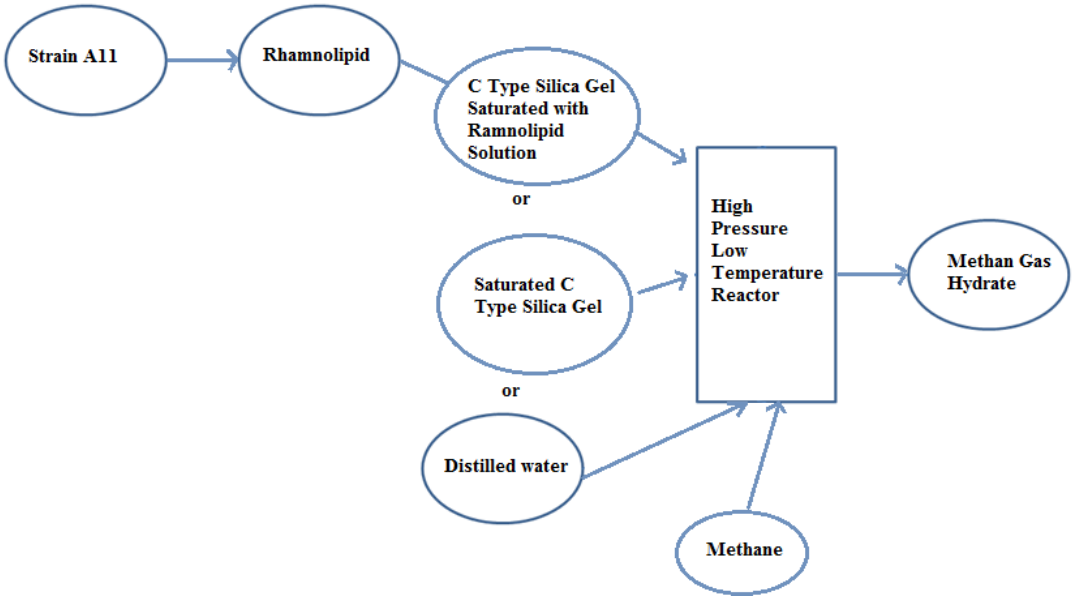

Figure 3.6.1: Microbial Surfactant Promotes Methane Hydrates Formation in Fixed Bed Porous Silica Gel System

3.7 Surfactin a Lipopeptide Biosurfactant Promoting Methane Hydrate Formation in Fixed Bed of Silica Gel: Thermodynamic and Kinetic Studies

The purpose of this set of experiment was to explore the feasibility of using Lipopeptides (Surfactin) type microbial surfactant as Methane Hydrate promoter. Study compares Methane Hydrate Formation in quiescent water and the fixed bed system consisting of Silica Gel in the

presence of different concentrations of biosurfactant. The thermodynamics and kinetics of Gas Hydrate Formation was compared under different aforementioned systems to have a better understanding of the process. Figure 3.7.1 Shows the experimental programme for studying the Role of surfactin as Biosurfactant in Methane Gas Hydrate Formation Kinetics.

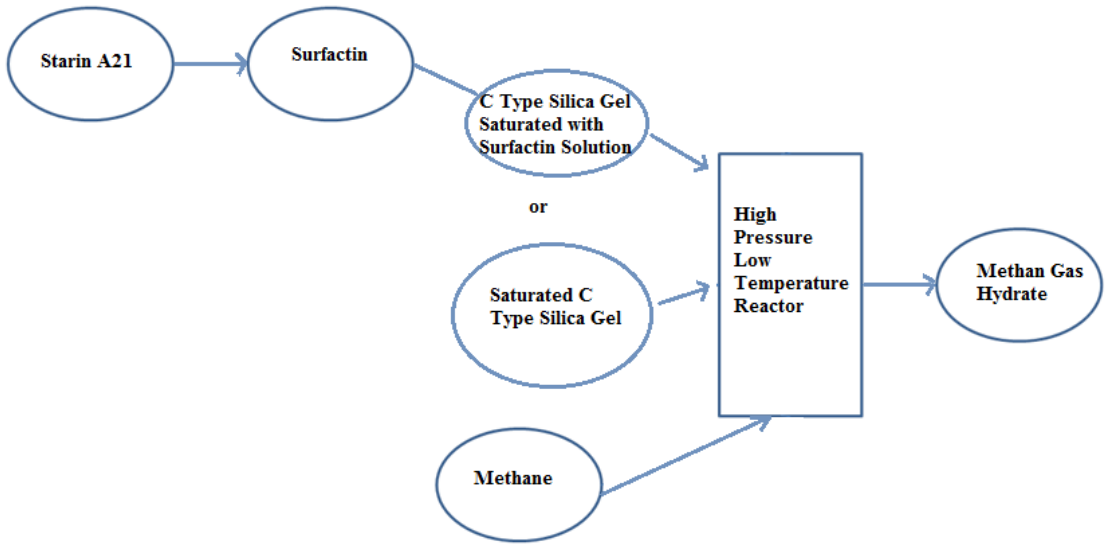

Figure 3.7.1: Role of surfactin as Biosurfactant in Methane Gas Hydrate Formation Kinetics

3.8 Characterization of Biosurfactant Calcium LignoSulphonate (CaLS)

Figure 3.8.1 Shows the experimental programme for studying the Characterization of Calcium LignoSulphonate

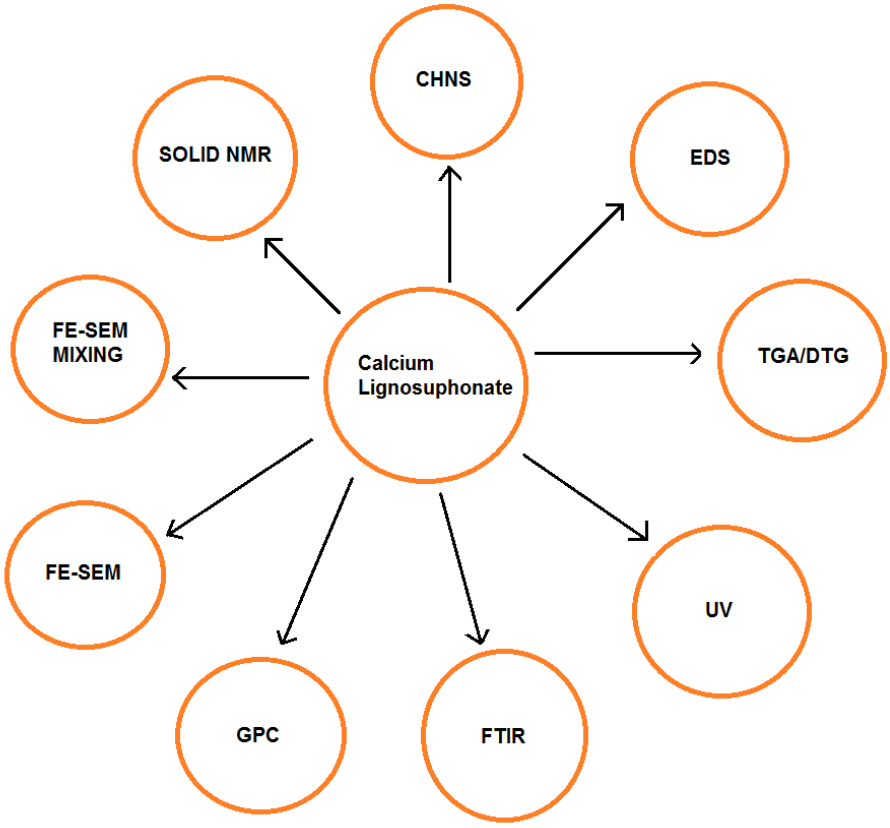

Figure 3.8.1: Characterization of Calcium LignoSulphonate

3.9 Influence of Biosurfactant i.e. Calcium LignoSulphonate as Inhibitor on Formation of Natural Gas Hydrate and Methane Hydrate

The goal of this set of experiment was to investigate the influence of Calcium LignoSulphonate a biosurfactant on the inhibition of Methane and Natural Gas Hydrate Formation. There is strong motivation for moving toward low dosage and green biodegradable economic Hydrate inhibitors. In the present study, we have investigated experimentally a biosurfactant i.e. Calcium LignoSulphonate (CaLS) generated from waste of pulp and paper for inhibiting the nucleation or growth of Gas Hydrate Formation. Different dosage (0, 0.1, 1 and 5 wt. %) of biosurfactant was used in Hydrate Formation in presence of Methane and Natural Gas. The inhibition of CH_4 and Natural Gas Hydrates in Presence of Calcium LignoSulphonate is as shown in Figure 3.9.1. Figure 3.9.1 Shows the experimental programme for studying the Inhibition of Methane and Natural Gas Hydrates in Presence of Calcium Ligno Sulphonate.

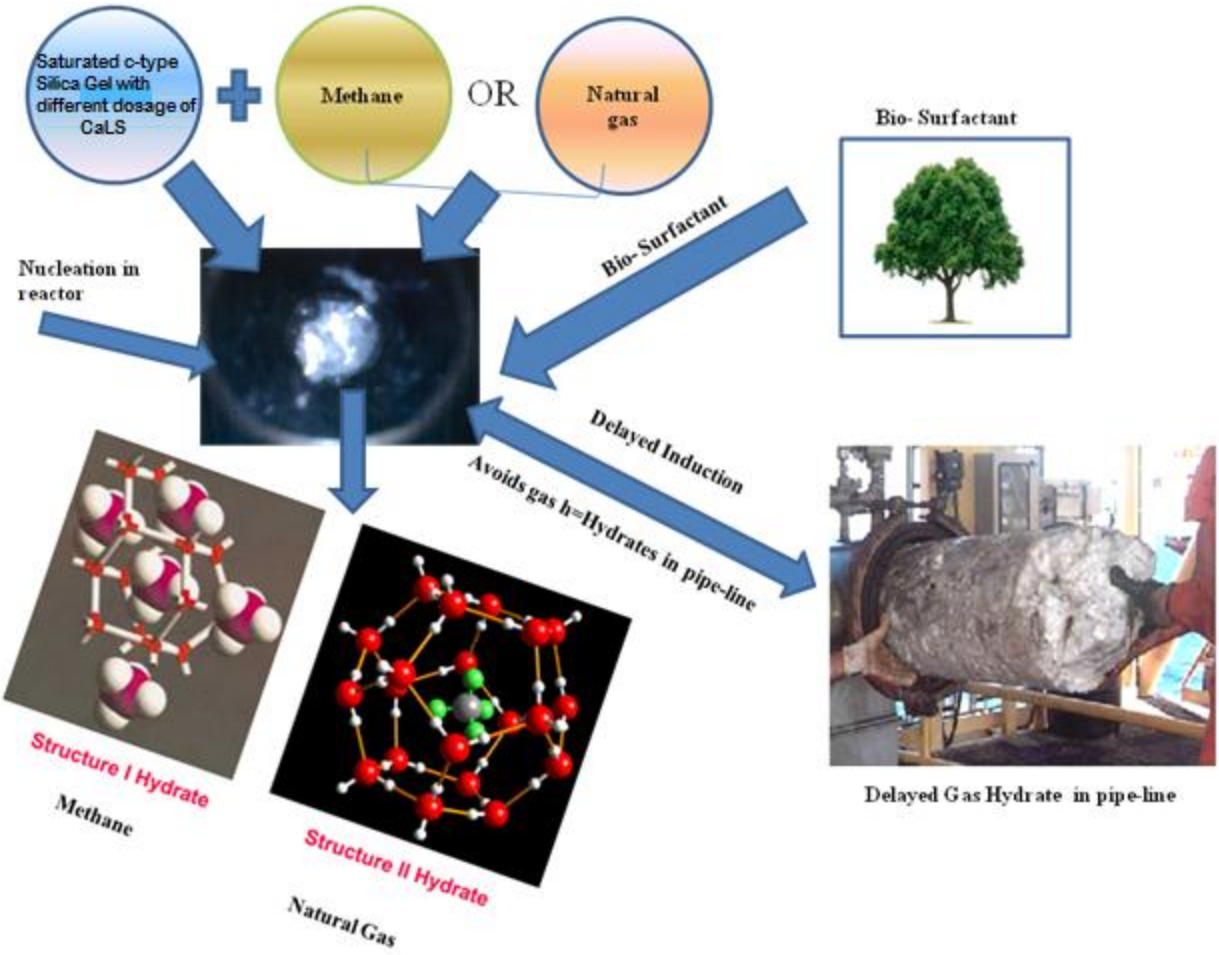

Figure 3.9.1: Inhibition of Methane and Natural Gas Hydrates in Presence of Calcium LignoSulphonate

CHAPTER - 4

EXPERIMENTAL SETUP

4.1 Effect of Different Fixed Bed Media on the Performance of Sodium Dodecyl Sulphate for Hydrate Based CO_2 Capture

4.1.1 *Apparatus and Hydrate Formation procedure*

Line diagram of the fixed bed apparatus is shown in Figure 4.1.1. A fixed quantity of liquid solution (50 cm^3) was used along with a calculated quantity of packing material (Silica sand or zeolite 5A or zeolite 13X) in a 500 cm^3 SS-316 crystallizer (CR). CR was securely sealed and put inside a water bath in which temperature was controlled. The temperature inside the CR was measured using a thermocouple having an accuracy of ±0.1K. CR was flushed with the pure CO_2 Gas (at 274.65 K) by repeating a cycle of pressurization (~ 0.5 MPa) and depressurization before the experiment. The cooling of the CR to the experimental temperature of 274.65 K was achieved by circulating a glycol/water mixture. On reaching the required temperature, the CR was pressurized by pure CO_2 Gas to the pre-determined experimental pressure (3.0 MPa). After reaching this stage, Gas uptake measurements were started. All the Gas uptake measurements were done in batch mode with pure CO_2 at a fixed temperature of ~274.65 K. CR was attached with a pressure transducer having a range of 0-16 MPa and accuracy of 0.075% of the span. Pressure and temperature of the reactor were noted every 5 seconds by a data acquisition system connected to a computer. There is a drop in pressure of the CR when Hydrate Formation takes place as the Gas inside the CR starts to move from the Gaseous phase to the solid Hydrate phase. This was used to measure the moles of Gas engaging in the Hydrate Formation experiment (moles of Gas uptake). An experiment was also carried out with dry zeolite (5A) to evaluate the CO_2 adsorption capacity of zeolite.

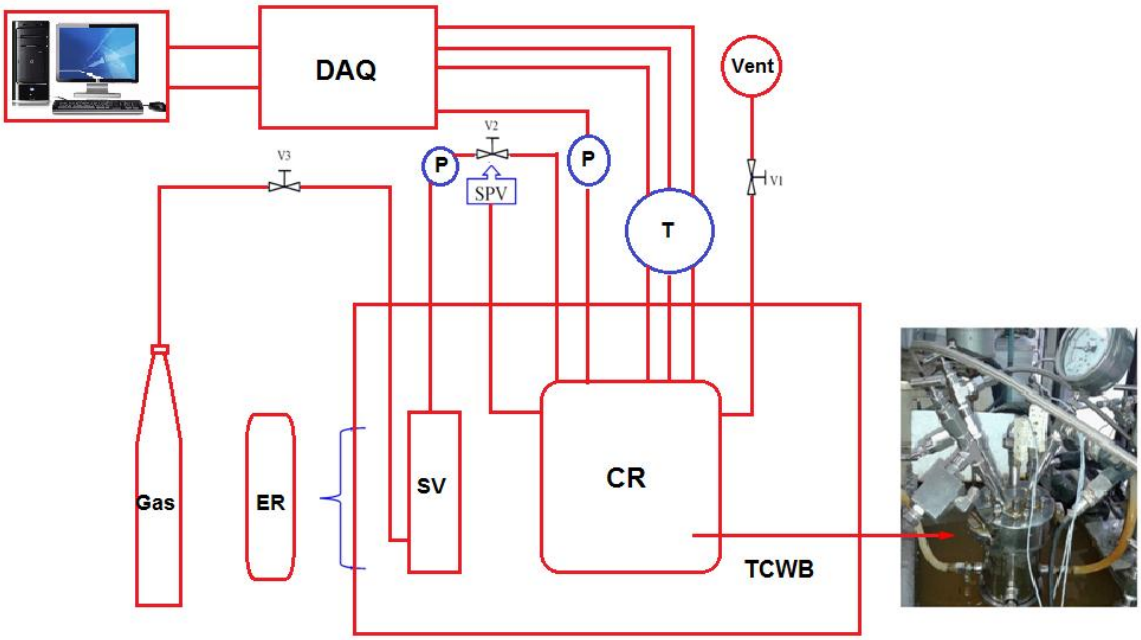

Figure 4.1.1: Line diagram of Experimental Setup to Study the Effects of Zeolite 5A, Zeolite 13X, Silica Sand on CO_2 Hydrate Formation

CR	Crystallizer
SV	Supply Vessel
P	Pressure Transducer
T	Thermocouples
DAQ	Data Acquisition System
ER	External Refrigerator
SPV	Safety Pressure Valve
TCWB	Temperature Controlled Water Bath

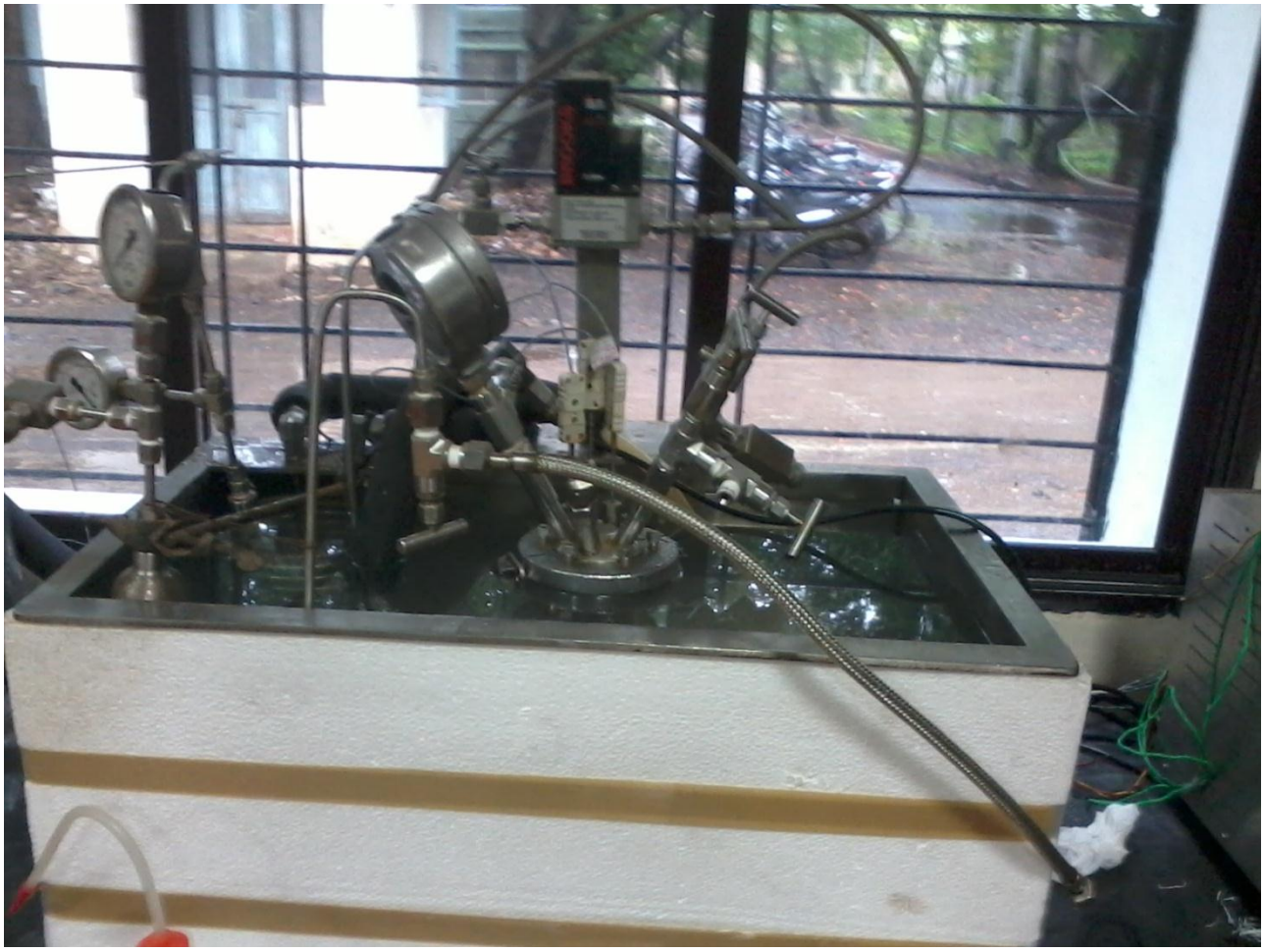

Figure 4.1.2: Experimental Setup to Study the Effects of Zeolite 5A, Zeolite 13X, Silica Sand on CO_2 Hydrate Formation

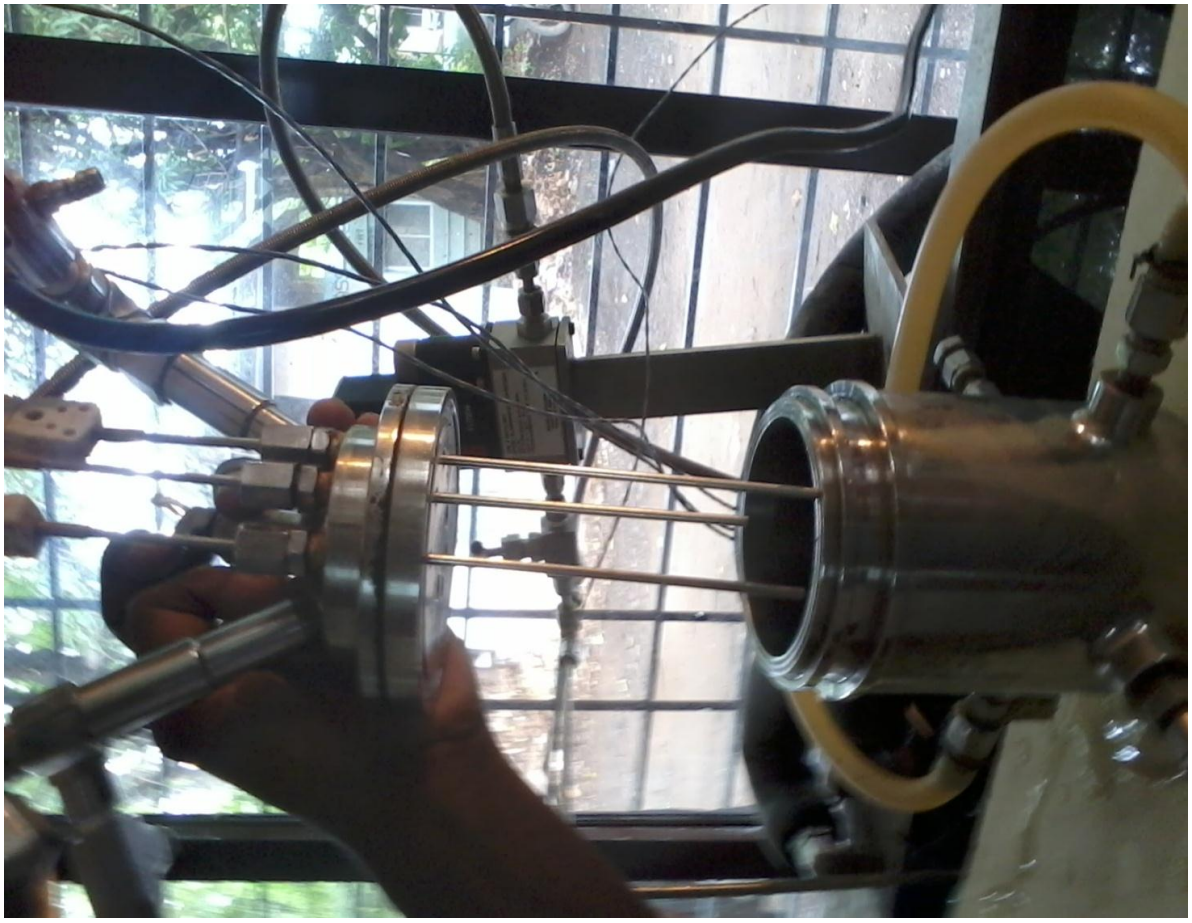

Figure 4.1.3: Showing the Location of Three Thermocouples in the Reactor used in present study.

4.2 Carbon dioxide Hydrate Formation in Fixed Bed and Stirred Tank Reactor Systems

Apparatus and Hydrate Formation procedure

4.2.1 *Fixed bed reactor (FBR)*

Line diagram of the fixed bed apparatus is shown in Figure 4.2.1. Briefly, the process is as follows. A fixed amount of water was used along with a calculated quantity of packing material (Silica sand, Silica Gel and Silica Gel-zeolite blend) in a 500 cm^3 SS-316 crystallizer (CR). CR was tightly closed and put inside the water bath whose temperature is controlled by an external chiller (Julabo). After reaching to the desired temperature (274.5K), the CR was pressurized by pure CO_2 Gas to the pre-determined experimental pressure (3.0 MPa). After this stage, Gas uptake measurements were started. All the Gas uptake measurements were carried out in batch mode. Pressure and temperature of the reactor were noted every 5 seconds through a data acquisition system connected to a computer.

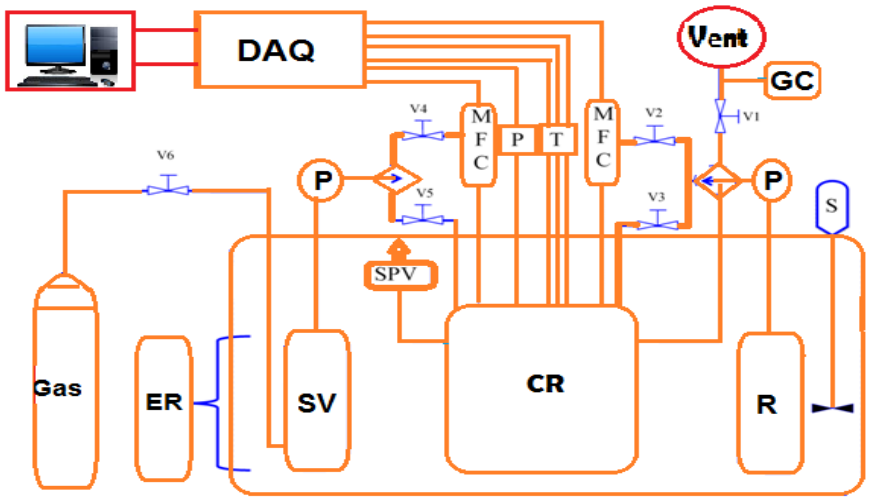

Figure 4.2.1: Line diagram of the Experimental Setup for studying the Effects of Silica Sand, Silica Gel (5nm and 100nm) and Zeolite 5A on CO_2 Hydrate Formation

CR	Crystallizer
SV	Supply Vessel
GC	Gas Chromatography
P	Pressure Transducer
T	Thermocouples
S	Stirrer
R	Reservoir
MFC	Mass Flow Controller
DAQ	Data Acquisition System
ER	External Refrigerator
SPV	Safety Pressure Valve

4.2.2 *Stirred tank reactor (STR)*

Line diagram of STR is shown in Figure 4.2.2. CR with volume 250 mL is equipped with a set of polycarbonate windows for visual identification of Hydrate crystals. Hydrate Formation experiments were carried out in batch mode with a fixed amount of water (50 mL). The pressure inside the CR starts falling upon Hydrate Formation until the driving force for Hydrate Formation becomes insufficient to sustain further production of Hydrates. This drop in pressure was measured to calculate the Gas uptake. Gas uptake measurements were done at constant temperature of ~274.5 K and pressure 3.0 MPa. The stirrer was set to 400 RPM for all experiments conducted. Pressure and temperature inside the reactor were noted every 5 seconds through a data acquisition system connected to a computer.

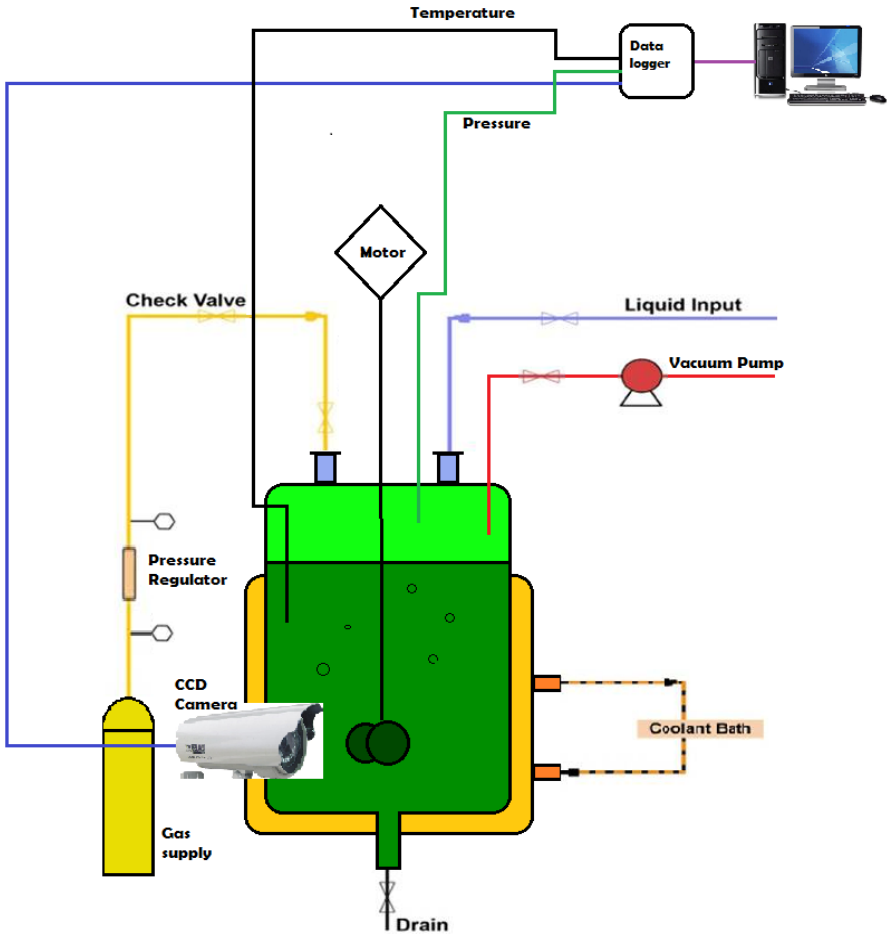

Figure 4.2.2: Line diagram of Stirred Tank Reactor for CO_2 Hydrate Formation

Figure 4.2.3: Experiment set up of Stirred Tank Reactor (STR) Along with Transparent Window used in present study

4.3 Influence of 3A and 5A Zeolites in Presence of Silica Gel on Carbon Dioxide Gas Hydrate Formation

4.3.1 *Experimental Setup*

Total volume of stainless steel reactor used was 325 millilitre (ml). Pressure Transducers were used to measure pressure readings. Reactor and supply vessel was immersed in external refrigerator which was filled with 50/50 wt. % of glycol/water mixture to keep the temperature constant. Pressure transducer and thermocouple was attached to data collection system. The desired amount of Silica Gel and zeolite after saturating with distilled water was put into reactor which was then placed in water bath maintained at constant temperature. Pure CO_2 Gas was introduced into the reactor at required pressure of 30 bar. The temperature in the water bath was maintained 274.15K. The pressure drop was measured by Data Acquisition System in order to calculate moles of CO_2 Gas consumed during Formation of Hydrate. The schematic diagram of experimental set up used in the present study is shown in Figure 4.3.1 as follows:

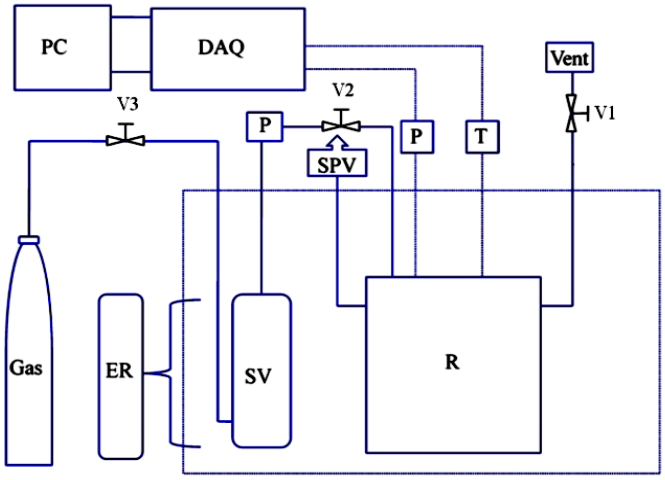

Figure 4.3.1: Line diagram of Experimental Setup for Influence of 3A and 5A Zeolites in Presence of Silica Gel on Carbon Dioxide Gas Hydrate Formation

R	Reactor
SV	Supply vessel
P	Pressure Transducer
T	Thermocouples
DAQ	Data Acquisition system
ER	External Refrigerator
SPV	Safety pressure Valve
V1	Valve 1
V2	Valve 2
V3	Valve 3

4.4 The Experimental Setup for Methane Gas Hydrate Formation and Dissociation in Presence of Biosurfactants namely Rhamnolipids, Surfactin, Calcium LignoSulphonate (CaLS) using Large Reactor: Thermodynamics and Kinetic Studies

The Formation and Dissociation of Gas Hydrate was investigated in the mercury free video Hydrate cell designed by Vinci Technology, France. Data acquisition was performed by built in software available with the system. The experiments were conducted in quiescent water system and porous C type Silica Gel saturated (90%) with distilled water containing different concentrations of biosurfactants i.e. Rhamnolipids and Surfactin (0, 100 and 1000ppm) and 1wt% Calcium LignoSulphonate.

The apparatus consisted of a constant volume Hydrate cell having capacity of 250 cm^3 (diameter =8 cm and height 2.5 cm) with pressure rating up to 3000 psi. A bed height of 2.5 cm was prepared by using 64.7g of C type Silica and was 90% saturated with 52.41ml of aqueous solution containing different dose of biosurfactant. The quantity of H_2O needed for saturation of the bed was calculated based on the pore volume of the C type Silica Gel (Merck) which was determined by BET analysis to be 0.9cm^3/g. Thermostatic bath was used to control the cell temperature. Cell pressure was measured by pressure transducer.

4.4.1 *Experimental Setup for Hydrate Formation and Dissociation Procedure*

The test sample was maintained at a fixed temperature by immersing it into a temperature controlled bath. A mixture of water and ethylene glycol (25%) was used as a liquid for bath. The air in the cell was expunged from the cell before pressurizing Methane Gas in the cell by vacuum pump. CH_4 Gas up to the desired pressure was pressurized in the cell.

Firstly, Hydrate stability zone experiments were performed and then kinetics experiments were performed afterwards. In order to conduct the Hydrate stability zone experiment, step wise cooling (1K/h) of the programmable bath was performed and sufficient time was given in order to acquire the equilibrium conditions at each temperature. There is gradual decrease in the pressure but at certain point a sharp decrease in pressure with simultaneously increases in temperature was observed which confirms the Hydrate Formation because Hydrate Formation is an exothermic process. Afterwards the temperature was decreased further slowly in order to measure the growth of Hydrate. When there is insignificant pressure drop it confirms the

completion of Hydrate Formation. The system is allowed to stay in at the same temperature for 5 hours to gain a state of equilibrium. After the Hydrate Formation, the complete chamber was heated at a rate of 1 K/h (Quiescent Water, Silica Gel containing different dose of Rhamnolipids and Surfactin) or 0.5 K/h calcium LignoSulphonate (CaLS). When the temperature was enhanced, the decomposition of Hydrates was seen with substantial increase in pressure. The pressure and temperature data during the experiments are kept in the computer and was also displayed as online graphs. The chamber has a video camera which continuously records the pictures of the system during the different phases of Formation of Gas Hydrate.

Kinetics experiments of the same test specimen were carried out to compute induction time and rate of Hydrate Formation after pressurizing the test sample present in the cell at Methane Hydrate Formation condition noted in the stability experiment. The test sample was placed in Hydrate cell immersed into a temperature controlled bath to maintain a fixed temperature. The Hydrate Formation was confirmed by fall of sudden pressure and increase of temperature simultaneously. Online video pictures were also used for confirming the Hydrate Formation. Insignificant pressure drop shows the completion of Hydrate Formation process.

The schematic diagram used for the above studies is shown in Figure 4.4.1 as per follows:

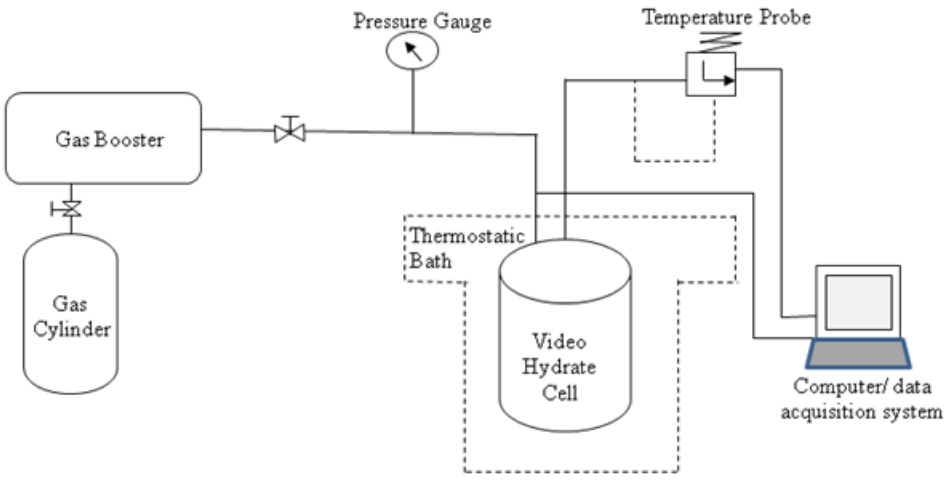

Figure 4.4.1: Line diagram of the Experimental Setup for Methane Hydrate Formation for Various Experimental Conditions.

Gas booster is also attached to autoclave set up in order to build up high pressure inside Hydrate cell. The Experiment setup of Methane Hydrate Formation is shown in Figure 4.4.2 as follows.

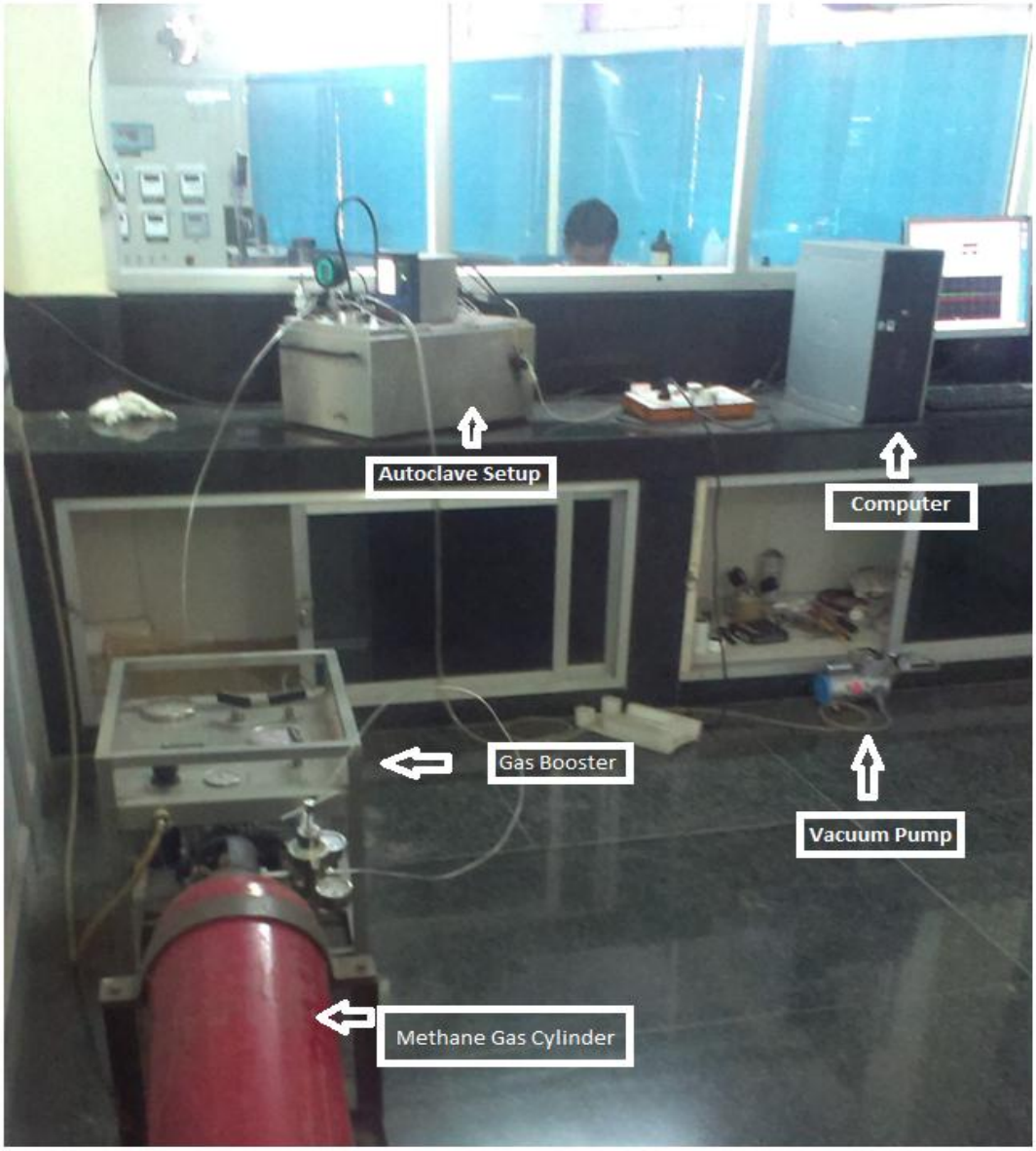

Figure 4.4.2: Experimental setup of Methane Hydrate Formation

4.4.2 *Instrumentation Section*

There are three main parts in the instrument namely: Cell, Thermostatic bath and Software to monitor the experiment and record temperature, pressure and time data while the experiment is going on. These parts are explained as follows:

(A) Cell

The cell is shown in closed condition in Figure 4.4.3 and in open condition in Figure 4.4.4. It is made up of stainless steel and equipped with a PT100 (temperature sensor) in order to measure temperature through the port. The operating conditions of video Hydrate cell reactor is shown in Table 4.4.1 as follows:

Table 4.4.1: Reactor Parameter

Description	Operating Conditions
Operating Pressure	3,000 psi
Pressure accuracy	0.1% Full Scale
Volume of Cell	250 cm^3
Operating Temperature	-10 ^{0}C to 60 ^{0}C
Temperature accuracy	0.1^{0}C
Process Fluid	Methane and Water
Fixed Bed	C Type Silica Gel (Merck)

Figure 4.4.3: Hydrate Cell in Close Condition

Figure 4.4.4: Hydrate Cell in Open Condition

(B) Thermostatic bath

The thermostatic bath without cell is shown in Figure 4.4.5 and with cell is shown in Figure 4.4.6. The bath is having dimension of 225×370× 429mm, the fluid capacity is 2.7 L. The thermostatic fluid (water and glycol at 25%) are used in order to achieve working temperature. Its operation is very simple in order to get an excellent thermal stabilization and control of temperature while the processes of chilling or heating is going on.

(C) Software

A colour graphics screen is shown in Figure 4.4.7 which exhibits Information like: set point temperature of bath, actual measured temperature of process fluid inside the cell. RS232 interface enables to monitor and record data (pressure, temperature and time) from AppliLab interface while Methane Hydrate Formation is as shown in Figure 4.4.7 and online video pictures of Methane Hydrate Formation after Nucleation are shown in Figure 4.4.8 as follows.

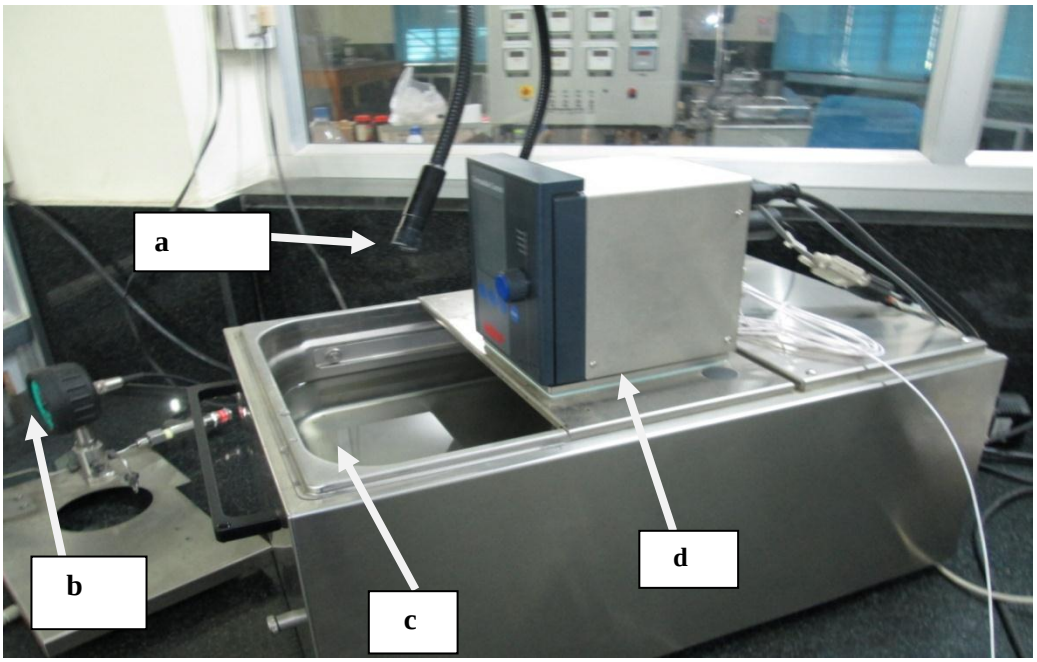

a Camera, b Pressure Gauge, c Bath, d Compatible Control-Thermostat

Figure 4.4.5: Thermostatic bath for both cooling and heating

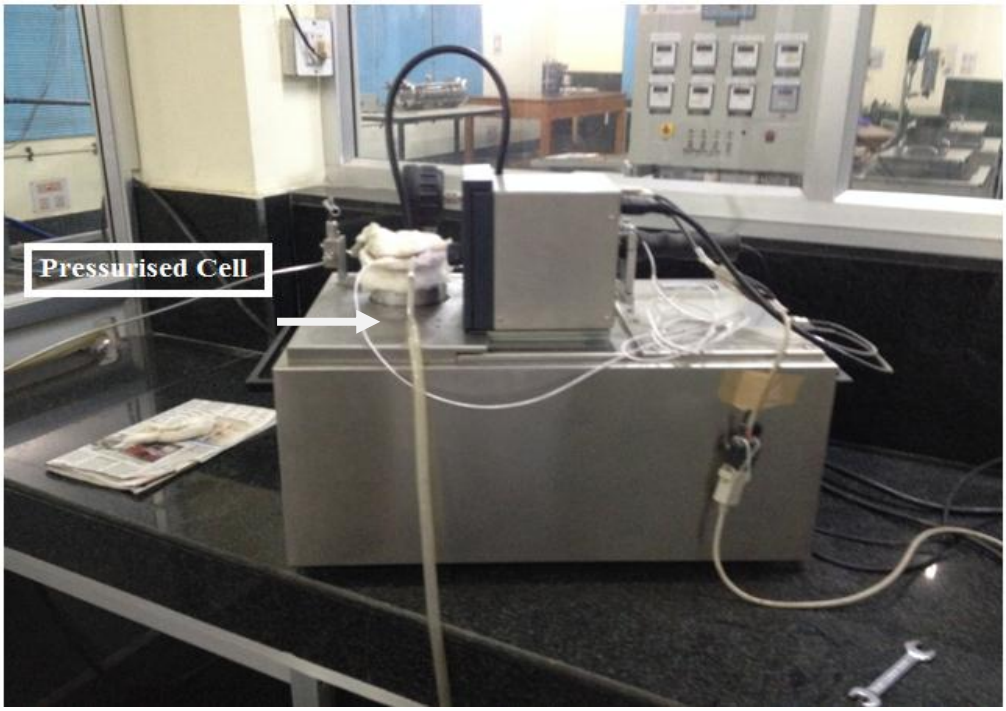

Figure 4.4.6: Thermostatic Bath Containing Cell in Pressurised Conditions

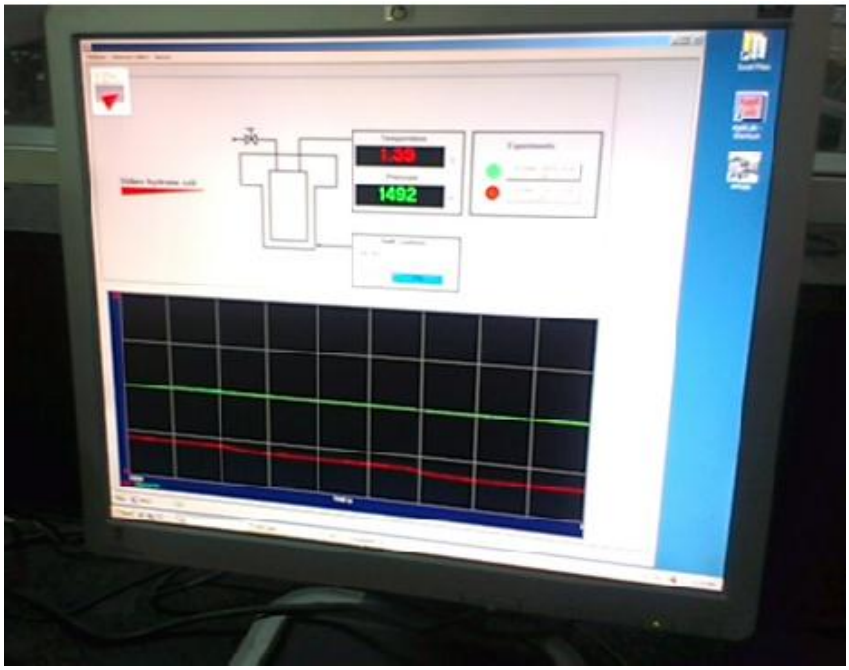

Figure 4.4.7: Display of Pressure, Temperature and Bath Set Point Temperature while Methane Hydrate Formation on Computer

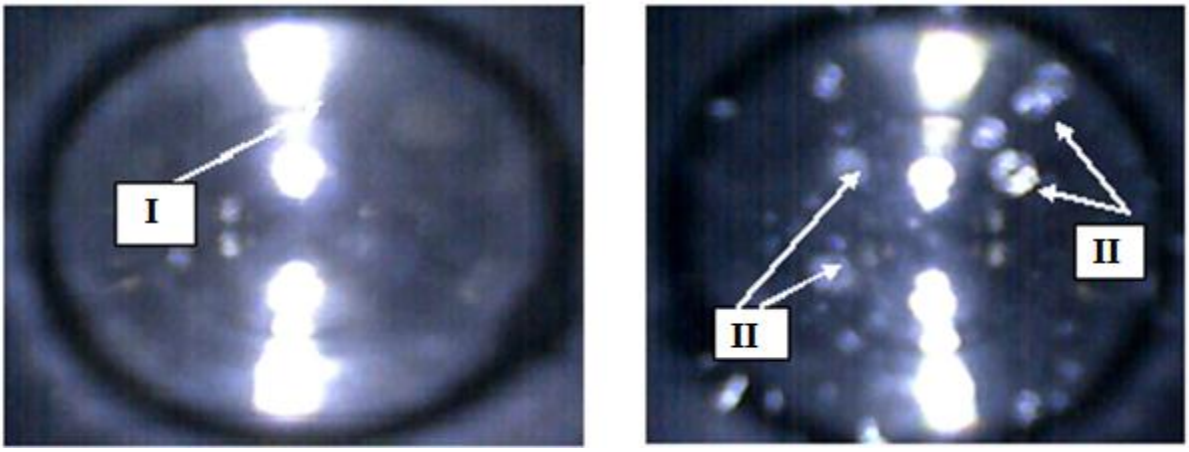

I-Reflected Light **II-Methane Hydrate Crystals**

Figure 4.4.8: Online video pictures of Methane Hydrate Formation after Nucleation

4.4.3 ***The pictorial representations of various material used are shown in the following figures***

Figure 4.4.9: C-type Silica Gel (Merck)

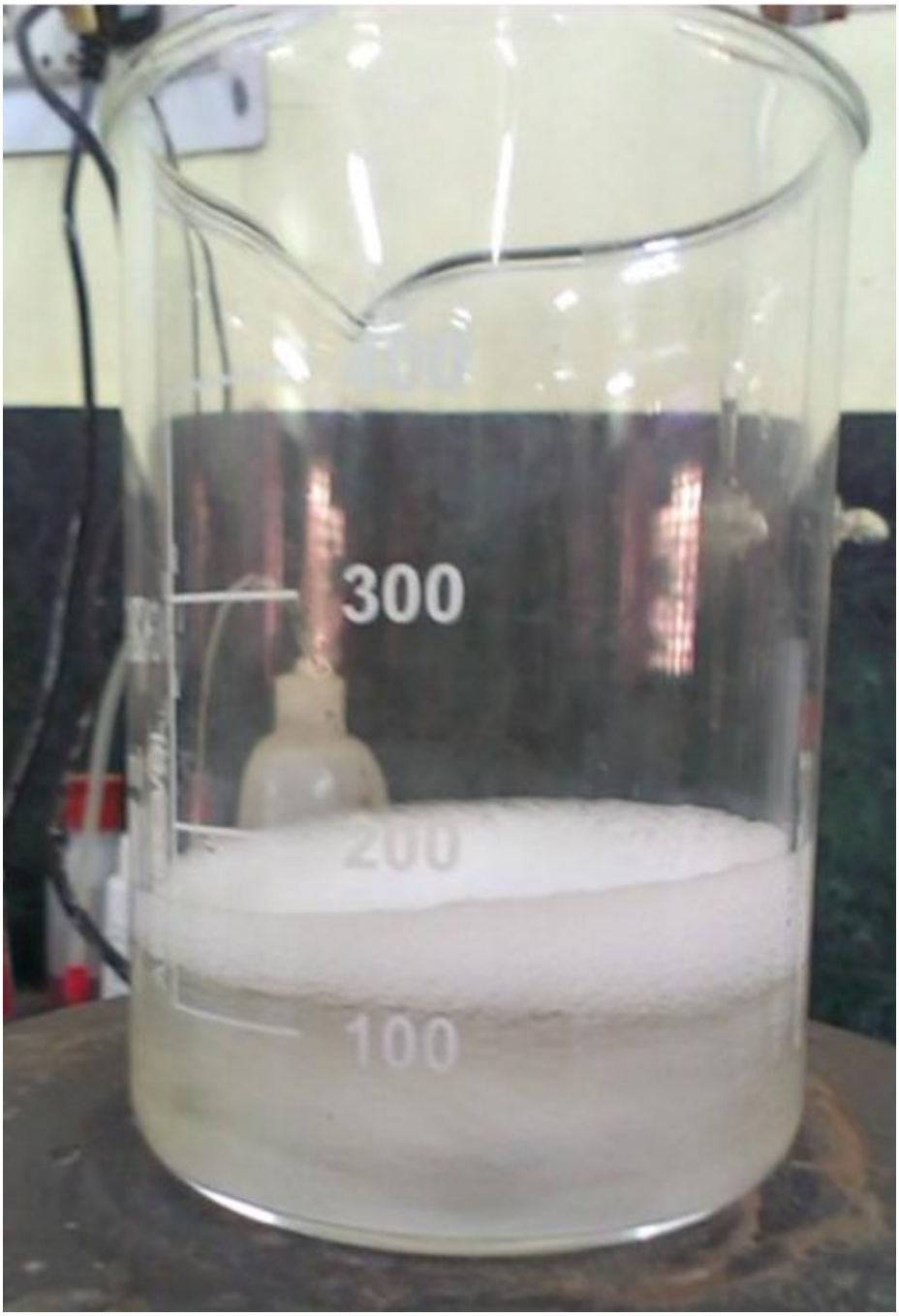

Figure 4.4.10: A Solution of 1000 ppm Rhamnolipids

Figure 4.4.11: C-type Silica Gel (Merck) getting saturated with 1000 ppm Rhamnolipids Solution

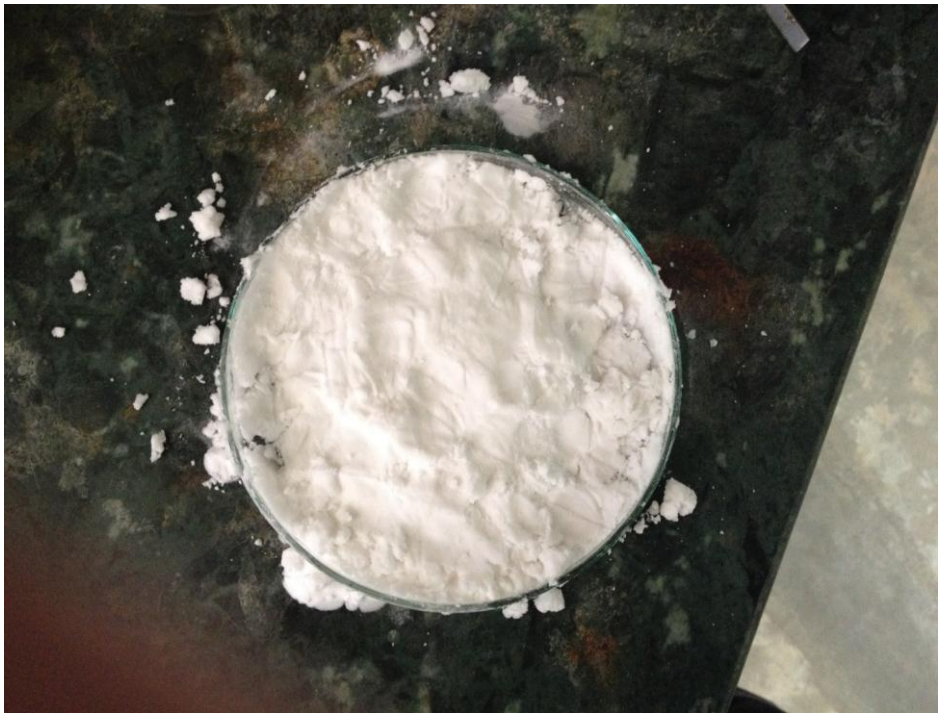

Figure 4.4.12: C-type Silica Gel (Merck) Saturated with 1000 ppm Rhamnolipids Solution

Figure 4.4.13: Fixed Bed of C-type Silica Gel (Merck) Saturated with 1000 ppm Rhamnolipids Solution

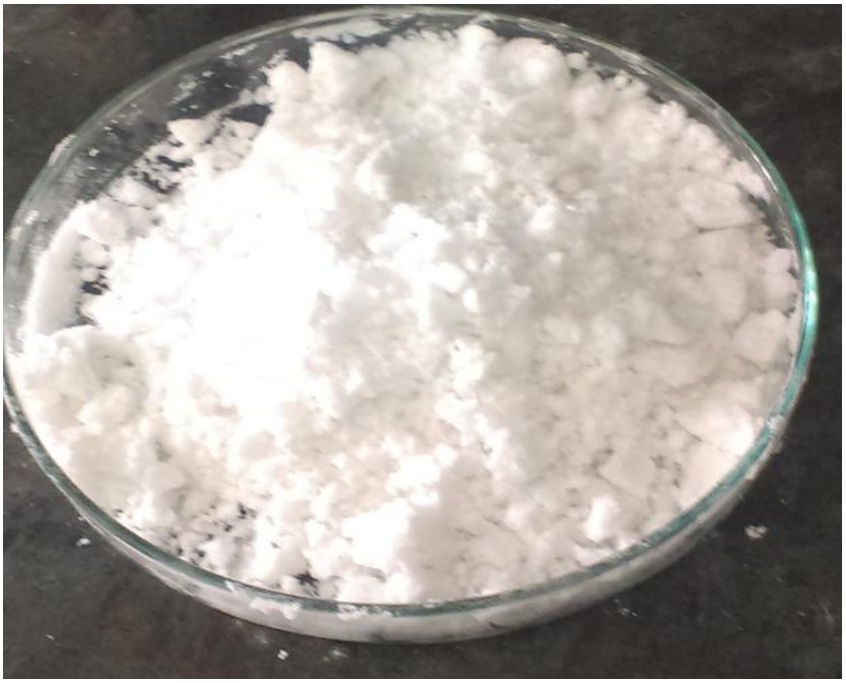

Figure 4.4.14: C-type Silica Gel (Merck) Saturated with distilled water

Figure 4.4.15: Fixed Bed of C-type Silica Gel (Merck) Saturated with distilled water

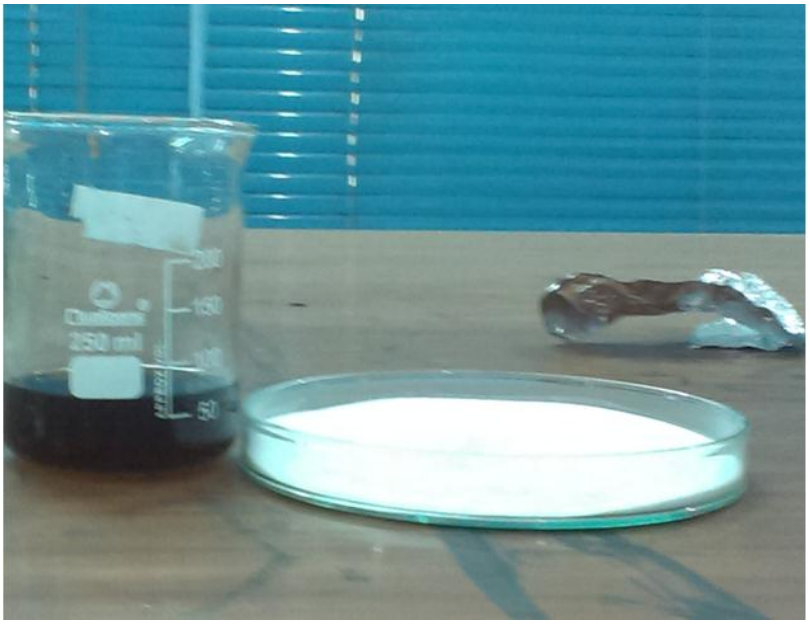

Figure 4.4.16: Solution of 1 wt. % Calcium LignoSulphonate and C-type Silica Gel (Merck)

Figure 4.4.17: Fixed bed of C-type Silica Gel (Merck) Saturated with 1 wt. % Calcium LignoSulphonate

Figure 4.4.18: C-type Silica Gel (Merck) after going through Methane Hydrate Formation Experience

4.4.4 *The Experimental Setup for Methane and Natural Gas Hydrate Formation in Presence of Biosurfactant Calcium LignoSulphonate (CaLS) using Medium Reactor*:

The experiments were conducted in medium reactor. Total volume of medium stainless steel reactor used was 69 ml. Pressure measurements are made with pressure transducers, with a range of 0-100 bar and accuracy of less than 0.075% of the span Reactor and supply vessel was immersed in external refrigerator which was filled with 50/50 wt. % of glycol/water mixture to keep the temperature constant. The temperature of the crystallizers as well as the supply vessel is maintained at a fixed temperature with the help of chillers (Julabo-FS18) which maintains the temperature in the Hydrate crystallizer and the supply vessel (SV) constant. Pressure transducer and thermocouple was attached to data collection system. The schematic diagram of Medium Reactor experimental set up used in the present study is shown in Figure 4.4.19 as follows.

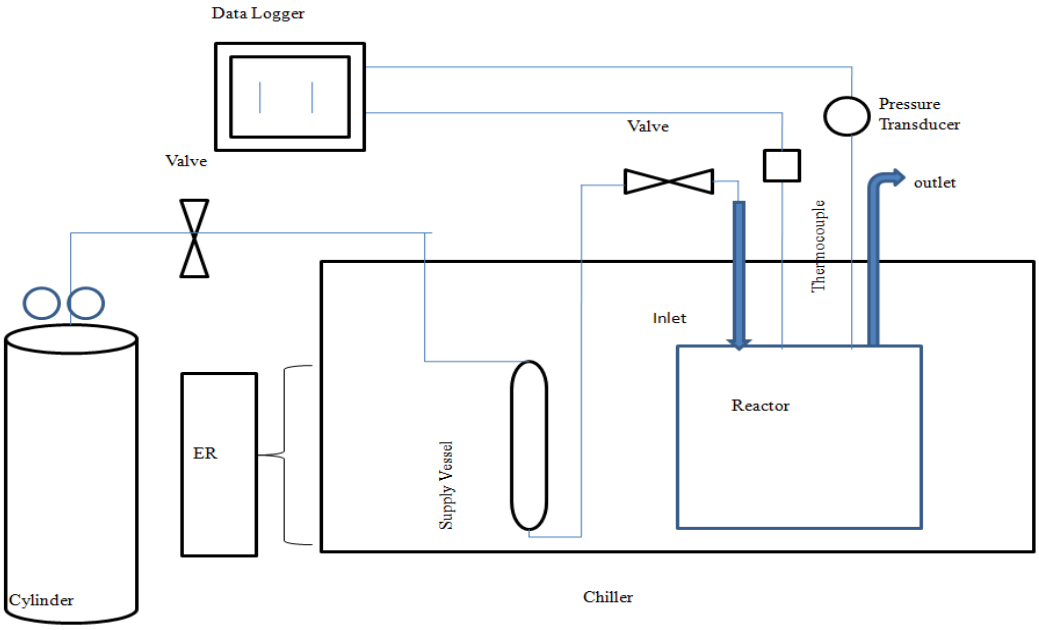

Figure 4.4.19: Line diagram of Experimental Setup for Methane and Natural Gas Hydrate Formation in Presence of Biosurfactant Calcium LignoSulphonate (CaLS) using Medium Reactor

R	Reactor
SV	Supply vessel
P	Pressure Transducer
DAQ	Data Acquisition system
ER	External Refrigerator

The method for the experiment is as follows. The quantity of C-type Silica Gel (Rankem) used for each experiment was 20g saturated with 90% distilled water or 0.1,1, 5 wt. % of CaLS. Pore volume of C type Silica Gel (Rankem) was determined by BET analysis to be 0.89 cm^3/g. Different dosage (0.1, 1 and 5 wt. %) of biosurfactant i.e. CaLS in presence of both Natural Gas and Methane is used in Hydrate Formation. After the reactor is charged with water saturated Silica Gel, the reactor was cooled to a required temperature (1^oC) and time was allowed to pass for temperature to be stabilized. The reactor was then pressurized to a desired experimental pressure i.e. 30 bar for Natural Gas and 50 bar for Methane through SV. As Hydrate Formation starts causing pressure drop in reactor which is recorded by DAQ.

CHAPTER-5

MATERIALS AND METHODS

5.1 Effect of Different Fixed Bed Media on the Performance of Sodium Dodecyl Sulphate for Hydrate Based CO_2 Capture

5.1.1 *Materials*

The materials used in the present study are shown in table 5.1.1. All the materials were used as such without treating them further. Distilled and Deionized water was used for the experiments.

Table 5.1.1: Materials used along with suppliers used in the present study

S. No	Materials Used	Supplier
1	Silica Sand	Sakalchand & Company Pune, India
2	SDS(SQ Grade,98% Purity)	Fisher Scientific Ltd. India.
3	Zeolite 5A	Sorbead India, Vadodara
4	Zeolite13x	Sorbead India, Vadodara
5	Pure CO_2 (99.9%)	Vadilal Gases Ltd, Baroda

5.1.2 *Zeolites*

Zeolites are one such porous media which have crystalline solid structure comprising of silicon aluminium and oxygen which can trap or reside small molecules or water and Gases within their cavities often considered as molecular sieves. They have definitive pore structure, high internal surface area and can adsorb hydrocarbons [Dhar, 2008].

5.1.3 *Field Emission Scanning Electron Microscopy FE-SEM of 5A and 13X Zeolites*

Field emission scanning electron microscopy (Carl Zeiss, Ultra Plus) equipped with EDS accessory (Model Oxford, X-Max, United Kingdom) was used to obtain the surface morphology for FE-SEM analysis, zeolite samples were sprinkled on the carbon tape mounted on the aluminium stub and the sample was kept in sputtering chamber for coating of a thin layer of gold for 30 s at 30 μA current to make the sample conducting. Silver paste was used to make contact of the sample with the aluminium sample holder. The samples were scanned under 15 kV accelerating voltage to record their surface morphology at different magnifications.

Energy dispersive X-Rays (EDX) studies of the specimen were done to examine the elemental distribution in the samples at any particular point or in a selected area using FESEM.

5.1.4 *Zeolite 5A*

The chemical formula of zeolite 5A found in literature is as follows:

$$0.7CaO.0.30Na_2O.Al_2O_3.2.0SiO_2.4.5H_2O$$

There is a good match of elements between formula of 5A and composition from EDS analysis except presence of few impurities in the sample and absence of hydrogen which cannot be determined using this machine as shown in table 5.1.2 and figure 5.1.1. The morphology of the as procured sample Zeolite 5A is shown in figure 5.1.2. The morphology depicts the uniform distribution of particles in zeolite 5A with an average size of about 2 μm.

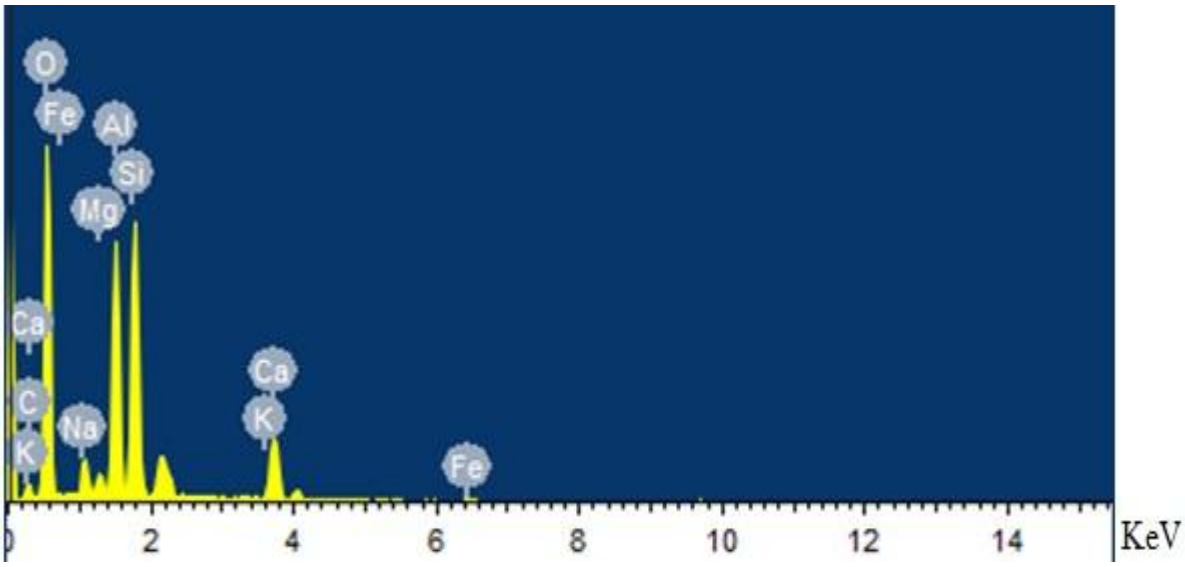

Figure 5.1.1: EDS Analysis of Zeolite 5A

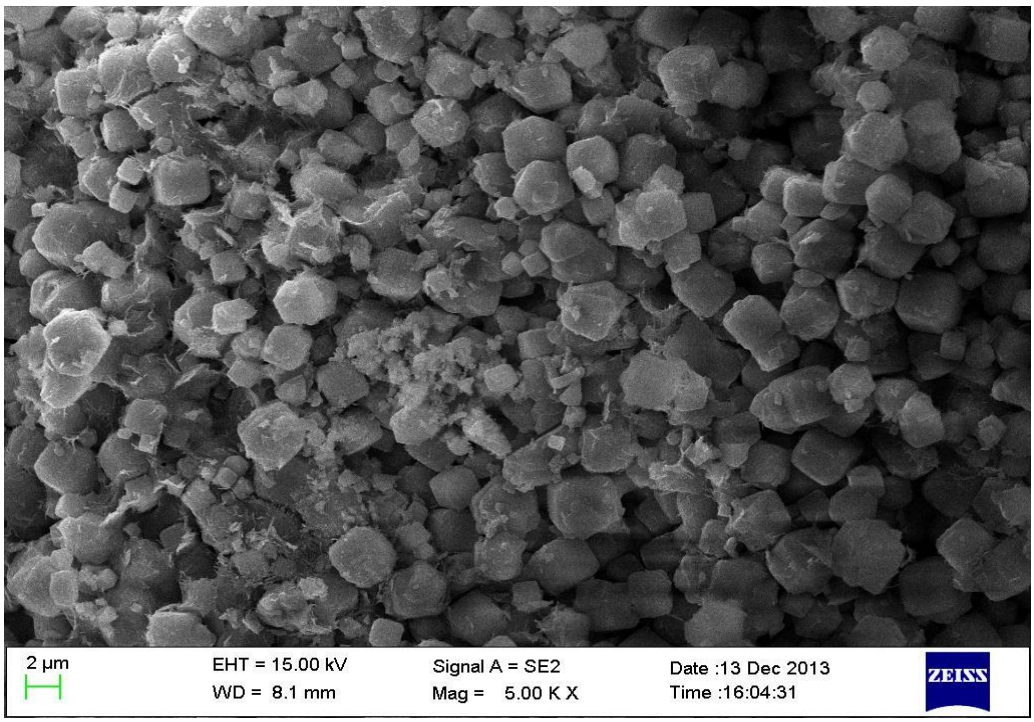

Figure 5.1.2: The morphology of the procured sample Zeolite 5A

Table 5.1.2: The Weight % and Atomic % of different elements in 5A

Elements	Wt%	Atomic%
O K	52.35	62.88
Si K	16.46	11.26
Al K	12.73	9.07
Ca K	7.92	3.80
Na K	2.32	1.94
C K	6.19	9.90
Mg K	0.96	0.76
Fe K	0.87	0.30
K K	0.20	0.10
Totals	100	100

Where K stands for K shell,

Where C, Mg, Fe, and K are impurities in the sample

5.1.5 *Zeolite 13X*

The chemical formula of zeolite 13X as expressed in literature is

$NaO.Al_2O_3.2.5\ SiO_2.6.2\ H_2O$

There is a good match of elements between formula of 13X and composition from EDS analysis except presence of few impurities in the sample and absence of hydrogen which cannot be determined using this machine as shown in table 5.1.3 and figure 5.1.3. The morphology of the procured sample Zeolite 13X is shown in figure 5.1.4. The morphology depicts the uniform distribution of particles in zeolite 13X with an average size of particles less than 2 μm.

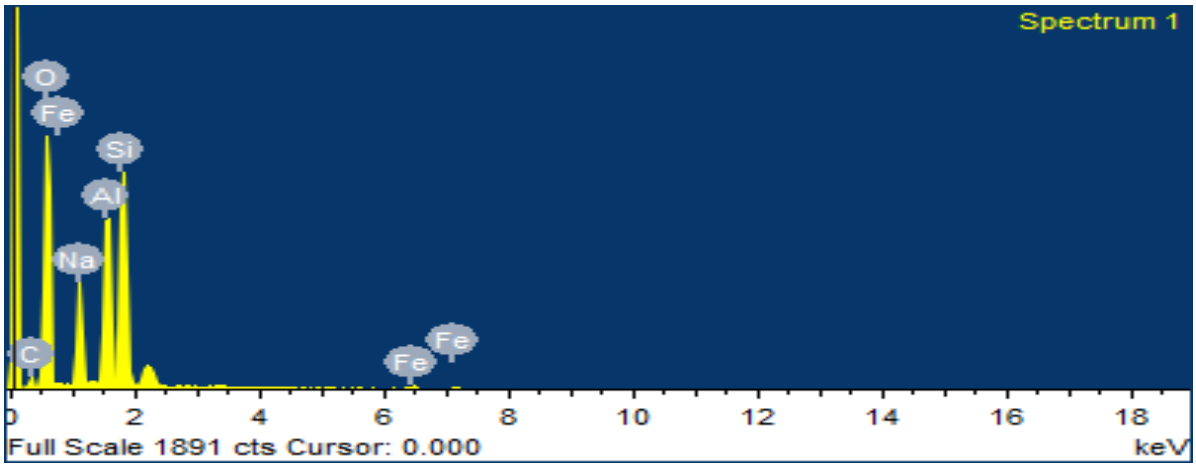

Figure 5.1.3: EDS Analysis of Zeolite 13X

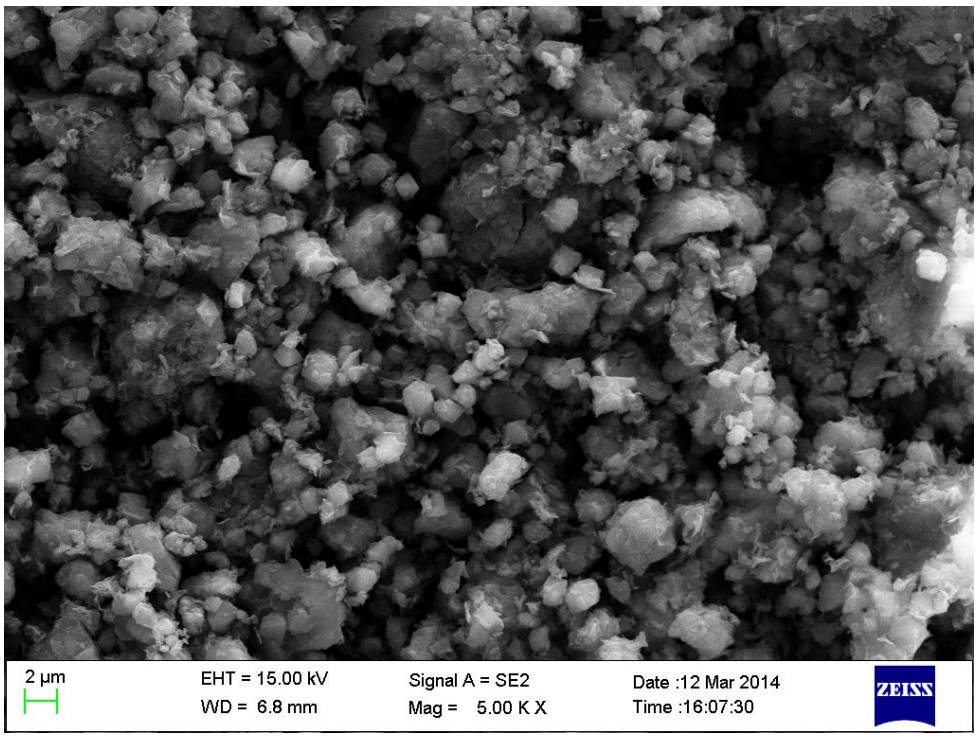

Figure 5.1.4: The morphology of the procured sample Zeolite 13X

Table 5.1.3: The Weight % and Atomic % of Different Elements in 13 X

Element	Wt. %	At. %
O K	47.85	56.67
Si K	19.92	13.44
Al K	13.25	9.30
Na K	10.03	8.27
C K	7.50	11.83
Fe K	1.46	0.49
Mg K	0.43	0.36

Where K stands for k shell

Where C, Fe and Mg are impurities

5.1.6 *Summary of the systems used in the present study is as shown in table 5.1.4.*

Table 5.1.4: Summary of the systems used in the study

System	Mass of packing,(g)	Amount of Water Used (cm^3)	Amount of SDS (wt %)
Zeolite 5A	130	-	-
Zeolite 5A/water	130	50	-
	130	50	-
Zeolite 13X/water	108	50	-
	108	50	-
	108	50	-
Zeolite 13X/SDS/water	108	50	0.5
	108	50	0.5
Silica sand/Water	250	50	-
	250	50	-
	250	50	-
Silica sand/SDS/ Water	250	50	0.5
	250	50	0.5
	250	50	0.5

The Zeolite 5A and 13X used in the present study is as shown in figure 5.1.5 and 13X Zeolite saturated with distilled water is as shown in figure 5.1.6.

Figure 5.1.5: The Zeolite 5A and 13X used in the present study

Figure 5.1.6: The 13X Zeolite saturated with distilled water

5.2 Carbon dioxide Hydrate Formation in Fixed Bed and Stirred Tank Reactor Systems

5.2.1 *Materials*

Details of the system used for experiments have been presented in table 5.2.1.

The particle size distribution of Silica sand varies from 30–400μm. The quantity of the water essential to fulfil the void space between the sand particles was 0.20 cm^3/g[Kumar et al, 2015]. Silica Gel used in the present study was having pore diameter ~5 nm, particle size distribution 40–65μm and pore volume of 0.89 cm^3/g as shown below. Another Silica Gel used in the present study having pore diameter ~100nm, particle size distribution of 200-500 μm and pore volume of 0.83cm^3/g [Kumar et al, 2014]. All the materials were used as such without treating them any further. Distilled and Deionized water was used for the experiments.

Table 5.2.1: Materials used along with suppliers used in the present study

S.No	Materials Used	Supplier
1	Silica Sand	Sakalchand & Company Pune, India
2	Spherical Silica Gel 100 nm pore diameter	SiliCycle, Canada
3	Silica Gel 5 nm pore diameter	Rankem Ltd.
4	Zeolite 5A	Sorbead India,Vadodara
5	Pure CO_2 (99.9%)	Vadilal Gases Ltd, Baroda

5.2.2 *The Summary of the systems used in present study*

Table 5.2.2: Summary of the systems used in the present study

System	Amount of packing (g)	Amount of Water* (ml)	Amount of Zeolite as additive (g)
Silica Sand (75% Saturated)	180	27	0
Silica Gel with 100 nm (100% Saturated)	33	27	0
Silica Gel with 5nm (50% Saturated)	43.47	20	0
Stirred Tank reactor	-	50	0
Silica Gel with 5 nm (50% Saturated) + 50wt% Zeolite 5A	43.47	20	21.47
Silica Gel with 5nm (50% Saturated) + 30wt% Zeolite 5A	43.47	20	13.04

*Water saturation is based on the pore volume of concerned material

5.2.3 *Brunauern - Emmett - Teller (BET) analysis of C type Silica Gel (Rankem)*

Nitrogen adsorption-desorption isotherms were plotted using a conventional volumetric nitrogen adsorption apparatus (Quantachrome Instrument Autosorb1 system). The claimed sample was degassed at 250^{o}C for 12 h at 0.00133 Pa, before the measurements. The sample was cooled to –196^{o}C by liquid nitrogen and the sorption of nitrogen was done at different equilibrium

pressures. The specific surface area of the sample was obtained using Brunauer, Emmett, and Teller (BET) method. The pore size distribution was calculated using the Barret- Joyner-Halenda (BJH) pore size model applied to the adsorption branch of the isotherm as shown in figure 5.2.1. The isotherms were classified as the type IV adsorption desorption defined by IUPAC which gives useful information through its hysteresis loop as shown in figure 5.2.2. The Surface characteristics are also shown in table 5.2.3.

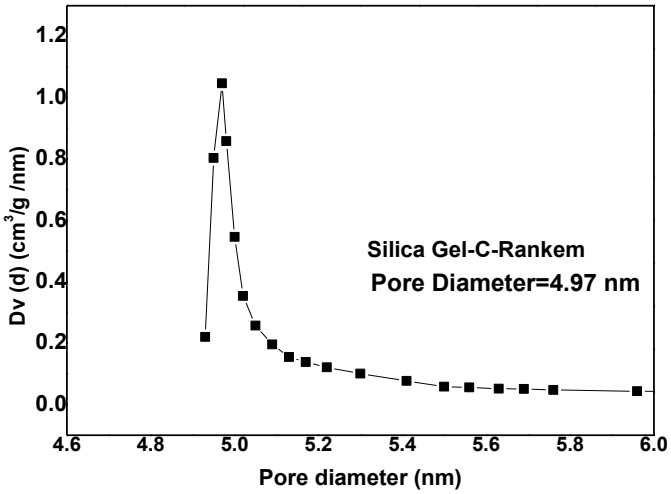

Figure 5.2.1: Pore Diameter of 5 nm pore size Silica Gel

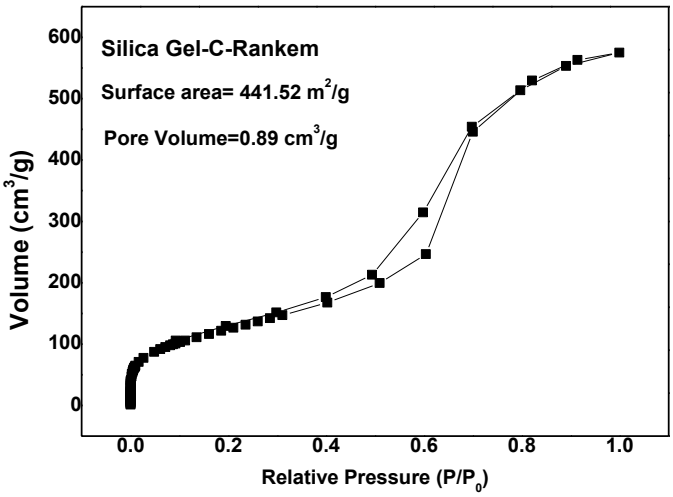

Figure 5.2.2: Pore Volume and Surface Area of 5 nm pore size Silica Gel

Table 5.2.3: Surface characteristics of the C- type Silica Gel (Rankem)

Catalyst	S_{BET} [a] ($m^2 g^{-1}$)	V_{Pore} [b] ($cm^3 g^{-1}$)	Average pore Diameter [c] (Å)	Pore Diameter (Å)
Silica Gel-C- (Rankem)	441.52	0.89	78	49.7

a- BET surface area

b- Total pore volume by Langmuir method

c- Average pore diameter by Langmuir method

5.3 Influence of Zeolites on Carbon Dioxide Gas Hydrate Formation

Zeolite 3A and Zeolite 5A were used as bead form in present study. 3A represents pore diameter of 3 Angstrom and 5A represents pore diameter of 5 Angstrom.

5.3.1 *Materials*

The various materials which are used in the experiments along with their supplier are shown in table 5.3.1.

Table 5.3.1: Materials used and their suppliers

Material	Supplier
PureCO_2	Vadilal Gases Ltd, Baroda
C Type Silica Gel	Rankem Ltd, Pune, India
Zeolite 3A	Sorbead India, Vadodara
Zeolite 5A	Sorbead India, Vadodara

The sample of 3A, 5A and C type Silica Gel zeolite used in present study is shown in figure 5.3.1(a), 5.3.1(b) and 5.3.1(c).

Figure 5.3.1(a): Sample of 3A Zeolite

Figure 5.3.1(b): Sample of 5A Zeolite

Figure 5.3.1(c): Sample of C-type Silica Gel(Rankem)

5.3.2 *Field Emission Scanning Electron Microscopy FE-SEM of 3A Zeolite*

Field emission scanning electron microscopy (Carl Zeiss, Ultra Plus) equipped with EDS accessory (Model Oxford, X-Max, United Kingdom) was used to obtain the surface morphology for FESEM analysis Energy dispersive X-Rays (EDX) analysis of the samples was done to examine the elemental distribution in the samples at any particular point or in a selected area using FESEM.

5.3.3 *Zeolite 3A*

The chemical formula of zeolite 3A as expressed in literature is

$$\frac{2}{3}K_2O.\frac{1}{3}Na_2O.Al_2O_3.2SiO_2.\frac{9}{2}H_2O$$

There is a good match of elements between formula of 3A and composition from EDS analysis except presence of few impurities in the sample and absence of hydrogen which cannot be determined using this machine as shown in figure 5.3.2 and table 5.3.2. The morphology of the procured sample Zeolite 3A is shown in figure 5.3.3. The morphology depicts the uniform distribution of particles in zeolite 3A with an average size of particles more than 2 μm.

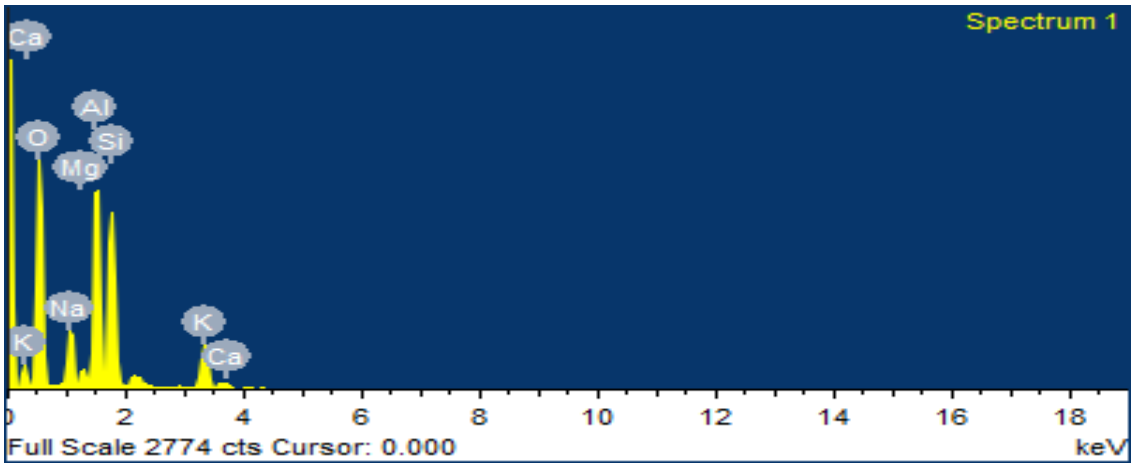

Figure 5.3.2: EDS Analysis of 3A Zeolite

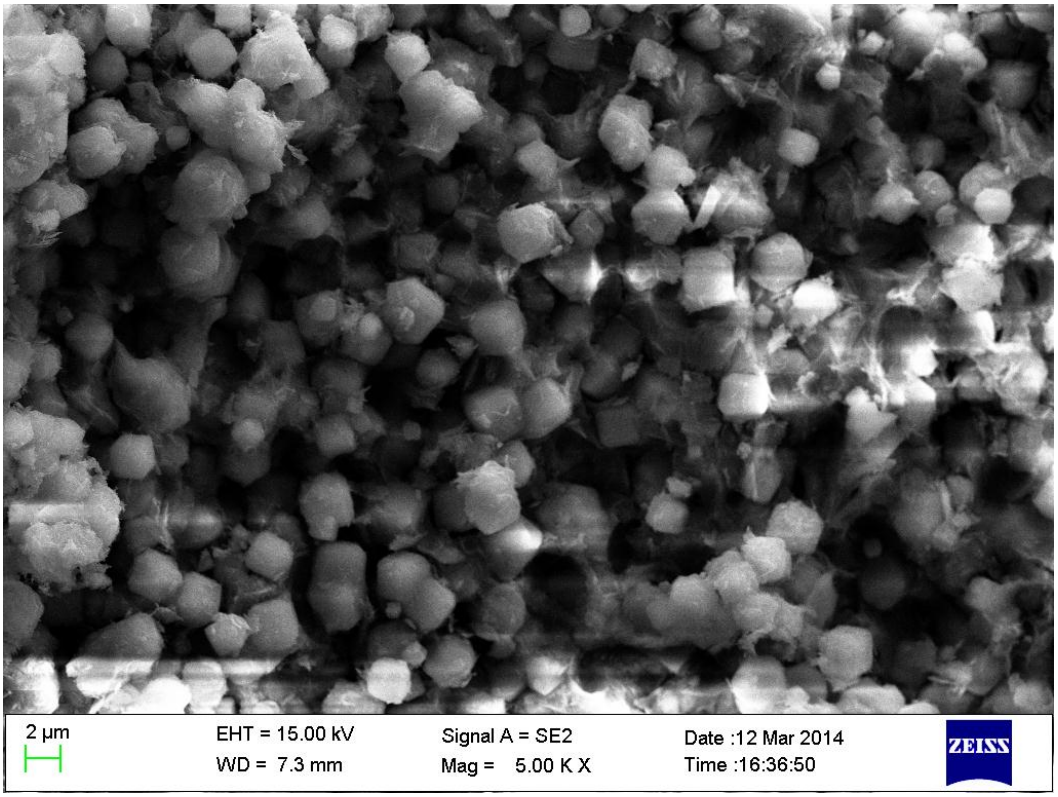

Figure 5.3.3: The morphology of the procured sample Zeolite 3A

Table 5.3.2: The Weight % and Atomic % of different elements in Zeolite 3A

Elements	Wt%	Atomic%
O K	50.91	64.66
Si K	17.82	12.89
Al K	16.26	12.24
K K	7.56	3.93
Na K	5.57	4.92
Mg K	1.23	1.02
Ca K	0.66	0.33

Where k stands for k shell,

Where Ca and Mg are impurities

5.3.4 ***The Summary of the systems used in present study is shown in table 5.3.3.***

Table 5.3.3: Summary of the systems used in the present study

System	Amount of Silica Gel (g)	Amount of Water* (ml)	Amount of Zeolite as additive (g)
Silica Gel	43.47	40 (100% sat.)	0
Silica Gel	43.47	20 (50% sat.)	0
Silica Gel + 30 wt. % Zeolite 3A	43.47	40 (100% sat.)	13.04
Silica Gel + 30 wt. % Zeolite 3A	43.47	20 (50% sat.)	13.04
Silica Gel + 30 wt. % Zeolite 5A	43.47	40 (100% sat.)	13.04
Silica Gel + 30 wt. % Zeolite 5A	43.47	20 (50% sat.)	13.04

For 100% saturation, moles of water = 2.22

For 50% saturation, moles of water = 1.11

*Water saturation is based on the pore volume of Silica Gel.

5.4 Biosurfactant Rhamnolipids as a Promoter of Methane Hydrate Formation: Thermodynamic and Kinetic Studies

5.4.1 *Materials*

All the high purity grade available chemicals and reagents are used. The various materials which are used in the experiments along with their supplier are shown in table 5.4.1.

Table 5.4.1: Materials used and their suppliers

Material	Supplier
Methane with purity of 99.99%	Chemtron Science Laboratory, Mumbai, India
C Type Silica Gel	Merck Specialties Pvt. Limited, Mumbai, India
Distilled Water	De-ionized (Milli-Q equipment, Millipore, Bedford, MA) and had a resistivity of 18 MΩ.
Microbiological growth media	HiMedia, India
Rhamnolipids	Synthesized in the laboratory from *Pseudomonas aeruginosa* strain A11

5.4.2 ***Pseudomonas aeruginosa strain A11 growing on nutrient agar plate as shown in figure 5.4.1***

Figure 5.4.1: *Pseudomonas aeruginosa* strain A11growing on nutrient agar plate

5.4.3 *Microorganism and growth medium composition*

In the present study Biosurfactant-producing microorganism *Pseudomonas aeruginosa* strain A11 was used which was isolated from rhizosphere of wild plant *Parthenium hysterophorus* growing at Dalma Wildlife Sanctuary, Jamshedpur, India [Singh et al, 2013]. For the production of biosurfactant, the minimal salt medium (MSM) used for the aerobic growth of the bacterium supplemented with 4% (w/v) glycerol as a carbon source is consisted of 2 g KH_2PO_4, 4 g Na_2HPO_4, 1.028 g $(NH_4)_2SO_4$, 0.8 g $MgSO_4.7H_2O$, 0.1% (w/w) Yeast Extract and 1 ml of trace element solution (TES) per litre. TES consisted of 0.1 g Al $(OH)_3$, 0.05 g $SnCl_2 \cdot 2H_2O$, 0.05 g KI, 0.08 g $MnCl_2 \cdot 4H_2O$, 0.05 g LiCl, 0.5 g H_3BO_3, 0.1 g $ZnSO_4 \cdot 7H_2O$, 0.1 g $CoCl_2 \cdot 6H_2O$, 0.1 g $NiSO_4 \cdot 6H_2O$, 0.05 g $BaCl_2$, and 0.05 g (NH_4) I in 1 L of the solution. The pH of MSM was maintained to 7.0 ± 0.5 with help of 1 Normal sodium hydroxide (NaOH) and 1 Normal hydrochloric acid (HCl).

5.4.4 *Biosurfactant production and purification*

Shake Flask Experiments were performed for the production of the biosurfactant. Incubation with the 2 % (v/v) inoculums of Erlenmeyer flasks (2L) containing 500 mL aliquots of MSM was done. For the preparation of Inoculums bacterium were grown in NB and then adjusting the OD with NB to ~0.5 at 600nm wavelength. The incubation of flasks were done at 30°C for 72h with agitation rate of 200rpm in Multi-stack shacking Incubator (Labtech, India). The monitoring of bacterial growth and biosurfactant production by strain A11 were done by withdrawing samples after every 12 h interval. Biosurfactant purification was performed following method reported by Sanchez et al, 2007 with slight modification. In brief, cell-free supernatant (CFS) was obtained by centrifuging the culture broth at 8,000 x g for 10 min at 4°C. The CFS was acidified to pH 2 with 6N HCl and incubated overnight at 4°C. The white precipitate was collected by centrifugation (10,000 x g for 10 minute). The precipitate was dissolved in 50mM sodium bicarbonate ($NaHCO_3$) buffer (pH 8.6) and again re-precipitated with 6N HCl. From precipitate the biosurfactant was obtained by solvent (2:1 chloroform and methanol) extraction at ambient temperature. Solvent was evaporated under reduced pressure to obtain honey coloured viscous biosurfactant.

Concentrated viscous biosurfactant was dissolved in chloroform (5mg/ml) and then purified by activated Silica-Gel 60, column (2x40 cm). Column was loaded and its washing was done at a flow rate of ~1 ml/min, by chloroform till neutral lipids were totally eluted. Then column was washed with chloroform/methanol 50:50, and pure methanol to elude the rhamnolipids congeners. The composition of each fraction was analysed by thin layer chromatography (TLC) on Silica Gel plates. Fractions containing rhamnolipids were concentrated using rotary evaporator. Concentrated biosurfactant was lyophilized to obtain white powder.

5.4.5 Determination of Biomass and Biosurfactant Concentration

Cell growth was monitored by measuring the absorbance at (600 nm) of the specimen using UV-1800 UV-Vis Spectrophotometer (Shimadzu, Japan). For determining the biomass concentration (g/l) calibration curves of dry weight (g/l) versus absorbance at 600nm was used. Biosurfactant concentration in culture broth was determined by quantifying hydrolysis released rhamnose by orcinol method after ethyl acetate extraction and acid hydrolysis of the specimens [Chandrasekaran et al, 1980]. Monod equation was used to measure specific growth rate (μ) of strain A11 in glycerol supplemented MSM [Monod et al, 1949].

The photographs taken while production of Rhamnolipids i.e. Biosurfactant from *Pseudomonas aeruginosa* strain A11 is shown from figure 5.4.2 to figure 5.4.8.

Figure 5.4.2: Bottles Containing Mother Liquor and Biomass after Centrifugation

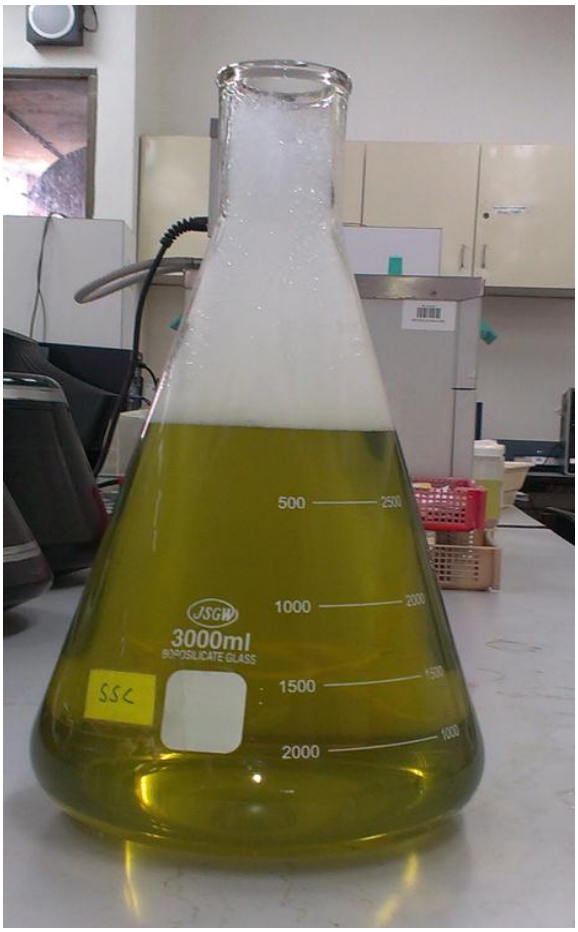

Figure 5.4.3: Mother Liquor Collected from all bottles as shown above

Figure 5.4.4: Bottles Containing Biomass after collecting Mother Liquor

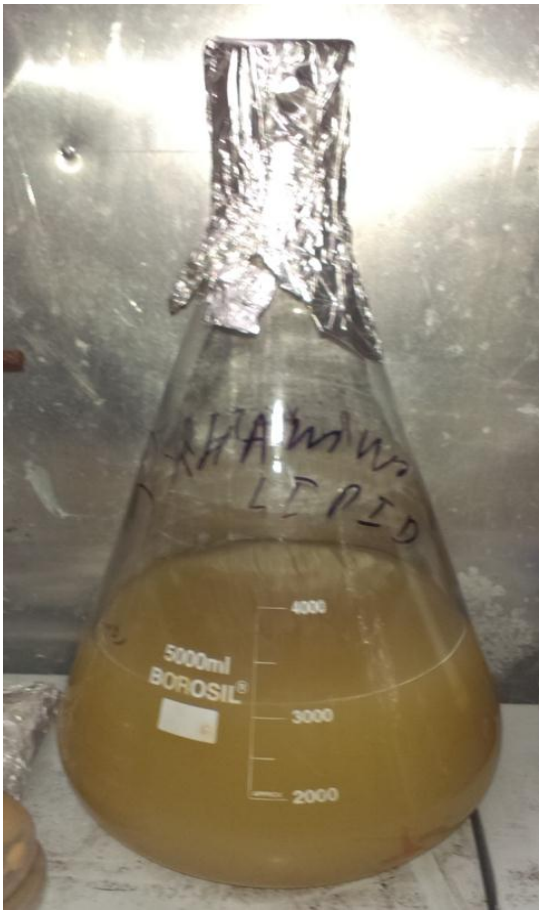

Figure 5.4.5: Acidified Mother Liquor kept in cold room over night

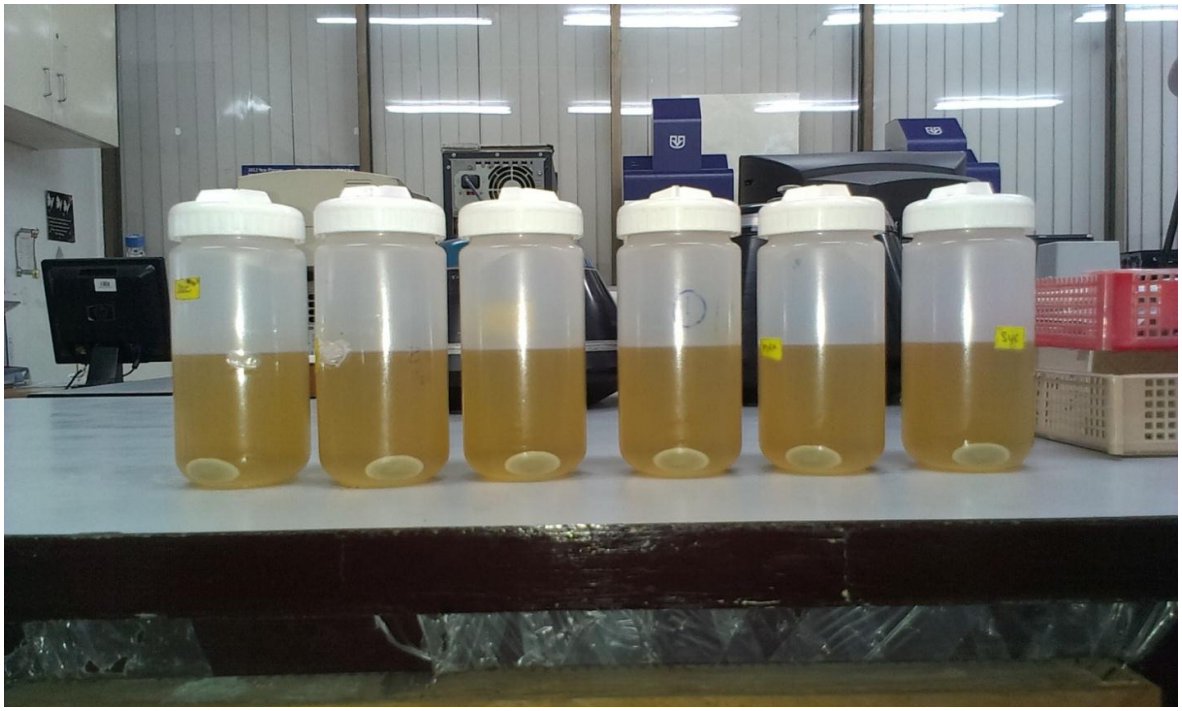

Figure 5.4.6: The bottles containing Mother Liquor as shown above and crude Biosurfactant after centrifugation

Figure 5.4.7: Rotary Dryer for Solvent removal

Figure 5.4.8: Lyophilizer used for Lyophilization of Biosurfactants

5.4.6 *Surface tension and Critical micelle concentration (CMC)*

Surface tension was determined at 25°C using a dunouy meter (CSC Scientific Company Inc., USA) based on platinum-iridium ring detachment method. For the calibration of the instrument ultrapure water (72 mN/m) and pure ethanol (22.7 mN/m) was used to make sure accuracy over the complete range of surface tension measurements. Un-inoculated growth medium was used as negative control. The CMC was found by plotting the surface tension as a function of biosurfactant concentration and point of a sudden change in the surface tension was designated as CMC. For measuring CMC the biosurfactant solution (500mg/L) was serially diluted and measurement of surface tension in triplicate of each dilution was done.

Figure 5.4.9: DuNouy Tensiometer for measurement of Surface Tension of Biosurfactants

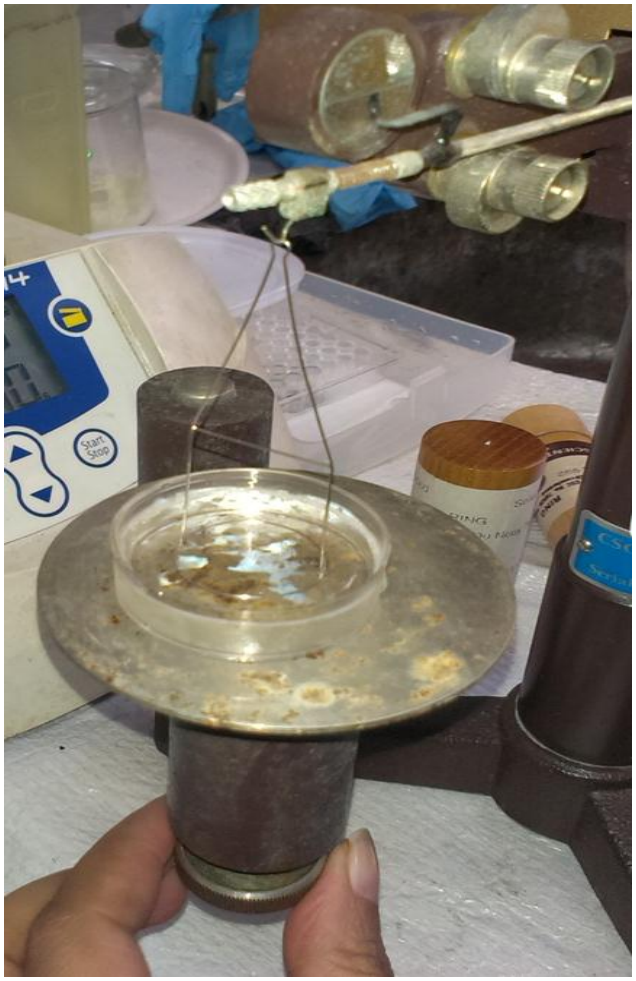

Figure 5.4.10: Platinum-Iridium Ring Detachment Method for measuring Surface Tension of Biosurfactants

5.4.7 *Characterization of Biosurfactant namely Rhamnolipids*

Purified Rhamnolipids were subjected to the following techniques for Characterization.

5.4.7.1 *TLC*

Initial characterization of glycolipids type biosurfactant i.e Rhamnolipids was performed by TLC Silica Gel 60 F254, plate (Merck, Darmstadt , Germany) using chloroform (65): methanol (25): water (4) as mobile phase. The plates were developed using a 50:1:0.05 mixtures of the solution of glacial acetic acid–sulphuric acid–anisaldehyde and heating for 30minutes at the temperature of 90 °C for detecting the glycolipids. Rhamnolipids purchased from Sigma Aldrich, USA served as standard.

5.4.7.2 *FTIR*

The FTIR analysis was performed by using a Nicolet, 6700 FT-IR spectrometer (Thermo Fisher Scientific, USA) in the mid IR range (4000 cm^{-1} - 500 cm^{-1}) Lyophilized biosurfactant powder (~2-5 mg) was mixed with 200 mg of KBr and then a thin pellet is made by compression with the support of a hydraulic press with specimen scattered in the pellets of KBr. The spectrometer was purged with dry nitrogen for approximately 60 minutes to eliminate traces of CO_2 before to spectral measurements. The spectral measurements were done in the transmittance mode with a resolution of 4 cm^{-1}. Prior to recording the FTIR Spectrum of each sample background correction was made.

5.4.7.3 *NMR*

Both ^{1}H NMR and ^{13}C NMR spectra of purified Rhamnolipids were obtained at 300 K in $CdCl_3$ with a NMR Bruker Instrument 500 MHz NMR spectrophotometer. Chemical shifts are provided on the δ- scale relative to tetramethyl silane (TMS).

5.4.7.4 *LC-MS*

Purified biosurfactant Rhamnolipids was characterized by analysing on hybrid Quadrupole-Orbitrap Mass Spectrometer (Q-Exactive, Thermo Fisher Scientific, Austria) coupled to ultra high performance liquid chromatography (UHPLC) system consisting of a LC-pump (Accela), degasser and auto sampler. Chromatographic separation was achieved using Hypersil Gold C_{18} (8µm, 150x4.6mm) reverse phase column. Mobile Phase system consisted of 40% acetonitrile (ACN) and 60% water with 0.1% formic acid for initial four minutes, following next

four minutes percentage of ACN was gradually increased from 40% to 90%, and for rest of run (22 minutes) the percentage of mobile phase was maintained at 90% ACN at a constant flow rate of 500µL/min, at ambient temperature. The auto sampler was set to inject 5µL of sample with a chromatographic run time of 30min. The tuning parameters for the MS were set as follows: capillary temperature 320˚C, spray voltage 3.60 kV, heater temperature 350˚C, sheath Gas flow rate 45, auxiliary Gas flow rate 10 and sweep Gas flow rate is 2. All mass spectra were acquired in the full scan positive ionization mode from m/z 400 to 900 m/z. Data acquisition and processing were performed using Thermo Xcalibur Qual browser (Version 2.2).

5.4.7.5 MALDI-TOF

MALDI-TOF analysis of purified biosurfactant was performed with the 5800 MALDI ToF/ToF ^{TM}system (AB Sciex, MA, USA). Alpha cyano 4-hydroxy cinnamic acid (α-CHCA) was used as MALDI matrix. A 10 mg/mL CHCA solution was prepared in 1:1 (v/v) acetonitrile–0.1% trifluoroacetic acid and Biosurfactant solution (1mg/mL) prepared in methanol was mixed with matrix solutions in the ratio of 1:5. From this mixture 0.5 µL of sample solution containing 0.83µg of biosurfactant was spotted on to the pre-cleaned 384 wells MALDI plate and dried at room temperature. Samples were then analysed in positive ion reflection mode. The equipment was equipped with Nd-YAG, 355nm laser, 1000 Hz laser speed and delayed extraction source. The laser energy (349nm, 8-12 micro joules) was optimized to achieve a good signal to noise ratio and extraction delay time was set at 180ns. The intensity of light was at 60 W/cm^2. Acquisition mass range was 100-1000Da. The data was acquired using TOF/TOF series explorer software and processed by Data Explorer Software.

5.4.7.6 Zeta potential measurements

The zeta potential of biosurfactant measurements were carried out for determining the ionic nature of biosurfactant. Aqueous solution of biosurfactant was prepared in the range of CMC to 5CMC and the solution was subjected to zeta potential measurement at 25 ± 1°C by Zetasizer (Malvern Instruments Ltd., UK).

5.4.7.7 Micelle Size

Micelle size of biosurfactant was determined by Dynamic Light Scattering method by Zetasizer (Malvem instruments Ltd., UK) in aqueous phase.

5.5 Brunauer–Emmett–Teller (BET) Analysis of C-type of Silica Gel (Merck)

Explained in 5.2.3. The surface characteristics are also shown in table 5.5.1.

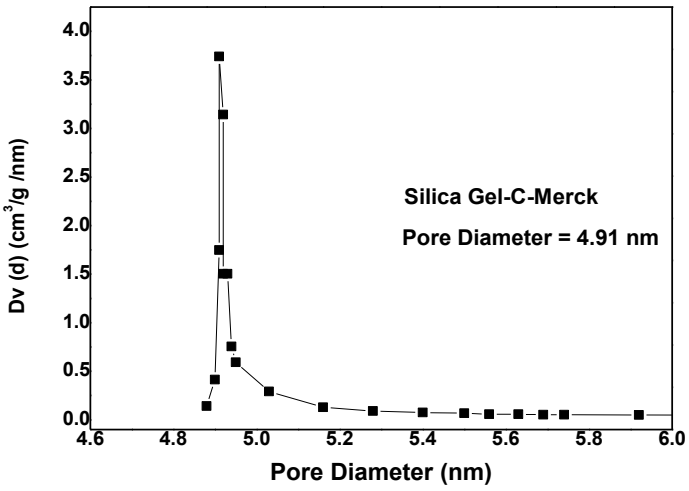

Figure 5.5.1: Pore Diameter of C Type Silica Gel (Merck)

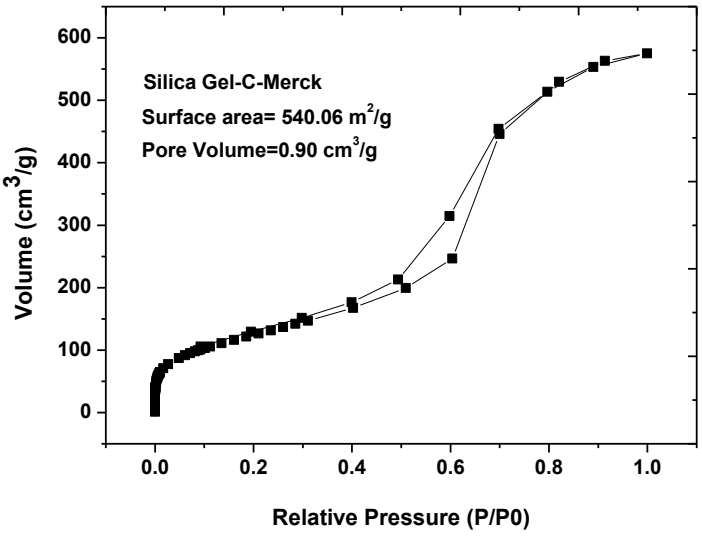

Figure 5.5.2: Pore Volume and Surface Area of C- type Silica Gel (Merck)

Table 5.5.1: Surface characteristics of C-type Silica Gel (Merck)

Catalyst	S_{BET} [a] ($m^2 g^{-1}$)	V_{Pore} [b] ($cm^3 g^{-1}$)	Average pore Diameter [c] (Å)	Pore Diameter (Å)
Silica Gel-C-(Merck)	540.06	0.90	64	49.1

a- BET surface area

b- Total pore volume by Langmuir method

c- Average pore diameter by Langmuir method

5.6 Lipopeptide Biosurfactant Surfactin Promoting Methane Hydrate Formation in Fixed Bed of Silica Gel: Thermodynamic and Kinetic Studies

5.6.1 Materials

Highest purity grade chemicals were used in the present study. The Silica Gel was used as porous media for fixed bed system. Type C Silica Gels used in the present study have mesh size of 230–400. The various materials which are used in the experiments along with their supplier are shown in table 5.6.1.

Table 5.6.1: Materials used and their suppliers

Material	Supplier
Methane with purity of 99.99%	Chemtron Science Laboratory, Mumbai, India
C Type Silica Gel	Merck Specialties Pvt. Limited, Mumbai, India
Distilled Water	Water used in the study was De-ionized in Milli-Q equipment (Millipore, Bedford, MA) and had a resistivity of 18 MΩ.
Microbiological growth media	HiMedia, India
Surfactin	Synthesized in the laboratory from *Bacillus subtilis* strain A21

5.6.2 Bacillus subtilis strain A21 *growing on nutrient agar plate as shown in figure 5.6.1*

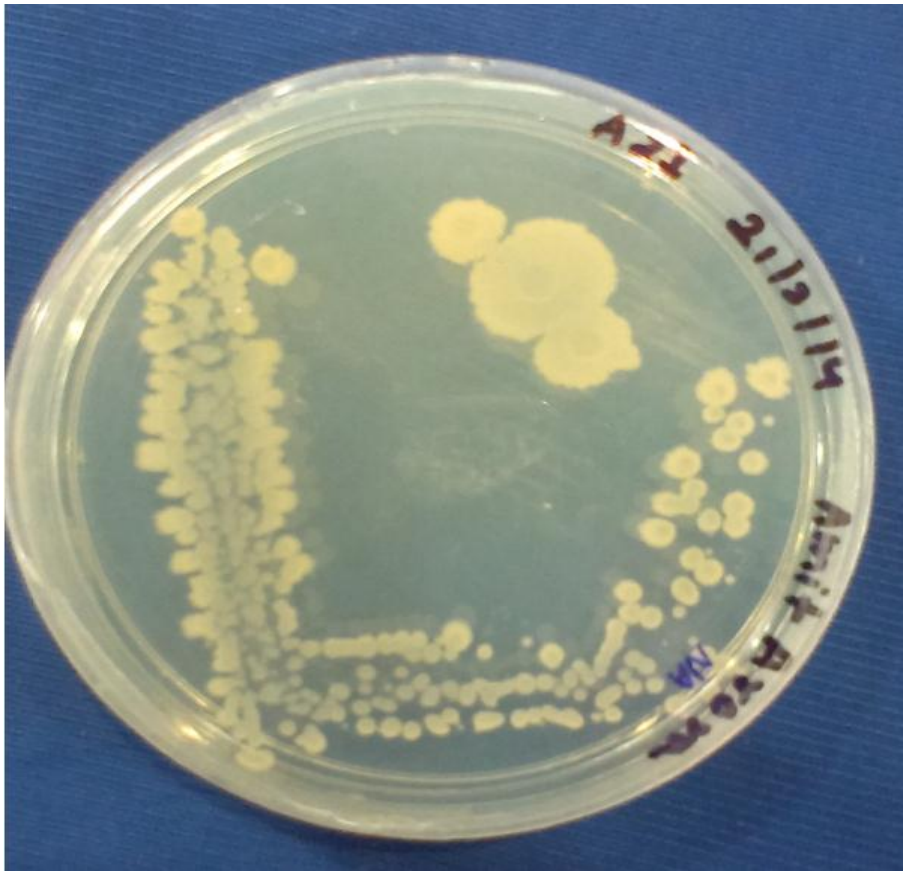

Figure 5.6.1: *Bacillus subtilis* strain A21 growing on nutrient agar plate

5.6.3 Microorganism and growth medium composition

The biosurfactant producing microorganism *Bacillus subtilis* strain A21 was separated from rhizosphere of wild plant *Parthenium hysterophorus* growing at Dalma Wildlife Sanctuary, Jamshedpur, India [Singh et al, 2013]. For the production of the biosurfactant from strain A21 the minimal salt medium (MSM) used for the aerobic growth of the bacterium supplemented with 4%(w/v) sucrose as a carbon source is consisted of 4 g L^{-1} NH_4NO_3, 4 g L^{-1} KH_2PO_4, 5.68 g L^{-1} Na_2HPO_4, 0.78 mg $^{-1}$ $CaCl_2$, 197.18 mg L^{-1} $MgSO_4$, 1.112 mg L^{-1} $FeSO_4$, 00148mg/l Ethylenediaminetetraacetic acid (EDTA). The pH of MSM was maintained to 7.0 ± 0.5 with help of 1 N NaOH and 1 N HCl.

5.6.4 Biosurfactant production and purification

The biosurfactant production was carried out in Erlenmeyer flasks (2l) containing 500 ml aliquots of MSM. The MSM was inoculated (2%) with bacterial suspension prepared by growing bacterium in nutrient broth (NB) for 12 h and then adjusting the optical density with NB to ~0.5 at 600nm wavelength. The flasks were incubated at 30°C for 48h with agitation rate of 200 rpm in Multi-stack shacking Incubator (Labtech, India). The samples were taken after every 12 h interval for monitoring bacterial growth and biosurfactant production.

The growth of strain A21 was determined by measuring the absorbance at 600 nm using UV-1800 UV-Vis Spectrophotometer (Shimadzu, Japan). For the determining biomass concentration (g/l) calibration curves of dry weight (g/l) verses absorbance at 600nm was used. The production of the biosurfactant was found by calculating surface tension of growth medium. Biosurfactant yield was determined by weighting the acid precipitated mass.

5.6.5 Biosurfactant purification

Earlier mentioned processes [Sanchez et al, 2007] with slight modification were used for the Purification of biosurfactant. In short, the cell suspension was centrifuged at 8,000×g for 10 min in order to prepare the cell-free supernatant (CFS) at 4 °C. The acidification of CFS was done with 6 N HCl to pH 2 and incubated overnight at 4 °C. To collect the precipitated biosurfactant centrifugation (15,000×g for 20 minute) was done which was then dissolved in methanol. Afterwards the evaporation of methanol using rotary evaporator, was done, then the lyophilization of biosurfactant was done in order to obtain the off white powder. Biosurfactant

was then re-dissolved in methanol and further, purification was carried out using Gel filtration on Sephadex LH-20 column (60 cm x 1cm) with methanol as the eluent [Kim et al, 2009]. Thin layer chromatography on Silica Gel plates was used in order to check the composition of each fraction. Fraction having biosurfactant i.e. Surfactin were concentrated by rotary evaporator and then lyophilized to get obtain the white powder biosurfactant.

5.6.6 Surface tension and CMC

Explained in 5.4.6

5.6.7 Characterization of Biosurfactant Surfactin

Purified surfactin was subjected to the following techniques for Characterization.

5.6.7.1 TLC

Biosurfactant i.e Surfactin was characterized by TLC Silica Gel 60 F254, plate (Merck, Darmstadt, Germany). The mobile phase used was chloroform (65%): methanol (25%): water (4%). The development of the plates was done by spraying the plate with water. Surfactin purchased from Sigma Aldrich, USA served as standard. TLC of Surfactin synthesized from strain A21 and standard from Sigma Aldrich, USA is shown in figure 5.6.2.

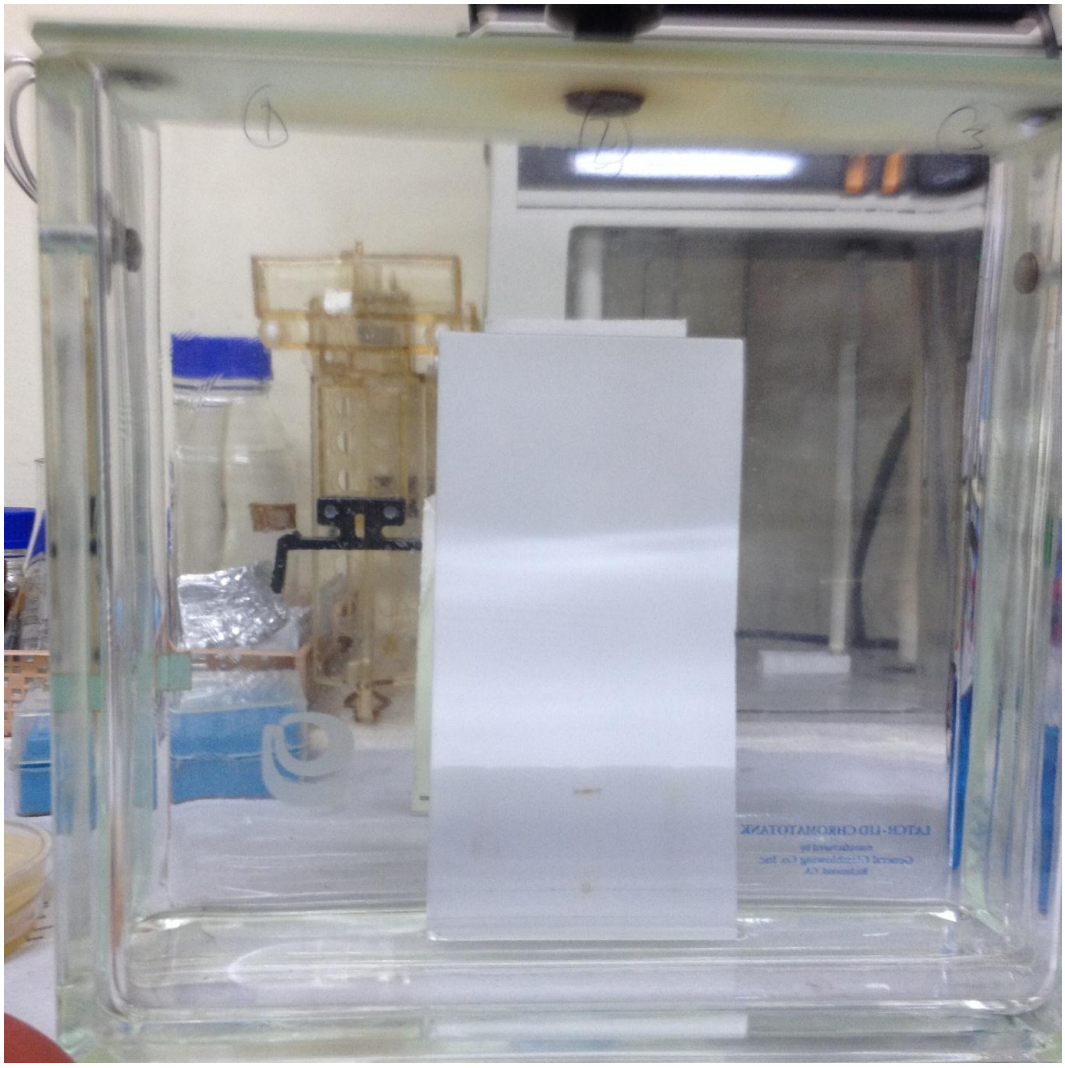

Figure 5.6.2: TLC of Surfactin synthesized from strain A21 and standard from Sigma Aldrich, USA

5.6.7.2 *FTIR*

Explained in 5.4.7.2.

5.6.7.3 *NMR*

Both ^{1}H NMR and ^{13}C NMR spectra of purified biosurfactant i.e Surfactin produced by strain A21 were obtained in deuterated Dimethyl sulfoxide (DMSO) with a 500 MHz Bruker NMR spectrophotometer Instrument. Chemical shifts are given on the δ-scale relative to TMS.

5.6.7.4 *MALDI-TOF*

Explained in 5.4.7.5.

5.6.7.5 *Amino acid analysis*

Amino acid analysis of lipopeptide biosurfactant i.e Surfactin was found using waters amino acid analyser (Waters Corporation USA) after complete hydrolysis of the sample in 6N HCL at $105^{0}C$ for 24 hours.

5.6.7.6 *HPLC*

HPLC of purified surfactin was performed on Waters HPLC System (Water Corporation U.S.A). Stationary phase was Phenomax C-18 Column (250mmx 4.6mmx5 μm). A mixture of 3.8 mm trifluoroacetic acid (TFAA) (30 vol %) and acetonitrile (ACN) flowing at 1ml/min. was used as mobile phase.

5.6.7.7 *Zeta potential measurements*

Explained in 5.4.7.6.

5.6.7.8 *Micelle Size*

Explained in 5.4.7.7.

5.7 Influence of a Novel Green Kinetic Inhibitor on Formation of Natural Gas Hydrate and Methane Hydrate

5.7.1 *Materials*

The materials used in the present study along with their suppliers are shown as per the following **table 5.7.1**.

Table 5.7.1: Materials used in present study

Material	Supplier
Natural Gas with composition 88.009% Methane, 7.234% Ethane, 4.757% Propane	Vadilal Gases Ltd, Baroda
Pure Methane	Chemtron Science Laboratory, Navi Mumbai, India
C Type Silica Gel	Rankem
C Type Silica Gel	Merck
Distilled Water	Prepared in Laboratory
Bio-Surfactant Calcium LignoSulphonate i.e. CaLS	Rass Sidh, Mumbai Costing Rs 500/Kg

The various materials used in the present study are also shown in Figures 5.7.1 and Figure 5.7.2.

Figure 5.7.1: Sample of Calcium LignoSulphonate

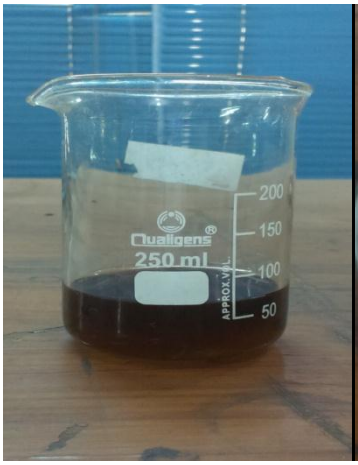

Figure5.7.2(a): Distilled water containing 1 wt. % CaLS

Figure5.7.2(b): C-type Silica Gel(Merck)

Figure5.7.2(c): Reactor Packed with 90% saturated (Distilled water with 1wt % CaLS) Silica Gel (Merck).

The distilled water containing 5wt. %, 1wt. %, 0.1 wt. % of CaLS is shown in figure 5.7.3.

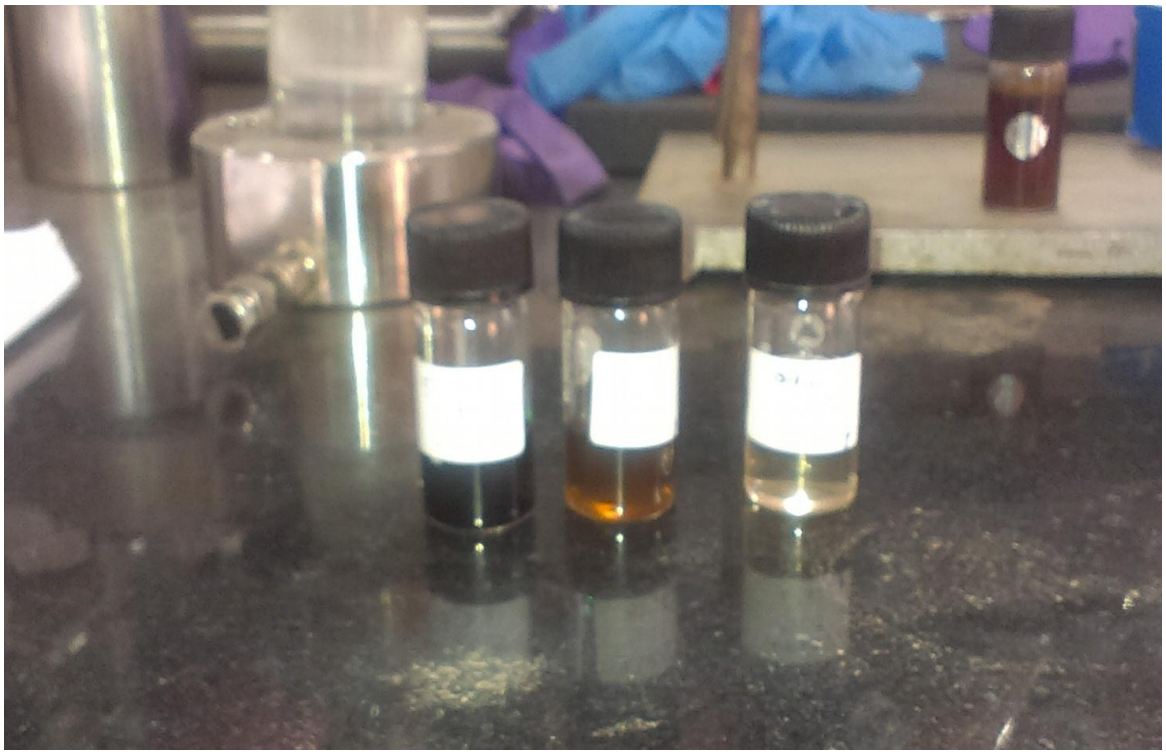

Figure 5.7.3: The distilled water containing 5wt. %, 1wt. %, 0.1 wt. % of CaLS

5.7.2 *Method of Gas Chromatography of Natural Gas*

The setup was equipped with a Gas chromatograph (GC-2014AT, Shimadzu), Column, was SHIN Carbon, dimensions was 1/ 16 inch dia, 3 m length carrier Gas helium; temperature of column was 60^0C and injector temperature 200^oC, detector was Thermal Conductivity Detector (TCD) temperature of detector was 150 ^{o}C, flow of carrier Gas 10ml/ minute.

5.7.3 *Characterization of Calcium LignoSulphonate*

CaLS was characterized with FTIR, UV, CHNS, GPC, FE-SEM, EDS, FE-SEM MIXING, DTG and Solid NMR as explained below:

5.7.3.1 *FTIR*

Explained in 5.4.7.2.

5.7.3.2 *Ultra Violet Spectroscopy*

Absorption spectra (250- 700 nm) of CaLS were recorded on SHIMADZU 1800 machine. The optical absorption spectrum was recorded on UV-VIS double beam spectrophotometer of Shimadzu 1800. Prior to recording UV Spectrum of sample baseline correction was made.

5.7.3.3 *CHNS*

CHNS of CaLS was carried on Elementar, Vario Micro Cube Machine. The carrying Gas used in the test was helium. The temperature of combustion tube was 1150 ^{0}C and reduction tube temperature was 850 ^{0}C.

5.7.3.4 ICPMS

The percentage of the elements Na, Mg, K and Ca in the Calciumn LignoSulphonate sample was determined using NEXION 300 Inductively Coupled Plasma- Mass Spectrometry (ICP-MS) from M/S Perkin Elmer. The instrument was calibrated with the help of multi elemental standard

solution procured from Perkin Elmer and the calibration plots for these elements are also shown. The sample was injected through a peristaltic pump equipped with Tygon tubing at a flow rate of 24µL/ min. Nebulization of samples was performed by means of a concentric nebulizer. The other parameters during ICPMS analysis are: the nebulization Gas, outer Gas flow and auxiliary Gas flow rate were 0.75 L/ minute, 13.5 L/ minute and 1.8 L / minute, respectively. Plasma power was set at 1350 W and ion lens voltages were adjusted in order to get the maximum intensity for analyte.

5.7.3.5 GPC

Molecular weight and molecular weight distribution of biosurfactant i.e CaLS was determined using a GPC system (Model: 2414; Make: Waters (I) Pvt. Ltd., USA) (Das et al, 2013). We have used aqueous GPC with HSPGel^{TM} column of dimension 6.0×150 mm. The GPC Column of HSPGel^{TM} AQ series was used for room temperature analysis of CaLS. Two Columns were connected with each other to measure the molecular weight of polymeric compounds. The first column was HSPGel^{TM} AQ 4.0, Part no. 186001787 of Waters in which molecular weight range was between 10,000 to 4,00,000 and the other column was HSPGel^{TM} AQ 6.0, Part no. 186001789 has molecular weight range between 1,00,000 to 1,00,00,000. The mobile phase was present in the aqueous solution (for this study HPLC grade water was used). Before injecting the sample solution into the column its filtration was done using Whatman syringe filter (0.45µm). The flow rate of injection was fixed at 0.6 mL/min, and the column temperature was kept at 30 ^{0}C during the study.

5.7.3.6 FE-SEM

FE-SEM analysis of CaLS was carried on FE-SEM Supra 55 (Carl Zeiss, Germany) equipped with Energy Dispersive Microanalysis (Oxford Liquid Nitrogen free SDD X MAX 50 EDS), The samples were scanned under 5 kV accelerating voltage to record their surface morphology at different magnification. EDAX analysis and Elemental Mapping of different samples were done. The powder samples were coated with platinum for microscopic measurement. Platinum coated

sample were placed under vacuum maintained in main chamber, pictures were taken at different magnification, different scales, different locations.

The samples were scanned under 5 kV accelerating voltage to record their surface morphology at different magnifications. Samples were sprinkled on the carbon tape mounted on the aluminium stub and the sample was kept in sputtering chamber for coating of a thin layer of platinum for 30 s at 30 µA current to make the sample conducting. Carbon tape was used to (Coater) make contact of the sample with the aluminium sample holder. The samples were scanned under 15 kV accelerating voltage with 30mm Aperture and made greater than 5.5mm working distance to record their surface morphology at different magnifications.

Energy dispersive X-Rays (EDX) analysis of the samples was done to examine the elemental distribution in the samples at any particular point or in a selected area using FESEM.

5.7.3.7 TGA

Thermo-gravimetric analysis of CaLS was carried out using EXSTAR TG/DTA 6300 instruments. Thermogravimetric / Differential Thermal Analysis (TG / DTA) of the sample was carried out on SII 6300 EXSTAR having the features of operating in either DSC or DTA mode. It was equipped with horizontal differential type balance with a programmable heating rate (0.01 to 100°C / minute) in the temperature range of ambient to 1500°C. The sample was loaded in the pan with pan material of alumina and pan volume size 45µL. The sample was heated in Air with a flow rates 200 ml/minute. Range / sensitivity of TG and DTA measurements are: 200 m/0.2 µg and +1000 µV / 0.06 µV, respectively. The data is analysed using the muse software.

5.7.3.8 NMR

Solid state C-13 NMR of CaLS was carried on JEOL 4OO machine

5.8 Analysis of C-type Silica Gel (Merck) before and after growing through Methane Hydrate Formation Experience

5.8.1 *FTIR of C-type Silica Gel (Merck) before and after growing through Methane Hydrate Formation Experience*

The FTIR analysis of C-type Silica Gel (Merck) before and after growing through Methane Hydrate Formation Experience was performed using the above explain method.

5.8.2 *Scanning Electron Microscopy (SEM) of C- type Silica Gel (Merck) before and after going for Gas Hydrate Formation experience*

A scanning electron microscope, SEM (HITACHI, Japan; Model: S-3400N) was used to determine the morphology of samples. The powder samples were coated with gold by plasma prior to measurement.

CHAPTER-6

RESULTS AND DISCUSSION

6.1 Effect of Different Fixed Bed Media on the Performance of Sodium Dodecyl Sulphate for Hydrate Based CO_2 Capture

6.1.1 *Induction Time and Gas Consumption*

Table 6.1.1 abridges all the examinations done during this study significant data including trial temperature & pressure, induction time, span of tests, moles of Gas consumed at the completion of the reaction is shown in **Table 6.1.1**. Working temperature of 274.65 K and pressure 3.0 MPa at this temperature was assessed from CSMGEM (software). Equilibrium Hydrate Formation pressure at 274.65 K was observed to be 1.49 MPa [Sloan et al, 2008].

Table 6.1.1: Summary of experiments: induction time and Gas consumption; experimental pressure and temperature used were 3.0 MPa and 274.65 K respectively. Amount of water used for all the experiment was 50 cm^3 except experiment-1(no water). Amount of SDS used was 0.5 wt. %.

System	Exp. No.	Mass of packing, (g)	Induction time (IT) (min)	End of Experiment		
				Time* (min)	Mol of Gas consumed	Mol of Gas/mol of water
Zeolite 5A	1	130	-	500	0.300	-
Zeolite 5A/water	2	130	4	500	0.074	0.027
	3	130	10	500	0.069	0.024
Zeolite 13X/water	4	108	300	500	0.084	0.030
	5	108	500	500	0.081	0.029
	6	108	10	400	0.082	0.029
Zeolite 13X/SDS/water	7	108	10	230	0.088	0.032
	8	108	8	300	0.091	0.033
Silica sand/Water	9	250	35	300	0.091	0.033
	10	250	10	300	0.090	0.032
	11	250	20	300	0.114	0.041
Silica sand/ SDS/ Water	12	250	25	300	0.196	0.070
	13	250	10	300	0.181	0.065
	14	250	50	300	0.201	0.072

After Induction Time*

6.1.2 *Typical Hydrate Formation-Dissociation Curve along with Pressure and Temperature Profile Acquired from Zeolite 5A/Water System*

Figure 6.1.1 shows the Hydrate Formation or decomposition curves along with temperature profile acquired from zeolite 5A/water system in which CR is immersed into the temperateture controlled water bath at 274.65 K and pressurized at the experimental pressure (3.0 MPa). The inset in Figure 6.1.1(a) shows the location of three thermocouples placed in the reactor. All the experiments were done in batch mode. Throughout the Hydrate Formation process, pressure keeps on dropping and this involves Gas dissolution, nucleation and Hydrate growth stages. As shown in the figure, nucleation occurs after about 4 minutes. At the nucleation point, as shown in Figure 6.1.1(a), there is a sharp drop in the pressure profile accompanied with a rapid rise in temperature [Figure 6.1.1(b)] as Hydrate nucleation is an exothermic in nature. Hydrate Formation continued until no drop in the pressure of the reactor was observed. At this point, temperature of water bath was increased up to 288.15K. Due to the additional heat supply Hydrates start to dissociate and the system once again reaches the initial pressure.

6.1.3 *The comparison of Gas consumption for Hydrate growth measured in a fixed bed media of zeolite 5A and 13X with the Gas consumption without any Hydrate growth in dry zeolite 5A*

The amount of Gas consumed is calculated by using equation 1 & 2 from annexure.

Figure 6.1.2 shows the comparison of Gas consumption for growth of Gas Hydrate calculated in a fixed bed media of zeolite 5A and 13X with the Gas consumption without any Hydrate growth in dry zeolite 5A. Time zero in the curve correlates to induction time for the Hydrate Formation. An experiment was carried out to evaluate the CO_2-capture efficiency of dry zeolite (5A) at Gas Hydrate Formation conditions (pressure and temperature). In this experiment dry zeolite was used as a fixed bed media. As can be seen in Figure 6.1.2, at Hydrate Formation conditions, the amount of Gas that gets adsorbed in dry zeolite is very small. However it is reported in literature, that at high temperatures, zeolites show significant Gas consumption [Phan et al, 2010, Kim et al, 2015, Park et al, 2012, Zang et al, 2009, Smith et al, 2001, Dicharry et al, 2013]. On the other hand, according to our observations, at Hydrate Formation conditions, the consumption of Gas in presence of water is significantly higher than that in case of dry zeolite. This is attributed to the Formation of Gas Hydrates, as the experimental conditions being employed here are highly favourable for CO_2 Hydrate Formation.

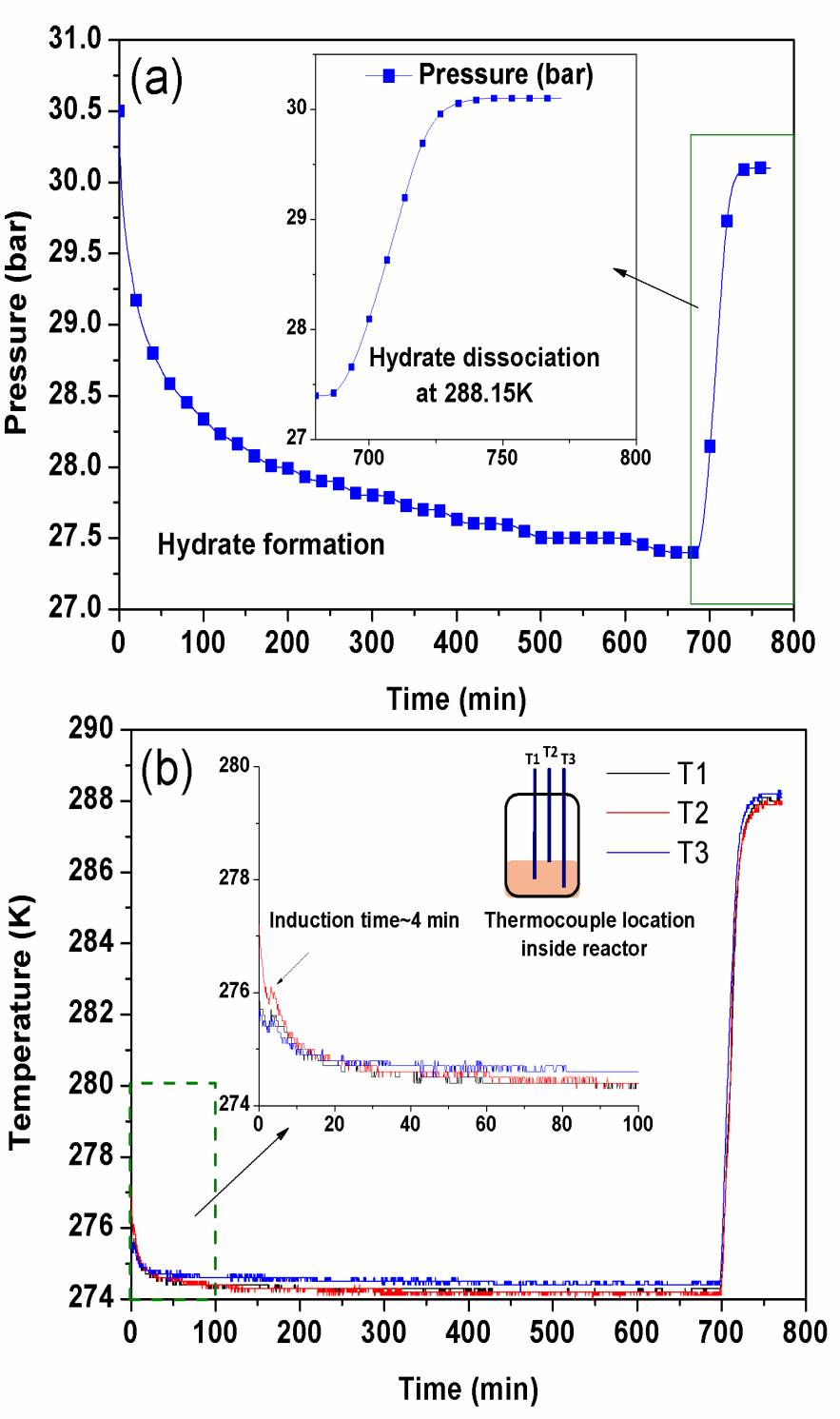

Figure 6.1.1: Typical Hydrate Formation-Dissociation curve along with temperature profile (Experimental pressure and temperature was 3.0 MPa and 274.65K. Inset shows the location of three thermocouples inside the reactor)

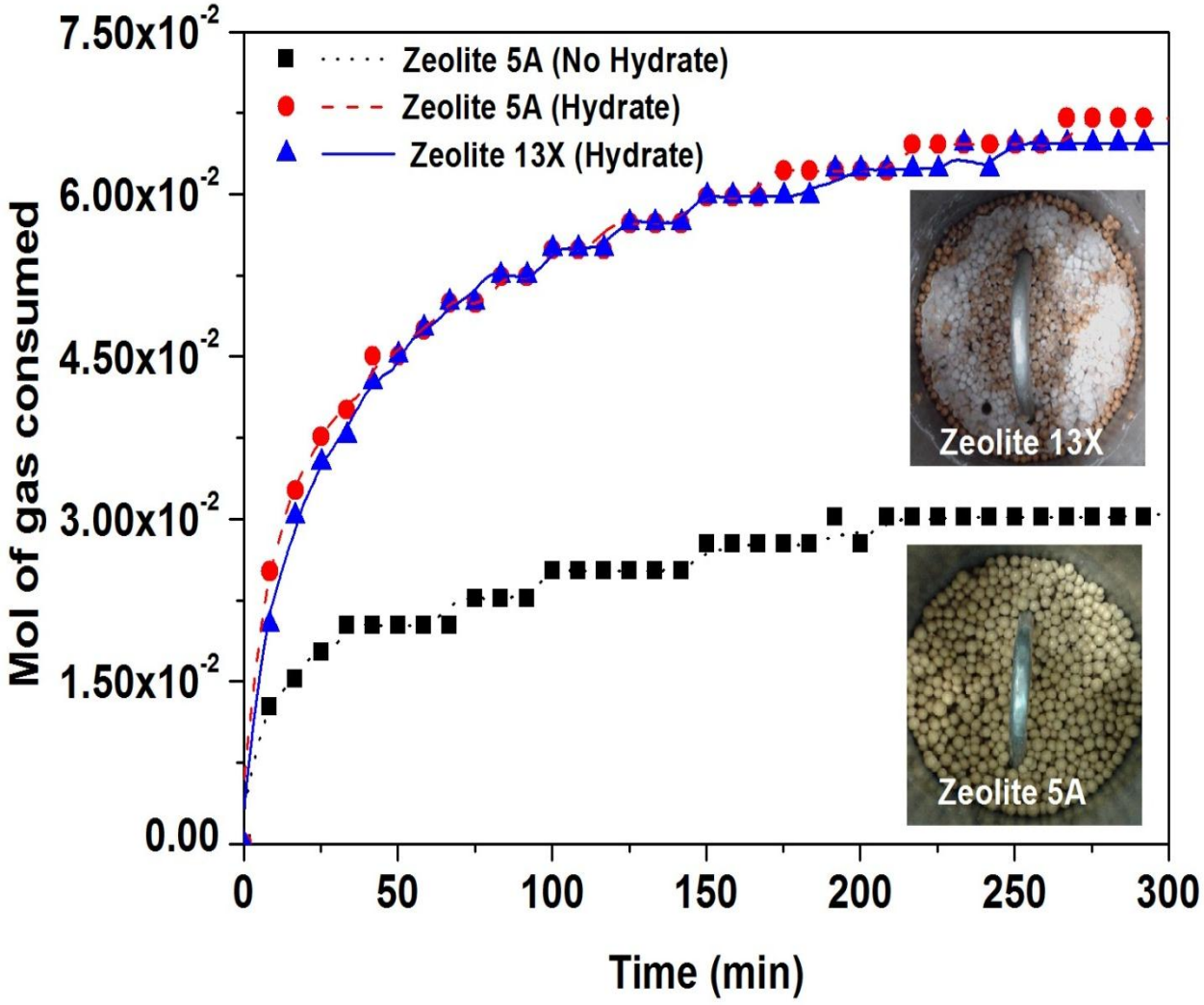

Figure 6.1.2: Comparison of Gas consumption for Hydrate growth measured in a fixed bed media of zeolite 5A and 13X with the Gas consumption in dry zeolite 5A. Time zero in the curve corresponds to nucleation point (induction time) for the Hydrate experiments.

6.1.4 *The comparison of Gas uptake for Hydrate growth measured in fixed bed media of zeolite 13X and Silica sand in presence /absence of SDS*

The amount of Gas consumed is calculated by using equation 1 & 2 from annexure.

Figure 6.1.3 shows the comparison of Gas uptake for Hydrate growth measured in fixed bed media of zeolite 13X and Silica sand in absence or presence of SDS. A constant amount of SDS (0.5 wt. %) was used for both the experiments. Time zero in the curve corresponds to nucleation point (induction time) for the experiments. As shown in the figure, the addition of SDS enhances the rate and Gas consumption in case of both the fixed bed media being studied. However, the

effect of SDS in presence of Silica sand is much more drastic as compared to zeolite. It was found that the Gas consumption in sand/SDS system is ~ 4 times greater than that in a system with pure sand. In the absence of any surfactant, Hydrates and closed water form a slushy Hydrate mass this hinders the mass transfer of Gas through the Gas or water interface [Linga et al, 2012]. This problem can be bypassed in the presence of SDS. It has been reported in literature that the promotion in water to Hydrate conversion is due to capillary driven supply of the water which diffuses through the porous Hydrate layer in presence of SDS. Due to this, there is more contact between water and the Hydrate forming Gases, even in the presence of solid Hydrate phase on the interface [Dicharry et al, 2013, Gayet et al, 2005, Okutani et al, 2008, Pang et al, 2007].

It can also be seen from Figure 6.1.3 that even in the absence of SDS, Silica sand shows improved Gas uptake kinetics as compared to zeolite. This enhanced rate of Gas uptake in Silica sand can be explained on the basis of shift of the Gas in the fixed bed, movement of water particles in the fixed bed, the presence of twisting paths in the bed and also the capillary effect of water movement in the porous Hydrate.

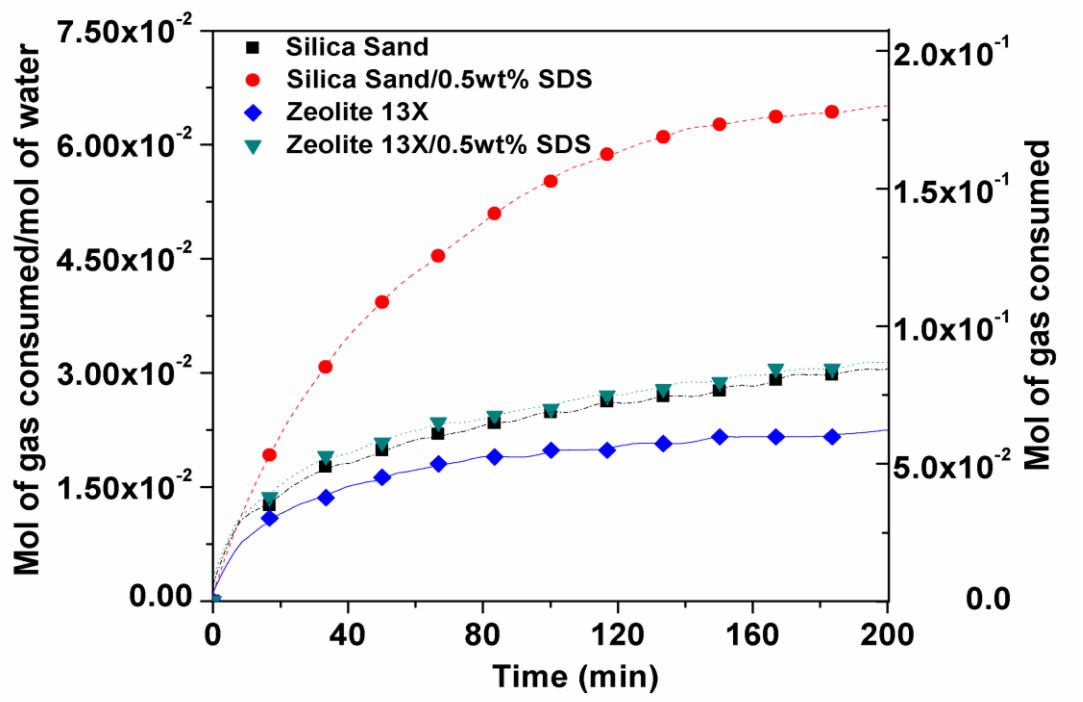

Figure 6.1.3: Comparison of Gas consumption for Hydrate growth measured in a fixed bed media of zeolite 13X and Silica sand in presence or absence of SDS. Time zero in the curve corresponds to nucleation point (induction time) for the experiments.

In the case of zeolite (porous media), the size of the pores may have a significant role to play in the Hydrate Formation process. Zeolite 13X has a pore size of ~12 Å. When water comes in contact with zeolite particles a large amount of the water gets trapped inside the pores present on the surface of the particles. The size of the pores however, is too small to accommodate Hydrate crystals as the size of the cages in Hydrate crystals is bigger than the pore size available on the surface of zeolite particles. This renders the water inside the pores unavailable to participate in the Hydrate Formation process and thus very low water to Hydrate conversions are observed in case of systems using zeolite as a fixed bed medium. The induction time in Gas Hydrate Formation is vital parameter for kinetic studies of the same. Table 1 shows the induction time for CO_2 Hydrate Formation experiments in presence of Silica sand and zeolite. As induction time is a stochastic phenomenon, it changes a lot even if operating conditions are same. Zeolite 13X shows the highest induction time compared to the other fixed bed media studied here. Table 6.1.1 also shows the effect of SDS (0.5 wt. %) on induction times obtained using Silica sand and zeolite 13X as fixed bed media. It can be seen that the occurrence of SDS in the system reduces the induction time. This indicates that the nucleation of Gas Hydrates was promoted in the occurrence of SDS. This study will be helpful in the selection of suitable fixed bed media for Hydrate based Gas separation (HBGS) process.

6.1.5 *Conclusion of this Task*

The impact of sodium dodecyl sulphate on carbon dioxide capture by Gas Hydrate Formation in presence of different fixed bed (Silica sand and zeolite) was investigated. A fixed amount of SDS (0.5 wt. %) was used. It was found that the effect of SDS is media dependant. In the case of Silica sand, SDS greatly impacted the Hydrate Formation kinetics whereas it did not have such a marked effect in the case of zeolite. Presence of SDS in the system was found to lower the induction time. A fixed bed reactor is more cost effective than a stirred tank reactor if used for commercial applications.

6.2 Carbon dioxide Hydrate Formation in Fixed Bed and Stirred Tank Reactor Systems

6.2.1 *Typical pressure-temperature curve (P-T profile) of CO_2 Hydrate Formation in a fixed bed of spherical Silica Gel (pore size 100 nm) at 3.0 MPa and 274.5 K*

All the experiments in this study were performed at same temperature and pressure conditions. Operating temperature of 274.5 K and pressure 3.0 MPa was estimated from literature. Figure 6.2.1 presents the Hydrate Formation curves with temperature profile (P-T Curve) obtained with pure CO_2 in a fixed bed reactor of spherical Silica Gel (pore size 100 nm) in which CR is immersed into the temperateture controlled water bath at 274.5 K and pressurized at the experimental pressure (3.0 MPa). All experiments were done in batch mode. This curve was divided in to three main stages:

(a) Gas dissolution: When CO_2 comes in contact with water; some CO_2 will get dissolved in the water. The amount that dissolves at a particular temperature depends on the experimental pressure which is highly favourable for dissolution and hence, in Hydrate Formation. As can be seen in figure 6.2.1, a significant number of moles of CO_2 gets dissolved in the water.

(b) Nucleation: A new thermodynamic phase forms in the first phase. Hydrate nucleation is said to be a statistical process taking place in a well-controlled environment. A nucleation site is a point at which a phase transition takes place and in Formation of Hydrates the solid is formed from a fluid phase. Nucleation is defined as the process that tells how much long a viewer has to wait before the new phase appears. Nucleation can be heterogeneous or homogeneous. Heterogeneous nucleation takes place at nucleation sites on surfaces in the system. Homogenous nucleation occurs away from the surface [Pruppacher et al, 1997]. As shown in the curve, nucleation takes place at the 125 minute mark. At the nucleation point, as shown in the curve, a sharp drop in the pressure profile and a rapid growth in the temperature (due to the exothermic nature of Hydrate nucleation) is observed [Babu et al, 2013]. Nucleation is a highly stochastic process, so even for two same systems, nucleation can occur after widely different time periods [Kumar et al, 2015].

***(c) Hydrate growth*:** Hydrate growth is a final stage of a Hydrate crystallization process and results into the final characteristic settlement of a crystalline Bravais lattice. The action of crystal growth yields a crystalline solid which is a close packed, with settled positions in space relative to each other. In the present case, the Hydrate forming guest, CO_2 forms structure I Hydrate in

conjunction with water molecules. As can be seen in figure 6.2.1, after Hydrate nucleation, the pressure of the CR continues to drop until there is no more driving force for Hydrate Formation and further drop in the pressure of the reactor is not observed.

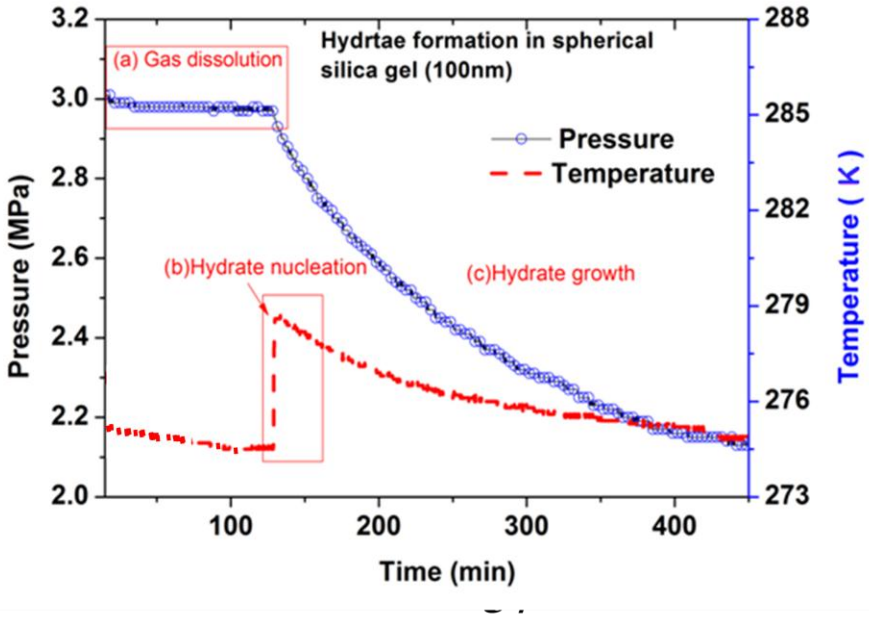

Figure 6.2.1: Typical pressure-temperature curve (P-T profile) of CO_2 Hydrate Formation in a fixed bed of spherical Silica Gel (100 nm) at 3.0 MPa and 274.5 K.

6.2.2 *Hydrate Formation curves (pressure profile) along with visualization of Hydrates obtained with pure CO_2 in a stirred tank reactor*

Figure 6.2.2 presents the Hydrate Formation curves (pressure profile) along with visualization of Hydrates obtained with pure CO_2 in a stirred tank reactor. Profile is again similar to that obtained using FBR systemn as shown in Figure 6.2.1. In the inset figures, one can see that at the initial stage only water and Gas is present in the reactor, however after hydrtae growth a solid mass of hydrtae is formed which looks like ice (inset figure 6.2.2).

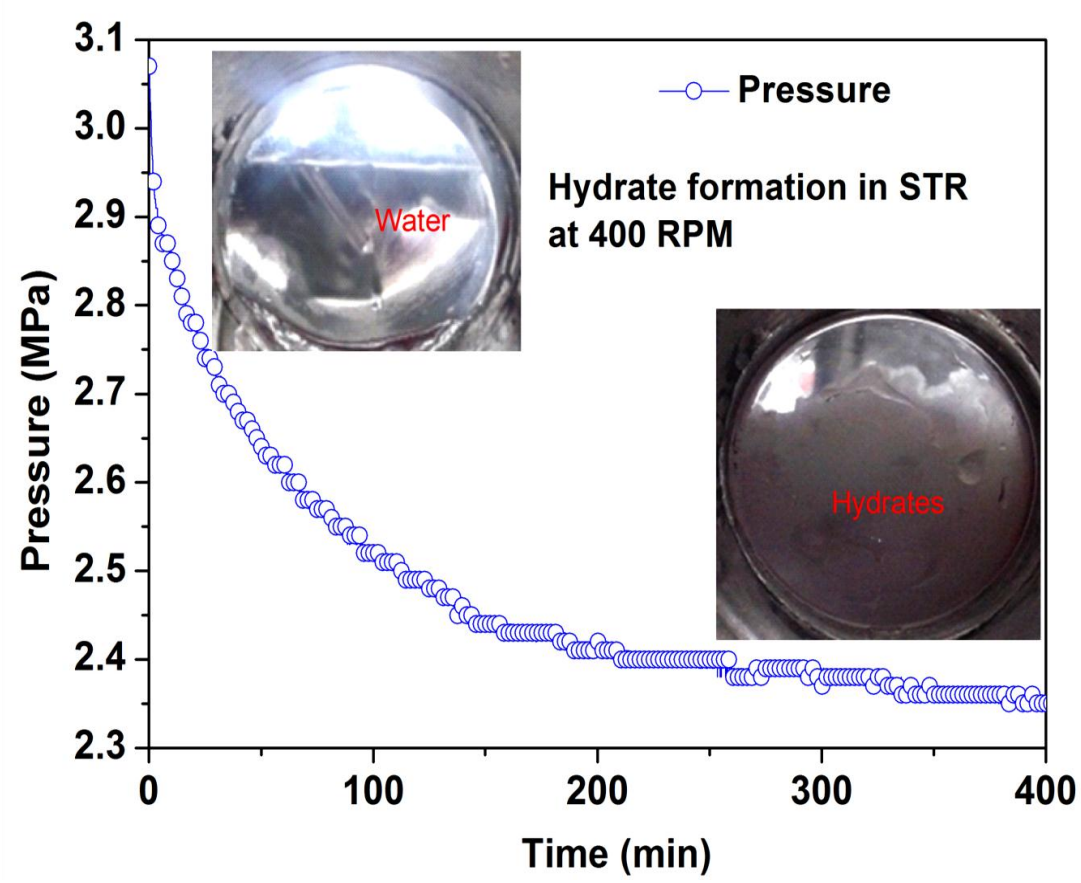

Figure 6.2.2: Pressure profile obtained during CO_2 Hydrate Formation in a stirred tank reactor at 400 rpm along with visual presentation of Hydrates at 3.0 MPa and 274.5 K

6.2.3 *The comparison of Gas consumption during Hydrate growth (mol of Gas/mol of water) in fixed bed of Silica Gel (pore size 100 nm), Silica Sand and stirred tank reactor systems*

The amount of Gas consumed is calculated by using equation 1 & 2 from annexure.

Figure 6.2.3 shows the comparison of consumption of Gas during Hydrate growth (mol of Gas/mol of water) in fixed bed and stirred tank reactor systems. Silica Gel (pore size 100 nm) and Silica sand was used as a porous media in the fixed bed setup. Time zero in the curve represents the nucleation point (induction) for the experiments. As shown in the figure, the initial rate of Formation of Hydrate for first 20 minutes is almost similar for all the systems while after some time the Hydrate growth curve gets saturated in the STR system culminating in low water to Hydrate transformation. However in the case of FBR system, the rate of Formation of Hydrate is continuously increasing. As shown in the curve, FBR shows enhanced rate and conversion

(water to Hydrate) and Silica Gel gives better results as compared to Silica sand. It is clearly shown in this study that porous media improves growth rate of Hydrate and attains maximum water to Hydrate transformation.

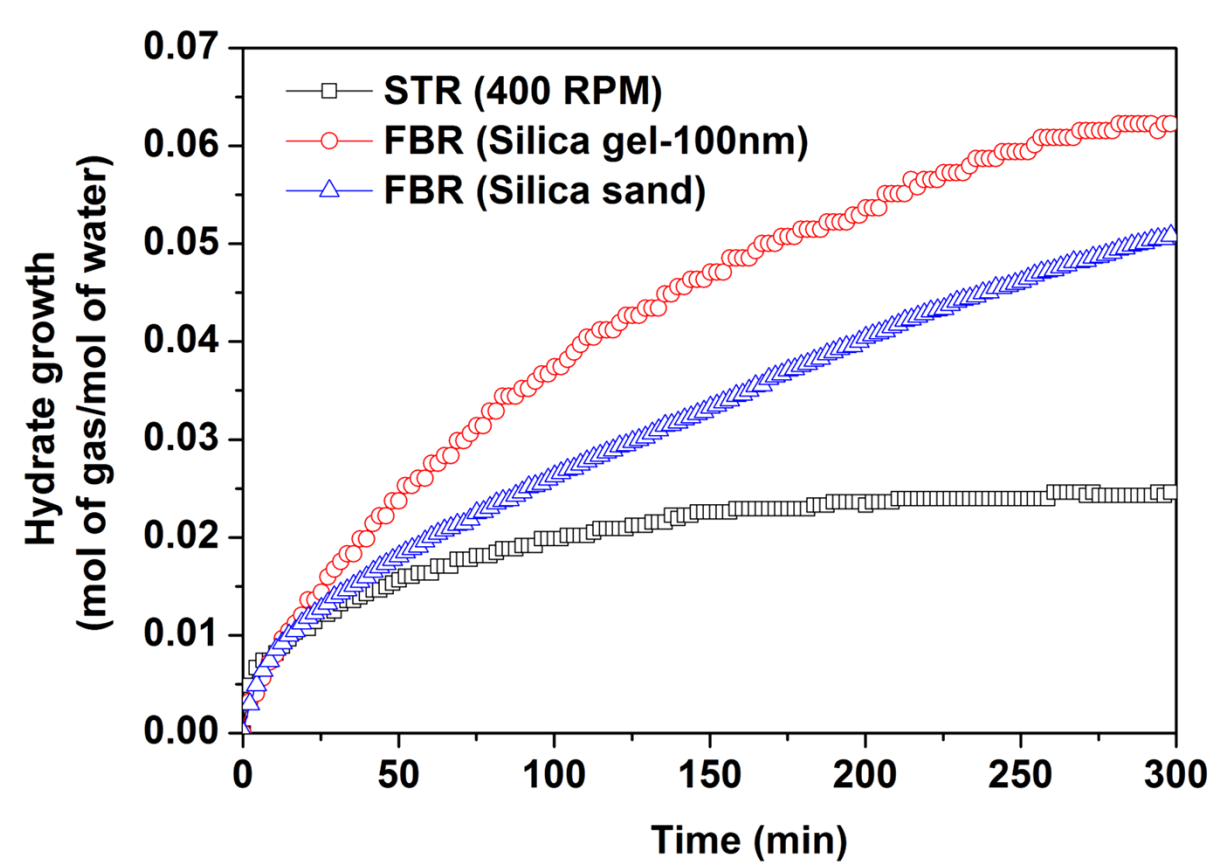

Figure 6.2.3: Comparison of Gas consumption during Hydrate growth (mol of Gas/mol of water) in FBR and STR systems. Time zero corresponds to induction for all the experiment.

6.2.4 Gas uptake curves received for the two types of water saturated Silica Gels having larger pore size (100 nm) and Silica Gel having lower pore size (5nm)

The amount of Gas consumed is calculated by using equation 1 & 2 from annexure.

Figure 6.2.4 shows the Gas uptake graphs received for the two kinds of water saturated Silica Gels for a duration of 200 min. Time zero in the curve represents the nucleation point (induction) for the experiments. This curve represents the kinetics of Hydrate Formation. The overall form of the plot matches with the Gas uptake curve explained in detail by Natarajan et al [Natarajan et al, 1994]. The scattered state of water in the Silica Gel pores is responsible for the more

consumption of Gas due to better Gas–water contact. As explained in figure the Gas uptake is more for the Silica Gel having larger pore size (100 nm) compared to the Silica Gel having lower pore size (5nm). Adeyemo et al, 2010 have also revealed that larger pore diameter is found to be effective for increased Hydrate Formation (water to Hydrate conversion ratio).

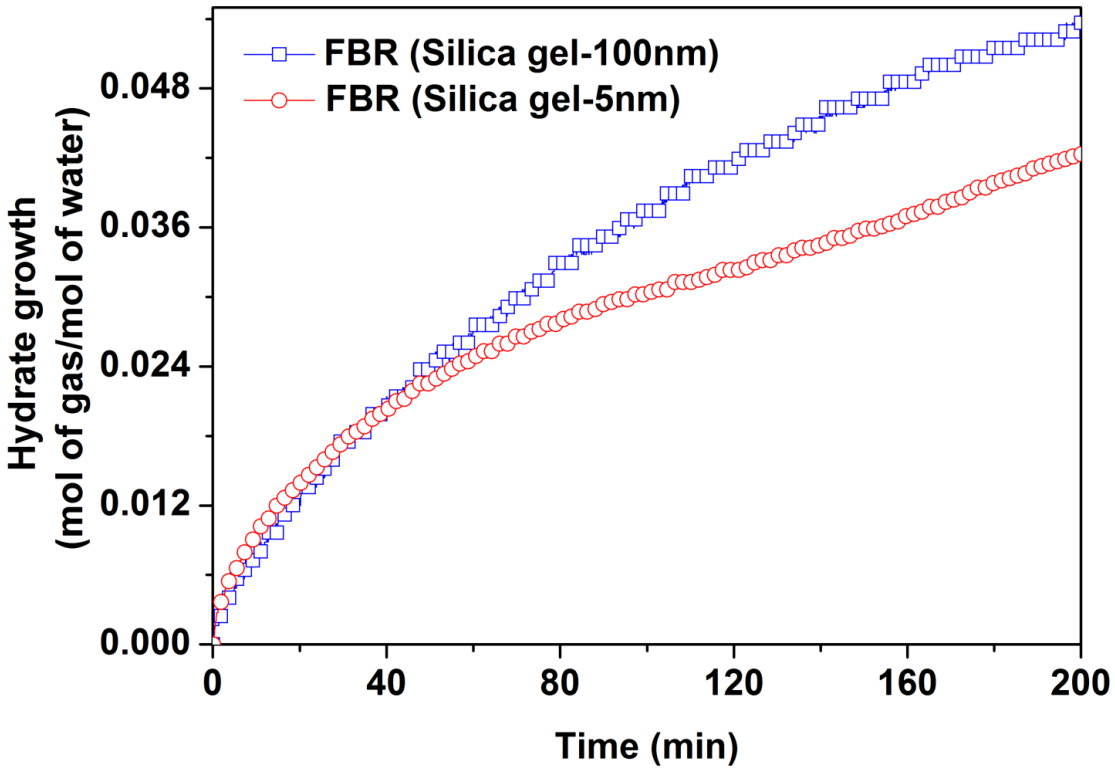

Figure 6.2.4: Comparison of Gas consumption during Hydrate growth (mol of Gas/mol of water) in fixed bed reactor containing Silica Gel of different pore size (5 and 100 nm). Time zero corresponds to induction for all the experiment.

6.2.5 *Comparison of Gas uptake during Hydrate growth (mol of Gas/mol of water) in a fixed bed reactor containing Silica Gel (5 nm) and blend of Silica Gel with zeolite 5A*

The amount of Gas consumed is calculated by using equation 1 & 2 from annexure.

Figure 6.2.5 represents the comparison of Gas uptake during Hydrate growth (mol of Gas/mol of water) in a fixed bed reactor containing Silica Gel and blend of Silica Gel with zeolite 5A. Time zero in the curve stands for the nucleation point (induction) for the experiments. It is reported in the literature that zeolite promotes Formation of Hydrate [Zang et al, 2008, Zang et al, 2009]. But there is no data available in the literature which deals with the fixed bed arrangement using

zeolite for Hydrate based CO_2 capture. For the first time we are using a blend of Silica Gel with zeolite 5A as a porous packing in a fixed bed reactor system. As shown in figure 8, the rate of Hydrate Formation and conversion of Hydrate is slightly better in presence of zeolite compared to bare Silica Gel (5nm). Thus the presence of zeolite in a fixed bed of Silica Gel is not detrimental to the Hydrate based CO_2 capture and separation process.

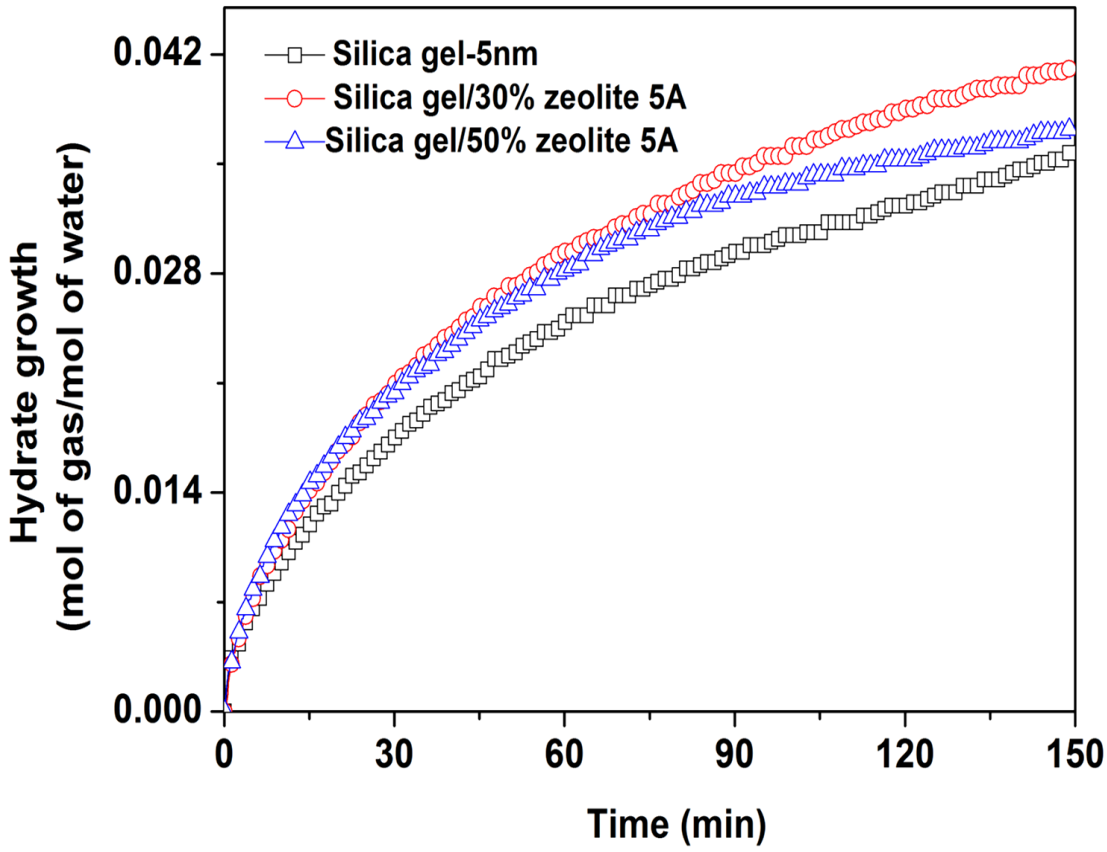

Figure 6.2.5: Comparison of Gas consumption during growth of Hydrate (mol of Gas/mol of water) in fixed bed reactor containing Silica Gel and blend of Silica Gel with zeolite 5A. Time zero relates to induction for all the experiment.

6.2.6 Water to Hydrate conversion of various systems investigated during this study

The water to CO_2 Hydrate conversion is calculated by using equation 7 & 8 from annexure.

Figure 6.2.6 summarizes the results obtained for water to Hydrate conversion of various systems investigated during this study. The data shown is for 3 hours of growth of Hydrate after nucleation. A comparison between the STR and FBR systems shows that there is a maximum

water to Hydrate transformation in case of FBR systems. The water to Hydrate conversion of 100 nm pore size Silica Gel in a FBR system was found to be ~28 mol% in first 3 hours whereas in the case of a STR system, it was found to be ~12 mol% in the first 3 hours. When various fixed bed media were compared, again 100 nm Silica Gel was found to provide higher conversion compared to other porous media such as Silica sand, Silica Gel with 5nm pore size and blend of Silica Gel with zeolite for each of them, the water to Hydrate conversion was more or less the same (18-20 mol%). It can be noted from this investigation that greater pore diameter accelerates the Hydrate Formation rate as well as conversion of water to Hydrate.

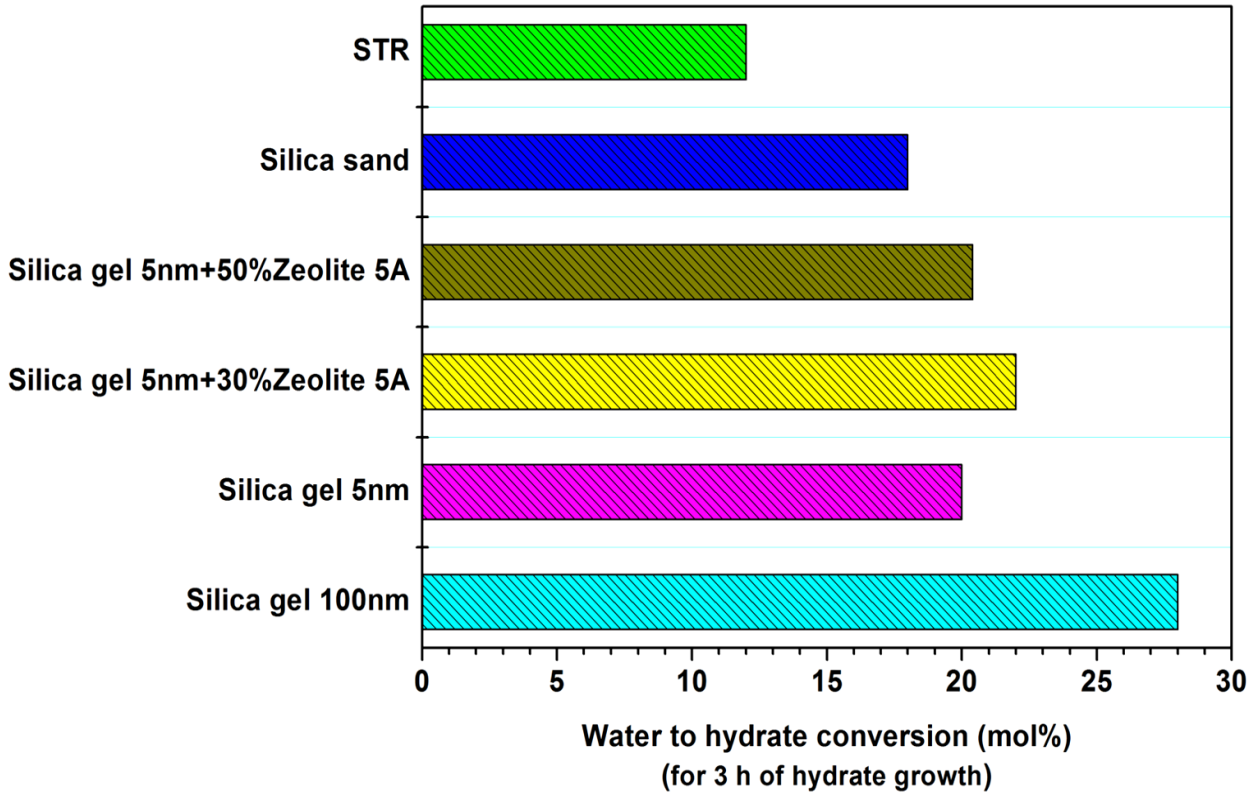

Figure 6.2.6: Comparison of water to Hydrate conversion for the different systems studied; the data shown is for 3 hours of Hydrate growth after nucleation.

6.2.7 Conclusion of this Task

Carbon dioxide Hydrate Formation experiments were performed with fixed temperature and in batch mode in various porous media (FBR) and STR systems. The Gas uptake for Formation of Gas Hydrate in a bed of Silica sand particles, Silica Gel and a blend of Silica Gel with zeolite 5A was compared with that in a stirred tank reactor. There was significant growth in the rate of

Formation of Hydrate in case of FBR whereas STR was observed to be not a suitable approach for scaling up the Hydrate based Gas capture and separation processes because the energy required for mechanical agitation is very significant and it is also plagued by other limitations such as the low Gas uptake and low water to Hydrate conversions.

6.3 Influence of 3A and 5A Zeolites in Presence of Silica Gel on Carbon Dioxide Gas Hydrate Formation

The results obtain for various experimental runs of CO_2 Gas Hydrates Formation at different saturations is explained as below

6.3.1 *Moles of CO_2 consumed in a fixed bed reactor containing Silica Gel (5 nm, Rankem) and blend of Silica Gel with zeolite 3A and 5A Zeolite*

The amount of Gas consumed is calculated by using equation 1 & 2 from annexure.

Moles of CO_2 consumed in various systems were compared in the study. Figure 6.3.1 shows the results with 100 % water saturation. It shows that Zeolite 3A has a positive effect on Hydrate Formation rate, as it shows better Gas uptake compared to other system under similar condition. However, no conclusive results were obtained at 50% water saturation which shows almost similar Gas uptake rate in presence of different zeolites as shown in Figure 6.3.2.

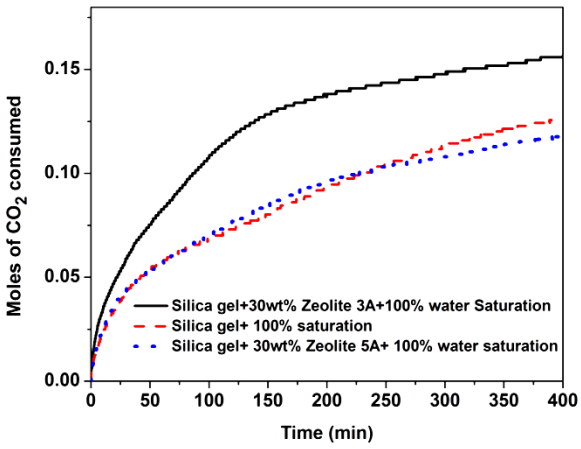

Figure 6.3.1: Comparison between 100% saturation of Silica Gel, Silica Gel+ 30 wt. % Zeolite 3A, Silica Gel+ 30 wt. % Zeolite 5A

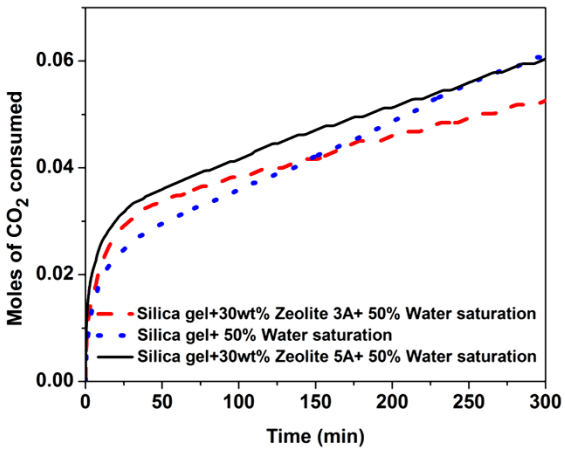

Figure 6.3.2: Comparison between 50% saturation of Silica Gel, Silica Gel+ 30wt. % Zeolite 3A, Silica Gel+ 30 wt. % Zeolite 5A

As discussed above, Zang et al, 2009 has carried out Methane Hydrate Formation in water adsorbed zeolites and they have concluded that 3A and 5A zeolite promotes Gas Hydrates Formation. However, it was not clear from their study whether enhanced Hydrate rate was due to better water to Gas contact as observed in other inert packing materials like Silica Gel and Silica sand or due to the catalytic effect of zeolite. This study clearly shows that zeolite might not have a very substantial effect on kinetics of Hydrate Formation.

6.3.2 *Moles of CO_2 consumed/ moles of water in a fixed bed reactor containing Silica Gel (5 nm, Rankem) and blend of Silica Gel with zeolite 3A and 5A Zeolite*

The amount of Gas consumed is calculated by using equation 1 & 2 from annexure.

Moles of CO_2, Moles of C02 consumed/moles of water and conversion i.e. water to Hydrate was compared in present study. Figure 6.3.3 shows the results with 100 % water saturation. It shows that Zeolite 3A has a promotional effect on Hydrate Formation rate, as its Gas uptake is better compared to other system under similar condition. However, no concluding results were obtained at 50% water saturation which shows almost same Gas uptake rate in presence of different zeolite as shown in Figure 6.3.4.

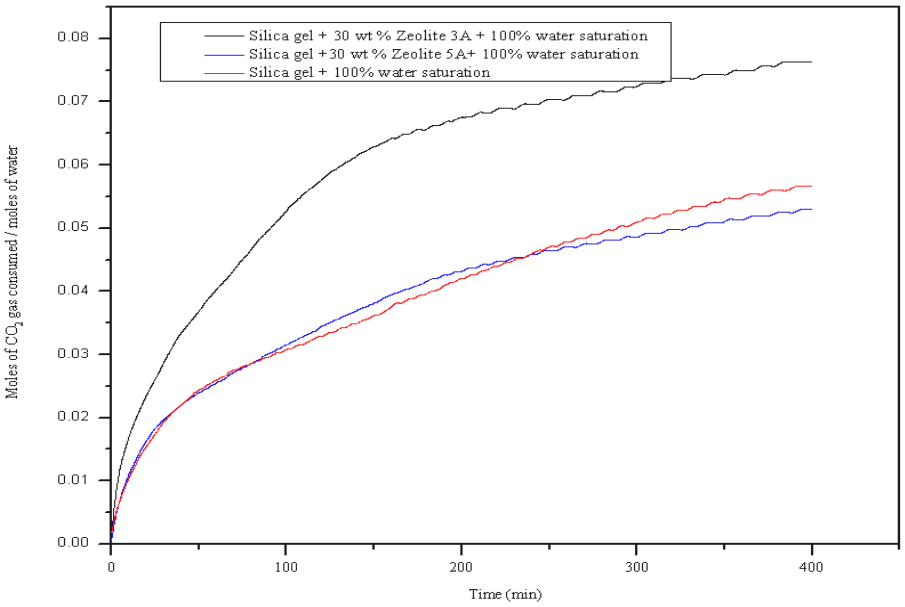

Figure 6.3.3: Comparison between 100% saturation of Silica Gel, Silica Gel+ 30wt. % Zeolite 3A, Silica Gel+ 30wt. % Zeolite 5A.

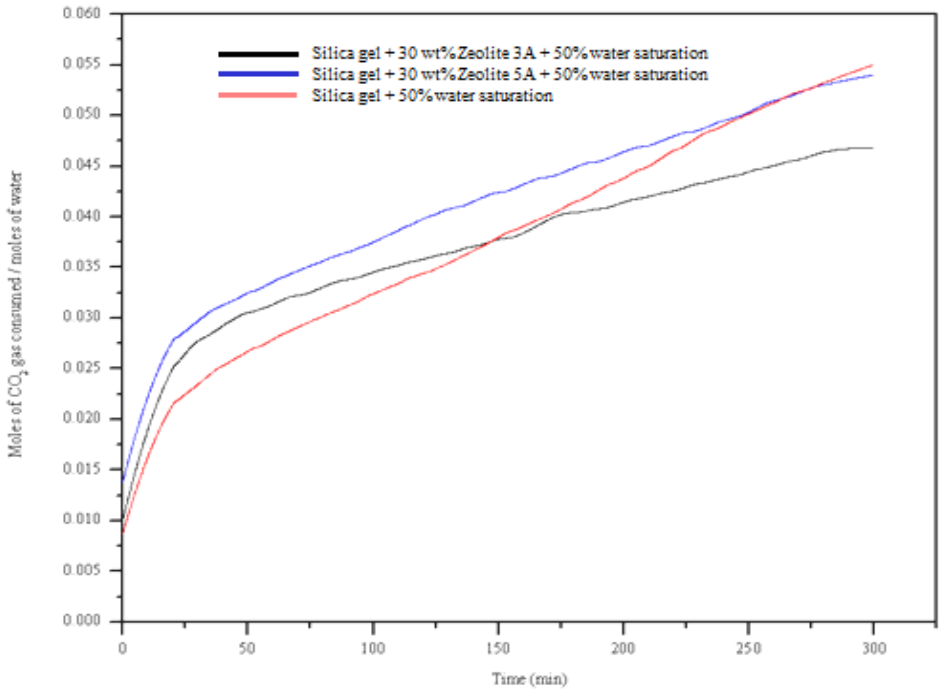

Figure 6.3.4: Comparison between 50% saturation of Silica Gel, Silica Gel+ 30wt% Zeolite 3A, Silica Gel+ 30wt% Zeolite 5A

6.3.3 *Percentage Conversion of water to Hydrate*

6.3.3.1 *Percentage conversion at 100% saturation*

The water to CO_2 Hydrate conversion is calculated by using equation 7 & 8 from annexure.

Percentage conversion for various experiments at 100% saturation is as shown in figure 6.3.5.

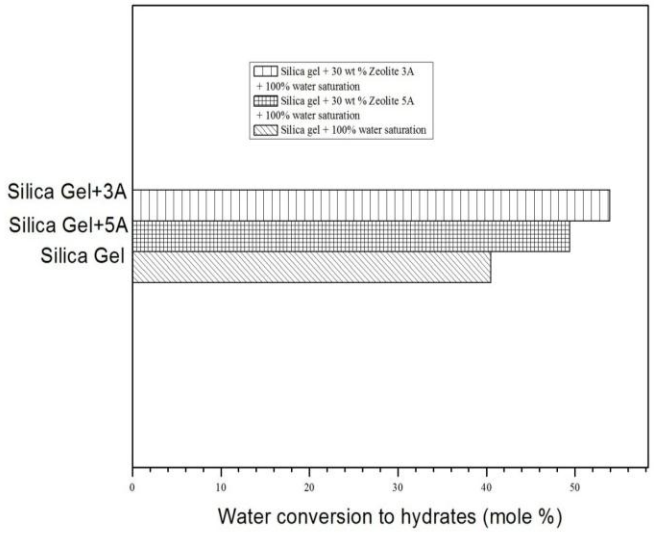

Figure 6.3.5: Comparison of water to Hydrate conversion for CO_2 Hydrate Formation at 100% saturation for 13.6 h

6.3.3.2 Percentage conversion at 50% saturation

Percentage conversion for various experiments at 50% saturation is as shown in figure 6.3.6:

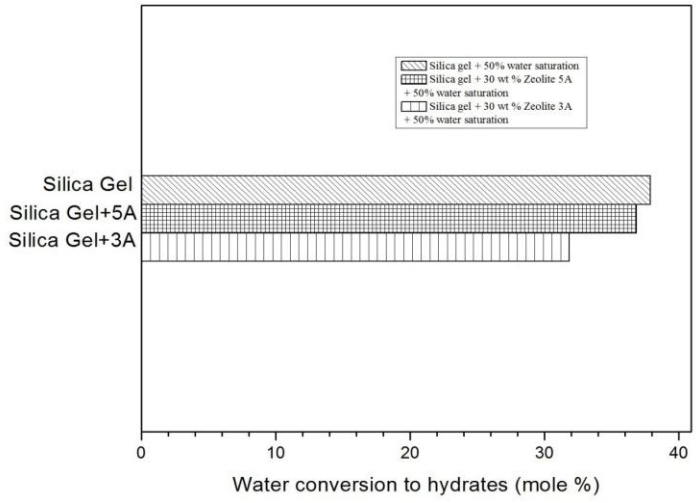

Figure 6.3.6: Comparison of water to Hydrate conversion for CO_2 Hydrate Formation at 50% saturation for 6.43 h.

6.3.3.3 *Percentage conversion for different experiments till the end of experiments*

It is as shown in table 6.3.1

Table 6.3.1: Percentage conversion for different experiments till the end of experiments

Serial no.	Name of Experiment	Saturation %	Time till the end of the experiment (min.)	% Conversion
1	Silica Gel	100	857.307	40.86471226
2	Silica Gel + 30 wt. % Zeolite 3A	100	817.965	53.95226
3	Silica Gel + 30 wt. % Zeolite 5A	100	930.098	40.676584
4	Silica Gel	50	385.535	37.89053
5	Silica Gel + 30 wt. % Zeolite 3A	50	817.965	46.25544234
6	Silica Gel + 30% wt. % Zeolite 5A	50	1069.704	62.1405418

From Figure 6.3.3 it can be concluded that 30wt. % zeolite 3A in presence of 100% saturated Silica Gel C has influenced the Gas Hydrate of CO_2 much more than 30wt. % zeolite 5A. This could be explained on the behalf of the reduction of nucleation randomicity as the Hydrate hydration process can occur separately on each tiny zeolite molecule. Moreover, 3A type zeolite is a kind of crystal silicon aluminates which have homogeneous aperture, polar absorption function and extremely high specific surface area. Figure 6.3.4 is not giving any conclusive remarks for 30wt. % zeolite 3A with 50% saturated Silica Gel C. This may be because of less absorption of water molecules on 3A type zeolite and hence, it can provide less nucleation grain which leads to less promotional effect of 3A type zeolite in this case. This is clear from Figure 6.3.5 and Figure 6.3.6 where maximum conversion took place in case of 3A zeolite with 100 %

saturation at a given time as shown in figure 6.3.5 and least conversion takes place in case of 3A zeolite with 50% saturation at a given time as shown in figure 6.3.6.

In case of 5A zeolite both water and carbon dioxide gets adsorbed and causes dual polar adsorption effects as the molecular dynamic diameter of carbon dioxide is more than 0.34 nm hence both 3A and 5A zeolites can adsorb water as its molecular diameter is 0.29 nm but only 5A can adsorb carbon dioxide. From Figure 6.3.3 no conclusive remarks can be obtained for 30wt. % zeolite 5A in presence of 100% Saturated C type Silica Gel. The carbon dioxide Hydrate Formation in presence of 5A zeolite becomes weak as large numbers of pores at 100% saturation are occupied by water and Carbon dioxide cannot occupy pores. From figure 6.3.4 it can be concluded that promotional effects of 30 wt. % 5A type zeolite at 50 % saturation are better than 30 wt. % 3A as in former case both water and carbon dioxide can get adsorbed and which facilitates a better mass transfer leading to more Hydrate Formation. This is clear from Figure 6.3.5 where more conversion in 3A took place in case100 % saturation at a given time and more conversion took place in case of 5A zeolite with 50% saturation at a given time as shown in figure 6.3.6.

As discussed above [Kim et al, 2014, Park et al, 2012, Zang et al, 2009] Methane Hydrate Formation has been carried out in water adsorbed zeolites and they have concluded that 3A and 5A zeolite promotes Gas Hydrates Formation. However, it was not clear from their study whether enhanced Hydrate rate was due to better water to Gas contact as observed in other inert packing materials like Silica Gel or due to the catalytic effect of zeolite.

6.3.4 *Conclusion of this Task*

This study clearly revealed that that zeolite performs as good as other porous materials like Silica Gel and enhance the Hydrate Formation rate.

6.4 Production of Biosurfactant Rhamnolipids from Strain A11 and its Characterization

6.4.1 *Biosurfactant producing microorganism*

Glycolipid type biosurfactant used in the present study was produced by *Pseudomonas aeruginosa* strain A11. Earlier strain A11 has been reported as plant-growth promoting (PGP) and multi-metal-resistant (MMR) bacterium capable of producing rhamnolipids while growing on glycerol supplemented minimal salt medium (MSM) [Singh et al, 2013]. Changing Abiotic

factors like growth media and conditions are known to influence rhamnolipids homologous and congeners composition [Bazire et al, 2009, Abdel-Mawgoud et al, 2009]. More knowledge to the rhamnolipids diversity has been added by the use of more sensitive and sophisticated analytical techniques [Ahmad et al 2010].

6.4.2 Biosurfactant production

Pseudomonas aeruginosa belongs to the class of Gammaproteobacteria is a well-known rhamnolipids producer [Abdel-Mawgoud et al, 2010]. Bacterium produces rhamnolipids as a blend of congeners that differs in composition according to the strain and media components [Abdel-Mawgoud et al, 2010, Singh et al, 2013]. Specific properties of rhamnolipids are thus influenced by the isolates used for biosurfactant production and the production process. In present study, rhamnolipids producing strain A11 was separated from rhizosphere of wild plant *Parthenium hysterophorus* [Singh et al, 2013]. Rhizosphere are endowed with distinctive nutrient rich microenvironment for its inhabitant. Thus, rhizobacteria have distinct physiological and metabolic capabilities with respect to bacteria from bulk soil [Singh et al, 2013].

Growth of strain A11 in glycerol supplemented medium was accompanied by decrease in surface tension of medium (Figure 6.4.1). Thus, suggesting that A11 is able to assimilate glycerol as a carbon source and produced biosurfactant. The maximum rhamnolipids production was detected during late log phase and stationary phase. Strain A11 produced 5020.4 ±9 .14 mg/lof rhamnolipids after 72 h of incubation with dry cell weight of 1600.78 ±105.0253 mg/l. Volumetric biomass productivity, volumetric rhamnolipids productivity and specific productivity were observed to be 22.23±1.46 mg/l/h, 69.72±0.12 mg/l/h and 3.14±0.20 mg/l/h respectively.

Rhamnolipids production on glycerol as carbon source has drawn attention of researchers as it provide effective strategies to curtail the cost of biosurfactant production [Muller et al, 2012, Abdel-Mawgoud et al, 2010, Singh et al, 2013, Silva et al, 2010].

In present study the growth and reduction in surface tension kinetics of strain A11 obtained is shown in figure 6.4.1 as per the following:

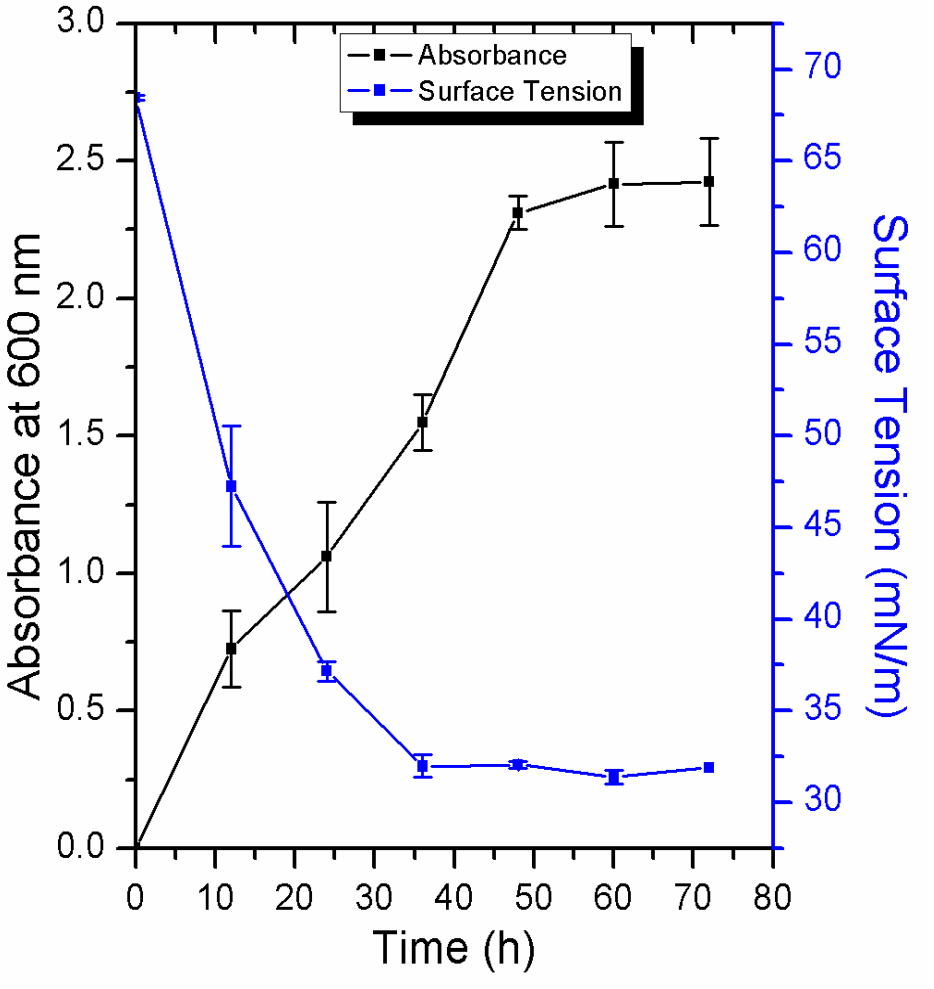

Figure 6.4.1: Growth kinetics of *Pseudomonas aeruginosa* A11. Time course of growth and surface tension reduction of growth medium.

As evident from figure 6.4.1 growth of strain A11 leads to reduction in surface tension of growth media suggesting production of biosurfactant. Maximum reduction in surface tension was observed after 12 hours of growth. The present study is in agreement with the work done by others [Singh et al, 2013, Anderson et al, 2015].

The dry cell mass and Rhamnolipids production of strain A11 is shown in Figure 6.4.2 as per following.

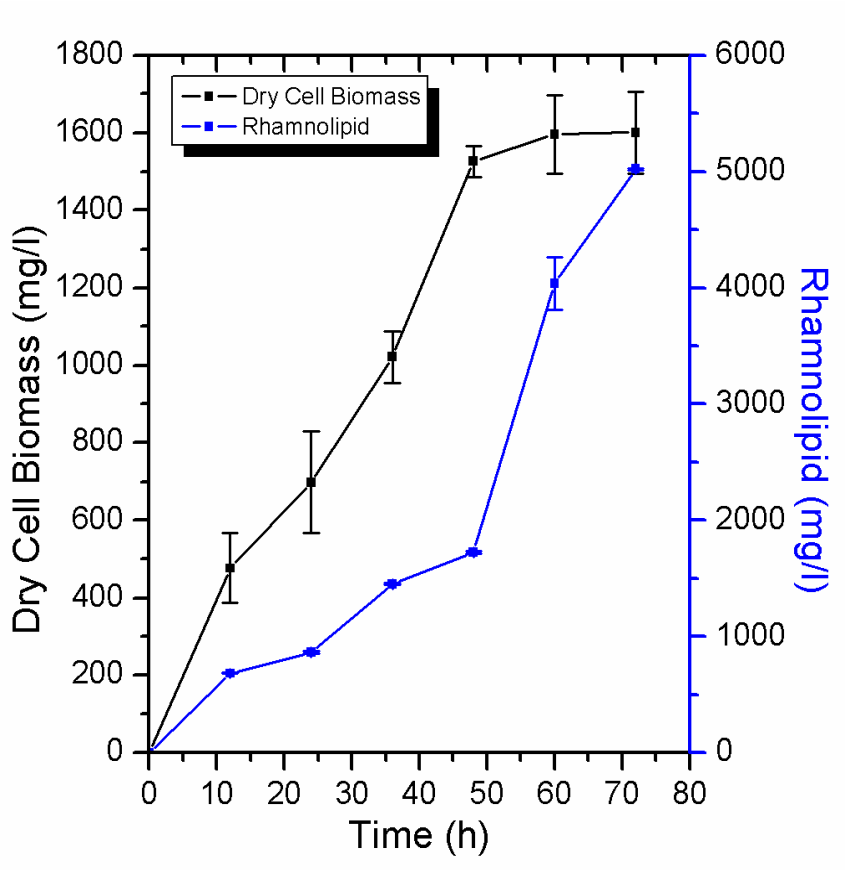

Figure 6.4.2: Growth kinetics of *Pseudomonas aeruginosa* A11.Time course of dry cell biomass and rhamnolipids yield. Strain A11 was grown in glycerol supplemented MSM containing TES at 30 ^{o}C with stirring done at 200 rpm. The values provided are mean ± S.D. of three independent experiments.

As evident from figure 6.4.2 Strain A11 produced 5020±9 mg/lRhamnolipids after 72 hours of growth. Maximum Rhamnolipids production was observed between 48 to 60 hours when strain was in stationary phase suggesting it to be a secondary metabolite. Specific growth rate was (µ) 22.2 ± 1.5 mg/l h while specific biosurfactant production rare was 3.14 ± 0.2. The amount of Rhamnolipids produced by strain A11 under given optimum condition is more than several reported strains [Moussa, et al 2014, Zhao et al, 2014].

Carbon source concentration in growth medium is one of the important parameters influencing the yield of biosurfactant [Abdel-Mawgoud et al, 2010, Silva et al, 2010]. Glycerol at 3% (v/v) concentration has been reported as most optimum concentration for biosurfactant production [Singh et al, 2013, Silva et al, 2010]. In present study, increasing the glycerol concentration to

4% (v/v) and supplementing growth medium with Trace Element Salts (TES) increased the rhamnolipids yield from 4,436.9 mg/l[Singh et al, 2013] to 5020.40 mg/l Specific growth rate and specific biosurfactant also increased as compared to the earlier report [Singh et al, 2013]. *Pseudomonas aeruginosa* EM1 isolate from oil-contaminated site was able to produce 4.93 g/l of rhamnolipids while growing on 4% glycerol as carbon source [Wu et al, 2008].

It has been known that conditions that limit growth support the production of rhamnolipids [Muller et al, 2012]. Limiting concentration of trace element salts can increase rhamnolipids yield [Guerra-Santos et al, 1986]. Contrarily, in present study addition of TES and increasing carbon source concentration increased biomass and subsequently the rhamnolipids yield. TES provided microorganisms the growth essential elements thus favouring luxuriant growth. The production economy of every microbial product is governed by three basic factors namely initial raw material costs, suitable and economic production and recovery procedures and the product yield. In the present work by slightly altering growth medium composition using inexpensive carbon source we achieved increased rhamnolipids yield. Thus making rhamnolipids produced by strain A11 an economically affordable green biosurfactant.

Specific growth rate (μ) was observed to be 22.2 ± 1.5 mg/l while specific biosurfactant production rate was 3.14 ± 0.2.

6.4.3 *Surface Tension, Critical Micelle Concentration (CMC) and stability of Biosurfactant*

Purified biosurfactant i.e Rhamnolipids from strain A11 decreased the surface tension of water from 72 mN/m to 36 mN/m with CMC of 70 mg/l. After 36 hours of growth, greatest reduction in surface tension of growth was seen, when strain A11 was in mid-log phase. Strain A11 decrease surface tension of growth medium from 68.4 ± 0.1 mN/m to 31.9 ± 0.1 mN/m. According to Mulligan, 2005, biosurfactant with ability to decrease surface tension of water from 72 mN/m to 35 mN/m or less is an efficient biosurfactant. Considering this Rhamnolipids produced by strain A11 is an efficient biosurfactant. As Rhamnolipids were able to decrease the surface tension of water to 36 mN/m. Bacteria produced rhamnolipids as a blend of congeners and homologues. Every single constituent of rhamnolipids mixture contributes differentially to physiochemical properties and biological activities. But due to problems in isolating the rhamnolipids constituents in to a single homologue, the particular contribution of each constituent has not been extensively explained in literature [Singh et al, 2013].

The CMC of different *Pseudomonas* rhamnolipids differs from 53 to 230 mg/l depending on the ratio and composition of rhamnolipids species [Abdel-Mawgoud et al, 2010]. Small change in the surface tension reduction ability and CMC may be attributed to change in the composition of the rhamnolipids and the content of fatty acid components. Costa et al, 2010 have reported changes in physiochemical properties of surfactant with change in chemical composition. The occurrence of the length of alkyl chains, unsaturated bonds, and the size of hydrophilic head group in rhamnolipids greatly impact the surface active characteristics of biosurfactants produced by *Pseudomonas* [Pornsunthorntawee et al, 2011, Nitschke et al, 2005].

Surface tension reducing ability of rhamnolipids remained intact even after being exposed to extreme temperature range of – 20 ^{0}C to 40 ^{0}C and in aqueous solution of pH range 7 to 10. Rhamnolipids produced by strain A11 retained its surface reducing ability even after exposure to extreme temperature (– 20 ^{0}C to 40 ^{0}C) and pH (range 7 to 10) as shown in figures 6.4.3 and figure 6.4.4. Rhamnolipids stability at extreme conditions is due to highly stable beta-glycosidic bond between sugar moiety and lipid chain [Abdel-Mawgoud et al, 2010].

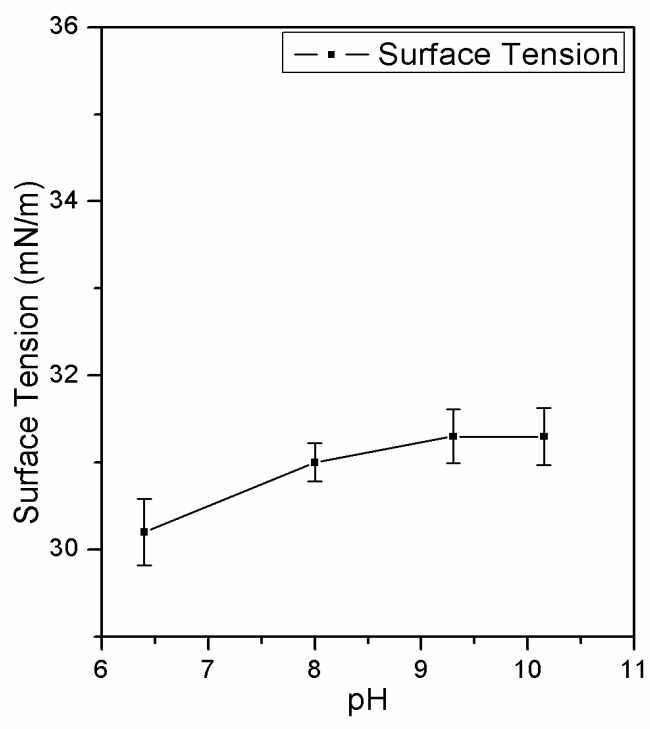

Figure 6.4.3: pH and reduction in surface tension relationship of Rhamnolipids produced from strain A11.

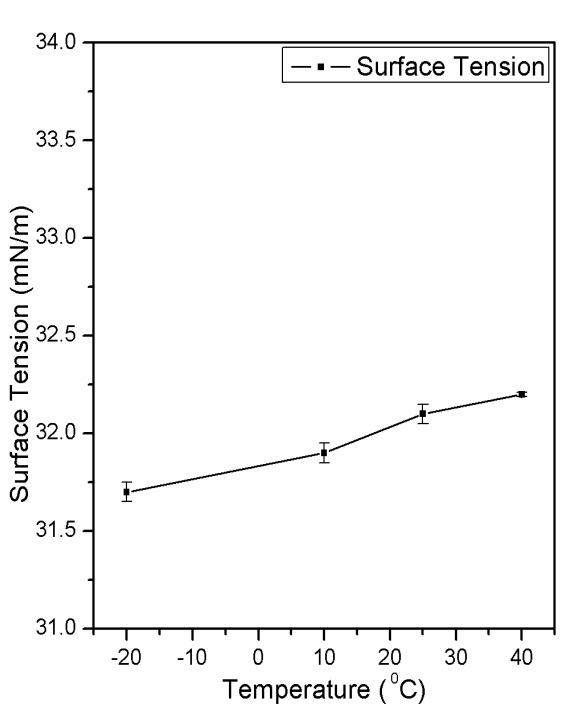

Figure 6.4.4: Temperature and reduction in surface tension relationship of Rhamnolipids produced from strain A11.

Following serial dilution method CMC of rhamnolipids was noted to be 70 mg/las shown in Figure 6.4.5. This is accordance to the earlier reported values [Abdel-Mawgoud et al, 2010].

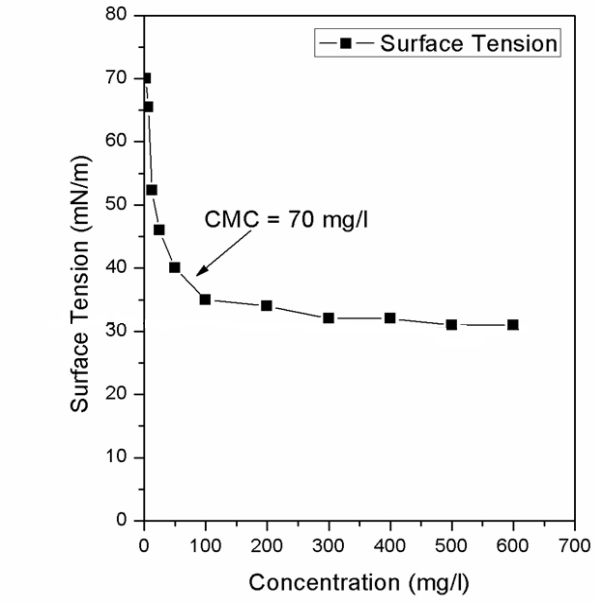

Figure 6.4.5: CMC of Rhamnolipids produced from strain A11.

6.4.4 *Characterization of Rhamnolipids Produced from Strain A11*

6.4.4.1 *TLC*

Initial characterization of the rhamnolipids was done by TLC as shown in Figure 6.4.6 . TLC profile of the biosurfactant showed 2 spots with *Rf* value of 0.45 and 0.69, respectively. Spots were positive for anisaldehyde demonstrating it to be glycolipids type surfactant [Satpute et al, 2010]. The two spots corresponded to dirhamnolipid and monorhamnolipid respectively. Wang et al, 2007 have also reported similar spots on TLC for rhamnolipids. TLC of purified biosurfactant with R_f = 0.45 indicates it to be a dirhamnolipid and R_f = 0.41 is obtained for standard by Sigma Rhamnolipid Eldrich USA which matches with the Rhamnolipid by A11 strain. R_F value of 0.69 indicates that monorhamnolipid is also present in the rhamnolipids of the biosurfactant produced from strain A11. Hence strain A11 produces rhamnolipids which is a mixture of mono Rhamnolipid and dirhamnolipid as shown in Figure 6.4.6.

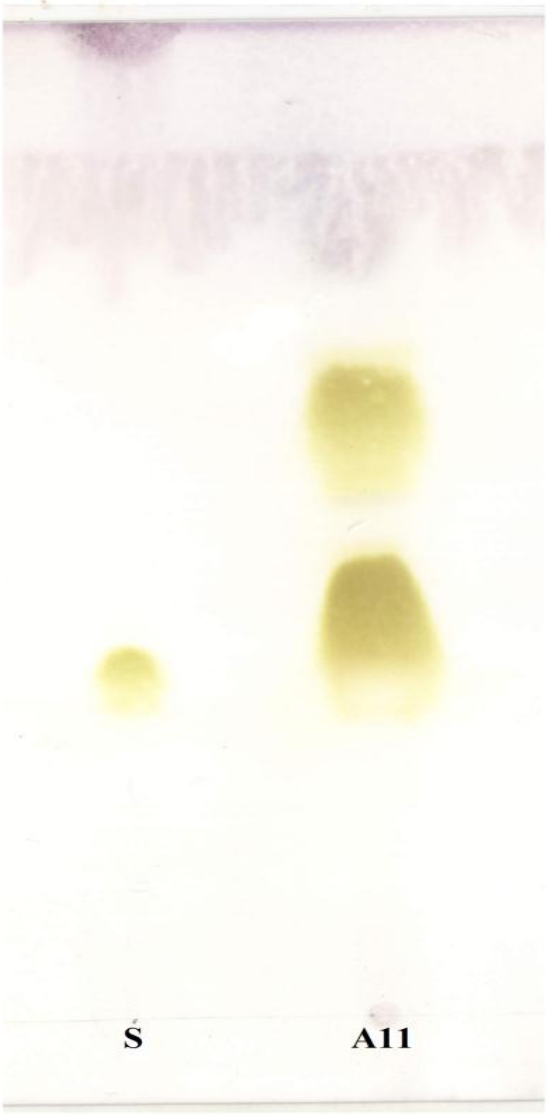

Figure 6.4.6: TLC of Rhamnolipids produced by standard and strain A11.

6.4.4.2 *FTIR*

FTIR was used to find the functional groups and the chemical bonds present in the biosurfactant as shown in figure 6.4.7. This help in confirming the chemical nature of biosurfactant. The FTIR spectrum of biosurfactant gave major peak at 3418 cm^{-1} due to the –OH stretching vibration. Peaks at 1741, 1112, 1058 cm^{-1} were also observed and these corresponded to carbonyl stretching frequencies of ester group as well as to acid groups. The observed peaks at 2922, 2856, 1466, 1388 cm^{-1} may be attributed for the C-H, $-CH_2$ and $-CH_3$ stretching vibrations. Peaks between 914 - 980 cm^{-1} and 815 - 848 cm^{-1} may be attributed to pyranyl-I and α-pyranyl –II stretching vibrations respectively [Zhang et al, 2007, Leitermann et al, 2008, Singh et al, 2013].

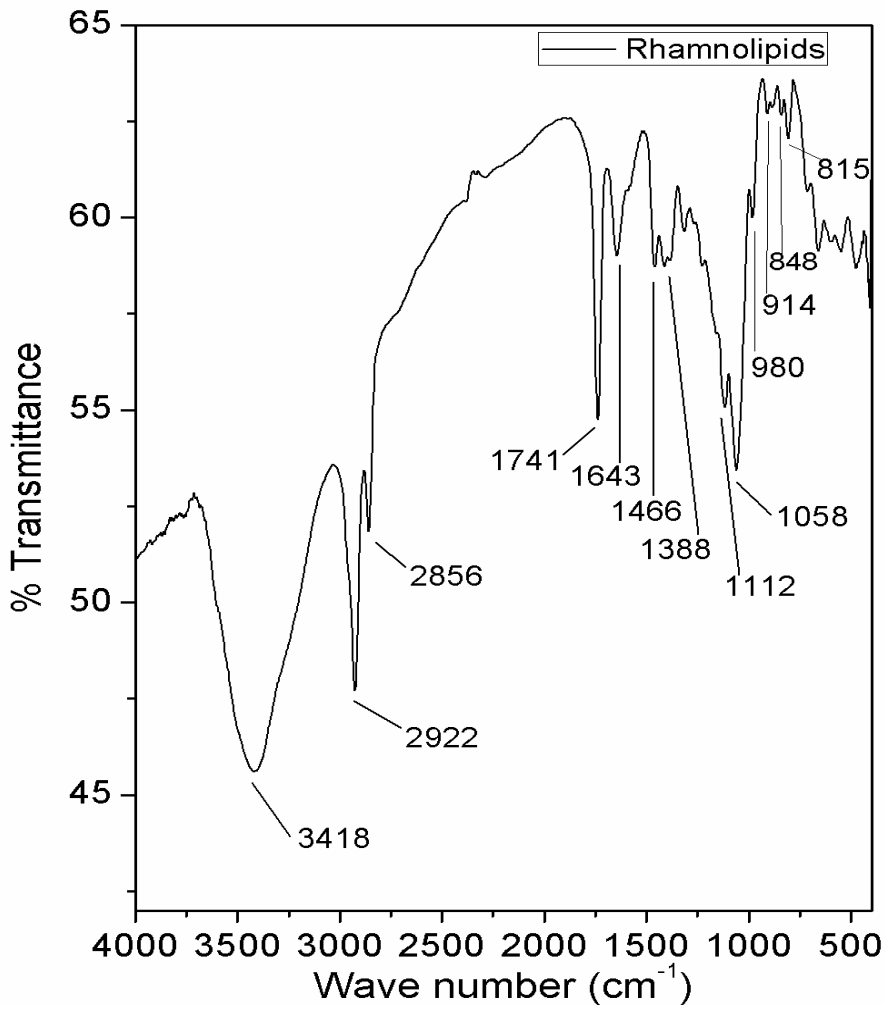

Figure 6.4.7: FTIR spectrum of Rhamnolipids produced from strain A11.

6.4.4.3 NMR

The *[1]H* and [13]C NMR were performed for biosurfactant characterizations.

(a) [1]H-proton NMR

As evident from figure 6.4.8 the proton NMR spectrogram exhibited Triplet at δ 0.82 suggesting the presence of $–CH_3$ in lipid chain. Broad signals at δ 1.13 to 1.24 is due to the presence of $–CH_2$ in lipid chains. Peaks at δ 2.37 is may be attributed to $–CH_2$ of the ester carbonyl and peak at δ 2.47 is due to the $– CH_2$ attached to the acid carbonyl. Peaks from δ 3.91 to δ 3.98 exhibits the – CH Protons in the rhamnose moiety. Peak at δ 4.82 is because of the –CH attached to the -O- of ester moiety. The peak at δ 5.33 is due to the hydrogen on anomeric carbon while peak at δ 10.0 shows the presence of acidic proton of lipid moiety [Choe et al, 1992, Raza et al, 2009, Jadhav et al, 2011]. The proton NMR of Rhamnolipids produced by strain A11 is shown in Figure 6.4.8 as follows.

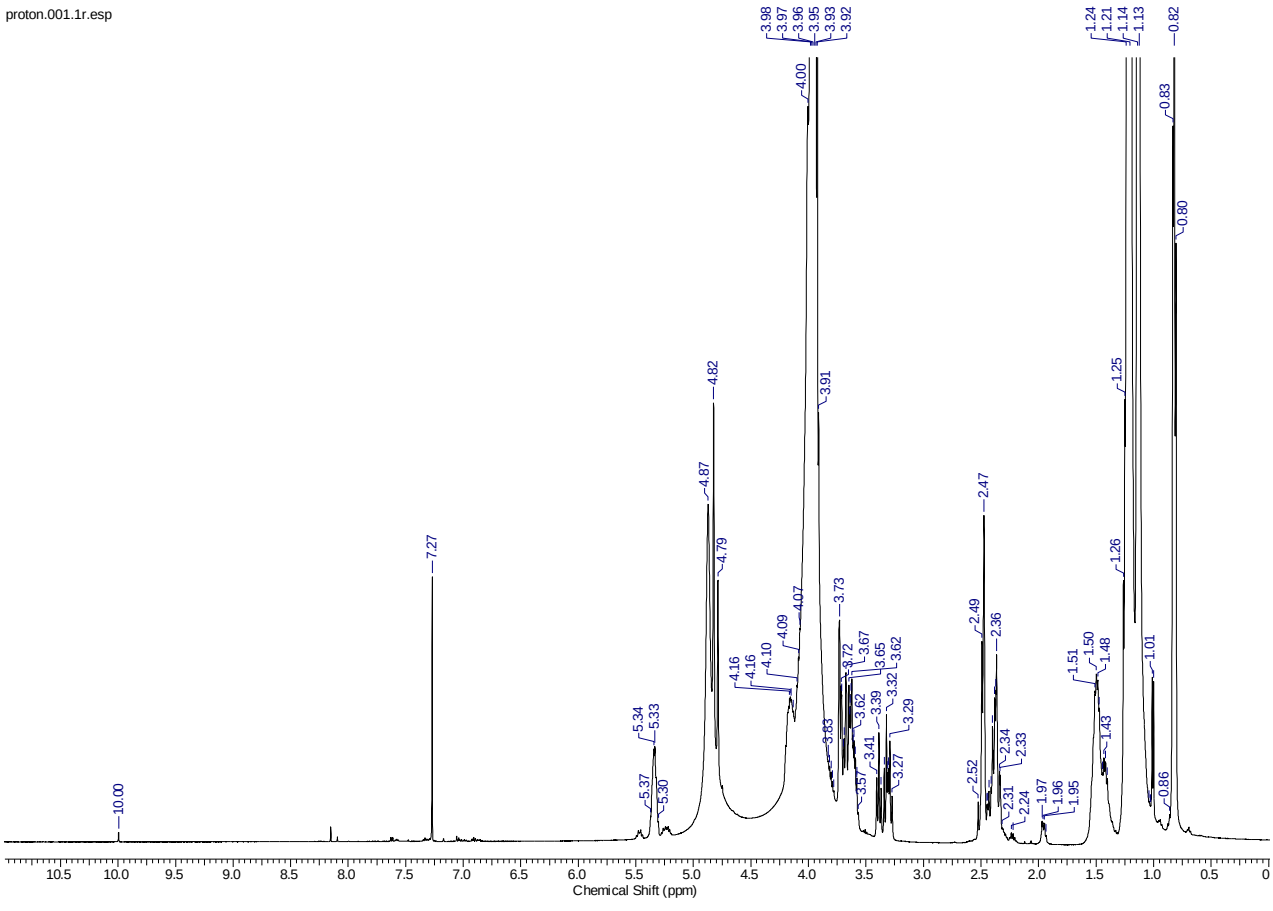

Figure 6.4.8: [1]H NMR of Rhamnolipids produced by strain A11.

(b) ^{13}C NMR

The ^{13}C NMR spectrogram exhibited peak at δ 13.9 is due to $–CH_3$ in lipid chain is shown in Figure 6.4.9. Peaks at δ 22.4, 24.3, 24.9, 28.9, 29.2, 29.5, 31.5, 34.2. 38.9, and 39.4 may be attributed to the $–CH_2$ in the lipid chain. The peak at δ 64.0 may be due to the -CH attached to the O of ester moiety. The peaks between δ 68.0 to 73.1 is due to the presence of de-shielded –CH in rhamnose moiety. Peaks at δ 79.2 and δ 102.4 is due to the linkage of two rhamnose moieties. The linkage of rhamnose moiety and lipid unit is demonstrated by the peak at δ 95.8. The peak at δ 171.3 and δ 173.3 is confirming the presence of ester and acid in lipid unit, respectively [Jadhav et al, 2011, Lotfabad et al, 2010, Choi et al, 2011]. The ^{13}C NMR of rhamnolipids produced by strain A11 is as shown in Figure 6.4.9.

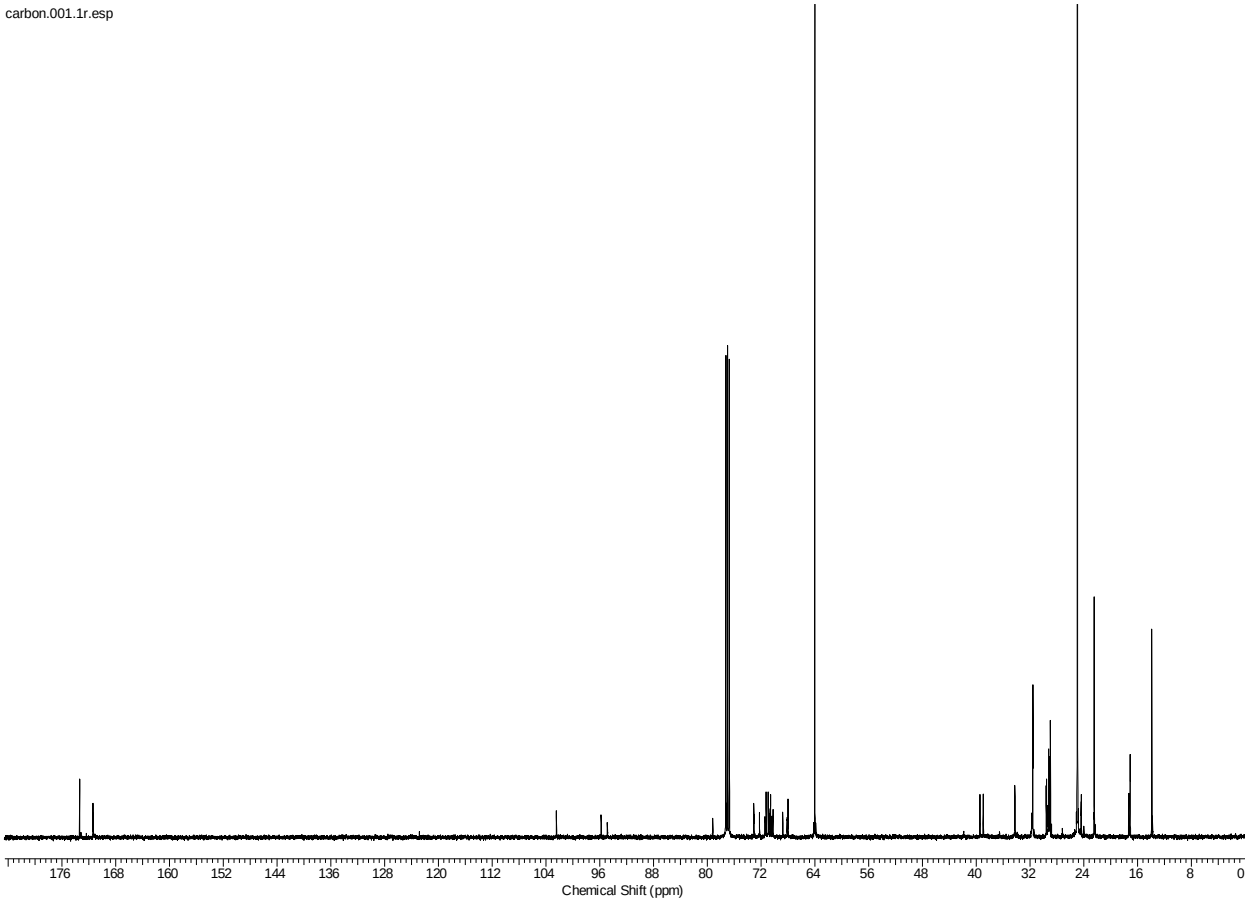

Figure 6.4.9: ^{13}C NMR of Rhamnolipids produced by strain A11.

6.4.4.4 *LC-MS*

Liquid Chromatography-Mass Spectrometry (LC-MS) chromatogram of purified biosurfactant suggested strain A11 produced rhamnolipids as a mixture of congeners and homologues (Figure 6.4.10). Most abundant rhamnolipids congener observed was dirhamnolipids ($RhaRhaC_{10}C_{10}$; α-L-rhamnopyranosyl -α-L-rhamnopyranosyl -β-hydroxydecanoyl -β-hydroxydecanoate) consisting of lipid chain length of C-10. Most abundant monorhamnolipid congener was $RhaC_{10}C_{10}$ (L-rhamnosyl -β -hydroxydecanoyl- β -hydroxydecanoate). Interestingly, olefinic rhamnolipids $RhaC_{22}$, $RhaC_{12}C_{10}$/$RhaC_{10}C_{12}$, $RhaRhaC_{10}C_{10}$ and $RhaRhaC_{12}C_{10}$ / $RhaRhaC_{10}C_{12}$ were also observed in the chromatogram. Rarely reported long chain monorhamnolipid congener $RhaC_{22}$ was observed at m/z ratio of 523.36. The present work is in tune with the previously reported work [Ahmad et al, 2010, Singh et al, 2013]. Liu et al, 2014 has reported $RhaC_{10}C_{10}$ as most abundant rhamnolipids congener. The present study confirmed that for each diarhamnolipids identified the corresponding monorhamnolipids congeners should also be identified. Chromatogram of rhamnolipids produced by *Pseudomonas aeruginosa* strain A11 is shown figure 6.4.10. The LCMS of rhamnolipids produced by strain A11 is shown from Figure 6.4.11 to Figure 6.4.15. Table 6.4.1 also exhibits the list of Rhamnolipids congeners with molecular formula, molecular weight and relative abundance present in rhamnolipids strain A11 as per following.

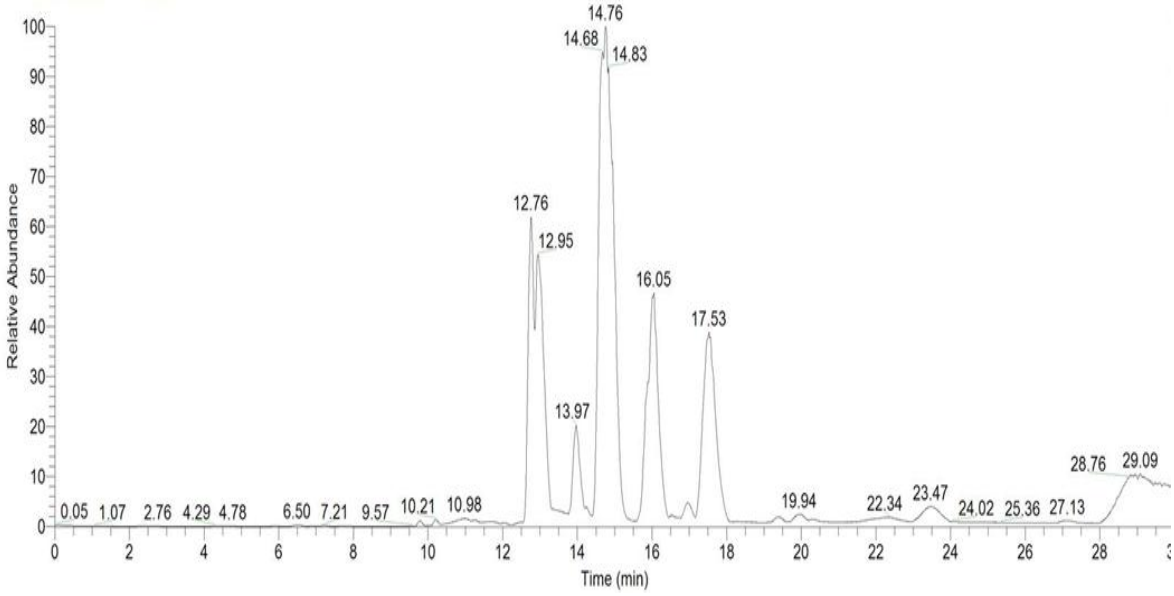

Figure 6.4.10: Chromatogram of rhamnolipids produced by *Pseudomonas aeruginosa* strain A11.

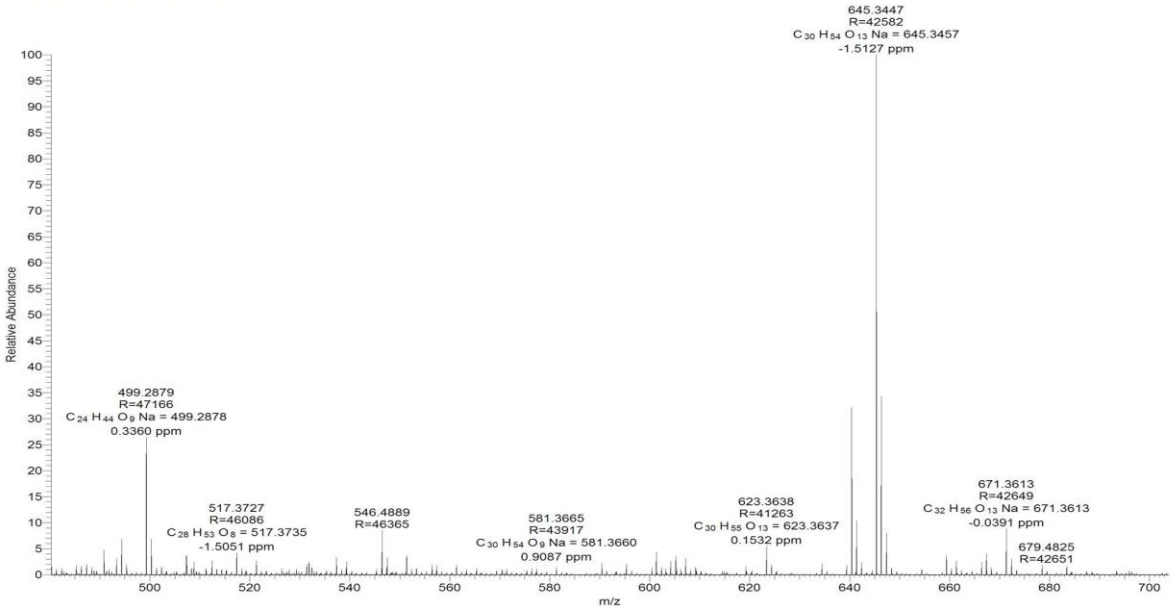

Figure 6.4.11: LCMS of purified rhamnolipids produced by *Pseudomonas aeruginosa* A11 while growing in glycerol supplemented MSM containing TES

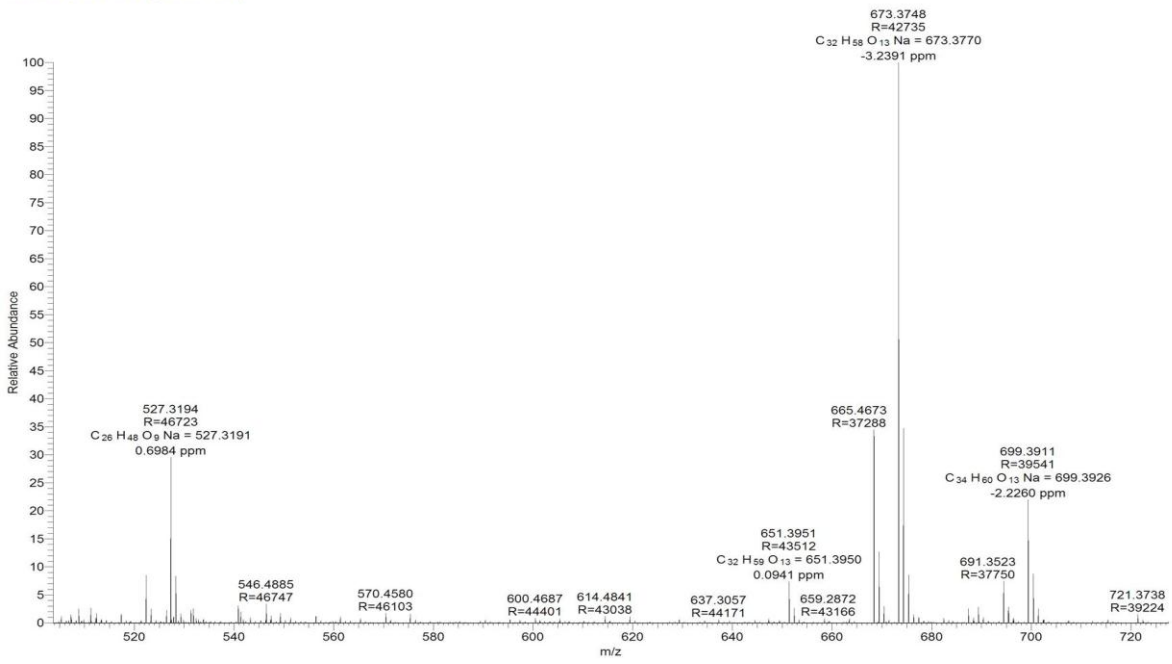

Figure 6.4.12: LCMS of purified rhamnolipids produced by *Pseudomonas aeruginosa* A11

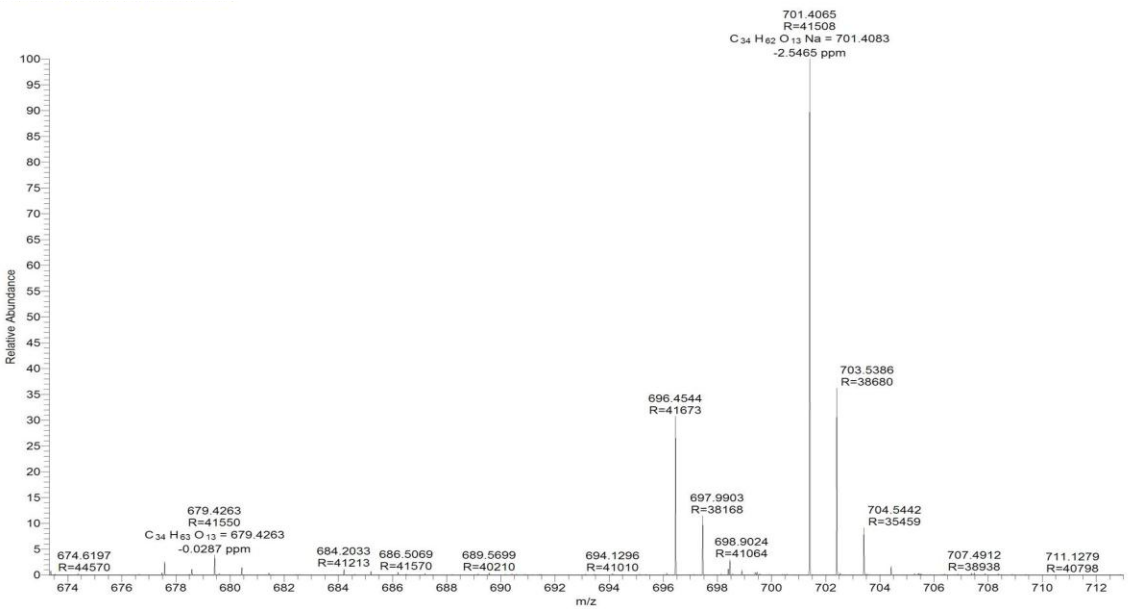

Figure 6.4.13: LCMS of purified rhamnolipids produced by *Pseudomonas aeruginosa* A11

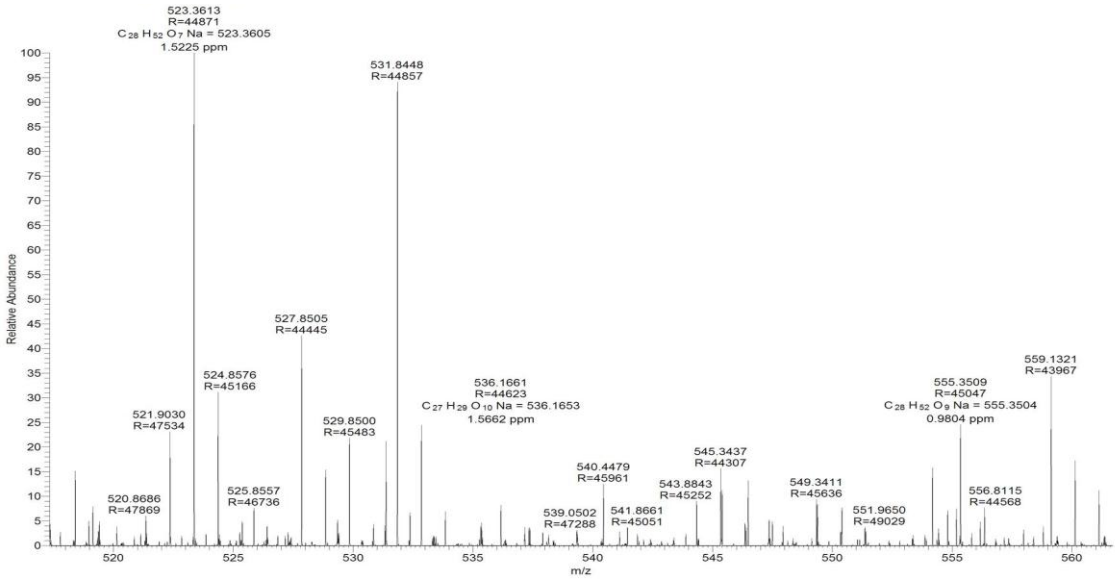

Figure 6.4.14: LCMS of purified rhamnolipids produced by *Pseudomonas aeruginosa* A11

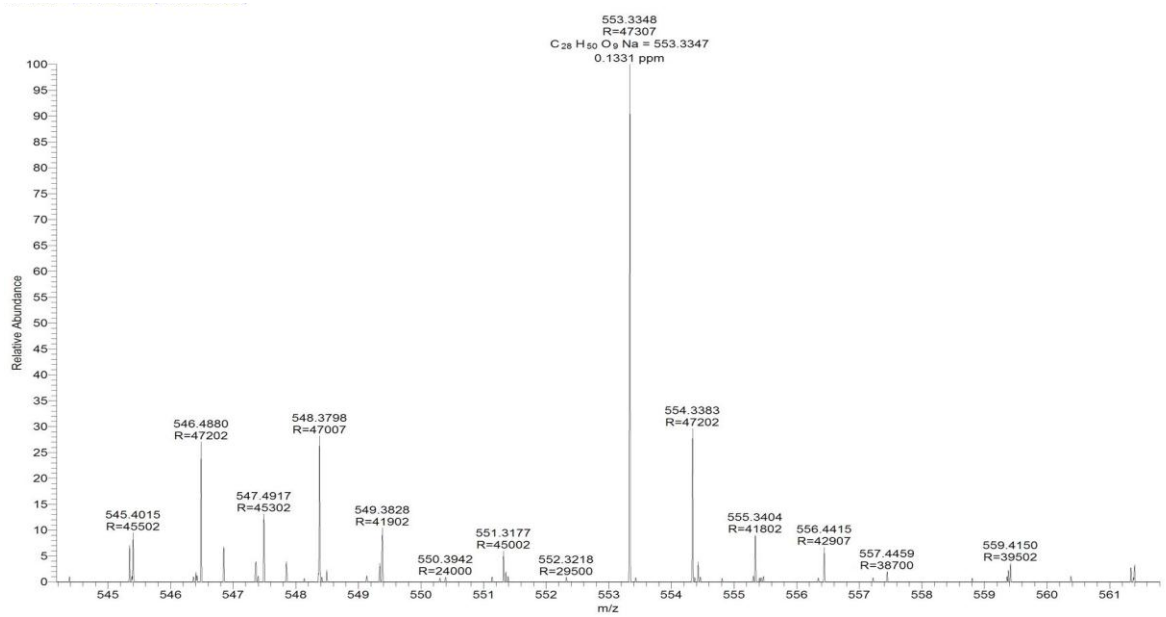

Figure 6.4.15: LCMS of purified rhamnolipids produced by *Pseudomonas aeruginosa* A11

The most abundant rhamnolipids formed by strain A11 in present study is RhaRha$C_{10}C_{10}$ (α-L-rhamnopyranosyl-α-L-rhamnopyranosyl-β-hydroxydecanoyl-β-hydroxydecanoate) as shown in Figure 6.4.16.

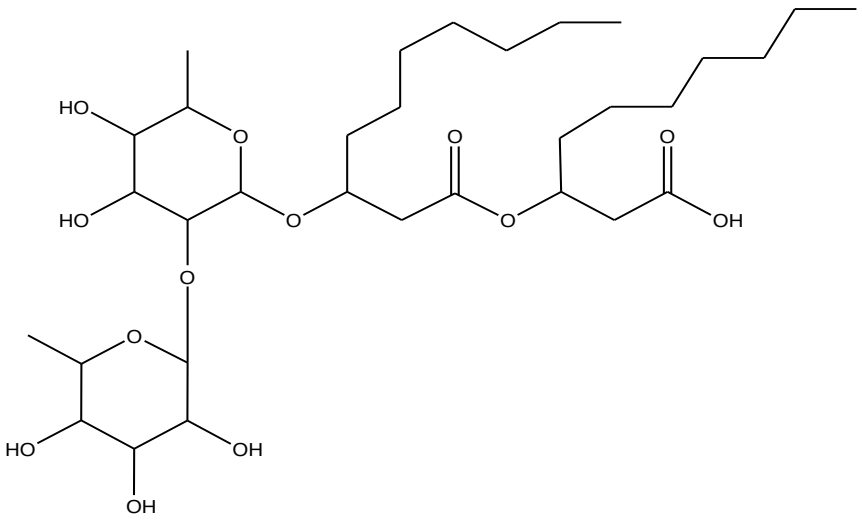

Figure 6.4.16: Structure of Rha Rha C_{10} C_{10}.

Table 6.4.1: Assignment of all rhamnolipids mass peaks found by LCMS mass spectrometry of biosurfactant produce by *Pseudomonas aeruginosa* strain A11 while growing on glycerol supplemented MSM containing TES.

Congener	Pseudomolecular mass (m/z)	Retention Time (min.)	Molecular Formula	Relative Abundance (%)
$RhaC_{10}C_8/RhaC_8C_{10}$	499.28	13.97	$C_{22}H_{44}O_9$	3.4
*$RhaC_{22}$	523.36	23.47	$C_{28}H_{52}0_7$	2.07
$RhaC_{10}C_{10}$	527.32	16.05	$C_{26}H_{48}O_9$	9.76
*$RhaC_{12}C_{10}$/ $RhaC_{10}C_{12}$	553.33	17.45	$C_{28}H_{50}O_9$	1.13
$RhaC_{12}C_{10}$/ $RhaC_{10}C_{12}$	555.35	19.42	$C_{28}H_{52}O_9$	0.46
$RhaRhaC_{10}C_8/RhaRhaC_8C_{10}$	645.34	12.95	$C_{30}H_{54}O_{13}$	12.16
*$RhaRhaC_{10}C_{10}$	671.36	13.88	$C_{32}H_{56}O_{13}$	1.35
$RhaRhaC_{10}C_{10}$	673.37	14.76	$C_{32}H_{58}O_{13}$	32.12
*$RhaRhaC_{12}C_{10}/RhaRhaC_{10}C_{12}$	699.39	15.94	$C_{34}H_{60}O_{13}$	7.49
$RhaRhaC_{12}C_{10}/RhaRhaC_{10}C_{12}$	701.4	17.53	$C_{34}H_{62}O_{13}$	11.83
* Olefinic Rhamnolipids				

6.4.4.5 *MALDI*

The MALDI-TOF mass spectra of rhamnolipids displayed peaks which can be attributed to the sodium and potassium adducts [Rooney et al, 2009]. The results of MALDI-TOF mass spectrometric analyses revealed that both mono- and dirhamnolipid moieties were present in the rhamnolipids produced by strain A11 as shown in Table 6.4.2. Most abundant rhamnolipid was observed at m/z 527.23 and this corresponds to dirhamnolipid ($RhaRhaC_{10}C_{10}$; α-L-rhamnopyranosyl -α-L-rhamnopyranosyl -β-hydroxydecanoyl -β-hydroxydecanoate) consisting of lipid chain length of C-10. Most abundant monorhamnolipid congener was $RhaC_{10}C_{10}$ (L-rhamnosyl -β -hydroxydecanoyl- β -hydroxydecanoate). Interestingly, olefinic rhamnolipids $RhaC_{22}$, $RhaC_{12}C_{10}/RhaC_{10}C_{12}$, $RhaRhaC_{10}C_{10}$ and $RhaRhaC_{12}C_{10}$ / $RhaRhaC_{10}C_{12}$ were also observed. Rarely, reported long chain monorhamnolipid congener $RhaC_{22}$ was observed at m/z of 523.36. The present study is an agreement with the study carried by Nie et al, 2010. The MALDI of Rhamnolipids as shown in Figure 6.4.17 and Figure 6.4.18.

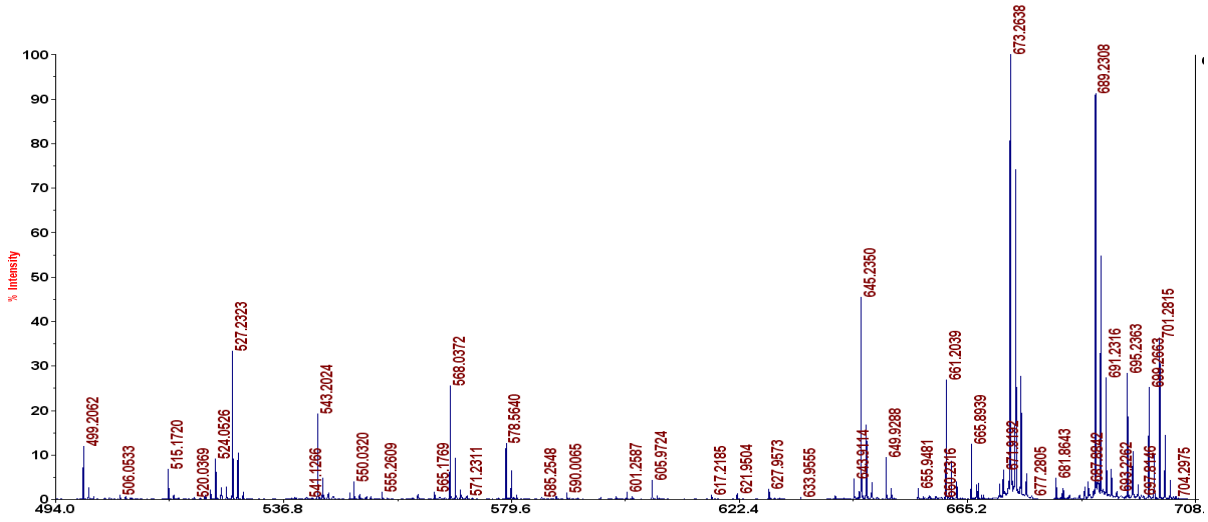

Figure 6.4.17: MALDI-TOF mass spectra of purified rhamnolipids produced by *Pseudomonas aeruginosa* A11

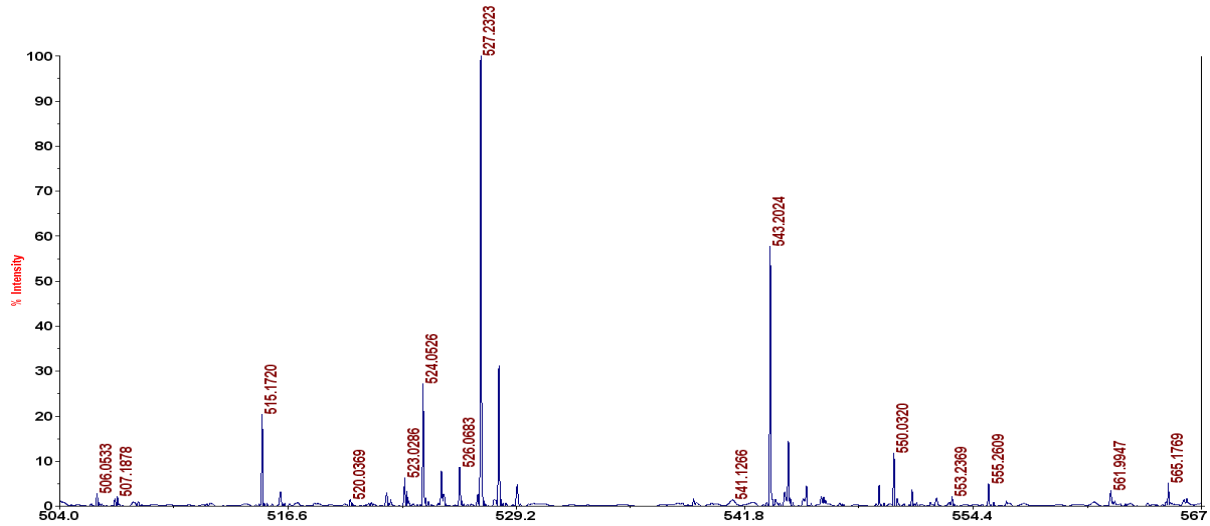

Figure 6.4.18: MALDI-TOF mass spectra of purified rhamnolipids produced by *Pseudomonas aeruginosa* A11

Table 6.4.2: Assignment of all rhamnolipids mass peaks obtained by MALDI-TOF mass spectrometry of biosurfactant produce by *Pseudomonas aeruginosa* strain A11

Mass Peak	Assignment	Molecular Formula
499.20, 515.17	$RhaC_{10}C_8/RhaC_8C_{10}$ $[M+ Na]^+$, $RhaC_{10}C_8/RhaC_8C_{10}$ $[M+K]^+$	$C_{22}H_{44}O_9$
523.02	*$RhaC_{22}[M+ Na]^+$	$C_{28}H_{52}0_7$
527.23,543.20	$RhaC_{10}C_{10}$ $[M+ Na]^+$, $RhaC_{10}C_{10}$ $[M+K]^+$	$C_{26}H_{48}O_9$
553.23	*$RhaC_{12}C_{10}$/ $RhaC_{10}C_{12}[M+ Na]^+$	$C_{28}H_{50}O_9$
555.26, 571.23	$RhaC_{12}C_{10}$/ $RhaC_{10}C_{12}[M+ Na]^+$, $RhaC_{12}C_{10}$/ $RhaC_{10}C_{12}[K+ Na]^+$	$C_{28}H_{52}O_9$
645.23,661.20	$RhaRhaC_{10}C_8/RhaRhaC_8C_{10}[M+ Na]^+$, $RhaRhaC_{10}C_8/RhaRhaC_8C_{10}[M+K]^+$	$C_{30}H_{54}O_{13}$
671.91,687.88	*$RhaRhaC_{10}C_{10}[M+ Na]^+$, *$RhaRhaC_{10}C_{10}[M+K]^+$	$C_{32}H_{56}O_{13}$
673.26,689.23	$RhaRhaC_{10}C_{10}[M+ Na]^+$, $RhaRhaC_{10}C_{10}[M+K]^+$	$C_{32}H_{58}O_{13}$
699	*$RhaRhaC_{12}C_{10}/RhaRhaC_{10}C_{12}[M+ Na]^+$	$C_{34}H_{60}O_{13}$
701.28	$RhaRhaC_{12}C_{10}/RhaRhaC_{10}C_{12}[M+ Na]^+$	$C_{34}H_{62}O_{13}$
*(olefinic Rhamnolipids)		

In rhamnolipids synthesis pathway, $RhaC_{10}C_{10}$ serves as a precursor for $Rha_2C_{10}C_{10}$. Thus, indicating that for each dirhamnolipids revealed, the corresponding monorhamnolipids congeners should also be revealed, but that is not what happens all the time [Manso et al, 1993]. In recent past our knowledge about the rhamnolipids diversity has increased primarily due to use of more sensitive and sophisticated analytical techniques [Abdel-Mawgoud et al, 2010]. Earlier Singh and Cameotra have reported that biosurfactant produced by strain A11 predominantly consisted of dirhamnolipids with single monorhamnolipids congener [Zhang et al, 2007]. However in the present study, with the help of better sophisticated analytical method more homologous and congeners were observed. The observed difference between components and fatty acids content

of rhamnolipids may be due to the difference in the culture condition and the analysing techniques [Abdel-Mawgoud et al, 2010].

TLC, FTIR, ^{1}H NMR and ^{13}C NMR, LCMS and MALDI suggested biosurfactant produced by strain A11 to be Rhamnolipids.

6.4.4.6 *Zeta Potential (Charge on Biosurfactant)*

Zeta potential studies were carried to determine net charge of rhamnolipids in aqueous solution. Zeta potential tells the potential difference between stationary layer of fluid attached to the scattered particle and the dispersion medium. The zeta potential value relates to the stability of colloidal dispersions. Colloids which have high zeta potential (positive or negative) are stabilized electrically while colloids which have low zeta potentials have the tendency to coagulate. Zeta potential studies of rhamnolipids aqueous solution indicated it to be anionic surfactants. Zeta potential of rhamnolipids changed with concentration and attained stable value after CMC.

Aqueous solution of rhamnolipids gave a negative zeta potential suggesting it to be anionic surfactant. The zeta potential varied in the range of-26.2 mV to -35.1 mV depending upon rhamnolipids concentration. There was gradual increase in zeta potential till CMC was reached after CMC the zeta potential became stable at -35.1 mV. Negative potential of Rhamnolipids observed in present study is in accordance with Pornsunthorntawee et al, 2011, Mendes et al, 2015.The net negative potential of rhamnolipids may be due to presence of carboxylic groups.

Rhamnolipids have better surface active properties than several synthetic surfactants like Sodium Dodecyl Sulphate, Triton X100 [Liu et al, 2011, Pedrazzani et al, 2012]. Moreover, the synthetic surfactants have been documented to exhibit toxic effect on living organism [Pedrazzani et al, 2012, Poremba et al, 1991]. Contrarily, rhamnolipids have lesser toxicity to toward living organisms thus making it an environment compatible alternative [Poremba et al, 1991].

6.4.4.7 *Micelle Size*

Micelle Size of Rhamnolipids was determined by Dynamic Light Scattering method by Zetasizer (Malvern Instruments Ltd., USA) in aqueous phase. Rhamnolipids mixtures were supposed to give two peaks, each one corresponding to monorhamnolipids and diarhamnolipids but instead of

this a single peak was identified. The reason for the may be because of combined contribution of monorhamnolipid and dirhamnolipids in the Formation of micelles of rhamnolipids. Diameter of Rhamnolipids Micelle was determined to be 499.7 nm by Dynamic Light Scattering method. The size in this range for rhamnolipids has been also reported by Anderson et al (2015). DLS analysis

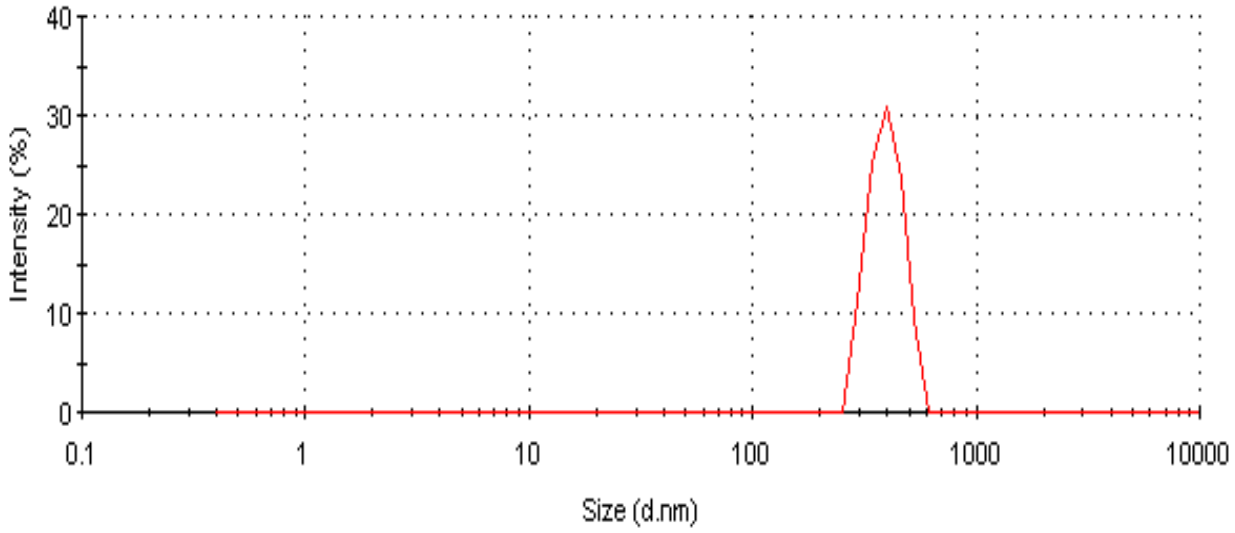

of rhamnolipids is shown in Figure 6.4.19 as follows.

Figure 6.4.19: DLS analysis of Rhamnolipids produced from strain A11.

6.5 Production of Biosurfactant Surfactin from Strain A21 and its Characterization

6.5.1 *Biosurfactant producing microorganism*

Lipopeptides type biosurfactant used in the present study was produced by *Bacillus subtilis* strain A21. Earlier strain A21 has been reported to produce lipopeptides type biosurfactant while growing on minimal salt medium (MSM) containing sucrose as a carbon source [Singh et al, 2013]. Sucrose is one of the best carbon source reported for biosurfactant production by *Bacillus subtilis* [Sandrin et al, 1990]. Members of Bacillus species have invertase enzyme enabling them to utilization sucrose for growth and metabolite production [Fernandes, 2010].

6.5.2 *Biosurfactant Production*

In present study the growth and reduction in surface tension kinetics of strain A21 is as shown in Figure 6.5.1.

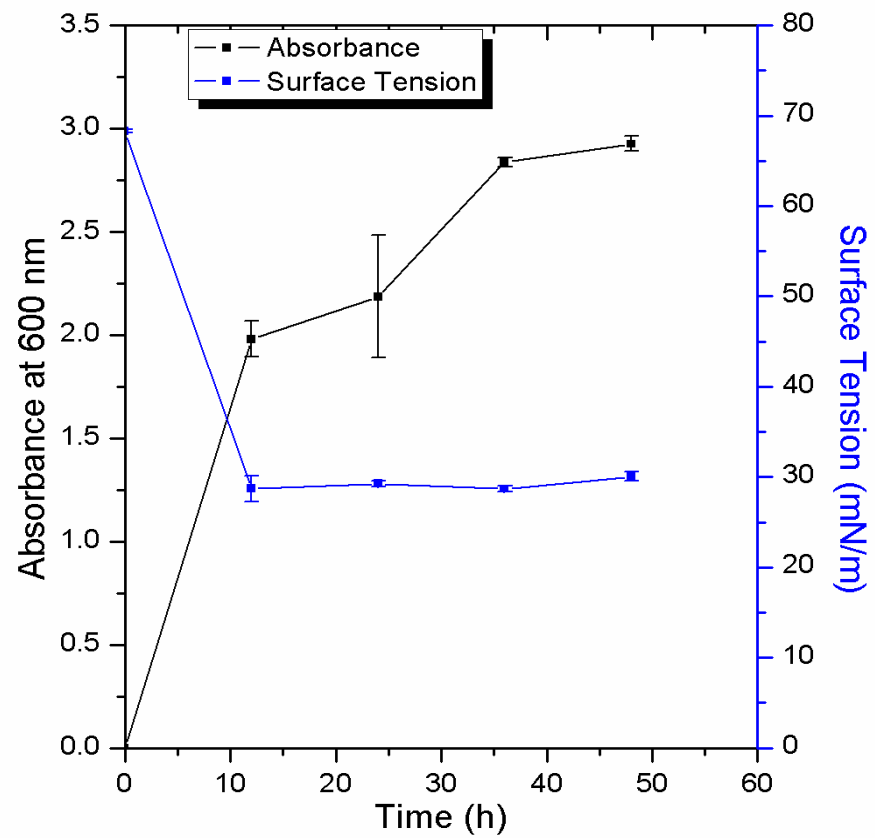

Figure 6.5.1: Growth and surface tension reduction kinetics of *Bacillus subtilis* strain A21. Strain A21 was grown in sucrose supplemented mineral salt medium at 30^{o} C with stirring done at 200 rpm. Values given are mean ± S.D. of three independent experiments

In present study the strain A21 decreased the surface tension of growth medium from 68 mN/m to 29 mN/m within 12 h of growth when the bacterium was in early exponential growth phase as shown in Figure 6.5.1. suggesting production of Surfactin. After 48 h of growth decline in cell mass was observed suggesting bacterium to entry death phase of growth. Bacillus species produce several amphiphilic cyclic lipopeptides molecules that are non-ribosomally synthesized by a multifunctional enzyme system [Arrebola et al, 2009]. Among all known cyclic lipopeptides, surfactin is the most studied molecules for its diverse applications. The present

study is an agreement with the work done in literature earlier [De Faria et al, 2011, Gudiña et al, 2015].

The dry cell mass and surfactin production of strain of A21 is as shown in Figure 6.5.2.

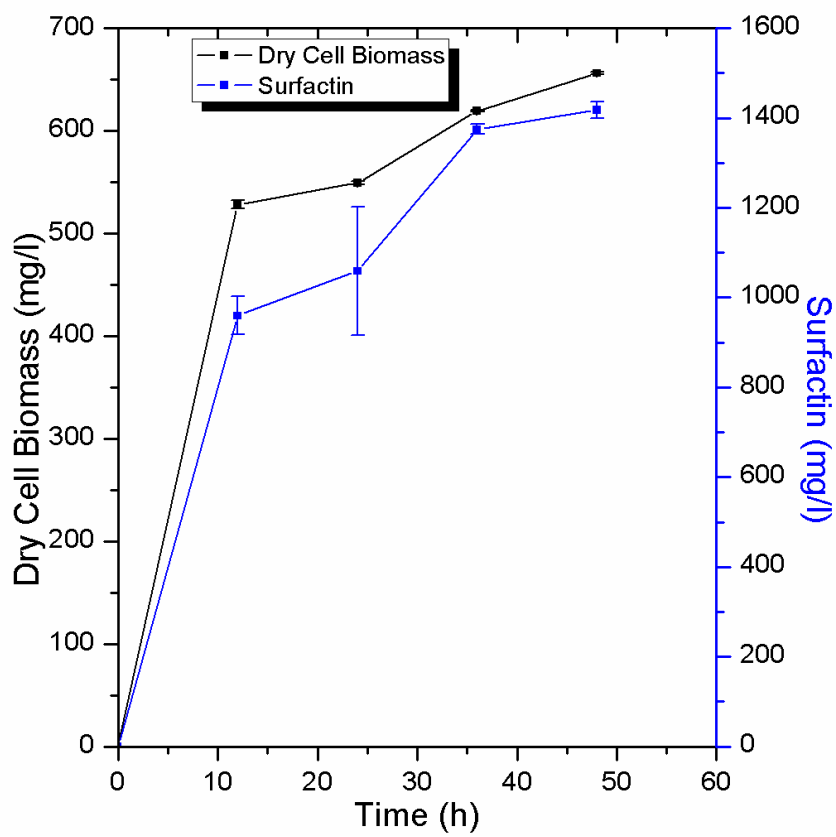

Figure 6.5.2: Time course of growth and surfactin production from *Bacillus subtilis* strain A21. Strain A21 was grown in sucrose supplemented mineral salt medium at 30 °C with stirring done at 200 rpm. Values given are mean ± S.D. of three independent experiments.

As it is clear from Figure 6.5.2 Strain A21 produced 1418±18 mg/l surfactin after 48 hours of growth with dry cell mass of 656.0 ± 0.98 mg/l. The amount of Surfactin produced by strain A21under given optimum condition is more than several reported strains [Pereira et al, 2013, Makkar et al, 1997].

Strain A21 exhibited good growth on MSM containing sucrose as a carbon source. According to Sandrin et al, 1990, fructose, sucrose and glucose are the best carbon substrates for synthesising surfactin [Sandrin et al, 1990]. Members of *Bacillus* family produce a wide variety of cyclic

lipopeptides having diverse biological function for its producer as well as for mankind [Pacwa-Plociniczak et al, 2011, Mnif et al, 2015].

6.5.3 Surface tension, Critical Micelle Concentration (CMC) and Stability of Biosurfactant

Surfactin has been reported to be one of the most powerful surfactant of biological origin. It can reduce surface tension of water to 25mN/m, an interfacial tension < 1.0mN/m and a CMC of 25 mg/l[Cooper et al, 1981]. The biosurfactants produced by strain A21 were capable of reducing the surface tension of water from 72 to 29 mN/m with CMC of 33 mg/l. Surface tension, and CMC observed in this study suggested it to be an efficient biosurfactant for environmental application [Mulligan et al, 2005, Sekhon et al, 2012]. Earlier, surface reducing activity and metal chelating ability of lipopeptides produced by strain A21 has been exploited for removing heavy metals and petroleum hydrocarbons from contaminated soil [Singh et al, 2013].

According to [Mulligan, 2005] biosurfactant with capability to decrease surface tension of water from 72mn/m to 35mN/m or less is an efficient biosurfactant. Considering this Surfactin produced by strain A21 is an efficient biosurfactant as Surfactin was capable to decrease the surface tension of water to 29 mN/m. From figure 6.5.3 and figure 6.5.4 it can be seen that Surface tension reducing capability of Surfactin under extreme conditions of pH (7.5 to 9) and temperature (-20 to 40 ^{o}C), remains stable. Lipopeptides type biosurfactant particularly surfactin has been reported to be stable under wide extreme conditions of pH and temperature [Sabate et al, 2013, Liu et al, 2015]. Thus, considered to be applicable for environmental and food industry applications.

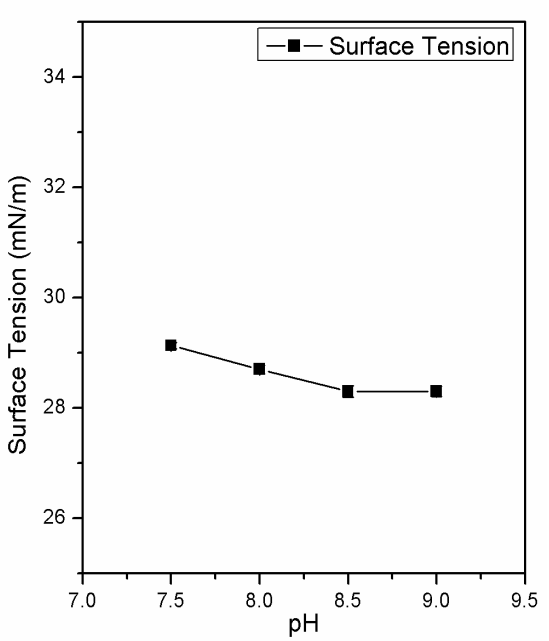

Figure 6.5.3: pH and reduction in surface tension relationship of Surfactin produced from strain A21.

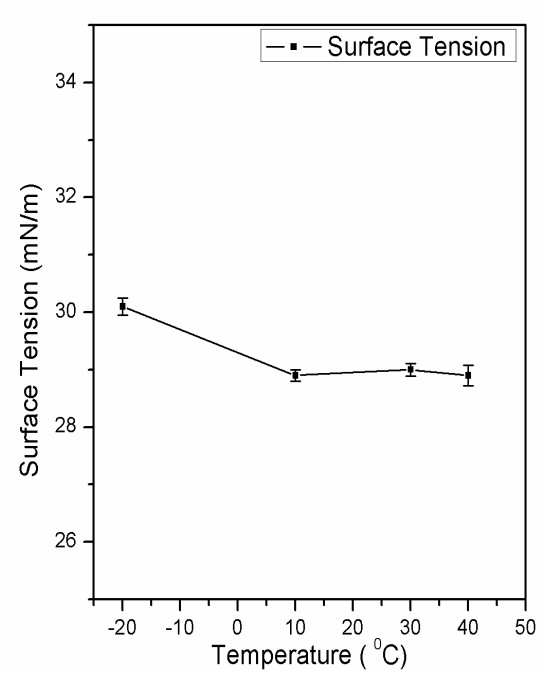

Figure 6.5.4: Temperature and reduction in surface tension relationship of Surfactin produced from strain A21.

Following serial dilution method CMC of surfactin was observed to be 33 mg/las shown in Figure 6.5.5. This is as per the earlier reported values [De Faria et al, 2011, Whang et al, 2008].

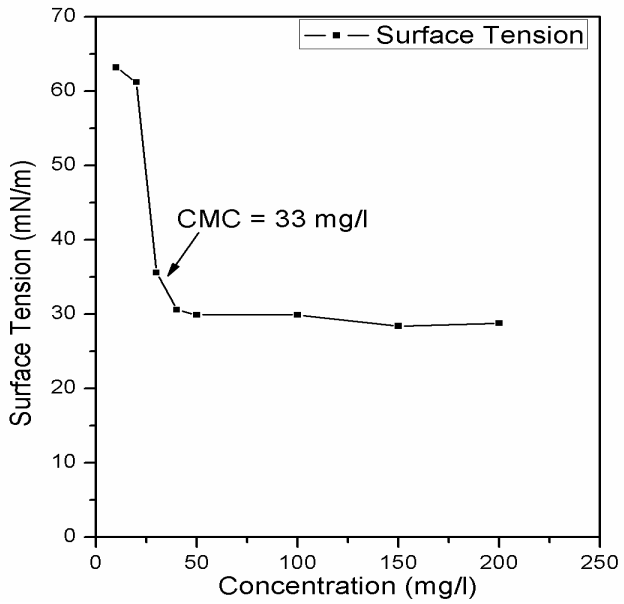

Figure 6.5.5: CMC of Surfactin produced from strain A21.

Lipopeptide type biosurfactant is one of the most powerful surfactant of biological origin [Cooper et al, 1981]. CMC defines efficiency of biosurfactant and is concentration above which biosurfactant molecules start to form micelles. Micelles Formation enables biosurfactant reduce to the surface tension and interfacial tension thus increasing solubility of hydrophobic compound. Efficient biosurfactant has lower CMC meaning that less amount of biosurfactant is required in order to decrease the maximum surface tension.

6.5.4 *Characterization of Biosurfactant surfactin produced by Bacillus subtilis strain A21*

6.5.4.1 *TLC*

Biosurfactant purified from *Sephadex LH-20 was initially characterized by Thin Layer Chromatogram (TLC).* The TLC profile of purified biosurfactant and surfactin standard purchased from Sigma Aldrich, USA gave single spot corresponding to *Rf* value of 0.76 and 0.77 after developing with water, respectively. Thus, suggesting that surfactant produced by strain A21 is surfactin. Arrebola et al. 2009 has also reported Rf value of 0.75 for the surfactin produced by *B. amyloliquefaciens [Arrebola et al, 2009,* Al Ajlani et al, 2007, Huszcza et al, 2006].

Figure 6.5.6: TLC of Surfactin produced by standard and strain A21.

6.5.4.2 FTIR

FTIR helped in characterizing the functional groups and the chemical bonds occurring in the biosurfactant produced by strain A21 (Figure 6.5.7). FTIR Spectrum exhibited a broad absorbance with wave numbers ranging roughly from 3600 cm^{-1} to 3011 cm^{-1}having its maxima at 3414 cm^{-1}. Absorbance in this region is responsible for C–H stretching vibrations and N–H stretching vibrations and is a typical property of carbon-containing compounds with amino groups. An absorbance in this region also confirms the occurrence of intramolecular hydrogen bonding. Two other sharp absorbance peaks were also seen at 2928 and 2851 cm^{-1} suggesting the presence of C–CH_3 bonding or long alkyl chains. The peak at 1650 cm^{-1} shows the occurrence of peptide group in the molecule. The peak at 1552 cm^{-1} indicates the presence of C=O bonds and is caused due to C=O stretching vibrations. A peak at 1464 cm^{-1} signifies C–H bending vibrations and is common in compounds with alkyl chains whereas peak at 1242 cm^{-1} suggest presence of C–O–C vibrations in esters. Peaks at 1066 cm^{-1} confirms the acidic carbonyl groups in the molecule. Overall FTIR spectrum confirms lipopeptide nature of biosurfactant produced by strain A21 [Das et al, 2008].

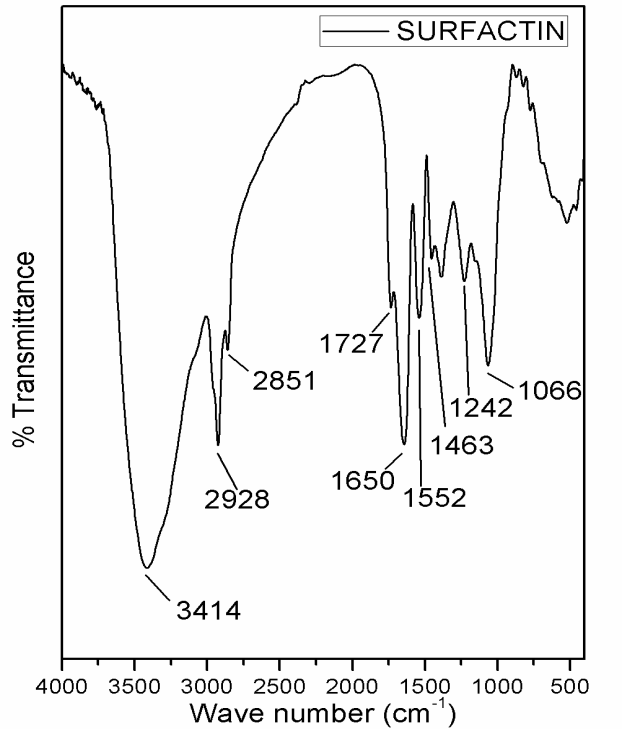

Figure 6.5.7: Fourier transform infrared spectrum of purified surfactin produced by *Bacillus subtilis* strain A21.

6.5.4.3 *HPLC*

An aliquot of sample was injected (20 µl) and analysed using UV-VIS detector (Shimadzu, Japan) at 205 nm. Surfactin purchased from Sigma Aldrich, USA served as standard. As evident from figure the chromatograms of standard and sample are nearly similar suggesting that strain A21 is producing Surfactin. The various peaks seen in both chromatograms corresponds to surfactin isoforms. The HPLC matching the present study is reported by [Yang et al, 2015]. The HPLC chromatograms is as shown in figure 6.5.8.

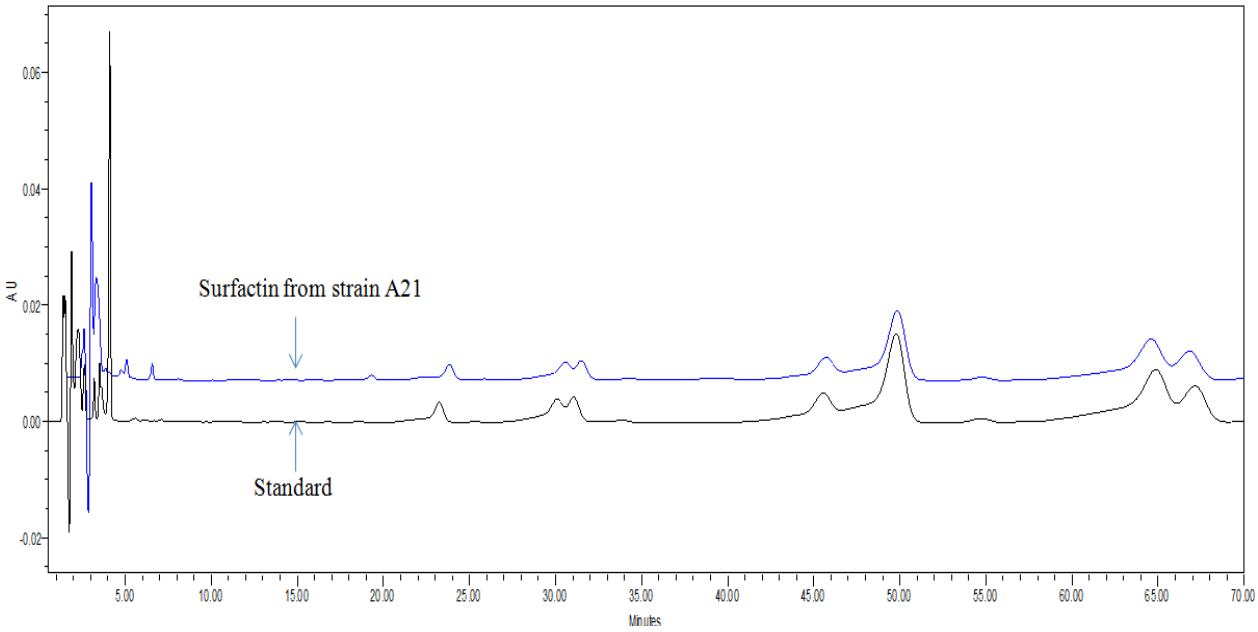

Figure 6.5.8: HPLC of Surfactin from Strain A21 and Standard.

6.5.4.4 MALDI

MALDI-TOF-Mass Spectrometry has been used widely for detecting the lipopeptides produced by *Bacillus Subtilus* [Vater et al, 2002, Savadogo et al, 2011]. As evident form figure 6.5.9, MALDI-TOF-MS spectrum exhibited cluster of peaks with mass/charge (m/z) ratios between 1036 and 1058, which could be accredited to surfactin isoforms. The most prominent peak was observed at m/z ratio 1044.76, corresponding to the mass of $[M+Na]^+$ ion of surfactin with a fatty acid chain length of 14 carbon atoms. Surfactin isoforms produced by strain A21 varied in fatty acid chain length of 13 to 15 carbon atoms (Table 6.5.1) and the isoforms observed are in

accordance with the available literature [Singh et al, 2013, Al Ajlani et al, 2007, Vater et al, 2002]. Lipopeptides produced by Bacillus species may differ in the composition and length of the lipids moiety as well as in the number, type and configuration of amino acids in the peptide chain [Raaijmakers et al, 2010].

Table 6.5.1 exhibits the mass peak, assignments and molecular formula of Surfactin identified in the Maldi of strain A21. Figures 6.5.9 shows the Maldi of surfactin from strain A21 as per the following. The present study is an agreement with the study carried by [Singh et al, 2014, Vater et al, 2002, Al-Ajlani et al, 2007, Singh et al, 2013].

As evident from table and figure 6.5.9 most abundant surfactin isoform is with carbon chain C_{14}.

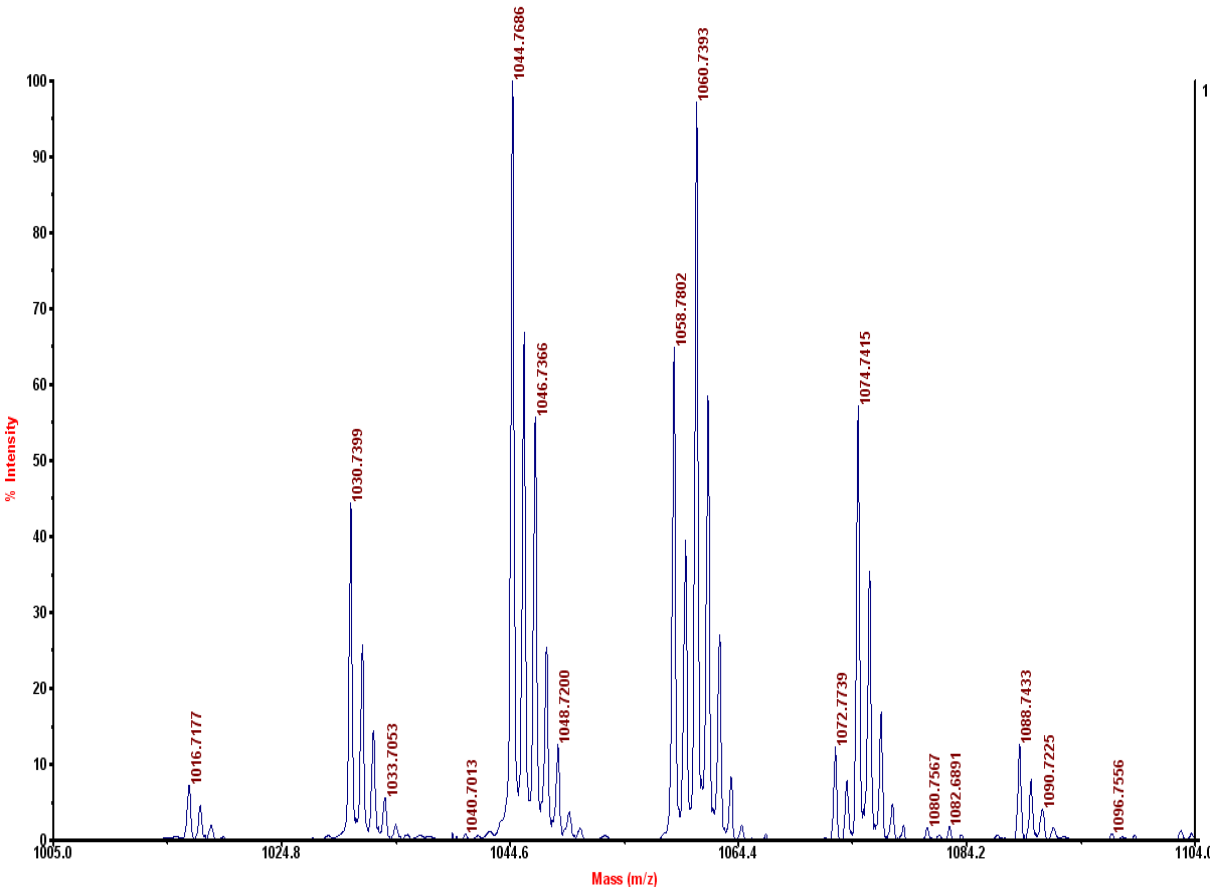

Figure 6.5.9: MALDI-TOF mass spectrum of purified surfactin produced by *Bacillus subtilis* strain A21

Table 6.5.1: Exhibits the mass peak and assignments of Surfactin identified in the MALDI of strain A21.

Mass Peak	Assignment	References
1016 .71	C_{13} surfactin Val-7 $[M + Na]^+$	Vater et al, 2002
1030.73	C_{13} surfactin Leu/Ile-7 $[M + Na]^+$	Vater et al, 2002
1044 .76	C_{14} surfactin Leu/Ile-7 $[M + Na]^+$	Vater et al, 2002, Savadogo et al, 2011
1046 .73	C_{13} surfactin Leu/Ile-7 $[M +K]^+$	Vater et al, 2002
1060 .73	C_{14} surfactin Leu/Ile-7 $[M +K]^+$	Vater et al, 2002
1058.78	C_{15} surfactin Leu/Ile-7 $[M + Na]^+$	Vater et al, 2002, Savadogo et al, 2011
1074.74	C_{15} surfactin Leu/Ile-7 $[M +K]^+$	Vater et al, 2002, Savadogo et al, 2011
1072 .77	C_{15} surfactin Leu/Ile-7 $[M-2H+K]^+$	Present Study
1088.74	C_{16} surfactin Leu/Ile-7 $[M +K]^+$	Present Study

6.5.4.5 *NMR*

Proton (^{1}H NMR) and Carbon-13 (^{13}C NMR) nuclear magnetic resonance were performed for determining the structural details of purified biosurfactant as shown in Figure 6.5.10. NMR of surfactin produced from strain A21 was carried by 500 MHz Brucker and explained as follows:

(a) ^{1}H NMR

Earlier, NMR has been successfully applied for characterizing biosurfactants produced by *B. subtilis* strains [Liu et al, 2009, Tang et al, 2007, De Faria et al, 2011, Pereira et al, 2013]. The ^{1}H NMR of biosurfactant exhibited peaks between δ 0.79 to δ 1.11 which confirms the presence

of –CH_3 of lipid chain and amino acids in the ring. The δ 1.22 to δ 1.53 shows the presence of –CH_2 in lipid chain. The δ 1.90 to δ 2.10 is because of –CH_2 of all leucines δ 2.58 to δ 2.90 shows the –CH_2 of aspartic acid and glutamic acid . The δ 3.40 to δ 5.08 confirms the – CH of amino acids while δ 7.04, 7.58, 7.84. 8.05, 8.18, 8.27 and 8.43 confirms the – NH of peptide linkage. The δ 11.55 and 11.64 shows the acidic proton of aspartic acid and glutamic acid respectively [Tang et al, 2007, De Faria et al, 2011, Pereira et al, 2013] as shown in Figure 6.5.10.

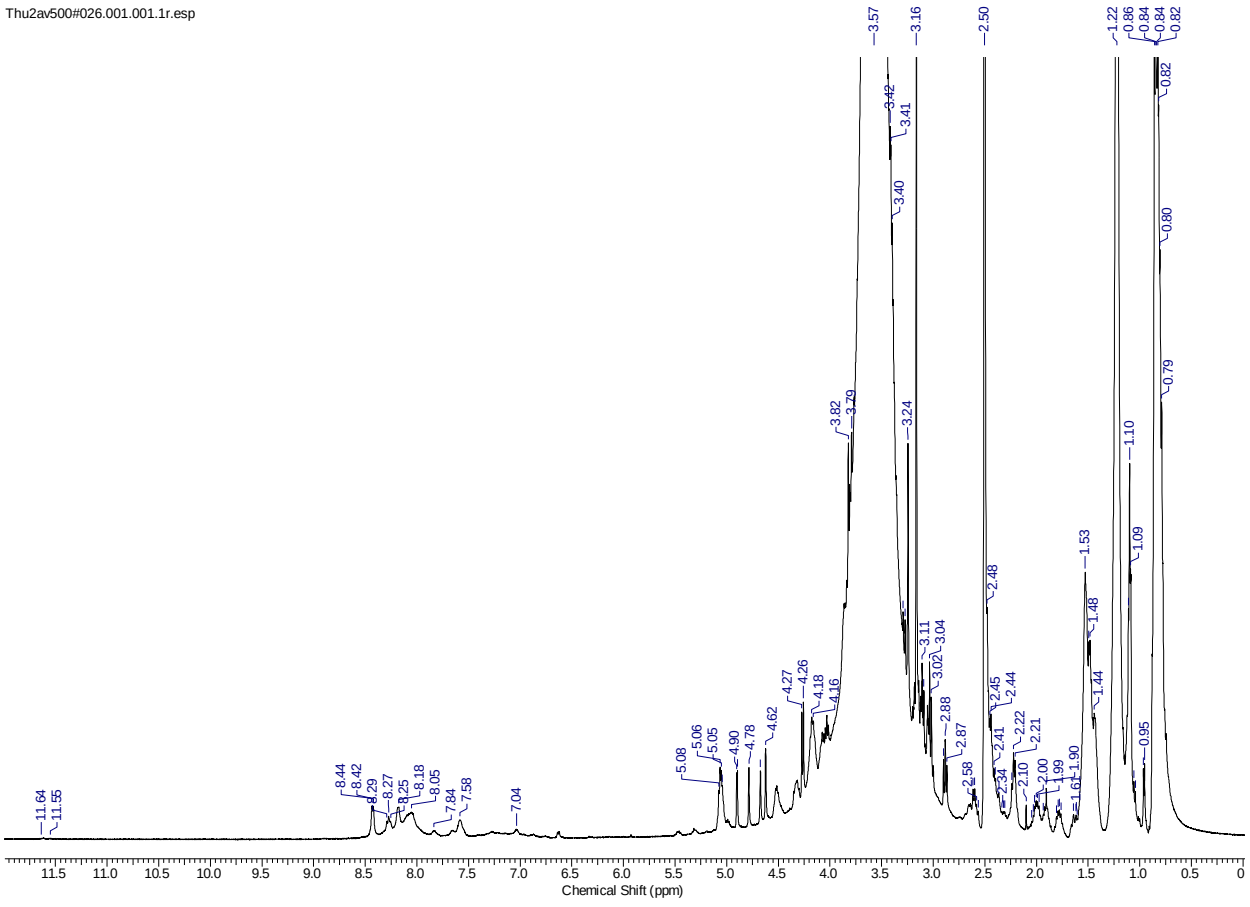

Figure 6.5.10: ^{1}H NMR of biosurfactant i.e Surfactin produced by *Bacillus subtilis* strain A21.

(b) ^{13}C NMR

δ 11.5 to 19.5 is because of carbon of – CH_3 of lipid chains. δ 21.5 to 23.4 shows the carbon of – CH_3 of all leucines and valine. δ 24.5 to 24.9 is because of carbon of –CH_2 of lipid chain. δ 27.2 to 33.7 shows the carbon in –CH_2 of leucines. δ 49.0 to 64.7 is due to the – carbon in – CH_2 of aspartic acid and glutamic acid. δ 68.2 to 104.5 is showing the carbon of –CH of all amino acids in ring. δ 170.1 to 171.2 is due to the amide carbonyl in amino acids in the ring. δ 171.7 and δ 171.8 due to acid carbonyl in aspartic acid and glutamic acid in ring [Tang et al, 2007, De Faria et al, 2011] is shown in Figure 6.5.11.

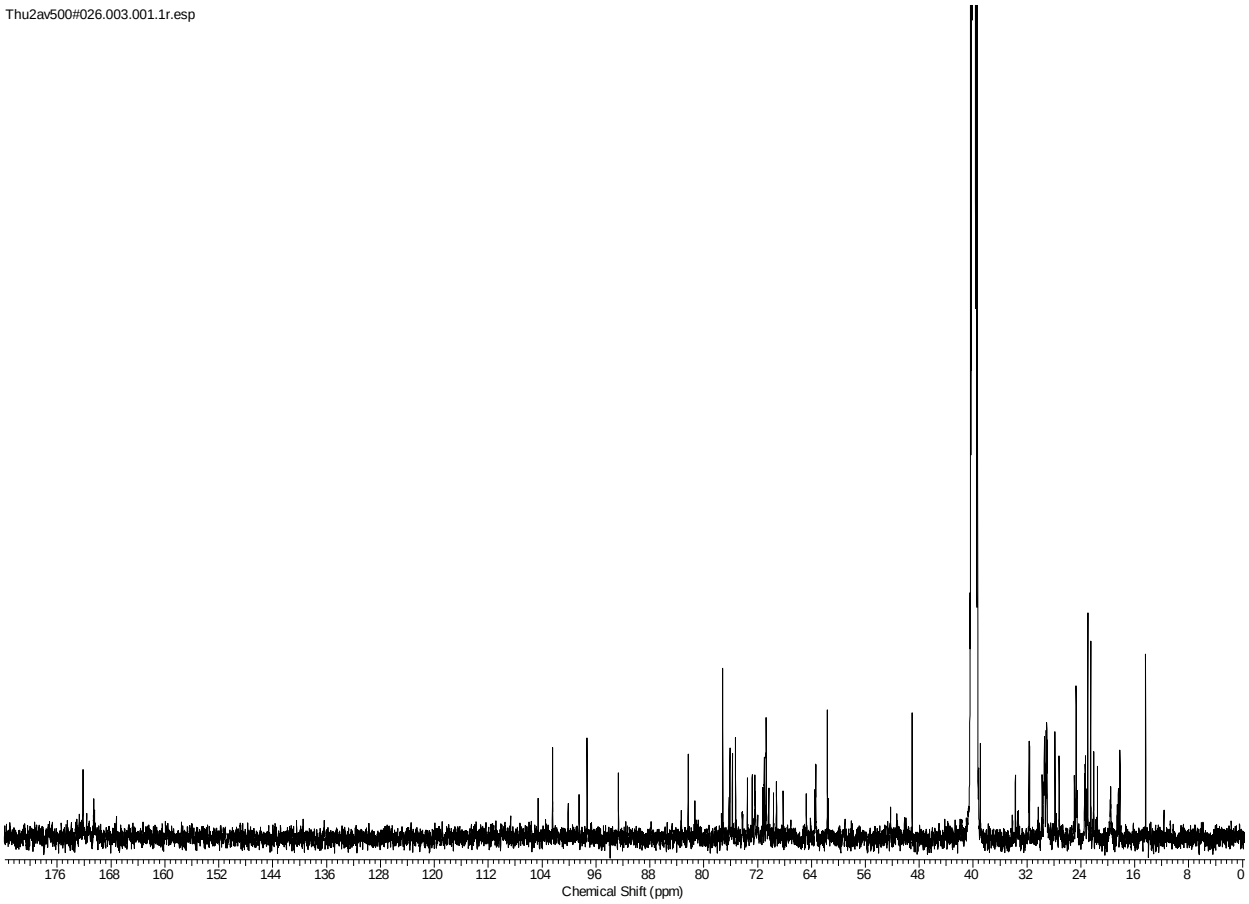

Figure 6.5.11: ^{13}C NMR of biosurfactant i.e Surfactin produced by *Bacillus subtilis* strain A21.

6.5.4.6 Amino Acids Analysis

The amino acids detected in biosurfactant synthesized from strain A21 are aspartic acid (Asp), glutamic acid (Glu) , leucines (Leu) and valine (Val), these has been reported to be present in surfactin [Singh et al, 2013, Baumgart et al, 1991] as shown in Figure 6.5.12.

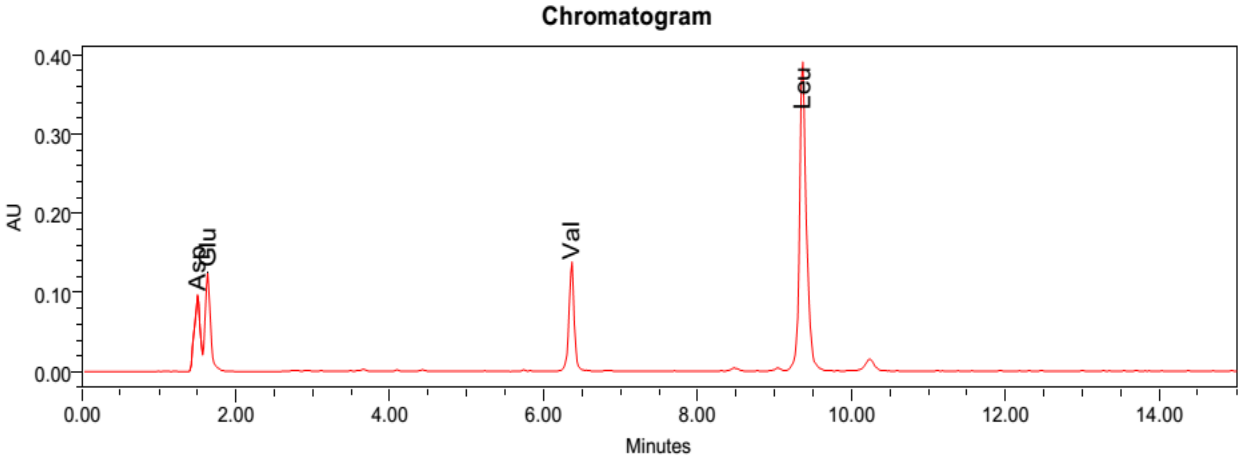

Figure 6.5.12: Chromatogram of amino acid analysis of Surfactin produced by *Bacillus subtilis* strain A21

.

TLC, FTIR, HPLC, MALDI, ^{1}H NMR and ^{13}C NMR and amino acid analysis suggested biosurfactant produced by strain A21 to be surfactin.

6.5.4.7 *Zeta Potential (Charge on Biosurfactant)*

The zeta potential studies suggested Surfactin to be anionic in nature. Zeta Potential of Surfactin varied in the range of-27.5 mV to -38.2 mV depending upon its concentration. Anionic nature of surfactin is in accordance with literature [Chen et al, 2008, Arutchelvi et al, 2014, Fan et al, 2014]. The negative potential observed for biosurfactant may be due to presence of anionic amino acids namely aspartic acid and glutamic acid [Singh et al, 2013].

There was gradual increase in zeta potential till CMC was reached after CMC the zeta potential become stable at a value of -38.2 mV. The net negative potential of surfactin may be due to presence of two acidic amino acids namely aspartic acid and glutamic acid.

6.5.4.8 *Micelle Size*

Diameter of Surfactin Micelle was determined to be 1075 nm by Dynamic Light Scattering method. The Micelle size of surfactin produced from strain A21 is in agreement with the micelle size reported by [Isa et al, 2007]. Figure 6.5.13 shows the diameter of the surfactant as follows:

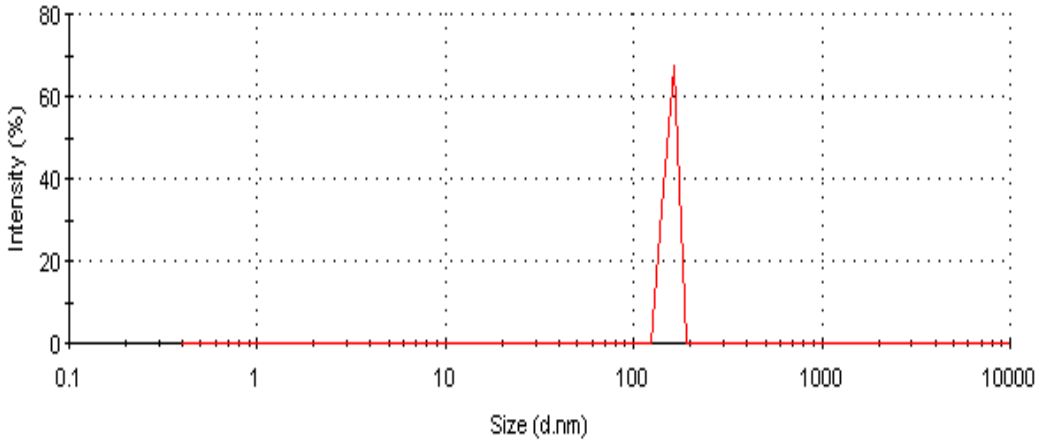

Figure 6.5.13: Diameter of surfactin produced from strain A21.

6.6 Characterization of a Novel Green Kinetic Inhibitor Calcium LignoSulphonate (CaLS)

Calcium LignoSulphonate was analysed using the following techniques.

6.6.1 *FTIR of CaLS*

As shown in Figure 6.6.1 in the FTIR spectrum of CaLS, it has been observed that the peaks at 3408 cm^{-1} and 2922 cm^{-1} are due to –OH and C-H stretching vibration respectively. The peak at 1640 cm^{-1} is because of the presence of acidic carbonyl groups that are intramolecular hydrogen bonded. Besides the peaks at 1420, 1176, 1044 and 652 cm^{-1} suggests the presence of sulfonate group in CaLS.

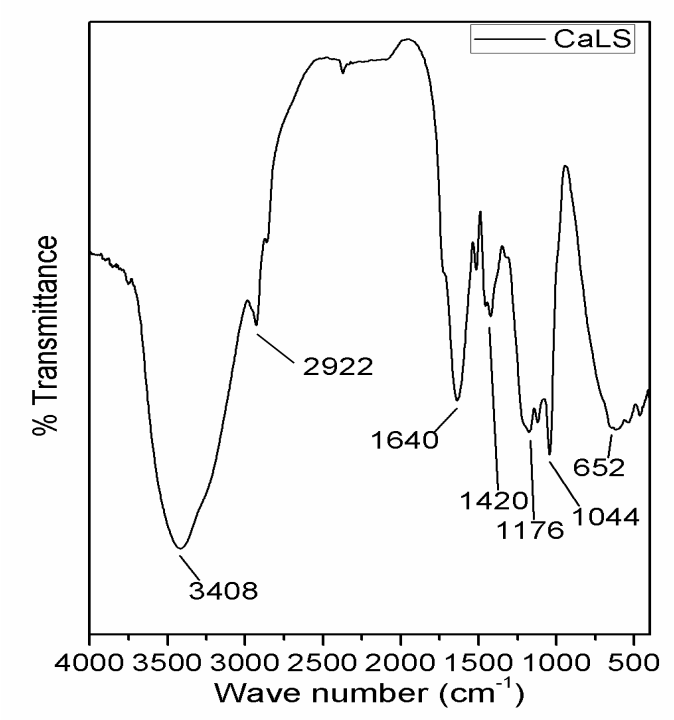

Figure 6.6.1: FTIR of CaLS

6.6.2 *UV of CaLS*

As shown in figure 6.6.2 In the UV-VIS spectrum of CaLS, a broad peak between 300 - 375 nm indicates the presence of aromatic moiety in CaLS

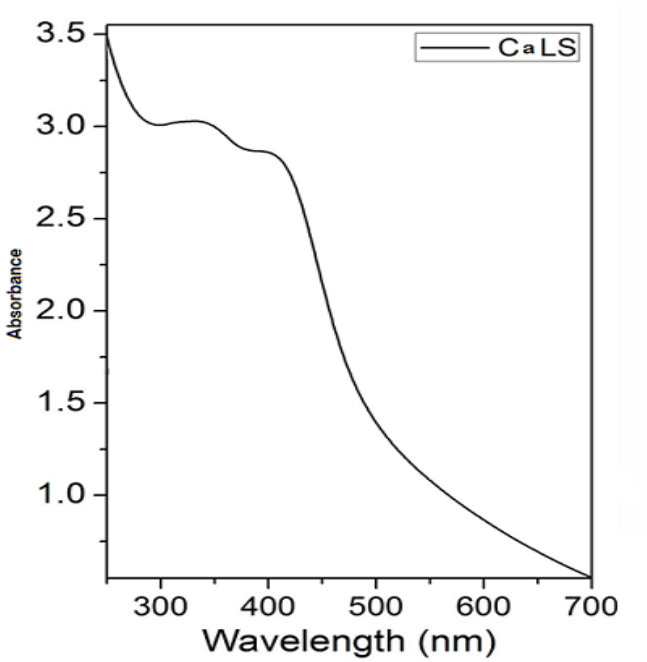

Figure 6.6.2: UV of CaLS

6.6.3 *CHNS Analysis of CaLS*

The results obtained are as described in the table 6.6.1.

Table 6.6.1: CHNS of CaLS

Name of the biosurfactant	%C	%N	%H	%S
CaLS	29.340	0.000	6.624	0.753

From the C, H, N, S analysis of CaLS it has been noticed that it contains C, H, S elements in the network besides oxygen.

6.6.4 *ICPMS*

For the analysis of Calcium LignoSulphonate sample, it was prepared by dissolving 0.08 gm in 10 ml of 10 % HNO_3 and was further diluted to 25 ml. One ml of this is diluted to 100 ml by double distilled water. The calibration curve of Sodium, Magnesium, Potassium and Calcium are shown from figure 6.6.3 to figure 6.6.6.

From this analysis the percentage of the elements found in CaLS is as follows:

Na= 0.33%, Mg= 6.08%, K=0.3%, Ca= 0.2%.

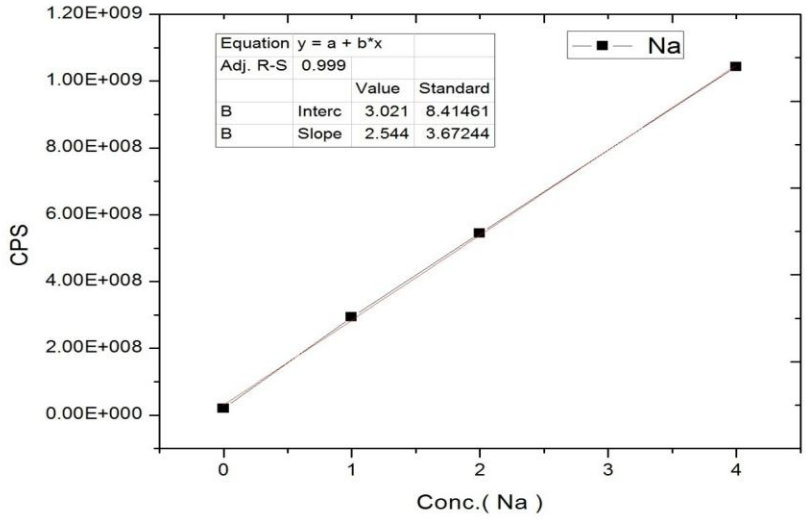

Figure 6.6.3: Calibration Curve of Sodium (Na)

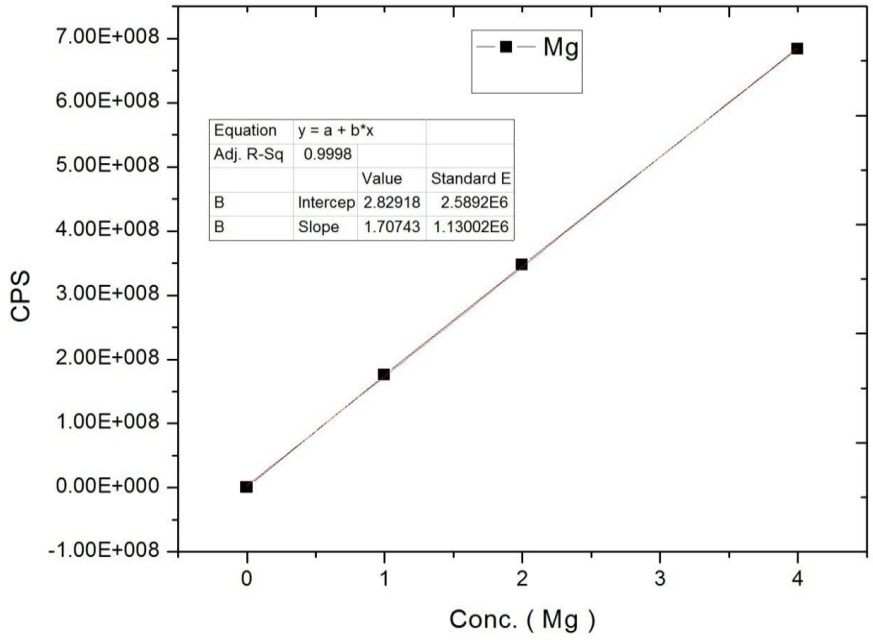

Figure 6.6.4: Calibration Curve of Magnesium (Mg)

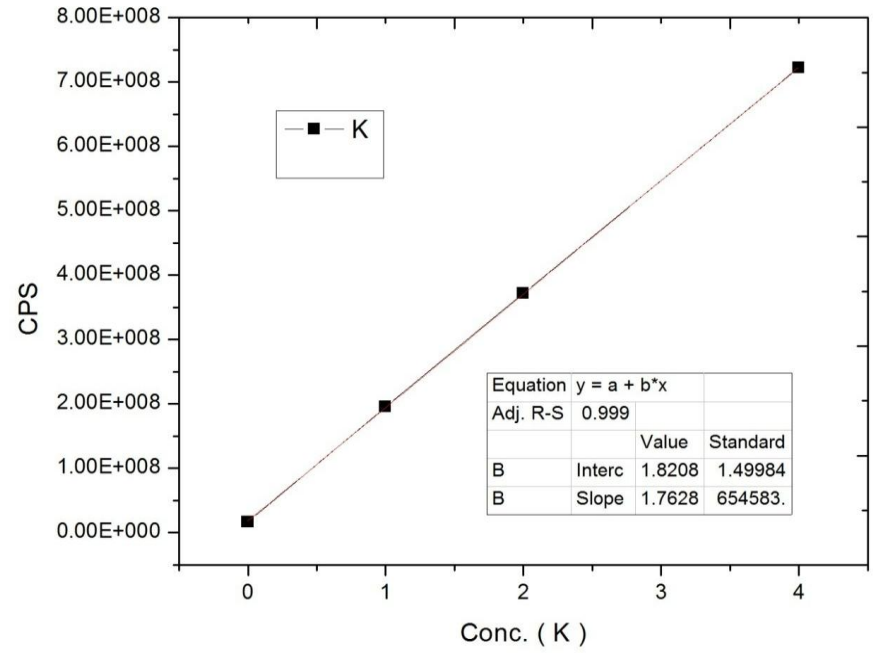

Figure 6.6.5: Calibration Curve of Potassium (K)

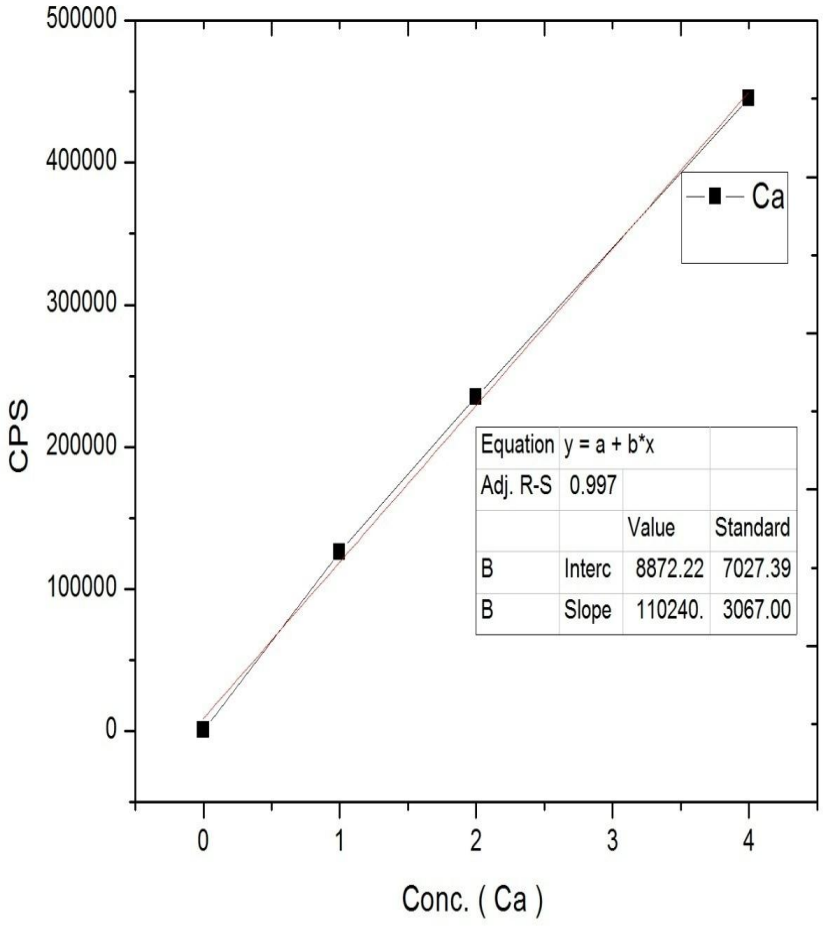

Figure 6.6.6: Calibration Curve of Calcium (Ca)

6.6.5 *GPC*

The molecular weight distribution of CaLS were found by GPC analysis and the results are shown in Figure 6.6.7 as well as in Table 6.6.2. It is obvious from the results Figure 6.6.7 & Table 6.6.2 that CaLS have higher molecular weight (Mw = 282377) due to Formation of polymeric network.

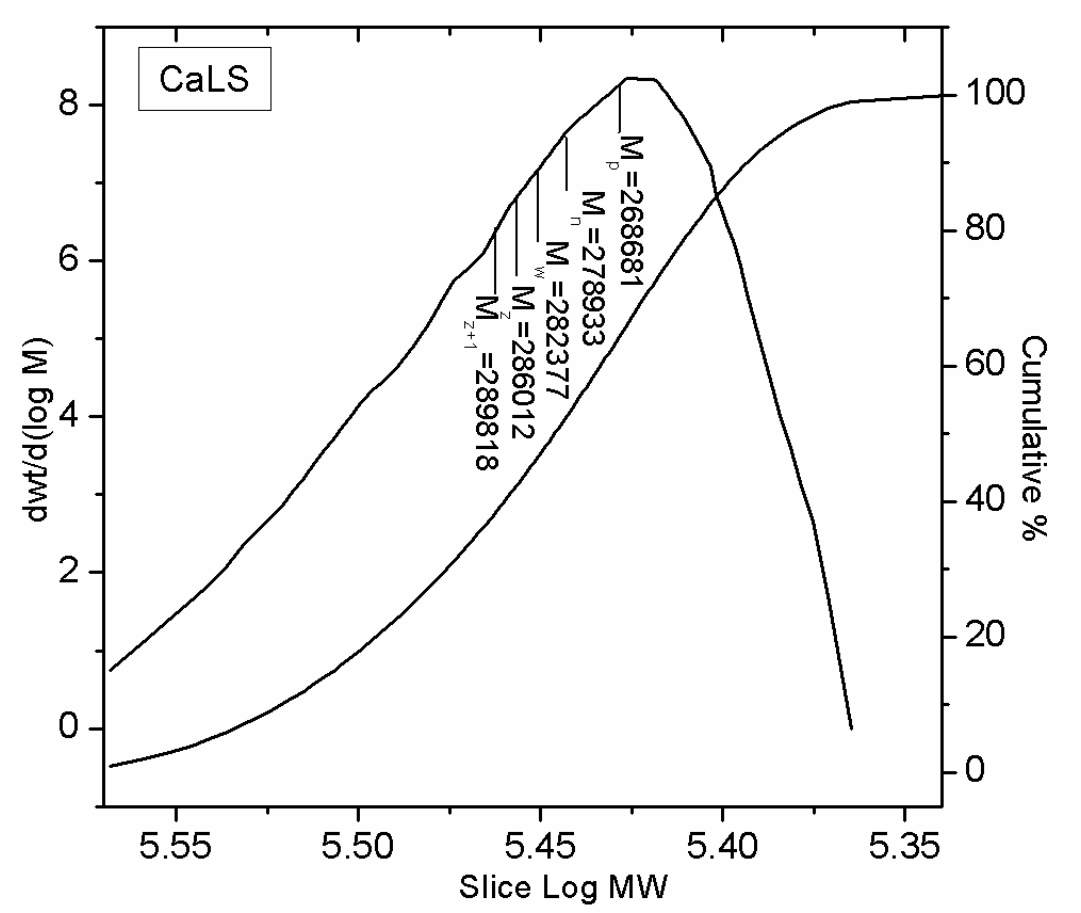

Figure 6.6.7: Gel Permeation Chromatography of CaLS

Table 6.6.2: Gel Permeation Chromatography of CaLS

Name of the biosurfactant	Mn	Mw	Mp	Mz	Mz+1	Polydispersity (Mw/Mn)
CaLS	278933	282377	268681	286012	289818	1.012347

M_n : Number average molecular weight

M_w : Weight average molecular weight

M_p : Molecular weight of highest peak M_z,

M_{z+1} : The higher average molecular weights

6.6.6 FE-SEM and Mapping

6.6.6.1 FE-SEM

The surface morphology of CaLS has been studied by FE- SEM analysis. From image in Figure 6.6.8, it has been observed that it has uneven, irregular porous structure with variable pore size.

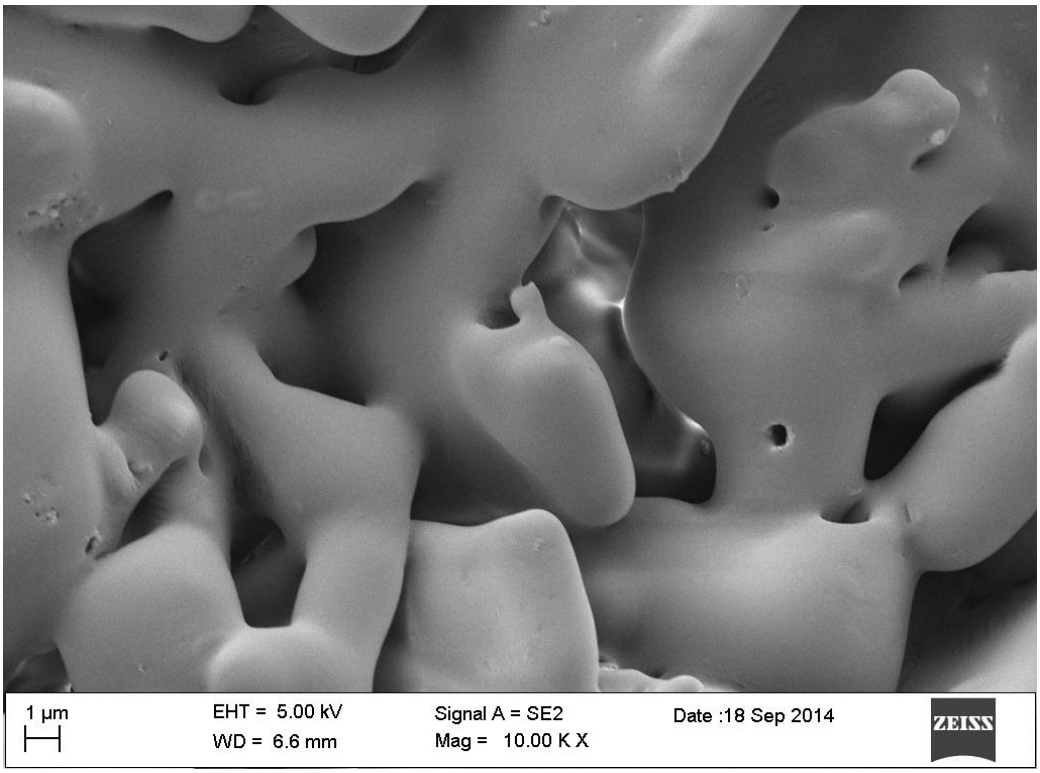

Figure 6.6.8: FE-SEM of CaLS

6.6.6.2 FE-SEM Mapping

Various elements found while mapping of CaLS are displayed in figure 6.6.9 and figure 6.6.10 respectively. In the mapping images various colors represent different elements (Carbon, Oxygen, Sulphur and Calcium).

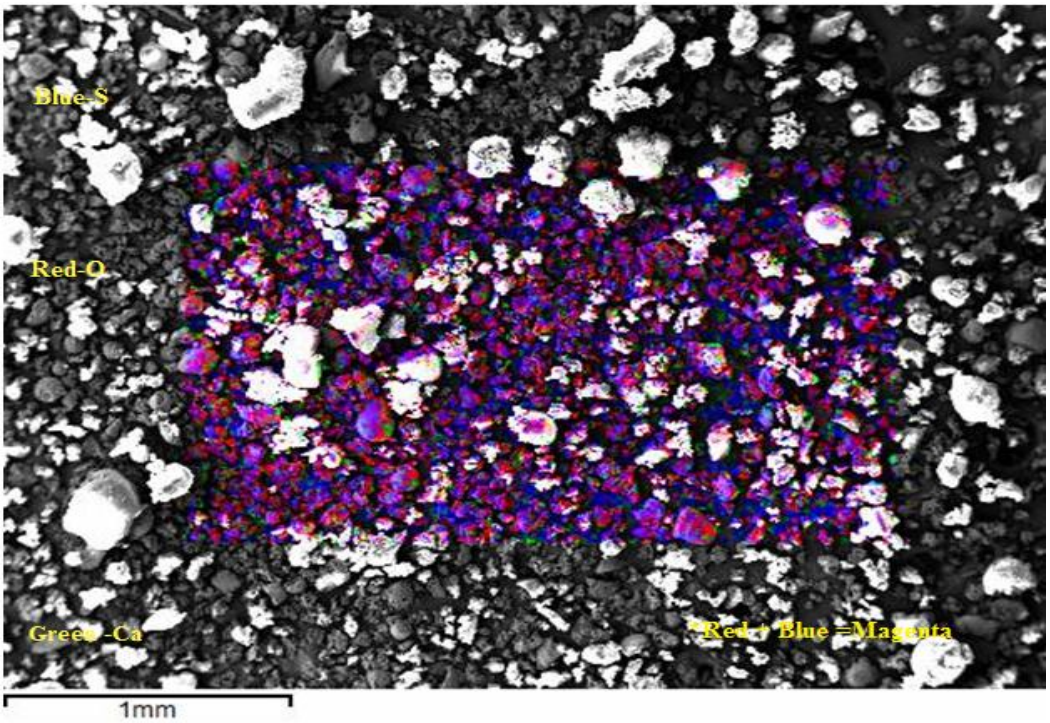

Figure 6.6.9: FE-SEM showing mapping of various elements of CaLS where Blue, Red, Green are Sulphur, Oxygen, Calcium respectively where Red + Blue = Magenta (showing the presence of Oxygen and Sulphur)

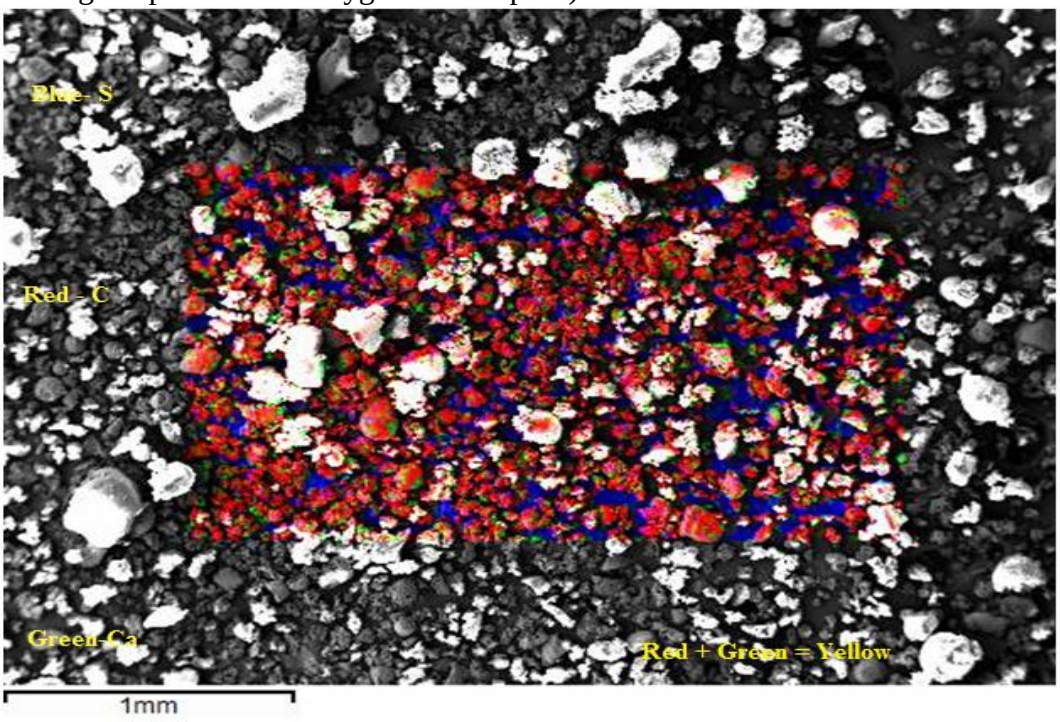

Figure 6.6.10: FE-SEM showing mapping of various elements of CaLS where Blue, Red, Green are Sulphur, Carbon, Calcium respectively where Red+ Green = Yellow (showing the presence of Carbon and Calcium).

6.6.7 *EDS*

From the EDS analysis Figure 6.6.11 & Table 6.6.3, it is seen that CaLS contains Carbon, Oxygen, Sulphur and Calcium as its components. Platinum is there because of coating of sample is done with it.

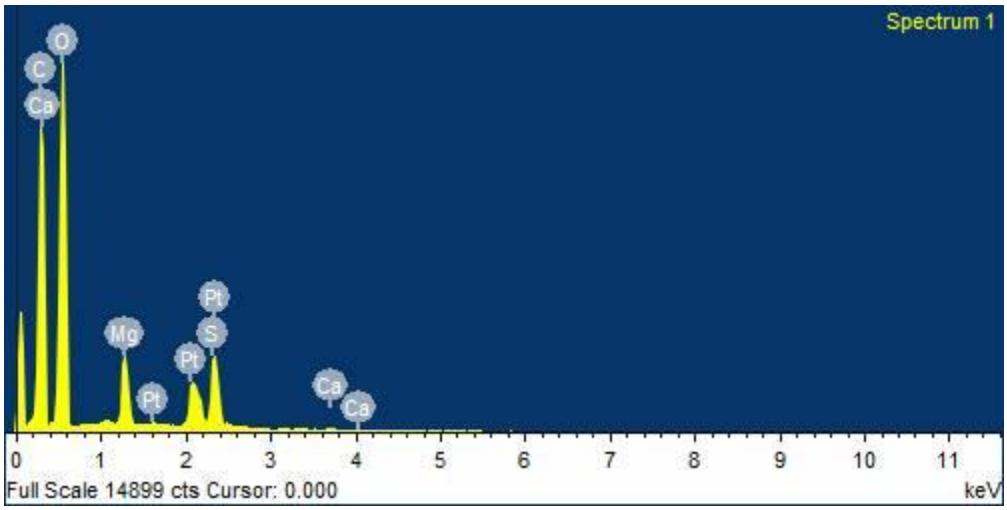

Figure 6.6.11: Electron Dispersive Spectroscopy of CaLS

Table 6.6.3: Electron Dispersive Spectroscopy analysis of CaLS

Element	Weight (%)	Atomic (%)
CK	38.80	52.97
OK	39.28	40.26
MgK	3.37	2.27
SK	6.74	3.44
CaK	0.20	0.08
PtK	11.61	0.98
Total	100	100

6.6.8 *TGA*

As shown in Figure 6.6.12, the DTG curves of CaLS exhibited significantly different decomposition pattern. The difference in the thermal behaviour can be well observed from the DTG peaks Figure 6.6.12. Degradation peaks in five major temperature regions can be observed in the DTG curves of the CaLS. Weight loss at 72°C attributed to the loss of moisture from lignin [Xiao et al, 2001, Jakab et al, 1995]. A broad peak at 106°C is due to the dehydration process in CaLS. The third peak at 284°C indicates the degradation of xylose moiety in the CaLS and a forth peak at 596°C is due to the decomposition of aromatic ring. Then CaLS release CO at 700°C is due to the cracking of C-O-C and C=O bonds [Tejado et al, 2007, Sun et al, 2000].

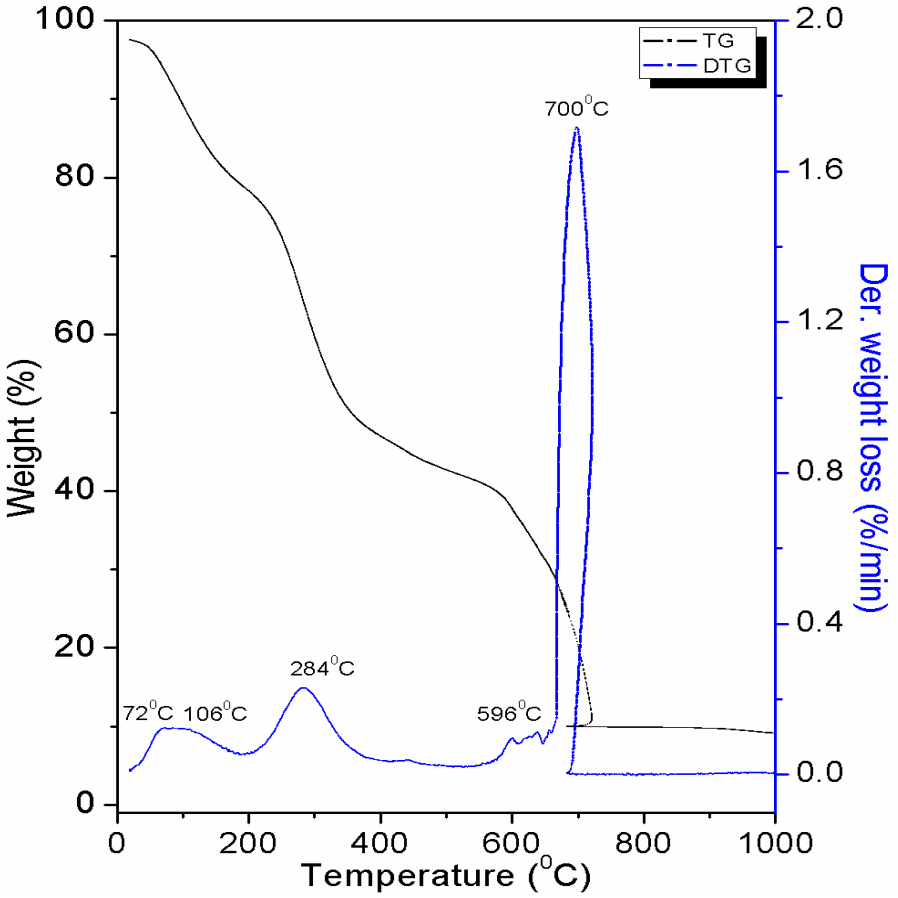

Figure 6.6.12: DTG Analysis of CaLS

6.6.9 *NMR*

The trends of solid NMR of CaLS obtained are as explained in Figure 6.6.13 and Table 6.6.4.

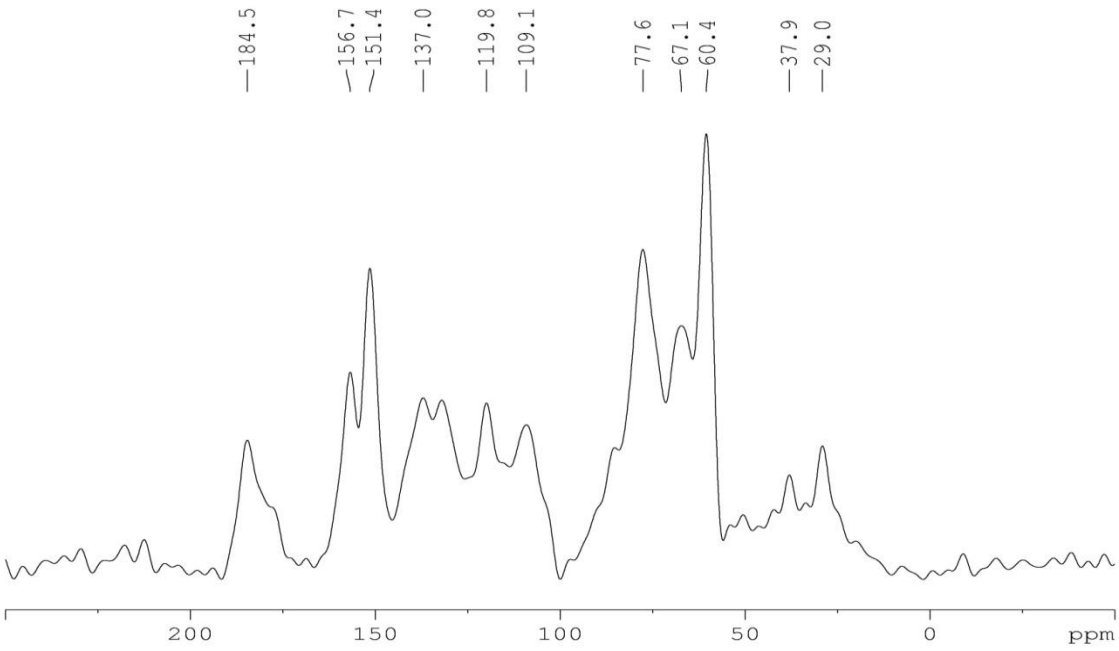

Figure 6.6.13: Nuclear Magnetic Resonance ^{13}C of CaLS

Table 6.6.4: Nuclear Magnetic Resonance ^{13}C of CaLS

Serial No.	Chemical Shift (ppm)	Moiety
1	109.1	Aromatic
2	119.8	Aromatic
3	137.0	Aromatic
4	151.4	Aromatic
5	156.7	Aromatic
6	60.4	C-SO_3
7	67.1 , 77.6	C-O , C-OH
8	29.0 , 37.9	Alkyls
9	184.5	COOH

6.7 Biosurfactant Rhamnolipids as a Promoter of Methane Hydrate Formation: Thermodynamic and Kinetic Studies

6.7.1 *Thermodynamic Study*

6.7.1.1 *Methane Hydrate Formation-Dissociation*

The experiment was done with 99.99 % of pure CH_4 first with quiescent water, then in presence of fixed bed made of C-type Silica Gel 90% saturated with distilled water and afterwards C type Silica Gel 90% saturated with distilled water containing different dosage of rhamnolipids. Pore volume was found by BET analysis. Firstly the pressure of the system decreased for a number of hours without forming Hydrate which is because of dissolution of Gas till the liquid is saturated with the Gas. Thus the concentration of Gas in liquid is increased and it becomes super-saturated resulting to clustering of water molecules. At a certain temperature shown as nucleation point (277.16 K) in Figure 6.7.1 rapid decrease of pressure at a greater rate was seen indicating Hydrate nucleation. A sharp discontinuity was seen in the Formation curve due to encapsulation of Gas in the cage of water molecules with a rise in the temperature due to the heat released while Hydrate Formation. It is found that Formation of Hydrate does not take place in a single stage but in multiple stages.

The temperature and pressure of the reactor were noted for the Formation of Hydrate. Temperature of the system was kept constant when sudden pressure drop was observed. Then temperature was further decreased slowly to 271.15 K to observe pressure drop due to growth of Hydrate. At 271.15 K, no significant pressure drop was observed indicating the completion of Hydrate Formation of Hydrate. The system is permitted to stay at the same temperature for 3h to attain a state of equilibrium. The temperature of the system was increased slowly at the rate of 1K/h so that equilibrium of the system could disturb. Dissociation was also studied in similar way by enhancing the temperature. When the temperature reached a threshold value (285.72 K) there is sudden increase in pressure which informs the start of Dissociation of Hydrate Figure 6.7.1. Hydrate Dissociation completed at 289.52 K called Dissociation point as shown in figure 6.7.1. The Dissociation point is the highest temperature where all the three phases are in equilibrium is known as the Dissociation point after that Hydrate is not observed.

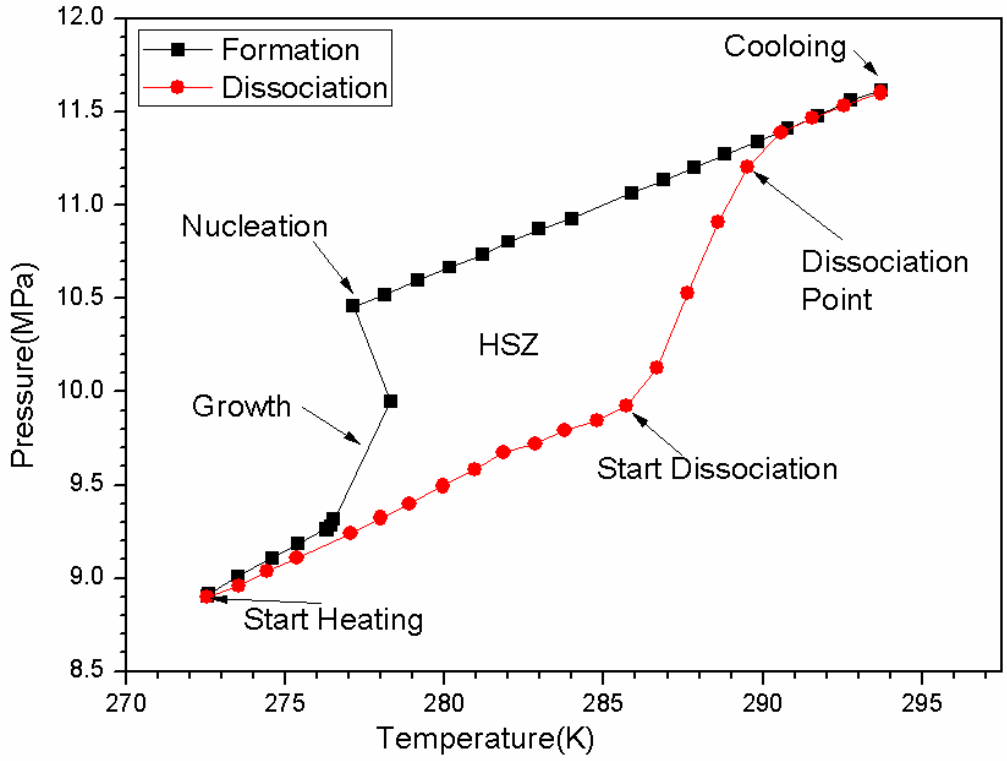

Figure 6.7.1: Temperature and Pressure profile of Methane Hydrate Formation and Dissociation in presence of C- type Silica Gel (Merck).

Our objective in the present study is to examine the effect of biosurfactant rhamnolipids on Methane Hydrate Formation and Dissociation. Different concentrations of rhamnolipids were used to observe the influence on the Formation and Dissociation of Methane Hydrate.

Under same conditions the cell was then packed with 90% saturated C-type Silica Gel (Merck) containing 100 ppm rhamnolipids. At temperature (277.37 K) rapid decrease of pressure at a greater rate was observed indicating Hydrate nucleation Figure 6.7.2. When the temperature reached a threshold value (285.88 K) there is sudden increase in pressure which confirms the start of Dissociation of Hydrate Figure 6.7.2. Hydrate Dissociation completed at 290.74 K known as Dissociation point as shown in figure 6.7.2. The Dissociation point is the highest temperature where all the three phases are in equilibrium is known as the Dissociation point after that Hydrate is not observed.

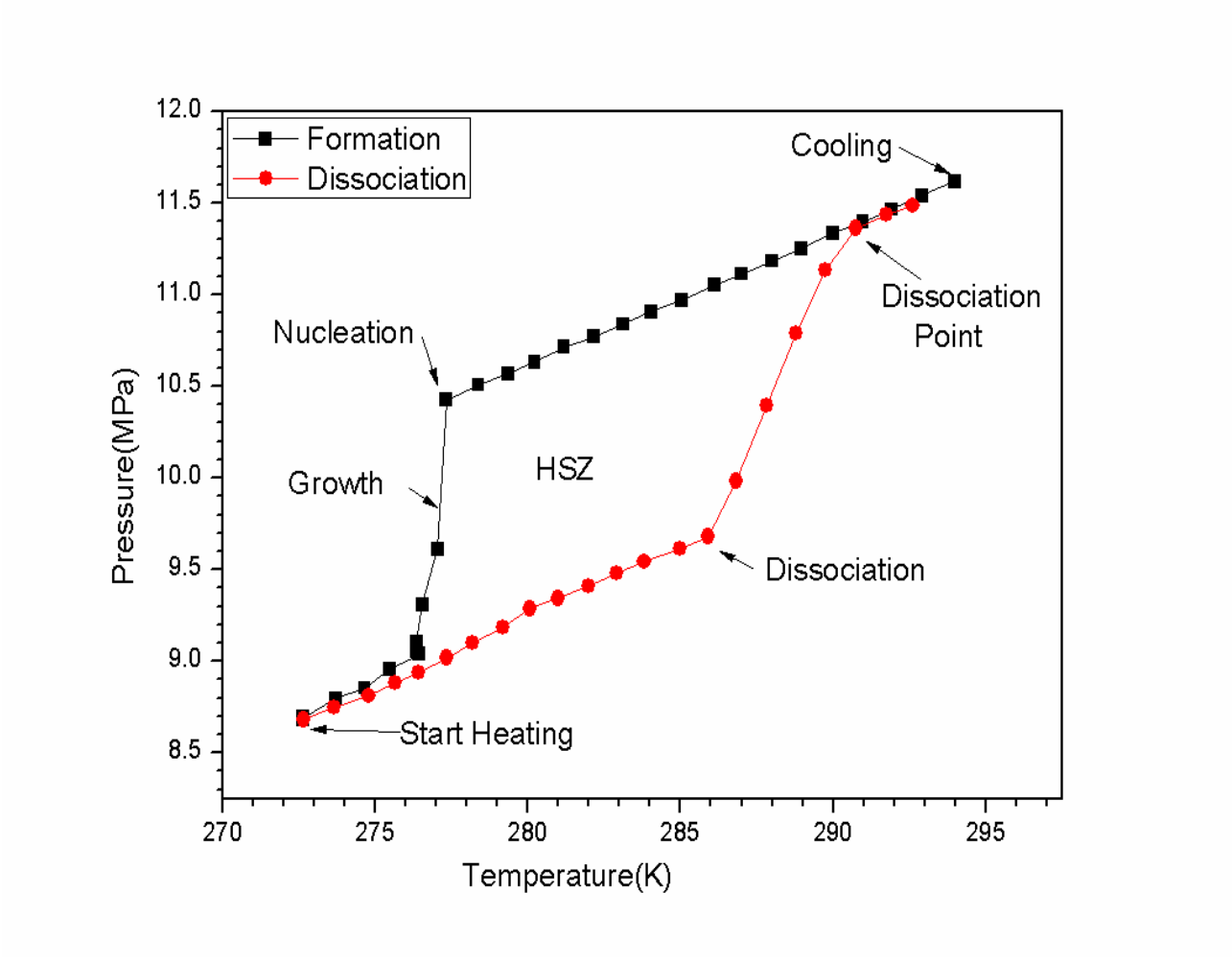

Figure 6.7.2: Temperature and Pressure profile of Methane Hydrate Formation and Dissociation in presence of C- type Silica Gel (Merck) containing 100 ppm Rhamnolipids

Afterwards under similar conditions test sample containing 1000 ppm rhamnolipids was investigated. At temperature (278.59 K) rapid decrease of pressure at a greater rate was observed indicating Hydrate nucleation Figure 6.7.3. Dissociation was also studied in same way by increasing the temperature. When the temperature reached a threshold value (286.09 K) there is sudden increase in pressure which shows the start of Dissociation of Hydrate Figure 6.7.3. Hydrate Dissociation completed at 290.79 K known as Dissociation point as shown in figure 6.7.3.

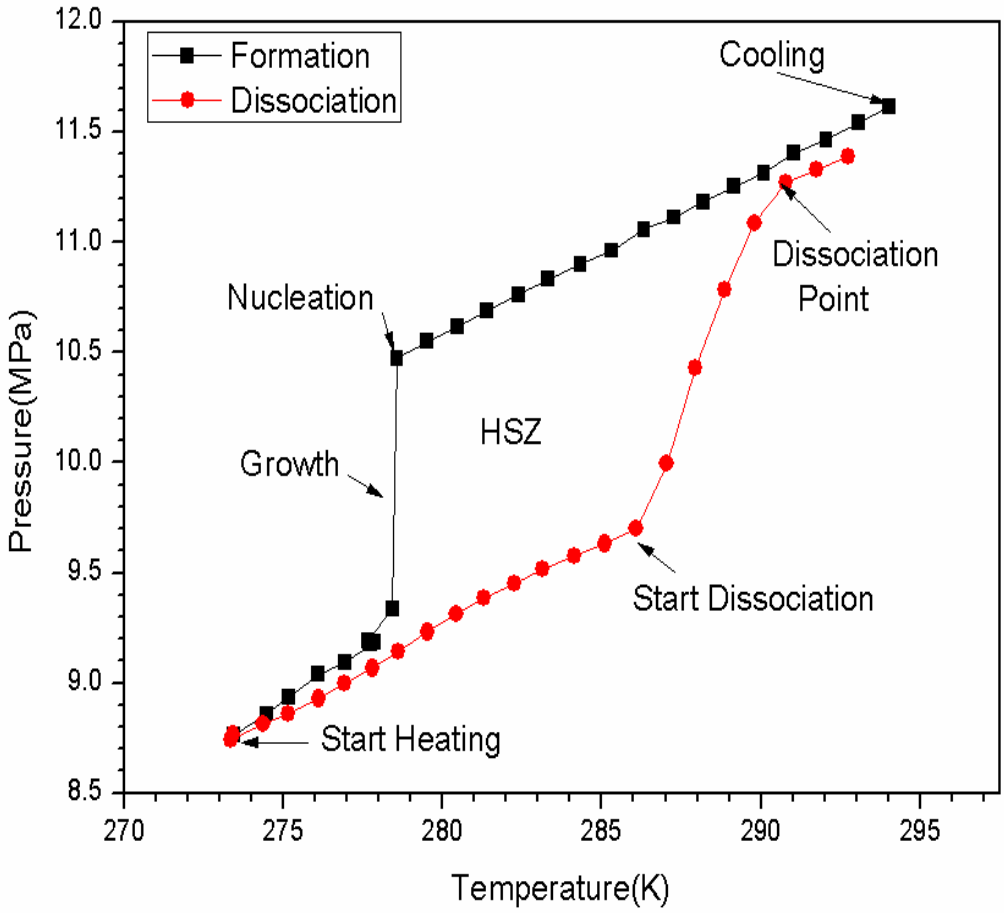

Figure 6.7.3: Temperature and Pressure profile of Methane Hydrate Formation and Dissociation in presence of C- type Silica Gel (Merck) containing 1000 ppm Rhamnolipids.

The thermodynamic parameters of Hydrate Formation and Dissociation are substantially influenced by the variation in concentration of rhamnolipids Table 6.7.1. When the concentration of rhamnolipids increased from 100 ppm to 1000 ppm, the nucleation temperature of Hydrate Formation is shifted to higher values and also less sub cooling is required to initiate Hydrate Formation. It is found that the nucleation temperature of Hydrate Formation is increased to higher values at 1000 ppm of rhamnolipids. The pressure drop of Hydrate Formation is also influenced on the addition of rhamnolipids as shown in Table 6.7.1 as per following:

Table 6.7.1: Methane Hydrate Formation and Dissociation parameters in presence of different test sample

Test sample	Initial cell Pressure P (MPa)	Nucleation Tempera-ture T(K)	Nucleation Pressure P(MPa)	Pressure drop Δp (MPa)	Equilibrium Tempera-ture T_{equ}(K)	Subcooling ΔT(°C) $\Delta T=T_{equ}$ - T	Dissociation Temperature (K)
Quiescent water	11.62	271.73	10.09	0.64	290.00	18.27	286.54
C-type Silica Gel without presence of Rhamnolipids	11.62	277.16	10.46	1.14	289.52	13.43	285.72
C-type Silica Gel containing 100 ppm Rhamnolipids	11.62	277.37	10.42	1.38	290.74	13.37	285.88
C-type Silica Gel containing 1000 ppm Rhamnolipids	11.62	278.59	10.47	1.14	290.79	12.2	286.09

6.7.1.2 *Comparison of nucleation temperature of Methane Hydrate Formation for different Systems*

Figure 6.7.4 exhibits the Hydrate Formation temperature under different combinations used in the study. As evident from the figure the nucleation temperature for C type Silica was 277.16K and it almost coincided with the nucleation temperature (277.37K) of 100 ppm rhamnolipids containing Silica Gel. However, maximum shift was observed in the presence of C type Silica Gel saturated with distilled water containing 1000 ppm of rhamnolipids.

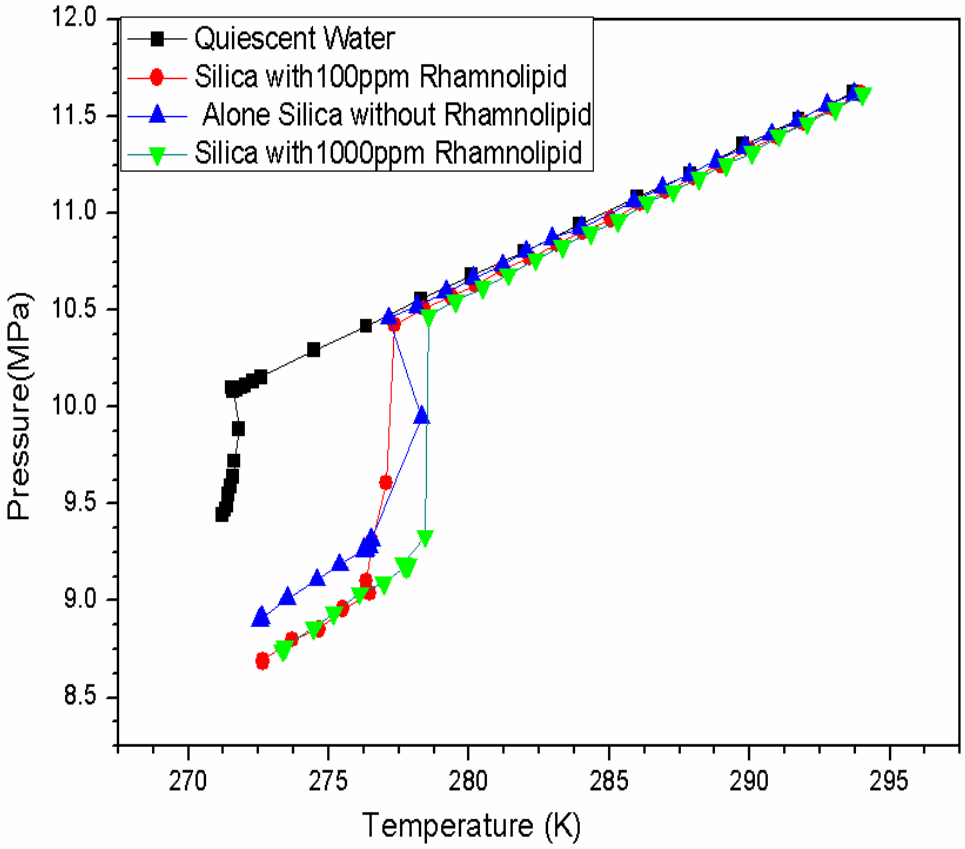

Figure 6.7.4: Comparison of Methane Hydrate Formation nucleation temperature.

6.7.1.3 ***Comparison of phase equilibrium of Methane Hydrate Formation for different Systems***

Figure 6.7.5 shows phase equilibrium of Methane Hydrate at different concentration of rhamnolipids. As evident from the figure the phase equilibrium graphs got shifted to high temperature region in presene of water-Silica Gel system containing rhamnolipids as compared to the water-Silica Gel system without rhamnolipids. However, no significant shift of phase equilibrium curve was observed by varing the concentration of rhamnolipids. This suggests that rhamnolipids thermodynamically promotes the Hydrate Formation shown as per following in Figure 6.7.5.

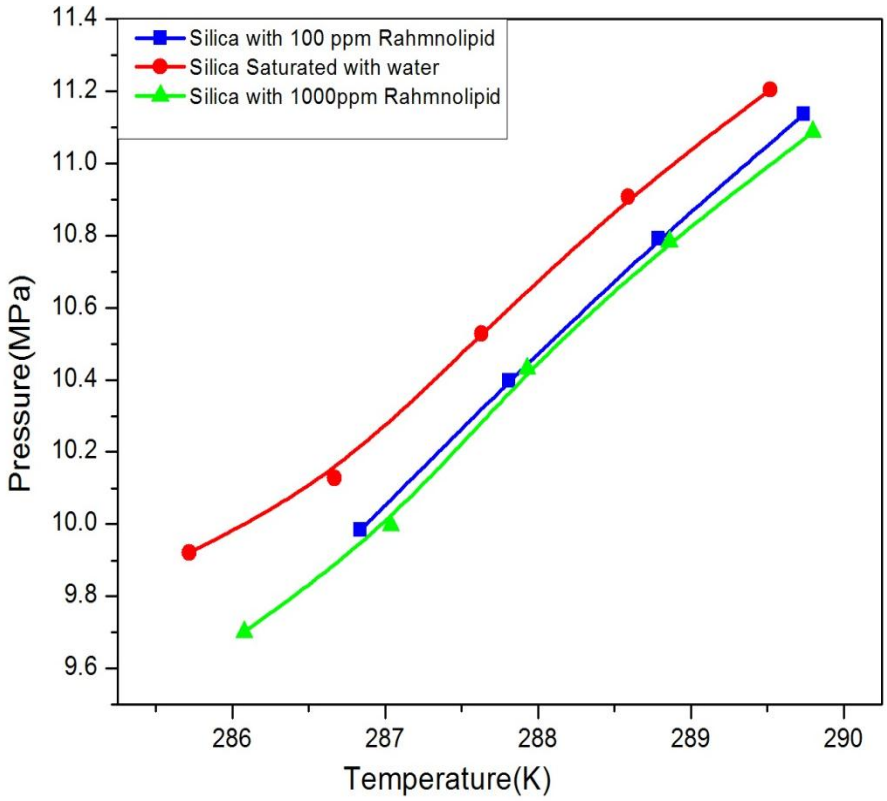

Figure 6.7.5: Comparison of phase equilibrium parameters.

6.7.1.4 *Dissociation enthalpy of Methane Hydrate*

The Dissociation enthalpy data of NGH is very vital for establishing a production scheme. The Dissociation enthalpies of Methane Hydrates in the presence of C type Silica Gel saturated with distilled water containing different concentration of rhamnolipids were calculated via Clausius-Clapeyron equation using equation 3 from annexure and shown in Table 6.7.2 based upon the measured phase equilibrium data. No significant difference was observed in the value of enthalpy of Dissociation in the presence and absence of rhamnolipids, suggesting that the heat required for dissociating Methane Hydrate in presence and absence of rhamnolipids is almost similar. The enthalpy of Dissociation of Methane Hydrates in the C type Silica Gel without rhamnolipids was in the range of 11.8 kJ/ mol to 18.0 kJ/ mol. Under that influence of rhamnolipids enthalpy of Dissociation was observed in the range of 17.2 kJ/ mol to 23.0 kJ/ mol. The Formation and Dissociation of Methane Hydrates can be shown by:

$$CH_4 \cdot nH_2O \leftarrow\rightarrow CH_4\,(g) + nH_2O \qquad (1)$$

Dissociation enthalpies of Gas Hydrates are usually calculated by direct calorimetric measurement and indirectly calculated via the Clapeyron or Clausius-Clapeyron equation by differentiating of phase equilibrium pressure-temperature data. If the system while Dissociation is assumed to be at the state of equilibrium, then temperature-pressure data of the Dissociation period can be used to calculate the enthalpy change of Gas component while Dissociation. Calorimetric method is the most precise method for calculating the heat of Dissociation (H_d) of Hydrate Formation reaction. These experimental measurements are laborious. Other way for finding the heat of Dissociation is by the Clausius-Clapeyron equation.

Several groups [Handa1986, Rueff et al, 1988, Kang et al, 2001, Gupta et al, 2008] have revealed calculation of enthalpy by calorimetric method. Handa et al, (1988) revealed that calorimetric method for calculation of enthalpy is tough because these compounds are stable at high pressures or low temperatures, although the calorimetric measurement is better than the results obtained from phase equilibrium data. It has been observed that the values of enthalpy calculated by Clausius-Clapeyron equation in the present work are close to that calculated by direct measurement method. The data of Dissociation enthalpy of pure Methane Hydrate calculated for various test samples using Clayperon equation is in agreement with the results obtained by other research groups like [Kakati et al, 2014] and presented in Table 6.7.2 as follows:

Table 6.7.2: Equilibrium temperature, pressure and Dissociation enthalpy calculated by Clausius-Clapeyron equation

Type of sample	P (Dissociation) (MPa)	Ln(P) (MPa)	T (dissociat-ion) (K)	1000/T (k^{-1})	Z factor	ΔH_d KJ (mol^{-1})
C-type Silica Gel without presence of Rhamnolipids	9.9215	2.2947102	285.7	3.49993	0.8071	-
	10.128	2.3153434	286.6	3.488332	0.80086	11.84493
	10.528	2.3540659	287.6	3.476689	0.7989	16.96316
	10.907	2.3894515	288.5	3.465124	0.79771	18.05239
	11.203	2.4162691	289.5	3.45137	0.79739	17.54297
C-type Silica Gel containing 100 ppm Rhamnolipids	9.98361	2.3009447	286.8	3.486264	0.8028	-
	10.39729	2.3415452	287.8	3.474514	0.8007	23.003
	10.7903	2.3786476	288.7	3.462724	0.79931	21.93559
	11.13503	2.410096	289.7	3.45137	0.7986	20.76912
C-type Silica Gel containing 1000 ppm Rhamnolipids	9.70092	2.2722207	286.08	3.495526	0.8043	---
	9.9974	2.3023251	287.04	3.483835	0.8044	17.22145
	10.43177	2.344856	287.93	3.473066	0.8007	21.5293
	10.7834	2.3780079	288.86	3.461885	0.7995	20.90218
	11.08677	2.4057525	289.8	3.450656	0.7992	19.77393

The (P, T) data of equilibrium are plotted as lnP vs 1000/T and shown in Figure 6.7.6.

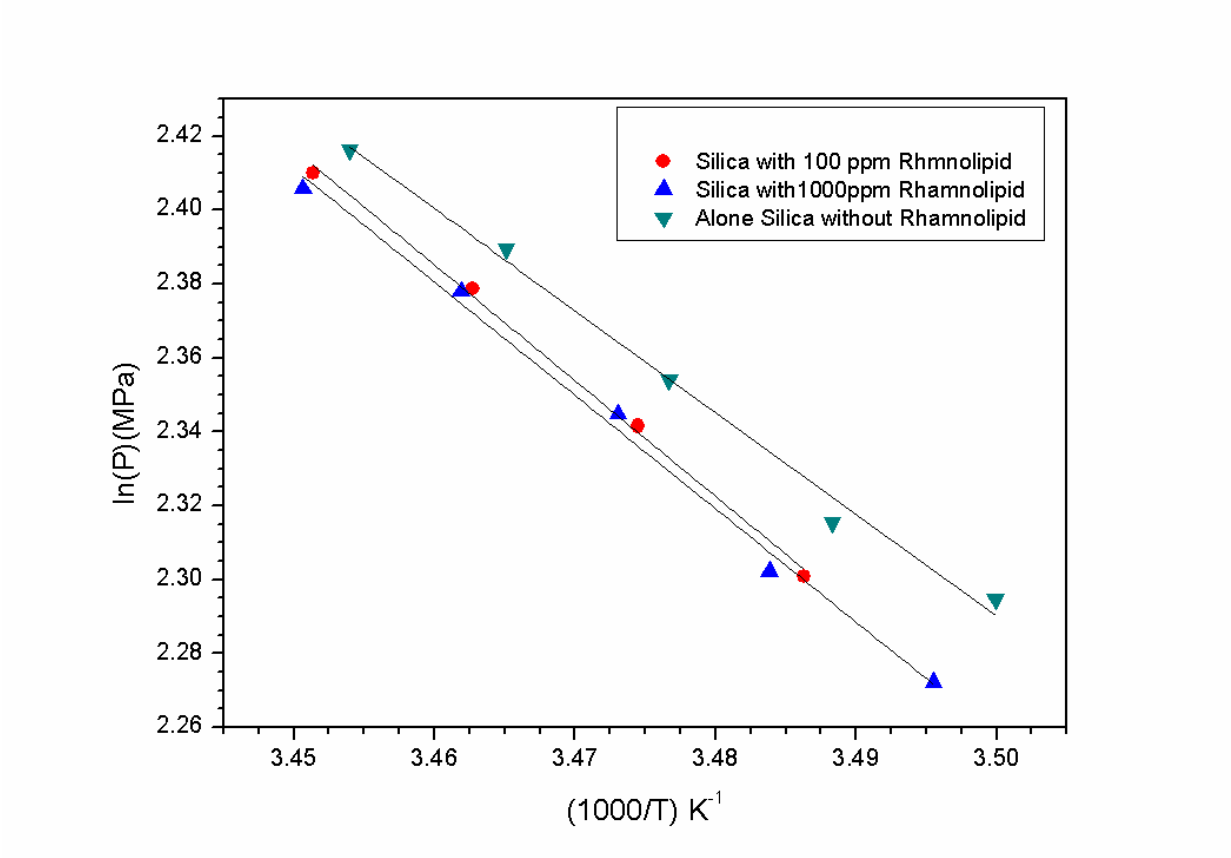

Figure 6.7.6: The (P, T) data of equilibrium are plotted as lnP vs 1000/T.

As can be observed from Figure 6.7.6, lnP vs 1000/T shows a good linear relation. The phase equilibrium pressure rises with rise in temperature.

6.7.2 *Kinetic Study*

The kinetic of Methane Hydrate Formation for various experimental condition is as explained below:

6.7.2.1 *Induction Time*

The induction time t_i, is the time elapsed from the beginning of the experiment at t_s to the commencement of Hydrate Formation t_o and it is one of the kinetic parameter of Hydrate Formation. Various groups [Kashchiev et al, 1991, Kashchiev et al, 2003] have given different definitions of the induction time. A temperature spike is seen as the latent heat is released

because of Gas Hydrate Formation [Karaaslan et al, 2002] which is shown in figures 6.7.7 to figure 6.7.10. During Hydrate growth, the temperature rises to the highest value and then it slowed down to the original temperature. Initially, the Gas and water molecules are in complete disorder. When crystallization process begins the molecules reorder themselves into orderly crystal structure of Gas Hydrate. During this process, a lot of heat is generated which leads to rapid rise in the temperature of the cell, since crystallization is an exothermic process [Handa et al, 1986]. The induction time for various experimental conditions is as shown in table 6.7.3 and from figures 6.7.7 to figure 6.7.10 as follows.

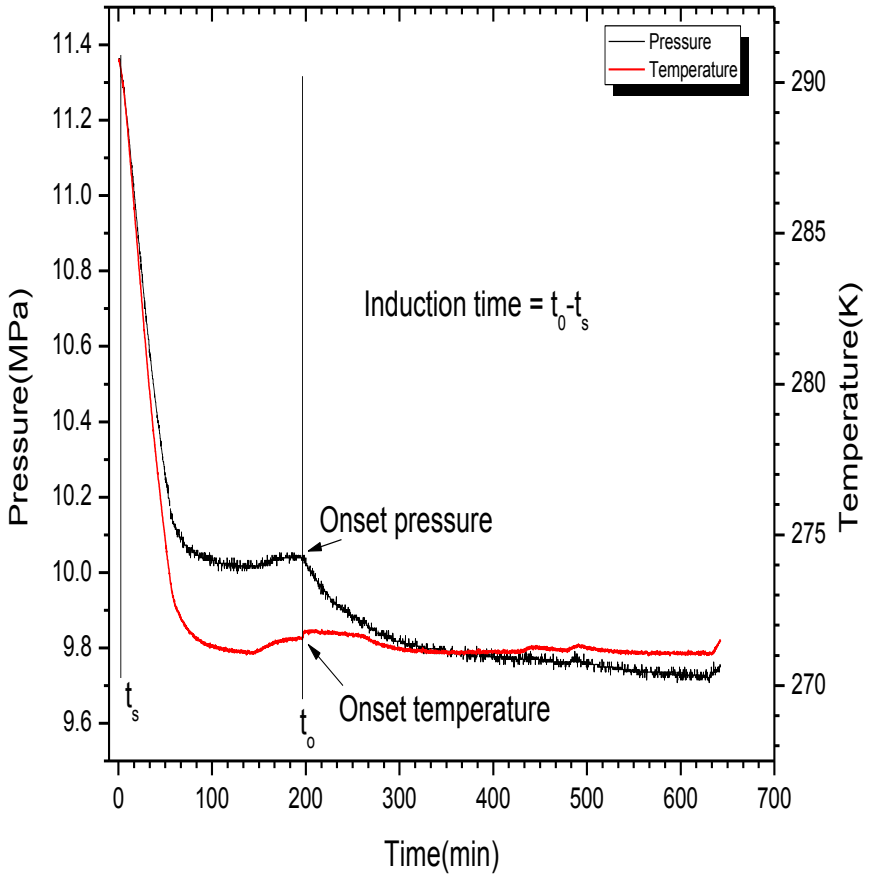

Figure 6.7.7: Induction Time for Methane Hydrate Formation in quiescent water.

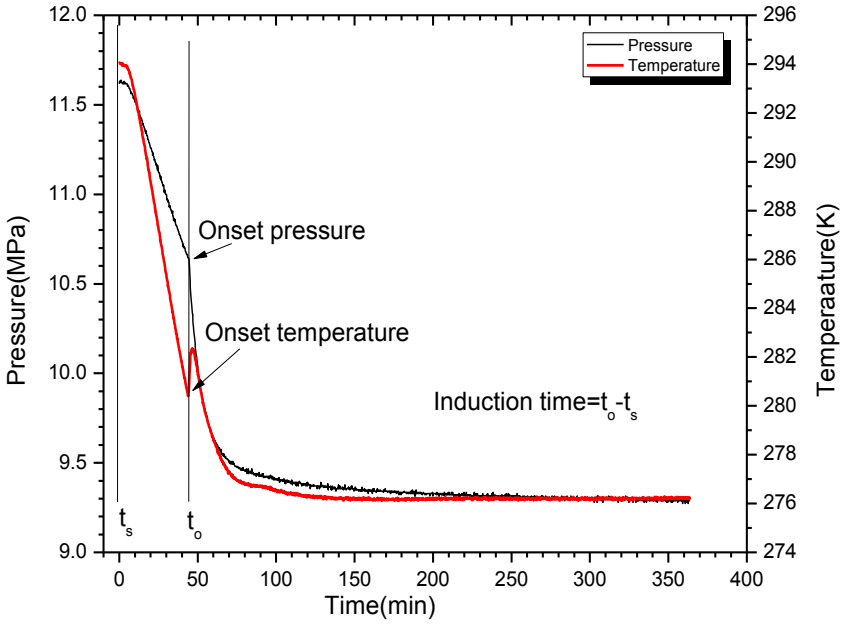

Figure 6.7.8: Induction Time for Methane Hydrate Formation in C-type Silica Gel (Merck).

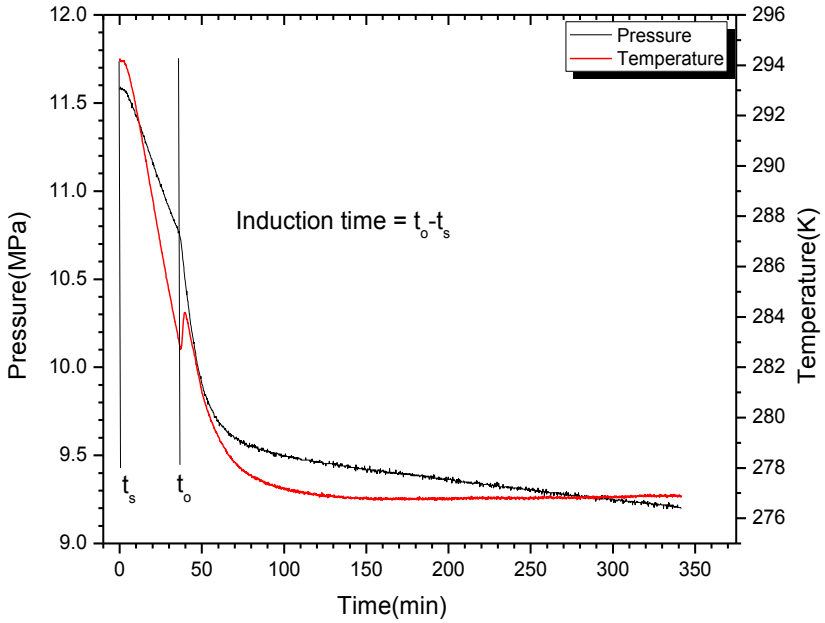

Figure 6.7.9: Induction Time for Methane Hydrate Formation in C-type Silica Gel (Merck) containing 100 ppm Rhamnolipids.

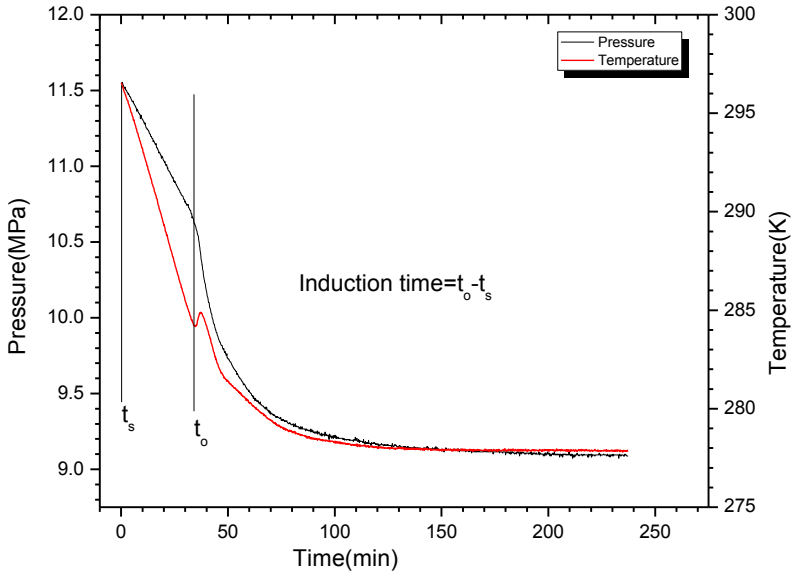

Figure 6.7.10: Induction Time for Methane Hydrate Formation in C-type Silica Gel (Merck) containing 1000 ppm Rhamnolipids.

The measured induction time of Methane Hydrate Formation in occurrence of different concentration of rhamnolipids is given in Table 6.7.3. It is noticed that the induction time of Hydrate Formation is reduced in presence of Rhamnolipids. However there is not much effect on increasing the concentration of rhamnolipids on induction time as shown in Table 6.7.3 and from Figures 6.7.7 to Figure 6.7.10.

Table 6.7.3: Induction time for various experiments

Type of sample	Experiments conducted at Sub-cooling (°C)	Induction Time (min.)
Quiescent water	17.61	196.70
C-type Silica Gel (Merck) without presence of surfactant	13.36	44.24

C-type Silica Gel (Merck) containing 100 ppm Rhamnolipids	12.98	36.91
C-type Silica Gel (Merck) containing 1000 ppm Rhamnolipids	12.01	34.23

A specific amount of time is required to start Hydrate nucleation when constituents which form the Hydrates are placed in appropriate temperature and pressure region. The induction time is found by calculating the time system takes to reach the Hydrate onset temperature (where detectable volume of Hydrate is observed). The induction time of Hydrate Formation was calculated in quiescent water system and in C type Silica Gel consisting of different concentration of rhamnolipids. During Hydrate Formation initially there was a gradual decrease in pressure with temperature before Hydrate Formation started. Afterwards a sharp peak is seen due to sudden rise in temperature with simultaneous decrease in pressure confirming Hydrate Formation. The difference of Hydrate onset time and the time of start of experiment is the induction time of Hydrate Formation.

Substituting synthetic surfactants with microbial surfactants for enhancing Gas Hydrate generation can make the process environment compatible. The C type Silica Gel having mesh size of 230-400 has been reported to perform better than A type and B type Silica Gel (60– 120 and 100–200 mesh respectively) for CO_2 clathrate Formation [Kumar et al, 2013]. In the present study the rhamnolipids produced by A11 was used for promoting Formation of Methane Hydrate in fixed bed system consisting of C type Silica Gel.

The induction time in Methane Hydrate crystallization is a significant kinetics parameter. According to Volmer (1939) induction time of Gas Hydrate Formation is the appearance of very first Hydrate cluster of super -nucleus size capable of spontaneously outgrowing to a macroscopic size [Volmer et al, 1939]. Certain promoters can decrease the induction time which is desirable as it will decrease the time required for growing Methane Hydrate crystal and thus, hastening the crystal growth [Wang et al, 2012]. In present work Gas uptake studies were carried out to measure the induction time of Methane Hydrate Formation at suitable temperature and pressure condition conducive for Hydrate Formation and growth. Figures 6.7.7 to 6.7.10 measures the variation of pressure and temperature during measurement of induction time. As expected the pressure of the system decreased with temperature drop. A rapid decrease in pressure and simultaneous sharp increase in temperature indicates Hydrate nucleation event

during a Gas uptake measurement. The difference of Hydrate nucleation time and the time of start of experiment is the induction time. A temperature spike observed in figures 6.7.7 to figure 6.7.10 may be attributed to the latent heat released as an outcome of the Methane Hydrate Formation. In present study, saturated C type Silica Gel with 1000 ppm aqueous solution of rhamnolipids shortened induction time significantly. Among all the tested conditions the longest induction time was observed in quiescent water system.

6.7.2.2 *Moles of Methane consumed*

The amount of Gas consumed is calculated by using equation 1 & 2 from annexure.

The pattern of Gas consumed during Formation of Hydrate is shown in Figure 6.7.11. It can be observed that the amount of Gas consumed is much more in presence of 1000ppm Rhamnolipids.

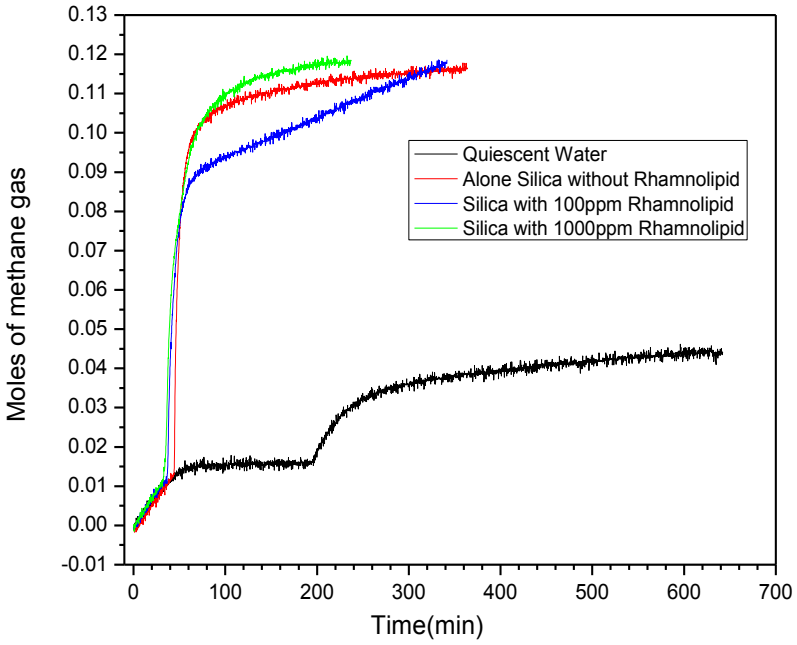

Figure 6.7.11: Moles of Methane consumed while Methane Hydrate Formation for various experimental conditions.

6.7.2.3 *Moles of Methane consumed per mole of water*

The amount of Gas consumed is calculated by using equation 1 & 2 from annexure.

Figure 6.7.12 displays the Gas uptake measurement graph (moles of Methane consumed per mole of water in the system) of a Methane Hydrate Formation experiment. The general characteristic of Methane uptake curve in quiescent water does not look like that of Hydrate Formation in Silica system saturated with water or water-rhamnolipids solution. As compared to quiescent water system the number of moles of Methane consumed per water molecule was significantly more in Silica system. There was nearly 2.6 times more Methane Gas consumption in Silica system saturated with water. Presence of rhamnolipids in the Silica system further increased Methane Gas consumption per water molecule during Methane Hydrates Formation.

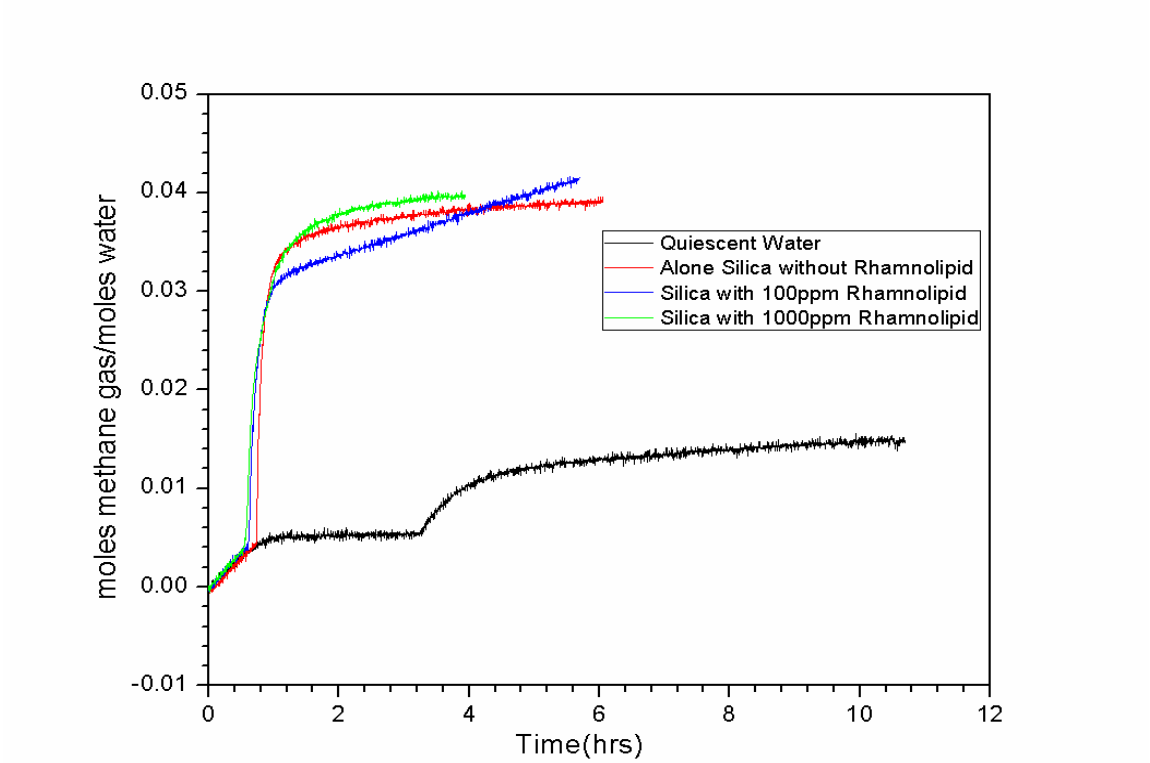

Figure 6.7.12: Moles of Methane/Moles of Water consumed while Methane Hydrate Formation takes place for various experimental runs.

6.7.2.4 *The growth curve of Methane Hydrate Formation for different Systems*

Figure 6.7.13 to Figure 6.7.16 shows Gas consumed and pressure drop as a function of time. The growth and Gas consumption region exhibits the two symmetric plots that could be explained as conservation of mass during the Hydrate growth. Number of Methane molecules leaving the Gas

phase to Hydrate phase is shown by the pressure drop, whereas the number of Methane molecules entering in the Hydrate cages is shown by the Gas consumption plot. As mass must be conserved in an isochoric system, the two plots are showing symmetry about an axis passing through the intersection of the two plots and parallel to the time axis. As shown in Figure 6.7.13-6.7.16, the process is divided into five regions. First region is started at time zero where the consumption of the Gas is less in the system and pressure slightly decreases due to dissolution of Gas. Second region is after the induction time where Gas consumption increases, this can be explained because of the Hydrate growth. From the third region to fifth region, as the Hydrate is formed, consumption of Gas is as shown in figure 6.7.13-6.7.16.

Figure 6.7.13-6.7.16 demonstrate plot of Methane consumed with respect to pressure and time during Formation of Hydrate. In all the experimental runs, there is a linear relation in the beginning and then the kinetic curve flattens in the growth stage as the pressure becomes constant due to very minute change in Gas consumption. Methane Hydrate Formation was accompanied by increase in the moles of Methane consumed and subsequent reduction in pressure (Fig. 6.7.13-6.7.16). Most rapid increase in Methane consumption was observed in C type Silica Gel saturated with 1000 ppm rhamnolipids solution whereas most slow Methane consumption was observed in quiescent system. Gas consumed during Methane Hydrate generation gets trapped into cages like lattice structure of water molecule. Such structures are formed by water under high pressure and low temperature [Sloan et al, 1998]. For a quiescent system, Gas Hydrates larGely begin to crystallize at the Gas-liquid interface but not in the bulk phase of water. Thus, nucleation and growth takes place in the liquid film at the Gas liquid-interface only. This results in slow Formation of Hydrate in a non-stirring setup as thin film of Hydrate gets formed on water surface, prevents mass transfer across the film subsequently slowing kinetics and lowering water to Hydrate transformation [Kumar et al, 2013]. It has been shown that the impeding Hydrate film Formation does not form if surfactants are added to the aqueous phase and agitation is used in the system [Kumar et al, 2013, Carvajal et al, 2013]. It is expected from a Hydrate promoting agent that it will enhance the solubility of Hydrate forming Gas in water. Use of surfactant above the CMC is expected to increase the solubility of Hydrate forming Gas, while at the surfactant concentration below or around the CMC, the Gas solubility remains similar to that of pure water [Rogers et al, 2003]. Carvajal et al, 2013 reported that overall, consumption of Methane was more in biosurfactant and biosurfactant–smectite

experiments system than smectite–clay experiments. Zhong et al, 2000 reported that there is a rise in consumption of ethane when Hydrates were formed from solutions containing 284 ppm synthetic surfactant i.e sodium dodecyl sulphate.

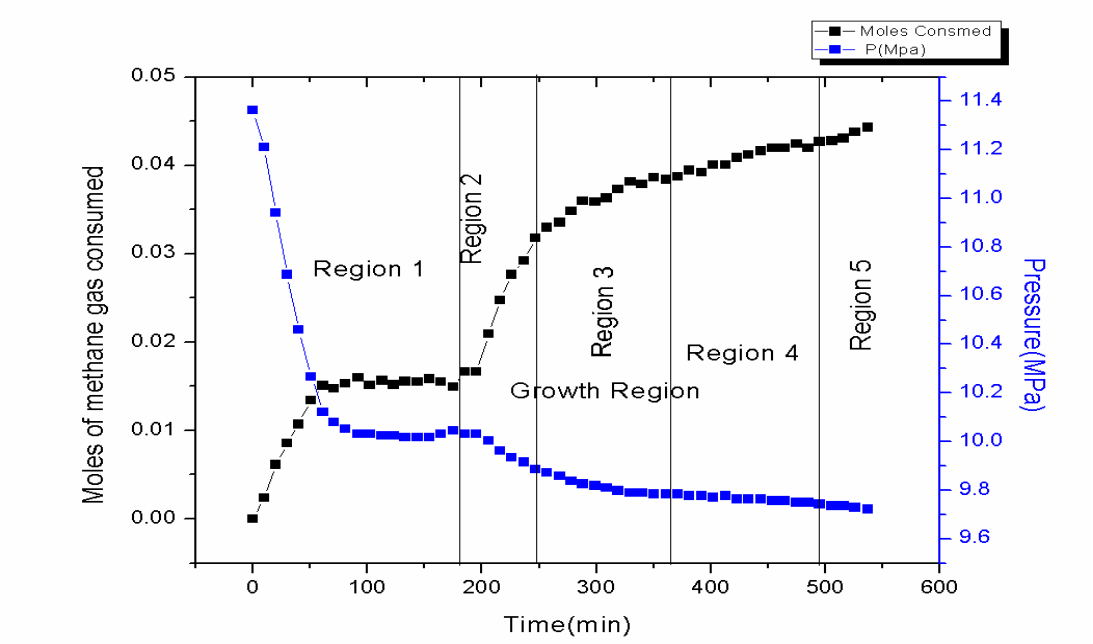

Figure 6.7.13: The growth curve of Methane Hydrate Formation for Quiescent water.

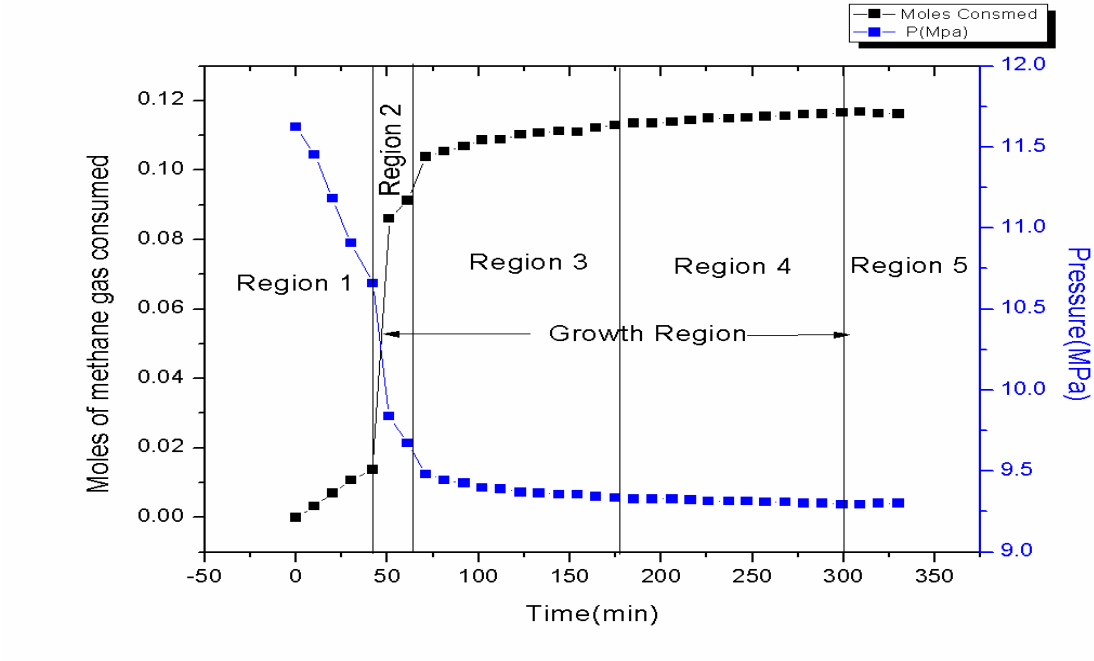

Figure 6.7.14: The growth curve of Methane Hydrate Formation in presence of C- type Silica Gel.

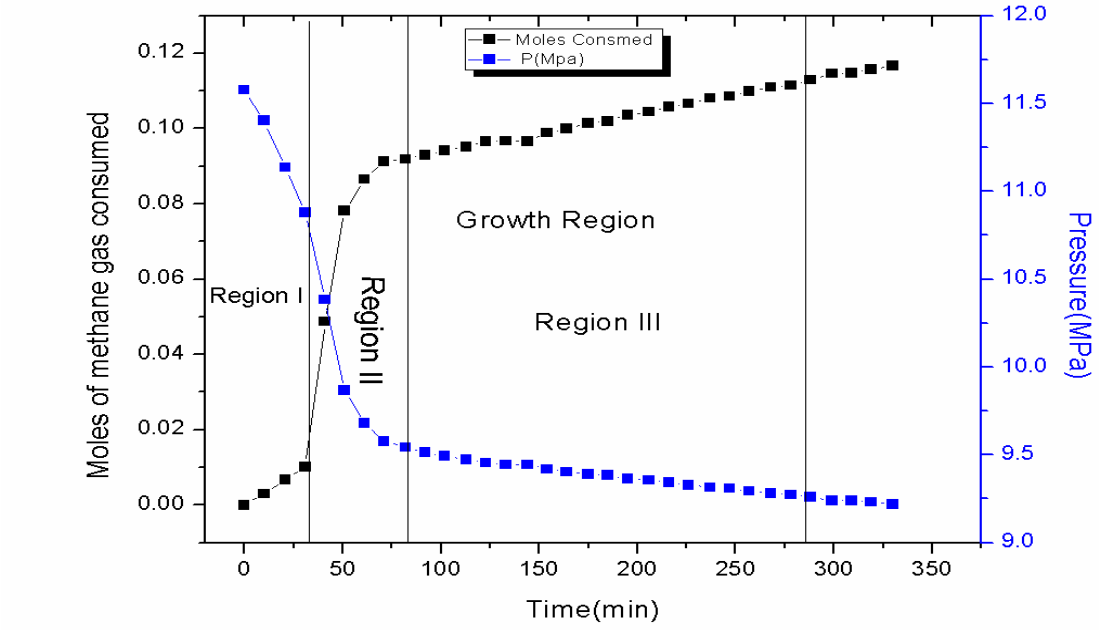

Figure 6.7.15: Growth curve of Methane Hydrate Formation in C- type Silica Gel in presence of 100 ppm Rhamnolipids.

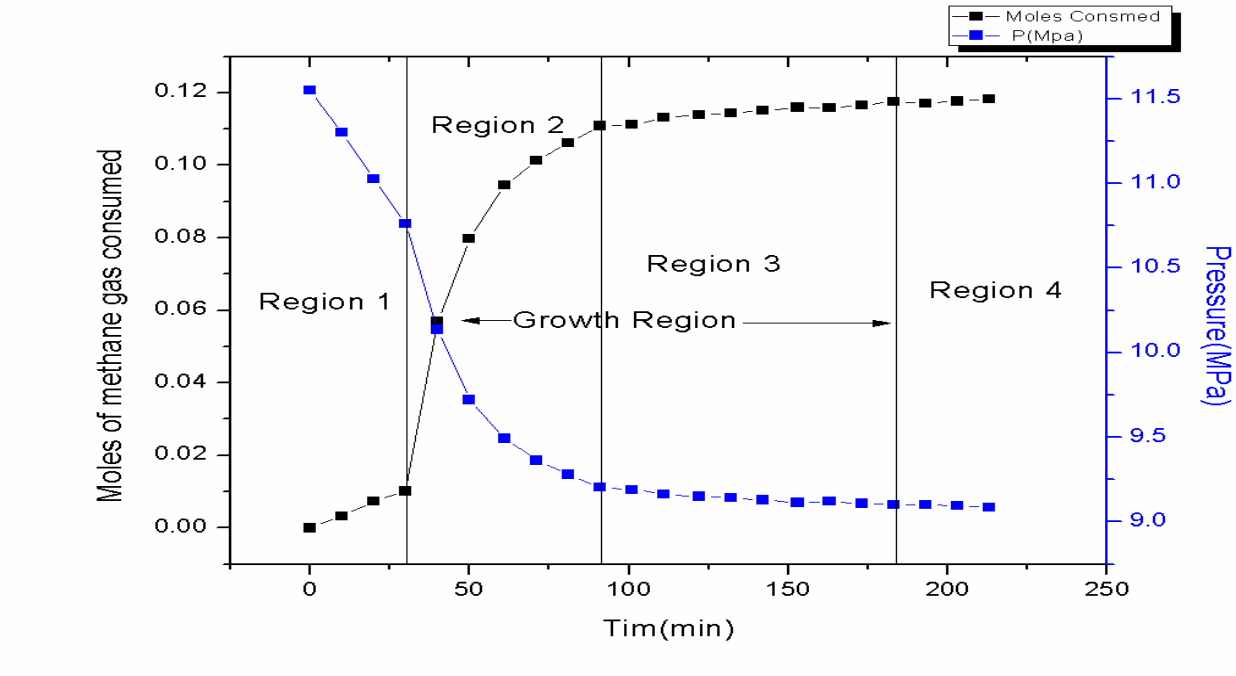

Figure 6.7.16: The growth curve of Methane Hydrate Formation in C- type Silica Gel containing 1000 ppm Rhamnolipids.

6.7.2.5 ***The rate of Methane Hydrate Formation for different experimental conditions***

As seen from Figures 6.7.17, 6.7.19, 6.7.21, 6.7.23, the slope of the curves after nucleation shows an exponential behaviour from which it can be assumed that it is a first order reaction. A first order reaction is defined by the equation 4 from annexure.

The rate constant (k) of Hydrate Formation can be obtained from the slope of the curve of ln (N/N_0) vs time using equation 5 from annexure. The Hydrate Formation from region 2 onwards Figure 6.7.13, 6.7.14, 6.7.15, 6.7.16 was divided into five zones of time as shown in Figure 6.7.18, 6.7.20, 6.7.22, 6.7.24 (0-20, 20-40, 40-80, 80-160, 160-260 min.) after nucleation. This may be because of different rate of Hydrate Formation which gives different reaction rate and hence different rate constant. The data of these five zones are used to calculate the rate constant of Hydrate Formation in each zone. The Formation rate is usually considered by the rate by which the amount of Methane molecule is converted to Hydrate [Hussain, 2006]. Hydrate Formation rate is calculated by putting the values of slopes i.e. rate constant k calculated from figures 6.7.18, 6.7.20, 6.7.22, 6.7.24 using equation 6 from annexure.

Figures 6.7.18, 6.7.20, 6.7.22, and 6.7.24 show change in moles of Methane during Hydrate Formation. Hydrate growth phase in Figure 6.7.18, 6.7.20, 6.7.22, 6.7.24 is divided into five zones (0-20, 20-40, 40-80, 80-160, 160-260 min.) after nucleation. The Gas uptake data of these five zones are used to calculate the rate constant of Hydrate Formation in each zone. The Formation rate is usually considered by the rate by which the amount of Methane molecule is converted to Hydrate [Hussain et al, 2006]. The number of moles Methane consumed in presence of rhamnolipid in present study at 1000 ppm is 9.70×10^{-7} mole/sec as shown in table 6.7.4 which is more than its synthetic counter parts (nonylphenol ethoxalate, quaternary ammonium salt and linear alkyl benzene sulfonic acid) at 1000 ppm for Natural Gas containing 89.47% Methane [Karaaslan et al, 2000].

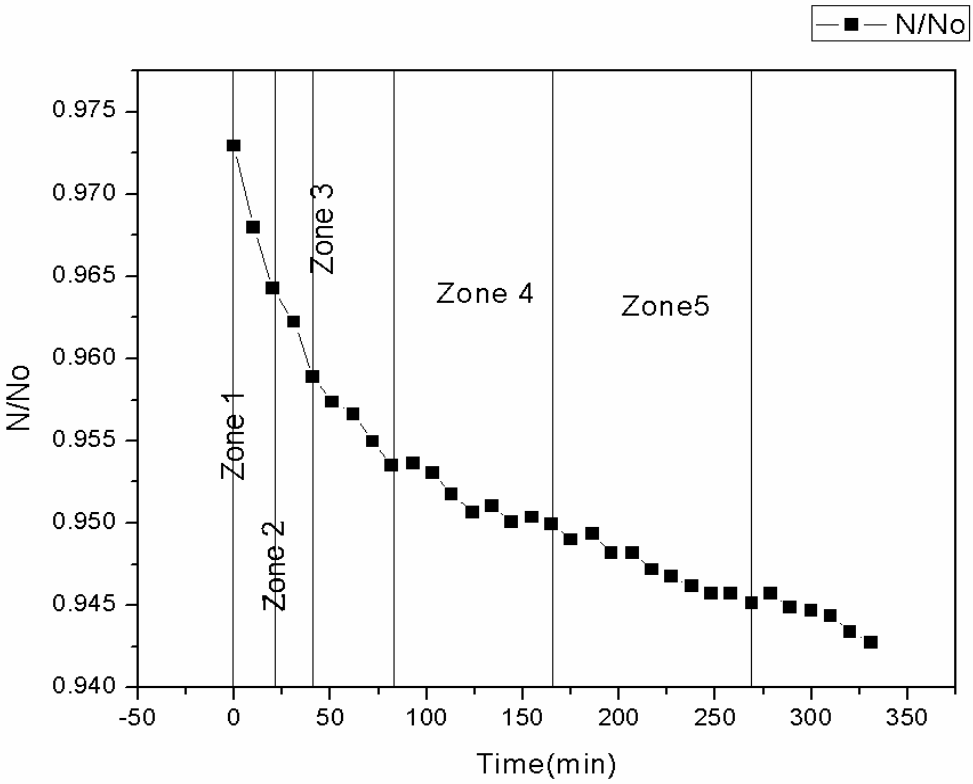

Figure 6.7.17: N/No vs Time Plot for Methane Hydride Formation with quiescent water.

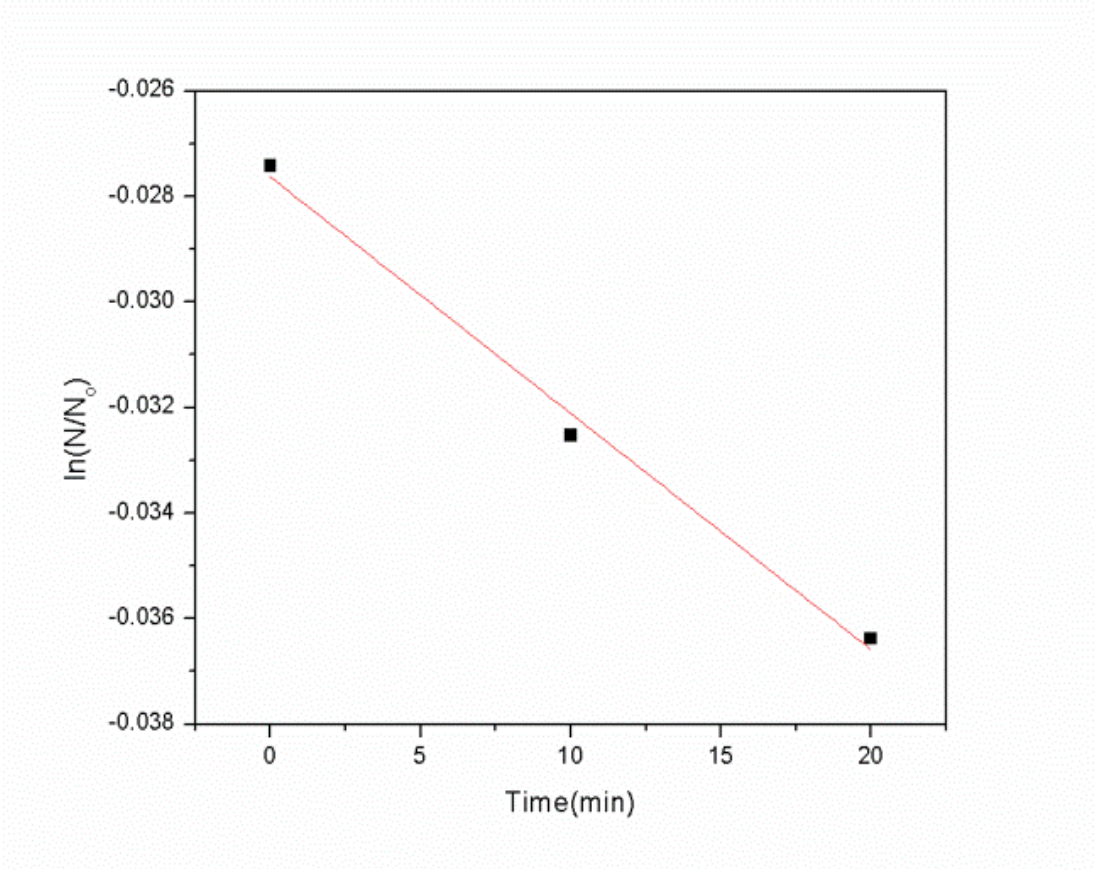
-0.026
-0.028
-0.030
-0.032
-0.034
-0.036
-0.038
ln(N/N$_o$)
0
5
10
15
20
Time(min)

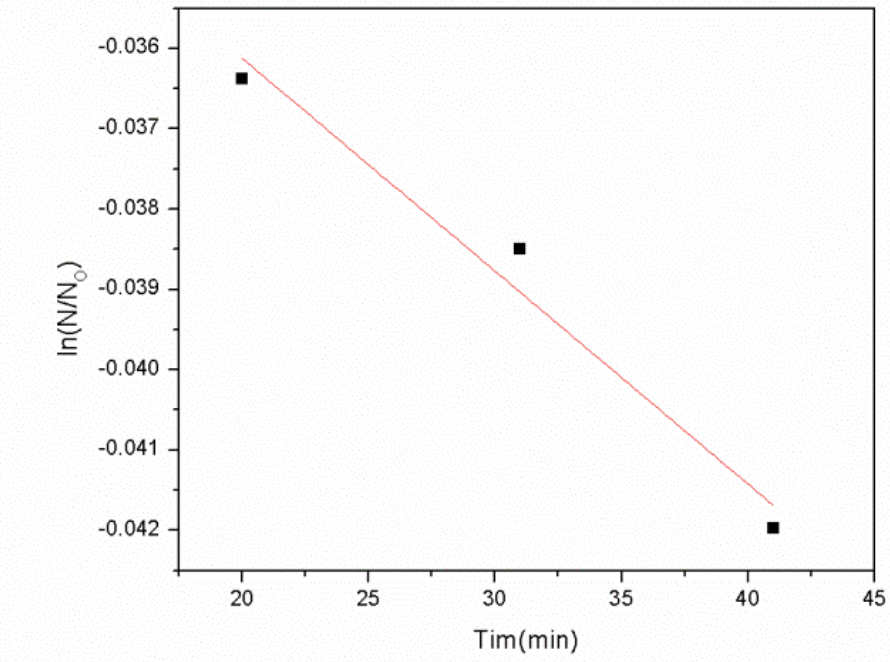
-0.036
-0.037
-0.038
-0.039
-0.040
-0.041
-0.042
ln(N/N$_o$)
20
25
30
35
40
45
Tim(min)

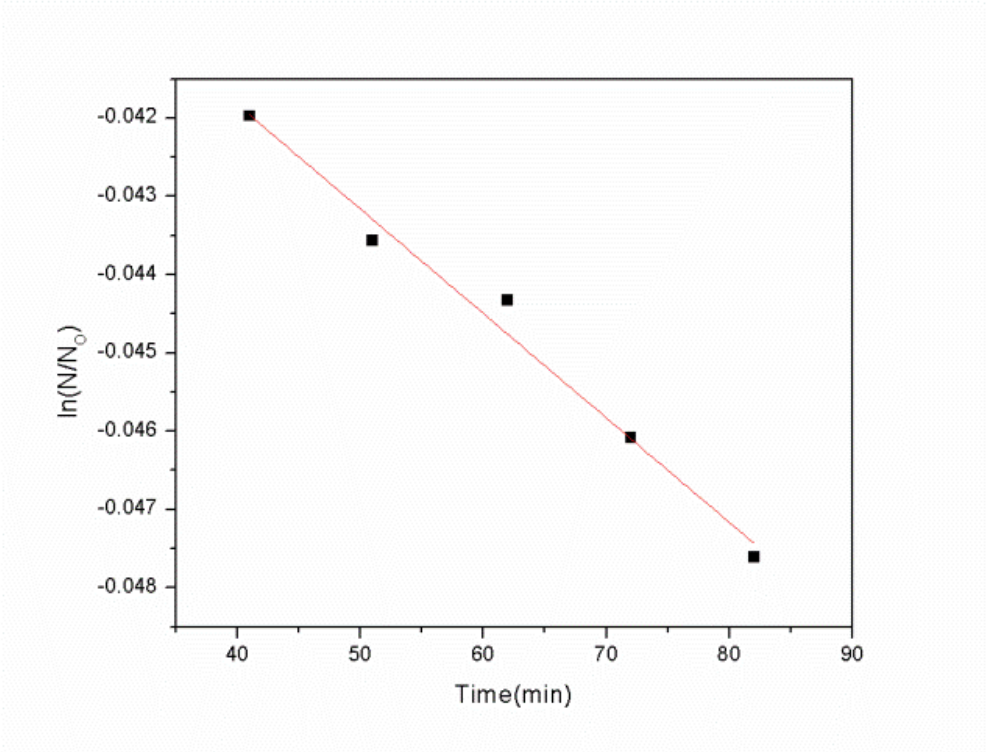
-0.042
-0.043
-0.044
-0.045
-0.046
-0.047
-0.048
ln(N/N$_O$)
40
50
60
70
80
90
Time(min)

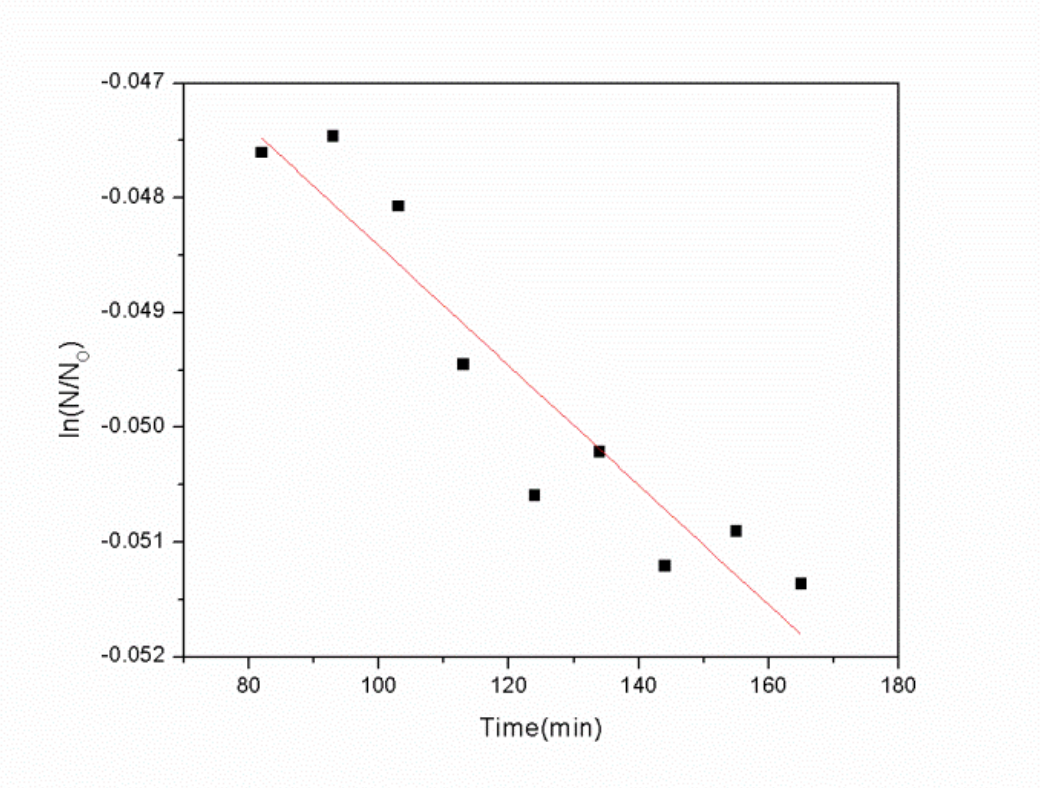
-0.047
-0.048
-0.049
-0.050
-0.051
-0.052
ln(N/N$_O$)
80
100
120
140
160
180
Time(min)

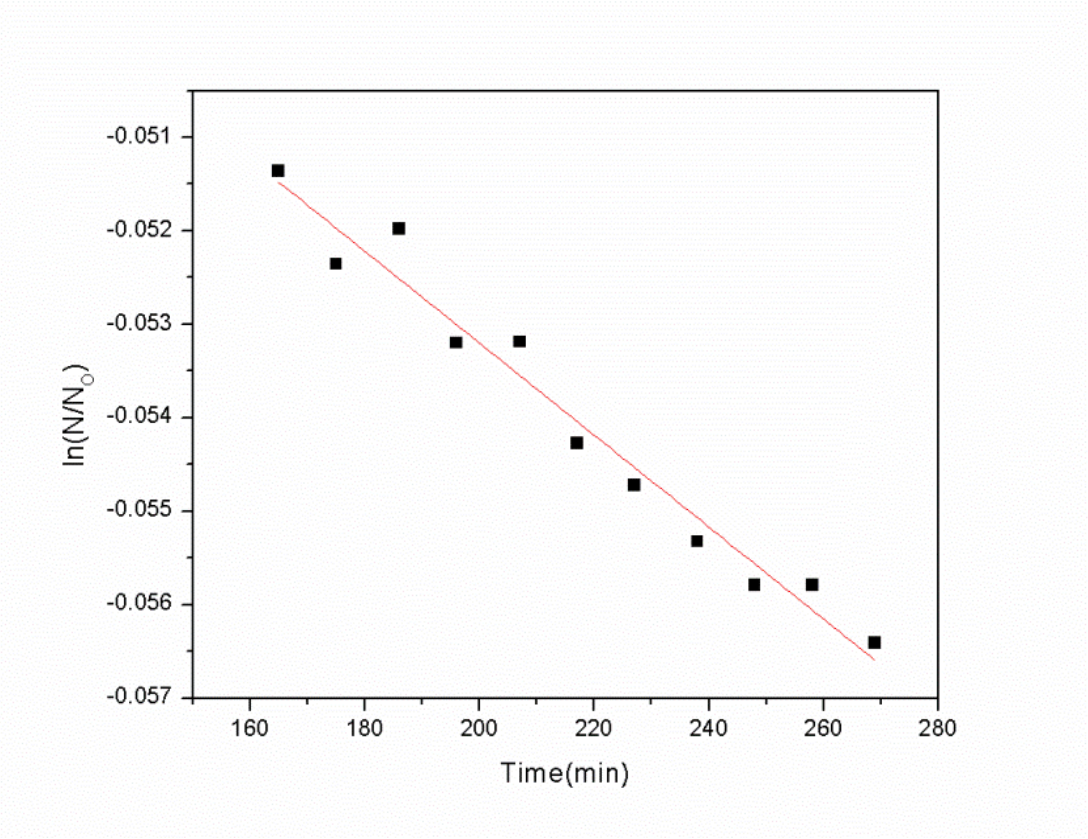

Figure 6.7.18: Semi-logarithmic plot of change of moles of Gas while Methane Hydrate Formation with quiescent water

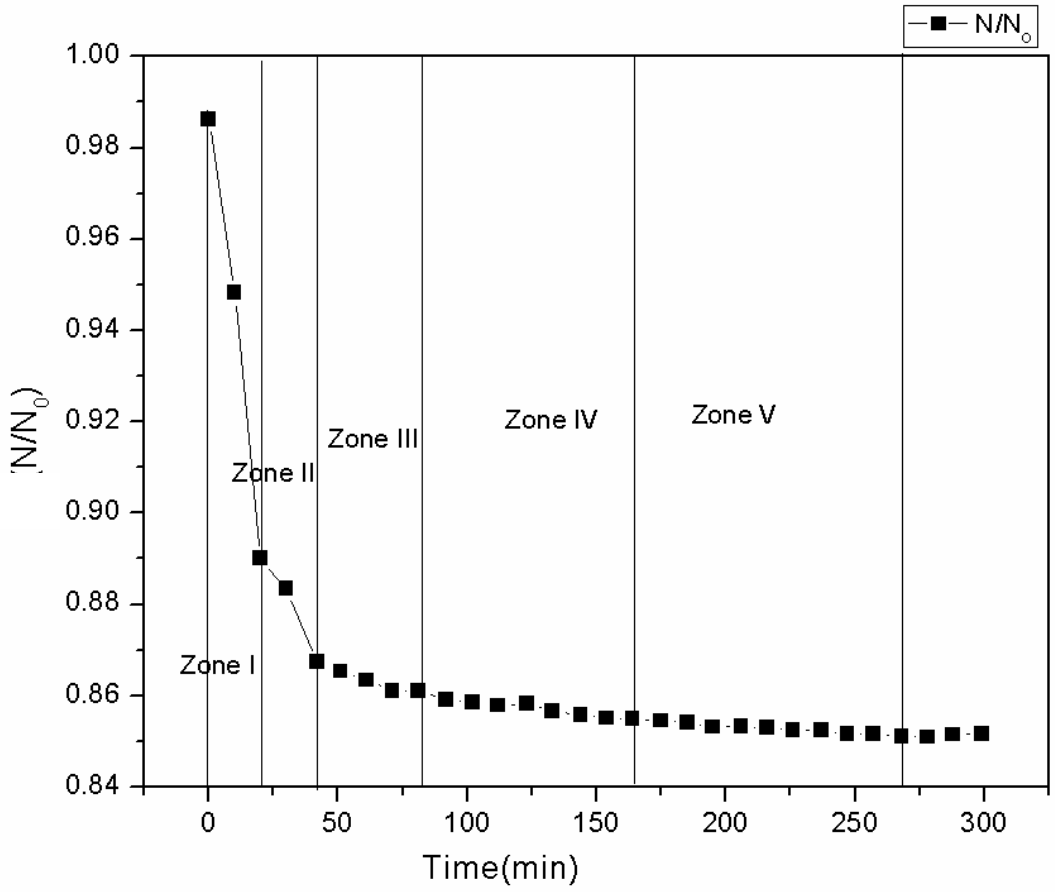

Figure 6.7.19: N/N0 vs Time Plot for Methane Hydrate Formation in presence of C- type Silica Gel.

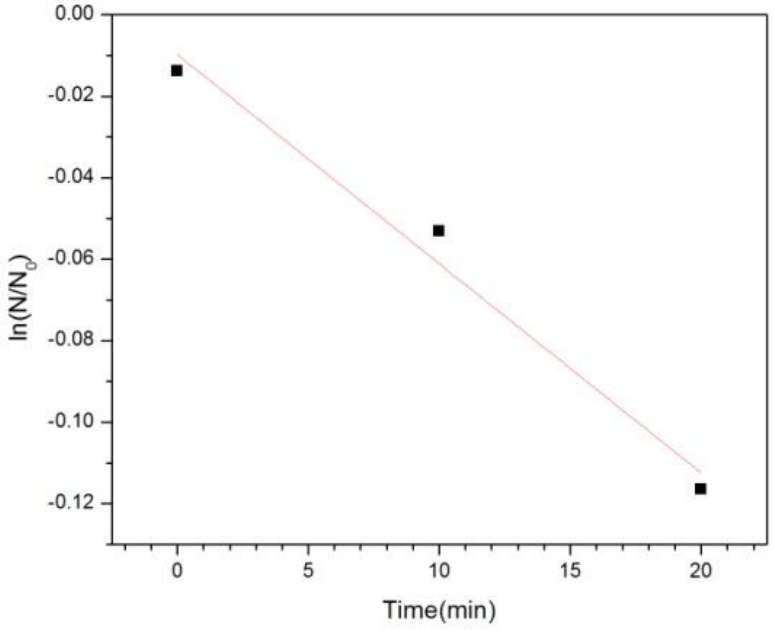
0.00
-0.02
-0.04
-0.06
-0.08
-0.10
-0.12
ln(N/N0)
0
5
10
15
20
Time(min)

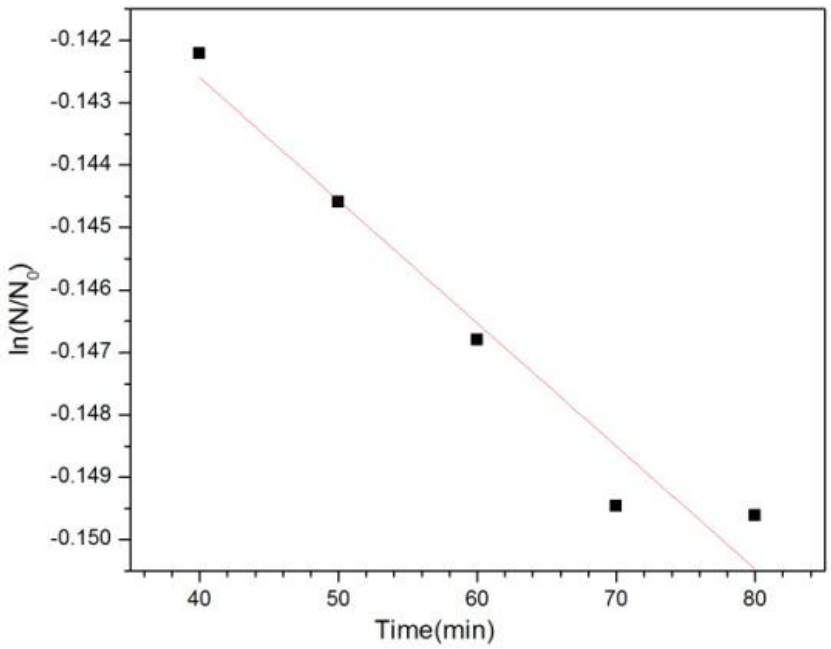
-0.142
-0.143
-0.144
-0.145
-0.146
-0.147
-0.148
-0.149
-0.150
ln(N/N0)
40
50
60
70
80
Time(min)

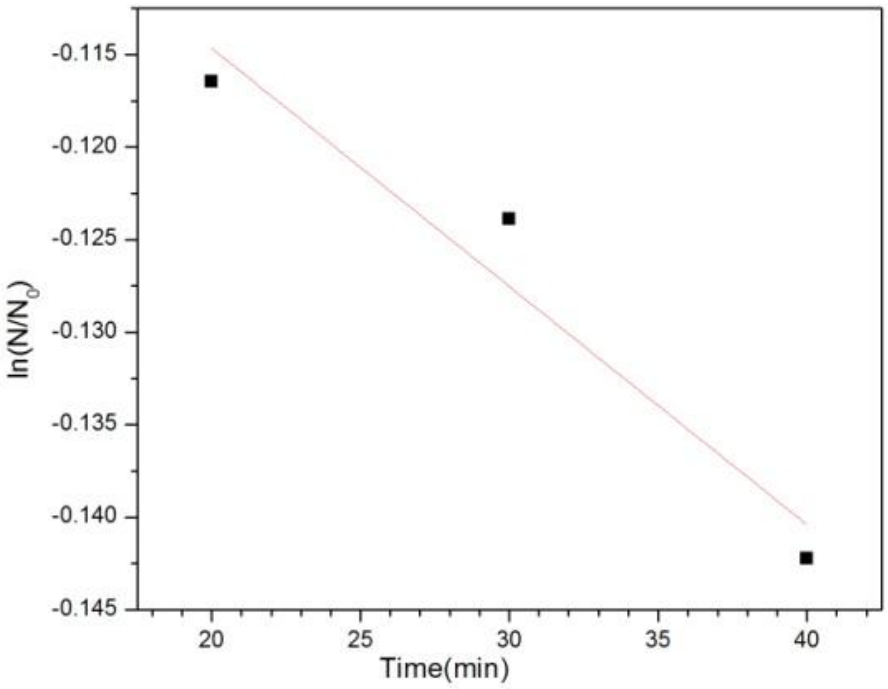
-0.115
-0.120
-0.125
-0.130
-0.135
-0.140
-0.145
ln(N/N0)
20
25
30
35
40
Time(min)

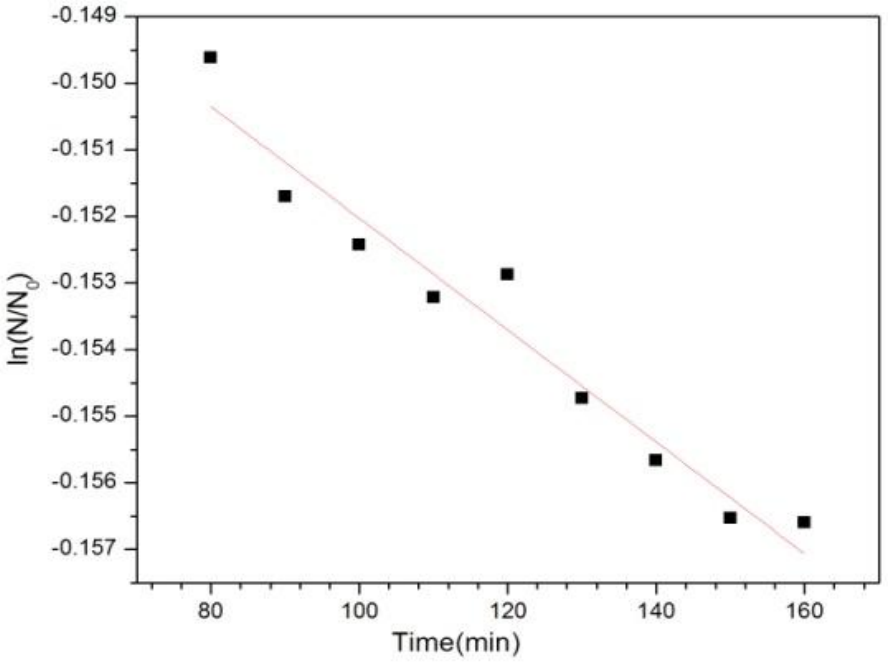
-0.149
-0.150
-0.151
-0.152
-0.153
-0.154
-0.155
-0.156
-0.157
ln(N/N0)
80
100
120
140
160
Time(min)

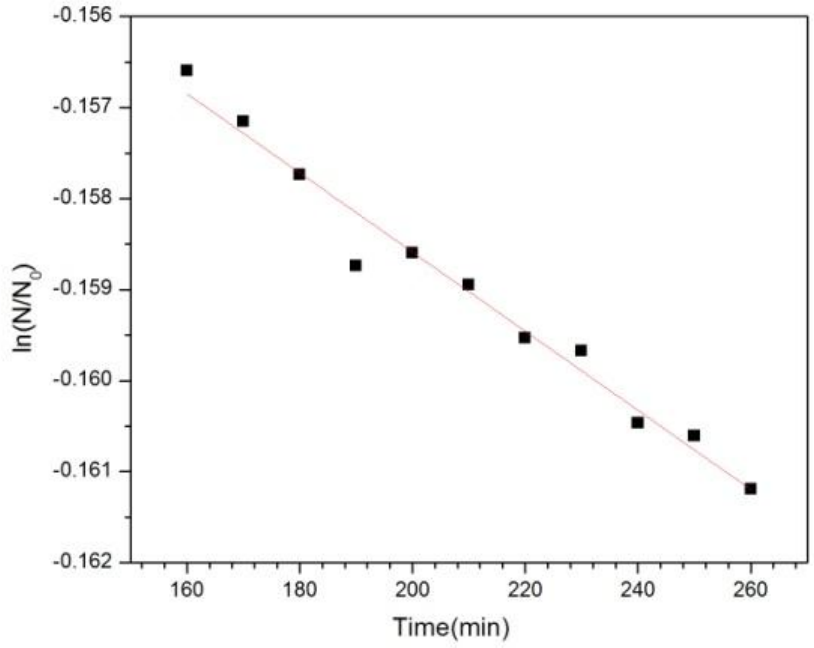

Figure 6.7.20: Semi-logarithmic plot of change of moles of Gas while Methane Hydrate Formation in presence of C-type Silica Gel.

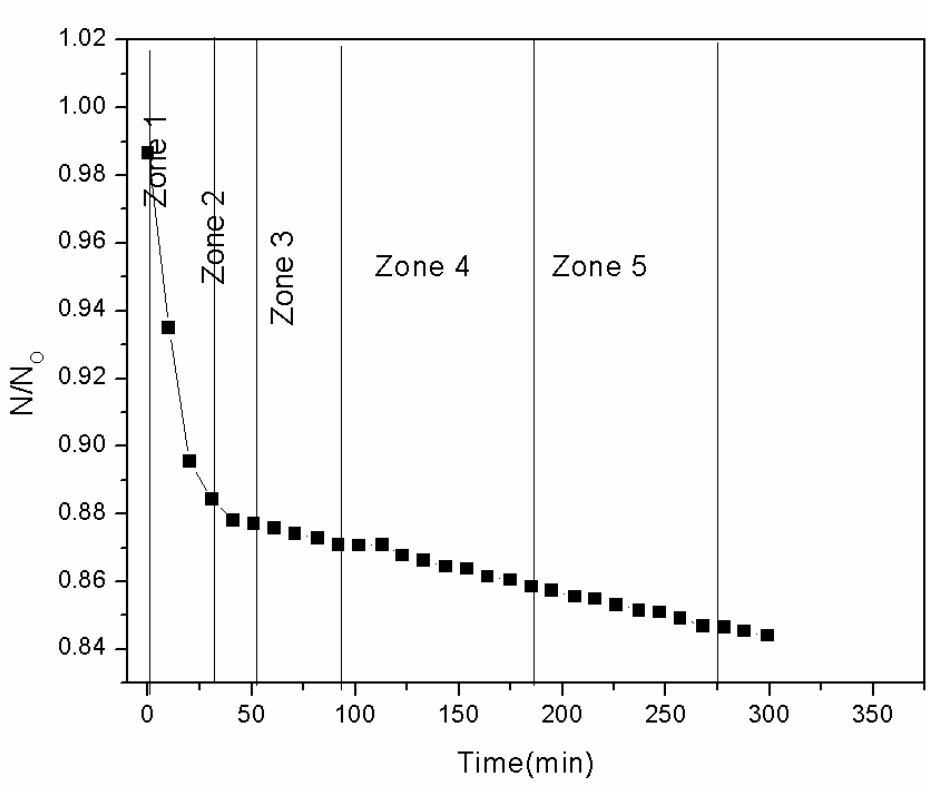

Figure 6.7.21: N/N_0 vs Time Plot for Methane Hydrate Formation in presence of C- type Silica Gel containing 100 ppm Rhamnolipids.

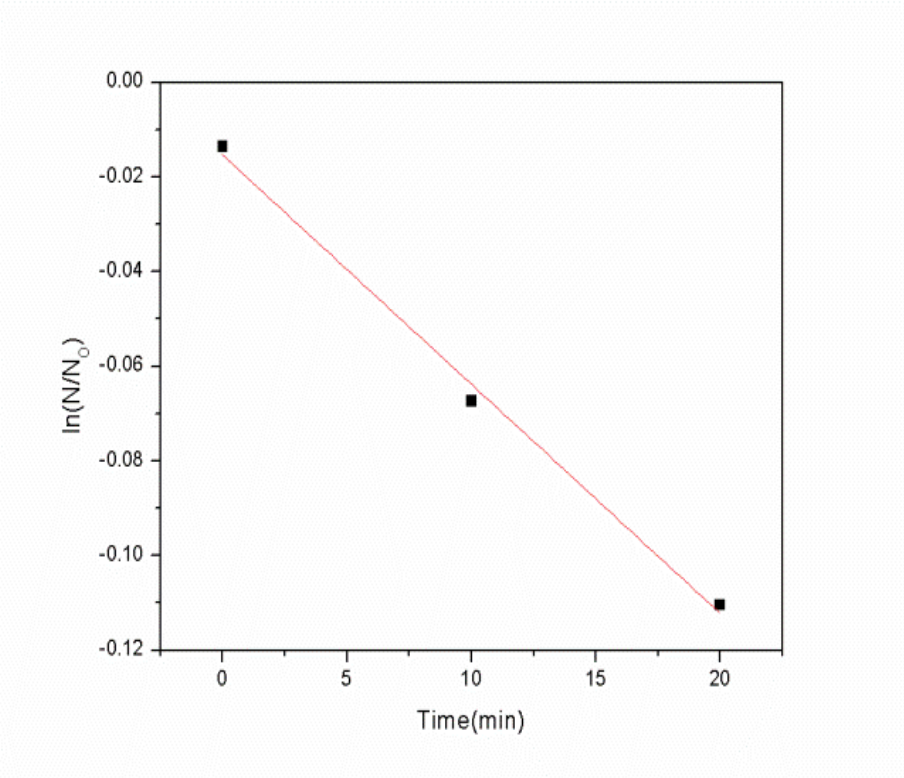
0.00
-0.02
-0.04
-0.06
-0.08
-0.10
-0.12
ln(N/N$_O$)
0
5
10
15
20
Time(min)

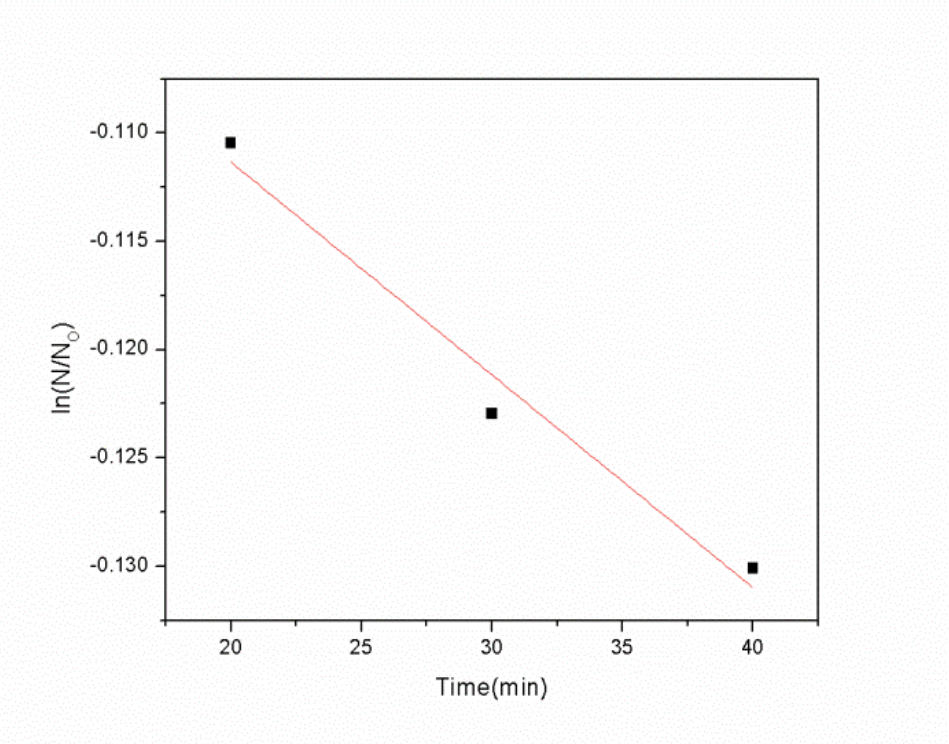
-0.110
-0.115
-0.120
-0.125
-0.130
ln(N/N$_O$)
20
25
30
35
40
Time(min)

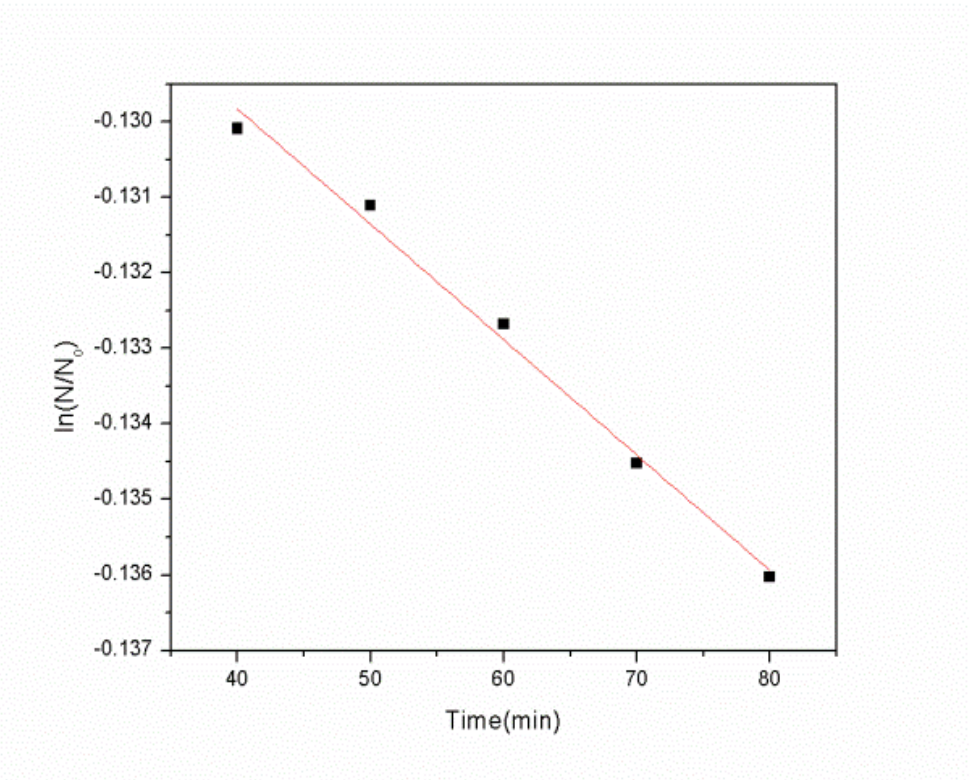
-0.130
-0.131
-0.132
-0.133
-0.134
-0.135
-0.136
-0.137
ln(N/N0)
40
50
60
70
80
Time(min)

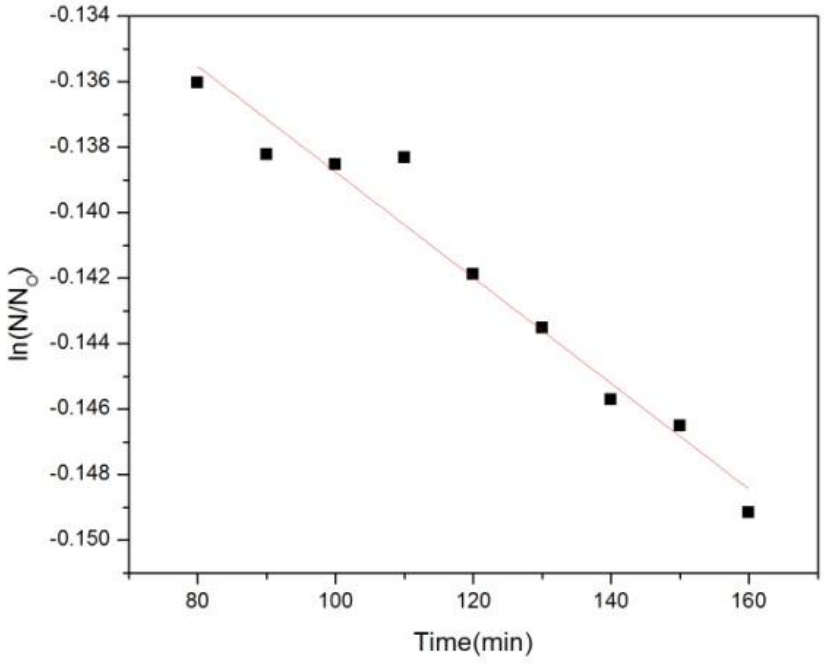
-0.134
-0.136
-0.138
-0.140
-0.142
-0.144
-0.146
-0.148
-0.150
ln(N/N0)
80
100
120
140
160
Time(min)

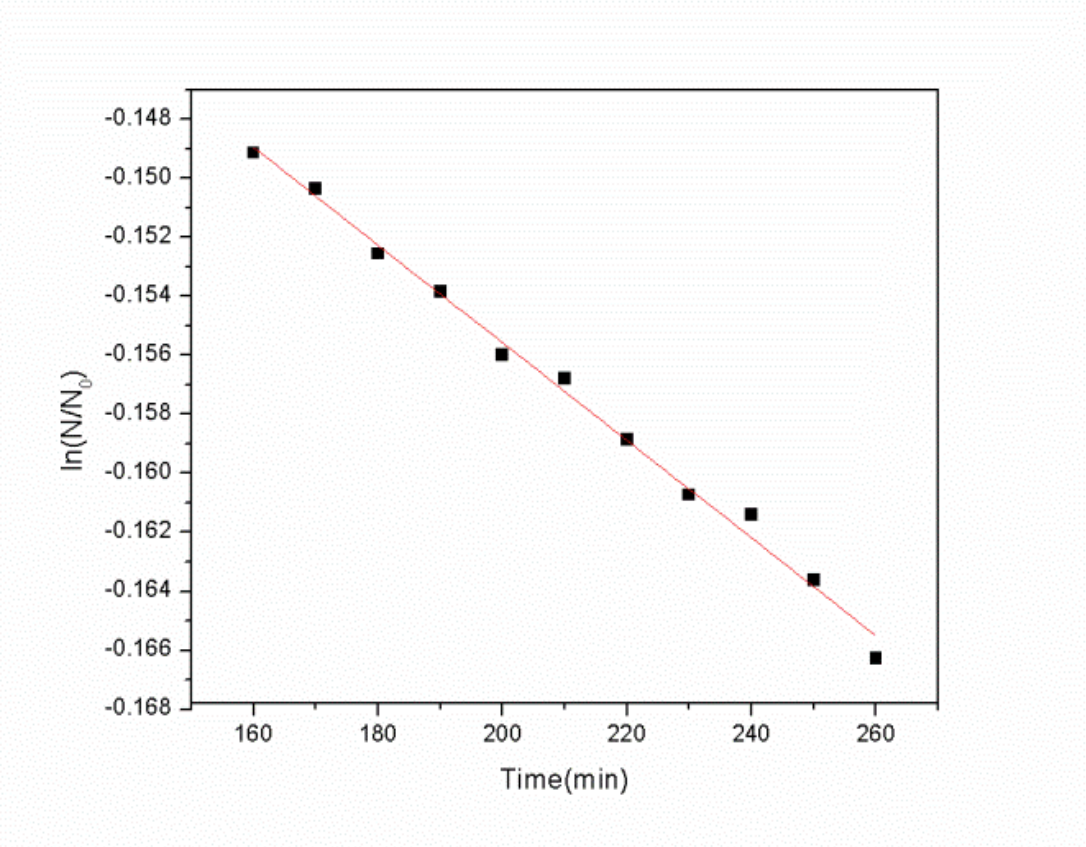

Figure 6.7.22: Semi-logarithmic plot of change of moles of Gas while Methane Hydrate Formation in presence of C- type Silica Gel containing 100 ppm Rhamnolipids.

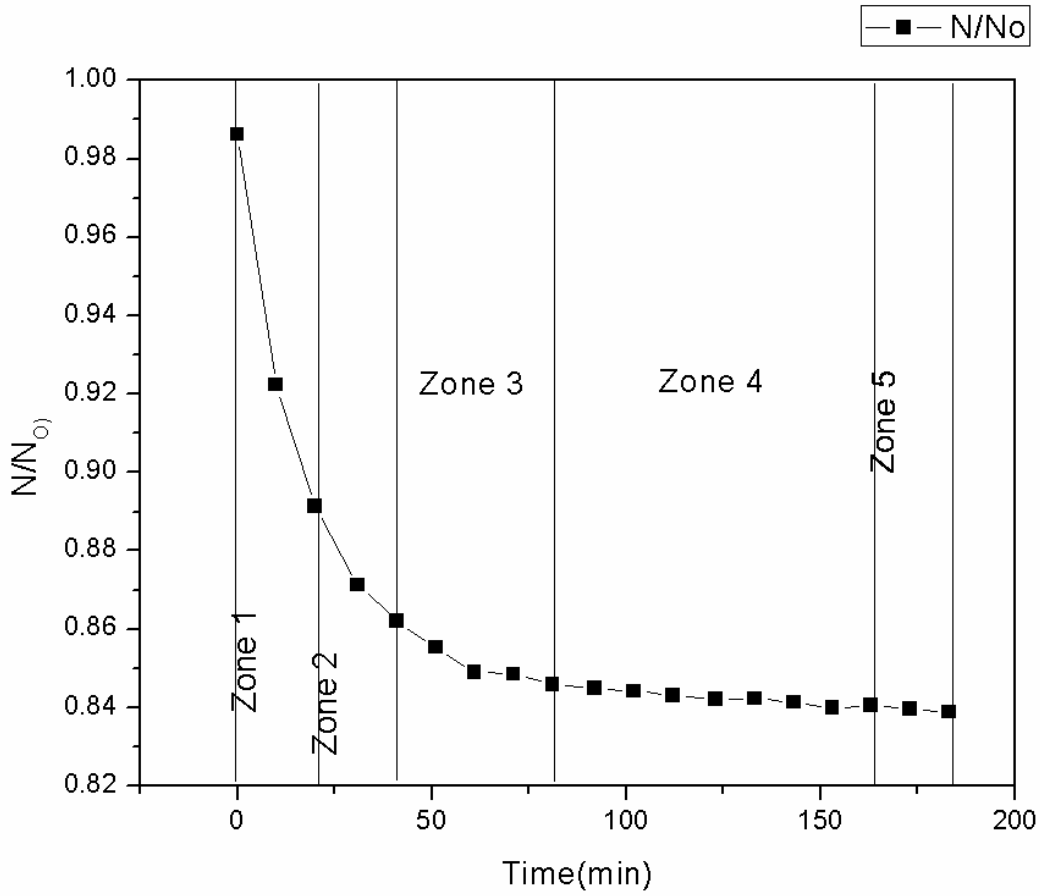

Figure 6.7.23: N/N_0 vs Time Plot for Methane Hydrate Formation in presence of C- type Silica Gel containing 1000 ppm Rhamnolipids.

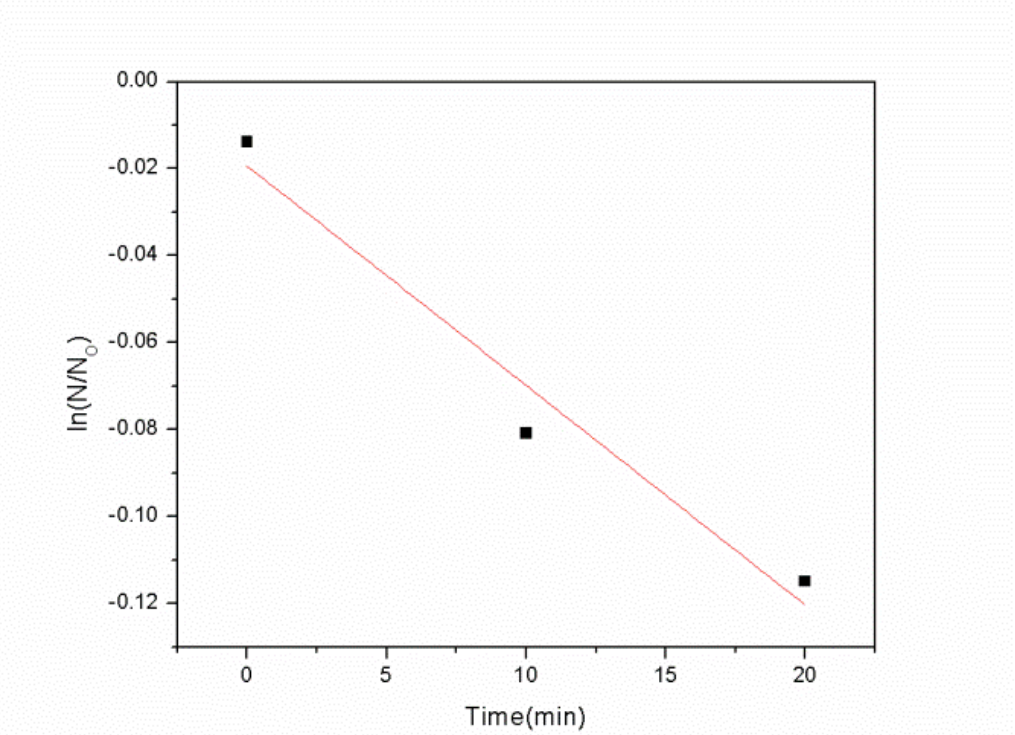
0.00
-0.02
-0.04
-0.06
-0.08
-0.10
-0.12
ln(N/N0)
0
5
10
15
20
Time(min)

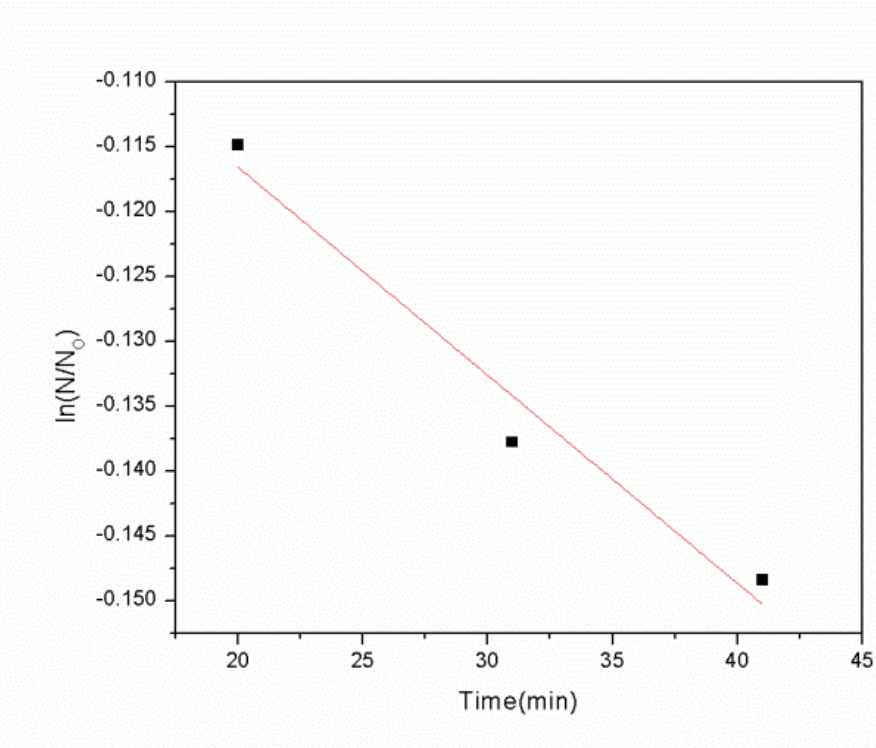
-0.110
-0.115
-0.120
-0.125
-0.130
-0.135
-0.140
-0.145
-0.150
ln(N/N0)
20
25
30
35
40
45
Time(min)

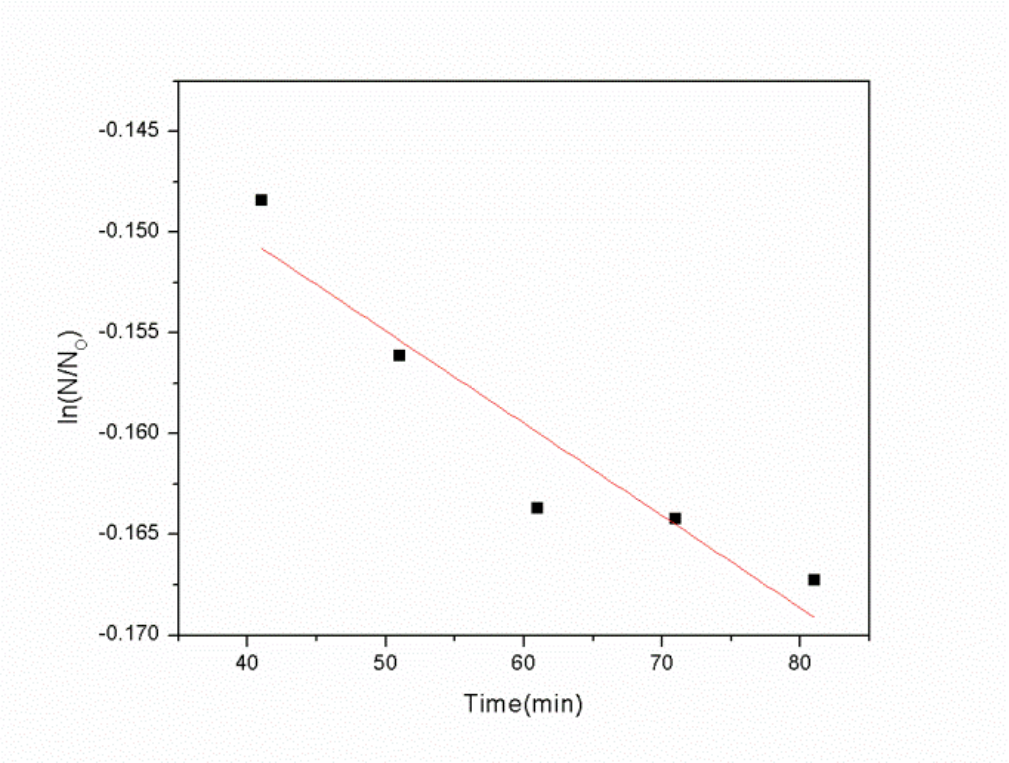
-0.145
-0.150
-0.155
-0.160
-0.165
-0.170
ln(N/N$_O$)
40
50
60
70
80
Time(min)

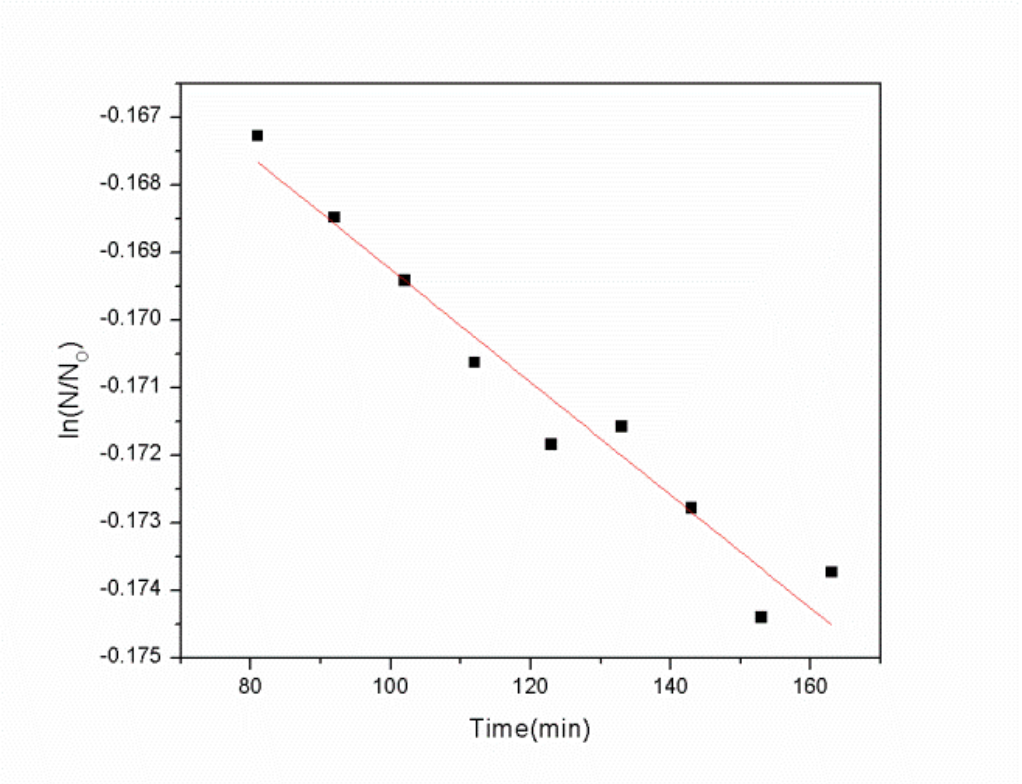
-0.167
-0.168
-0.169
-0.170
-0.171
-0.172
-0.173
-0.174
-0.175
ln(N/N$_O$)
80
100
120
140
160
Time(min)

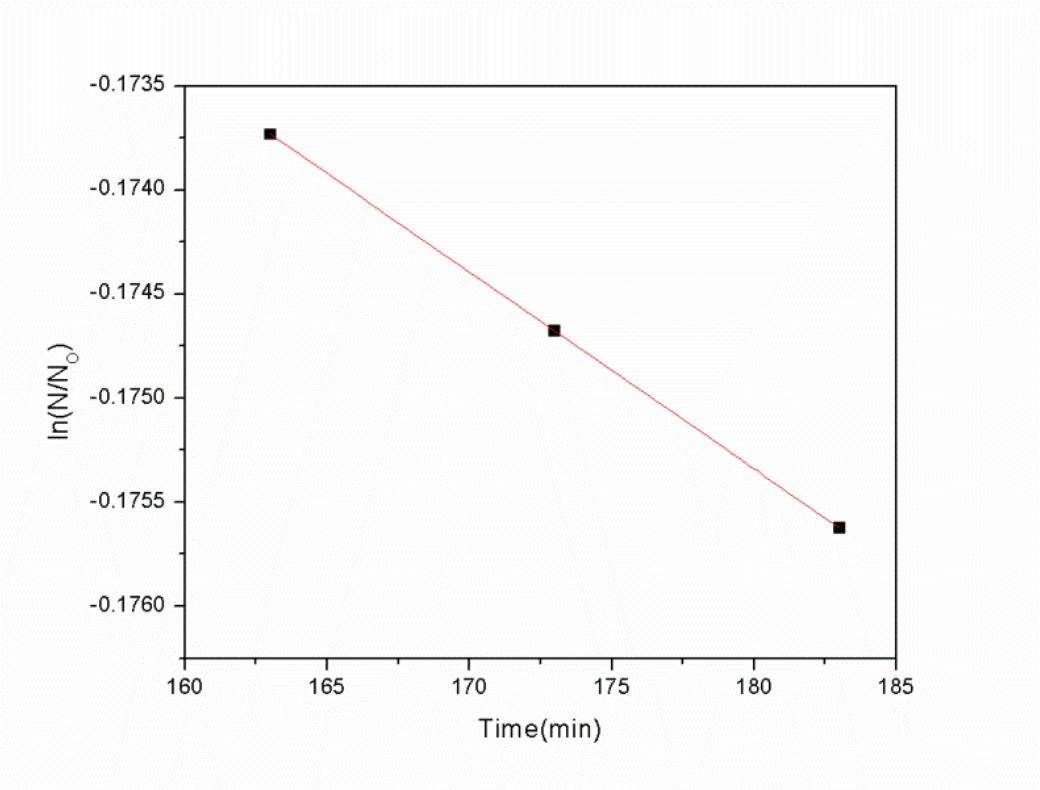

Figure 6.7.24: Semi-logarithmic plot of change of moles of Gas while Methane Hydrate Formation in presence of C- type Silica Gel containing 1000 ppm Rhamnolipids.

The rate of Methane Hydrate generation in 0-20 minutes time frame in C type Silica Gel saturated with water is better than the C type Silica Gel saturated with water-rhamnolipids solution. However, after aforementioned time frame, presence of rhamnolipids in the system enhanced the rate of Hydrate Formation.

Initially it is noted that the rate of Formation of Hydrate is almost same. But during the growth of Hydrate the rate was observed to depend on the concentration of rhamnolipids. The growth rate of Hydrate is enhanced by the presence of rhamnolipids many more times as compared to the absence of rhamnolipids. It is observed that 100 ppm rhamnolipids enhances the overall rate of Hydrate growth relatively more. This enhancement of rate in the present study is an agreement with work carried out by others [Rogers et al, 2003, Rogers et al, 2003, Woods el al, 2004]. Methane Hydrate Formation rates are calculated and are shown from Figures 6.7.25 to 6.7.30 and table 6.7.4, which shows that there are much variation in the presence of Rhamnolipids for Methane Hydrate Formation rate.

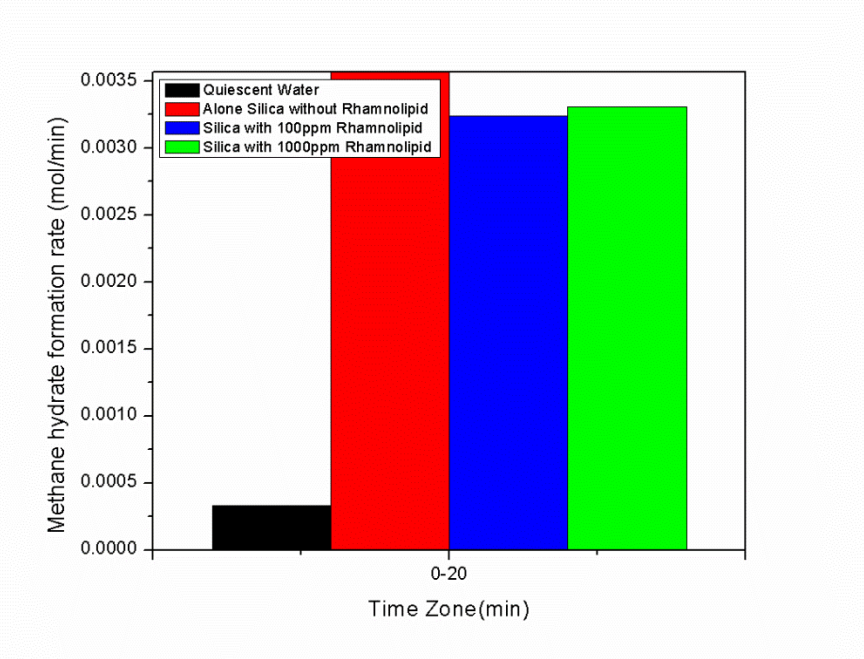

Figure 6.7.25: Methane Hydrate Formation rate for time zone 0 to 20 minutes.

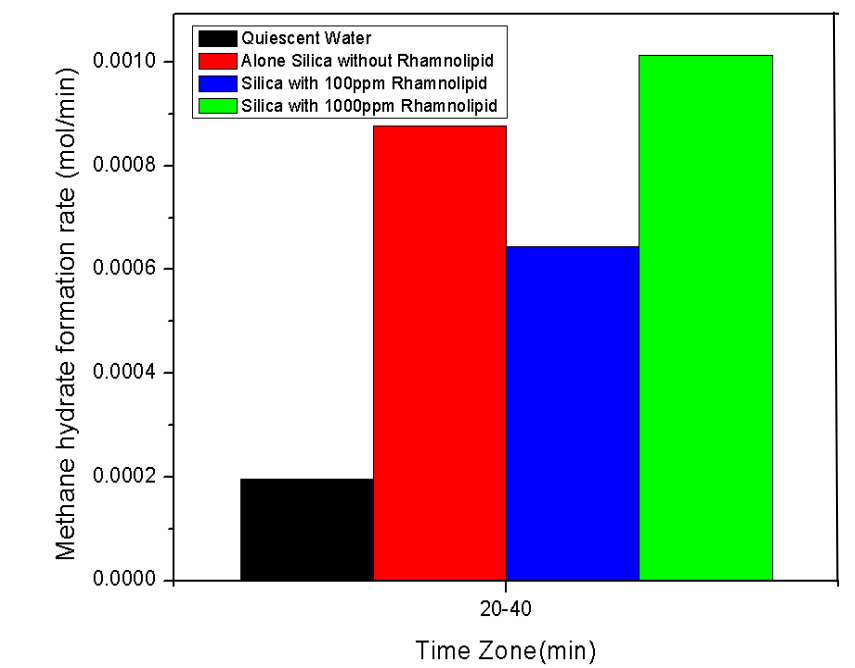

Figure 6.7.26: Methane Hydrate Formation rate for time zone 20 to 40 minutes.

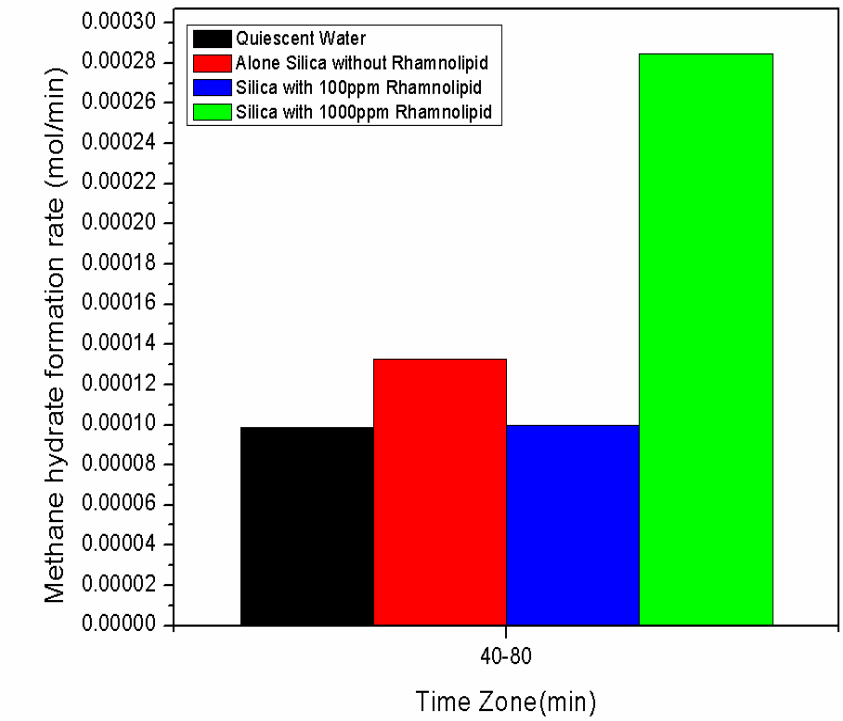

Figure 6.7.27: Methane Hydrate Formation rate for time zone 40 to 80 minutes.

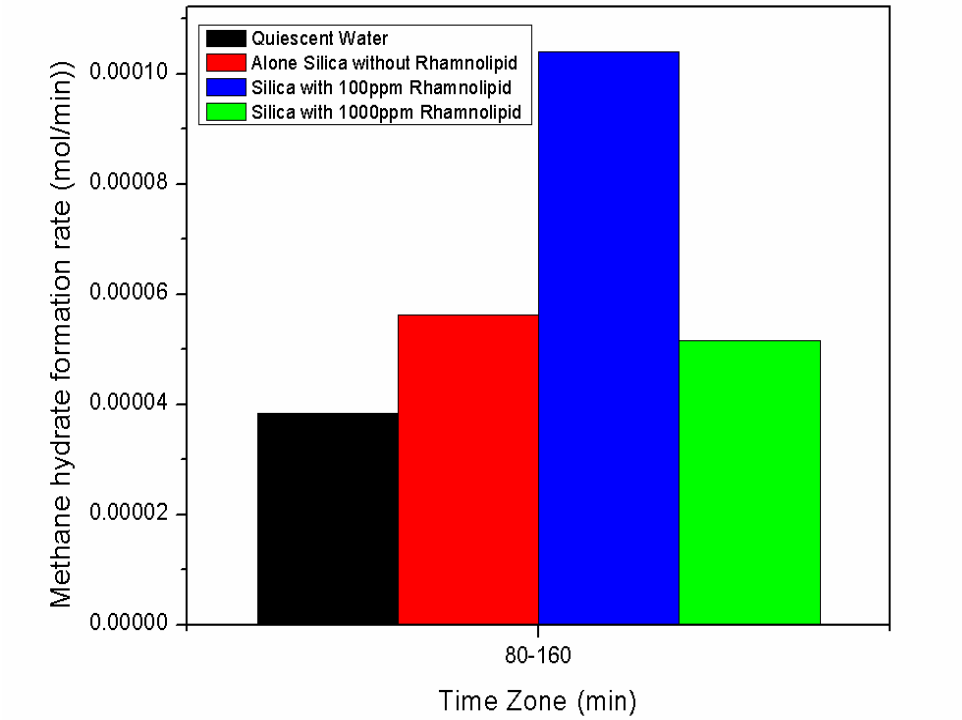

Figure 6.7.28: Methane Hydrate Formation rate for time zone 80 to 160 minutes.

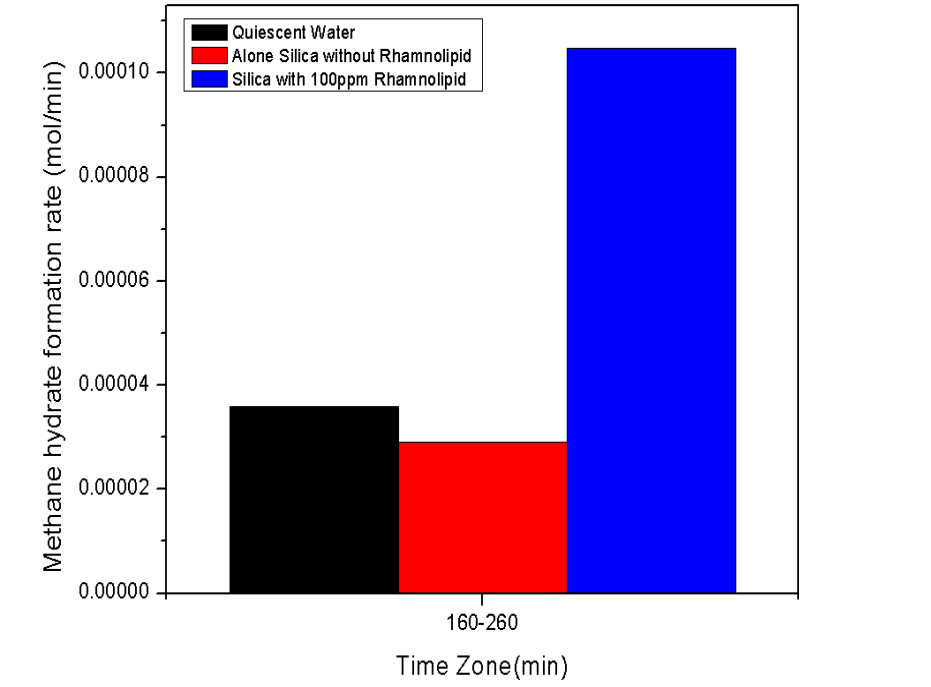

Figure 6.7.29: Methane Hydrate Formation rate for time zone 160 to 260 minutes.

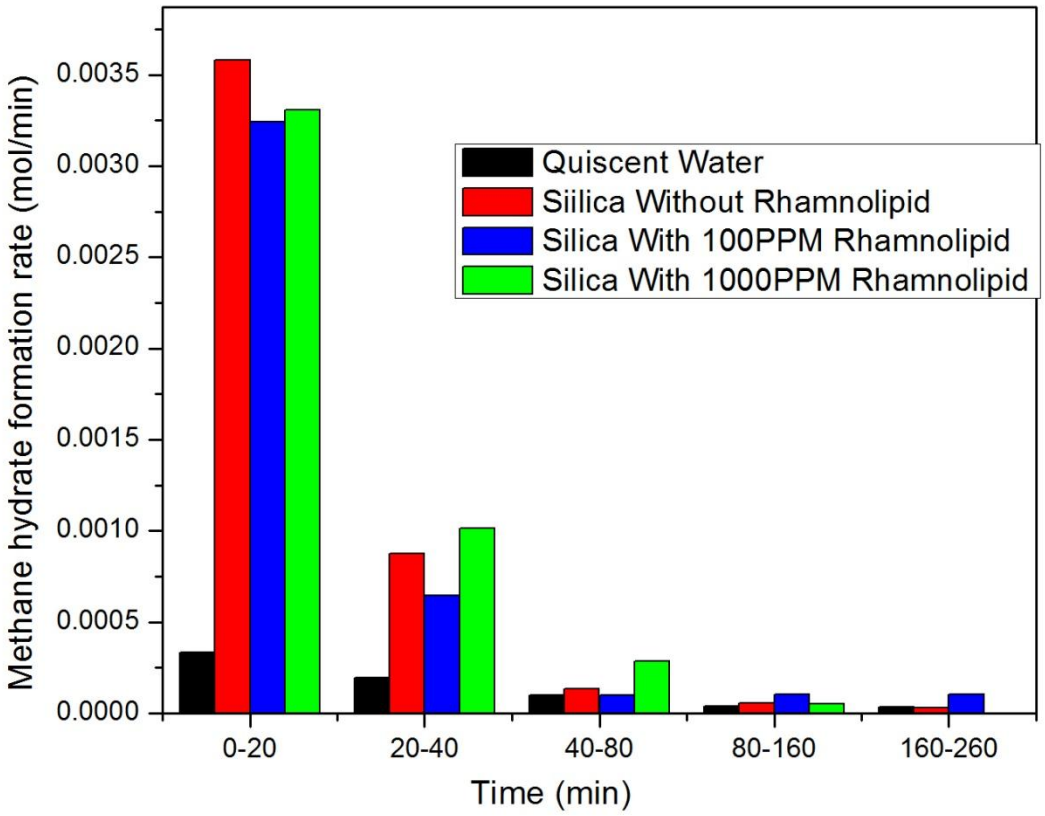

Figure 6.7.30: Comparison of rates of Methane Gas Hydrate Formation for different time zone in different experiment condition

Table 6.7.4: The rate of Methane Gas Hydrate Formation for different experimental condition

Type of sample	Time Zone (Min)	Rate constant K (min^{-1})	Formation rate (mole/min)	% over all increased rate with respect to Silica
C-type Silica Gel without presence of bio- surfactant	0-20	0.00514	0.003583383	
	20-40	0.00892677	0.000876474	
	40-80	1.33E-04	0.0001327	
	80-160	5.65E-05	5.62E-05	
	160-260	2.91E-05	2.92E-05	
C-type Silica Gel containing 100 PPM Rhamnolipids	0-20	0.00484	0.003241392	57.08272969
	20-40	9.82E-04	0.000645076	
	40-80	1.53E-04	9.9753E-05	
	80-160	1.61E-04	0.000103977	
	160-260	1.65E-04	0.0001047	
Quiescent water	0-20	4.48E-04	3.34E-04	-40.35750586
	20-40	2.65E-04	1.97E-04	
	40-80	1.33E-04	9.85E-05	
	80-160	5.21E-05	3.83E-05	
	160-260	4.92E-05	3.60E-05	
C-type Silica Gel containing 1000 PPM Rhamnolipids	0-20	0.00505	3.31E-03	42.97473456
	20-40	0.0016	1.01E-03	
	40-80	4.58E-04	2.84E-04	
	80-160	8.36E-05	5.16E-05	
	160-183	9.45E-05	5.82E-05	

6.7.2.6 *Water to Hydrate conversion*

The amount water to Methane Hydrate conversion is calculated by using equation 7 & 9 from annexure.

The percentage conversion till 237.5 minutes is given as per the following in Figure 6.7.31:

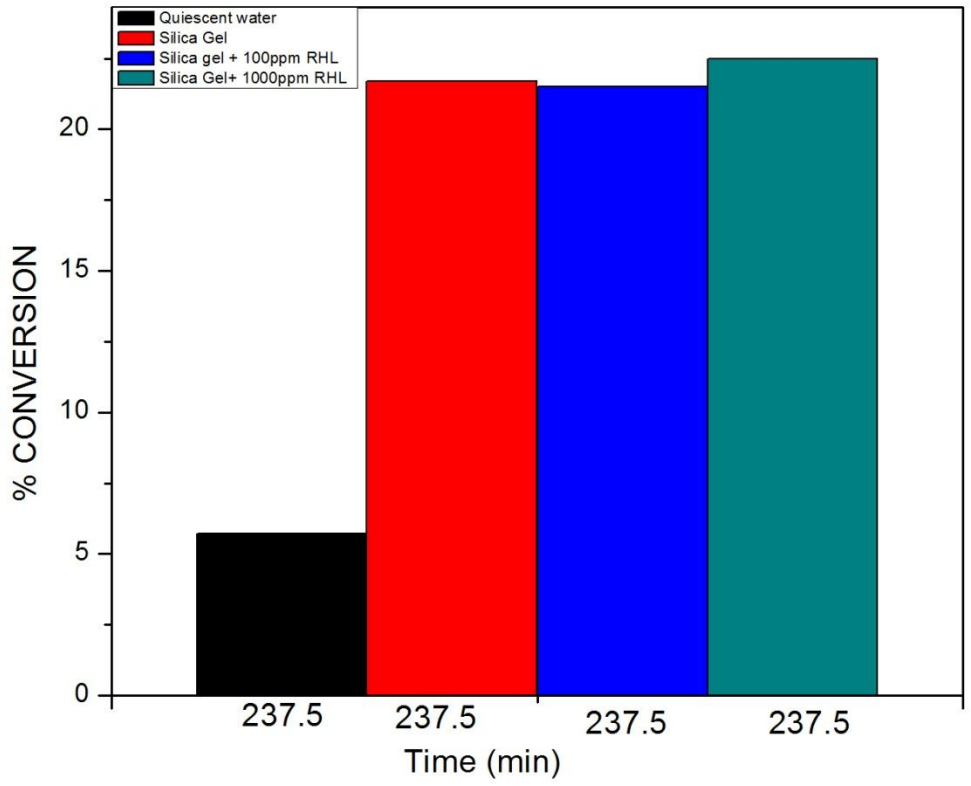

Figure 6.7.31: % Conversion of Methane Hydrate for various experiments.

At a given time the percentage of Hydrate conversion is found more in presence of 1000 ppm rhamnolipids whereas the conversion till end of the reaction is maximum for 100 ppm rhamnolipids and reported to be 23.6 percent for 341.5 minutes. The conversion till the end of the reaction for quiescent water is 8.43 percent for 642.1 minutes, for Silica Gel without the presence of rhamnolipids the conversion is 22.2 for 363 minutes, and the conversion till end of the reaction for 1000 ppm rhamnolipids is 22.5 for 237.5 minutes.

The percentage conversion till 237.5 minutes is given in Figure 6.7.31. Conversion reported by Zhang et al, 2013 in presence of Silica Gel powders is around 8% till 5 hours. The Silica Gel used in this work shows far better water to Hydrate conversion rate which further improves in presence of rhamnolipids.

Biosurfactant is regarded as a next generation surfactant for its environment-friendly nature and versatile potential applications [Muller et al, 2012]. Use of biosurfactant in NGH Formation can make process environment-friendly and more acceptable to environmentalist and policy makers.

In the present study biosurfactant used was obtained from strain A11. Strain A11 produced rhamnolipids while growing on relatively inexpensive carbon substrate glycerol. In the present situation, usage of glycerol for the production of biotechnologically valued products is gaining impetus as it is comparatively economical [Da Silva et al, 2009]. Moreover the quantity of waste glycerol production is rising every year due to increase in production of biodiesel and other oleo chemicals [Morita et al, 2007]. The amount of rhamnolipids produced by strain A11 under given condition is more than several others reports [Moussa et al, 2014, Zhao et al, 2014]. Previously strain A11 has been reported to produce 4,436.9 mg/lof biosurfactant after 120 h of incubation [Singh et al, 2013]. However, in the present study yield was increased by adding Trace Element Salts (TES) and increasing carbon source concentration in growth medium. The conditions that limit growth are known to promote rhamnolipids production. Limiting concentration of multivalent ions such as Mg, Ca, K, Na, and trace element salts are known to increase rhamnolipids yield [Guerra-Santos et al, 1986]. High yield, efficient purification and low substrate cost can make biosurfactant economically viable for industrial applications.

In recent past our knowledge about the rhamnolipids diversity has increased primarily due to use of more sensitive and sophisticated analytical techniques [Abdel-Mawgoud et al, 2010]. Changing abiotic factors like growth media and conditions are known to influence rhamnolipids homologous and congeners composition [Costa et al, 2010, Yin et al, 2009]. Earlier [Singh et al, 2013] have reported that strain A11 produced biosurfactant predominantly consisting of dirhamnolipids with single monorhamnolipids congener. However in the present study, with the help of more sophisticated analytical method unrecorded homologous and congeners were also observed. Usually $RhaRhaC_{10}C_{10}$ is the most abundant rhamnolipids congener [Muller et al, 2012]. Literatures suggest that the observed difference between components and content of fatty

acids can be attributed to change in culture condition and the analysis techniques [Muller et al, 2012, Abdel-Mawgoud et al, 2010].

The purified rhamnolipids reduced the surface tension of water to 29 mN/m with CMC of 83 mg/l [Singh et al, 2013]. However, a small change in the surface tension reduction ability and CMC was observed in the present study as compared to the previous report. This may be attributed to change in the composition of the biosurfactant and the content of fatty acid components. Similar changes have also been highlighted earlier [Costa et al, 2010].

The CMC is a vital parameter of any surfactant as it signifies the efficacy of surfactants. Lower CMC surfactants are considered much more suitable as the concentration of surfactant needed for decreasing the surface tension is very less. Every one of the constituents of rhamnolipids mixture impact differentially towards CMC but as it is very difficult to separate the rhamnolipids components in to a single homologue, the individual involvement of each constituent in CMC has not been explained. The CMC of different *Pseudomonas* rhamnolipids vary from 53 to 230 mg/l depending on the ratio and composition of rhamnolipids species [Guerra-Santos et al, 1986]. Literature suggests that rhamnolipids is more efficient than most common synthetic surfactants like Sodium Dodecyl Sulphate (SDS), Triton [Thangamani et al, 1994, Churchill et al, 1995].

Stability of rhamnolipids at extreme conditions can be attributed to highly stable bond between sugar moiety and lipid chain. Similar observations have been reported by Singh and Cameotra [Singh et al, 2013]. Generally pH of sea water ranges from 7.5 to 8.4 whereas temperature can reach minimum up to subzero levels and maximum up to 36 ^{0}C depending upon surrounding conditions. Stability observed under aforementioned condition suggests that rhamnolipids can be successfully used in the marine conditions.

Lanoil et al, 2001 reported direct physical interaction between microbes and Gas Hydrate. They hypothesized that aforementioned interaction can have significant consequences for Gas Hydrate composition, stability and geochemistry. Members of gammaproteobacteria have been reported in Gulf of Mexico Gas Hydrates samples [Lanoil et al, 2001]. Thus, anticipation that secondary metabolites from gammaproteobacteria like *Pseudomonas aeruginosa* may have beneficial effect on Gas Hydrate Formation would not be an exaggeration. It was expected that rhamnolipids, a glycolipids type biosurfactant produced by *Pseudomonas aeruginosa* strain A11 can execute

beneficial influence on Gas Hydrate Formation by improving interfacial interaction between water and Methane.

In present study, for making the NGH technology environment-friendly along with microbial surfactant, environment compatible porous media was also used. Earlier, Linga et al, 2009 highlighted the need for studying the dynamics of Hydrate Formation and decomposition in Natural pores media as there are very few reports in literature. As compared to quiescent water system rate of Hydrate generation was rapid in C-type Silica Gel due to better Gas-water contact [Kumar et al, 2013]. The C- type Silica Gel has smaller particle size and higher specific surface area as compared type-A and type-B Silica Gel, thus has better Hydrate transformation ratio [Kumar et al, 2013]. Combination of larger pore diameter and higher surface area enhance the rate of Formation of Hydrate and water to Hydrate transformation ratio considerably. In a porous matrix Hydrates Formation takes place within the pores and in between the interstitial sites. Larger pores promotes the dispersion of Gases into the interstitial sites while high surface area allows more contact between the water and Gas thus, resulting in better Hydrate conversion.

Information on kinetics of NGH Formation is vital for storage, transportation and effective utilization of NGH hence, received considerable attention in the recent past. In present study, the chemical additives significantly increase the rate of Hydrate Formation as compared to quiescent water system. Comparatively better Methane Hydrate Formation kinetics in C- type Silica can be attributed to the large surface area and large pore diameter which facilitated the relatively better mass transfer between two phases leading to large pressure drop due to nucleation and growth. Faster growth kinetics at a later period in the presence of surfactants can be attributed to lower interfacial tension allowing better contact between Methane and water thus better mass transfer between the two phases.

The induction time in Methane Hydrate crystallization is an important property of the kinetics studies. The induction time is a measure of the nucleation period in which Gas and water molecules in the metastable region interact to form nuclei of a critical size, from which the Gas Hydrate growth can proceed [Sloan et al, 1998]. Release of energy due to hydrogen bond Formation during Hydrate nucleation is responsible for this sudden rise in reactor cell temperature [Handa et al, 1986]. Shorten induction time as observed in the presence of Silica Gel

is attributed to higher surface area of C- type Silica Gel. Silica Gel allowed an improved contact between the Gas and water phase resulting in lesser induction time.

Replacing energy intensive process of agitation with fixed bed system decreases over all energy requirement and confiscates the requirements for specially designed system. Autoclave used in the present study was earlier used by [Saw et al, 2014] for studying the kinetics of Methane Hydrate Formation and its Dissociation in the presence of Tergitol with agitation of 1000 rpm. Interestingly the fixed bed system of C-type Silica Gel used in the present study was found to be better than the combination of agitation and surfactant in terms of induction time of Methane Hydrate Formation.

In present study saturating C-type Silica with water-rhamnolipids further favoured Methane Hydrate Formation as compared to condition when only water was used for preparing Silica bed. Presence of rhamnolipids shifted Methane Hydrate Formation temperature to higher value. The equilibrium temperature and pressure of Methane Hydrate Formation shifted to higher and lower values, respectively. The rate of Hydrate Formation increased as well as the induction time of Hydrate Formation got reduced in the presence of rhamnolipids suggesting rhamnolipids as Methane Hydrate promoter.

Earlier few groups have carried studies on the effects of biosurfactants on Gas Hydrate Formations and highlighted them as promoters [Rogers et al, 2003, Rogers et al, 2003, Woods, 2004, Wang et al, 2012]. Rogers et al, (2003) reported that addition of commercially available rhamnolipids increased the Hydrate Formation rate by 96% and decreased the induction time by 58% as compared to the system where surfactant was not used.

Recently, Wang et al, 2012 reported use of clathrates of biological origin for accelerating Hydrate Formation kinetics. They reported the nucleation temperature in the presence of fungi to be 279K. Present study also reports almost same temperature (278.59K) in Silica bed containing 1000 ppm rhamnolipids solution.

In quiescent water system the number of moles of Methane per mole of water consumed is minimum mainly because of Hydrate layer Formation on the water surface subjecting inadequate interaction between the Gas-bulk water. On the contrary use of porous C-type Silica Gel in present study increased the Gas uptake primarily by providing more surfaces for interaction.

Further use of biosurfactant solution with C-type Silica Gel favoured the Methane consumption by reducing the surface tension of water.

Chemical nature and concentration of surfactant have significant influence on Natural Gas Hydrate's promoter activity of surfactants. Anionic surfactants are more effectual than non-ionic and cationic surfactants in enhancing the rate of Hydrate Formations [Sun et al, 2003]. Karimi et al, (2013) studied influence of three synthetic surfactants namely dodecyl trimethyl ammonium bromide (DTAB, cationic surfactant), TritonX-100 (non-ionic surfactant) and sodium dodecylbenzenesulfonate (SDBS, anionic surfactant) on ethane Hydrate generation. They observed that SDBS are more effective in promoting the ethane Hydrate Formation rate at varied concentrations. Cationic surfactant DTAB has the contrasting effect on the ethane Hydrate Formation rate, which reduced with increasing DTAB concentration. Non-ionic surfactant Triton X-100 also enhanced the ethane Hydrate Formation rate but was not as effective as SDBS.

Biosurfactant concentrations above CMC are more effective in fastening the rate of NGH Formation than the concentrations below CMC [Rogers et al, 2003]. The biosurfactant promote the NGH Formation by associating water to hydrophilic head and hydrocarbon Gas to hydrophobic tail [Woods, 2004] and also by "Surfactant micelle hypothesis" suggested by Rogers and his co-workers [Zhong et al, 2000, Kothapalli et al, 2002, Rogers et al, 2003, Rogers et al, 2004, Rogers et al, 2005]. Micelles are considered as colloidal aggregates which are formed by surfactants in solution when the concentration of the surfactant exceeds CMC. The Natural inclination of micelles to gather large masses of structured water and hydrocarbon Gas at a common site increases their likelihood of promoting Hydrate Formation. Micelle plays the role of nucleation point which increases the solubility of hydrocarbon Gas in the aqueous phase. It leads to the Formation of Hydrate crystals around the micelle.

The above hypothesis was challenged by Watanabe et al, 2005. He proposed that several surfactants including SDS cannot form micelles at a Hydrate forming temperature. The lowest temperature at which the micelles can be formed is known as Kraft's point or the point of intersection of solubility and CMC curve known as Kraft Point. The rhamnolipids are in the form of congener consisting of monorhamnolipids and dirhamnolipids. The kraft point of rhamnolipids having more dirhamnolipids is below 0^0 C [Chen et al, 2008]. In the present study the relative abundance of dirhamnolipids is far greater then monorhamnolipids and it can help in

reaching the kraft point at Hydrate Formation conditions. Moreover, their observation was based on HFC-32 fluorohydrocarbon-Gas/water/ SDS system at low pressure. The results were then extrapolated to Methane/water/SDS system which their group did not evaluate [Zhang et al, 2007].

The interactions of two systems would be quite different. The SDS micelle core of associated alkyl groups readily solubilized the Natural Gas but the core doesn't have the affinity for the HFC-32 because of strong polarity of flouric Gas molecules. With non-polar Methane Sun et al, 2004 revealed that CMC of SDS decreases at Hydrate Formation temperatures under Methane pressure. Moreover, the kraft point of SDS reported by various groups Weil et al, 1963, Lange et al, 1968 range from 16 ^{0}C to 8 ^{0}C indicate that kraft point is very much sensitive to test conditions. It should be also lowered by surfactant solute interactions. [Sun et al, 2004], with pendant-drop method of surface tension calculation it was revealed that CMC of SDS is also decreased 500 ppm under the pressure of Methane at 273.3 K, in comparison to CMC of SDS at ambient conditions is 2500 ppm as measured by Flockhart, 1961 and moreover Zhong et al, 2000 filmed ethane as well as Natural Gas Hydrates crystals which reveals miceller forming SDS. This hypothesis of possible miceller enhancement of Hydrates was supported by sun et al, 2004, So it is very tough to agree with Watanabe's conclusion, 2005 that no micelles is formed at Hydrate forming conditions in SDS water and hydrocarbon Gas system. In the present study rhamnolipids forms micelles at very low concentration which is of the order of magnitude lower than this CMC of SDS.

Literature suggests that among all the currently known synthetic surfactants, SDS has been widely reported as NGH promoter [Moraveji et al, 2010, Mandal et al, 2008]. Relatively better know how of SDS as NGH promoter makes it as forerunner among the synthetic surfactants for industrial application. However, SDS toxicity cannot be ignored towards living organisms. SDS reaches living organism by food chain, gets accumulated and induce toxic effect by damaging biological macromolecules like protein, lipids, phospholipid membranes and DNA. Substituting SDS with environment compatible anionic rhamnolipids is a good option. Moreover, CMC of rhamnolipids is ~ 100 times lower than that of SDS thus making former a more efficient surfactant [Mendes et al, 2015].

The above results suggest that rhamnolipids shifts the Methane Hydrate Formation temperature to higher value compared to Hydrate Formation without presence of rhamnolipids. Also it is found that the equilibrium temperature and pressure of Methane Hydrate Formation is shifted to higher and lower value respectively. It is also found that the induction time of Hydrate Formation is reduced in presence of rhamnolipids. The rate of Hydrate Formation is found to increase many time. Therefore it is suggested from the results the Methane Hydrate Formation is promoted in presence of rhamnolipids. The above study is in agreement with the studies carried out on biosurfactant by Rogers, 2003, Rogers, 2003 , Woods , 2004 and moreover these results are also supported by various studies carried out on synthetic anionic surfactants like SDS [Mandal et al, 2008, Fazlali et al 2013], LABS [Ganji et al 2006)], SDBS Dai et al 2014].

The rhamnolipids act as a promoter because of the Formation of biosurfactant micelles. The spherical micelle is formed by long chain carbon alkyl groups which solubilises hydrocarbon Gases [MacKerell, 1995]. Water associates around the circumference of the micelle near the solubilized Gas which facilitates to act micelles as nucleation sites for Hydrate crystals and accelerates the Hydrate Formation. The rhamnolipids synthesized from strain A11 has reduced the surface tension of water from 72mN/m to 36 mN/m with CMC of 70 mg/l which in turn facilitates the cages of water and encapsulation of Methane Gas and converting them to Hydrate. The CMC of Rhamnolipids is much lower than even Sodium Dodecyl Sulphate [Herman et al, 2002, Thangamani et al, 1994, Churchill et al, 1995] and they can be also adsorbed on sediment particle surfaces, [Banat et al, 1995, Herman et al, 2002]. Micelles can migrate through porous media [Herman et al, 2002, Bai et al, 1997]. Rhamnolipids micelles size is lesser than micelles size of SDS [Champion et al, 1995, MacKerell, 1995], which facilitates it in migrating through porous media and moreover with the increase in concentration of the surfactant the surface tension of the aqueous phase will be reduced leading to acceleration of Hydrate Formation [Daimaru et al, 2007].

When the concentration of the surfactant is more than the CMC, the micelle is formed which can help in restricting the Gas molecules and making clusters with water molecules which in turn accelerate the Formation of crystal nuclei leading to Hydrate nucleation where the Hydrate crystals grow to a critical size for continued growth [Sloan, 1998]. In the present study the CMC of Rhamnolipids is very very less i.e. 70mg/lin comparison to SDS.

Rhamnolipids has also decreased the surface tension of water from 72mN/m to 36 mN/m which facilitates the transport of Gas in contact with water. It was proposed that micelles cannot be formed by many surfactants including SDS at a temperature where Hydrate is formed. The lowest temperature at which the micelles can be formed is known as krafts point.

Rhamnolipids act as promoter which can help in synthesizing Gas Hydrates. Industry is looking on Gas Hydrates not because of their energy potentials rather Gas Hydrate is becoming a technology these days because of their other applications such as transportation and storage of Gas, desalination of water etc. The present study has also addressed the issue of more energy consuming mechanism of synthesizing Gas Hydrate via agitation by synthesizing Gas Hydrate using fixed bed media of C-type Silica Gel and showing the performance of fixed bed media at par with the agitation method. So the above study has given biodegradable green biosurfactant which is performing at par with the synthetic surfactant. It has also clarified role of rhamnolipids a biosurfactant as promoter in Natural Gas Hydrate sites.

Biomass derived Gas Hydrate promoter, to support rapid Formation of high capacity Methane Hydrate with a small induction time is very much desirable for commercial exploitation of Natural Gas Hydrates. Chemical additives of biological origin like rhamnolipids [Rogers et al, 2003], surfactin [Rogers et al, 2003] have been reported to shorten the induction time. Roger et al, 2003 observed 58% reductions in induction time under influence of 1000 ppm rhamnolipids [Rogers et al, 2003].

The mechanism of surfactant promoting Hydrate nucleation is still poorly understood [Saw et al, 2012]. The induction time for Hydrate nucleation in a quiescent system is influenced by super-saturation, the presence of additives and foreign particles, interfacial tension of Hydrate-liquid, etc. [Carvajal et al, 2013]. The C type Silica Gel has smaller particle size and higher specific area [Kumar et al, 2013]. Combination of larger pore diameter and higher surface area enhances the rate of Hydrate Formation by decreasing the induction period. Kumar et al, 2013 reported that in a porous matrix Gas Hydrates Formation takes place within the pores as well as in between the interstitial sites [Kumar et al, 2013]. Further application of surfactant solution decreases interfacial tension between Gas-liquid and thus favouring interfacial interaction between Gas and water [Wang et al, 2012, Kashchiev et al, 2003]. The induction time reduces with decreasing

interfacial tension of Hydrate-liquid, by facilitating better interfacial interaction between Gas and water [Kashchiev et al, 2003, Wang et al, 2012].

The zeta potential of Rhamnolipids synthesized in the present study from strain A11 was found to be negative, hence it is anionic surfactant and much of work in literature on anionic surfactants such as SDS etc. on Gas Hydrate Formation has been reported. Zeta potential is the potential difference between the stationary layer of the fluid attached to the dispersed particle and the dispersion medium. The zeta potential value relates to the stability of colloidal dispersion. Colloids with high zeta potential are stabilized electrically. Anionic nature of rhamnolipids observed in the present study is in accordance with the earlier report [Pornsunthorntawee et al, 2008].

These results are in agreement with various studies reported on synthetic anionic surfactants like SDBS [Dai et al, 2014], LABS [Ganji, 2006, Fazlali et al, 2013, Saw et al, 2014].

The above results are indicating that rhamnolipids act as promoter which can help in synthesizing Gas Hydrates. Industry is looking on Gas Hydrates not because of their energy potentials rather it is becoming a technology these days because of their other applications such as transportation and storage of Gas, desalination of water, Cool Storage applications, Separation of Gases, CO_2 Capture . The present study is clarifying role of rhamnolipids a biosurfactant as promoter in Natural sites and giving a green biodegradable promoter as much of work as promoter of Gas Hydrates is reported on synthetic surfactants however the above study has given a replacement of synthetic surfactant by a green biosurfactant.

If Natural Gas Hydrate from the ocean floor becomes a viable Natural resource in future than fundamental understanding of their Formation, environment and decomposition will be of great importance. The significance of microorganisms and their metabolites is shown. Biosurfactant are produced in the ocean floor which promotes the Gas Hydrates Formation so the above thesis has lighten the Formation of Gas Hydrates in marine conditions and given the better understanding of the Formation of Natural Gas Hydrates in ocean floor.

6.7.3 *Conclusion of this task*

The kinetics and thermodynamics of Methane Hydrate Formation and its Dissociation has been studied in presence of rhamnolipids produced by *Pseudomonas aeruginosa* strain A11 with C-type Silica Gel as fixed bed media and found that Rhamnolipids act as dual promoter i.e. thermodynamic as well as kinetic promoter for Methane Hydrate Formation. Hydrate Formation rate is appreciably increased by the presence of rhamnolipids. The induction time of Hydrate Formation is reduced. Phase equilibrium graph moves to high temperature and lower pressure region in presence of rhamnolipids. These results suggest that rhamnolipids promote Hydrate Formation kinetically as well as thermodynamically. The performance of fixed bed media i.e. C-type Silica Gel is found to be at par with the agitation media for Methane Hydrate Formation. Thus small dosages of rhamnolipids produced by *Pseudomonas aeruginosa* strain A11 must clearly affect the Gas Hydrate Formation kinetics in Natural sites (as in Gulf of Mexico). Rhamnolipids is a green biodegradable promoter for Gas Hydrates Formation capable of replacing the synthetic surfactants.

Glycolipids type biosurfactant rhamnolipids were produced by rhizobacteria *Pseudomonas aeruginosa* A11. Modifying earlier reported MSM by adding TES and increasing glycerol concentration in growth medium increased rhamnolipids yields. Rhamnolipids produced by strain A11 has dirhamnolipids ($RhaRhaC_{10}C_{10}$) as most dominant congener. Apart from $RhaRhaC_{10}C_{10}$ olefinic rhamnolipids $RhaC_{22}$, $RhaRhaC_{10}C_{10}$/ $RhaRhaC_{10}C_{12}$, $RhaRhaC_{10}C_{10}$ / $RhaRhaC_{10}C_{12}$ were also produced by strain A11. Methane Hydrate Formation in C-type Silica Gel saturated with 1000 ppm rhamnolipids solution increased the rate of Methane Hydrated Formation as compared to quiescent water system and water saturated C-type Silica Gel. Rhamnolipids decreased the induction time by favouring better interaction between Methane and water. By decreasing the interfacial tension between Gas and water, surfactant increased the Methane Hydrate conversion percentage as well increased the number of moles of Methane consumed during Hydrate Formation. Overall results suggest that surfactant and C-type Silica Gel combination can be used for enhancing the Methane Hydrate Formation rate. Rhamnolipids has potential to act as Methane Hydrate Formation environment-friendly promoter in fixed C-type Silica Gel system.

The above study clearly indicates the role of rhamnolipids in the Formation of Methane Gas Hydrate Formation as promoter, thus small dosages of rhamnolipids produced by *Pseudomonas aeruginosa* strain A11 must clearly enhance the Formation rate of Gas Hydrate kinetics in Natural sites (as in Gulf of Mexico). Rhamnolipids are green biodegradable promoter for Gas Hydrates Formation which can substitute the synthetic surfactant which are used presently as promoter for the Formation of Gas Hydrates.

6.8 Lipopeptide Biosurfactant Surfactin Promoting Methane Hydrate Formation in Fixed Bed of Silica Gel: Thermodynamic and Kinetic Studies

6.8.1 *Thermodynamic Study*

6.8.1.1 *Methane Hydrate Formation-Dissociation*

Our objective in the present study is to examine the effect of biosurfactant Surfactin on Methane Hydrate Formation as well as Dissociation. Different concentrations of surfactin are used to observe the influence on Methane Hydrate Formation and Dissociation.

100 ppm dose of surfactin is made in distilled water then it is filled in C-Type Silica Gel in order to get 90% saturated C-type Silica Gel with this 100 ppm dose of surfactin. The cell was then packed with 90% saturated C-type Silica Gel (Merck) containing 100 ppm surfactin and then placed in temperature controlled bath under similar conditions. At temperature (277.31 K) sudden decline of pressure at a higher rate was seen confirming Hydrate nucleation Figure 6.8.1. When the temperature reaches a threshold value (285.83 K) there is sudden increase in pressure which shows the start of Dissociation of Hydrate Figure 6.8.1. Hydrate Dissociation is completed at 290.53 K called Dissociation point as shown in figure 6.8.1.

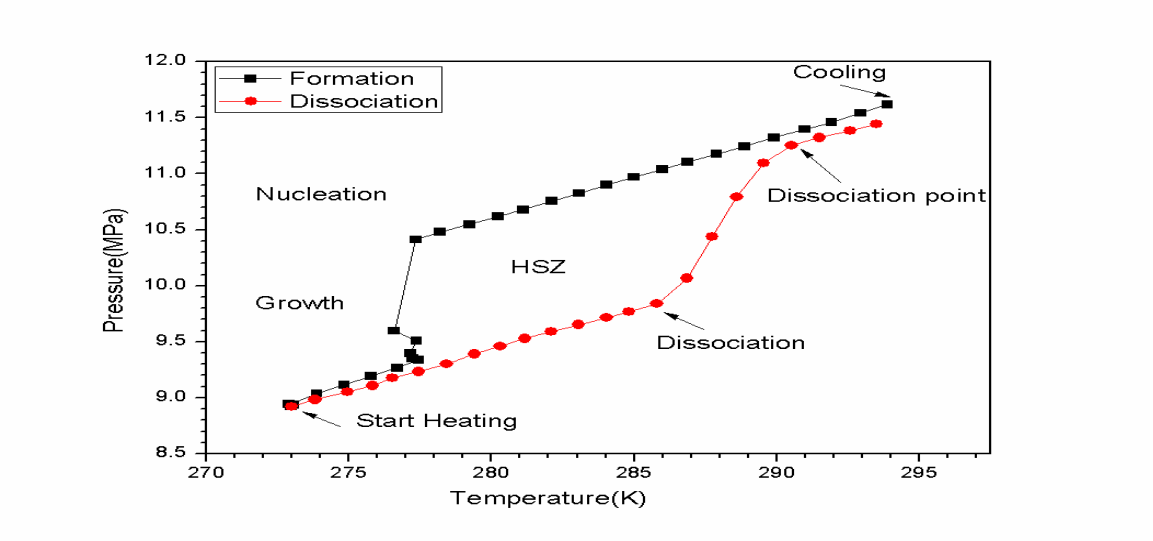

Figure 6.8.1: Temperature and Pressure profile of Methane Hydrate Formation and Dissociation in presence of C-type Silica Gel containing 100 ppm surfactin.

Afterwards under similar conditions 90% saturated C-type Silica Gel test sample containing 1000 ppm surfactin was examined. At temperature (279.24 K) sudden decline of pressure at a higher rate was seen confirming Hydrate nucleation Figure 6.8.2. Decomposition was also studied in similar way by rising the temperature. When the temperature reached a threshold value (286.57 K) there is sudden rise in pressure which confirms the start of decomposition of Hydrate Figure 6.8.2. Hydrate Dissociation is completed at 290.29 K called Dissociation point as shown in figure 6.8.2.

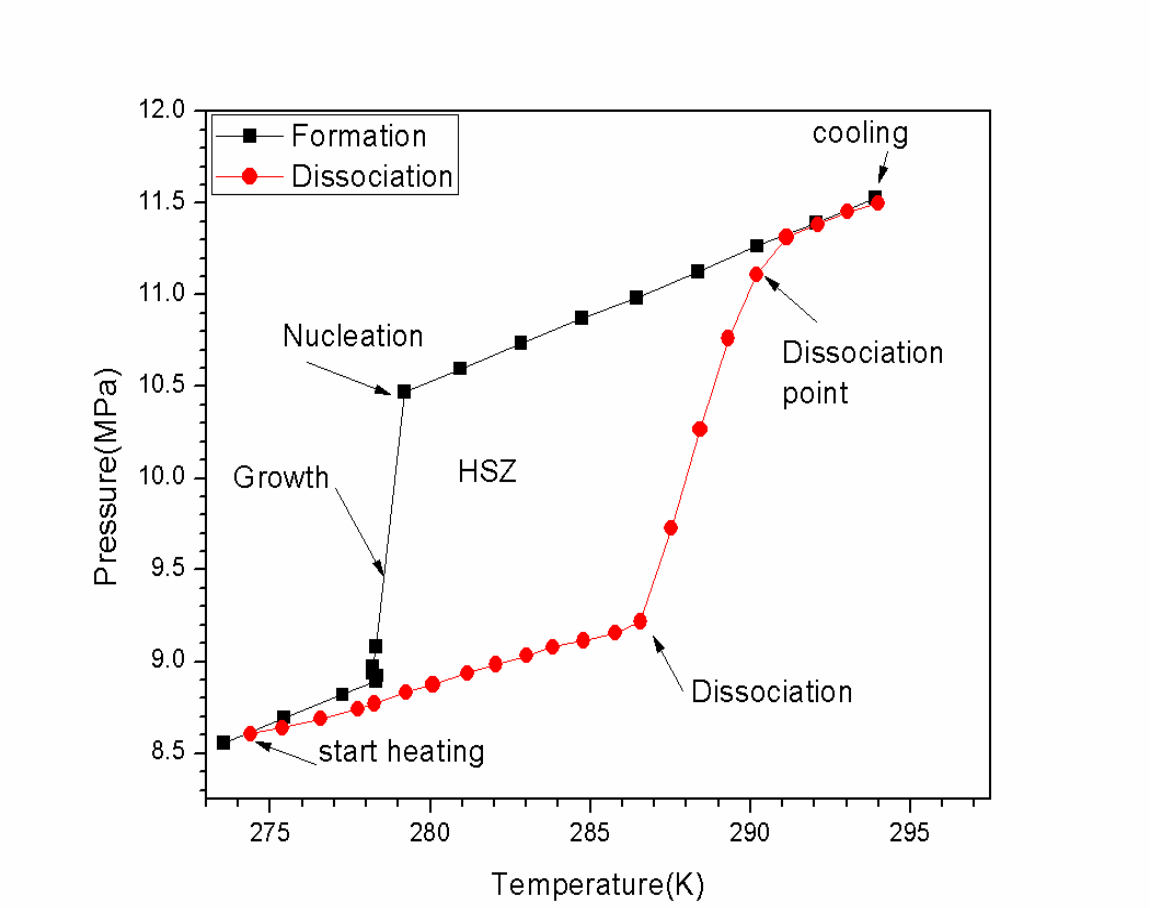

Figure 6.8.2: Temperature and Pressure profile of Methane Hydrate Formation and Dissociation in presence of C- type Silica Gel containing 1000 ppm surfactin.

The variation of concentration of surfactin the appreciably effects the thermodynamic parameters of Hydrate Formation and Dissociation Table 6.8.1. When the concentration of surfactin increased from 100 ppm to 1000 ppm, the nucleation temperature of Hydrate Formation is transferred to higher value and also less sub-cooling is needed to initiate Hydrate Formation. It is seen that nucleation temperature of Hydrate Formation shifts to higher value in case of 1000 ppm of surfactin. The addition of surfactin also effect the pressure drop of Hydrate Formation Table 6.8.1.

Table 6.8.1: Methane Hydrate Formation and Dissociation parameters in presence of different test sample

Test sample	Initial cell pressure P (MPa)	Nucleation tempera-ture T(K)	Nucleation pressure P(MPa)	Pressure drop Δp (MPa)	Equilibrium temperature T_{equ}(K)	Subcooling ΔT(°C) $\Delta T=T_{equ}$ - T	Dissoci-ation tempera ture (K)
C-type Silica Gel (Merck) containing 100 ppm Surfactin	11.62	277.31	10.41	1.08	290.74	13.22	285.83
C-type Silica Gel (Merck) containing 1000 ppm Surfactin	11.62	279.24	10.47	1.55	290.29	11.05	286.57

Fixed bed system of bentonite clay has been reported as a thermodynamic promoter for Methane Hydrate Formation [Saw et al, 2013, Saw et al, 2014] .Saw et al, 2014, reported change in nucleation temperature on changing the surfactant concentration. Nucleation temperature of Methane Hydrate Formation is shifted to higher values [Saw et al, 2014].

6.8.1.2 ***Comparison of nucleation temperature of Methane Hydrate Formation for different Systems***

Comparison of nucleation Methane Hydrate Formation parameters are shown in figure 6.8.3. As evident from the figure maximum shift was observed in the presence of Silica Gel saturated with distilled water containing 1000 ppm of surfactin. The comparative study of Formation of Methane Hydrate in absence as well as presence of surfactin is shown figure 6.8.3. It can be seen that the Hydrate Formation temperature is transferred to higher value upon adding surfactin.

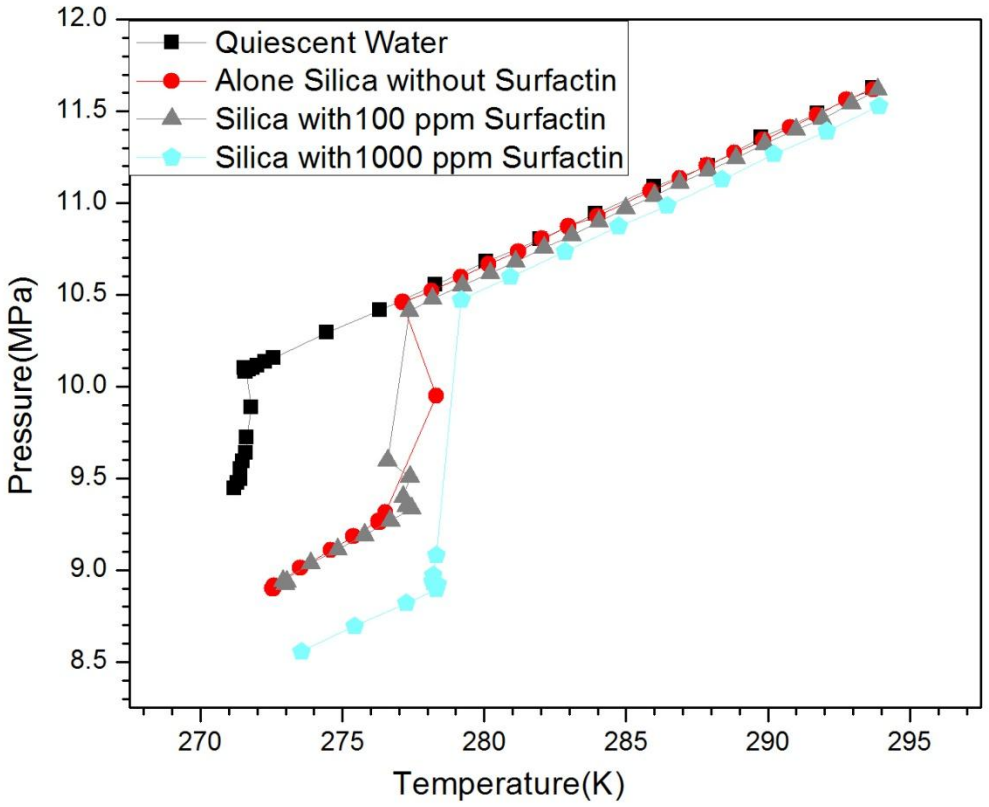

Figure 6.8.3: Methane Hydrate Formation parameters in presence of different test samples.

6.8.1.3 *Comparison of phase equilibrium of Methane Hydrate Formation for different Systems*

Similarly the phase equilibrium curves got shifted to high temperature region in the presence of Silica Gel containing 1000 ppm biosurfactant as compared to the water-Silica Gel system without surfactin.

The phase equilibrium of Methane Hydrate without surfactin and in presence of differentg concentration of surfactin is shown as per figure 6.8.4. The phase equilibrium curves shift to higher temperature zone on addition of surfactin. This recommends that surfactin is thermodynamic promoter of Methane Hydrate Formation.

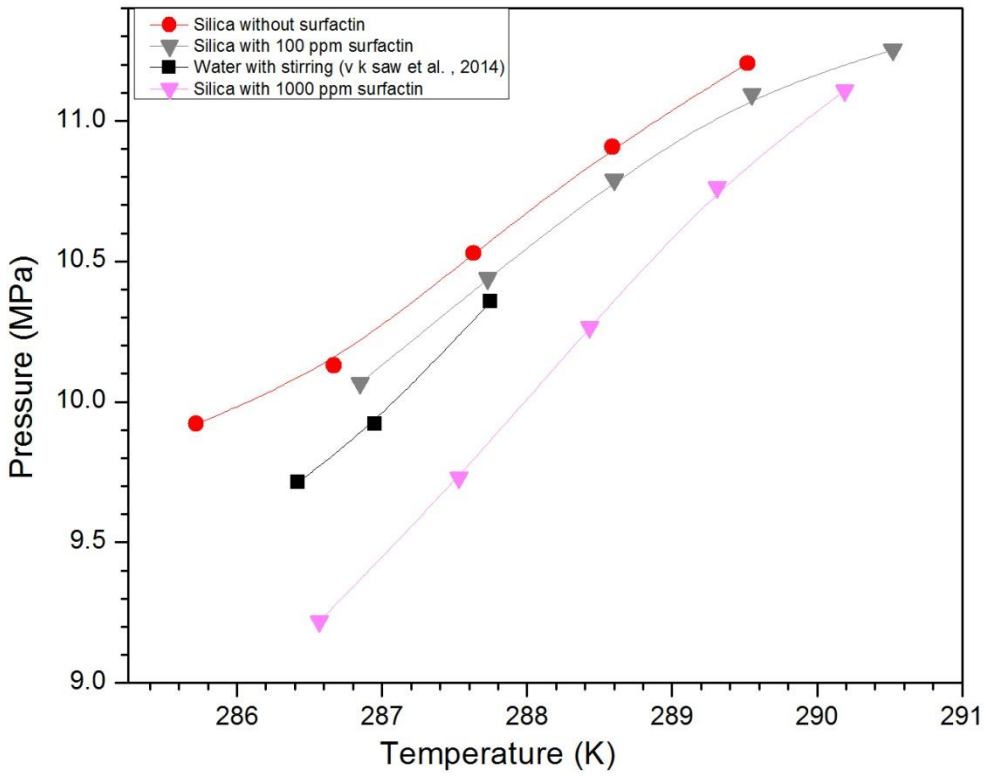

Figure 6.8.4: Phase Equilibrium conditions for various test samples

Thus suggesting that lipopeptides type surfactant is thermodynamic promoter of Methane Hydrate Formation. Interestingly saturating Silica Gel with 1000 ppm surfactin solution performed better than earlier reported agitation mode in presence of tergitol on same system

[Saw et al, 2014]. As phase equilibrium temperature and pressure got shifted to higher and lower values respectively. The results of fixed bed i.e. C-type Silica Gel were also matched with quiescent water with stirring and it was observed that on addition of surfactin, the performance of fixed bed is better than stirring system (v.k.et al.) as shown in Figure 6.8.4.

6.8.1.4 *Dissociation enthalpy of Methane Hydrate*

The Dissociation enthalpies of Methane Hydrates Formation was calculated via Clausius-Clapeyron equation using equation 3 from annexure by differentiating of phase equilibrium pressure-temperature data as shown in Table 6.8.2. For calculating the system while Dissociation is assumed to be at the state of equilibrium and then temperature-pressure data of the Dissociation period can be used to calculate the enthalpy change of Gas component while Dissociation.

The Dissociation enthalpies of Methane Hydrates in presence of C-type Silica Gel saturated surfactin were calculated via Clausius-Clapeyron equation as shown in Table 6.8.2 based upon the measured phase equilibrium data.

Table 6.8.2: Equilibrium temperature, pressure and calculated enthalpy of Dissociation (using Eqn 3)

Type of sample	P (Dissociation) (MPa)	Ln(P) (MPa)	T (Dissociation) (K)	1000/T (k^{-1})	Z factor	ΔH_d (KJ mol^1)
C-type Silica Gel (Merck) containing 100 ppm Surfactin	10.06635	2.309198	286.85	3.486143	0.80195	-
	10.43866	2.345516	287.73	3.47548	0.80082	22.67904
	10.7903	2.378648	288.6	3.465003	0.79881	21.81902
	11.09366	2.406374	289.55	3.453635	0.79843	19.84352
	11.25224	2.420567	290.52	3.442104	0.79957	16.81109
C-type Silica Gel (Merck) containing 1000 ppm Surfactin	9.2189	2.2219	286.57	3.4894	0.8207	-
	9.7285	2.2756	287.53	3.4779	0.8125	30.598
	10.262	2.3286	288.43	3.4674	0.8046	31.345
	10.767	2.3768	289.31	3.4565	0.7975	30.426
	11.104	2.4071	290.19	3.4461	0.7926	27.655

The (P, T) data of equilibrium Figure are plotted as lnP vs 1000/T in Figure 6.8.5. As it is evident from Figure 6.8.5 that, lnP vs 1000/T shows a good linear relationship. The phase equilibrium pressure rises with the rise in temperature.

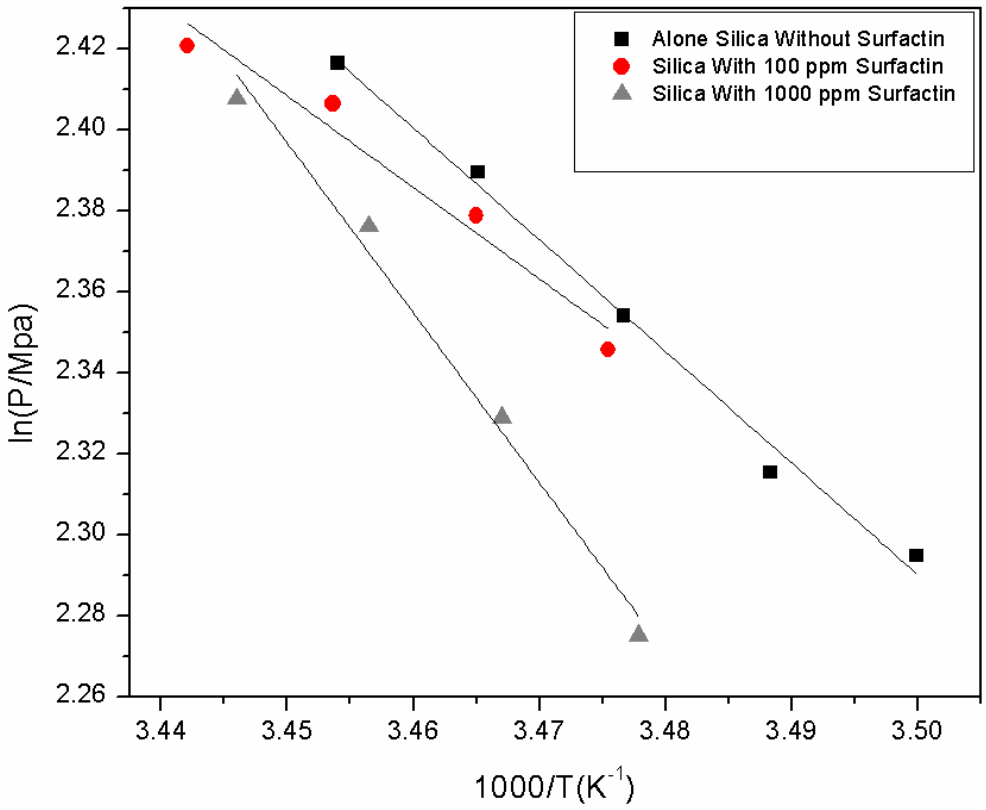

Figure 6.8.5: The (P, T) data of equilibrium are plotted as lnP vs 1000/T.

The data of Dissociation enthalpy of pure Methane Hydrate obtained using Clayperon equation is represented in Table 6.8.2.

As evident from table 6.8.2 presence of surfactin at 100ppm concentration increased the enthalpy of Dissociation as compared to Silica system without surfactin. The enthalpy of Dissociation of Methane Hydrates in the C-type Silica Gel containing surfactin was observed in the range of 16.81 kJ/ mol to 30.59 kJ/mol.

6.8.2 *Kinetic Study*

The kinetic of Methane Hydrate Formation for various experimental condition is as explained below:

6.8.2.1 *Induction Time*

During Hydrate growth, the temperature rapidly rises to a maximum and then it slowly decreases to an initial temperature in Figure 6.8.6. The induction time for various experimental conditions is as shown in table 6.8.3 and Figure 6.8.6 to 6.8.7 as follows.

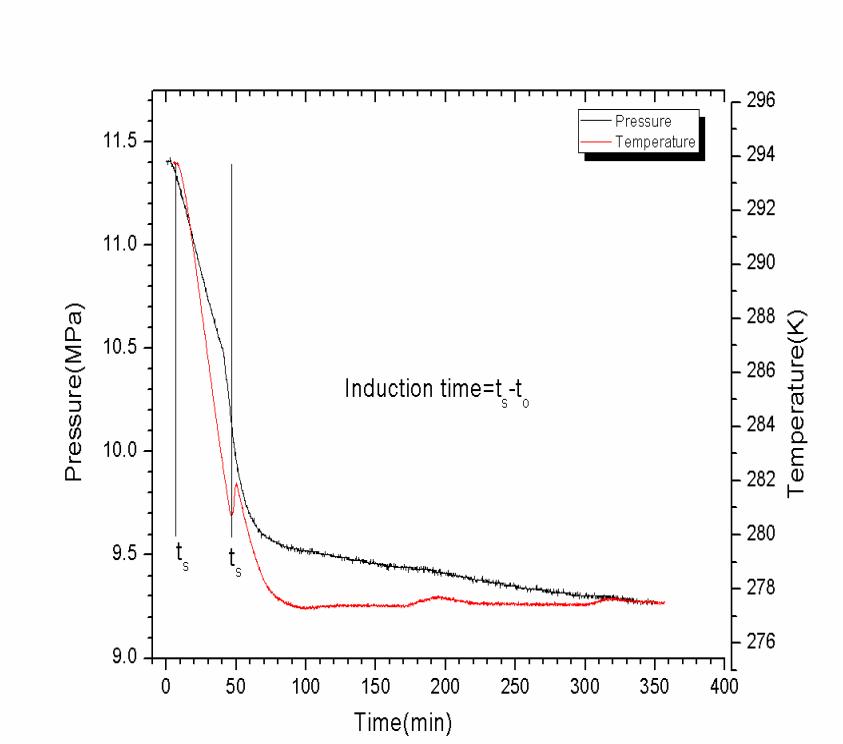

Figure 6.8.6: Induction Time for Methane Hydrate Formation in C-type Silica Gel (Merck) containing 100ppm Surfactin

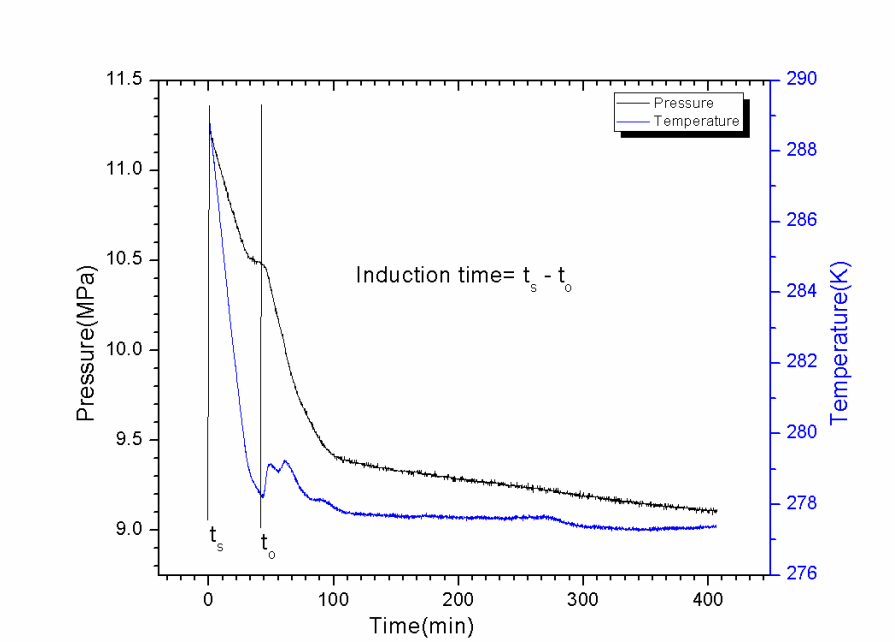

Figure 6.8.7: Induction Time for Methane Hydrate Formation in C-type Silica Gel (Merck) containing 1000 ppm Surfactin

The measured induction time of Hydrate Formation in presence of different concentration of surfactin is given in Table 6.8.3. It is observed that the induction time of Methane Hydrate Formation is decreased in presence of surfactin. However, there is not much effect on increasing the concentration of surfactin on induction time as it is evident from Table 6.8.3. The present study is an agreement with studies by others. Rogers et al (2003) Rogers et al (2003), Woods et al 2004].

Table 6.8.3: Induction time for various experiments

Type of sample	Experiments conducted at Sub-cooling (°C)	Induction Time (min.)
Quiescent water	17.61	196.70
C-type Silica Gel (Merck) without presence of surfactant	13.36	44.24
C-type Silica Gel (Merck) containing 100 ppm surfactin	13.22	41.73
C-type Silica Gel (Merck) containing 1000 ppm surfactin	11.05	39.60

Gas Hydrate promoter of biological origin that can reduce induction time is important for commercial exploitation of Natural Gas Hydrates. Well known microbial surfactants namely rhamnolipids and surfactin, has been reported to decrease the induction times by 58% to 71% relative to the control system without surfactants [Rogers et al, 2003]. The C-type Silica Gel used in the present study has smaller particle size and higher specific area which allowed better interfacial interaction between liquid-Gas phases, thus favoring Hydrate Formation by decreased the induction period. In a porous matrix Hydrates Formation takes place within the pores and in between the interstitial sites [Kumar et al, 2013]. Addition of surfactin solution to C-type Silica Gel decreases interfacial tension between Gas-liquid and subsequently further enhancing the interfacial interaction between Gas and water [Wang et al, 2012, Kumar et al, 2013]. Radich et al, 2009 has observed a synergistic effect between *Bacillus subtilis* surfactin, cells and bentonite in a slurry matrix. Use of aforementioned combination decreased the induction times essential for Formation of Hydrate relative to tests without bentonite. *Bacillus subtilis* has been associated with seafloor Gas Hydrates and surrounding sediments [Lanoil et al, 2001]. Smectite clays in association with biosurfactants such as surfactin, provides heterogeneous nucleation sites of localized high Gas concentrations [Dearman et al, 2007]. Adsorption of surfactin, Natural Gas, and *Bacillus subtilis* to the active smectite surfaces generated a structure-related ordering effect of Gas and water that resulted in reduced and stable induction times [Dearman et al, 2007].

6.8.2.2 *Moles of Methane consumed*

The moles of Methane Gas consumed are calculated by using equation 1 & 2 from annexure.
The pattern of Gas consumed during Formation of Hydrate is shown in Figure 6.8.8. It can be observed that the amount of Gas consumed is greater in presence of 1000 ppm Surfactin.

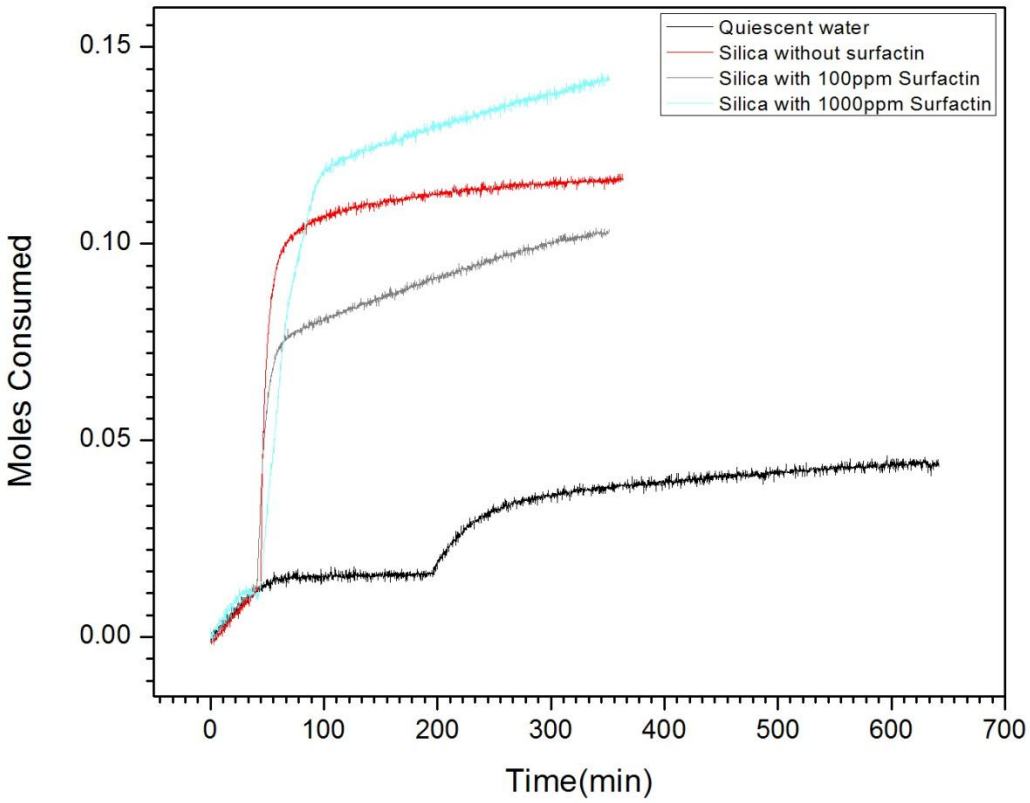

Figure 6.8.8: Moles of Methane consumed while Methane Hydrate Formation for various experimental conditions.

6.8.2.3 *Moles of Methane consumed per mole of water*

The moles of Methane Gas consumed are calculated by using equation 1 & 2 from annexure.

Figure 6.8.9 compares the moles of Methane consumed per moles of water molecules in different systems used in the present study. The Gas uptake in 1000 ppm surfactin solution saturated system was nearly 1.5 times higher than in 100 ppm surfactin solution saturated system. Fixed bed system has been favored several research groups over agitation based system for Hydrate generation as it is energetically affordable means of Methane Hydrate generation [Kumar et al, 2015, Linga et al, 2012]. As compared to quiescent water system rate of Hydrate generation in Silica Gel is rapid due to better Gas-water contact [Kumar et al, 2015]. Earlier, Kumar et al,

2013 has reported that C-type Silica Gel which has smaller particle size and higher specific surface area as compared type-A and type-B C-type Silica Gel leading to better Hydrate conversion. Combination of larger surface area and higher pore diameter promote the rate of Hydrate conversion [Kumar et al, 2015]. Further addition of surfactant increase solubility of Gas molecule in water and thus supporting better interaction between water-Gas systems. This allows easy entry of Gas molecules into Hydrate cages thus supporting better Gas consumption as compared to fixed bed of C-type Silica Gel saturated with water.

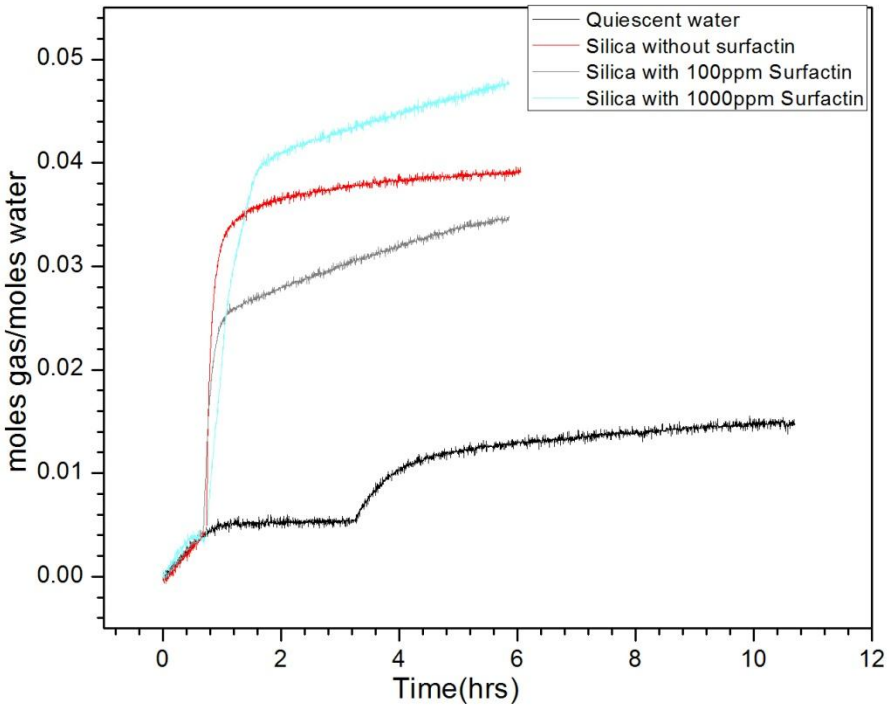

Figure 6.8.9: Moles of Methane consumed / moles of water consumed while Methane Hydrate Formation for various experimental conditions

6.8.2.4 *The growth curve of Methane Hydrate Formation for different Systems*

Figure 6.8.10 to 6.8.11 Shows consumption of Gas and pressure drop as a function of time. The growth and Gas consumption region is exhibiting two symmetric plots that could be interpreted as conservation of mass while the Hydrate growth. Number of Methane molecules escaping from the Gas phase to Hydrate phase is expressed by the pressure drop, whereas the number of

Methane molecules inserting in the Hydrate cages is expressed by the Gas consumption plot. As mass must be conserved in an isochoric system, the two plots display symmetry about an axis passing through the intersection of the two plots and parallel to the time axis. As shown in Figure 6.8.10 to 6.8.11, the process is splitted into five regions. First region is starts at time zero where the system has less consumption of Gas and pressure slightly decreases because dissolution of Gas. Second region is after the induction time where consumption of Gas increases, this is due to the Hydrate growth. From the third region to fifth region, as the Hydrate is formed, consumption of Gas is as shown in figure 6.8.10 to 6.8.11.

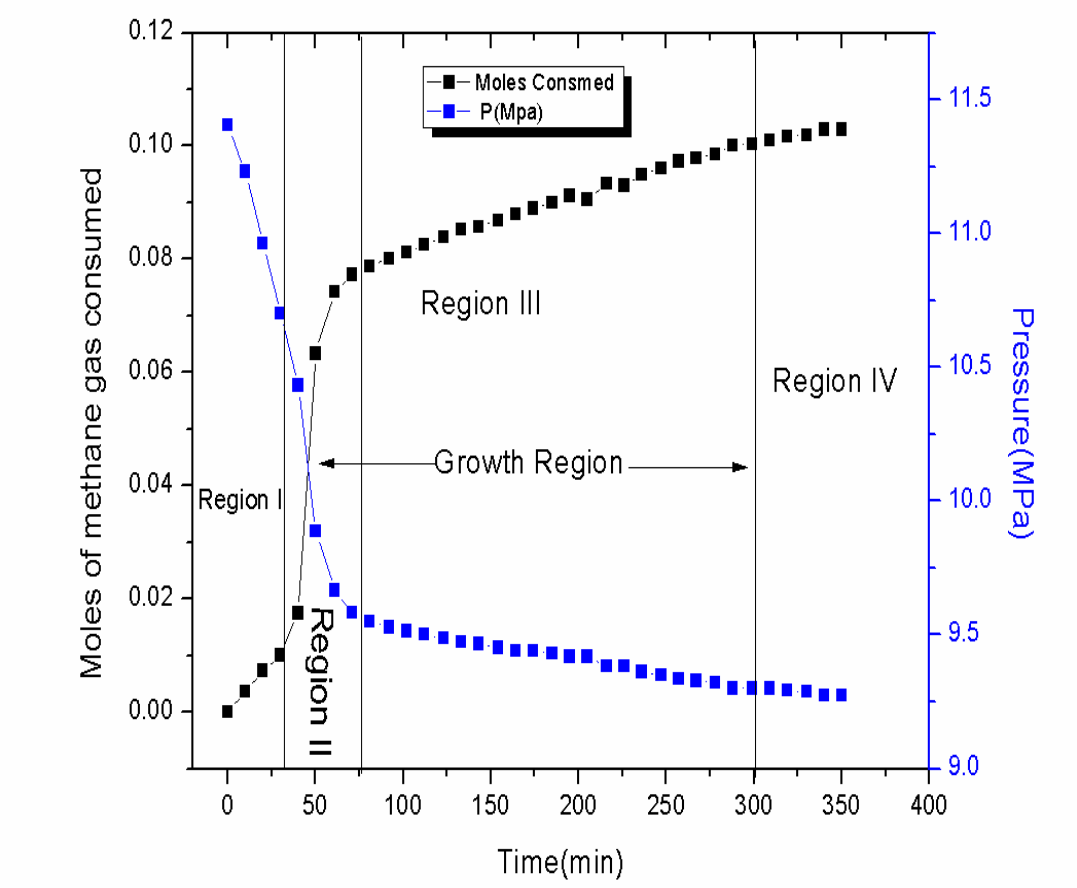

Figure 6.8.10: Growth curve of Methane Hydrate Formation in C-type Silica Gel in presence of 100 ppm Surfactin.

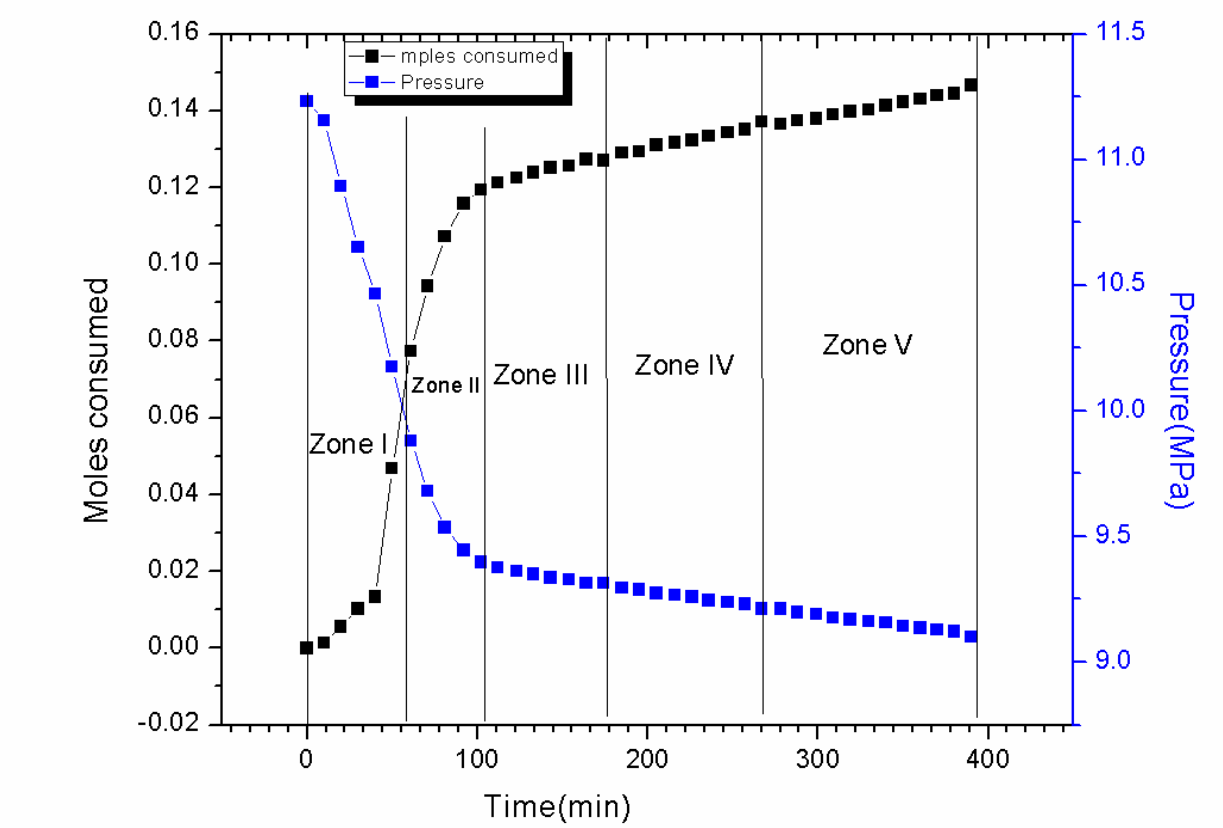

Figure 6.8.11: The growth curve of Methane Hydrate Formation in C-type Silica Gel containing 1000 ppm Surfactin.

6.8.2.5 *The rate of Methane Hydrate Formation for different experimental conditions*

As seen, the slope of the curves after nucleation exhibits an exponential behaviour Figures 6.8.12 and 6.8.14, from which we can assume that it is a first-order reaction. A first order reaction is defined by the equation 4 from annexure.

Rate of constant k of Hydrate Formation can be calculated from the slope of the curve of ln (N/N_0) vs t using equation 5 from annexure. The Hydrate Formation from region 2 onwards of figures 6.8.12 and 6.8.14 was splitted into five zones of time as shown in Figures 6.8.13 and

6.8.15 (0-20, 20-40, 40-80, 80-160,160-260 min) after nucleation. This may be because of different rate of Hydrate Formation that gives different reaction rate and hence different rate constant. The data of these five zones are used to determine the rate constant of Hydrate Formation in each zone. The Formation rate is usually indicated by the rate by which the amount of Methane molecule is converted to Hydrate. Hydrate Formation rate is calculated by placing the values of slopes i.e. rate constant k obtained from figure 6.8.13 and 6.8.15 in equation 6 from annexure.

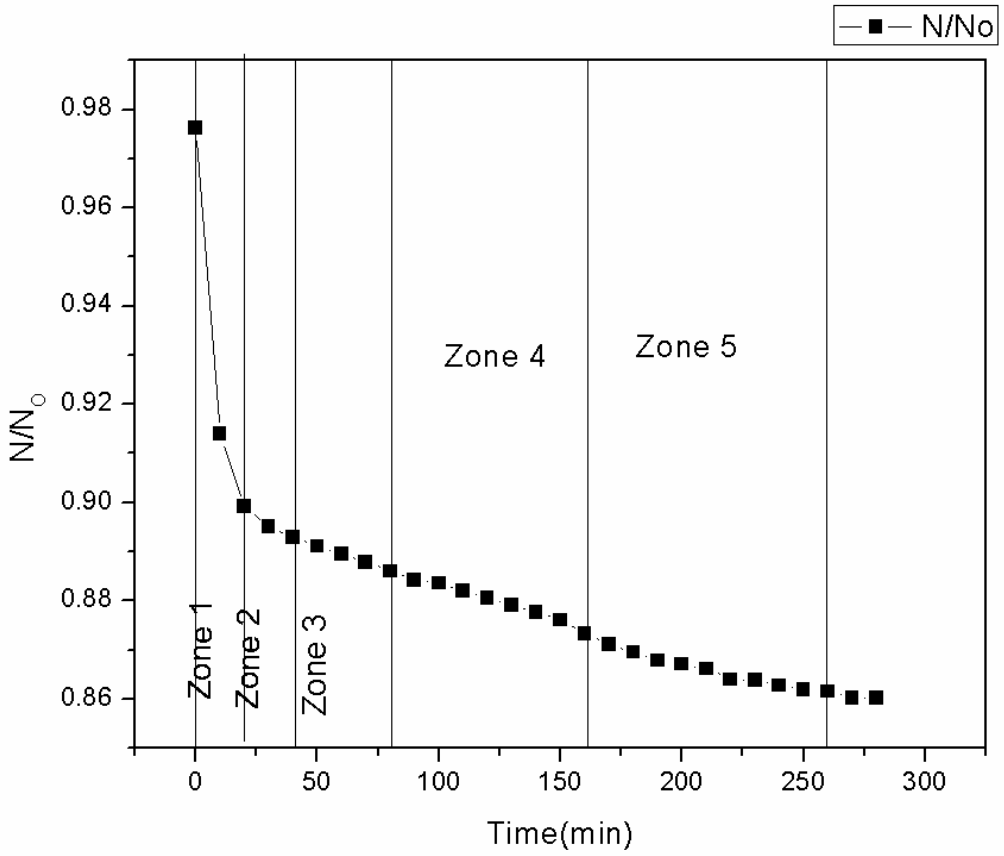

Figure 6.8.12: N/N_0 vs Time Plot for Methane Hydrate Formation in presence of C-type Silica Gel (Merck) containing 100 ppm Surfactin.

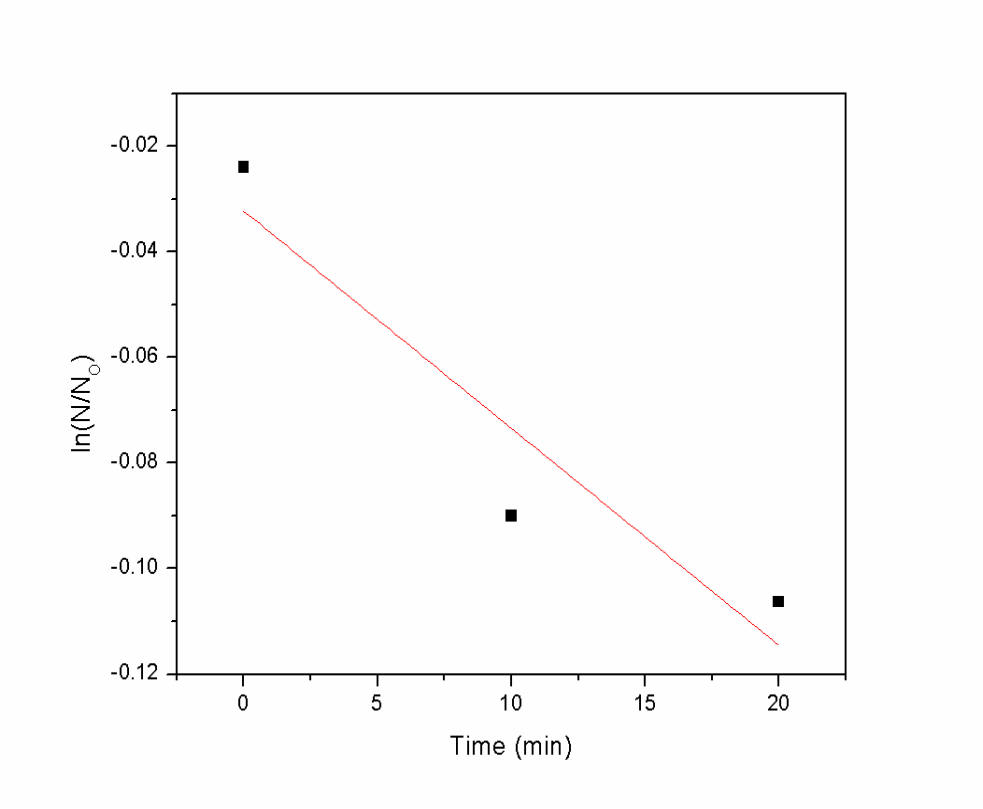
-0.02
-0.04
-0.06
-0.08
-0.10
-0.12
ln(N/N$_O$)
0
5
10
15
20
Time (min)

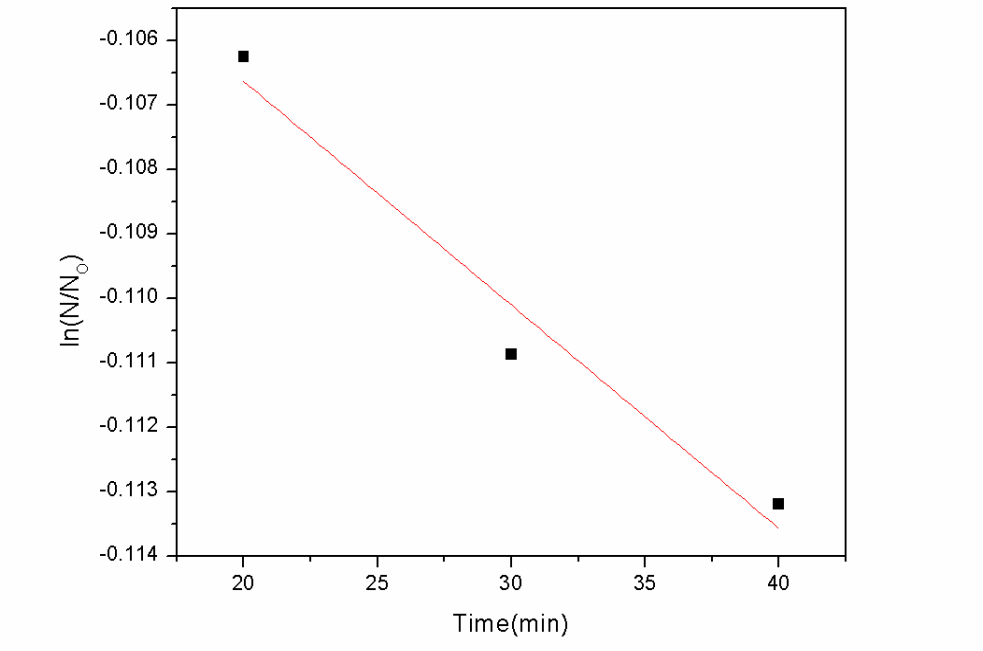
-0.106
-0.107
-0.108
-0.109
-0.110
-0.111
-0.112
-0.113
-0.114
ln(N/N$_O$)
20
25
30
35
40
Time(min)

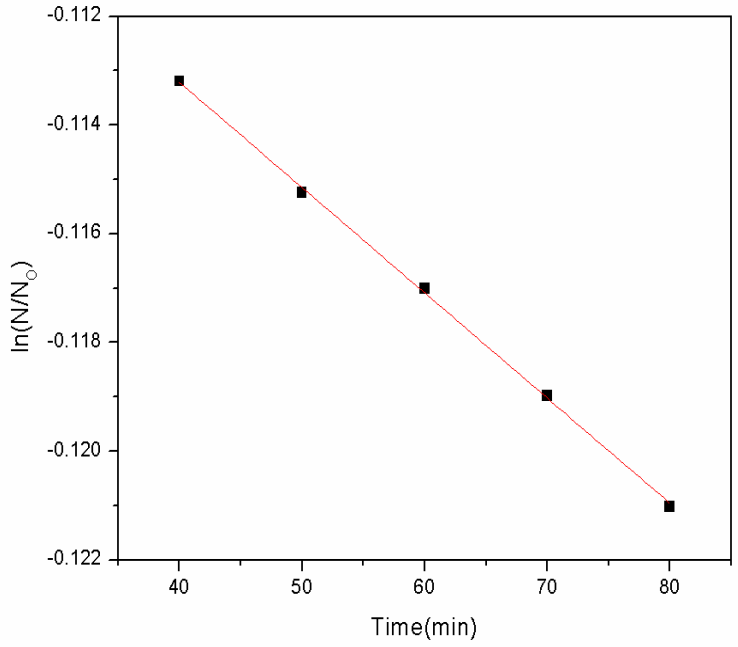
-0.112
-0.114
-0.116
-0.118
-0.120
-0.122
ln(N/N$_O$)
40
50
60
70
80
Time(min)

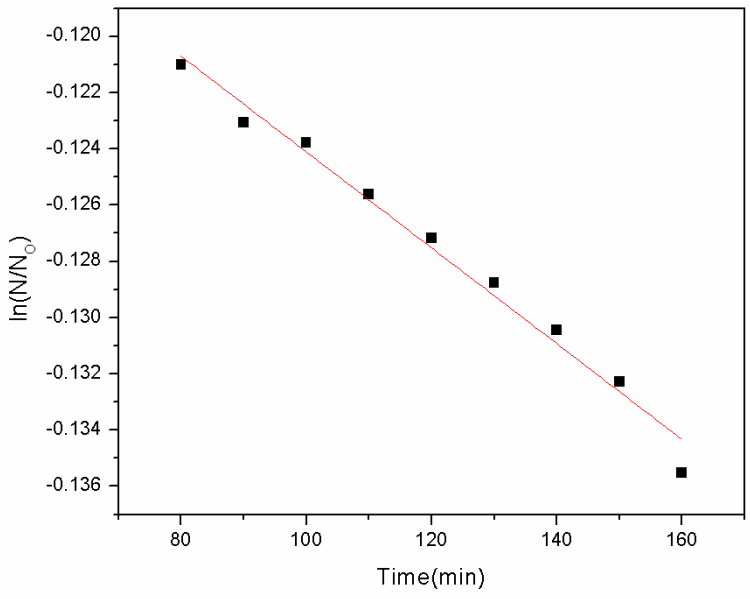
-0.120
-0.122
-0.124
-0.126
-0.128
-0.130
-0.132
-0.134
-0.136
ln(N/N$_O$)
80
100
120
140
160
Time(min)

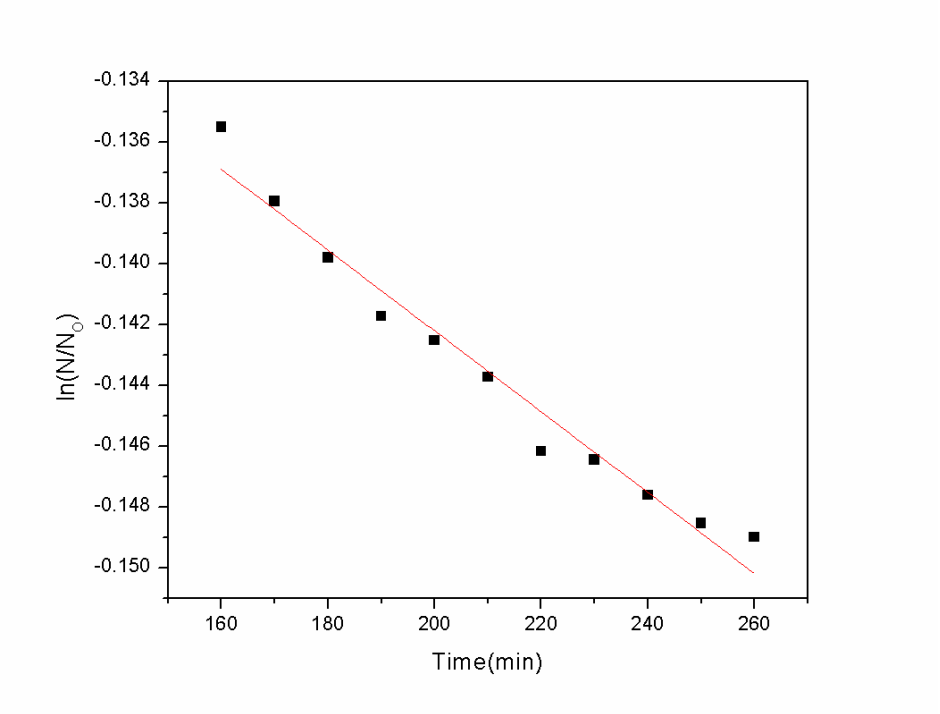

Figure 6.8.13: Semi-logarithmic plot of change of moles of Gas while Methane Hydrate Formation in presence of C-type Silica Gel (Merck) containing 100 ppm Surfactin.

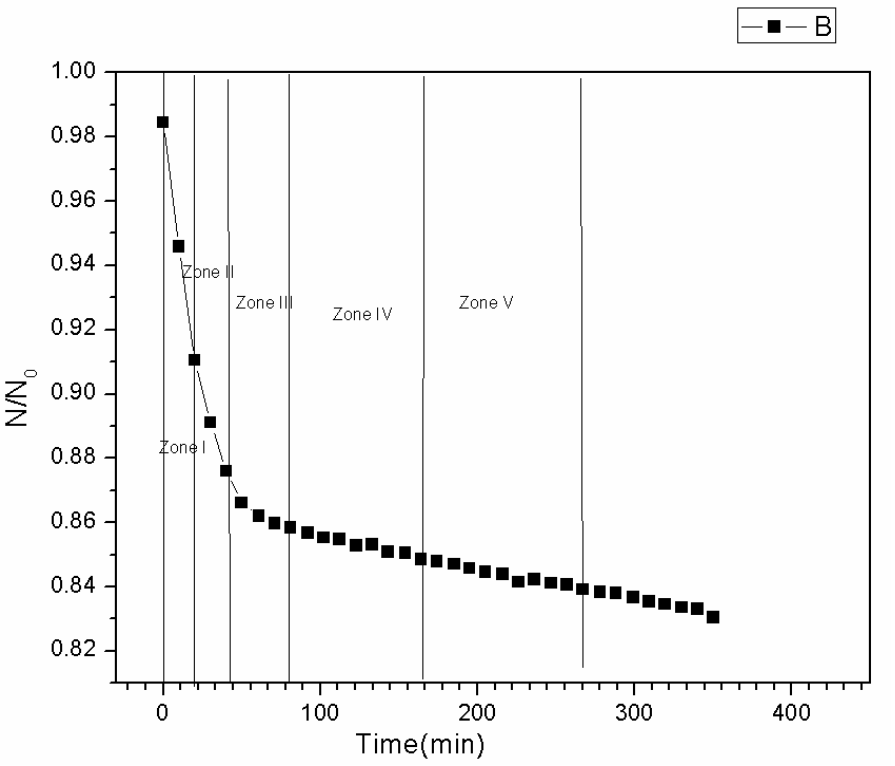

Figure 6.8.14: N/N_0 vs Time Plot for Methane Hydrate Formation in presence of C-type Silica Gel containing 1000 ppm Surfactin.

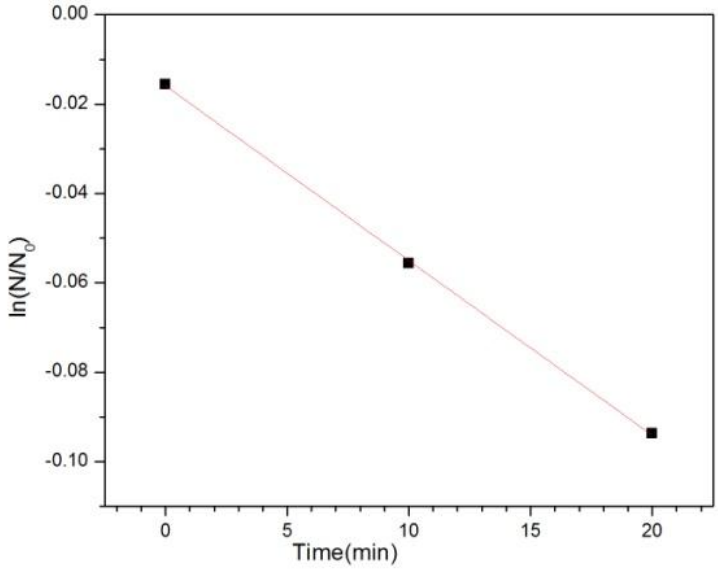
0.00
-0.02
-0.04
-0.06
-0.08
-0.10
ln(N/N0)
0
5
10
15
20
Time(min)

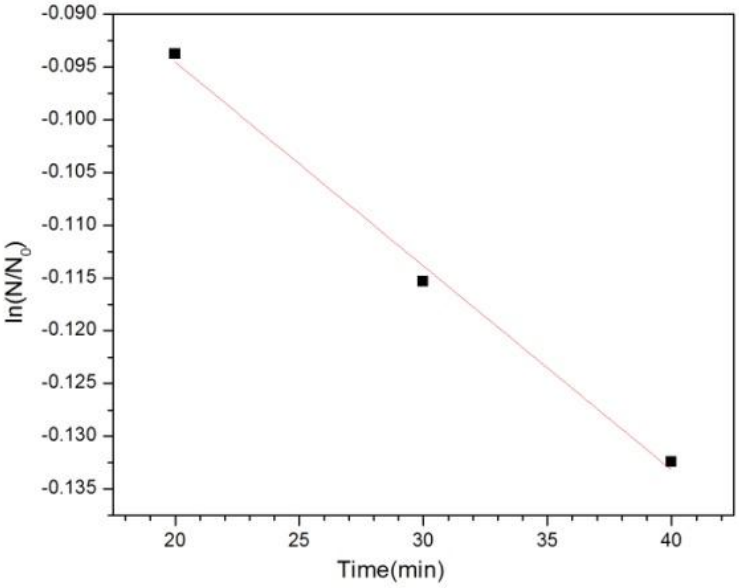
-0.090
-0.095
-0.100
-0.105
-0.110
-0.115
-0.120
-0.125
-0.130
-0.135
ln(N/N0)
20
25
30
35
40
Time(min)

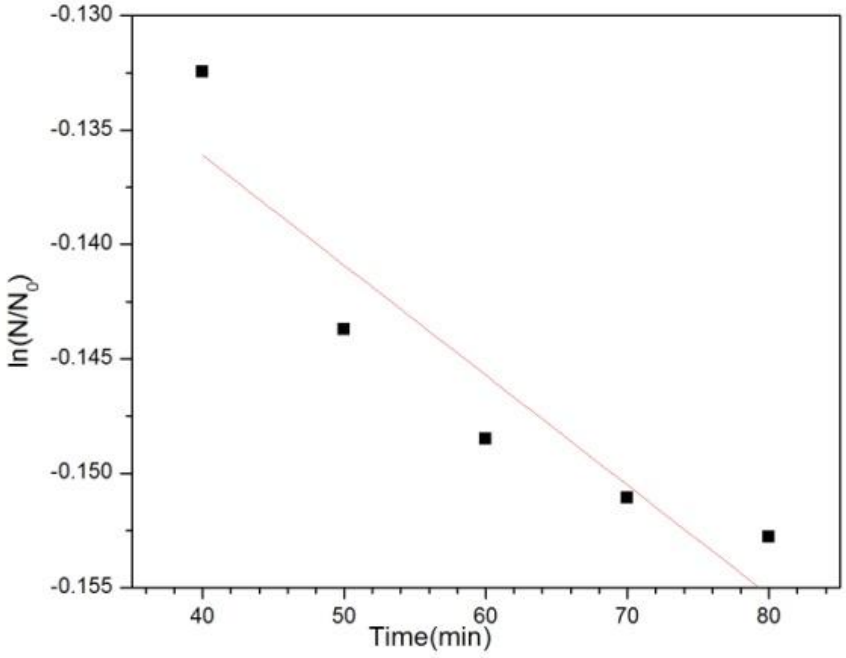
-0.130
-0.135
-0.140
-0.145
-0.150
-0.155
ln(N/N0)
40
50
60
70
80
Time(min)

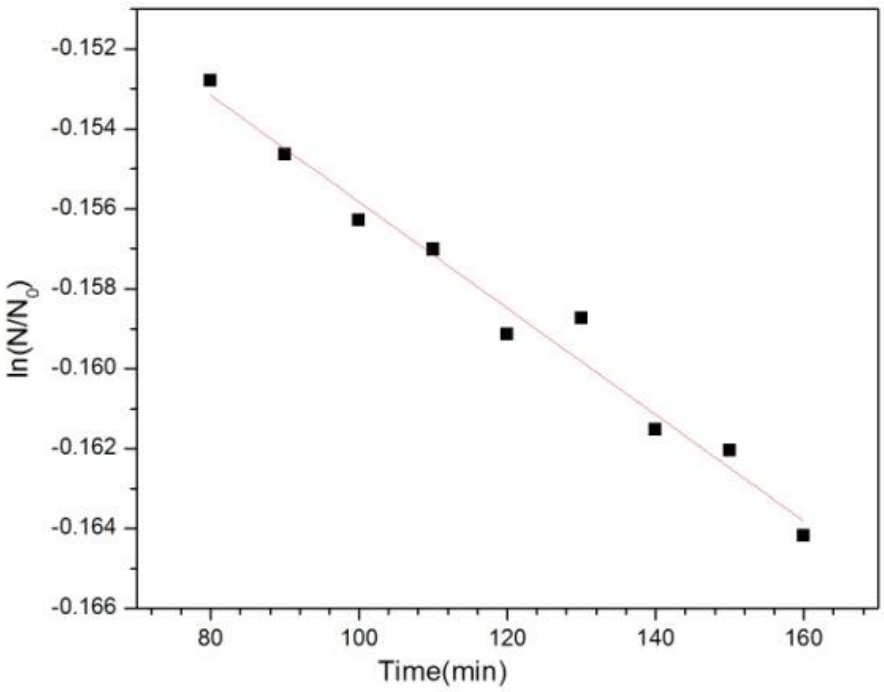
-0.152
-0.154
-0.156
-0.158
-0.160
-0.162
-0.164
-0.166
ln(N/N0)
80
100
120
140
160
Time(min)

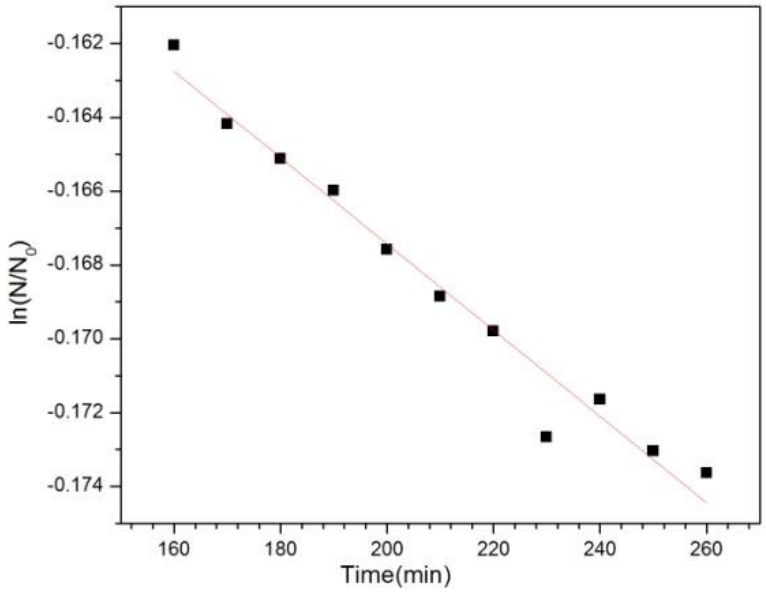

Figure 6.8.15: Semi-logarithmic plot of change of moles of Gas while Methane Hydrate Formation in presence of C-type Silica Gel containing 1000 ppm Surfactin.

Firstly it is observed that the rate of Hydrate Formation is almost same. But while the growth rate of Hydrate was found to depend on the concentration of surfactin. The rate of Hydrate growth is increased by the presence of surfactin many more times as compared to the absence of surfactin. It is noticed that 1000 ppm surfactin increased the overall rate of Hydrate growth relatively more. This enhancement of rate in the present study is an agreement with work carried out by others (Rogers et al (2003), Rogers et al (2003), Woods (2004). Rogers et al (2004). Methane Hydrate Formation rates are determined and are shown from Figures 6.8.16 to 6.8.21 and in table 6.8.4, which exhibits that there are much variation in the presence of surfactin in Methane Hydrate Formation rate.

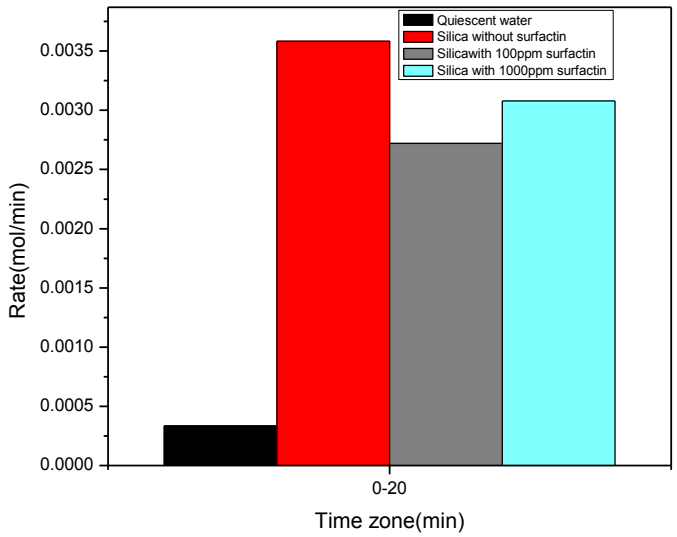

Figure 6.8.16: Methane Hydrate Formation rate for time zone 0 to 20 minutes.

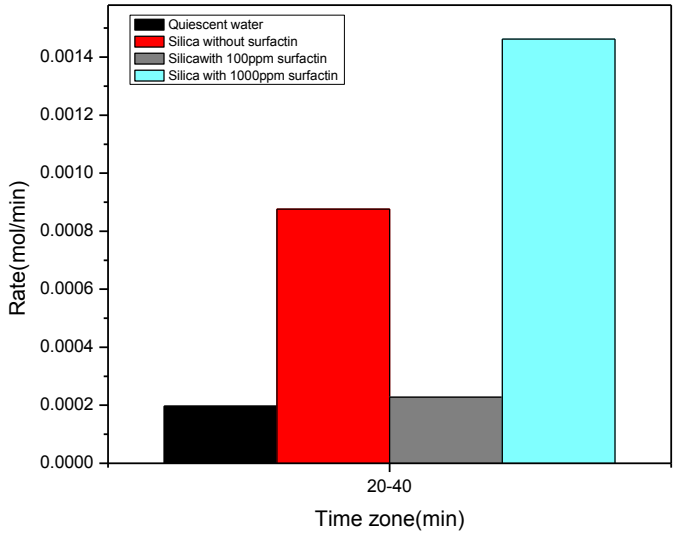

Figure 6.8.17: Methane Hydrate Formation rate for time zone 20 to 40 minutes.

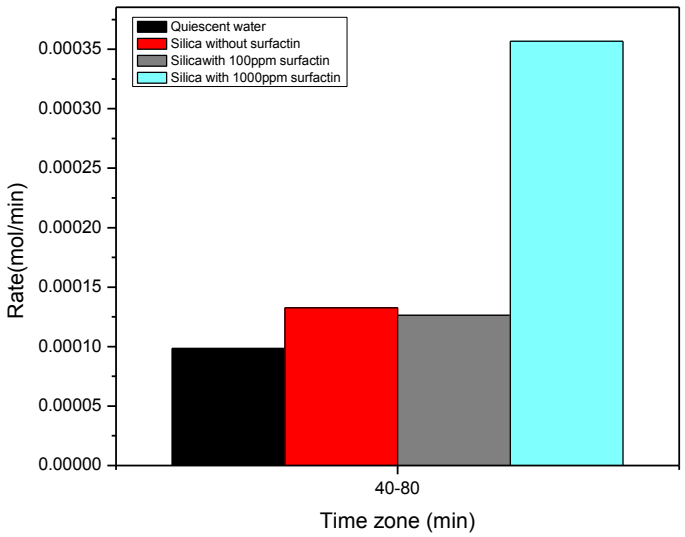

Figure 6.8.18: Methane Hydrate Formation rate for time zone 40 to 80 minutes.

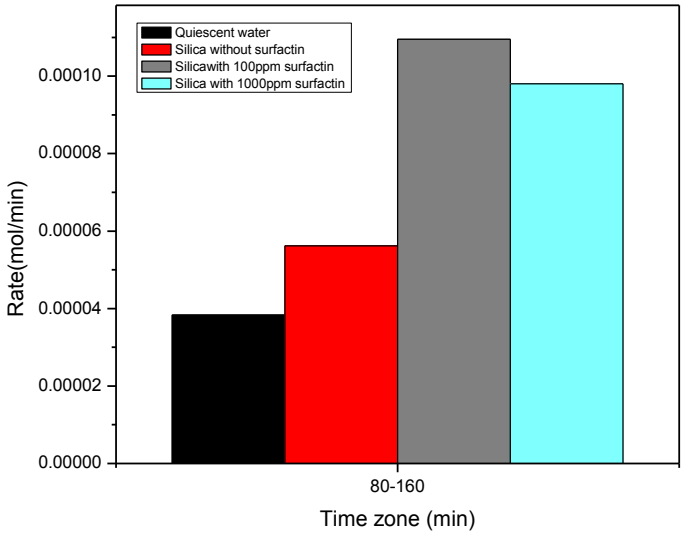

Figure 6.8.19: Methane Hydrate Formation rate for time zone 80 to 160 minutes.

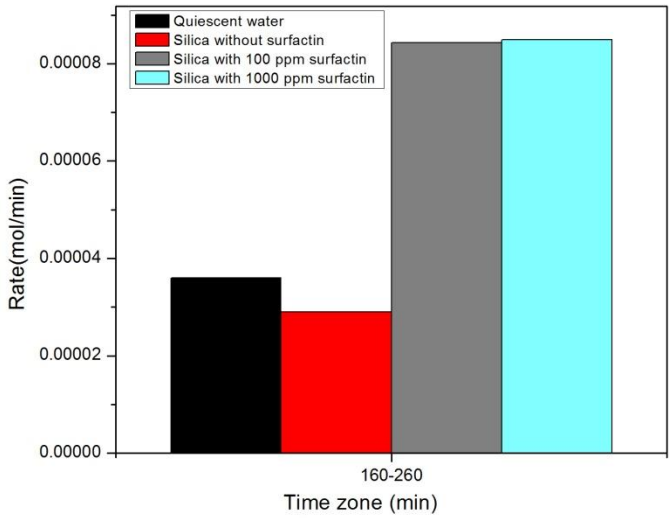

Figure 6.8.20: Methane Hydrate Formation rate for time zone 160 to 260 minutes

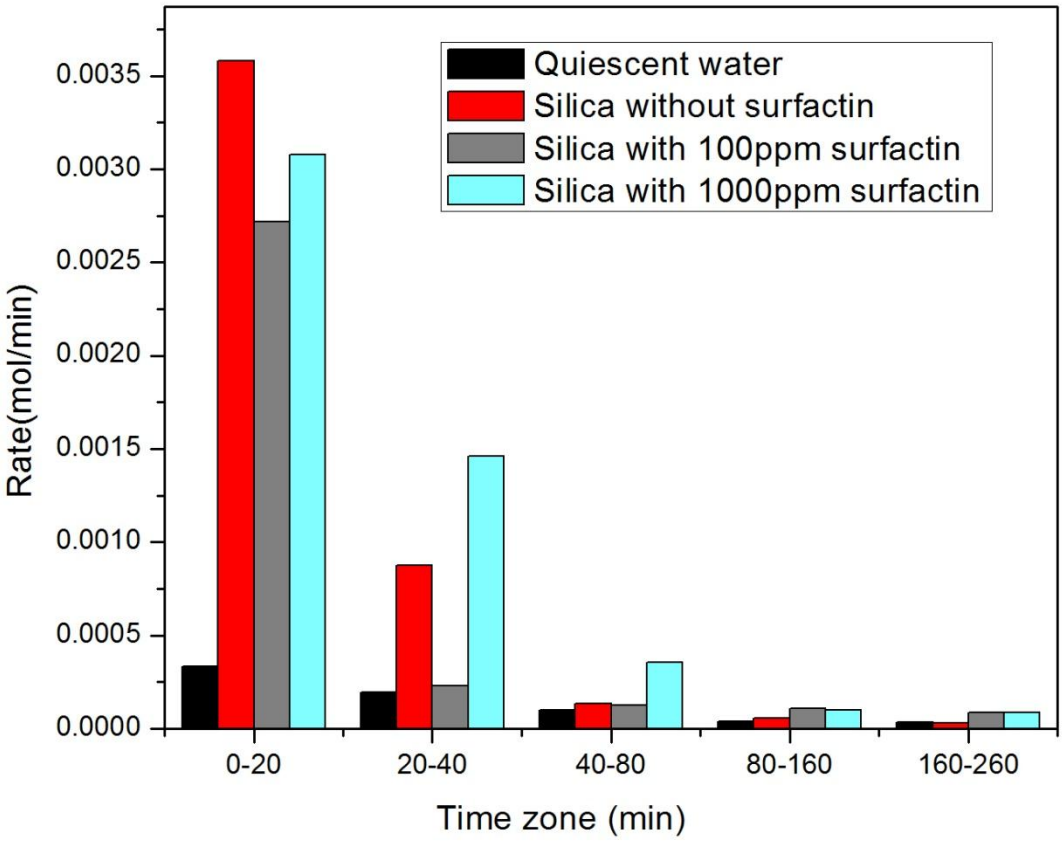

Figure 6.8.21: Comparison of rates of Methane Gas Hydrate Formation for different time zone in different experiment condition

Table 6.8.4: The rate of Methane Gas Hydrate Formation for different experimental condition

Type of sample	Time Zone (Min)	Rate constant K (min^{-1})	Formation rate (mole/min)	% over all increased rate with respect to Silica
C-type Silica Gel containing 100 PPM Surfactin	0-20	4.11E-03	2.72E-03	36.58579174
	20-40	3.47E-04	2.28E-04	
	40-80	1.94E-04	1.26E-04	
	80-160	1.70E-04	1.10E-04	
	160-260	1.33 E-04	8.43E-05	
C-type Silica Gel containing 1000 PPM Surfactin	0-20	3.91E-03	0.003079427	97.83
	20-40	1.93E-03	.001462369	
	40-80	4.81E-03	0.000356753	
	80-160	1.33E-04	9.86208E-05	
	160-260	1.17E-04	8.49792E-05	

6.8.2.6 *Water to Hydrate conversion*

The water to Methane Hydrate conversion is calculated using equation 7 & 9 from annexure.

Figure 6.8.22 compares the percentage conversion till 330.0 minutes for quiescent water, Silica Gel saturated with distilled water without surfactant; water saturated C-type Silica Gel with 100 ppm and 1000 ppm surfactin solution. As it is evident from figure 6.8.22 at the same time i.e. 330 minutes the % conversion is 7.28 % for quiescent water, 22.16 % for C-type Silica Gel saturated with water without biosurfactant, 19.6 % for water saturated C-type Silica Gel with 100 ppm surfactin solution and 26.71 % for water saturated C-type Silica Gel for 1000 ppm surfactin solution. The conversion for C-type Silica Gel in presence of 100 ppm surfactin solution is 19.6 %. This is because of at lower dose i.e. 100 ppm surfactin the behaviour of the system matches with the fixed bed media of C-type Silica Gel and it influences on the system is not much more pronounced.

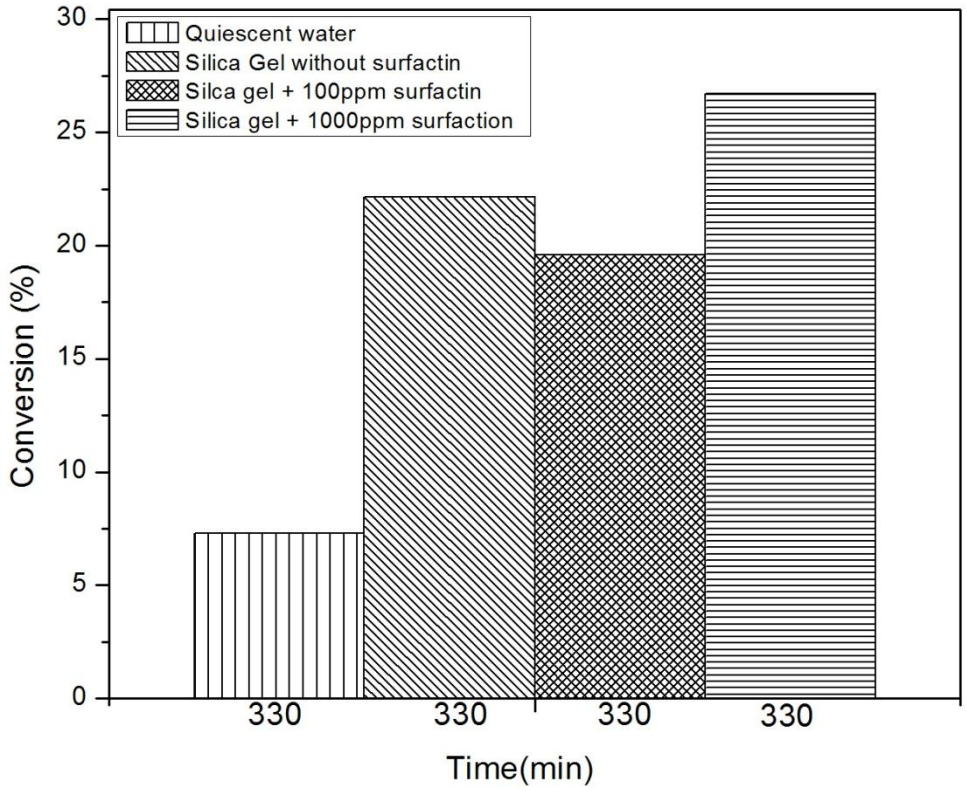

Figure 6.8.22: Conversion (%) of Methane Hydrate for various experiments

At a given time the percentage of Hydrate conversion is more in presence of 1000 ppm surfactin and the conversion till end of the reaction is also maximum for 1000 ppm surfactin and is reported to be 27.9 percent for 390 minutes. The conversion till the end of the reaction for quiescent water is 8.43 percent for 642.1 minutes, for C-type Silica Gel without the presence of surfactin the conversion is 22.2 for 363 minutes and the conversion till end of the reaction for 100 ppm surfactin is 19.78 for 350 minutes.

Adding surfactant at concentration above CMC to Gas Hydrate forming system increases Gas solubility in water. However, the surfactant concentration below or around the CMC, the solubility of the Gas remains similar to that of pure water [Rogers et al, 2003]. In present study the Methane Hydrate promotion activity at 1000 ppm surfactin solution was better than 100 ppm surfactin solution. Surfactin used in the study have CMC of 33mg/l at 25°C. It was observed that 1000 ppm surfactin solution shows better water to Hydrate conversion probably due to better Gas water solubility compared to100 ppm surfactin solution.

The Formation rate is usually considered by the rate by which the amount of Methane molecule is converted to Hydrate. Hydrate Formation process was accompanied by growth in the number moles of Methane consumed and subsequent reduction in the pressure. Initially (0-20 min), the most rapid Methane consumption was observed in water saturated C-type Silica Gel system whereas slowest Methane consumption was observed in quiescent water system. However, for rest of the time rate of Methane Hydrate Formation in terms of moles of Methane consumed was maximum in 100 ppm and 1000 ppm surfactin saturated C-type Silica Gel systems.

Gas consumed during Methane Hydrate generation gets trapped into cages like lattice structure of water molecule formed by water under high pressure and low temperature. In non-stirring system Methane Hydrates primarily begin to crystallize at the Gas-liquid interface and not in the bulk phase of water. Hence, nucleation and growth occur at surface which further preventing the mass transfer across the film and subsequently slowing kinetics and lowering water to Hydrate conversion [Wang et al, 2012].

"Surfactant micelle hypothesis" was proposed by Rogers and his co-workers [Zhong et al, 2000, Kothapalli, 2002, Rogers et al, 2003, Woods, 2004, Rogers et al, 2004, Taylor et al, 2004, Rogers et al, 2005, Rogers et al, 2007]. Micelles are made up of colloidal aggregates which are formed by surfactants in solution when the concentration of the surfactant is exceeds CMC. This above hypothesis was augmented by Watanabe et al, 2005 and it was suggested that micelles cannot be formed by many surfactants including SDS at a Hydrate Formation temperature. The minimum temperature at which the micelles can be formed is called krafts point the point. The krafft point of lipopeptide is around 0 ^{0}C i.e. 273 K. Nnanna et al 2001 that means surfactin can for micelle around 0 ^{0}C which is the Hydrate Formation temperature in current study which supports the micelle Formation in the current study. However, Watanabe et al 2005 conclusion was withdrawn from HFC-32 fluorohydrocarbon-Gas/water/ SDS system at low pressure. The results were then extrapolated to Methane/water/SDS system which was not evaluated by Watanabe. The interactions of these two system would be quite different. The SDS micelle core of associated alkyl groups solubilized the Natural Gas but the core don't have the affinity for the HFC-32 because of strong polarity of flouric Gas molecules. With non-polar Methane Sun et al 2004 concluded that CMC of SDS decreases at Hydrate Formation temperatures under Methane pressure. Moreover, the kraft point of SDS revealed by various groups i.e Weil et al, 1963, Lange et al, 1968 range from 16 ^{0}C to 8 ^{0}C point out that kraft point is very much sensitive to

conditions of test. It gets lowered by surfactant solute interactions. Sun et al 2004 with pendant-drop method of surface tension has reported that CMC of SDS is also decreased 500 ppm under the pressure of Methane at 273.3 K in comparison with CMC of SDS at ambient conditions around 2500 ppm [Flockhart, 1961]. Moreover Zhong et al, 2000 filmed ethane as well as Natural Gas Hydrate crystals which reported miceller forming SDS. This hypothesis of possible miceller enhancement of Hydrates was also supported by Sun et al, 2004, So it is very much unrealistic to agree with Watanabe's conclusion, 2005 that there is absence of micelles at Hydrate forming conditions in SDS water and hydrocarbon Gas system.

Surfactin produced by strain A21 was used as a low dosage additive for enhancing Methane Hydrate Formation in fixed bed system consisting of C-type Silica Gel. Earlier, Kumar et al, 2013 has observed that the use of synthetic surfactant in combination with C-type Silica Gel favours higher Gas consumption as well as reduces the induction time of CO_2 Hydrate Formation. The induction time in Methane Hydrate crystallization is one of the important parameters used to describe kinetics. Induction time of Gas Hydrate Formation is the appearance of very first Hydrate cluster of super-nucleus size capable of spontaneously outgrowing to a macroscopic size [Volmer, 1939]. Chemical additives such as surfactants has been reported to decrease the induction time, thus decreasing the time required for growing Methane Hydrate crystal and consequently hastening the crystal growth [Ando et al, 2012].

Onset of Hydrate Formation coincides with a spike in temperature profile as Hydrate Formation is an exothermic process [Karaaslan et al, 2002]. Formation of hydrogen bonded crystalline structure releases heat which appears as a sudden increase in reactor temperature [Handa et al, 1986]. Using aqueous solution of surfactin for saturating C-type Silica Gel reduced induction time significantly as compared to the unstirred water system and water saturated C-type Silica Gel system.

Reduction in induction time is important for commercial exploitation of Gas Hydrate based technologies like Hydrate based Gas separation process [Eslamimanesh et al, 2012], Hydrate based desalination [Cha et al, 2013] or storage and transportation of Natural Gas in Hydrate form [Wang et al, 2012]. Biosurfactant like rhamnolipids, surfactin, has been reported to decrease the induction times by 58% to 71% relative to the control system without surfactants [Rogers et al, 2003]. The induction time for Hydrate nucleation in a quiescent system is effected by super-

saturation, the presence of additives and foreign particles, interfacial tension of Hydrate-liquid, etc [Kashchiev et al, 2003]. The C-type Silica Gel used in the present study has smaller particle size and higher specific area which allowed better interfacial interaction between liquid-Gas phases, thus favouring Hydrate nucleation by decreasing the induction period. In a porous matrix Hydrates Formation takes place within the pores and in between the interstitial sites [Kumar et al, 2013]. Addition of surfactin solution to C-type Silica Gel decreases interfacial tension and subsequently enhances the contact between Gas and water [Kumar et al, 2013, Wang et al, 2012].

Radich et al, 2009 has observed a synergistic effect between *Bacillus subtilis* surfactin, cells and bentonite in a slurry matrix. Use of aforementioned combination reduced the induction times necessary for Hydrate Formation relative to tests without bentonite. *Bacillus* subtilis has been associated with seafloor Gas Hydrates and surrounding sediments [Lanoil et al, 2001]. Smectite clays in association with biosurfactants such as surfactin, provides heterogeneous nucleation sites of localized high Gas concentrations [Dearman, 2007, Wang et al, 2012]. Surfactin, Natural Gas, and *Bacillus subtilis* tends to get absorbed to active smectite surface for generating a ordered structure that causes reduction in induction time during Hydrate Formation [Dearman, 2007, Wang et al, 2012].

The Formation rate is usually considered by the rate by which the amount of Methane molecule is converted to Hydrate. Hydrate Formation process was accompanied by increase in the moles of Methane consumed and subsequent decrease in the pressure. The most rapid Methane consumption was observed in 1000 ppm surfactin solution saturated C-type Silica Gel system. Table 6.8.4 compares the rate of Methane Gas Hydrate Formation in fixed bed system of C-type Silica Gel saturated with different concentration of surfactin solution. The use of 100 ppm and 1000 ppm surfactin solution increased the overall Methane Hydrate Formation rate by 36.5% and 97.8% respectively.

It is possible that excessive addition of surfactant may decrease Hydrate Formation rate as surfactant molecules may cover the water-Gas interface, which in turn reduces contact between the guest molecule and water, ultimately reducing the effective surface area for Hydrate Formation. However, in fixed bed media as used in this study no such effects was observed at 1000ppm surfactin concentration. Ganji et al. 2006, has observed that linear alkyl benzene sulfonate (LABS) decreased Hydrate Formation rate at 300 ppm but enhanced the same at

500ppm and 1000ppm. Similarly, cetyltrimethyl ammonium bromide (CTAB) and ethoxylated nonylphenol (ENP) decreased Hydrate Formation at 300 and 500ppm but supported Hydrate Formation rate at 1000 ppm [Ganji et al, 2006].

Carvajal et al, 2013 reported that overall, consumption of Methane was higher in biosurfactant (surfactin and rhamnolipids) and biosurfactant–smectite experiments system than smectite–clay experiments. Surfactin was observed to be better than rhamnolipids as overall Methane consumption in rhamnolipids system was almost similar to that of surfactin containing system even though the surfactin concentration was nearly ten times lower [Carvajal et al, 2013]. Zhong et al, 2000, reported that there is an increase in ethane consumption when Hydrates were formed from solutions containing 284 ppm synthetic surfactant SDS.

Surfactin change the Methane Hydrate Formation temperature to higher value compared to Hydrate Formation without presence of surfactin figure 6.8.3. Also it is observed that the equilibrium temperature and pressure of Methane Hydrate Formation is also shifted to far higher and lower values respectively Figure 6.8.4. It is also observed that the induction time of Hydrate Formation is reduced in presence of surfactin Table 6.8.3. The rate of Hydrate Formation is found to increase many more times in presence of surfactin Table 6.8.4. Therefore it is concluded from above results that the Methane Hydrate Formation is promoted thermodynamically and kinetically both in presence of surfactin. 1000 ppm of surfactin in presence of C-type Silica Gel has shifted the equilibrium curve of Methane Hydrate Formation towards the higher temperature and lower pressure zone than the result obtain in the agitation mode as reported by Saw et al, 2014 for the same system. At 1000 ppm the performance of surfactin as thermodynamic promoter is better than 100 ppm of surfactin. Even the reduction in induction time and Gas uptake at 1000 ppm surfactin is far better than 100 ppm surfactin. The above study is in agreement with the studies carried out on biosurfactant [Rogers et al, 2003, Woods, 2004, Rogers et al, 2004, Rogers et al, 2007, Rogers et al, 2011] and moreover these results are also supported by various studies carried out on synthetic anionic surfactants like SDS, LABS, SDBS by various groups [Saw et al, 2014, Mandal et al, 2008, Karaaslan et al, 2000, Dai et al, 2014].

The work with synthetic surfactants put the question: Is the role of microbes in ocean sediments is to produce the biosurfactants that would catalyse Gas Hydrate Formation and influence their

accumulation on specific porous media surfaces [Rogers et al, 2004] which has been satisfactorily answered by present study.

Water-borne microbes in soils mixed with relatively water insoluble hydrocarbons may synthesize a surfactant to solubilize and make available the carbon source Bai et al, 1997. Lipopeptide surfactin from the *Bacillus subtilis* microorganism is the most powerful biosurfactants, and it can reduced surface tension of water to as low as 27 mN/m [Nakanao et al, 1988]. The CMC of surfactin is reported to be 25 ppm Rosenberg et al, (1993). In the present study surfactin has lowered the surface tension of water from 70 mN/m as low as 29 Mn/m and CMC to 33 ppm. The promotional effects of surfactin are observed due to the Formation of biosurfactant micelles. Thus, extremely small concentrations of biosurfactant in pore waters of ocean sediments can reach the CMC as it is very low and can promote Gas Hydrate Formation.

Water branches around the periphery of the micelle in close proximity to the solubilized Gas. Thus, micelles plays the role of nucleation sites for Hydrate crystals and promotes the Hydrate Formation. The surfactin synthesized from strain A21 has reduced the surface tension of water and CMC both which in turn aids the cages of water and encapsulation of Methane Gas and changing them to Hydrate. Surfactin act as promoter which can help in synthesizing Gas Hydrates. This phenomenon may be used to develop a cost effective procedure for Natural Gas storage in Gas Hydrates for industrial applications such as to supply fuel for electrical power plants at peak loads, a feasible Natural Gas storage process is in demand for other applications as well. The present study has found the performance of fixed bed media of C-type Silica Gel better than agitation mode of synthesizing Gas Hydrates. Moreover the performance of this fixed bed media of C-type Silica Gel as promoter has increased many folds in presence of a biosurfactant surfactin synthesized from stain A21.

If Natural Gas Hydrate from the ocean floor will become a feasible Natural resource in future then fundamental understanding of their Formation, environment and decomposition will be very much significant. The present study reports the significance of microorganisms and their metabolites. Biosurfactant are produced in the ocean floor which catalyses the Gas Hydrates Formation so the above thesis has lighten the Formation of Gas Hydrates in marine conditions and given the better understanding of the Formation of Natural Gas Hydrates in ocean floor.

Surfactin is a green biodegradable biosurfactant substitute to synthetic surfactants used extensively for Gas Hydrate Formation in present context.

6.8.3 *Conclusion of this task*

The kinetics and thermodynamics of Methane Hydrate Formation and its Dissociation has been studied in presence of surfactin produced by *Bacillus subtilis* strain A21 with C-type Silica Gel as fixed media and found that surfactin act as dual promoter i.e. thermodynamic as well as kinetic promoter for Methane Hydrate Formation. Lipopeptide biosurfactant was produced by *Bacillus subtilis* strain A21. Biosurfactant was characterized as surfactin. It reduced surface tension of water to 29 mN/m, thus, signifying its efficiency. Addition of surfactin solution to C-type Silica Gel bed changed the Methane Hydrate Formation temperature to higher value as compared to Hydrate Formation in water saturated C-type Silica Gel. Equilibrium temperature and pressure of Methane Hydrate Formation shifted to higher values in presence of surfactin. Presence of surfactin increased the rate of Hydrate Formation and reduced induction time by enhancing Methane solubility in water. The overall results suggested that lipopeptide biosurfactant like surfactin can be used as a thermodynamic and kinetic promoter for Methane Hydrate Formation.

Hydrate Formation rate is increased many more times by the presence of surfactin. The induction time of Hydrate Formation is reduced. The performance of 1000 ppm surfactin as promoter is better than at 100 ppm surfactin. The performance of fixed media i.e. C-type Silica Gel in presence of surfactin is found to be better than the agitation media reported by other research groups for Methane Hydrate Formation.

Methane Hydrate Formation in Silica Gel saturated with 1000 ppm surfactin solution increased the rate of Methane Hydrated Formation as compared to quiescent water system and water saturated C-type Silica Gel. Surfactin decreased the induction time by favouring better interaction between Methane and water. By decreasing the interfacial tension between Gas and water, surfactin increased the Methane Hydrate conversion percentage as well increased the number of moles of Methane consumed during Hydrate Formation. Overall results suggested that surfactin in combination with C-type Silica Gel can be used for enhancing the Methane Hydrate Formation rate. Surfactin has potential to act as Methane Hydrate Formation promoter in fixed bed system of C-type Silica Gel.

From the present study it can be concluded that surfactin act as both thermodynamic and kinetic promoter as in the presence of surfactin the induction time for Methane Hydrate is reduced and the same can be formed at higher temperature with respect to alone C-type Silica Gel when the surfactin is absent. Thus small doses of surfactin getting produced from *Bacillus subtilis* must clearly affect the Gas Hydrate Formation kinetics in Natural sites (as in Gulf of Mexico).

Natural Gas Hydrates are seen as future energy resource which is present in permafrost and marine sediments. The conditions of low temperature and high pressure for the Formation of Gas Hydrates can be overcome by addition of few surfactants. Hydrate technology is seen as future technology for transportation and storage of Natural Gas, new generation desalination, Gas mixture separation will be based on Hydrate technology. So future studies are required so that this resource of energy can be exploited and some novel technologies can be developed for the storage and transportation of Natural Gas, desalination and aforesaid applications of Gas Hydrates. Surfactin is found to be green biodegradable promoter for Gas Methane Hydrates Formation capable of replacing the synthetic surfactants for Gas Hydrate Formation.

6.9 Influence of a Novel Green Kinetic Inhibitor Calcium LignoSulphonate (CaLS) on Formation of Natural Gas Hydrate and Methane Hydrate

The results obtain for medium reactor and large reactor are as follows:

6.9.1 *Results for Medium Reactor*

The induction time and normalised growth for Natural Gas Hydrate Formation and induction time for Methane Hydrate Formation are here by explained.

6.9.1.1 *Induction Time for Natural Gas Hydrate Formation*

The induction time for saturated C-type Silica Gel without presence of CaLS and for various dosage of biosurfactant i.e. CaLS is measured in presence of Natural Gas. As it is evident from the graph shown in figure 6.9.1 the induction time when the biosurfactant CaLS is not present in saturated C type Silica Gel is 6 minutes which increases to 19 minutes when the CaLS is present in 0.1 wt. %, it further increase to 42 minutes when the CaLS is present in 1 wt. % and finally it goes to 144 minutes when the CaLS is present in 5 wt. %. This clearly explains that CaLS is acting as inhibitor for Natural Gas Hydrate Formation which is shown in figure 6.9.1.

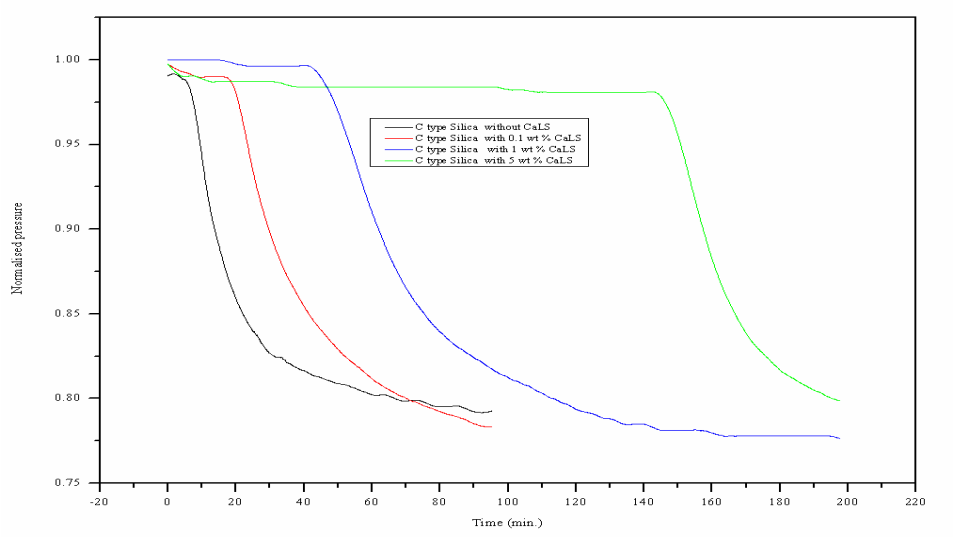

Figure 6.9.1: Induction time of Natural Gas Hydrate Formation for various experimental conditions.

6.9.1.2 *Normalized growth of Natural Gas Hydrate Formation*

The trends obtained for normalized growth is as shown in figure 6.9.2.

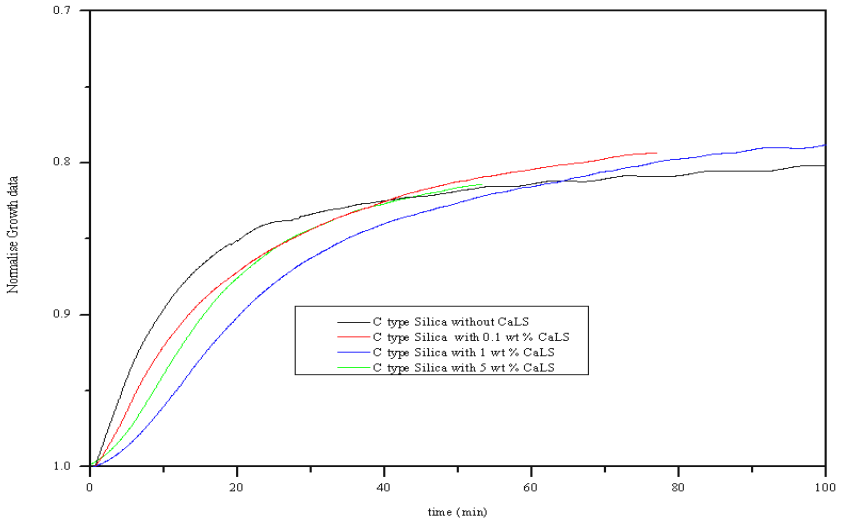

Figure 6.9.2: Normalized growth of Natural Gas Hydrate Formation for various experimental conditions.

6.9.1.3 *Induction Time for Methane Hydrate Formation*

The induction time for saturated C-type Silica Gel (Rankem) without presence of CaLS and for various dosage of biosurfactant i.e. CaLS is measured in presence of Methane Gas. As it is evident from the graph shown in figure 6.9.3 the induction time when the biosurfactant is not present in C type Silica Gel is 40 minutes which increases to 134 minutes when CaLS is present in 1 wt. % which finally reaches to 194 minutes when CaLS is present in 5 wt. %. The above study proves CaLS to be inhibitor for Methane Gas Hydrate Formation.

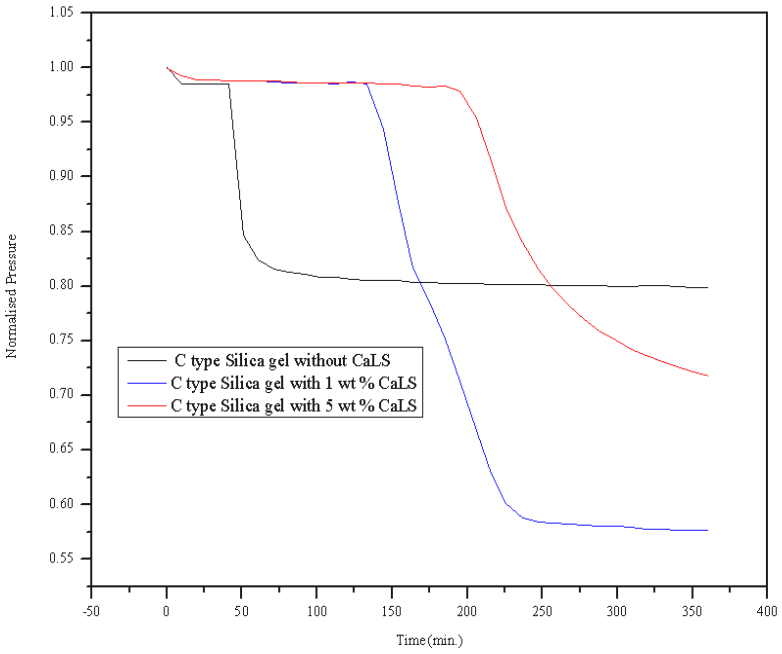

Figure 6.9.3: Induction time of Methane Hydrate Formation for various experimental conditions.

6.9.2 *Results for Large Reactor*

6.9.2.1 *Thermodynamics Study*

6.9.2.1.1 *Methane Hydrate Formation and Dissociation in large reactor in presence of CaLS*

The Formation and Dissociation behaviour of pure Methane Hydrate formed in saturated C-type Silica Gel in presence of 1 wt. % CaLS is shown in Figure 6.9.4. Firstly the pressure of the system decreases for a lot of hours without Formation of Hydrate. This happens because of

dissolution of Gas. This period ends when the Gas saturates the liquid. Thus the concentration of Gas in liquid rises and becomes super-saturated which leads to grouping of water molecules around Gas molecules with rapid decrease in pressure at constant temperature (277.53 K). This decrease in pressure at a specific temperature is due to Hydrate nucleation as shown in Figure 6.9.4 with appearance of turbidity in liquid phase and consequent growth of Gas Hydrates. A sharp discontinuity is seen in the Formation curve due to encapsulation of Gas in the cage of water molecules, with a small rise in the solution temperature because of the heat release during the stable Hydrate Formation. Our interest in the present study is to investigate the effect of Bio-Surfactant i.e. CaLS on Methane Hydrate Formation. Therefore the experiments were conducted with its presence in dosage 1 wt. % and without its presence in C type Silica Gel (Merck). Figure 6.9.4 shows the pressure–temperature profile during the process of Methane Formation and Dissociation in presence of 1 wt. % CaLS. Various Methane Hydrate parameters for various experimental conditions are given in table 6.9.1 which shows that Nucleation pressure and nucleation temperature are approximately same in C type Silica Gel (Merck) Table 6.7.1 with the presence of CaLS and without its presence.

Table 6.9.1: Methane Hydrate Formation parameters for various types of samples

Type of sample	Initial cell pressure, P (MPa)	Nucleation Temperature, T (K)	Nucleation pressure P (MPa)	Sub cooling (^{0}C)
C-type Silica Gel (Merck) containing 1 wt.% CaLS	11.70	277.53	10.32	11.47

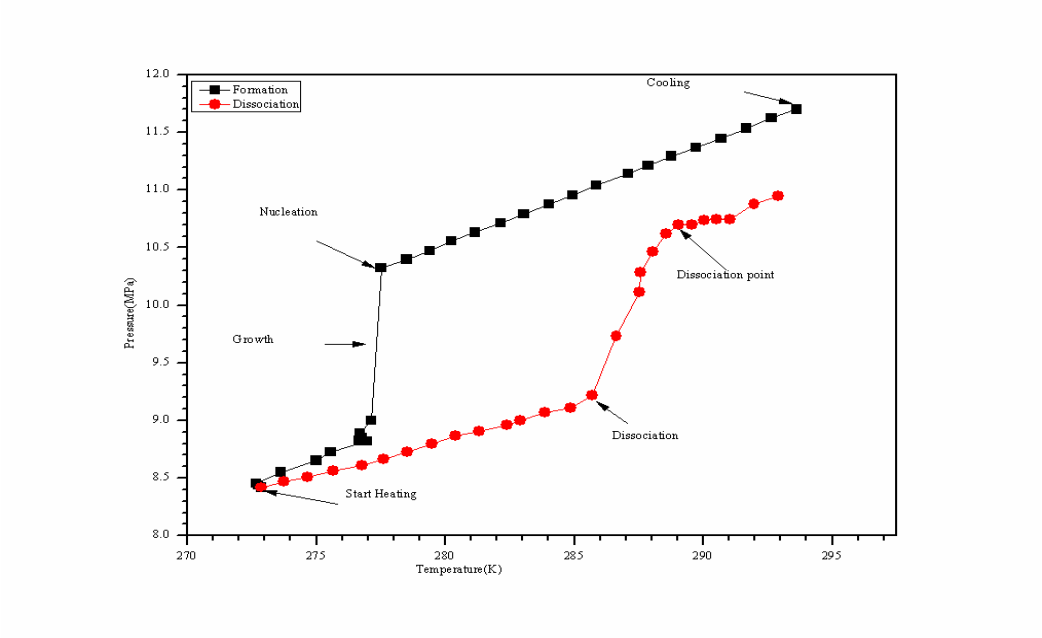

Figure 6.9.4: Temperature and pressure profile of Methane Hydrate Formation and Dissociation in presence of 1 wt. % CaLS

The nucleation temperature of Silica Gel without CaLS and with 1 wt. % CaLS is matching, hence CaLS is not influencing Formation of Methane Hydrate thermodynamically.

6.9.2.1.2 *Dissociation enthalpy of Methane Hydrate*

The Dissociation enthalpies of Methane Hydrates in presence of C-type Silica Gel saturated with distilled water containing 1wt.% CaLS were determined via Clausius-Clapeyron equation using equation 3 from annexure are as shown in Table 6.9.2 based on the measured phase equilibrium data.

Table 6.9.2: Equilibrium temperature, pressure and calculated Dissociation enthalpy (using Eq3)

Type of sample	P (Dissociation) (MPa)	Ln(P) (MPa)	T (Dissociation) (K)	1000/T (k^{-1})	Z factor	ΔH (KJ mol^{-1})
C-type Silica Gel containing 1 wt.% CaLS	9.7285	2.27506	286.6	3.488818	0.80541	-
	10.11461	2.313981	287.5	3.477777	0.8032	23.53956
	10.28698	2.330879	287.5	3.477535	0.80132	32.95851
	10.46624	2.348155	288.0	3.47162	0.80067	28.29131
	10.61793	2.362544	288.5	3.465604	0.8004	25.07778
	10.70066	2.370305	289.0	3.459848	0.80084	21.89044

6.9.2.2 *Kinetic Study*

The kinetic of Methane Hydrate Formation for various experimental condition is as explained below:

6.9.2.2.1 *Induction Time*

Figure 6.9.5 demonstrates the induction time for Methane Hydrate Formation in presence of 1 wt. % CaLS. The induction time in presence of CaLS and without its presence is shown in table 6.9.3.

Table 6.9.3: Induction Time for various experiments

Type of sample	Experiments conducted at Sub-cooling (˚C)	Induction Time (min.)
C-type Silica Gel without presence of surfactant	13.36	44.24
C-type Silica Gel containing 1 wt% CaLS	12.34	672.95

The induction time was compared with various polymeric compounds and Anti-Freeze proteins. Daraboina et al, 2011 has revealed that induction time is delayed from 48 minutes to more 10 to 20 minutes in presence of PVP and AFP and more than 1.5 hours with H1W85281. So in comparison to this our compound can delay it to 11.2 hours.

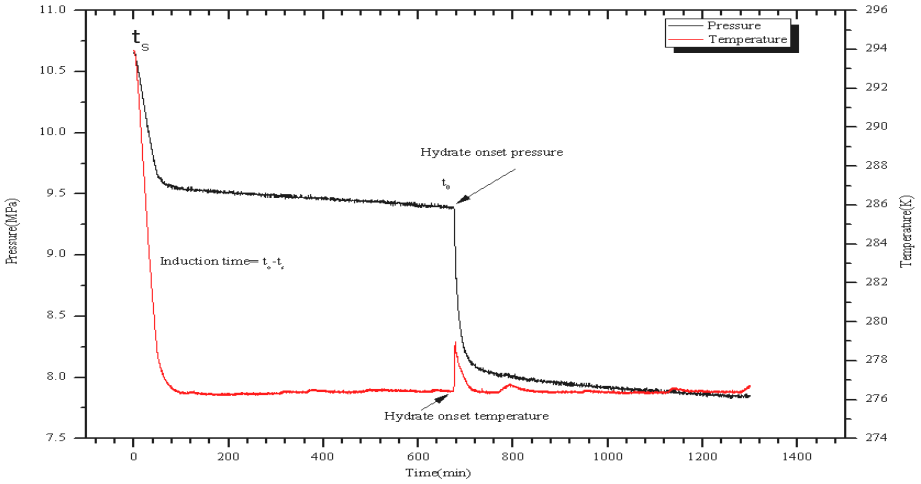

Figure 6.9.5: Induction time for Methane Hydrate Formation in presence of 1 wt. % CaLS.

6.9.2.2.2 ***Gas consumption***

The amount of Methane Gas consumed is calculated by using equation 1 & 2 from annexure. During the beginning of Hydrate Formation, there was a decrease in pressure accompanied by an increase in cell temperature. This pressure drop is due to the consumption of Gas when Methane Gas molecules occupy unoccupied water cavities during Hydrate Formation process. Typical pattern of Gas consumption during Formation of Hydrate is shown in Figure 6.9.6.

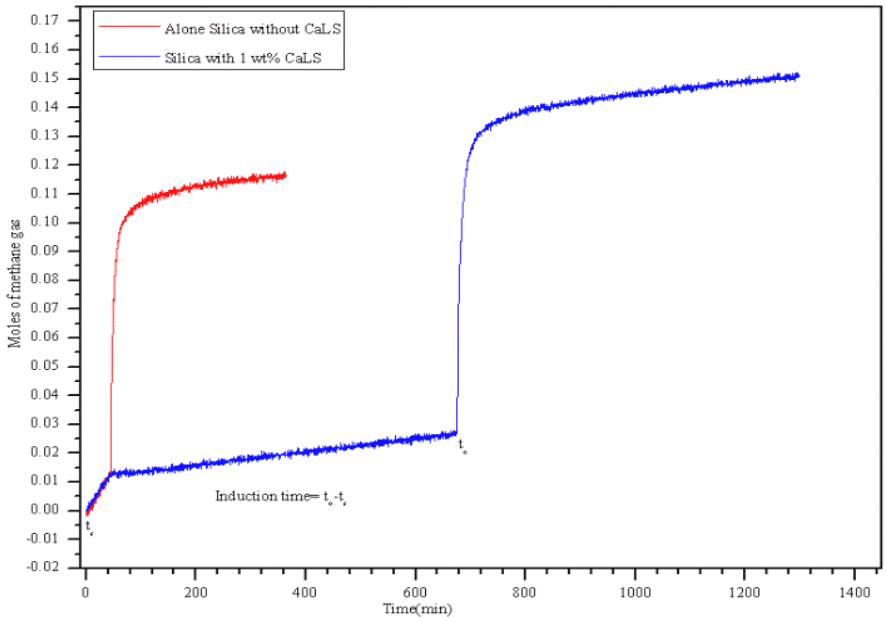

Figure 6.9.6: Moles of Methane Gas consumed.

Figure 6.9.7 Shows Gas consumption and pressure drop as a function of time. The growth and Gas consumption region is showing two symmetric plots that could be interpreted as conservation of mass during the Hydrate growth. Number of Methane molecules leaving the Gas phase to Hydrate phase is represented by the pressure drop, whereas the number of Methane molecules entering in the Hydrate cages is represented by the Gas consumption plot. Since mass must be conserved in an isochoric system, the two plots shows symmetry about an axis passing through the intersection of the two plots and parallel to the time axis. As shown in Figure 6.9.7, the process is divided into five regions. First region is started at time zero where the system has less consumption of Gas and pressure slightly decreases due to dissolution of Gas. Second region is after the induction time where Gas consumption increases, this is because of the Hydrate growth. From the third region to fifth region, since the Hydrate is formed, consumption of Gas is as shown in figure 6.9.7.

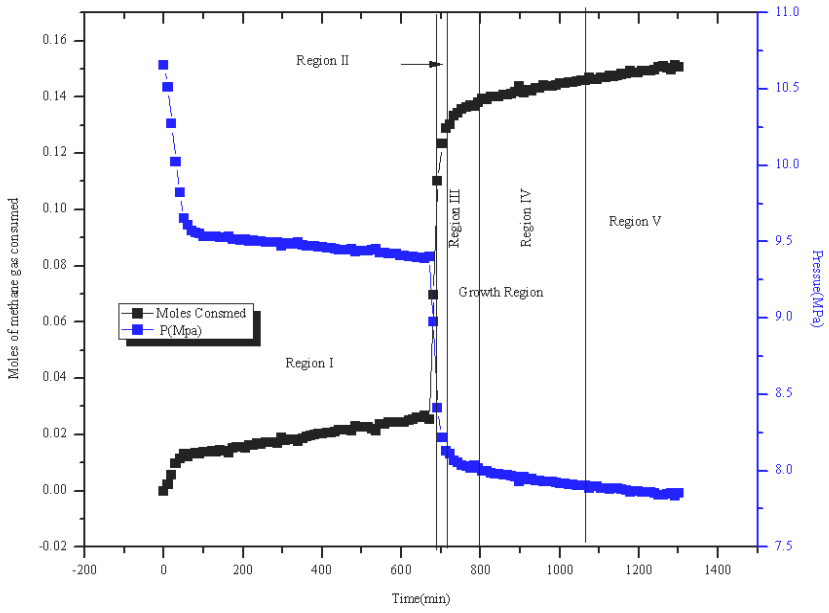

Figure 6.9.7: Methane Gas consumption and Pressure drop as function of time in presence 1 wt. % CaLS

6.9.2.2.3 *The rate of Methane Gas Hydrate Formation for different experimental conditions*

As observed, the slope of the curves after nucleation exhibits an exponential behaviour Figure 6.9.8 from which we can assume that it is a first-order reaction. A first order reaction is defined by the equation 4 from annexure.

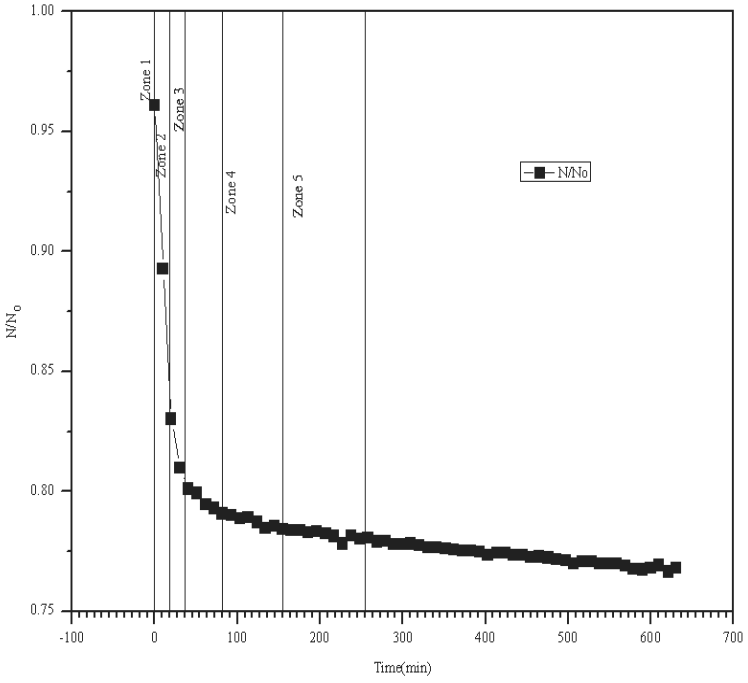

Figure 6.9.8: Change of moles of Methane during Methane Hydrate Formation in presence of 1 wt. % CaLS.

The slope of the curve of ln (N/N_0) vs. t gives the rate constant (k) of Hydrate Formation using equation 5 from annexure. The Hydrate Formation from region 2 Figure 6.9.7 was divided into five zones of time as shown in Figure 6.9.8 (0-20, 20-40, 40-80, 80-160,160-260 min.) after nucleation. This may be due to different rate of Hydrate Formation which gives different reaction rate and hence different rate constant. The data of five zones are used to estimate the rate constant of Hydrate Formation in each zone. The Formation rate is usually expressed by the rate by which the amount of Methane molecule is converted to Hydrate [Hussain et al, 2006]. Hydrate Formation rate is calculated by putting the values of slopes i.e. rate constant k obtained from figure 6.9.9 using equation 6 from annexure:

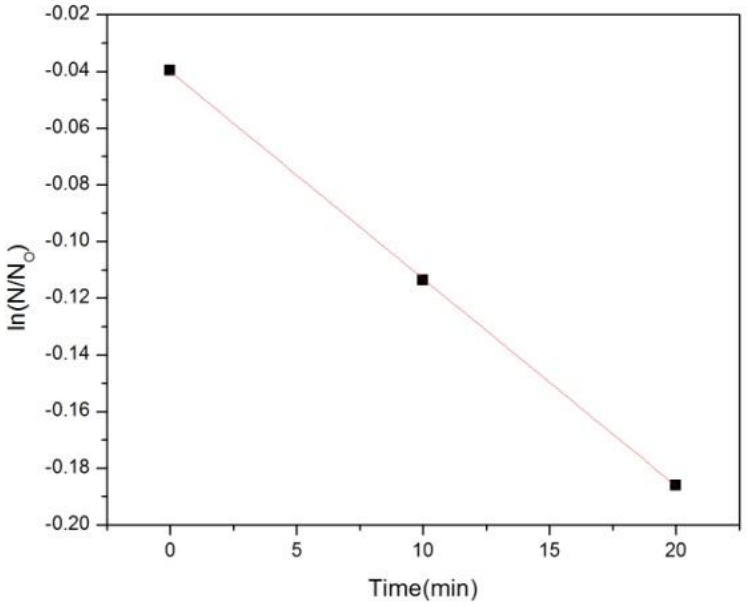
-0.02
-0.04
-0.06
-0.08
-0.10
-0.12
-0.14
-0.16
-0.18
-0.20
ln(N/N$_O$)
0
5
10
15
20
Time(min)

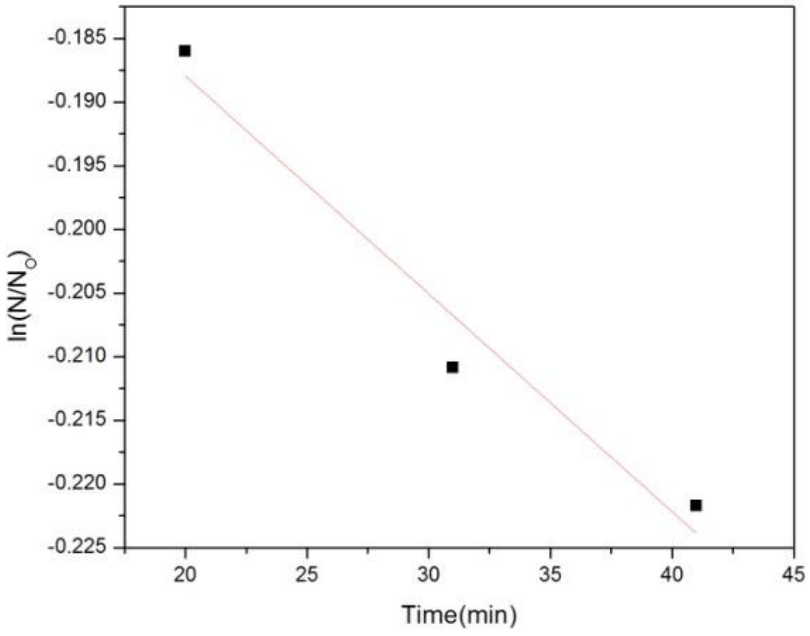
-0.185
-0.190
-0.195
-0.200
-0.205
-0.210
-0.215
-0.220
-0.225
ln(N/N$_O$)
20
25
30
35
40
45
Time(min)

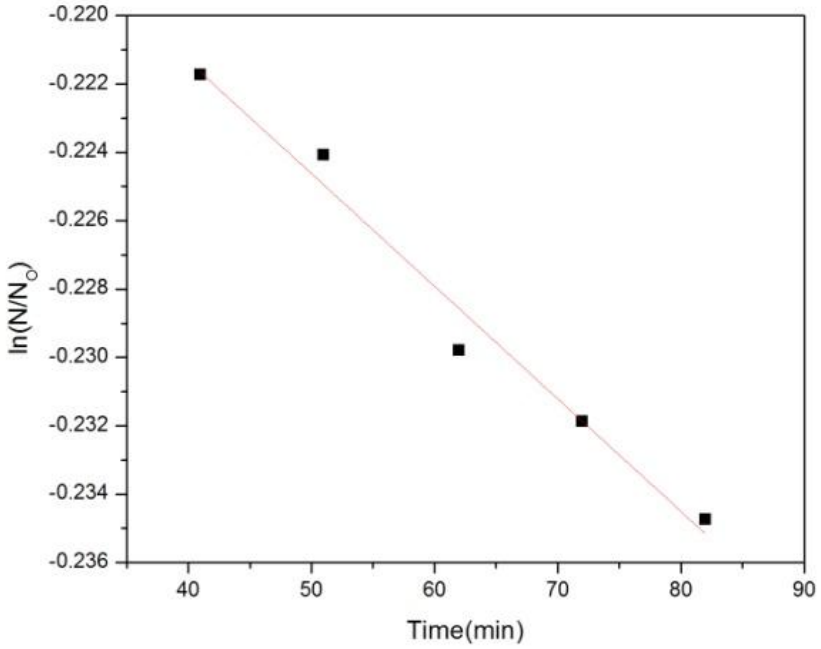
-0.220
-0.222
-0.224
-0.226
-0.228
-0.230
-0.232
-0.234
-0.236
ln(N/N$_o$)
40
50
60
70
80
90
Time(min)

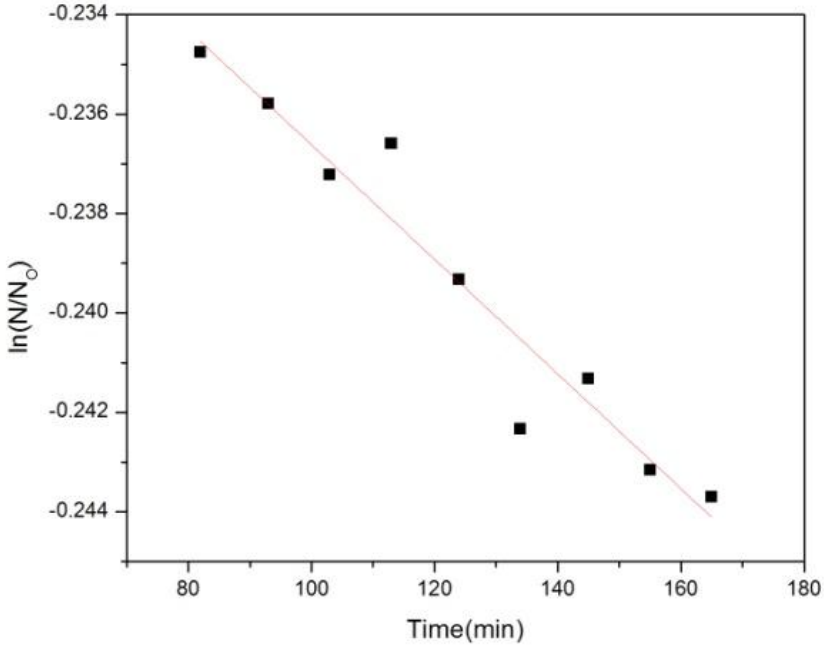
-0.234
-0.236
-0.238
-0.240
-0.242
-0.244
ln(N/N$_o$)
80
100
120
140
160
180
Time(min)

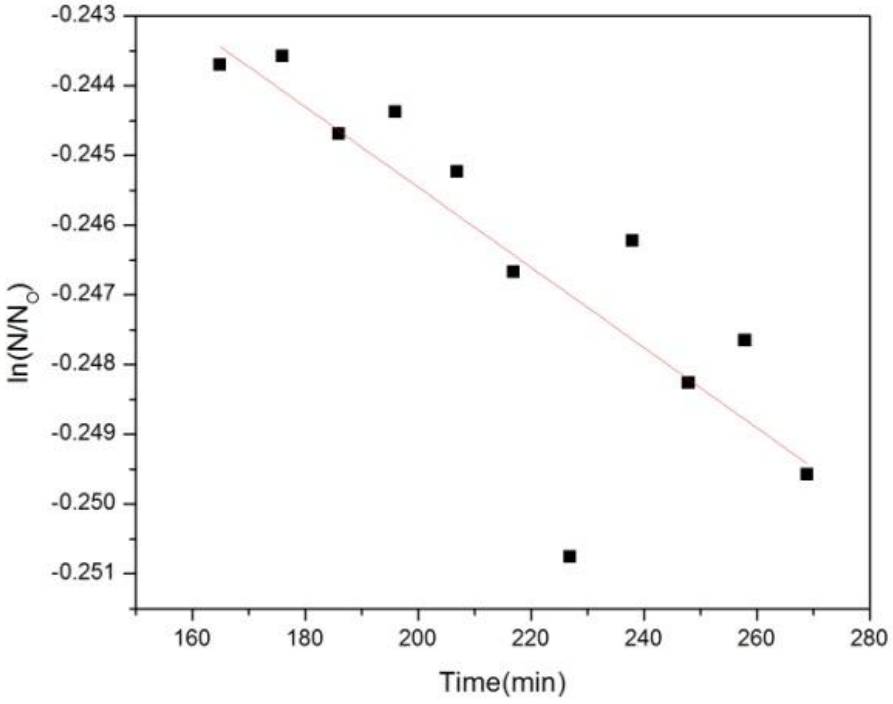

Figure 6.9.9: Semi-logarithmic plots of change of moles of Gas during Hydrate Formation in presence of 1 wt. % CaLS.

Methane Hydrate Formation rates are calculated and are shown from Figures 6.9.10 to 6.9.15 and in table 6.9.4, which shows that there are no much variation in Methane Hydrate Formation rate in presence of biosurfactant i.e. CaLS.

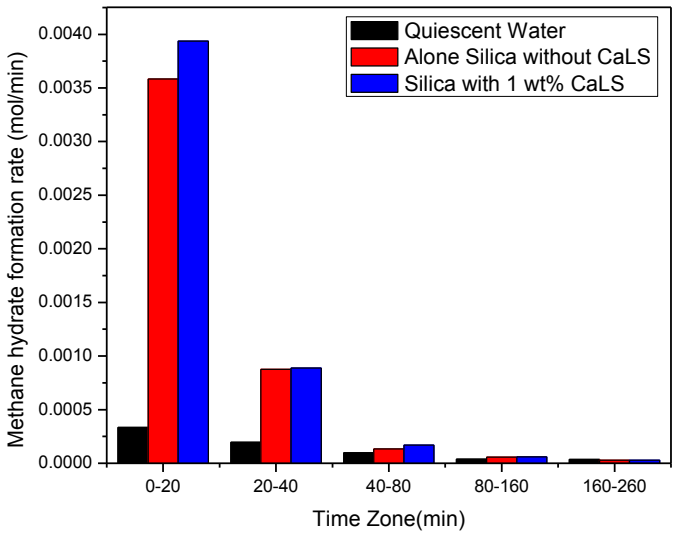

Figure 6.9.10: Comparison of rates of Methane Gas Hydrate Formation for different time zone in different experiment condition

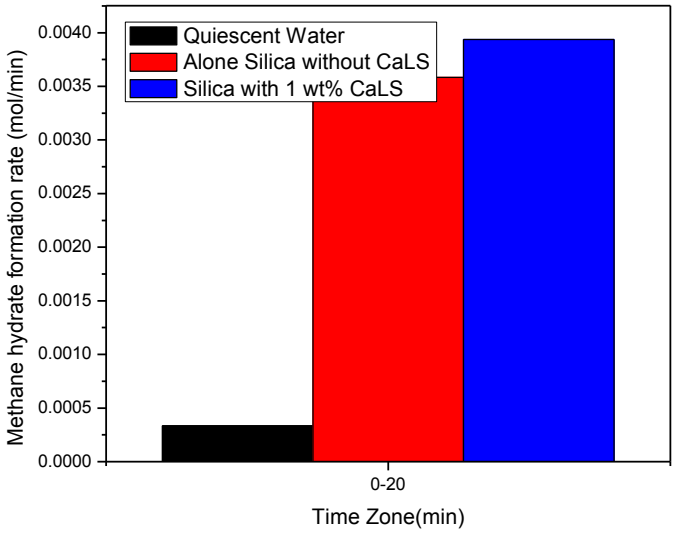

Figure 6.9.11: Comparison of rates of Methane Gas Hydrate Formation for time zone (0-20 min) in different experiment condition.

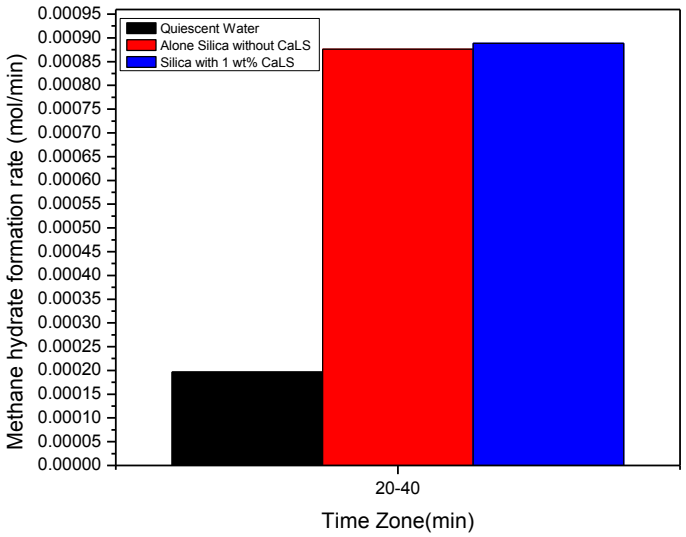

Figure 6.9.12: Comparison of rates of Methane Gas Hydrate Formation for time zone (20-40 min) in different experiment condition.

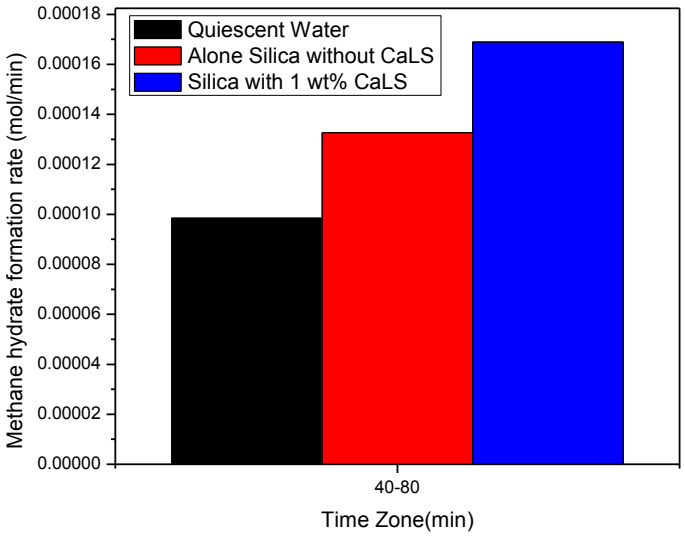

Figure 6.9.13: Comparison of rates of Methane Gas Hydrate Formation for time zone (40-80 min) in different experiment condition.

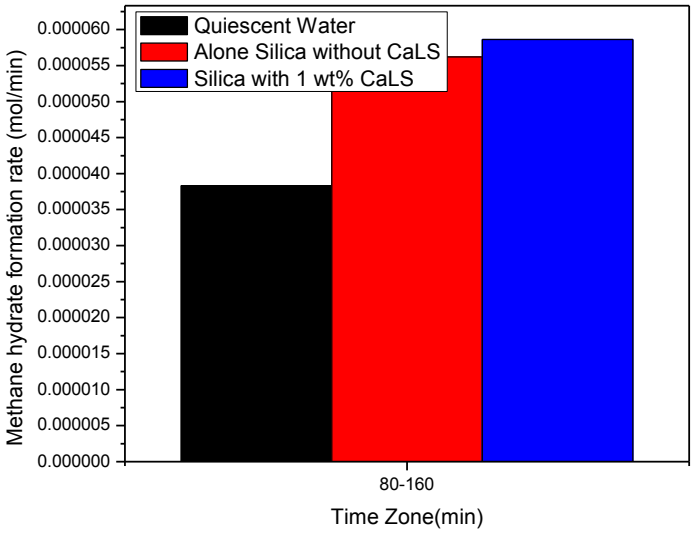

Figure 6.9.14: Comparison of rates of Methane Gas Hydrate Formation for time zone (80-160 min) in different experiment condition

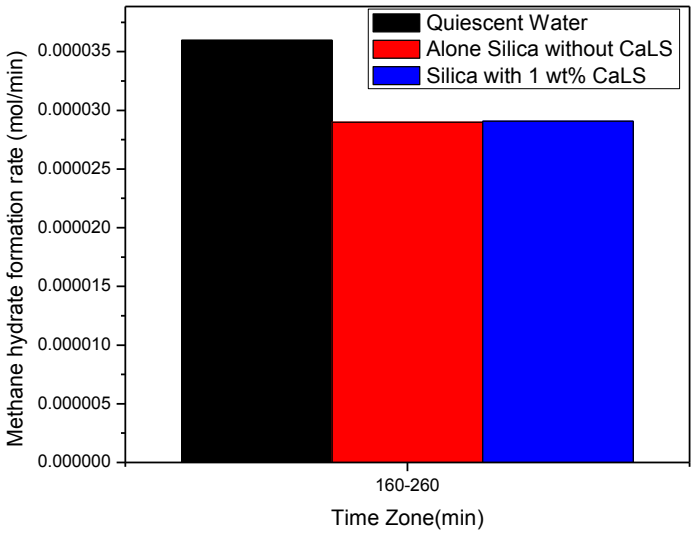

Figure 6.9.15: Comparison of rates of Methane Gas Hydrate Formation for time zone (160-280 min) in different experiment condition.

Table 6.9.4: The rate of Methane Gas Hydrate Formation for different experimental condition

Type of sample	Time Zone (Min)	Rate constant K (min^{-1})	Formation rate (mole/min)	% over all increased rate with respect to Silica
C-type Silica Gel	0-20	0.00731	0.003937094	
containing 1 wt%	20-40	0.00171	0.000888661	8.631082224
CaLS	40-80	3.29E-04	0.000168923	
	80-160	1.15E-04	5.86258E-05	
	160-260	5.75E-05	2.90742E-05	

The result of Methane uptake and rate of Methane Hydrate Formation is not influenced much in presence of CaLS which further justifies its role as kinetic inhibitor.

6.9.3 *FTIR of Silica C type Silica Gel (Merck)*

Figure 6.9.17 compares FTIR spectrum of C-type Silica Gel before and after Methane Hydrate Formation. C-type Silica Gel (Merck) gave characteristics spectrum with broad absorption band at 1084 cm^{-1} that can be attributed to stretching vibration of Si-O- Si and a less intense band at 799 cm^{-1} may be attributed to Si-O- Si symmetric stretching vibration. Broad spectrum band at 3465 is due to O-H bond present on C-type Silica Gel [Roldan et al, 2004]. After Methane Hydrate Formation the FTIR spectrum was very similar to that of C-type Silica Gel before Hydrate Formation. The band at 2924 cm^{-1} is of interest as it signifies C-H stretching of alkane. This may be due to very small amount Methane left in the pores of Silica.

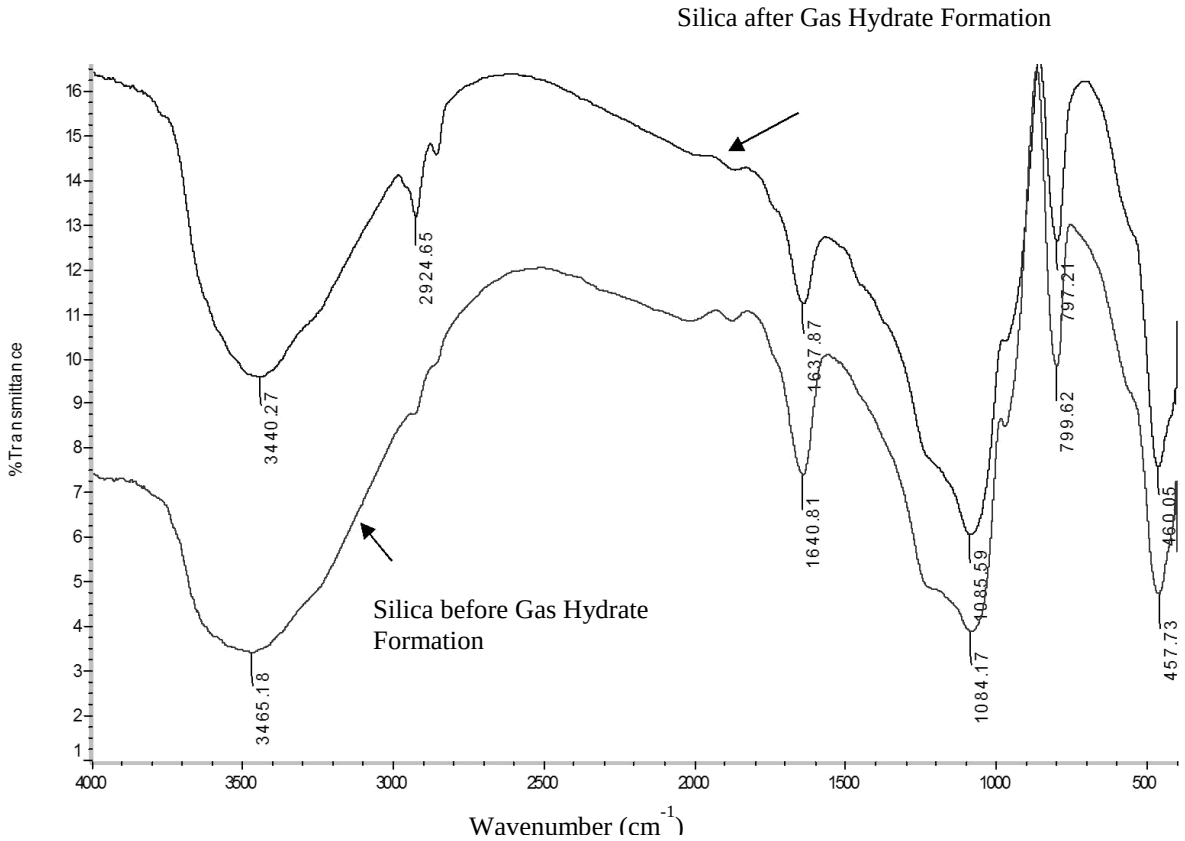

Figure 6.9.16: FTIR of C-Type Silica Gel before and after Going for Gas Hydrate Experience.

6.9.4 *Scanning Electron Microscopy (SEM)*

The surface morphology of bare Silica Gel and Silica Gel in which Methane Hydrate were formed and then dissociated has been studied by SEM analysis. As evident from FE-SEM image analysis bare Silica Gel has smooth, irregular nonporous structure Figure 6.9.18(a). However after going through Hydrate Formation and Dissociation experience swollen Silica Gel with smooth regular nonporous structure was observed in FE-SEM Figure 6.9.18(b). This may be due to the Hydrate Formation in the pores of Silica.

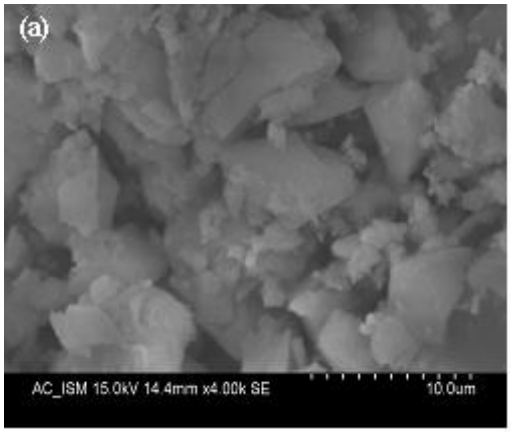

Fig. 6.9.17(a) Scanning Electron Microscopic Image of C-Type Silica Gel before Hydrate Formation

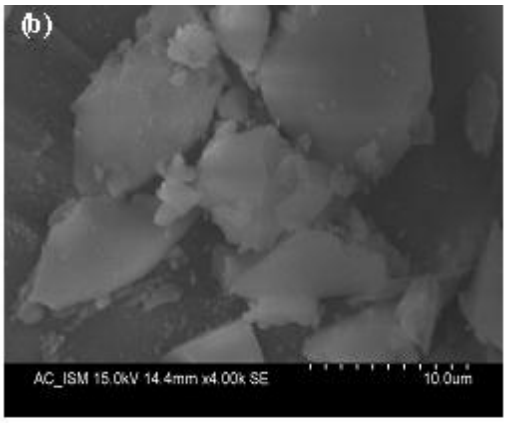

Fig. 6.9.17(b) Scanning Electron Microscopic Image of C-Type Silica Gel after Hydrate Formation

6.9.5 *Conclusion of this task*

Calcium LignoSulphonate was characterized by FTIR, UV, CHNS, GPC, FE-SEM, EDS, FE-SEM MIXING, DTG and Solid NMR which is found to be same i.e. Calcium LignoSulphonate (CaLS). All techniques have given signatures of various elements present in Calcium LignoSulphonate and the molecular weight determined from Gel permeation chromatography has confirmed its polymeric nature.

The above compound is a byproduct from pulp and paper waste industry and is found to be a very novel, economic, biodegradable green low dose inhibitor for Natural Gas Hydrate and Methane Hydrate. It has delayed the induction time of Methane Gas Hydrate from 44 minutes when it is not present to 11.2 hours when it is present in 1 wt. %. It is available at very low cost in market and has a potential to replace synthetic polymers and very high costly Anti-Freeze Proteins inhibitor used for flow assurance at present by oil and Gas industry.

CHAPTER – 7

CONCLUSIONS

1. An economic and less energy intensive fixed bed media of Silica Gel (100 nm) was found to be more efficient amongst fixed bed of Silica sand, Silica Gel (5 nm), blend of Silica Gel (5nm) and Zeolites and Stirred tank rectors for Hydrate based carbon dioxide capture. Fixed bed media are capable of replacing the expensive and energy intensive method of mechanical agitation used for Gas Hydrate Formation due to which Hydrate Formation technology is not commercialized for various applications such as carbon dioxide capture, cool storage applications, Gas separation, desalination and storage and transport of Natural Gas. Fixed bed media of Silica Gel (100nm) was found to be very effective for carbon dioxide capture which can help in designing an economic Hydrate based technology for carbon dioxide capture.

2. Biosurfactant synthesized from strain A11 was found to be Rhamnolipids after characterizing with techniques such as TLC, FTIR, NMR, LC-MS, MALDI. Purified Rhamnolipids produced by strain A11 can reduce the surface tension of water from 72 mN/m to 36 mN/m with CMC of 70 mg/l.

3. Biosurfactant synthesized from strain A21 was found to be Surfactin after characterizing with techniques such as TLC, FTIR, HPLC, MALDI, NMR, Amino Acids Analysis. Purified Surfactin produced by strain A21 can reduce the surface tension of water from 72 mN/m to 29 mN/m with CMC of 33 mg/l.

4. Rhamnolipids and Surfactin were found to be dual promoters i.e. kinetic as well as thermodynamic promoter for Methane Hydrate Formation. The induction time, rate of Methane Hydrate Formation and moles of Methane consumed has proved both the biosurfactants i.e. Rhamnolipids and Surfactin as kinetic promoters for Methane Hydrate Formation. The shift in the nucleation temperature towards higher side at higher dose has proved both the biosurfactants i.e. Rhamnolipids and Surfactin as thermodynamic promoters. The equilibrium temperature and pressure curves got shifted to higher and lower zones respectively for both the biosurfactants i.e. Rhamnolipids and Surfactin which further justify them to be thermodynamic promoters. These biosurfactants are

capable of replacing their counter parts i.e. synthetic surfactants which are toxic, non-environment friendly and non-biodegradable. Hence these biosurfactants can help in designing a green, clean, biodegradable and environment friendly technology for promoting the Formation of Natural Gas Hydrate which have enormous applications..

5. Methane Gas Hydrates are fuels of the future generation provided an economical viable technology is developed for their exploitation. Thermal stimulation technique is found to be very effective for Dissociation of Methane Hydrates.
6. The above thesis lightens the significance of microorganisms and their metabolites in the generation of Gas Hydrates in marine conditions, thus the small dosage of Rhamnolipids produced by *Pseudomonas aeruginosa* Strain A11 and Surfactin produced by *Bacillus subtilis* Strain A21 must clear the role of these biosurfactants as promoters in Natural Gas Hydrates sites (as in Gulf of Mexico).
7. Calcium LignoSulphonate was characterized by FTIR, UV, CHNS, GPC, FE-SEM, EDS, FE-SEM MIXING, DTG and Solid NMR which is found to be same i.e. Calcium LignoSulphonate (CaLS). All techniques have given signatures of various elements present in Calcium LignoSulphonate and the molecular weight determined from Gel permeation chromatography has confirmed its polymeric nature.
8. Calcium LignoSulphonate (CaLS) is found to be an economic, low dose, green and biodegradable kinetic inhibitor for Methane as well as Natural Gas Hydrates which can replace synthetic polymers and as well as very expensive low dose antifreeze proteins (AFP) used currently by industry for inhibition of Natural Gas Hydrates by oil and Gas industry.
9. If Natural Gas Hydrate from the ocean floor will become a feasible Natural resource in future then fundamental understanding of their Formation and Dissociation will be very much significant. The above thesis has addressed the Formation and Dissociation issue of Methane Hydrates in detail. Few learning can be applied from the above thesis in understanding the basics of Formation and Dissociation of Methane Hydrates.

CHAPTER – 8

SCOPE FOR FUTURE WORK

This thesis has reported the designing of Silica Gel as a fixed bed media for the Formation of Gas Hydrates which can replace the expensive method of Gas Hydrate Formation i.e. agitation. The thesis has also investigated the biosurfactant promoters for Gas Hydrate Formation capable of replacing their counter parts. The thermal stimulation technique for Methane Hydrate Dissociation has also being studied. On the bases of results obtained and observation made the scope of future work in this area is listed as below:

1. Hydrate Formation and Dissociation may be studied using other hydrocarbon Gases such as ethane, propane, butane, mixture of carbon dioxide and Methane in presence of fixed bed media of Silica Gel as well as in presence of biosurfactants studied i.e. Rhamnolipid and Surfactin.
2. Most of the marine sediments consist of clays like bentonite, montmorillonite, kaolinite, illite etc. So, further research is required to study the Hydrate Formation and Dissociation behaviour using different clays in presence of different hydrocarbon Gases. The Natural sediments from Krishna – Godavari (KG) Basin, Kerela-Konkan (KK) basin or other Natural Hydrates occurring sites may also be investigated in presence of Methane, Natural Gas or other hydrocarbon Gases.

3. Hydrates are not only seen as future generation fuels but Hydrates are more or less seen as a technology for applications such as Separation Processes, Marine Carbon Dioxide Sequestration, Cool Storage Application, Natural Gas Storage and Transportation etc. Hence an economic means of their Formation has been suggested i.e. fixed bed media which can help in commercializing Hydrate based technology but still the stability of Hydrates which is an important parameter for industrial applications may also be studied in presence of more fixed bed media as well as other biosurfactants.

4. In the current study Calcium LignoSulphonate (CaLS) has been found an economic, biodegradable green inhibitor for Methane and Natural Gas Hydrate Formation. The more biomass based materials may be further investigated as inhibitor for Natural Gas Hydrate Formation which can replace the very expensive inhibitors such as antifreeze proteins (AFP) used currently for transportation of oil and Gas by the industry.

   The overall scope of the proposed future work can be divided into three major areas of Natural Gas Hydrates research field.

- First area is related to designing an economic technology for the storage and transport of Natural Gas which can be addressed by exploiting few more fixed bed media capable of replacing the more energy intensive method of formulation of Gas Hydrates.

- Secondly the understanding of carbon dioxide capture in fixed bed media of marine like conditions can help in carbon dioxide sequestration of Methane Hydrates and it can achieve two objectives at a time i.e. production of energy resource with simultaneous decrease in global warming.

- Thirdly other than thermal stimulation exploitation techniques of Gas Hydrates can also be studied in detail which can help in designing feasible technology of production of Methane from Gas Hydrates.

PUBLICATIONS

Patent Filed, Papers Published, Accepted and Communicated in Journals, Awards, Papers Published in International/ National Conference Proceedings, Papers / Posters Presented in International and National Conferences

(A) Patent Filed

1. Patent Filed by **Amit Arora**, Chandrajit Balomajumder, Rajnish Kumar, Pushpendra Kumar, Asheesh Kumar and Sukumar Laik on Inhibition of Gas Hydrate Formation by a Novel Green Kinetic Inhibitor.

(B) Paper Published In Journals

2. **Amit Arora**, Swaranjit Singh Cameotra, Rajnish Kumar, Chandrajit Balomajumder, Anil Kumar Singh, B. Santhakumari, Pushpendra Kumar and Sukumar Laik, Biosurfactant as a Promoter of Methane Hydrate Formation: Thermodynamic and Kinetic Studies. Journal of **Scientific Reports- Nature** 6: 20893 (2016).
3. **Amit Arora**, Asheesh Kumar, Gaurav Bhattacharjee, Pushpendra Kumar and Chandrajit Balomajumder, Effect of different fixed bed media on the performance of sodium dodecyl sulfate for hydrate based CO_2capture. **Journal of Material and Design** 90: 1186-1191 (2016).
4. **Amit Arora**, Swaranjit Singh Cameotra, Rajnish Kumar, Pushpendra Kumar and Chandrajit Balomajumder, Effects of Biosurfactants on Gas Hydrates. Journal of Petroleum and Environmental Biotechnology 5(2):170 (2014).
5. **Amit Arora**, Swaranjit Singh Cameotra and Chandrajit Balomajumder, Natural Gas Hydrate as an Upcoming Resource of Energy. Journal of Petroleum and Environmental Biotechnology 6(1):199 (2015).
6. **Amit Arora**, Swaranjit Singh Cameotra and Chandrajit Balomajumder, Techniques for Exploitation of Gas Hydrate (Clathrates) an Untapped Resource of Methane Gas. Journal of Microbial & Biochemical Technology 7(2):108-111 (2015).

7. **Amit Arora**, Swaranjit Singh Cameotra and Chandrajit Balomajumder, Natural Gas Hydrate (Clathrates) as an Untapped Resource of Natural Gas. Journal of Petroleum and Environmental Engineering 6(4):234 (2015).

8. **Amit Arora**, Swaranjit Singh Cameotra and Chandrajit Balomajumder, Field Testing of Gas Hydrates- An Alternative to Conventional Fuels. Journal of Petroleum and Environmental Engineering 6(5):235 (2015).

(C) Book Chapter Published

9. Amit Arora, Swaranjit Singh Cameotra, Rajnish Kumar, Anil Kumar Singh, **Pushpendra Kumar,** Chandrajit Balomajumder and Sukumar Laik, (2015) "Role Of Rhamnolipid A Bio-Surfactant in Methane Gas Hydrate Formation Kinetics," **Springer Proceeding on Energy of First International Conference on Recent Advances in Bio-Energy Research ICRABR**, at Sardar Swaran Singh National Institution of the Renewable Energy, Kapurthala, Punjab, India, pp 333-343.

(D) Publication in Referred International/ National Conference

10. **Amit Arora**, Chandrajit Balomajumder, Asheesh Kumar, Rajnish Kumar, Pushpendra Kumar and Manit Kaur, Influence of Zeolites on Carbon dioxide Gas Hydrate Formation, Proceedings of the 8th International Conference on Gas Hydrate (ICGH 2014), Beijing, China 28th July – 1st August 2014.
11. **Amit Arora**, Vikash Kumar Saw, Chandrajit Balomajumder, Effects of Surfactants on Gas Hydrate Formation- A Review, Proceedings of National Conference on Advances in Manufacturing Systems Technology, Materials and Management (CAMS-2014), SBSSTC, Firozpur, India 5th-6th September 2014.
12. **Amit Arora**, Anil Kumar Singh, Swaranjit Singh Cameotra, Rajnish Kumar, Pushpendra Kumar, Chandrajit Balomajumder, Sukumar Laik, Role of Surfactin a Bio-Surfactant in Natural Gas Hydrate Formation Kinetics, Proceedings of International Conference on Chemical Engineering- Emerging Dimensions And Challenges Ahead & Indo Japanese

Symposium on Separation Technology For Green Environment, CHEMCON 2014, Chandigarh, India 27th-30th December 2014.

(E) Ready For Communication in Journals

13. **Amit Arora**, Swaranjit Singh Cameotra, Rajnish Kumar, Chandrajit Balomajumder, Anil Kumar Singh, Asheesh Kumar, Pushpendra Kumar and Sukumar Laik, Lipopeptide Biosurfactant Promoting Methane Hydrate Formation in Fixed Bed of Silica Gel in **Scientific Reports – Nature.**
14. **Amit Arora**, Swaranjit Singh Cameotra, Rajnish Kumar, Chandrajit Balomajumder, Anil Kumar Singh, B. Santhakumari, Pushpendra Kumar and Sukumar Laik, Rhamnolipids promotes methane hydrates formation in fixed bed Porous Silica gel system

(F) Under Preparation

15**.** **Amit Arora**, Asheesh Kumar, Gaurav Bhattacharjee, Pushpendra Kumar and Chandrajit Balomajumder, Carbon Dioxide Hydrate Formation in Fixed Bed and Stirred Tank Reactor System .
16. **Amit Arora**, Swaranjit Singh Cameotra, Rajnish Kumar, Chandrajit Balomajumder, Anil Kumar Singh, B. Santhakumari, Pushpendra Kumar and Sukumar Laik, Methane Hydrate Formation in Fixed Bed Silica Gel System with Surfactin acting as Promoter.

(G) Awards by Presenting Oral Papers / Posters at International / National Conferences

17. **Amit Arora**, Rajnish Kumar, Pushpendra Kumar and Chandrajit Balomajumder, Awarded **Consolation Prize** by Presenting Poster Titled Effects of Zeolites on CO_2 Gas Hydrate Formation at First International Seminar on Nanotechnology in Conventional and Alternate Energy Systems A Global Status and Pathway at UPES Campus, Dehradun, India **Conducted by Indian Oil, R&D, ONGC, CSIR India during 12th-13th August 2013**.
18. **Amit Arora**, Swaranjit Singh Cameotra, Rajnish Kumar, Pushpendra Kumar , Chandrajit Balomajumder and Sukumar Laik, **Award of EUR 100 by Springer and SSS NIRE for**

First Position by Presenting Paper TitledRole Of Rhamnolipid A Bio-Surfactant In Methane Gas Hydrate Formation at First International Conference on Recent Advances in Bio-Energy Research **ICRABR-2015 at Sardar Swaran Singh National Institution of the Renewable Energy, Kapurthala, Punjab, India from 14th-17th March 2015**.

19. **Amit Arora**, Swaranjit Singh Cameotra and Chandrajit Balomajumder, **First Prize** for Presenting Poster entitled Influence of Biosurfactants on Gas Hydrate Formation at Chandigarh University on National Seminar on Sustainability of New & Renewable Energy A Present Scenario- **SUNREAPS 2015 Sponsored by Ministry of New & Renewable Energy, New Delhi on17th April, 2015.**

20. **Amit Arora**, Asheesh Kumar, Rajnish Kumar Gaurav Bhattacharjee, Pushpendra Kumar and Chandrajit Balomajumder, **Best Paper Award** by presenting the poster paper titled Carbon Dioxide Hydrate Formation in Fixed Bed and Stirred Tank Reactor System in **6th World Renewable Energy Technology Congress, New Delhi, India 21st – 23rd August, 2015.**

(H) Oral Papers / Posters Presented in International and National Conferences

21. **Amit Arora** and Chandrajit Balomajumder, Oral Paper Titled "Influence of Surfactants on Gas Hydrates Formations" Presented at National Seminar on Recent Advances in Pollution and Abatement (RAPA) at Meerut Institute of Engineering And Technology Chemical Engineering Department, Meerut, India on 14th- 15th February 2014.

22. **Amit Arora** and Chandrajit Balomajumder, Oral Paper Titled "Role of Porous Materials in the Formation of Gas Hydrates" at Second International Conference on Innovative Trends in Applied Physical, Chemical, Mathematical, Statistical Sciences and Emerging, Energy Technology for Sustainable Development" (APCMSET-2014) Organized by "Social Welfare Foundation in Association with Krishi Sanskriti" at Jawaharlal Nehru University, New Delhi on 19th – 20th July 2014, Abstract Published in Innovations & Research in Physico-Chemical Sciences-A Step towards Sustainability : 121.

23. **Amit Arora** and Chandrajit Balomajumder, Oral Paper Titled "Gas Hydrates as Upcoming Source of Energy" at Second International Conference on Innovative Trends in Applied Physical, Chemical, Mathematical, Statistical Sciences and Emerging, Energy

Technology for Sustainable Development" (APCMSET-2014) Organized by "Social Welfare Foundation in Association with Krishi Sanskriti" at Jawaharlal Nehru University, New Delhi on 19th – 20th July 2014. Abstract Published in Energy Technologies, Climate Change and Environmental Sustainability Innovative Perspective: 75.

24. **Amit Arora** and Chandrajit Balomajumder, Oral Paper Titled "Role of Surfactants in the Formation of the Gas Hydrates" at Second International Conference on Innovative Trends in Applied Physical, Chemical, Mathematical, Statistical Sciences and Emerging, Energy Technology for Sustainable Development" (APCMSET-2014) Organized by "Social Welfare Foundation in Association with Krishi Sanskriti" at Jawaharlal Nehru University, New Delhi on 19th – 20th July 2014, Abstract Published in Innovations & Research in Physico-Chemical Sciences-A Step towards Sustainability :122.

25. **Amit Arora** and Chandrajit Balomajumder, Oral Paper Titled "Gas Hydrates as a problem for oil and gas pipelines" at Second International Conference on Innovative Trends in Applied Physical, Chemical, Mathematical, Statistical Sciences and Emerging, Energy Technology for Sustainable Development" (APCMSET-2014) Organized by "Social Welfare Foundation in Association with Krishi Sanskriti" at Jawaharlal Nehru University, New Delhi on 19th – 20th July 2014, Abstract Published in Innovations & Research in Physico-Chemical Sciences-A Step towards Sustainability :120.

26. **Amit Arora**, Asheesh Kumar, Chandrajit Balomajumder, SuKumar Laik, Paper Titled "A Novel Green Kinetic Hydrate Inhibitor: Special emphasis on flow assurance" was Selected for Oral Presentation at Chemeca 2014 Conference at Australia Perth during 28th September to 1st October 2014 but could not be presented because of lack of funding.

27. **Amit Arora**, Rajnish Kumar, Swaranjit Singh Cameotra, Pushpendra Kumar, Chandrajit Balomajumder and SuKumar Laik, Poster Titled "Role of Biosurfactants In Natural Gas Hydrates Formation Kinetics" was Presented at 9th International Methane Hydrate R&D (IMHRD) Workshop, Organized by CSIR, National Geophysical Research Institute, Hyderabad, India from 9th- 12th November 2014, Abstract Published in FIERY ICE 2014:105.

REFERENCES

1. Aaron, D. and Tsouris, C. Separation of CO_2 from flue gas a review. *Sep Sci Technol* 40:321–348 (2005).
2. Abdel-Mawgoud, A.M., Aboulwafa, M. and Hassouna, N. Characterization of Rhamnolipid Produced by *Pseudomonas aeruginosa* Isolate Bs20. *Appl Biochem Biotechnol* 157:329-345 (2009).
3. Abdel Mawgoud, A.M., Lepine, F. and Deziel, E. Rhamnolipids: diversity of structures, microbial origins and roles. *Appl Microbiol Biotechnol* 86(5):1323-1336 (2010).
4. Adeyemo, A., Kumar, R., Linga, P., Ripmeester, J. and Englezos, P. Capture of carbon dioxide from flue or fuel gas mixtures by clathrate crystallization in a silica gel column. *Int J Greenh Gas Control* 4:478–485 (2010).
5. Ahmad, M.A.M. and Dézie, F.L.E. Rhamnolipids: diversity of structures, microbial origins and roles. *Appl Microbiol Biotechnol* 86:1323–1336 (2010).
6. Aittomaki, A. and Lahti, A. Potassium formate as a secondary refrigerant. *Int J Refrig* 20(4):276–282 (1997).
7. Akiya, T., Owa, M., Nakaiwa, M., Kawasaki, S., Ninemoto, M. and Ando, Y. Cool storage using gas hydrate. *27th International congress of refrigeration* Vienna, Austria 166–170 (1987).
8. Al Ajlani, M.M., Sheikh, M.A., Ahmad, Z. and Hasnain, S. Production of surfactin from *Bacillus subtilis* MZ-7 grown on pharmamedia commercial medium. *Microb Cell Fact* 6:17 (2007).
9. Alessandro, D.M.D., Smit, B. and Long, J.R. Carbon dioxide capture: prospects for new materials. *Angew Chem Int Ed* 49:6058–6082 (2010).
10. Amende, B. and Gordon, J. Literature and analyses reports on Snomax, York Snow Inc, Victor N Y, (1999).
11. Anderson, B., Boswell, R., Collett, T.S., Farrell, H., Ohtsuki, S., White, M. and Zyrianova M. Review of the Findings of the Iġnik Sikumi CO_2-CH_4 gas Hydrate Exchange.Field Trial. *8th ICGH* 28th July to 1st August: Beijing, China (2014).

12. Anderson, N.M., Lívia A.F., José C.P. and Marcio N. Physicochemical Properties of Rhamnolipid Biosurfactant from *Pseudomonas aeruginosa* PA1 to Applications in Microemulsions. *Journal of Biomaterials and Nanobiotechnology* 6:64-79 (2015).
13. Ando, N., Kuwabara, Y. and Mori Y.H. Surfactant effects on hydrate formation in an unstirred gas/liquid system an experimental study using methane and micelle forming surfactants. *Chem Eng Sci* 73:79-85 (2012).
14. Arechabala, B., Coiffard, C., Rivalland, P., Coiffard, L.J. and de Roeck Holtzhauer, Y. Comparison of cytotoxicity of various surfactants tested on normal human fibroblast cultures using the neutral red test, MTT assay and LDH release. *J Appl Toxicol* 19:163-165 (1999).
15. Arguelles, A.A., Ongena, M., Halimi, B., Lara, Y., Brans, A., Joris, B. and Fickers P. Bacillus amyloliquefaciens GA1 as a source of potent antibiotics and other secondary metabolites for biocontrol of plant pathogens. *Microbial Cell Factory* 8:63 (2009).
16. Arrebola, E., Jacobs, R. and Korsten, L. Iturin A is the principal inhibitor in the biocontrol activity of *Bacillus* amyloliquefaciens PPCB004 against postharvest fungal pathogens. *J Appl Microbiol* 108:386-395 (2009).
17. Arutchelvi, J., Sangeetha, J., Philip, J. and Doble, M. Self-assembly of surfactin in aqueous solution: Role of divalent counterions. *Colloid Surface B* 116:396-402 (2014).
18. Aya, I., Yamane, K. and Nariai, H. Solubility of CO_2 and density of CO_2 hydrate at 30 MPa. *Energy* 22(2–3):263–271 (1997).
19. Ayel, V., Lottin, O. and Peerhossaini, H. Rheology, flow behaviour and heat transfer of ice slurries a review of the state of the art. *Int J Refrig* 26(1):95–107 (2003).
20. Babu, P., Kumar, R. and Linga, P. A new porous material to enhance the kinetics of clathrate process: application to pre combustion carbon dioxide capture. *Environ Sci Technol* 47:13191–13198 (2013).
21. Babu, P., Kumar, R. and Linga, P. Medium pressure hydrate based gas separation (HBGS) process for pre-combustion capture of carbon dioxide employing a novel fixed bed reactor. *Int J Greenh Gas Control* 17:206–214 (2013).

22. Babu, P., Kumar, R. and Linga, P. Unusual behaviour of propane as a co-guest during hydrate formation in silica sand: Potential application to seawater desalination and carbon dioxide capture. *Chem Eng Sci* 117:342-351 (2014).
23. Babu, P., Yee, D., Linga, P., Palmer, A., Khoo, B.C., Tan, T.S. and Rangsunvigit, P. Morphology of Methane Hydrate Formation in Porous Media. *Energ Fuel* 27:3364−3372 (2013).
24. Bachu, S. and Adams, J.J. Sequestration of CO_2 in geological media in response to climate change capacity of deep saline aquifers to sequester CO_2 in solution. *Energy Convers Manage* 44:3151–3175 (2003).
25. Bai, G., Brusseau, M.S. and Miller, R.M. Influence of a rhamnolipid biosurfactant on the transport of bacteria through a sandy soil. *Appl Environ Microbiol* 63:1866-1873 (1997).
26. Banat, I.M. Biosurfactants production and possible uses in microbial enhanced oil recovery and oil pollution remediation a review. *Biores Technol* 51:1-12 (1995).
27. Banat, I.M., Franzetti, A., Gandolfi, I., Bestetti, G., Martinotti, M.G., Fracchia, L., Smyth, T.J. and Marchant, R. Microbial biosurfactants production, applications and future potential. *Appl Microbiol Biot* 87(2):427-444 (2010).
28. Banat, I.M., Satpute, S.K., Cameotra, S.S., Patil, R. and Nyayanit, N.V. Cost effective technologies and renewable substrates for biosurfactants production. *Front Microbiol* 5(697):1-18 (2014).
29. Banerjee, R., Furukawa, H., Britt, D., Knobler, C., O'Keefe, M. and Yaghi, O.M. Control of Pore Size and Functionality in Isoreticular Zeolitic Imidazolate Frameworks and their Carbon Dioxide Selective Capture Properties. J Am Chem Soc 131:3875–3877 (2009).
30. Banerjee, R., Phan, A., Wang, B., Knobler, C., Furukawa, H., O'Keefe, M. and Yaghi O.M. High-Throughput Synthesis of Zeolitic Imidazolate Frameworks and Application to CO_2 Capture. *Science* 319*:939-943 (*2008).
31. Barchas, R. and Davis, R. The Kerr-Mcgee abb lummus crest technology for the recovery of CO_2 from stack gases. *Energy Convers Manage* 33:333–340 (1992).
32. Barkay, T., Navon, V.S., Ron, E. and Rosenberg, E. Enhancement of solubilization and biodegradation of polyaromatic hydrocarbons by the emulsifier alasan. *Appl Environ Microb* 65:2697-2702 (1999).

33. Baumgart, F., Kluge, B., Ullrich, C., Vater, J. and Ziessow, D. Identification of amino acid substitutions in the lipopeptide surfactin using 2D NMR spectroscopy. *Biochem Biophys Res Commun* 177:998-1005 (1991).

34. Bazire, A., Diab, F., Taupin, L., Rodrigues, S., Jebbar, M. and Dufour, A. Effects of Osmotic Stress on Rhamnolipid Synthesis and Time-Course Production of Cell-To-Cell Signal Molecules by *Pseudomonas aeruginosa*. *Open Microbiol J* 3:128-135 (2009).

35. Begley, M., Cotter, P.D., Hill, C. and Ross, R.P. Identification of a novel two-peptide lantibiotic, lichenicidin, following rational genome mining for LanM proteins. *Appl Environ Microb* 75:5451-5460 (2009).

36. Bel, O. and Lallemand, A. Study of a two phase secondary refrigerant intrinsic thermophysical properties of an ice slurry. *Int J Refrig* 22(3):164–174 (1999).

37. Bezza, F.A. and Chirwa, E.M.N. Production and applications of lipopeptide biosurfactant for bioremediation and oil recovery by *Bacillus subtilis* CN2. *Biochem Eng J* 101:168-178 (2015).

38. Bhattacharjee, G., Kumar, A., Sakpal, T. and Kumar, R. Carbon Dioxide Sequestration: Influence of Porous Media on Hydrate Formation Kinetics. *A C S Sustainable Chem Eng* 3(6):1205-1214 (2015).

39. Bily, C. and Dick, J.W.L. Natural occurring gas hydrates in the Mackenzie Delta, N.W.T. . *B Can Petrol Geol* 74:340-352 (1974).

40. Bily, C., Guo, T., Zhu, T., Fan, S., Liang, D. and Zhang, L. Influence of volumetric flow rate in the crystallizer on the gas-hydrate cool-storage process in a new gas-hydrate cool storage system. *Appl Energ* 78:111–121 (2004)

41. Birchwood, R., Dai, J., Shelander, D., Boswell, R., Collett, T., Cook, A., Dallimore, S., Fujii, K., Fukuhara, M., Kusaka, K., Murray, D. and Saeki, T. Developments in Gas Hydrates. *Oilfield Review Spring Schlumberger* 22(1):18-33 (2010).

42. Bishnoi, P.R. and Dholabhai, P.D. Equilibrium conditions for hydrate formation for a ternary mixture of methane, propane and carbon dioxide and a natural gas mixture in the presence of electrolytes and methanol. *Fluid Phase Equilibr* 158–160:821-827 (1999).

43. Boswell, R. and Collett, T.S. Current perspectives on gas hydrate resources. *Energy & Environmental Science* 4:1206-1215 (2011).

44. Bosewell, R. Japan Completes First Offshore Methane Hydrate Production Test- Methane Successfully Produced From Deepwater Hydrate Layers. *Fire in the Ice* 13(2):1-30 (2013).
45. Bosewell, R., Robert, H., Collett, T.S., Digert, S.A., Steve, H. and Weeks, M. Investigation of Gas Hydrate-Bearing Sandstone Reservoirs at the "Mount Elbert" Stratigraphic test well, Milne point, Alaska. *6th ICGH* July 6th to july Vancouver, British Columbia, Canada, 10th (2008).
46. BP Statistical Review of World Energy June 2013. April 17, 2014. https://www.imf.org/external/np/res/commod/pdf/ppt/BP0613.pdf
47. Brewer, P.G., Friederich, G., Peltzer, E.T. and Orr Jr., F. M. Direct experiments on the ocean disposal of fossil fuel C_{O2}. *Science* 284(5416):943–945 (1999).
48. Bryant, E. Climate Process and Change, Cambridge University Press, UK 118 (1997).
49. Budzianowski, W.M. Engineering benefits of mass recirculation in novel energy technologies with CO_2 capture. *Rynek Energii* 88:151–158 (2010).
50. Buffett, B. and Archer, D. Global inventory of methane clathrate sensitivity to changes in the deep ocean. *Earth Planet Sci Lett* 227:185–199 (2004).
51. Candrasekaran, E.V. and Bemiller, J.N. Constituent analyses of glycosaminoglycans, In: Methods in Carbohydrate Chemistry, Academic Press, ed. Whistler, R.L. 89-96 (1980).
52. Carapellucci, R. and Milazzo, A. Membrane systems for CO_2 capture and their integration with gas turbine plants. *J Power Energy* 217:505–517 (2003).
53. Carbajo, J. J. A direct-contact-charged–direct-contact-discharged cool storage system using gas hydrate. *ASHRAE Trans, 91(Part 2A)* 258–266 (1985).
54. Carvajal, O.H. and Pratt, L.M. Effects of clay minerals and biosurfactants on isotopic and molecular characteristics of methane encaged in pressure vessel gas hydrates. *Org Geochem* 60:83-92 (2013).
55. Cha, J.H. and Seol, Y. Increasing Gas Hydrate Formation Temperature for Desalination of High Salinity Produced Water with Secondary Guests. *ACS Sustainable Chem Eng* 1(10):1218-1224 (2013).
56. Cha, M., Shin, K., Seo, Y., Shin, J.Y. and Kang, S.P. Catastrophic Growth of Gas Hydrates in the Presence of Kinetic Hydrate Inhibitors. *J Phys Chem A* 117:13988−13995 (2013).

57. Cha, S.B., Ouar, H., Wildeman, T.R. and Sloan, E.D. A third-surface effect on hydrate formation. *J Phys Chem* 92:6492-6494 (1988).

58. Chakma, A. CO_2 capture processes-opportunities for improved energy efficiencies. *Energ Convers Manage* 38:S51-S56 (1997).

59. Champion, J.T., Gilkey, J.C., Lamparski, H., Retterer, J. and Miller, R.M. Electron microscopy of rhamnolipid (biosurfactant) morphology: effects of pH, cadmium, and octadecane. *J Colloid Interface Sci* 170:569-574 (1995).

60. Chand, S., Priest, J.A., Gei, D., Minshull, T., Best, A. and Carcione, J.M. An Inversion Algorithm for Gas Hydrate Quantification. American Geophysical Union (2003).

61. Chandrasekaran, E.V. and BeMiller, J.N. Methods in carbohydrate chemistry, New York: Academic press, ed. Whistler R.L. editor 89 (1980).

62. Chatti, I., Delahaye, A., Fournaison, L. and Petitet, J.P. Benefits and drawbacks of clathrate hydrates: A review of their areas of interest. *Energ Convers Manage* 46(9-10):1333-1343 (2005).

63. *Chen, C., Park, D.W. and Ahn, W.S. CO_2 capture using zeolite 13X prepared from bentonite. Appl Surf Sci* 292:63–67 (2014).

64. Chen, H.L., Lee, Y.S., Wei, Y.H. and Juang, R.S. Purification of surfactin in pretreated fermentation broths by adsorptive removal of impurities. *Biochem Eng J* 40:452-459 (2008).

65. Chen, M., Thomas, R. and Penfold, J. Self-Assembly of Mono- and Di-Rhamnolipids in Solution Studied by Small Angle Neutron Scattering (SANS). McKimmon Conference Center, June 18, (2008).

66. Choe, B.Y., Krishna, N.R., Pritchard, D.G. and Proton, N.M.R. study on rhamnolipids produced by *Pseudomonas aeruginosa*. *Magn Reson Chem* 30(10):1025-1026 (1992).

67. Choi, M.H., Xu J., Gutierrez, M., Yoo, T., Cho, U.H. and Yoon, S.C. Metabolic relationship between polyhydroxyalkanoic acid and rhamnolipid synthesis in *Pseudomonas aeruginosa*: Comparative 13C NMR analysis of the products in wild-type and mutants. *Journal of Biotechnology* 151:30–42 (2011).

68. Choi, W.J., Choi, H.G. and Lee, W.H. Effects of ethanol and phosphate on emulsan production by Acinetobactercalcoaceticus RAG-1. *J Biotechnol* 45(3):217-225 (1996).

69. Chong, Z.R., Yang, S.H.B., Babu, P., Linga, P. and Li, X.S. Review of natural gas hydrates as an energy resource: Prospects and challenges. *Appl Energ* (2015). doi:10.1016/j.apenergy.2014.12.061

70. Chun-Gang X, Xiao-Sen L., Research progress of hydrate-based CO_2 separation and capture from gas mixtures. *RSC Adv* 4:18301-18316 (2014).

71. Churchill, S.A., Griffin, R.A., Jones, L.P. and Churchill, P.F. Biodegradation Rate Enhancement of Hydrocarbons an Oleophilic Fertilizer and a Rhamnolipid Biosurfactant. *J Environ Qual* 24(1):19-28 (1995).

72. Circone, S., Stern, L.A., Kirby, S.H., Durham, W.B., Chakoumakos, B.C. and Rawn, C.J. CO_2 hydrate: synthesis, composition, structure, dissociation behaviour, and a comparison to structure I CH_4 hydrate. *J Phys Chem B* 107(23):5529–5539 (2003).

73. Cirigliano, M. and Carman, G. Isolation of a Bioemulsifier from Candida lipodytica. *Appl Environ Microbiol* 48:747–750 (1984).

74. Clennell, M.B., Hovland, M., Booth, J.S., Pierre, H. and Winters, W.J. Formation of natural gas hydrates in marine sediments, Conceptual model of gas hydrate growth conditioned by host sediment properties. *J Geophys Res* 104:22985-23003 (1999).

75. Collett, T.S. Energy resource potential of natural gas hydrates. *AAPG Bull* 86:1971–1992 (2002).

76. Collet, T.S., Johnson, A.H., Knapp, C.C. and Boswell, R.M. Natural Gas Hydrates -- Energy Resource Potential and Associated Geologic Hazards, American Association of Petroleum Geologists Memoir, 89:137 (2009).

77. Cooper, D.G., Macdonald, C.R., Duff, S.J. and Kosaric, N. Enhanced Production of Surfactin from *Bacillus subtilis* by Continuous Product Removal and Metal Cation Additions. *Appl Environ Microbiol* 42:408-412 (1981).

78. Costa, S.G.V.A.O., Nitschke, M., Lepine, F., Daziel, E. and Contiero, J. Structure, properties and applications of rhamnolipids produced by *Pseudomonas aeruginosa* L2-1 from cassava wastewater. *Process Biochem* 45(9):1511-1516 (2010).

79. Cotter, P.D., Hill, C. and Ross, R.P. Bacteriocins: developing innate immunity for food. *Nature Reviews Microbiology* 3:777-788 (2005).

80. D'Alessandro, D.M., Smit, B. and Long, J.R. Carbon dioxide capture: prospects for new materials. *Angew Chem Int Ed* 49:6058–6082 (2010).

81. Da Silva, G.P., Mack, M. and Contiero, J. Isolation and partial characterization of a new strain of *Klebsiella pneumoniae* capable of high 1, 3 propanediol production from glycerol. *Biotechnol Adv* 27:30–39 (2009).

82. Dai, Y., Zhong, X., Jiang, X. and Wang, S. Experiment of New Additives Effect on Gas Hydrate Formation. *Energy and Power Engineering* 6:133-141 (2014).

83. Daimaru, T., Yamasaki, A. and Yanagisawa, Y. Effect of surfactant carbon chain length on hydrate formation kinetics. *J Petrol Sci Eng* 56:89-96 (2007).

84. Dallimore, S.R. and Collett, T.S. JAPEX/JNOG/GSC et al. Mallik 5L-38 gas hydrate production research well downhole well-log and core montages, Scientific Results from the Mallik 2002 Gas Hydrate Production Research Well Program Mackenzie Delta Northwest Territories Canada, eds., Dallimore SR and Collett TS, Geological Survey of Canada Bulletin, 585:23 (2005).

85. Dallimore, S.R., Uchida, T. and Collett, T.S. Scientific Results from JAPEX/JNOG/GSC Mallik 2L-38 Gas Hydrate Research Well Mackenzie Delta Northwest Territories Canada, Geological Survey of Canada Bulletin, 544:403 (1999).

86. Daraboina, N., Linga, P., Ripmeester, J., Walker, V.K. and Englezos, P. Natural Gas Hydrate Formation and Decomposition in the Presence of Kinetic Inhibitors. 2. Stirred Reactor Experiments. *Energ Fuel* 25(10):4384−4391 (2011).

87. Daraboina, N., Moudrakovski, I., Ripmeester, J.A., Walker, V.K. and Englezos, P. Assesing the Performance of Commercial and Biological Gas Hydrate Inhibitors Using Nuclear Magnetic Resonance Microscopy and a Stirred Autoclave. *Fuel* 105:630−635 (2013).

88. Daraboina, N., Perfeldt, M.C. and Solms, N.V. Synergistic kinetic inhibition of natural gas hydrate formation. *Fuel* 108:749–757 (2013).

89. Daraboina, N., Ripmeester, J., Walker, V.K. and Englezos, P. Natural Gas Hydrate Formation and Decomposition in the Presence of Kinetic Inhibitors. 1. High Pressure Calorimetry. *Energ Fuel* 25(10):4392−4397 (2011).

90. Das, P., Mukherjee, S. and Sen, R. Antimicrobial potential of a lipopeptide biosurfactant derived from a marine *Bacillus* circulans. *J Appl Microbiol* 104:1675-1684 (2008).

91. Das, R. and Pal, S. Hydroxypropyl methyl cellulose grafted with polyacrylamide Application in controlled release of 5-amino salicylic acid. *Colloid Surface B* 110:236-241 (2013).

92. Davidson, D.W., Clathrate hydrates, In water: a comprehensive treatise, Plenum press, Franks F, editor. New York 115-163 (1973).

93. Davidson, D.W., El-Defrawy, M.K., Fuglem, M.O. and Judge, A.S. Natural gas hydrates in northern Canada. *3rd International Conference on Permafrost* 1:938–943 (1978).

94. Davy, H. The Bakerian Lecture: On Some of the Combinations of Oxymuriatic Gas and Oxygene, and on the chemical Relations of these Principles, to Inflammable Bodies. *Phil Trans R Soc Lond* 101:1-35 (1811).

95. De Faria, A.F., Teodoro-Martinez, D.S., De Oliveira Barbosa, G.N., Vaz, B.G., Silva, I.S., Garcia, J.S., Totola, M.R., Eberlin, M.N., Grossman, M., Alves, O.L. and Durrant, L.R. Production and structural characterization of surfactin (C14/Leu7) produced by *Bacillus subtilis* isolate LSFM-05 grown on raw glycerol from the biodiesel industry. *Process Biochem* 46(10):1951-1957 (2011).

96. De Forcrand, R. Compt. Rend, 135:959 (1902).

97. Dearman, J.L. Gas Hydrate Formation in Gulf of Mexico Sediments, Mississippi State University, (2007).

98. Deaton, W.M. and Frost, E.M. Gas hydrates and their relation to the operation of Natural Gas Pipelines. US. Bureau of Mines, Monograph 8 (1946).

99. Del Villano, L.; Kommedal, R.; Kelland, M. A. Class of Kinetic Hydrate Inhibitors with Good Biodegradability. Energy Fuels,2008, 22(5): 3143−3149.

100. Demirbas, A. Methane Gas Hydrate, Springer-Verlag London (2010).

101. Demirbas, A. Methane hydrates as potential energy resource: Part 1 Importance, resource and recovery facilities. *Energ Conver Manage* 51:1547-1561 (2010).

102. Desai, A.J., Patel, R.M. and Desai, J.D. Advances in the production of biosurfactants and their commercial applications. *J Sci Ind Res* 53:619-629 (1994).

103. Desai, J.D. and Banat, I.M. Microbial production of surfactants and their commercial potential. *Microbiol Mol Biol R* 61(1):47-64 (1997).
104. Desideri, U. and Paolucci, A. Performance modelling of a carbon dioxide removal system for power plants. *Energ Convers Manage* 40(18):1899–915 (1999).
105. Dhar, V. Fe-Modified Zsm-5 Shape Selective Catalysts for The Synthesis of 2, 6-Dimethylnaphthalene. Thesis, Supervised by Song, C., Pisupati, S.V., Boehman, A.L. and Mathesws, J.P. (2008).
106. Dholabhai, P.D., Parent, J.S. and Bishnoi, P.R. Equilibrium conditions for hydrate formation from binary mixtures of methane and carbon dioxide in the presence of electrolytes, methanol and ethylene glycol. *Fluid Phase Equilibr* 141:235–246 (1997).
107. Dicharry, C., Duchateau, C., Asbaï, H., Broseta, D. and Torré, J.P. Carbon dioxide gas hydrate crystallization in porous silica gel particles partially saturated with a surfactant solution. *Chem Eng Sci* 98:88-97 (2013).
108. Dobryin, V.M., Korotavej, Y.P. and Plyuschev, D.V. Gas hydrates- a possible energy resource, in R.F. Meyer and J.C. Oslon, Eds. Long term energy resources. Pitman publishing, Boston, 727-729 (1981).
109. Duc, N.H., Chauvy, F. and Herri, J.M. CO_2 Capture by hydrate crystallization–a potential solution for gas emission of steelmaking industry. *Energ Converse Manage* 48(4):1313–1322 (2007).
110. Duncum, S.N., Edwards, A.R., and Osborne, C.G. European patent. 0536950 Al, (1993).
111. Durham, W.B., Kirby, S.H., Stern, L.A. and Zhang, W. The strength and Rheology of methane clathrate hydrate. *J Geophys Res* 108:2182 (2003).
112. Elgibaly, A. and Elkamel, A. Optimal hydrate inhibition policies with the aid of neural networks. *Energ Fuel* 13:105–113 (1999).
113. Englezos, P. and Bishnoi, P.R. Prediction of gas hydrate formation conditions in aqueous electrolyte solutions. *Aiche J* 34(10):1718–1721 (1988).
114. Englezos, P. and Lee, J.D. Gas hydrates: a cleaner source of energy and opportunity for innovative technologies. *Korean J Chem Eng* 22:671–681 (2005).
115. Englezos, P. Clathrate hydrates. *Ind Eng Chem Res* 32:1251–1274 (1993).
116. Englezos, P. Computation of the incipient equilibrium carbon dioxide hydrate formation conditions in aqueous electrolyte solutions. *Ind Eng Chem Res* 31(9):2232–2237 (1992).

117. Englezos, P. Nucleation and growth of gas hydrate crystals in relation to‘‘kinetic inhibition’’. *Oil Gas Sci Technol* 51(6):789-795 (1996).
118. Eslamimanesh, A., Mohammadi, A.H., Richon, D., Naidoo, P. and Ramjugernath, D. Application of gas hydrate formation in separation processes. A review of experimental studies. *J Chem Thermodyn* 46:62-71 (2012).
119. Fan, H.Y., Nazari, M., Raval, G., Khan, Z., Patel, H. and Heerklotz, H. Utilizing zeta potential measurements to study the effective charge, membrane partitioning, and membrane permeation of the lipopeptide surfactin. *Biochim Biophys Acta* 1838:2306–2312 (2014).
120. Fan, S.S. Storage and Transportation Technologies of Natural Gas Hydrate, Chemical Industry Press: 1st ed., Beijing, China 1–2 (2005).
121. Farkhondeh, M. and Gheisi, A.R. An introduction to natural gas hydrate transportation. Methane gas hydrate report, Tehran University, (2002).
122. Fazlali, A., Kazemi, S.A., Moraveji, M.K. and Mohammadi, A.H. Impact of Different Surfactants and their Mixtures on Methane-Hydrate Formation. *Energy Technology* 1:471–477 (2013).
123. Felse, P.A., Shah, V., Chan, J., Rao, K.J. and Gross, R.A. Sophorolipid biosynthesis by Candida bombicolafrom industrial fatty acid residues. *Enzyme Microb Tech* 40:316-323 (2007).
124. Fernandes, P. Enzymes in Food Processing: A Condensed Overview on Strategies for Better Biocatalysts. *Enzyme Research* 862537 (2010).
125. Flockhart, B.D. The effect of temperature on the critical micelleconcentration of some paraffin-chain salts. *Journal of ColloidScience* 16(5):484–492 (1961).
126. Forni, C., Braglia, R., Harren, F.J. and Cristescu, S.M. Stress responses of duckweed (Lemna minor L.) and water velvet (Azolla filiculoides Lam.) to anionic surfactant sodium-dodecyl-sulphate (SDS). *Aquat Toxicol* 111:107-113 (2012).
127. Fournaison, L., Delahaye, A., Chatti, I. and Petitet, J.P. CO_2 hydrates in refrigeration processes. *Ind Eng Chem Res* 43(20):6521–6526 (2004).
128. Freer, E. and Sloan, E.D. An engineering approach to kinetic inhibitor design using molecular dynamics simulations. Gas Hydrates. Challenges Future. *Ann Ny Acad Sci* 912:651-657 (2000).

129. Ganji, H., Manteghian, M. and Rahimi Mofrad, H. Effect of mixed compounds on methane hydrate formation and dissociation rates and storage capacity. *Fuel Process Technol* 88:891–895 (2007).
130. Ganji, H., Manteghian, M., Sadaghiani, Z.K., Omidkhaha, M.R. and Mofrad, R.H. Effect of Different surfactant on methane hydrate formation rate, stability and storage capacity. *Fuel* 86:434–441 (2006).
131. Gargulak, J.D. and Lebo, S.E. Lignin Historical, Biological and Materials Perspectives. *American Chemical Society* 742:304–320 (1999).
132. Gayet,P., Dicharry,C., Marion,G., Graciaa,A., J. Lachaise and A. Nestrov. Experimental determination of methane hydrate dissociation curve up to 55 MPa by using a small amount of surfactant as hydrate promoter. *Chem. Eng. Sci.* 60 (2005)
133. Georgiou, G., Lin, S.C. and Sharma, M.M. Surface active compounds from microorganisms. *Biotechnology* 10(1):60-65 (1992).
134. Gerami, S. and Pooladi-Darvish, M. Material balance and boundary dominated flow models for hydrate-capped gas reservoirs. *SPE Annual Technical Conference and Exhibition* 24TH-27th September: San Antonio, Texas, USA (2006).
135. Gilbert, J.A., Davies, P.L., Laybourn-Parry, J., A hyperactive Ca2+-dependent antifreeze protein in an Antarctic bacterium. *FEMS Microb Lett* 245:67–72 (2005).
136. Gnanendran, N. and Amin, R. The effect of hydrotopes on gas hydrate formation. *J Petrol Sci Eng* 40:37–46 (2003).
137. Goel, N. In situ methane hydrate dissociation with carbon dioxide sequestration: Current knowledge and issues. *J Petrol Sci Eng* 51:169–184 (2006).
138. Gonsalves, M.J., Fernandes, C.E.F., Fernandes, S.O., Kirchman, D.L. and Bharathi, P.A.L. Effects of composition of labile organic matter on biogenic production of methane in the coastal sediments of the Arabian Sea. *Environ Monit Assess* 182:385-395 (2011).
139. Goodnow, R.A., Harrison, M.D., Morris, J.D., Sweeting, K.B. and Laduca, R.J. Fate of ice nucleation- active *Pseudomonas syringae* strains in alpine soils and waters and in synthetic snow samples. *Appl Environ Microb* 56:2223-2227 (1990).

140. Gordienko, R., Ohno, H., Singh, V.K., Jia, Z., Ripmeester, J.A. and Walker,V.K. Towards a Green Hydrate Inhibitor: Imaging Antifreeze Proteins on Clathrates. *Plos One* 5(2):e8953 (2010).
141. Gornitz, V. and Fung, I. Potential distribution of methane hydrates in the world's oceans. *Global Biogeochem Cy* 8:335–347 (1994).
142. Grauls, D. Gas hydrates: importance and applications in petroleum exploration. *Mar Petrol Geol* 18:519-523 (2001).
143. Gray, M.L., Soong, Y., Champagne, K.J., Baltrus, J., Stevens, R.W. and Toochinda P. CO_2 capture by amine-enriched fly ash carbon sorbents. *Sep Purif Technol* 35(1):31–36 (2004).
144. Gudiña, E.J., Fernandes, E.C., Rodrigues, A.I., Teixeira, J.A. and Rodrigues, L.R. Biosurfactant production by *Bacillus subtilis* using corn steep liquor as culture medium. *Front Microbiol* 6:59 (2015).
145. Gudmundsson, J.S. and Børrehaug, A. Frozen hydrate for transport of nature gas. *2nd International Conference on Nature Gas Hydrate* Toulouse, France 439–446 (1996).
146. Gudmundsson, J.S. and Graff, O.F. Hydrate Non-Pipeline Technology for Transport of Natural Gas. *22nd World Gas Conference* 1st June to 5th June:Tokyo, (2003).
147. Gudmundsson, J.S., Andersson, V., Levik, O.I. and Mork, M. Hydrate technology for capturing stranded gas, challenges for the future, gas hydrates. *Ann N Y Acad Sci* 912:403-410 (2000).
148. Gudmundsson, J.S., Andersson, V., Levik, O.I. and Mork, M. Hydrate Technology for Capturing Stranded Gas. *3rd International Conference on Gas Hydrates* 18th July to 22nd July:Salt Lake City, (1999).
149. Gudmundsson, J.S., Andersson, V., Levik, O.I. and Parlaktuna, M. Hydrate Concept for Capturing Associated Gas. Society of Petroleum Engineering, European Petroleum Confrence 20th – 22nd October: Hague, Netherlands, (1998).
150. Gudmundsson, J.S., Parlaktuna, M., Levik, O.I. and Andersson, V. Laboratory for Continuous Production of Natural Gas Hydrates. *Ann N Y Acad Sci* 912:851−858 (2006).
151. Guerra-Santos, L., Kappeli, O. and Fiechter, A. Dependence of *Pseudomonas aeruginosa* continous culture biosurfactant production on nutritional and environmental factors. *Appl Microbiol Biot* 24(6):443-448 (1986).

152. Guo, W., Sun, Y., Li, B., Zhang, Y., Li, K., Wang, P., Jia, R. and Qu, L. Comparative Analysis of Production Trial and Numerical Simulations of Gas Production From Multilayer Hydrate Deposits in the Qilian Mountain Permafrost. Oil and Gas Survey, China Geological Survey, *Proceedings of Permafrost-associated Gas Hydrate in China* 162-175 (2014).
153. Gupta, A.K. Marine gas hydrates: their economic and environmental importance. *Curr Sci India* 86:1198–1199 (2004).
154. Gupta, A., Lachance, J., Sloan, E.D. and Koh, C.A. Measurements of methane hydrate heat of dissociation using high pressure differential scanning calorimetry. *Chem Eng Sci* 63:5848-5853 (2008).
155. Hammerschmidt, E.G. Formation of gas hydrates in natural gas transmission lines. *Ind Eng Chem* 26(8):851–855 (1934).
156. Hammerschmidt, E.G. The oil and gas journal, May 11, 66-72 (1939).
157. Handa, Y.P. A Calorimetric study of naturally occurring gas hydrates. *Ind Eng Chem Res* 27:872-874 (1988).
158. Handa, Y.P. and Tse, J.S. Thermodynamics properties of empty lattices of structure I and structure II clathrate hydrates. *J Phys Chem* 90:5917-5921 (1986).
159. Handa, Y.P.J. Compositions, enthalpies of dissociation, and heat capacities in the range 85 to 270 K for clathrate hydrates of methane, ethane, and propane, and enthalpy of dissociation of isobutane hydrate, as determined by a heat-flow calorimeter *J Chem Therodyn* 18(10):915–921 (1986).
160. Haq, B.U. Gas hydrates; greenhouse nightmare? Energy panacea or pipe dream?. *Geological Society of America (GSA) Today* 8(11):1-6 (1998).
161. Harrison, W.J., Wendlandt, R.F. and Sloan, E.D. Geochemical interactions resulting from carbon dioxide disposal on the seafloor. *Appl Geochem* 10(4):461–475 (1995).
162. Harvey, L.D.D. and Huang, Z.J. Evaluation of the potential impact of methane clathrate destabilization on future global warming. *J Geophys Res-Atmos* 100(D2):2905-2926 (1995).
163. Hendriks, C.A. and Blok, K. Underground storage of carbon dioxide. *Energy Convers Manage* 34(9–11):949–957 (1993).

164. Heriot - Watt University Hydrate model, http://www.pet.hw.ac.uk/ research/hydrate/ (accessed July 2007).

165. Herman, D.C. and Maier, R.M. Biosynthesis and Applications of Glycolipid and Lipopeptide Biosurfactants. In Lipid Biotechnology, Marcel Dekker, Eds. H. W. Gardner, T. M. Kuo, New York (USA), 629–654 (2002).

166. Hester, K.C. and Brewer, P.G. Clathrate Hydrates in Nature. *Annual Review of Marine Science* 1:303-327 (2009).

167. *Hicks, J.C., Drese, J.A., Fauth, D.J., Gray, M.L., Qi, G. and Jones, C.W. Designing Adsorbents for CO_2 Capture from Flue Gas-Hyperbranched Aminosilicas Capable of Capturing CO_2 Reversibly. J Am Chem Soc 130:2902–2903 (2008).*

168. *Hill Bembenic, M.A. The Chemistry Of Subcritical Water Reactions Of A Hardwood Derived Lignin And Lignin Model Compounds With Nitrogen, Hydrogen, Carbon Monoxide And Carbon Dioxide. Thesis, Supervised by Clifford, C.E.B., Schobert, H.H., Pisupati, S.V., Brown, N.R. and Yeboah, Y.D. (2011)*

169. Hirohama, S., Shimoyama, Y., Wakabayashi, A., Tatsuta, S. and Nishida, N. Conversion of CH_4-Hydrate to CO_2, Hydrate in Liquid CO_2. *J Chem Eng Japan* 29(6):1014-1020 (1996).

170. Hisatsuka, K., Nakahara, T., Sano, N. and Yamada, K. Formation of rhamnolipid by *Pseudomonas aeruginosa* and its function in hydrocarbon fermentation, *Agr Biol Chem Tokyo* 35:686-692 (1971).

171. Holder, G.D., Cugini, A.V. and Warzinski, R.P. Modeling clathrate hydrate formation during carbon dioxide injection into the ocean. *Environ Sci Technol* 29:276–278 (1995).

172. Holder, G.D., Malone, R.D. and Lawson, W.F. Effects of Gas Composition and Geothermal Properties on the Thickness and Depth of Natural-Gas-Hydrate Zones. *J Petrol Technol* 39(9):1147-1152 (1987).

173. Hunter, R.B., Collett, T.S., Boswell, R., Anderson, B.J., Digert, S.A., Pospisil, G., Baker, R. and Weeks, M. Mount Elbert Gas Hydrate Stratigraphic Test Well Alaska North Slope Overview of scientific and technical program. *Mar Petrol Geol* 28(2):295-310 (2011).

174. Hussain, S.M.T., Kumar, A., Laik, S., Mandal, A. and Ahmad, I. Study of the kinetics and morphology of gas hydrate formation. *Chem Eng Technol* 29(8):937–943 (2006).

175. Huszcza, E. and Burczyk, B. Surfactin Isoforms from *Bacillus* coagulans, Verlag der Zeitschrift für Naturforschung. *Tübingen* 900:727-733 (2006).
176. Igboanusi, U.P., Okere, J.U., Natural Gas Hydrates–A Review of the Resources Offshore Nigeria and around the Globe. *Journal of Engineering Research in Africa* 4:27-33 (2011).
177. Ignik Skumi Gas Hydrate exchange trial project team. *Fire in the Ice* 12(1) (2012).
178. Inaba, H. New challenge in advanced thermal energy transportation using functionally thermal fluids. *Int J Therm Sci* 39(9-11):991–1003 (2000).
179. Isa, M.H.M., Coraglia, D.E., Frazier, R.A. and Jauregi, P. Recovery and purification of surfactin from fermentation broth by a two-step ultrafiltration process. *J Membrane Sci* 296:51-57 (2007).
180. Jadhav, M., Kalme, S., Tamboli, D. and Govindwar, S. Rhamnolipid from *Pseudomonas* desmolyticum NCIM-2112 and its role in the degradation of Brown 3REL. *J Basic Microbiol* 51(4):385-396 (2011).
181. Jager, M.D., Peters, C.J. and Sloan, E.D. Experimental determination of methane hydrate stability in methanol and electrolyte solutions. *Fluid Phase Equilibr* 193(1–2):17–28 (2002).
182. Jakab, E., Faix, O., Till, F. and Szelkely, T. Thermogravimetry/mass spectrometry study of six lignins within the scope of an international round robin test. *J Anal Appl Pyrol* 35:167-169 (1995).
183. Jakosky, B.M., Henderson, B.G. and Mellon, M.T. Chaotic obliquity and the nature of the Martian climate. *J Geophys Res* 100:1579-1584 (1995).
184. Jean-Baptiste, P. and Ducroux, R. Potentiel des me´thodes de se´paration et stockage du CO_2 dans la lutte contre l'effet de serre: the role of CO_2 capture and sequestration in mitigation of climate change. *C R Geoscience* 335:611–625 (2003).
185. Jiafei, Z., Kun, X., Yongchen, S., Weiguo, L., Weihaur, L., Yu, L., Kaihua, X., Yiming, Z., Xichong, Y. and Qingping, L. A Review on Research on Replacement of CH_4 in Natural Gas Hydrates by Use of CO_2. *Energies* 5:399-419 (2012).
186. Jin, Y., Konno, Y. and Nagao, J. Growth of Methane Clathrate Hydrates in Porous Media. *Energ Fuel* 26:2242−2247 (2012).
187. Kakati, H., Kar, S., Mandal, A. and Laik, S. Metahne Hydrate Formation and Dissociation in Oil-in-water. *Energ Fuel* 28:4440-4446 (2014).

188. Kang, H., Koh, D.Y. and Lee, H. Nondestructive natural gas hydrate recovery driven by air and carbon dioxide. *Scientific Reports* 4 (2014).
189. Kang, S.P. and Lee, H. Recovery of CO_2 from flue gas using gas hydrate thermodynamic verification through phase equilibrium measurements. *Environ Sci Technol* 34:4397–43400 (2000).
190. Kang, S.P. and Lee, J.W. Formation Characteristics of Synthesized Natural Gas Hydrates in Meso and Macroporous Silica Gels. *J Phys Chem B* 114:6973–6978 (2010).
191. Kang, S.P. and Lee, Y.W. Kinetic behaviour s of CO_2 hydrate in porous media and effect of kinetic promoter on the formation kinetics. *Chem Eng Sci* 65:1840–1845 (2010).
192. Kang, S.P. and Seo, Y. kinetics of methane and carbon dioxide hydrate formation in silica gel pores. *Energ Fuel* 23:3711–3715 (2009).
193. Kang, S.P. and Seo, Y. Natural Gas Storage in Mesoporous Media Using Gas Hydrate. *Internation Gas union Research Confrence* 8^{th} – 10^{th} October: Parish (2008).
194. Kang, S.P., Lee, H. and Ryu, B.J. Enthalpies of dissociation of clathrate hydrates of carbon dioxide, nitrogen, (carbon dioxide plus nitrogen), and (carbon dioxide plus nitrogen plus tetrahydrofuran). *J Chem Thermodyn* 33(5):513-521 (2001).
195. Karaaslan, U. and Parlaktuna, M. PEO-a new hydrate inhibitor polymer. *Energ Fuel* 16:1387–1391 (2002).
196. Karaaslan, U. and Parlaktuna, M. Promotion Effect of Polymers and Surfactants on Hydrate Formation Rate. *Energ Fuel* 16:1413-1416 (2002).
197. Karaaslan, U. and Parlaktuna, M. Surfactants as hydrate promoters?. *Energ Fuel* 14:1103-1107 (2000).
198. Karaaslan, U., Uluneye, E., and Parlaktuna, M. Effect of an anionic surfactant on different type of hydrate structures. *J Petrol Sci Eng* 35:49-57 (2002).
199. Karimi, R., Varaminian, F., Izadpanah, A.A. and Mohammadi, A.H. Effects of Different Surfactants on the Kinetics of EthaneHydrate Formation: Experimental and Modeling Studies. *Energy Technology* 1:530-536 (2013).
200. Karisiddaiah, V.M., Vora, S.M., Wagle, K.G. and Almeida, F. Detection of gas-charged sediments and gas hydrate horizons along the western continental margins of India, Geological Society Special Publication London, eds., JP Henriet and J Mienert, 137:239-253 (1998).

201. Kashchiev, D. and Firoozabadi, A. Induction time in crystallization of gas hydrates. *J Cryst Growth* 250(34):499-515 (2003).
202. Kashchiev, D., Verdoes, D. and Van Rosmalen, G.M. Induction time and metastability limit in new phase formation. *J Crystal Growth* 110:373-380 (1991).
203. Kelkar, S.K., Selim, M.S. and Sloan, E.D. Hydrate dissociation rates in pipelines. *Fluid Phase Equilibr* 150–151:371–382 (1998).
204. Kelland, M.A. History of the development of low dosage hydrates inhibitors. *Energ Fuel* 20:825–847 (2006).
205. Kelland, M.A., Svarta, T.M. and Andersen, L.D. Gas HydrateAnti Agglomerant Properties of Polypropoxylates and Some Other Demulsifiers. *J Petrol Sci Eng* 64:1−10 (2009).
206. Kikkinides, E.S., Yang, R.T. and Cho, S.H. Concentration and recovery of CO_2 from flue-gas by pressure swing adsorption. *Ind Eng Chem Res* 32:2714–2720 (1993).
207. Kim, J., Lin, L.C., Swisher, J.A., Haranczic, M. and Smit, B. Predicting Large CO_2 Adsorption in Aluminosilicate Zeolites for Postcombustion Carbon Dioxide Capture. J Am Chem Soc 134:18940–18943 (2012).
208. Kim, K.M., Lee, J.Y., Kim, C.K. and Kang, J.S. Isolation and characterization of surfactin produced by Bacillus polyfermenticus KJS-2. *Arch Pharm Res* 32:711-715 (2009).
209. Kim, N.J., Lee, J.H., Cho, Y.S. and Chun, W. Formation Enhancement of Methane Hydrate for Natural Gas Transport and Storage. *Energy* 35:2717−2722 (2010).
210. Kim, N.J., Park, S.S., Shin, S.W., Hyun, J.H. and Chun, W. An experimental investigation into the effects of zeolites on the formation of methane hydrates. *Int. J.Energy Res* 39:26–32 (2014).
211. Klara, S.M. and Srivastava, R.D. US DOE integrated collaborative technology development program for CO_2 separation and capture. *Environmental Progress & suitable Energy* 21:247–253 (2002).
212. Klauda, J.B. and Sandler, S.I. Global distribution of methane hydrates in ocean sediment. *Energ Fuel* 19:459–470 (2005).
213. Klauda, J.B. and Sandler, S.I. Phase behaviour of clathrate hydrate: a model for single and multiple gas component hydrates. *Chem Eng Sci* 58(1):27-41 (2003).
214. Klauda, J.B. and Sandler, S.I. Predictions of gas hydrate phase equilibria and amounts in natural sediment porous media. *Mar Pet Geol* 20:459–470 (2003).

215. Klein Nagelvoort R., Large-Scale GTL–A Commercially Attractive Alternative to LNG. *Natural Gas Technology Workshop* 28th -29th November: NorwegianUniversity of Science and Technology Trondheim (2000).

216. Kocherla, M. and Pillai, S. Methane- Derived Authigenic Carbonates-A Proxy for Gas Hydrate Exploration: A Comparative Study From the Continental Margins of India. *51st Aanual Convention on Earth Sciences and Society*, Indian Geophysical Union, 19th – 21st November: Kurukeshetra University 72-77 (2014).

217. Kocherla, M., Teichert, B.M.A., Surabhi, P., Satyanarayanan, M., Ramamurty, P.B., Patil, D.J. and Rao, A.N. Formation of methane-related authigenic carbonates in a highly dynamic biogeochemical system in the Krishnae-Godavari Basin, Bay of Bengal. *Mar Petrol Geol* 64:324-333 (2015)

218. Koh, C.A., Sloan, E.D., Sum, A.K. and Wu, D.T. Fundamentals and applications of gas hydrates. *Annu Rev Chem Biomol Eng* 2:237-257 (2011).

219. Koh, C.A. Towards a fundamental understanding of natural gas hydrates. *Chem Soc Rev* 31:157–167 (2002).

220. Koh, C.A., Westacott, R.E., Zhang, W., Hirachand, K., Creek, J.L. and Soper, A.K. Mechanisms of gas hydrate formation and inhibition. *Fluid Phase Equilibr* 194–197:143–151 (2002).

221. Kojima, R., Yamane, K. and Aya, I. Dual nature of CO_2 solubility in hydrate forming region. *Fourth international conference on gas hydrates* 286–289 (2002).

222. Kosaric, N. Biosurfactants and Their Application for Soil Bioremediation. *Food Technol Biotech* 39:295-304 (2001).

223. Kothapalli, C.R. Catalysis of gas hydrates by Biosurfactants in seawater-saturated Sand/Clay, M.S. Thesis, Dave C. Swalm School of Chemical Engineering, Mississippi State University, 43–61 (2002).

224. Kuhs, W.F., Klapproth, A., Gotthardt, F., Techmer, K. and Heinrichs, T. The formation of meso and macroporous gas hydrates. *Geophys Res Lett* 27:2929-2932 (2000).

225. Kumar, A., Kumar, R. and Linga, P. Carbon dioxide capture from a flue gas and fuel mixture by hydrate formation in silica gel and silica sand media. Proceedings of the *8th International Conference on Gas Hydrates*, 28th July – 1st August (2014).

226. Kumar, A., Sakpal, T. and Kumar, R. Influence of Low Dosage Hydrate Inhibitor on Methane Clathrate Hydrate Formation and Dissociation Kinetics. *Energy Technology* 3(7):717-725 (2015).
227. Kumar, A., Sakpal, T., Linga, P. and Kumar, R. Enhanced carbon dioxide hydrate formation kinetics in a fixed bed reactor filled with metallic packing. *Chem Eng Sci* 122:78-85 (2015).
228. Kumar, A., Sakpal, T., Linga, P. and Kumar, R. Impact of Fly Ash Impurity on the Hydrate-Based Gas Separation Process for Carbon Dioxide Capture from a Flue Gas Mixture. *Ind Eng Chem Res* 53:9849−9859 (2014).
229. Kumar, A., Sakpal, T., Linga, P. and Kumar, R. Influence of contact medium and surfactants on carbon dioxide clathrate hydrate kinetics. *Fuel* 105:664-671 (2013).
230. Kumar, A., Sakpal, T., Roy, S. and Kumar, R. Methane hydrate formation in a test sediment of sand and clay at various level of water saturation. *Can J Chem Eng* (2015). DOI: 10.1139/cjc-2014-0537
231. Kumar, P., Collett, T.S., Boswell, R., Cochran, J.R., Lall, M., Mazumdar, A., Ramana, M.V., Ramprasad, T., Riedel, R., Sain, K., Sathe, A.V., Vishwanath, K., and Yadav, U.S. NGHP Expedition 01 Scientific Party, Geologic implications of gas hydrates in the offshore of India: Krishna-Godavari Basin, Mahanadi Basin, Andaman Sea, Kerala-Konkan Basin. *Mar Petrol Geol* 58:29-98 (2014).
232. Kumar, R., Englezos, P., Moudrakovski, I. and Ripmeester, J.A. Structure and composition of $CO_2/H_2$and $CO_2/H_2/C_3H_8$hydrate in relation to simultaneous CO_2 capture and H_2 production. *Aiche J* 55:1584–1594 (2009).
233. Kumar, R., Lee, J.D., Song, M. and Peter, E. Kinetic inhibitor effects on methane/propane clathrate hydrate-crystal growth at the gas/water and water/n-heptane interfaces. *J Cryst Growth* 310:1154–1166 (2008).
234. Kumar, R., Linga, P., Ripmeester, J.A. and Englezos, P. Two-Stage Clathrate Hydrate/Membrane Process for Pre-combustion Capture of Carbon Dioxide and Hydrogen, *J Environ Eng-Asce* 135:411-417 (2009).
235. Kumar, S.V., Kumar, M.G., Udayabhanu, G., Mandal, A. and Laik, S. Kinetics of methane hydrate formation and its dissociation in presence of non-ionic surfactant Tergitol. *Journal of Unconventional Oil and Gas Resources* 54–59 (2014).

236. Kvenvolden, K.A. A primer on the geological occurrence of gas hydrate. *Geological Society Special Publication London* 137:9–30 (1998).
237. Kvenvolden, K.A. and McMenamin, M.A. Hydrates of natural gas: a review of their geologic occurrence. *US Geological Survey* Circular 825 1–11 (1980).
238. Kvenvolden, K.A. Estimates of the methane content of worldwide gas-hydrate deposits, methane hydrates: resources in the near future, 20th –22nd October: Japan (1988).
239. Kvenvolden, K.A. Gas hydrates as a potential energy resource—a review of their methane content, Ed., Howerll, D. G., The future of energy gases : U.S. Geological Survey Professional Paper 1570, 555-561 (1993).
240. Kvenvolden, K.A. Gas hydrates-Geological perspective and global change. *Rev Geophys* 31:173-187 (1993).
241. Kvenvolden, K.A. Methane hydrate- A major reservoir of carbon in the shallow geosphere?. *Chem Geol* 71:41–51 (1988).
242. Kvenvolden, K.A. Potential effects of gas hydrate on human welfare. *Proc Natl Acad Sci* 96:3420-3426 (1999).
243. Kwon, Y.Ah., Park, J.M., Jeong, K.E., Kim, C.U., Kim, T.W., Chae, H.J., Jeong, S.Y., Yim, J.H., Park, Y.K. and Lee, J.d. Synthesis of anionic multichain type surfactant and its effect on methane gas hydrate formation. *J Ind Eng Chem* 17:120–124 (2011).
244. Lai, C.C., Huang, Y.C., Wei, Y.H. and Chang, J.S. Biosurfactant-enhanced removal of total petroleum hydrocarbons from contaminated soil. *J Hazard Mater* 167:609-614 (2009).
245. Lange, H. and Schwuger, M.J. Mizellbildung und Krafft-Punkte inder homologen Reiche der Natriium-n-alkyl-sulfate einschlieβ lich der ungeradzahligen Glieder. *Kolloid-Zeitschrift und Zeitschrift für Polymere* 223:45–149 (1968).
246. Lanoil, B.D., Sassen, R., La Duc M.T., Sweet, S.T. and Nealson, K.H. Bacteria and Archaea Physically Associated with Gulf of Mexico Gas Hydrates. *Appl Environ Microb* 67(11):5143-5153 (2001).
247. Lederhos, J.P., Long, J.P., Sum, A., Christiansen, R.L. and Sloan, E.D. Effective kinetic inhibitors for natural gas hydrates. *Chem Eng Sci* 51(8):1221-1229 (1996).

248. *Lee, H., Seo, Y., Seo, Y.T., Moudrakovski, I.L. and Ripmeester, J.A. Recovering methane from solid methane hydrate with carbon dioxide. Angew Chem Int Edit 115:5202–5205 (2003).*

249. Lee, J.D. and Englezos, P. Unusual kinetic inhibitor effects on gas hydrate formation. *Chem Eng Sci* 61:1368-1376 (2006).

250. Lee, J.D., Hong, S.Y., Park, K., Kim, J.H. and Yun, J.H. A new method for seawater desalination via gas hydrate process and removal characteristics of dissolved minerals. *7th ICGH* 17th – 21st July: Scotland, United Kingdom 17–21 (2011).

251. Lee, J. Experimental study on the dissociation behaviour and productivity of gas hydrate by brine injection scheme in porous rock. *Energ Fuel* 24:456-463 (2010).

252. Lee, J.W. and Kang, S.P. Phase equilibria of natural gas hydrates in the presence of methanol, ethylene glycol, and NaCl aqueous solutions. *Ind Eng Chem Res* 50:8750–8755 (2011).

253. Lee, M.W. and Collett, T.S. In-situ gas hydrate hydrate saturation estimated from various well logs at the Mount Elbert Gas Hydrate Stratigraphic Test Well Alaska North Slope. *Mar Petrol Geol* 28:439-449 (2011).

254. Lee, S., Liang, L., Riestenberg, D., West, O.R., Tsouris, C. and Adams, E. CO_2 hydrate composite for ocean carbon sequestration. *Environ Sci Technol* 37:3701–7308 (2003).

255. Lee, S., Zhang, J., Mehta, R., Woo, T.K. and Lee, J.W. Methane Hydrate Equilibrium and Formation Kinetics in the Presence of an Anionic Surfactant. *J Phys Chem C* 111:4734-4739 (2007).

256. Leitermann, F., Syldatk, C. and Hausmann, R. Fast quantitative determination of microbial rhamnolipids from cultivation broths by ATR-FTIR Spectroscopy. *Journal of Biological Engineering* 2(1):13 (2008).

257. Levy, N., Bar, Y. and Magdassi, S. Flocculation of Bentonite Particles by a Cyanobacterial Bioflocculant. *Colloid Surface* 48:337-349 (1990).

258. Lin, W.W.K., Chen, G.J., Sun, C.Y. and Yang, L. Effect of surfactant on the formation and dissociation kinetic behaviour of methane hydrate. *Chem. Eng. Sci* 59(21):4449-4455 (2004).

259. Linga, P., Daraboina, N., Ripmeester, J.A. and Englezos, P. Enhanced rate of gas hydrate formation in a fixed bed column filled with sand compared to a stirred vessel. *Chem Eng Sci* 68:617-623 (2012).
260. Linga, P., Haligva, C., Nam, S.C., Ripmeester, J.A. and Englezos, P. Gas Hydrate Formation in a Variable Volume Bed of Silica Sand Particles. *Energ Fuel* 23(11):5496-5507 (2009).
261. Linga, P., Kumar, R. and Englezos, P. The clathrate hydrate process for post and pre combustion capture of carbon dioxide. *J Hazard Mater* 149:625–629 (2007).
262. Linga, P., Kumar, R., Lee, J.D., Ripmeester, J. and Englezos, P. A new apparatus to enhance the rate of gas hydrate formation: application to capture of car bon dioxide. *International Journal of Greenhouse gas Control* 4(4):630–637 (2010).
263. Link, D.D., Ladner, E.P., Elsen, H.A. and Taylor, C.E. Formation and dissociation studies for optimizing the uptake of methane by methane hydrates. *Fluid Phase Equilibr* 211:1-10 (2003).
264. Liro, C.R., Adams, E.E. and Herzog, H.J. Modeling the release of CO_2 in the deep ocean. *Energ Convers Manage* 33(5–8):667–74 (1992).
265. Liu, J., Shi, J., Li, J. and Yuan, X. Characterization of the interaction between surfactants and enzymes by fluorescence probe. *Enzyme Microb Tech* 49(4):360-365 (2011).
266. Liu, J.F., Wu, G., Yang, S.Z. and Mu, B.Z. Structural characterization of rhamnolipid produced by *Pseudonomas aeruginosa* strain FIN2 isolated from oil reservoir water. *World J Microb Biot* 30:1473–1484 (2014).
267. Liu, Q., Lin, J., Wang, W., Huang, H. and Li, S. Production of surfactin isoforms by *Bacillus subtilis* BS-37 and its applicability to enhanced oil recovery under laboratory conditions. *Biochem Eng J* 93:31-37 (2015).
268. Liu, W., Ji, C., Li, Y., Song, Y., Zhu, Y. and Zhang, L. Effects of the addition of a surfactant on methane hydrate formation. *ICGH8* 28th july- 1st Augest: Beijing, China (2014).
269. Liu, X.Y., Yang, S.Z. and Mu, B.Z. Production and characterization of a C15-surfactin-O-methyl ester by a lipopeptide producing strain *Bacillus subtilis* HSO121. *Process Biochem* 44:1144-1151 (2009).

270. Lorenson, T.D., Collett, T.S. and Hunter, R.B. Gas geochemistry of the Mount Elbert Gas Hydrate Stratigraphic Test Well Alaska North Slope Implications for gas hydrate exploration in the Arctic. *Mar Petrol Geol* 28(2):343-360 (2011).

271. Lotfabad, T.B., Abassi, H., Ahmadkhaniha, R., Roostaazad, R., Masoomi, F., Zahiri, H.S., Ahmadian, G., Vali, H. and Noghabi, K.A. Structural characterization of a rhamnolipid-type biosurfactant produced by *Pseudomonas aeruginosa* MR01: Enhancement of di-rhamnolipid proportion using gamma irradiation. *Colloid Surface B* 81(2):397-405 (2010).

272. Loveday, J.S., Nelmes, R.J., Guthrie, M., Belmonte, S.A., Allan, D.R., Klug, D.D., Tse, J.S. and Handa, Y.P. Stable methane hydrate above 2 GPa and the source of Titan's atmospheric methane. *Nature* 410:661–663 (2001).

273. Lubert-Martin, M., Darbouret, M. and Herri, J.M. Rheological study of two-phase secondary fluids for refrigeration and air-conditioning. *9e`me Congre`s de la SFGP* 27th September: Saint-Nazaire, France, (2003).

274. *Lu, C., Bai, H., Wu, B., Su, F. and Hwang, J.F. Comparative Study of CO_2 Capture by Carbon Nanotubes, Activated Carbons, and Zeolites. Energ Fuel 22:3050–3056 (2008).*

275. Lu, S.M. A global servey of gas hydrate development and reserves: Specifically in the marine field. *Renewable and Sustainable Energy Reviews* 41:884-900 (2015).

276. Lugo, R., Fournaison, L., Chourot, J.M. and Guilpart, J. An excess function method to model the thermophysical properties of one-phase secondary refrigerants. *Int J Refrig* 25(7):916–23 (2002).

277. Lunine, J.I. and Stevenson, D.J. Thermodynamics of clathrate hydrate and low and high pressures with application to the outer solar system. *Astrophys J Suppl S* 58:493-531 (1985).

278. MacKerell, A.D. Molecular dynamics simulation analysis of a sodium dodecyl sulfate micelle in aqueous solution: decreased fluidity of the micelle hydrocarbon interior. *J Phys Chem* 99:1846 (1995).

279. Maekawa, T. Equilibrium conditions for clatharate hydrates formed from methane and aqueous propanol solutions. *Fluid Phase Equilibr* 267:1-5 (2008).

280. Mahajan, D., Taylor, C.E. and Mansoori, G.A. An introduction to natural gas hydrate/clathrate: the major organic carbon reserve of the Earth. *J Petrol Sci Eng* 56:1–8 (2007).

281. Mahmoodaghdam, E. and Bishnoi, P.R. Equilibrium data for methane, ethane, and propane incipient hydrate formation in aqueous solutions of ethylene glycol and diethylene glycol. *J Chem Eng Data* 47(2):278–81 (2002).
282. Makkar, R.S. and Cameotra, S.S. Biosurfactant production by a thermophilic *Bacillus subtilis* strain. *J Ind Microbiol Biot* 18:37–42 (1997).
283. Makogon, Y.F., Holditch, S.A. and Makogon, T.Y. Natural gas-hydrates–a potential energy source for the 21st century. *J Petrol Sci Eng* 56:14–31 (2007).
284. Makogon, Y.F., Hydrates of hydrocarbons. Pennwell Publ, Comp Tulsa, Oklahoma, (1997).
285. Mandal, A. and Laik, S. Effect of the promoter on gas hydrates formation and dissociation. *Energ Fuel* 22(4):2527-2532 (2008).
286. Manso Pajarron A., De Koster C.G., Heerma, W., Schmidt, M. and Haverkamp, J. Structure identification of natural rhamnolipid mixtures by fast atom bombardment tandem mass spectrometry. *Glycoconjugate J* 10(3):219-226 (1993).
287. Masakorala, K., Turner, A. and Brown, M. Toxicity of Synthetic Surfactants to the Marine Macroalga, Ulva lactuca. *Water Air Soil Poll* 218(1-4):283-291 (2010).
288. Matsumoto, K., Namiki, Y., Okada, M., Kawagoe, T., Nakagawa, S. and Kang, C. Continuous ice slurry formation using a functional fluid for ice storage. *Int J Refrig* 27(1):73–81 (2004).
289. Matsumoto, R., Ryu, B.J., Lee, L.R., Lin, S., Wu, S., Sain, K., Pecher, I. and Riedel, M. Occurrence and exploration of gas hydrate in the marginal seas and continental margin of the Asia and Oceania region. *Mar Petrol Geol 28:1751-67 (2011).*
290. *Matsuo, K., Kurosaka, S., Yanagimori, Y., Asano, S. and Shinoda, J. Device and method for extracting a gas hydrate. U.S. Patent 6817427 B2 (2004).*
291. Max, M.D. and Pellenbarg, R.E. Desalination through Gas Hydrate. *U.S. Patent 6158239 A* (2000).
292. Max, M.D., Johnson, A. and Dillon, W.P. Economic Geology of Natural Gas Hydrate, Springer, Berlin Dordrecht 341 (2006).
293. Mazzini, A., Ivanov, M.K., Parnell, J., Stadnitskaia, A., Cronin, B.T., Poludetkina, E., Mazurenko, L., and van Weering, T.C.E. Methane-related authigenic carbonates from the

Black Sea: geochemical characterization and relation to seeping fluids. *Mar Geol* 212:153–181 (2004).

294. McIver, R.D. Gas hydrates, Long-term energy resources, Pitman, Boston, Meyer, R.F., Olson, J.C. eds. 713–726 (1981).
295. McKendry, P. Energy production from biomass (part 1) overview of biomass. *Bioresour Technol* 83:37-46 (2002).
296. Mekala, P., Babu, P., Sangwai, J.S. and Linga P. Formation and Dissociation Kinetics of Methane Hydrates in Seawater and Silica Sand. *Energ fuel* 28(4):2708−2716 (2014).
297. Mendes, A., Filgueiras, L., Pinto, J. and Nele, M. Physicochemical Properties of Rhamnolipid Biosurfactant from *Pseudomonas aeruginosa* PA1 to Applications in Microemulsions. *Journal of Biomaterials and Nanobiotechnology* 6:64-79 (2015).
298. Michael, A.L. Chronic and Sublethal Toxicities of Surfactants to Aquatic Animals: a review and risk assessment. *Water Res* 25(1):101-113 (1991).
299. Milkov, A.V., Claypool, G.E., Lee, Y.J., Xu, W.Y., Dickens, G.R. and Borowski, W.S. In situ methane concentrations, at Hydrate Ridge, offshore Oregon: new constraints on the global gas hydrate inventory from an active margin. *Geology* 31:833–836 (2003).
300. Milkov, A.V. Global estimates of hydrate-bound gas in marine sediments: how much is really out there. *Earth-Sci Rev* 66:183–197 (2004).
301. Miller, S.L. and Smythe, W.D. Carbon dioxide hydrate and floods on Mars. *Science* 170:531-533 (1970).
302. Mnif, I. and Ghribi, D. Review lipopeptides biosurfactants Mean classes and new insights for industrial, biomedical, and environmental applications. *Biopolymers* 104:129-147 (2015).
303. Mohammadi, A.H., Afzal, W. and Richon, D. Experimental Data and Predictions of Dissociation Conditions for Ethane and Propane Simple Hydrates in the Presence of Distilled Water and Methane, Ethane, Propane, and Carbon Dioxide Simple Hydrates in the Presence of Ethanol Aqueous Solutions. *J Chem Eng Data* 53:73–76 (2008).
304. Mohammadi, A.H. and Richon, D. Gas Hydrate Phase Equilibrium in the Presence of Ethylene Glycol or Methanol Aqueous Solution. *Ind Eng Chem Res* 49:8865-8869 (2010).

305. Mohammadi, A.H. and Richon, D. Phase Equilibria of Methane Hydrates in the Presence of Methanol and/or Ethylene Glycol Aqueous Solutions. *Ind Eng Chem Res* 49:925–928 (2010).
306. Monod, J. The growth of bacterial cultures. *Annu Rev Microbiol* 3:371-394 (1949).
307. Moraveji, M.K., Sadeghi, A., Fazlali, A. and Davarnejad, R. Effect of an Anionic Surfactant on the Methane Hydrate Formation: Induction Time and Stability. *World Appl Sci J* 9(10):1121-1128 (2010).
308. Mori, Y.H. and Isobe, F. A model for gas hydrate formation accompanying direct-contact evaporation of refrigerant drops in water. *Int Commun Heat Mass* 18(5):599–608 (1991).
309. Mori, Y.H. and Mori, T. Characterization of gas hydrate formation in direct-contact cool storage process. *Int J Refrig* 12:259–265 (1989).
310. Mori, Y.H. and Mori, T. Formation of gas hydrate with CFC alternative R-134a. *Aiche J* 35(7):1227–1228 (1989).
311. Moridis, G.J. and Collett, T. Strategies for gas production from hydrate accumulations under various geologic conditions. *TOUGH Symposium* 12th -14th May: Berkeley, CA (2003).
312. Moridis, G.J. and Sloan, E.D. Gas production potential of disperse low-saturation hydrate accumulations in oceanic sediments. *Energ Convers Manage* 48:1834-1849 (2007).
313. Moridis, G.J. Numerical studies of gas production from methane hydrates. *Gas Technology Symposium SPE* April 30th –May 2nd Calgary (2002).
314. Morita, T., Konishi, M., Fukuoka, T., Imura, T. and Kitamoto, D. Microbial conversion of glycerol into glycolipid biosurfactants, mannosylerythritol lipids, by a basidiomycete yeast, Pseudozyma antarctica JCM 10317T. *J Biosci Bioeng* 104:78–81 (2007).
315. Moussa, T.A.A., Mohamed, M.S. and Samak, N. Production and Characterization and di-Rhamnolipid Produced by *Pseudomonas aeruginosa* TMN. *Braz J Chem Eng* 31(4):867-880 (2014).
316. Muller, M.M., Kugler, J.H., Henkel, M., Gerlitzki, M., Hormann, B., Pohnlein, M., Syldatk, C. and Hausmann, R. Rhamnolipids--next generation surfactants?, *J Biotechnol* 162(4):366-380 (2012).
317. Mulligan, C.N. Environmental applications for biosurfactants. *Environ Pollut* 133:183-198 (2005).

318. Mulligan, C.N., Yong, R.N. and Gibbs, B.F. Remediation technologies for metal-contaminated soils and groundwater: an evaluation. *Eng Geol* 60(1-4):193-207 (2001).
319. Muthusamy, K., Gopalakrishnan, S., Ravi, T.K. and Sivachidambaram, P. Biosurfactants: properties, commercial production and application. *Curr Sci India* 94:736-774 (2008).
320. Najibi, H., Shayegan, M.M. and Heidary, H. Experimental investigation of methane hydrate formation in the presence of copper oxide nanoparticles and SDS. *Journal of Natural Gas Science and Engineering* 23:315-323 (2015).
321. Nakano, M.M., Marahiel, M.A. and Zuber, P. Identification of a genetic locus required for biosynthesis of the lipopeptide antibiotic Surfactin in *Bacillus subtilis*. *J Bacteriol* 170(12):5662-5668 (1988).
322. Natarajan, V., Bishnoi, P.R. and Kalogerakis, N. Induction phenomena in gas hydrate nucleation. *Chem Eng Sci* 49:2075–2087 (1994).
323. Ng, H.J. and Robinson D.B. Hydrate formation in systems containing methane, ethane, propane, carbon dioxide or hydrogen sulfide in the presence of methanol. *Fluid Phase Equilibr* 21(1–2):145–155 (1985).
324. Ng, H.J., Chen, C.J. and Saeterstad, T. Hydrate formation and inhibition in gas condensate and hydrocarbon liquid systems. *Fluid Phase Equilibr* 36:99–106 (1987).
325. Nie, M., Yin, X., Ren, C., Wangq Y., Xu, F. and Shen, Q. Novel rhamnolipid biosurfactants produced by a polycyclic aromatic hydrocarbon-degrading bacterium *Pseudomonas aeruginosa* strain NY3. *Biotechnol Adv* 28(5):635–643 (2010).
326. Nitschke, M. and Costa, S.G. and Contiero, J. Rhamnolipid Surfactants: An Update on the General Aspects of these Remarkable Biomolecules. *Biotechnol Progr* 21(6):1593-1600 (2005).
327. Nixdorf, J. Experimentelle und theoretische untersuchung der hydratbildung von erdgasen unter betriebsbedingungen, Dissertation, Universität Karlsruhe T.H., (1996).
328. Nnanna, I.A. and Xia, J. Protein-Based Surfactant, Synthesis, Physicochemical Properties and Applications, Marcel Dekker AG, New York, USA. 157 (2001).
329. Ochiai, K., Hayashi, M., Oikawa, N., Shimizu, S., Nakamizu, M., Yonezawa, T., Takayama, K., Hato, M., Baba, K. and Morita, S. The estimation for the resources of

methane hydrate in the Nankai Trough offshore Japan. *22nd World Gas Conference* 1st – 5th June: Tokyo (2003).

330. Ohgaki, K., Takano, K. and Moritoki, M. Exploitation of CH_4 Hydrates under the Nankai Trough in Combination with CO_2 Storage. *Kagaku Kogaku Ronbun* 20:121-123 (1994).
331. Ohgaki, K., Takano, K., Sangawa, H., Matsubara, T. and Nakano, S. Methane Exploitation by Carbon Dioxide from Gas Hydrates - Phase Equilibria for CO_2-CH_4 Mixed Hydrate System. *J Chem Eng Jpn* 29(3):478-483 (1996).
332. Ohno, H., Susilo, R., Gordienko, R., Ripmeester, J. and Walker, V.K. Interaction of Antifreeze Proteins with Hydrocarbon Hydrates. *Chem-Eur J* 16(34):10409−10417 (2010).
333. Okutani, K., Kuwabara, Y. and Mori, Y.H. Surfactant effects on hydrate formation in an unstirred gas/liquid system amendments to previous study using HFC-32 and sodiumdodecyl sulphate. *Chem Eng Sci* 62:3858–3860 (2007).
334. Okutani, K., Kuwabara, Y. and Mori, Y.H. Surfactant effects on hydrate formation in an unstirred gas/liquid system: an experimental study using methane and sodium alkyl sulphates. *Chem Eng Sci* 63:183-194 (2008).
335. Østergaard, K. K., Masoudi, R., Tohidi, B., Danesh, A. and Todd, A. C. A general correlation for predicting the suppression of hydrate dissociation temperature in the presence of thermodynamic inhibitors. *J. Pet. Sci. Eng*. 48:70–80 (2005).
336. Pacwa-Plociniczak, M., Plaza, G.A., Piotrowska-Seget, Z. and Cameotra, S.S. Environmental applications of biosurfactants: recent advances. *Int J Mol Sci* 12(1):633-654 (2011).
337. Pang, W.X., Chen, G.J., Dandekar, A., Sun, C.Y. and Zhang, C.L. Experimental study on the scale-up of gas storage in the form of hydrate in a quiescent reactor. *Chem Eng Sci* 62:2198-2208 (2007).
338. Park, S.S., Park, Y.B. and Kim, N.J. A Comparative Study on the Formation of Methane Hydrate Using Natural Zeolite and Synthetic Zeolite 5A. *New & Renewable Energy* 8(2):24-32 (2012).
339. Park, Y., Kim, D., Lee, J., Huh, D., Park, K., Lee, J. and Lee, H. Sequestering Carbon Dioxide Into Complex Structures Of Naturally Occurring Gas Hydrates. *Proc Natl Acad Sci U.S.A* 103(34):12690-1269 (2006).

340. Parrish, W.R. and Prausnitz, J.M. Dissociation pressures of gas hydrates formed by gas mixtures. *Ind Eng Chem Proc DD* 11(1):26-35 (1972).

341. Paull, C.K. and Dillon, W.P. Natural gas hydrates occurrence, distribution and detection. American Geophysical Union, Geophysical Monograph 124:315 (2000).

342. Pedrazzani, R., Ceretti, E., Zerbini, I., Casale, R., Gozio, E., Bertanza, G., Gelatti, U., Donato, F. and Feretti, D. Biodegradability, toxicity and mutagenicity of detergents, Integrated experimental evaluations. *Ecotox Environ Safe* 84:274-281 (2012).

343. Pereira, J.F.B., Gudia, E.J., Costa, R., Vitorino, R., Teixeira, J.A., Coutinho, J.o.A.P. and Rodrigues L.R. Optimization and characterization of biosurfactant production by *Bacillus subtilis* isolates towards microbial enhanced oil recovery applications. *Fuel* 111:259-268 (2013).

344. Perfeldt, C.M., Chua, P.C., Nagu, D., Friis, D., Kristiansen, E., Ramlov, H., Woodley, J.M., Kelland, M.A. and Solms, N.V. Inhibition of Gas Hydrate Nucleation and Growth Efficacy of an Antifreeze Protein from the Longhorn Beetle Rhagium mordax. *Energ Fuel* 28:3666−3672 (2014).

345. Peypoux, F., Bonmatin, J.M. and Wallah, J. Recent trends in the biochemistry of surfactin. *Appl Microbial Biot* 51:553-563 (1999).

346. Phan, A., Doonan, C.J., Uribe-Rono F.J., Knobler, C., Furukawa, H., O'Keefe, M. and Yaghi, O.M. Synthesis, Structure, and Carbon Dioxide Capture Properties of Zeolitic Imidazolate Frameworks. Accounts Chem Res 43:58–67 (2010).

347. Pinkert, S., Grozic, J.L.H. and Priest J.A. Strain-Softening Model for Hydrate-Bearing Sands. *Int J Geomech* (2015). DOI:10.1061/(ASCE)GM.1943-5622.0000477

348. Pooladi-Darvish, M. Gas production from hydrate reservoirs and its modelling. *J Petrol Technol* 56(6):65-71 (2004).

349. Poremba, K., Gunkel, W., Lang, S. and Wagner, F. Marine biosurfactants, III. Toxicity testing with marine microorganisms and comparison with synthetic surfactants. *Z Naturforsch C* 46(3-4):210-216 (1991).

350. Pornsunthorntawee, O., Arttaweeporn, N., Paisanjit, S., Somboonthanate, P., Abe, M., Rujiravanit, R. and Chavadek, S. Isolation and comparison of biosurfactants produced by *Bacillus subtilis* PT2 and *Pseudomonas aeruginosa* SP4 for microbial surfactant-enhanced oil recovery. *Biochem Eng J* 42:172-179 (2008).

351. Pornsunthorntawee, O., Chavadej, S. and Rujiravanit, R. Characterization and encapsulation efficiency of rhamnolipid vesicles with cholesterol addition. *J Biosci Bioeng* 112(1):102-106 (2011).

352. Poropokari, A.L., Babu, C.P. and Mascarenhas, A. New evidences for enhanced preservation of organic carbon in contact with oxygen minimum zone on the western continental margin of India. *Mar Geol* 111:7-13 (1993).

353. Priest, J.A., Clayton, C.R.I. and Rees, E.V.L. Potential impact of gas hydrate and its dissociation on the strength of host sediment in the KrishnaeGodavari Basin. *Mar Petrol Geol* 58:187-198 (2014).

354. Profio, P.D., Arca, S., Germani, R. and Savelli, G. Surfactant promoting effects on clathrate hydrate formation: Are micelles really involved?. *Chem Eng Sci* 60:4141–4145 (2005).

355. Pruppacher, H.R. and Klett, J.D. Microphysics of Clouds and Precipitation, Dordrecht: Kluwer Academic Publishers, 2nd ed., (1997).

356. Qiang, W.U. and Zhang, B.Y. Kinetic promotion of sodium dodecyl sulfate on formation rate of mine gas hydrate. *Procedia Earth and planetary Science* 1:648-653 (2009).

357. Raaijmakers, J.M., De Bruijn, I., Nybroe, O. and Ongena, M. Natural functions of lipopeptides from *Bacillus* and *Pseudomonas* more than surfactants and antibiotics. *FEMS Microbiol Rev* 34(6):1037-1062 (2010).

358. Radich, J., Rogers, R.E., French, W.T. and Zhang, G. Biochemical reaction and diffusion in seafloor gas hydrate capillaries Implications for gas hydrate stability. *Chem Eng Sci* 64:4278-4285 (2009).

359. Rahimi, M., Chae, I., Hawk, J.E., Mitra, S.K. and Thundat, T. Methane sensing at room temperature using photothermal cantilever deflection spectroscopy. *Sensors Actuat B-Chem* 221:564-569 (2015).

360. Rahman, K.S.M., Rahman, T.J., McClean, S., Marchant, R. and Banat, I.M. Rhamnolipidbiosurfactant production by strains of *Pseudomonas aeruginosa* using low-cost raw materials. *Biotechnol Prog* 18:1277-1281 (2002).

361. Ramana, M.V., Ramprasad, T., Paropkari, A.L., Borole, D.V., Rao, B.R., Karisiddaiah, S.M., Kocherla, M., Joao, H.M., Lokabharati, P., Gonsalves, M.J., Pattan, J.N., Khadge, N.H., Babu, C.P., Sathe, A.V., Kumar, P. and Sethi, A.K.

Multidisciplinary investigations exploring indicators of gas hydrate occurrence in the Krishna–Godavari Basin offshore, east coast of India. *Geo-Mar Lett* 29:25-38 (2009).

362. Ramesh, S., Vedachalam, N., Ramesh, R., Prasad, N.T., Ramadass, G.A. and Atmanand, M.A. An approach for methane hydrates reservoir dissociation in a marine setting, Krishna Godhavari Basin, east coast India. *Mar Petrol Geol* 58:540-550 (2014).
363. Randhawa, K.K.S. and Rahman, P.K.S.M. Rhamnolipid biosurfactants: past, present, and future scenario of global market. *Front Microbiol* 5:454 (2014).
364. Rawool, A.S. and Mitra, S.K. Role of green energy towards India's energy security. *1st International Green Energy Conference* 12th -16th June: Waterloo, Ontario Canada (2005).
365. Raza,Z.A., Khalid,Z.M. and Banat,I.M. Characterization of rhamnolipids produced by a Pseudomonas aeruginosa mutant strain grown on waste oils. *J Environ Sci. and Health, Part A: Toxic/Hazardous Subst and Environ Eng.* 44(13):1367-1373 (2009).
366. Riedel, M., Collett, T.S. and Shankar, U. Documenting channel features associated with gas hydrates in the Krishna–Godavari Basin, offshore India. *Mar Geol 279:1-11 (2011).*
367. Ripmeester, J.A. and Ratcliffe, C.I. Low temperature cross polarization/magic angle spinning carbon-13 NMR of solid methane hydrates structure cage occupancy and hydration number. *J Phys Chem* 92(2):337-339 (1988).
368. Ripmeester, J.A., Tse, J.A., Ratcliffe, C.I. and Powell, B.M. A new clathrate hydrate structure. *Nature* 325:135-136 (1987).
369. Risk Assessment report, Application A1030, Calcium Lignosulphonate (40-65) as a Food Aditive, Food Standards Australia & New Zealand.
370. Robinson, D.B. and Ng, H.J. Hydrate formation and inhibition in gas condensate streams. *J Can Pet Tech* 25(4):26-30 (1986).
371. Rock, A. Experimentelle und theoretische untersuchung zur hydratbildung aus gasgemischen in inhibitorhaltigen wässrigen lösungen, Dissertation, Universität Karlsruhe T.H., (2002).

372. Rogers, R., Radich, J. and Xiong, S. The multiple roles of microbes in the formation, dissociation and stabilite of seafloor gas hydrates. *7th international conference on gas hydrates (ICGH)* 17th -21st July: Edinburgh, Scotland, United Kingdom (2011).
373. Rogers, R., Zhang, G., Dearman, J. and Woods, C. Investigations into surfactant/gas hydrate relationship. *J Petrol Sci Eng* 56(1-3):82-88 (2007).
374. Rogers, R.E., Dearman, J.L. and Roberts, H.H. Enhancement of Gas Hydrate Formation in Gulf of Mexico Sediments, *Offshore Technology Conference* 5th –8th May: Houston, Texas, U.S.A. (2003).
375. Rogers, R.E., Kothapalli, C., Lee, M.S. and Woolsey, J.R. Catalysis of Gas Hydrates by Biosurfactants in Seawater-Saturated Sand/Clay. *Can J Chem Eng* 81(5):973-980 (2003).
376. Rogers, R.E., Zhang, G., Kothapalli, C. and French, W.T. Laboratory Evidence of Microbial-Sediment-Gas Hydrate Synergistic Interactions in Ocean Sediments. *14th International Offshore and Polar Engineering Conference*, 23th -28th May:Toulon, France I*nternational Society of Offshore and Polar Engineers* (2004).
377. Rogers, R.E., Zhong, Y., Etherridge, J.A., Kumar, R.A., Pearson, L.E. and Hogancamp, T.K. Micellar gas hydrate storage process. *5th International Conference on Gas Hydrates (ICGH)* 4036 (2005).
378. Roldan, P.S., Alcantara, I.L., Rocha, J.C., Padilha, C.C.F. and Padilha, P.M. Determination of Copper, Iron, Nickel and Zinc in fuel kerosene by FAAS after adsorption and pre concentration on 2 aminothiazole modified silica gel. *Eclet Quím* 29:33-40 (2004).
379. Rooney, A.P., Price, N.P., Ray, K.J. and Kuo, T.M. Isolation and characterization of rhamnolipid-producing bacterial strains from a biodiesel facility. *FEMS Microbiol Lett* 295(1):82-87 (2009).
380. Rosenberg, E. Microbial Diversity as a Source of Useful Biopolymers. *J Ind Microbiol* 11:131–137 (1993).
381. Rosenberg, E. Microbial Surfactants. *CRC Crit Rev Biotech* 3:109–132 (1986).
382. Rueff, R.M., Sloan, E.D. and Yesavage, V.F. Heat capacity and heat of dissociation of methane hydrates. *AIChE J* 34(9):1468-1476 (1988).
383. Sabate, D.C. and Audisio, M.C. Inhibitory activity of surfactin, produced by different *Bacillus subtilis* subsp. subtilis strains, against Listeria monocytogenes sensitive and bacteriocin-resistant strains. *Microbiol Res* 168:125-129 (2013).

384. Saeki, T., Hayashi, M., Fujii, T., Inamori, T., Kobayashi, T., Takano, O. and Nagakubo, S. Extraction of Methane Hydrate Concentrated Zone for Resource Assessment in the Eastern Nankai Trough Japan. *Offshore Technology Conference* 5th -8th May: Houston, Texas, USA (2008).

385. Sain, K. and Gupta, H.K. Gas Hydrates, A Major Energy Resource of India for the Next Generation. *J Ind Geophys Union* 18(1):11-18 (2014).

386. Sain, K. Gas-Hydrates-A probable Solution to India's Energy Crisis. *Int J Earth Sci and eng 5(2) (2012).*

387. Saito, A. Recent advances in research on cold thermal energy storage. *Int J Refrig* 25(2):177–89 (2002).

388. Sanchez, M., Aranda, F.J., Espuny, M.J., Marques, A., Teruel, J.A., Manresa, A. and Ortiz, A. Aggregation behaviour of a dirhamnolipids biosurfactant secreted by *Pseudomonas aeruginosa* in aqueous media. *J Colloid Interf Sci* 307(1):246-253 (2007).

389. Sandrin, C., Peypoux, F. and Michel, G. Coproduction of surfactin and iturin A, lipopeptides with surfactant and antifungal properties, by *Bacillus subtilis*. *Biotechnol Appl Bioc* 12:370-375 (1990).

390. Satoh, M., Maekawa, T. and Okuda, Y. Estimation of amount of methane and resources of gas hydrates in the world and around Japan. *Jour Geol Soc Japan* 102:959–971 (1996).

391. Satpute, S.K., Banpurkar, A.G., Dhakephalkar, P.K., Banat, I.M. and Chopade, B.A. Methods for investigating biosurfactants and bioemulsifiers: a review. *Crit Rev Biotechnol* 30(2):127-144 (2010).

392. Satyavani, N., Shankar, U., Thakur, N.K. and Reddi, S.I. Probable gas hydrate/free gas model over western continental margin of India. *Mar Geophys Res* 23:423-430, (2002).

393. Savadogo, A., Tapi, A., Chollet, M., Wathelet, B., Traore, A.S. and Jacques, P. Identification of surfactin producing strains in Soumbala and Bikalga fermented condiments using Polymerase Chain Reaction and Matrix Assisted Laser Desorption/Ionization Mass Spectrometry methods. *Int J Food Microbiol* 151:299-306 (2011).

394. Saw, V.K., Ahmad, I., Mandal, A., Udayabhanu, G. and Laik, S. Methane hydrate formation and dissociation in synthetic seawater. *Journal of Natural Gas Chemistry* 21(6):625-632 (2012).

395. Saw, V.K., Gudalaa, K.M., Udayabhanu, G., Mandal, A. and Laik, S. Kinetics of methane hydrate formation and its dissociation in presence of non-ionic surfactant Tergitol. *Journal of Unconventional Oil and Gas Resources* 6:54–59 (2014).

396. Saw, V.K., Udayabhanu, G., Mandal, A. and Laik, S. Methane Hydrate Formation and Dissociation in the Presence of Silica Sand and Bentonite Clay. *Oil Gas Sci Technol Rev IFP Energies nouvelles* (2014). http://dx.doi.org/10.2516/ogst/2013200.

397. Saw, V.K., Udayabhanu, G.N., Mandal, A. and Laik, S. Methane Hydrate Formation and Dissocition in the Presence of Bentonite Clay Suspension. *Chem Eng Technol* 36(5):810-818 (2013).

398. Schicks, J.M., Spangenberg, E., Giese, R., Heeschen, K., Priegnitz, M., Luzi-Helbing, M., Thaler, J., Abendroth, S., Kück, J. and Töpfer, M. Methane production from hydrate-bearing sediments via thermal stimulation using a counter-current heat-exchange reactor. *ICGH* 28th July – 1st August (2014).

399. Schoderbek, D., Farrell, H., Hester, K., Howard, J., Raterman, K., Silpngarmlert, S., Martin, K.L., Smith, B. and Klein, P. Conoco Phillips Gas Hydrate Production Test Final Technical Report, (2013).

400. Scott, D.R., Frederick, W., Mark, N.F., Masanori, K., Koji, Y., Tetsuya, F., Kasumi, F., Masaaki, N. and Masato, Y. Geologic and Porous Media Factors Affecting the 2007 Production Response Characteristics of the Jogmec/Nrcan/Aurora Mallik Gas Hydrate Production Research Well. *ICGH* July 6th to 10th (2008).

401. Sekhon,K.K., Khanna,S. and Cameotra,S.S. Biosurfactant Production and Potential Correlation with Esterase Activity. *J petroleum and environ biotechnology* 3(7):133 (2012).

402. *Seo, Y. and Lee, H. Multiple-phase hydrate equilibria of the ternary carbon dioxide, methane, and water. J Phys Chem B 105(41):10084–10090 (2001).*

403. Seo, Y.T., Moudrakovski, I.L., Ripmeester, J.A., Lee, J.W. and Lee, H. Efficient Recovery of CO_2 from Flue Gas by Clathrate Hydrate Formation in Porous Silica Gels. *Environ Sci Technol* 39:2315-2319 (2005).

404. Shankar, U. and Sain, K. Specific character of the bottom simulating reflectors near mud diapirs Western margin of India. *Curr Sci India* 93(7):997-1002 (2007).

405. Shankar, U., Sain, K. and Riedel, M. Assessment of gas hydrate stability zone and geothermal modeling of BSR in the Andaman Sea. *J Asian Earth Sci 79:358-365 (2014).*

406. Sherif, S.A., Barbir, F. and Veziroglu, T.N. Hydrogen Economy, Handbook of Hydrogen energy, ed., S.A. Sherif, D.Yogi Goswami, Elias K. Stefanakos, Aldo Steinfeld, CRC Press, 1-18 (2014).

407. Sherif, S.A**.**, Barbir, F. and Veziroglu, T.N. Hydrogen Energy Systems, Wiley Encyclopedia of Electrical and Electronics Engineering, John Wiley & Sons, Inc. (1999).

408. Sherif, S.A., Barbir, F. and Veziroglu, T.N. Principles of Hydrogen Energy Production, Storage and Utilization. *J Sci Ind Res India* 62(01-02):46-63 (2003).

409. Sherif, S.A., Barbir, F. and Veziroglu, T.N. Towards a Hydrogen Economy. *The Electricity Journal* 18(6):62-76 (2005)

410. Shipley, T.H., Houston, M.H., Buffler, R.T., Shaub, F.J., McMillen, K.J., Ladd, J.W. and Worzel, J.L. Seismic evidence for widespread possible gas hydrate horizons on continental slopes and rises. *Aapg Bull* 63, 2204–2213 (1979).

411. Shoham, Y. and Rosenberg, E. Enzymatic depolymerisation of Emulsan. *J Bacteriol* 156(1):161-167 (1983).

412. Siangsai, A., Rangsunvigit, P., Kitiyanan, B., Kulprathipanja, P. and Linga, P. Investigation on the roles of activated carbon particle sizes on methane hydrate formation and dissociation. *Chem Eng Sci* 126:383–389 (2015).

413. Silva, S.N., Farias, C.B., Rufino, R.D., Luna, J.M. and Sarubbo, L.A. Glycerol as substrate for the production of biosurfactant by *Pseudomonas aeruginosa* UCP0992. *Colloid Surface B* 79(1):174-183 (2010).

414. Singh, A. and Cameotra, S. Efficiency of lipopeptide biosurfactants in removal of petroleum hydrocarbons and heavy metals from contaminated soil. *Environ Sci Pollut Res* 20:7367-7376 (2013).

415. Singh, A. and Singh B.D. Methane Gas an unconventional energy resource. *Curr Sci India* 76:1533-1545 (1999).

416. Singh, A.K. and Cameotra, S.S. Rhamnolipids Production by Multi-metal-Resistant and Plant-Growth-Promoting Rhizobacteria. *Appl Biochem Biotech* 170:1038–1056 (2013).

417. Singh, A.K., Rautela, R. and Cameotra, S.S. Substrate dependentin vitro antifungal activity of *Bacillus* spstrain AR2. *Microb Cell Fact* 13:67 (2014).

418. Skirvina, R.M., Kohlerb, E., Steinerc, H., Ayersc, D., Laughnanc, A., Nortond, M.A. and Warmunde, M. The use of genetically engineered bacteria to control frost on strawberries and potatoes. Whatever happened to all of that research?. *Sci Hortic-Amsterdam* 84:179-189 (2000).
419. Sloan, E.D. and Fleyfel, F. Hydrate dissociation enthalpy and guest size. *Fluid Phase Equilibr* 76:123–40 (1992).
420. Sloan, E.D. and Koh, C.A. Clathrate hydrates of natural gases, CRC Press, 3rd edition, Taylor & Francis Group: Boca Raton, FL (2008).
421. Sloan E.D., Clathrate hydrate of natural gases, Marcel Dekker CRC press, New York, (1990).
422. Sloan, E.D. Clathrate hydrates of natural gases, Marcel Dekker CRC press, Second Ed., New York, (1998).
423. Sloan, E.D. Fundamental principles and applications of natural gas hydrates. *Nature* 426:353-363 (2003).
424. Sloan, E.D. Hydrate-plug remediation. SPE monograph hydrate engineering, (2000).
425. Sloan, E.D., Koh, C.A., Sum, A.K., Ballard, A.L., Shoup, G.J., McMullen, N., Creek, J.L. and Palermo, T. Hydrates State of the Art Inside and Outside Flowlines. *J Petrol Technol* 61:89−94 (2009).
426. Sloan, E.D., Natural Gas Hydrates in Flow Assurance, Gulf Professional Publishing Oxford, eds., Koh & Sum, U.K., (2011).
427. Sloan, E.D., US patent, US 5, 432, 292 (1995).
428. Smith, D.H., Seshadri, K. and Wilder, J.W. Assessing the Thermodynamic Feasibility of the Conversion of Methane Hydrate into Carbon Dioxide Hydrate in Porous Media. *1st National Conference on Carbon Sequestration*, National Energy TechnologyLaboratory (2001).
429. Smith, I.M. and Thambimuthu, K.V. Greenhouse gas emissions, abatement and control: the role of coal. *Energ Fuel* 7:7–13 (1993).
430. Smith, J.M., VanNess H.C. and Abbott, M.M. Introduction to chemical engineering thermodynamics, McGraw-Hill Inc, 7th ed., New York, 100-103 (2001).

431. Song, Y., Wang, X., Yang, M., Jiang, L., Liu, Y., Dou, B. and Wang, S. Study of selected factors affecting hydrate-based carbon dioxide separation from simulated fuel gas in porous media. *Energ Fuel* 27(6):3341-3348 (2013).
432. Stackelberg, M.V. and Muller, H.R. Feste Gas hydrate II. *Zeitschrift füer Elektrochem* 58:25-39 (1954).
433. Stackelberg, M.V. Feste Gas hydrate. *Naturwissenschaften* 11:327-359 (1949).
434. Stephen, A., Adebusuyi, A., Baldygin, A., Shuster, J., Southam, G., Budwill, K., Foght, J., Nobes, D.S., and Mitra, S.K. Bioconversion of coal: new insights from a core flooding study. *RSC Advances* 4:22779-22791 (2014).
435. Stern, L.A., Circone, S. and Kirby, S.H. Anomalous preservation of pure methane hydrate at 1 atm. *J Phys Chem B* 105:1756–62 (2001).
436. Stewart, C. and Hessami, M.A. study of methods of carbon dioxide capture and sequestration–the Sustainability of a photosynthetic bioreactor approach. *Energ Convers Manage* 46:403–420 (2005).
437. Suess, E., Bohrmann, G., Rickert, D., Kuhs, W.F., Torres, M.E., Thehu, A. and Linke, P. Properties and fabric or near-surface methane hydrates at hydrate ridge, Cassadia Margin. *4th International Conference On Gas Hydrates* 19th –23rd May: Yokohama (2002).
438. Sujith, P.P., Gonsalves, M.J.B.D., Rajkumar, V. and Sheba, M.B. Manganese cycling and its implication on methane related processes in the Andaman continental slope sediments. *Mar Pet Geol* 58(A):254-264 (2014).
439. Sun, C., Li, W., Yang, X., Li, F., Yuan, Q., Mu, L., Chen, J., Liu, B. and Chen, G. Progress in Research of Gas Hydrate. *Chinese J Chem Eng* 19(1):151-162 (2011).
440. Sun, C.Y., Chen, G.J. and Yang, L.Y. Interfacial tension of methane + water with surfactant near the hydrate formation conditions. *J Chem Eng Data* 49:1023 (2004).
441. Sun, R.C., Tomkinson, J. and Jones, G.L. Fractional characterization of ash-aq lignin by successive extraction with organic solvents from oil palm EFB fiber. *Polym Degrad Stabil* 68:111-119 (2000).
442. Sun, Z.G., Fan, S.S., Shi, L., Guo, Y.K. and Guo, K.H. Equilibrium conditions hydrate dissociation for a ternary mixture of methane, ethane, and propane in aqueous solutions of ethylene glycol and electrolytes. *J Chem Eng Data* 46(4).927–929 (2001).

443. Sun, Z., Ma, R., Fan, S., Guo, K. and Wang, R. Investigations on gas storage in methane hydrate. *Journal of Natural Gas Chemistry* 13:107-112 (2004).

444. Sun, Z.G., Ma, R.S., Wang, R.Z., Guo, K.H. and Fan, S.S. Experimental studying of additives effects on gas storage in hydrate. *Energ Fuel* 17(5):1180–1185 (2003).

445. Sun, Z., Wang R., Ma, R., Guo K., and Fan S. Effect of surfactants and liquid hydrocarbons on gas hydrates formation rate and storage capacity. *Int J Energ Res* 27(8):747-756 (2003).

446. Sun, Z.G., Wang, R., Ma, R., Guo, K. and Fan, S. Natural gas storage in hydrates with the presence of promoters. *Energ Convers Manage* 44(17):2733-2742 (2003).

447. Sung, W.M., Lee, H., Kim, S. and Kang, H. Experimental investigation of production behaviour s of methane hydrate saturated in porous rock. *Energ Source* 25(8):845-856 (2003).

448. Sutyak, K.E., Wirawan, R.E., Aroutcheva, A.A. and Chiindas, M.L. Isolation of the *Bacillus subtilis* antimicrobial peptide subtilosin from the dairy product derived *Bacillus* amyliquefaceiens. *J Appl Microbiol* 104:1067-1074 (2008).

449. Tajima, H., Yamasaki, A. and Kiyono, F. Energy consumption estimation for greenhouse gas separation processes by clathrate hydrate formation. *Energy* 29(11):1713–1729 (2004).

450. Takashashi, H. and Tsuji, Y. Multi well exploration program in 2004 for Natural Hydrate in Nankai Trough Offshore , Japan. *Offshore technology conference* OTC 17162 May 2-5: Houston , (2005).

451. Tanasawa, I. and Takao, S. Low-temperature storage using clathrate hydrate slurries of tetra-n-butylammonium bromide: thermophysical properties and morphology of clathrate hydrate crystals. *4th International Conference on Gas Hydrates* Yokohama, Japan, 963–967 (2002).

452. Tang, J.S., Gao, H., Hong, K., Yu, Y., Jiang, M.M., Lin, H.P., Ye, W.C. and Yao, X.S. Complete assignments of ^{1}H and ^{13}C NMR spectral data of nine surfactin isomers. *Magn Reson Chem* 45:792-796 (2007).

453. Tanino, M. and Kozawa, Y. Ice–water two-phase flow behaviour in ice heat storage systems. *Int J Refrig* 24(7):639–651 (2001).

454. Taylor, C., Kwan, J., Rogers, R., Zhong, Y., Etheridge, J. and Pearson, L. The MSU Micellar-Solution Gas Hydrate Storage Process for Natural Gas Advances in the Study of Gas Hydrates. *Springer US* 185-198 (2004).

455. Taylor, M. and Fitzgerald, A. The BG Hydrate Project–Technology Development, AIChE Spring National Meeting, 8 (2001).

456. Taylor, M. Fire and ice: gas hydrate transportation-a possibility for the Caribbean region. *SPE 8th Latin American and Caribbean petroleum engineering Conference*, 27th -30th April: Port of Spain, Trinidad (2003).

457. Tchapda, A.H. and Pisupati, S.V. A Review of Thermal Co-Conversion of Coal and Biomass/Waste. *Energies* 7:1098-1148 (2014).

458. Tejado, A., Pena, C., Labidi, J., Echeverria, J.M. and Mondragon, I. Physico-chemical characterization of lignins from different sources for used in phenol-formaldehyde resin synthesis. *Bioresource Technol* 98:1655-1663 (2007).

459. Thangamani, S. and Shreve, G.S. Effect of anionic biosurfactant on hexadecane partitioning in multiphase systems. *Environ Sci Technol* 28:1993-2000 (1994).

460. Thomas, S. and Dawe, R.A. Review of ways to transport natural gas energy from countries which do not need the gas for domestic use. *Energy* 28:1461–1477 (2003).

461. Tomlison, J.J. Clathrates a storage alternative to ice for residential cooling, In EPRI Cool storage Workshop, (1983).

462. Torré, J.P., Dicharry, C., Ricaurte, M., David, D.D. and Broseta, D. CO_2 capture by hydrate formation in quiescent conditions: in search of efficient kinetic additives. *Energy Procedia* 4:621–628 (2011).

463. Townson, I., Walker, V.K., Ripmeester, J.A. and Englezos, P. Bacterial Inhibition of Methane Clathrate Hydrates Formed in a Stirred Autoclave. *Energ Fuel* 26:7170−7175 (2012).

464. Trofimuk, A.A., Cherskii, N.V. and Tsaryov, V.P. The role of continental glaciation and hydrate formation on petroleum occurrences, The future supply of nature-made petroleum and gas, Pergamon Press, Meyer, R.F. eds., New York 919–926 (1977).

465. Tucholke, B.E., Bryan, G.M. and Ewing, J.I. Gas-hydrate horizons detected in seismic-profiler data from the western north atlantic. *AAPG Bull* 61:698–707 (1977).

466. Uchida, T., Takagi, A., Mae, S. and Kawabata, J. Dissolution mechanisms of CO_2 molecules in water containing CO_2 hydrates. *Energy Convers Manage* 38:S307–312 (1997).

467. USGS Fact Sheet Assessment of Gas Hydrate Resources on the North Slope Alaska, 2008-3073 (2008).

468. Vater, J., Kablitz, B., Wilde, C., Franke, P., Mehta, N. and Cameotra, S.S. Matrix-assisted laser desorption ionization time of flight mass spectrometry of lipopeptide biosurfactants in whole cells and culture filtrates of *Bacillus subtilis* c-1 isolated from petroleum sludge. *Appl Environ Microb* 68:6210-6219 (2002).

469. Vedachalam, N., Ramesh, S., Jyothi, V.B.N., Prasad, N.T., Ramesh, R., Sathianarayanan, D., Ramadass, G.A. and Atmanand, M.A. Evaluation of the depressurization based technique for methane hydrates reservoir dissociation in a marine setting, in the Krishna Godavari Basin, east coast of India. *Journal of Natural Gas Science and engineering* 25: 226-235 (2015).

470. Vedachalam, N., Srinivasalu, S. Rajendran, G., Ramadass, G.A. and Atmanand, M.A. Review of unconventional hydrocarbon resources in major energy consuming countries and efforts in realizing natural gas hydrates as a future source of energy. *Journal of Natural Gas Science and engineering* 26:163-175 (2015).

471. Veluswamy, H.P., Kumar, R. and Linga, P. Hydrogen storage in clathrate hydrates: Current state of the art and future directions. *Appl Energ* 122:112-132 (2014).

472. Verret, J. and Servio,P. Evaluating Surfactants and Their Effect on Methane Mole Fraction during Hydrate Growth. *Ind. Eng. Chem. Res 51* (40): 13144–13149 (2012).

473. Villano, L.D., Kelland, M.A., Miyake, G.M. and Chen, E. Effect of Polymer Tacticity on the Performance of Poly (N.Ndialkylacrylamides) as Kinetic Hydrate Inhibitors. *Energ Fuel* 24:2554−2562 (2010).

474. Villard, P. *Compt Rend* 111:302 (1890).

475. Villard, P. Sur quelques nouveaux hydrates de gaz. *Compt Rend* 106:1602-1603 (1888).

476. Vogt, P.R., Crane, K., Sundvor, E., Hjelstuen, B.O., Gardner, J., Bowles, F. and Cherkasher, G. Ground-Truthing 11 to 12 kHz side-scan sonar images in the Norwegian-Greenland Sea: Part II probable diapirs on the Bear Island fan slide valley margins and the Vering Plateau. *Geo-Mar Lett* 19:11-130 (1999).

477. Volmer, M. Kinetik der Phasenbildung, Steinkopff. Dresden Leipzig, (1939).

478. Wang, Q., Fang, X., Bai, B., Liang, X., Shuler, P.J., Goddard, W.A. 3rd. and Tang, Y. Engineering bacteria for production of rhamnolipid as an agent for enhanced oil recovery. *Biotechnol Bioeng* 98(4):842-853 (2007).

479. Wang, W., Huang, Z., Chen, H., Tan, Z., Chen, C. and Sun, L. Methane hydrates with a high capacity and a high formation rate promoted by biosurfactants. *Chem Commun* 48(95):11638-11640 (2012).

480. Wang, W., Ma, C., Lin, P., Sun, L. and Cooper, A.I. Gas storage in renewable bioclathrates. *Energy Environ Sci* 6(1):105-107 (2012).

481. Wang, W., Ma, C., Lin, P., Sun, L. and Cooper, A I.Gas storage in renewable bioclathrates. *Energy Environ Sci* 6:105-107 (2013).

482. Watanabe, K., Imai, S. and Mori, Y.H. Surfactant effects on hydrate formation in an unstirred gas/liquid system: An experimental study using HFC-32 and sodium dodecyl sulphate. *Chem Eng Sci* 60:4846-4857 (2005).

483. Wei, L., David, K., Jun, L., Brad, J., Yong, W. and Zhenguo, Y. Critical Material and Process issues for CO_2 separation from coal Powered Plants. *Material in Clean power Systems overview* 61:36-44 (2009).

484. Weil, J.K., Smith, F.S., Stirton, A.J. and Bistline, R.G. Longchain alkanesulfonates and 1-hydroxy-2-alkanesulfonates: structure and property elations. *J Am Oil Chem Soc* 40(10):538–540 (1963).

485. Whang, L.M., Liu, P.W.G., Ma, C.C. and Cheng, S.S. Application of biosurfactants, rhamnolipid, and surfactin, for enhanced biodegradation of diesel-contaminated water and soil. *J Hazard Mater* 151:155–163 (2008).

486. White, C.M., Strazisar, B.R., Granite, E.J., Hoffman, J.S. and Pennline, H.W. Separation and capture of CO_2 from large stationary sources and sequestration in geological formations Coalbeds and deep saline aquifers. *J Air Waste Manage* 53(6):645–715 (2003).

487. Wittstruck, T.A., Brey, W.S., Buswell, A.M. and Rodebush, W.H. Solid hydrates of some halomethanes. *J Chem Eng Data* 6(3):343–346 (1961).

488. Wood, W. and Jung, W. Modelling the extent of Earth's marine methane hydrate cryosphere. *6th International Conference on Gas Hydrates (ICGH)* 6th -10th July: Vancouver, British Columbia, Canada (2008).

489. Woods, C.E. Jr. Examination of the effects of biosurfactant concentration on natural gas hydrate formation in seafloor porous media. Thesis, Chemical engineering, Earth sciences, Dave C. Swalm School of Chemical Engineering, Mississippi State University 94–95 (2004).

490. Wright, J.F., Uddin, M., Dallimore, S.R. and Coombe, D. Mechanisms Of Gas Evolution And Transport In A Producing Gas Hydrate Reservoir An Unconventional Basis For Successful History Matching Of Observed Production Flow Data. *7th International Conference on Gas Hydrates* 17th to 21st July: Edinburgh, Scotland, U.K (2011).

491. Wu, J.Y., Yeh, K.L., Lu, W.B., Lin, C.L. and Chang, J.S. Rhamnolipid production with indigenous *Pseudomonas aeruginosa* EM1 isolated from oil-contaminated site. *Bioresource Technol* 99(5):1157-1164 (2008).

492. Xiao, B., Sun, X.F. and Cang, S.R. Chemical, structural and thermal characterization of alkali-soluble lignins and hemicelluloses, andcellulose from the maize stems, rye straw and rice straw. *Polym Degrad Stabil* 74:307-319 (2001).

493. Xu, S., Fan, S., Wang, Y. and Lang, X. An Investigation of Kinetic Hydrate Inhibitors on the Natural Gas from the south China Sea. *J Chem eng data* 60:311−318 (2015).

494. Yakimov, M., Amro, M. and Bock, M. The potential of *Bacillus* licheniformis strains for in situ enhanced oil recovery. *J Petrol Sci Eng* 18:147-160 (1997).

495. Yamamoto, K. and Dallimore, S. Aurora-Jogmec-Nrcan Mallik 2006-2008 Gas Hydrate Research Project Progress. *Fire in the ice* 8(3):1-5 (2008).

496. Yamamoto, K., Inada, N., Kubo, S., Fujii, T., Suzuki, K., Nakalsuka, Y., Ikawa, T., Seki, M., Konno, Y., Yoneda, J., Nagao, J. and Mizuguchi, Y. A Pressure Coring Operation On-board Analyses of Methane Hydrate-bearing Samples, *Offshore Technology Conference* 5th to 8th May: Houston Texas, USA 4(5):2425 (2014).

497. Yamasaki, A. An overview of CO_2 mitigation options for global warming–Emphasizing CO_2 sequestration options. *J Chem Eng Jpn* 36:361–375 (2003).

498. Yan, L.J., Chen, G.J., Pang, W.X. and Liu, J. Experimental and modeling study on hydrate formation in wet activated carbon. *J Phys Chem B* 109(12):6025-6030 (2005).

499. Yang, H., Li, X., Li, X., Yu, H. and Shen, Z. Identification of lipopeptide isoforms by MALDI-TOF-MS/MS based on the simultaneous purification of iturin, fengycin, and surfactin by RP-HPLC. *Anal Bioanal Chem* 407:2529–2542 (2015).

500. Yang, M., Liu, W., Song, Y., Ruan, X., Wang, X., Zhao, J. and Li, Q. Effects of additive mixture (THF/SDS) on the thermodynamic and kinetic properties of CO_2/H_2 hydrate in porous media. *Ind Eng Chem Res* 52(13):4911-4918 (2013).
501. Yang, M., Song, Y., Jiang, L., Liu, Y. and Wang, X. Behaviour of hydrate-based technology for H_2/CO_2 separation in glass beads. *Sep Purif Technol* 141:70-178 (2015).
502. Yang, M., Song, Y., Jiang, L., Zhu, N., Liu, Y., Zhao, Y. and Li, Q. CO_2 hydrate formation and dissociation in cooled porous media: A potential technology for CO_2 capture and storage. *Environ Sci Technol* 47(17):9739-9746 (2013).
503. Yang, S.O., Yang, I.M. and Lee, C.S. Measurement and prediction of phase equilibria for water + CO_2 in hydrate forming conditions. *Fluid Phase Equilibr* 175(1–2):75–89 (2000).
504. Yanhong, W., Xuemei, L. and Shuanshi, F. Hydrate capture CO_2 from shifted synthesis gas, flue gas and sour natural gas or biogas. *Journal of Energy Chemistry* 22(1):39-47 (2013).
505. Yin, H., Qiang, J., Jia, Y., Ye, J., Peng, H., Qin, H., Zhang, N. and He, B. Characteristics of biosurfactant produced by *Pseudomanas aeruginosa* S6 isolated from oil-containing wastewater. *Process Biochem* 44:302-308 (2009).
506. Yoslim, J., Linga, P. and Englezos, P. Enhanced growth of methane-propane clathrate hydrate crystals with sodium dodecyl sulfate, sodium tetradecyl sulfate, and sodium hexadecyl sulfate surfactants. *J Cryst Growth* 313(1):68-80 (2010).
507. Zang, X., Du, J., Liang, D., Fan, S. and Tang, C. Influence of A-type zeolite on methane hydrate formation. *Chinese J Chem Eng* 17(5):854–859 (2009).
508. Zang, X., Fan, S., Liang, D., Li, D. and Chen, G. Influence of 3A molecular sieve on tetrahydrofuran (THF) hydrate formation. *Sci China Ser B* 51(9):893–900 (2008).
509. Zang, X., Du, J., Liang,D., Fan, S. and Tang ,C. Influence of A-type Zeolite on Methane Hydrate Formation. *Chinese J Chem Eng*;17(5):854-859 (2009).
510. Zeng, H., Moudrakovski, I.L., Ripmeester, J.A. and Walker, V.K. Effect of antifreeze protein on nucleation, growth and memory of gas hydrates. *Aiche J* 52(9):3304-3309 (2006).
511. Zeng, H., Wilson, L.D., Walker, V.K. and Ripmeester, J.A. The Inhibition of Tetrahydrofuran Clathrate-Hydrate Formation with Antifreeze Protein. *Can J Phys* 81(1−2):17−24 (2003).

512. Zhang, B., Wu,Q. and Sun, D.L. Effect of surfactant Tween on induction time of gas hydrate formation. *J china univ mining & technol* 18(1):18-21 (2008).
513. Zhang, C.S., Fan, S.S., Liang, D.Q. and Guo, K.H. Effects of Additives on Formation of Natural Gas Hydrate. *Fuel* 83:2115-2121 (2004).
514. Zhang, G., Rogers, R.E., French, W.T. and Lao, W. Investigation of microbial influences on seafloor gas-hydrate formations. *Mar Chem* 103(3-4):359-369 (2007).
515. Zhang, J.S., Lee, S. and Lee, J.W. Does SDS micellize under methane hydrate-forming conditions below the normal Krafft point?, *J Colloid Interf Sci* 315:313–318 (2007).
516. Zhang, J.S., Lee, S. and Lee, J.W. Kinetics of Methane Hydrate Formation from SDS Solution. *Ind Eng Chem Res* 46(19):6353-6359 (2007).
517. Zhang, P., Wu, Q. and Yang, Y. Characteristics of Methane Hydrate Formation in Artificial and Natural Media. *Energies* 6(3):1233-1249 (2013).
518. Zhang, Z.G., Wang, Y., Gao, L.F., Zhang, Y. and Liu, C.S. Marine Gas Hydrates: Future Energy or Environmental Killer?. *Energy Procedia* 16(Part B):933-938 (2012).
519. Zhao, F., Shil, R., Zhao, J., Li, G., Bai, X., Han, S. and Zhang, Y. Heterologous production of *Pseudomonas aeruginosa* rhamnolipid under anaerobic conditions for microbial enhanced oil recovery. *J Appl Microbiol* 118:379-389 (2014).
520. Zhong, Y. and Rogers, R.E. Surfactant effects on gas hydrate formation. *Chem Eng Sci* 55:4175-4187 (2000).
521. Zhou, S.D., Wang, S.L. and Zhang, G.Z. Effect of Different Surfactants on Gas Hydrate Formation. *Advanced Materials Research* 645:146-149 (2013).

ANNEXURE

1. Amount of CO_2 and Methane Gas consumed during Hydrate Formation

As the Gas inside the crystallizer is consumed for Hydrate Formation, the pressure in the CR drops. The total number of moles of the Gas that were consumed for Hydrate Formation $\Delta n_{H,\downarrow}$ was calculated by following equation:

$$(\Delta n_{H,\downarrow})_t = V_{CR}\left[\frac{P}{zRT}\right]_0 - V_{CR}\left[\frac{P}{zRT}\right]_t \quad (1)$$

$$Z = 1 + \beta^0 \frac{P_r}{T_r} + \omega\beta^1 \frac{P_r}{T_r} \quad (2)$$

Where $\beta^0 = 0.083 - \frac{0.422}{T_r^{1.6}}$, $\beta^1 = 0.139 - \frac{0.172}{T_r^{4.2}}$

$\beta^0, \beta^1 =$ Empirical Constants

ω = Acentric factor

P_r = Reduced Pressure

T_r = Reduced Temperature

$$T_r = \frac{T_{\exp}}{T_{critical}}, \quad P_r = \frac{P_{\exp}}{P_{critical}}$$

Where z is the compressibility factor calculated by Pitzer's correlation [Smith et al, 2001]; z varies with time and is obtained from the Gas uptake data. V_{CR} is the volume of the Gas phase of the crystallizer; P & T are pressure and temperature of the crystallizer at the corresponding states.

2. Calculation of the heat of Methane Hydrate Dissociation

The Heat of Dissociation is measured by the Clausius-Clapeyron equation is as follows:

$$\ln\frac{P2}{P1} = \frac{\Delta H\,(dissociation)}{zR}\left(\frac{1}{T1}-\frac{1}{T2}\right) \quad (3)$$

Where P1 stands for initial pressure, P2 stands for final pressure, T1 stands for initial temperature, T2 stands for final temperature, z stands for compressibility factor for Gas, R stands for universal Gas constant(R=8.14 J mol^{-1} k^{-1}) and ΔH_{diss} stands for molar enthalpy of Dissociation of Methane Gas Hydrate.

3. Calculation of the Rate of Methane Hydrate Formation

The rate of Methane Hydrate Formation for different experimental conditions was assumed to be first-order reaction. A first order reaction is defined by the following Equations :

$$N = N_o e^{-kt} \quad (4)$$

$$\ln (N/N_o) = -kt \quad (5)$$

Where N stands for total number of moles at time t, N_0 stands for initial number of moles, k is the rate constant (min^{-1}) and t is time in minute. The rate constant (k) of Hydrate Formation can be obtained from the slope of the curve of ln (N/N_0) vs time. Hydrate Formation rate is calculated by putting the values of slopes i.e. rate constant k in the following equation:

$$dN/dt = -N_o k e^{-kt} \quad (6)$$

4. Calculation of the water to CO_2 and Methane Hydrate conversion

The equation for amount of water that converts to Hydrate has been shown as per following equation [Linga et al, 2010]:

$$\text{Conversion of water to hydrate(mol\%)} = \frac{\Delta n_{H\downarrow} \times HydrationNo.}{n_{H_2O}} \times 100 \quad (7)$$

Where $\Delta n_{H,\downarrow}$ the total number of moles of Gas consumed for Hydrate Formation process as determined from the Gas uptake measurements and n_{H_2O} is the total number of moles of water in the system.

Type I structure is formed by Pure CO_2 Hydrates (Sloan et al, 2008). Its unit cell is made up of 46 water molecules in the basic crystal having 6 large ($5^{12}6^2$) cavities (average cavity radius 4.33 Å) and 2 small (5^{12}) cavities (average cavity radius 3.95 Å). The ideal unit cell formula is 6 ($5^{12}6^2$) 2(5^{12}) 46 H_2O [Kang et al, 2000]. For an ideal sI Hydrates, if both large and small cavities were fully occupied then the hydration number will be equal to 46/8 but the actual hydration number depends on experimental condition. Kumar et al [Kumar et al, 2009] has reported cage occupancy of pure CO_2 Hydrate at moderate pressure range which is used in the present study. For simple Hydrates, the hydration number [Sloan et al, 2008] is dependent on the fractional occupancy of the large and small cavities, respectively. The hydration number N_h can be calculated from the following formula:

$$N_h = \frac{46}{6\theta_L + 2\theta_S} \tag{8}$$

Cage occupancy valve for pure CO_2 Hydrate can be calculated by combining results from infrared spectroscopy and Gas chromatography.

Where θ_S= 0.81, θ_L= 1.0 and putting in above equation 8 giving a hydration number of 6.04 for CO_2 [Kumar et al, 2009].

Type I structure is formed by Methane Hydrate. Its unit cell is made up of 46 water molecules in the basic crystal with 6 large ($5^{12}6^2$) cavities and 2 small (5^{12}) cavities. The ideal unit cell formula is 6 ($5^{12}6^2$). 2 (5^{12}). 46 H_2O [Davidson et al, 1973, Sloan et al, 2008]. For ideal sI Hydrates, if all of the cavities were filled the hydration number (water molecules per guest molecule) would be n =46/8. For simple Hydrates, the hydration number can be co-related to the fractional filling of the large and small cavities, θ_L and θ_S respectively [Sloan et al, 2008].

The hydration number n can be calculated from the following formula:

$$N_h = \frac{46}{6\theta_L + 2\theta_S} \tag{9}$$

Put θ_L= 0.97 and θ_S = 0.89 in Equation 9 [Ripmeester et al, 1988].

Nh= 6.05 for CH_4 [Ripmeester et al, 1988].